

THE UNIVERSITY OF MANITOBA

SOME ASPECTS OF THE MECHANISMS OF DIAGONAL

FAILURE OF REINFORCED CONCRETE BEAMS

by

ASAD A. SHAH

A THESIS

SUBMITTED TO THE FACULTY OF GRADUATE STUDIES

IN PARTIAL FULFILMENT OF THE REQUIREMENTS FOR THE DEGREE

OF DOCTOR OF PHILOSOPHY

DEPARTMENT OF CIVIL ENGINEERING

WINNIPEG, MANITOBA

October 1973



SOME ASPECTS OF THE MECHANISMS OF DIAGONAL
FAILURE OF REINFORCED CONCRETE BEAMS

By: Asad A. Shah

A dissertation submitted to the Faculty of Graduate Studies of
the University of Manitoba in partial fulfillment of the requirements
of the degree of

DOCTOR OF PHILOSOPHY

© 1973

Permission has been granted to the LIBRARY OF THE UNIVER-
SITY OF MANITOBA to lend or sell copies of this dissertation, to
the NATIONAL LIBRARY OF CANADA to microfilm this
dissertation and to lend or sell copies of the film, and UNIVERSITY
MICROFILMS to publish an abstract of this dissertation.

The author reserves other publication rights, and neither the
dissertation nor extensive extracts from it may be printed or other-
wise reproduced without the author's written permission.

ACKNOWLEDGEMENTS

I wish to acknowledge the valuable guidance and encouragement extended to me throughout this investigation by my supervisor, Dr. A. M. Lansdown, and for the many stimulating discussions we have had.

I am also thankful to Dr. K. R. McLachlan, Dr. B. N. Thadani and Dr. J. Cahoon for their technical assistance and advice during various stages of the work.

I would also like to acknowledge the assistance by the Civil Engineering Laboratory Staff, Mr. E. Lemke, Mr. J. Rodenhuis and Mr. Z. Fridrich in particular, during the experimental part of this investigation.

Finally, I would like to express my gratitude to my parents and my wife for their understanding for the considerable period that I was away from home working on this project.

ABSTRACT

In this study, the internal mechanisms of diagonal resistance of reinforced concrete beams without web reinforcement, subjected to flexural and shear loading, have been investigated. The main conclusion drawn from a detailed examination of the internal distribution of forces is that beam and arch action exist simultaneously in the shear spans of all such beams after flexural cracking occurs for the complete range of types of diagonal failure, regardless of the type and manner of loading. Flexural cracks on the tension side of a beam divide it into a number of blocks, which can be considered to be concrete cantilevers, loaded at their tips by the bond forces that are induced in the shear span. At the same time internal arching develops in the beam from the midspan region outwards along the flexural cracks which follow the lines of principal compressive stress trajectories. The extent of internal arching depends upon the extent of flexural cracking. As loading increases, the internal arching proceeds outwards. Complete arching over the entire span only takes place after the critical diagonal crack penetrates into the compression zone and is stabilized. At this stage, with non-yielding supports at the beam ends, the external arch develops. Resultant compressive force becomes significantly inclined above the diagonal crack and can be transferred to the supports directly through the external arch.

Before the appearance of the diagonal crack, the action

of concrete cantilevers predominates. Bond forces generate a moment at the roots of these cantilevers which is resisted by the flexural resistance of the concrete cantilevers, by shear transfer across the cracks through aggregate interlock and by the dowel action of the reinforcement. When the capacity of the concrete cantilevers is surpassed, a critical diagonal crack appears. If the beam is slender, high flexural-tensile stresses above this crack cause the critical crack to propagate rapidly leading to a sudden diagonal tension failure of the beam. However, if the beam is relatively short and deep, the diagonal crack becomes stable before failure takes place. At this stage, an interaction exists between the arch action and a modified beam action, with significant internal rotations taking place in the compression zone. In this case, final failure may result from either a shear-compression failure or a flexural-tension failure at a higher load.

A total of 22 beams were tested in this study. Variables examined were the shear-span/depth ratio, the percentage of longitudinal reinforcement and the manner and type of loading. The beams were extensively instrumented with electrical resistance strain gauges and demountable mechanical (DEMEC) strain gauges. Detailed test results were obtained and substantiated the failure hypothesis described above. The results included observations of longitudinal flexural strains for concrete and the reinforcement, bending of concrete cantilevers, opening of cracks, internal rotations and shifts in the centre of compression on inclined gauge lines.

The test results are analyzed to determine the effect of shear-span/depth ratio, the percentage of longitudinal reinforcement and to indicate the effect of type and manner of loading on the ultimate strength of reinforced concrete beams and on the mechanism of failure. Kani's Method of analysis [KANI (1964)] is used as a basis for discussion of the results, and to determine ultimate beam capacities. It is shown that his equations for beam action underestimate the capacity of the beams, while those for arch action may sometimes overestimate the strength.

NOTATION

A_s	=	area of flexural tension reinforcement
a	=	length of shear span or distance from plane of nearest concentrated load point to plane of the support
b	=	width of a rectangular beam
b'	=	width of the web of a beam
C	=	flexural compression force
ΔC	=	compression force in an internal arch
c_w	=	crack width measured at right angles to the direction of crack
D	=	total depth of beam
d	=	effective depth of beam, the distance between the centroid of the longitudinal tension reinforcement and the extreme compression fiber of the beam
E	=	modulus of elasticity
f'_c	=	compression strength of concrete measured on a standard cylinder
f'_t	=	tensile splitting strength of concrete measured on a standard cylinder
f_y	=	yield strength of reinforcement
\bar{f}_y	=	nominal yield strength of reinforcement
H_{ai}	=	horizontal component of shear transmitted across a crack by aggregate interlock
H_i	=	horizontal component of internal reaction on an internal arch
I	=	moment of inertia of cross section about neutral axis
j	=	ratio of distance between centroid of compression force and centroid of tension force to the effective depth of the beam
j_{dc}	=	value of j at diagonal cracking

j_f	= value of j at failure
K	= ratio of depth of compression zone to the effective depth of the beam or the coefficient of biaxility directly under the concentrated load point or the equivalent spring constant
L	= total length of a beam
l	= length of span of a beam
M	= bending moment acting on a beam
M_{cr}	= bending moment at the time the resistance of concrete cantilevers is broken
M_{fl}	= flexural capacity of the beam
\bar{M}_{fl}	= flexural capacity of the beam using nominal yield strength of reinforcement
M_u	= ultimate bending moment in midspan cross-section at failure
O	= perimeter of reinforcing bar
P	= applied load
P_c	= diagonal cracking load
P_u	= ultimate load at failure of the beam
p	= ratio (or percentage) of the area of flexural tension reinforcement to the area equal to the effective depth times the width of the beam (A_s/bd)
p_w	= ratio (or percentage) of the area of flexural tension reinforcement to the area equal to the effective depth times the width of the web of the beam ($A_s/b'd$)
p_x	= load intensity on the reinforcing bar at point x
R_i	= internal reaction on an internal arch
s	= distance from the centroid of reinforcement to top of cracks measured at right angles to longitudinal axis of beam
T	= flexural tension force
ΔT	= incremental tension force (bond force) acting at the ends of a concrete cantilever

u	= nominal bond stress of reinforcement
V	= total shear applied to the span of a beam
V_{ai}	= transverse component of the shear force transmitted across a crack by aggregate interlock
V_c	= shear force at the formation of a critical diagonal crack or the shear force carried by the compression gauge of the beam
V_d	= dowel shear force
V_i	= vertical component of internal reaction on an internal arch
V_u	= ultimate shear force at failure of a beam
ΔV	= shear force on an internal arch
v or v_n	= nominal shear stress ($\frac{V}{bjd}$)
v_c	= shear stress at critical diagonal cracking
v_h	= horizontal shear stress
v_u	= shear stress at ultimate collapse of a beam
Δx	= spacing of cracks at the reinforcement level
x	= distance measured along the beam from the support point
y	= distance measured from the neutral axis of the beam
α	= shear-span/depth ratio (a/d)
α_{min}	= shear-span/depth ratio where the beam strength is minimum
α_{TR}	= shear-span/depth ratio where full flexural capacity of beam is achieved
δ_h	= longitudinal component of movement in the opening of a crack
δ_s	= shear displacement, the component of movement in the opening of a crack measured in the direction of the crack
δ_v	= transverse component of movement in the opening of a crack
Δ	= total displacement of a point

- Δ_c = displacement of vertical section at reinforcement level
- θ = direction of crack measured from the longitudinal axis of the beam
- θ_1 = angle between the direction of movement of a particle and the perpendicular to the direction of crack
- θ_c = flexural rotation of compression zone of a beam between the centre lines of two adjacent concrete cantilevers, or flexural rotation of compression zone in the region of a beam containing a diagonal crack
- σ_1 = maximum principal stress
- σ_3 = minimum principal stress
- ϵ_{dc} = maximum compressive strain at compression face at diagonal cracking in a beam
- ϵ_f = maximum compressive strain at failure of a beam
- ϕ = capacity reduction factor (0.85)

TABLE OF CONTENTS

	Page
TITLE PAGE	i
ACKNOWLEDGEMENTS	ii
ABSTRACT	iii
NOTATION	vi
TABLE OF CONTENTS	x
 CHAPTER ONE - INTRODUCTION	 1
1.1 GENERAL	1
1.2 A REVIEW OF THE EXISTING RESEARCH	4
1.3 SCOPE OF THE PROJECT	11
1.4 TYPES OF DIAGONAL FAILURES	15
1.4.1 Diagonal Tension Failure	15
1.4.2 Shear Compression Failure	16
1.4.3 Shear Tension Failure	16
1.4.4 Failure by Shear Proper	18
1.4.5 Diagonal Compression Failure	18
1.4.6 Failures Discussed in this Study	18
1.5 FACTORS INFLUENCING RESISTANCE TO DIAGONAL FAILURE OF R. C. BEAMS	19
1.5.1 The a/d or $\frac{M}{Vd}$ Ratio	19
1.5.2 The Amount of Longitudinal Tension Reinforcement	20
1.5.3 The Compressive Strength of Concrete	21
1.5.4 The Manner of Load Application	21
1.5.5 Multiple and Uniform Loads	22

	Page
1.5.6 The Size of the Compression Zone	22
1.5.7 Bond Characteristics of Longitudinal Tension Reinforcement	23
1.5.8 Size of the Web	24
1.5.9 Longitudinal Compression Reinforcement	24
1.5.10 Absolute Size of the Beam	24
1.5.11 Width-Depth Ratio of the Beam	24
1.5.12 Web Reinforcement	25
CHAPTER TWO - SOME BASIC ASPECTS OF DIAGONAL RESISTANCE OF REINFORCED CONCRETE BEAMS	26
2.1 GENERAL	26
2.2 DEVELOPMENT OF CRACKS LEADING TO DIAGONAL FAILURE	26
2.3 PROPAGATION OF CRACKS IN CONCRETE	29
2.4 BEAM AND ARCH ACTION IN R. C. BEAMS	30
2.5 FLEXURAL RESISTANCE OF THE CONCRETE CANTILEVERS	34
2.6 SHEAR TRANSFER ACROSS CRACKS BY AGGREGATE INTERLOCK	37
2.7 DOWEL ACTION OF THE LONGITUDINAL REINFORCEMENT	39
CHAPTER THREE - A CONCEPTUAL MODEL OF THE DIAGONAL FAILURE OF AN R. C. BEAM	46
3.1 GENERAL	46
3.2 THE CONCEPTUAL MODEL	47
3.3 THE INFLUENCE OF VARIOUS FACTORS ON PROPOSED FAILURE MODEL	67
3.3.1 Rotations in the Compression Zone	67
3.3.2 The Method of Loading	71
3.3.3 Compressive and Tensile Strength of Concrete and the Area of Concrete in the Compression Zone of the Beam	76

	Page
3.3.4 The a/d or $\frac{M}{Vd}$ Ratio	78
3.3.5 The Percentage of Longitudinal Reinforcement and its Bond Characteristics	79
3.4 THE ROLE OF WEB REINFORCEMENT	80
CHAPTER FOUR - TEST PROGRAMME	85
4.1 GENERAL	85
4.2 PRELIMINARY SERIES OF TESTS	85
4.3 INFERENCES DRAWN FROM PRELIMINARY TESTS	86
4.4 MAIN TEST PROGRAMME	88
CHAPTER FIVE - EXPERIMENTAL RESULTS	91
5.1 GENERAL	91
5.2 DISTRIBUTION OF LONGITUDINAL FLEXURAL STRAINS IN CONCRETE	95
5.2.1 DEMEC Data	96
5.2.2 Electrical Resistance Strain Gauge Data	98
5.2.3 Results of Other Beams	99
5.3 DISTRIBUTION OF LONGITUDINAL FLEXURAL STRAIN IN THE REINFORCEMENT	102
5.4 DISTRIBUTION OF CONCRETE STRAINS OVER INCLINED GAUGE LINES	106
5.5 DISPLACEMENTS RESULTING FROM BENDING OF CONCRETE CANTILEVERS AND ROTATION OF THE COMPRESSION ZONE	108
5.6 CRACK WIDTHS AND INTERNAL ROTATIONS	110
5.6.1 Beam IA-1	112
5.6.2 Beam III-3	115
5.6.3 Results of Other Tests	116
5.7 INFLUENCE OF DIFFERENT VARIABLES ON BEAM STRENGTH AND THE MECHANISM OF FAILURE	118

	Page
5.7.1 The a/d Ratio	128
5.7.2 The Percentage of Longitudinal Reinforcement	129
5.7.3 Loading Through Secondary Beam	130
5.7.4 Uniform Loads	132
(a) Assuming $a = 1/4$	132
(b) Using Critical Cross-Section of Failure	132
5.7.5 The Compressive Strength of Concrete	133
5.8 DEFLECTIONS OF BEAMS	134
CHAPTER SIX - EXISTING RESEARCH AND PRESENT INVESTIGATION	136
6.1 GENERAL	136
6.2 CONCEPTUAL MODEL OF DIAGONAL FAILURE AND EXISTING RESEARCH	137
6.3 SHEAR STRESS AT DIAGONAL CRACKING AND COLLAPSE	140
6.4 EFFECT OF DIFFERENT VARIABLES ON DIAGONAL STRENGTH OF BEAMS	150
6.4.1 The Compressive Strength of Concrete	150
6.4.2 The a/d Ratio	151
6.4.3 The Percentage of Longitudinal Reinforcement	154
6.4.4 The Method of Loading	156
(a) Uniform Loads	156
(b) Secondary Beam Loading	156
6.5 COMPARISON OF TEST RESULTS WITH KANI'S ANALYTICAL SOLUTIONS	160
CHAPTER SEVEN - CONCLUSIONS AND SUGGESTIONS FOR FURTHER WORK	169
7.1 CONCLUSIONS	169
7.2 SUGGESTIONS FOR FURTHER WORK	175

	Page
BIBLIOGRAPHY	179
APPENDIX I - EXPERIMENTAL WORK	187
APPENDIX II - EXPERIMENTAL RESULTS	247
APPENDIX III - PRESENTATION OF EXPERIMENTAL RESULTS	353

LIST OF FIGURES

Fig.		Page
1.1	Typical Diagonal Failures in Reinforced Concrete Beams	17
2.1	Development of Cracking in the Shear Span of Beams	27
2.2	Internal Forces of Reinforced Concrete Beams [KANI (1964)]	32
2.3	Stress Distribution in a Concrete Cantilever	36
2.4	Dowel Test Arrangement of Various Research Workers	40
3.1	Flexural Cracking due to Bond Forces and Action of Concrete Cantilevers	50
3.2	Equilibrium of Forces before Critical Diagonal Cracking	50
3.3	Beam and Arch Action in Shear Span	50
3.4	Progressive Development of Internal Arching	52
3.5	Internal Forces at Critical Diagonal Cracking	55
3.6	Internal Force Distributions and Diagonal Failures	56
3.7	Compressive Stress Trajectories and Stress Distributions before Cracking	61
3.8	Stress Distribution along an Internal Arch	63
3.9	Development of Internal Arching and Compressive Force Distribution	63
3.10	Forces on an Internal Arch	63
3.11	Displacements Across a Crack	70
3.12	Internal Rotations and Diagonal Crack Width	70
3.13	Effect of Direct Loading on the Compression Face of the Beam	73

Fig.		Page
3.14	Function of Web Reinforcement	84
5.1(a)	Longitudinal Strain - DEMEC Data-Beam IIIA-3	100
5.1(b)	Longitudinal Strain - Electrical Resistance Strain Gauge Data - Beam IIIA-3	101
5.2	Longitudinal Strain in the Reinforcement - Beam IIIA-3	105
5.3	Concrete Strain Distribution on Inclined Gauge Lines - Beam IIIA-3	107
5.4	Horizontal Displacement of Concrete Cantilevers	109
5.5	DEMEC Rosettes and Diagonal Crack - Beam IA-3	112
5.6	DEMEC Rosettes and Diagonal Crack - Beam IIIA-3	115
5.7	Comparative Moment $\frac{M_u}{M_{f1}}$ vs. a/d or l/d	126
5.8	Comparative Moment $\frac{M_u}{M_{f1}}$ vs. a/d or l/d	127
6.1	Shear Stress vs. Shear-Span/Depth Ratio - Series IA	144
6.2	Shear Stress vs. Shear-Span/Depth Ratio - Series IA (Magnification of Fig. 6.1)	145
6.3	Shear Stress vs. Shear-Span/Depth Ratio - Series IB	146
6.4	Shear Stress vs. Shear-Span/Depth Ratio - Series IC	147
6.5	Shear Stress vs. Shear-Span/Depth Ratio - Series IIA	148
6.6	Shear Stress vs. l/d Ratio - Series IIIA	149
6.7	Bending Moment at Failure vs. a/d Ratio	152
	(a) MORROW and VIEST (1957)	
	(b) LEONHARDT and WALTHER (1961)	
	(c) KANI (1964)	
6.8	Effect of Percentage of Longitudinal Reinforcement on Beam Strength - KANI (1966)	155
6.9	Function of Concrete Cantilevers and the Remaining Concrete Arch - KANI (1964)	161

LIST OF TABLES

Table		Page
5.1	Test Results - Series IA	119
5.2	Test Results - Series IB	121
5.3	Test Results - Series IC	122
5.4	Test Results - Series IIA	123
5.5	Test Results - Series IIIA (Using $a = 1/4$)	124
5.6	Comparative Moments - Series IIIA (Using Actual Cross Section of Failure)	125
6.1	Shear Stress at Diagonal Cracking and Collapse	142
6.2	The Effect of Manner of Loading on Diagonal Strength of Beams - FERGUSON (1956)	158
6.3	The Influence of Manner of Loading on Diagonal Strength of Beams - TAUB and NEVELLE (1960)	159
6.4	Kani's Equation and Test Results (Using α_{TR} for each Series - Experimental Values)	167

C H A P T E R O N E

INTRODUCTION

1.1 GENERAL

In this chapter some basic aspects of the behaviour of a beam in the zone of flexure and shear are discussed. The work of some key research workers is examined and the scope of the present investigation is defined. This is followed by a description of the types of diagonal failures and factors influencing them.

When loads are transferred to the supports through the web, vertical stress caused by end shear combines with longitudinal stress from bending in the beam and produces tensile and compressive stress components. The tensile component is more critical because of the inherent weakness of concrete in resisting tensile stresses. This component is 'Diagonal Tension'. Since end shear is used as a measure of its magnitude, diagonal tension is commonly called shearing stress.

There has been a great deal of controversy in the literature about the nomenclature to be used and the terms 'Shear Failure' and 'Diagonal Tension' have frequently been employed. The writer considers that the use of the term 'Diagonal Failure' is more appropriate, a diagonal crack being the common feature of all failures which result from diagonal tension or shear-compression.

A theoretical analysis of the stresses in the web of a reinforced concrete beam is difficult due to the heterogeneous nature

of concrete. The classical shear formula is developed on the assumptions that no longitudinal tension is carried by the concrete and there is no slipping between concrete and steel. This gives the equation for the nominal shearing stress in a beam as:

$$v = \frac{V}{b_j d} \quad \dots\dots (1.1)$$

The term "bond" is used to describe the means by which the slip between concrete and steel is prevented or minimized. Wherever the tensile or the compressive stresses in a bar change, bond stresses must act along the surface to produce the change. Nominal bond stress, assuming uniform distribution of stress, is given by:

$$u = \frac{V}{\sum o_j d} \quad \dots\dots (1.2)$$

It is almost impossible to determine the "proper" shearing strength of concrete because of the difficulty of eliminating the accompanying tensile stresses during tests. A wide variation exists in test results which have been reported, depending on how successful the investigator has been in reducing the tensile stresses accompanying the shear. Tests by TALBOT* (1906) and RENSAA (1958) show the ratio of shearing strength to compressive strength varying from 0.37 to 1.04. Since the shearing strength is much higher than the pure tensile strength, there is very little possibility of initial failure by shear in normal beams.

In any beam subjected to shearing and bending stresses, the inclination of diagonal tension of any element below the neutral

* See bibliography (arranged alphabetically).

axis is less than 45° whereas that above the neutral axis is more than 45° . An analysis shows that in any section of a simply supported homogeneous beam, the intensities of diagonal tensions below the neutral axis are much larger than above the neutral axis. The highest probability of crack formation, therefore, exists in the region below the neutral axis and in a direction normal to the principal stress trajectories. In reinforced concrete beams, the longitudinal steel provides the concentration of tension in the steel reinforcement and the magnitude of tensile fiber stresses cannot be obtained very accurately.

For convenience in the design of web reinforcement, the nominal shearing stress is arbitrarily used as a measure of diagonal tension in common practice. Diagonal cracking is a much more complex problem, involving many variables, and cannot be described by simple, precise relationships. Considerations of shear alone as a measure of the principal stress intensity may be grossly misleading and this in fact has caused a great deal of misunderstanding of the actual conditions of internal stresses in reinforced concrete members. Further, some mathematical theories have employed the assumption that concrete has no tensile strength. However, if concrete did not have any tensile or shear strength, it would be entirely unsuited as a construction material.

1.2 A REVIEW OF THE EXISTING RESEARCH

RITTER (1899) published a study of the web reinforcement based on the "truss analogy". In this analogy, the compression zone of the beam forms the compression chord of the truss whereas flexural reinforcement is considered as the tension chord. Concrete in the web of the beam is assumed to provide the compression members in the web of the truss, with stirrups or bent-up bars forming the tension members. Ritter recognized the existence of diagonal tension as the cause for failure by noting that stirrups were stressed in tension.

SEWELL (1903) suggested that tests indicated a formation of cracks along the lines of the principal tensile stress in reinforced concrete beams. He advocated the design of stirrups to resist these principal stresses, which later became known as diagonal tension.

MORSCH (1903, 1907) indicated diagonal tension as the cause of diagonal failures and developed the classical equation for the nominal shearing stress. He postulated that at the formation of diagonal cracks, internal forces were redistributed, the applied shear being resisted primarily by the compression zone of the beam and to a lesser extent by the dowel action of the reinforcement.

TALBOT (1907, 1909) distinguished between various modes of failure and concluded that diagonal cracking was a function not only of shear but of moment and depth of the beam as well. He pointed out that "shearing strength" of concrete is a function of

concrete compressive strength, length of span and amount of longitudinal and web reinforcement. Since his results showed stirrup stresses consistently lower than those obtained from the truss analogy approach, he concluded that part of the shear was carried by the compressive zone of the concrete.

FABER (1916) was the first research worker to recognize that a shear force could be carried by arching action. He assumed that compression force becomes inclined between the load and the support points whereas the tension force remains constant between these two points. This type of arching requires extensive slippage between concrete and steel and effective elimination of bond resistance of the reinforcement.

During the mid 1940's, design on the basis of ultimate load capacity became more popular as the inadequacy of the working stress method became particularly obvious in the design of monolithic and other complex structural systems. Since the problem of diagonal failures was not solved from the theoretical point of view, an empirical approach was adopted. This approach took into account the major variables affecting diagonal strength as shown by the test results.

MORETTO (1945) proposed empirical equations for the ultimate and the yield point shear for beams with web reinforcement. CLARK (1951) developed the concept that the shear-span/effective depth ratio was an important variable in the study of diagonal failures. The shear span was taken as the distance between the load and the support points. This parameter, which is commonly referred to as

the "a/d ratio" (where a is the shear span and d, the effective depth of the beam) is applicable only to the simply supported beams. To express the slenderness of beams with uniformly distributed loads or continuous beams, the parameter M/Vd (where M and V are the moment and shear at the section considered), was introduced by later research workers which reduces to a/d ratio for concentrated loads on simply supported beams.

ZWOYER (1954), MOODY (1954-55) and LAUPA, SIESS and NEWMARK (1955) considered that the compression zone of concrete was destroyed above the diagonal crack at failure. Ultimate strength of beams could thus be expressed by equations of the same type as used for the ultimate capacity of a beam failing in flexure-compression.

BRESLER and PISTER (1958) and GURALNICK (1959-60) considered that the concrete in the compression zone failed under the combined action of the compression and shearing forces. WALTHER (1957) appreciated the problem of determining the size of the compression zone and considered the compatibility requirements of concrete and steel deformations in the region of a beam containing a diagonal crack. His compatibility equations, however, assumed a uniform distribution of compressive stresses above the diagonal crack, thus precluding the possibility of any local rotation.

FERGUSON (1956) developed a hypothesis of unrestrained failure, assuming each step in the cracking pattern as a tension failure which could be rationalized in terms of the combined stress formula. He also indicated that much of the increased capacity

associated with small shear spans is lost if the loads are applied as shear over the depth of the beam or if the reaction is applied as a shear.

During the late 1950's and early 1960's, a controversy developed over whether the load corresponding to the formation of a "critical diagonal tension crack" should be considered as the limit of useful capacity of the beam or the state of stress in the uncracked compression zone was the proper criterion. The ACI-ASCE COMMITTEE 426(326) [1962] recommended the adoption of the former.

KANI (1964) showed that flexural cracks in the shear span of the beam divide the tension zone into a number of concrete blocks which could be regarded as concrete teeth. These concrete teeth, separated by the flexural cracks, were acted upon by the bond forces which developed due to a variation in the tension force in the reinforcement along the span. The function of concrete teeth* could be conceived as that of a cantilever, anchored in the compression zone and loaded by the bond forces.

Kani considered that the magnitude of the bond forces was limited by the flexural capacity of the concrete section between the tops of adjacent flexural cracks. Flexural failure of the concrete cantilevers caused the cracks to extend in an inclined direction. He developed an expression which showed that the ultimate moment at failure was a linear function of the a/d ratio until the

* The term 'concrete cantilevers' is used throughout the thesis to describe the action of the concrete blocks.

full flexural capacity was attained. He further showed that when the resistance of the concrete teeth was destroyed, the active cross-section was reduced and only a tied arch remained. At this stage the tension force in the reinforcement was constant throughout the span length. For small a/d ratios, the capacity of the remaining arch was more than that of concrete cantilevers and failure occurred only when the remaining arch was destroyed. For intermediate range of a/d ratios, the beam capacity was governed by the strength of the concrete cantilevers and transformation into an arch could not take place resulting in sudden diagonal failure.

KANI(1966) presented his test results to show that the results conformed to his "rational theory". He concluded that the ratio of the ultimate moment at failure to the flexural capacity of the beam was a better indicator of the beam strength than the shear stress at failure. His results showed considerable influence of the longitudinal reinforcement on the beam strength and almost no effect of the compressive strength of concrete.

KANI (1969) developed the principle of "internal arches" from a study of stress trajectories and concluded that the function of web reinforcement was to produce supports for the internal arches and consequently there was no direct relationship between the shear force and the requirement for web reinforcement.

LORENTSEN (1965) reported on the theory for combined action of bending moment and shear in reinforced concrete beams showing that the shear was carried partly by beam action and partly by arch action.

KREFELD and THURSTON (1966) concluded that the horizontal development of the diagonal crack at its root above the longitudinal steel initiates failure in shear by causing the diagonal crack to propagate into the compression zone. The "reserve strength" after critical cracking was dependent on the amount of rotation and "rapidity of stress redistributions" after dowel resistance had reached maximum values. They considered critical cracking to be the maximum usable resistance.

IYENGAR and RANGAN (1967) presented a theory of diagonal failure based on the state of stresses existing at the critical point of failure and a failure criterion for concrete under compressive-tensile stresses. In their analysis, they neglected the contribution of the dowel action.

FENWICK and PAULAY (1966, 1968) concluded that shear could be resisted either by beam action or by arch action. When beam action governed, the concrete cantilevers were the important structural elements. Bending moments induced by the bond forces were resisted by flexural resistance of the concrete between the cracks, by shear transfer across the cracks due to aggregate interlock and dowel action of the reinforcement. They found that prior to diagonal cracking beam action predominated and arch action developed in beams with small a/d ratios only after the diagonal cracking. Further, they showed from their test results that the major contribution to the resistance of beam action was due to aggregate interlock. This accounted for about 60% of the bond

force moment, the balance being shared almost equally by the dowel action of the reinforcement and the flexural resistance of the concrete cantilevers. The authors considered arch action to be confined to areas near a load point and in the vicinity of the supports, complete arching developing over the entire span only when these two regions merged.

BROMS (1969) postulated that internal local rotation takes place close to the apex of the critical diagonal crack within members failing by shear compression. This rotation results in an increase of diagonal crack widths at subsequent stages of loading. If the location of the diagonal crack within the compression zone could be determined as well as the distribution of the compression force, the ultimate moment could be calculated by formulas similar to those for beams failing in flexure compression.

SWAMY, ANDRIOPOULOS and ADEPEGBA (1970) presented test data to show that there exist, until complete collapse, distinct tensile and compressive zones over the entire span of the beam. The tensile force is far from constant even after extensive diagonal cracking and arch action can develop only if the steel is completely unbonded between the supports and fully anchored at ends.

ACI-ASCE COMMITTEE 426(326) [1962] points out the fact that between 1899 and 1961, more than 2500 beams and frames have been tested and their results reported in no less than 450 papers. Since 1961 a great deal of further experimental work has been reported. With such a great deal of effort having been applied to

the problem, one would have expected the knowledge of the mechanism of diagonal failure to be fairly complete.

It is evident that though a large volume of test results are available and several empirical approaches exist, a clear understanding of the internal mechanisms of diagonal resistance has not yet been realized. Some investigators suggest that after diagonal cracking, the beam is transformed into a tied arch; others maintain that a beam continues behaving as a beam until failure.

Further, it is not yet clear whether the entire beam acts as an arch or whether beam and arch action are present simultaneously and if so whether the arch action is present over the entire range of diagonal failures. Significant advances in the understanding of diagonal failures can only be made if the above questions can be answered clearly.

1.3 SCOPE OF THE PROJECT

The ultimate load and the load-deformation characteristics of reinforced concrete beams in pure bending are now well understood and satisfactory procedures exist for estimating their flexural strength. However, where the final failure is not in the region of maximum moment but results from the interaction of moment and shear, neither an accurate description of the mechanism of resistance of a beam nor a completely satisfactory theory for the strength of such a failure has been developed as discussed above. The difficulties

in establishing a mechanism of collapse arise from the fact that in many of the diagonal failures, propagation of cracks and the ultimate failure is extremely rapid.

Extensive test data and empirical equations are now available to determine the diagonal resistance of reinforced concrete beams without web reinforcement. Many of the factors affecting diagonal resistance of beams interact with each other. It is apparent that any attempt to find the solution from a single series of tests, in which one factor is varied while keeping the others constant, may be misleading. Considerable skill is thus involved in the interpretation of the results and in establishing the inter-dependent relationships between different variables.

The increasing trend of employing ultimate strength design procedures emphasizes the need for a satisfactory solution of the problems associated with diagonal failure. The present design approach, which, although safe, ensures that a flexural failure must always develop before a diagonal failure, results in an uneconomic use of the materials. Since the mechanism of diagonal failure is not fully understood, the design of beams in the region of shear and flexure is based on semi-rational or empirical equations in many parts of the world. For example, the present ACI code (1971) shows no significant variation from the last code (1963), though it is recognized in the commentary to the code that some recent test data show that the ACI equations over-estimate the contribution of the compressive strength of concrete while under-estimating that of

the longitudinal reinforcement.

In the opinion of the writer, there has been an over-emphasis placed on finding formulas which would be universally applicable and not enough attention given to the mechanisms involved and the accuracy of the fundamental assumptions which form the basis of such formulas. The fact that reinforced concrete is not a homogeneous material and cannot be expected to be as fitted for generalization as more homogeneous materials like steel, should not be lost sight of at any stage when dealing with concrete.

The primary objective of the work presented in this thesis is to develop a rational understanding of mechanisms of diagonal failure. The internal force system at failure consisting of contributions of dowel action, aggregate interlock and uncracked compression zone of the beam is statically indeterminate and necessitates many simplifying assumptions. The writer considered it more important to study the overall mechanism of collapse rather than directing the main thrust of the work towards working out proportions of resistance of various modes in the mechanism. It was the purpose of this work to develop a hypothesis of diagonal failure for beams without web reinforcement for the entire range of diagonal failures and to study the interaction of the beam and arch action as the beam is loaded to failure.

In order to draw any significant conclusions from a limited number of tests, it is important to isolate the most important variables and to study their influence. A total of 22 beams were

tested. Primary variables consisted of the shear-span/depth or the a/d ratio and the percentage of longitudinal reinforcement. Type of loading and manner of loading were selected as secondary variables. The beams were extensively instrumented with both electrical resistance strain gauges and demountable mechanical (DEMEC) strain gauges throughout the span of the beams, enabling strain distributions at various stages of loading prior to collapse to be recorded. Details of experimental work and instrumentation are given in Appendix I. Results of the strain gauge data have been compiled into a separate report* but are summarized graphically for individual beam tests in Appendix III along with other plots. Other experimental results are given in Appendix II.

Some basic aspects of the mechanisms of diagonal resistance of reinforced concrete beams are discussed in Chapter 2. Development of cracks leading to a diagonal failure, based upon experimental observations is described. Some important aspects of the theory of rupture as applicable to the propagation of cracks in concrete are very briefly referred to. Further, beam and arch action are described in the context of existing research. So long as the beam action predominates, the important constituents of the internal force system consist of the flexural resistance of the concrete cantilevers, the transfer of shear across cracks by aggregate interlock and the dowel action of the flexural reinforcement. These three elements are described separately.

* See p. 91 , Chapter 5.

A conceptual model of the diagonal failure of a reinforced concrete beam is presented in Chapter 3. The test programme undertaken is described in Chapter 4 followed by a presentation of the experimental results (Chapter 5) to verify different aspects of the conceptual model. The relation of present investigation to existing research is described in Chapter 6. Conclusions drawn from the present investigation and suggestions for further work are given in Chapter 7.

1.4 TYPES OF DIAGONAL FAILURES

The types of diagonal failures observed in reinforced concrete beams loaded in shear fall into five general types.

- (a) diagonal tension failure
- (b) shear-compression failure
- (c) shear-tension failure
- (d) failure by shear proper and
- (e) diagonal compression failure

For purpose of reference, each is described briefly below.

1.4.1 Diagonal Tension Failure

In this case, failure is caused by a sudden extension of a diagonal crack through the compression zone of the beam accompanied by a split along the reinforcement. Prior to this sudden failure, the cracks are sharp and thin and the beam remains reasonably sound. Failure cracks generally extend from the outermost flexural cracks in the shear span of the beam. At failure, the two portions of the beam, separated by the critical diagonal crack may jump apart, suggesting a tensile failure of the concrete. A small crack may be

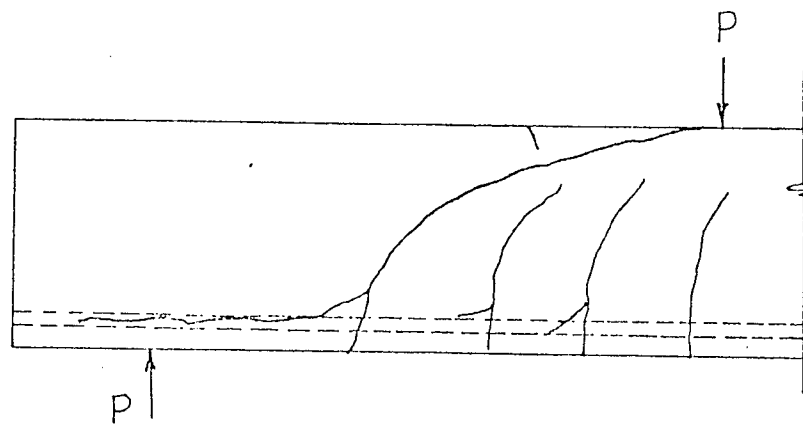
seen to extend from the top surface of the beam downwards above the diagonal crack, as shown in Figure 1.1(a). The section of concrete at this location may be lifted up at failure.

1.4.2. Shear-Compression Failure

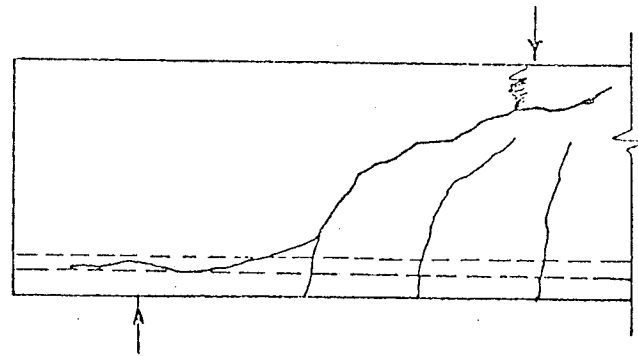
In this case, diagonal cracks form and extend in a manner similar to that described in the last sub-section. However, as the critical diagonal crack propagates into the compression zone, it becomes stabilized and the beam can support further increments of load. At this stage the critical diagonal crack propagates very slowly with a flatter trajectory. Final failure occurs at a much higher load than that causing diagonal cracking, when the concrete above the diagonal crack crushes. A typical case is shown in Figure 1.1(b).

1.4.3. Shear Tension Failure

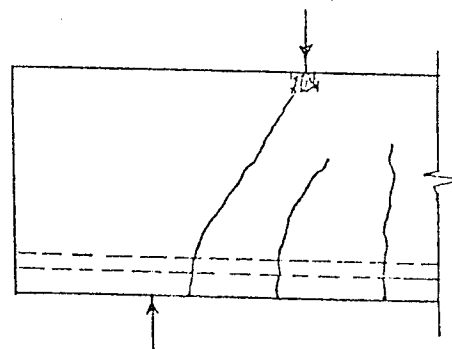
In this case, as the diagonal crack propagates into the compression zone, vertical displacements occur at the level of the reinforcement due to the opening of cracks. This induces dowel action in the reinforcement which may cause a splitting of concrete along the reinforcement leading to a shear tension failure as the splitting proceeds to the anchorage zone.



(a) Diagonal Tension Failure



(b) Shear-Compression Failure



(c) Shear Proper Failure

FIG. 1.1 TYPICAL DIAGONAL FAILURES IN REINFORCED CONCRETE BEAMS

1.4.4. Failure by Shear Proper

For very short beams ($a/d < 1$), failure may occur by crushing of concrete either near the load point or at the supports or by splitting of concrete between load and support points. Such a failure [Figure 1.1(c)], is very sensitive to the loading arrangement, especially the size of the bearing plates.

1.4.5. Diagonal Compression Failure

In T-beams containing web reinforcement, the inclined compression forces in the web may cause the failure of the web which is thin compared to the flanges.

1.4.6. Failures Discussed in this Study

Tests performed by the writer were confined to rectangular beams without web reinforcement. No beam had an a/d ratio less than unity. As a result, no shear proper failures or diagonal compression failures were observed in the tests. Furthermore, since in the tests splitting along the reinforcement occurred in both the shear compression and diagonal tension type of failures, shear tension failures have not been treated separately. Therefore, only two types of diagonal failures - diagonal tension and shear-compression - are referred to in subsequent chapters of this thesis. The specimens employed in the tests cover the practical range of a/d values for most rectangular beams.

1.5 FACTORS INFLUENCING RESISTANCE TO DIAGONAL FAILURE OF R. C. BEAMS

1.5.1 The a/d or M/Vd Ratio

Since CLARK (1951) introduced the parameter a/d (shear-span/depth ratio), its effect on the mechanism of failure as well as on the load carrying capacity of beams has been found to be very significant. Plots of ultimate moment in terms of a non-dimensional ratio, M_u/M_{fl} , where M_u is the ultimate moment of the beam and M_{fl} the flexural capacity of the beam, as a function of a/d ratio show that the diagonal capacity of a beam is lowest at a point occurring between a/d values of 2 and 3. On either side of this minimum point, the capacity of the beam increases. When the a/d ratio is less than that corresponding to the point of minimum strength, the type of failure to be expected is shear compression whereas beyond this value diagonal tension failure occurs until the full flexural capacity of the beam is attained.

For continuous beams, the slenderness ratio of the beam is expressed by M/Vd ratio, instead of a/d .

1.5.2. The Amount of Longitudinal Tension Reinforcement

The effect of longitudinal reinforcement on shear capacity has long been recognized and included in most of the empirical formulas. There seems to be a general agreement that an increase in the percentage of longitudinal reinforcement results in an increase in the beam capacity.

TAUB and NEVILLE (1960) concluded that the percentage of longitudinal reinforcement has a marked influence on the strength of beams failing by diagonal tension but becomes negligible for shear compression failures. Results of KREFELD and THURSTON (1966 - April) show that the diagonal strength of beams is improved by an increase in longitudinal reinforcement for all values of a/d ratios. However, none of their test beams had an a/d ratio of less than 2.35 and most of the failures observed by them were of the diagonal tension type..

KANI(1966) showed the considerable influence of the percentage of longitudinal reinforcement on the beam capacity. He showed that between a/d ratio of 1 and 6.5 a "valley of diagonal failure" of reduced strength exists in the M_u/M_{f1} versus a/d plot. This valley disappears totally for low ratios of percentage of longitudinal reinforcement and deepens with an increase in this ratio. The point where the full flexural capacity of the beam is attained is thus very much related to the percentage of longitudinal reinforcement in the beam. A better distribution of the reinforcement

is known to improve the diagonal strength of beams.

1.5.3. The Compressive Strength of Concrete

Many research workers* have found the compressive strength of concrete to have a significant influence on the diagonal resistance of beams, especially for concrete strengths below 5,000 psi. TAUB and NEVILLE (1960) considered the influence of a/d and concrete strength to be inter-related, there being significantly greater influence of concrete strength on the strength of beams failing in shear compression. KANI (1966), however, concluded that the "shear strength" of rectangular reinforced concrete beams does not depend on the concrete strength within the entire range of $f'_c = 2,500$ to 5,000 psi and $p = 0.50$ to 2.80% where f'_c is the compressive strength of concrete and p the percentage of longitudinal reinforcement. DIAZ DE COSSIO and LOERA (1966) reported experimental work suggesting that the contribution of concrete compressive strength is over-estimated in the ACI code equation at the expense of the percentage of longitudinal reinforcement.

1.5.4. The Manner of Load Application

FERGUSON (1956) showed that much of the increased capacity of the beams with small a/d ratios is lost if the main beam is loaded through secondary beams framing into it. He attributed this

* MOODY (1953); MORROW and VIEST (1957); TAUB and NEVILLE (1960) and VAN DER BERG (1962).

to the absence of high vertical compression under the load points on the main beam which stabilized the critical diagonal crack.

TAYLOR (1960) also concluded that there was no reserve strength in beams loaded through secondary beams beyond the diagonal cracking load. TAUB and NEVILLE (1960), on the other hand, found that there was only a very slight reduction in the ultimate load for beams loaded through secondary beams. However, Taub and Neville used stirrups in addition to the longitudinal reinforcement in the secondary beams. It is probable that a diagonal crack from the main beam crossed the line of these stirrups.

1.5.5. Multiple and Uniform Loads

FERGUSON (1956) showed that beams with multiple loads have a higher diagonal strength than those loaded by one or two concentrated loads. However, tests of KREFELD and THURSTON (1966) with uniform loads indicated that the "shearing strength" of the beams with uniformly distributed loads is higher than the corresponding beams with concentrated loads.

1.5.6. The Size of the Compression Zone

Several research workers* have concluded that an increase in the size of the compression zone has a beneficial influence on

* MOODY (1953); TAUB (1956); NEVILLE and LORD (1960).

the diagonal capacity of the beams. MOODY (1953) and TAUB (1956) considered that there is a close connection between the deflection of a beam and the crack development in it. The smaller the beam deflection, the later the crack forms and slower is its progress and vice versa. Tests of MOODY (1953) indicated that the deflections of T-beams were much smaller than those of corresponding rectangular beams and the diagonal cracks in T-beams also formed at higher loads than in rectangular beams. NEVILLE and LORD (1960) showed that the "ultimate shear strength" of T-beams was 13% to 60% higher than the corresponding rectangular beams.

1.5.7. Bond Characteristics of Longitudinal Tension Reinforcement

Tests of LEONHARDT and WALTHER (1962) indicate that beams reinforced with smooth polished bars showed only limited cracking and failed (either by crushing of the concrete in the compression zone or by failure of the anchorage) at a substantially higher load than the beams reinforced with deformed bars. SWAMY and others (1970) considered the effect of constant steel stress in beams reinforced with polished bars to be a "prestressing" effect so that the web of the beam remained essentially in compression. They showed that the increase in diagonal resistance of unbonded beams was very unreliable and was not always observed.

1.5.8. Size of the Web

Tests reported by TAUB and NEVILLE (1960) suggested that all other factors being the same, the "shear strength" is roughly proportional to the cross-sectional area of the web.

1.5.9. Longitudinal Compression Reinforcement

TAUB and NEVILLE (1960) reported a negligible effect of the compression reinforcement on the diagonal strength of beams without web reinforcement.

1.5.10. Absolute Size of the Beam

The work of KANI (1967) and MACGREGOR (1967) indicated that the "shear strength" decreases as the overall depth of the member increases. Tests of CHANG and KRESLER (1958) and LEONHARDT and WALTHER (1962) showed considerable scale effect. However, ALAMI and FERGUSON (1963) reported that the scale effect is relatively small.

1.5.11. Width-Depth Ratio of the Beam

The effect of this factor seems to be very small in beams of normal structural proportions.

1.5.12. Web Reinforcement

Various investigators* have found that the stirrup stress is lower than that compatible with the truss analogy, and increases only when a diagonal crack crosses the line of the stirrup. Inclusion of web reinforcement improves the dowel resistance of the longitudinal reinforcement, increases the load capacity, controls the diagonal crack width and provides resistance against opening of cracks at all stages of loading. KANI (1969) concluded that the function of stirrups is to provide support forces for internal concrete arches and to transfer them to the external supports. He also showed the importance of good anchorage conditions of the web reinforcement. Inclined compressive forces in the web of the beam are balanced by the tensile forces in stirrups and bond forces in the longitudinal reinforcement. If the stirrups are well anchored, they can perform better in resisting the inclined compressive forces.

* TALBOT (1909); RICHART (1927); LEONHARDT and WALTHER (1962).

C H A P T E R T W O

SOME BASIC ASPECTS OF DIAGONAL RESISTANCE OF REINFORCED CONCRETE BEAMS

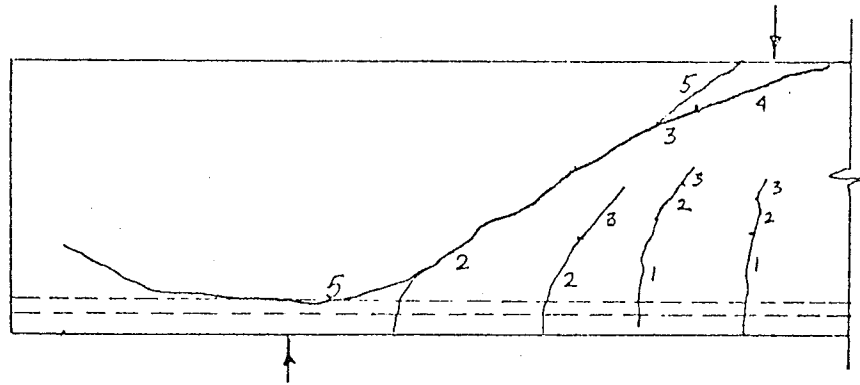
2.1. GENERAL

In this chapter, the development of cracks leading to a diagonal failure, as established through experimental observations is described. Attention is drawn to the heterogeneous nature of concrete and difficulties associated with the general problem of cracking in concrete. Prevalent concepts of beam and arch action are discussed. Then follows separate treatment of the flexural resistance of concrete cantilevers, the transfer of shear across cracks by aggregate interlock and the dowel action of the flexural reinforcement.

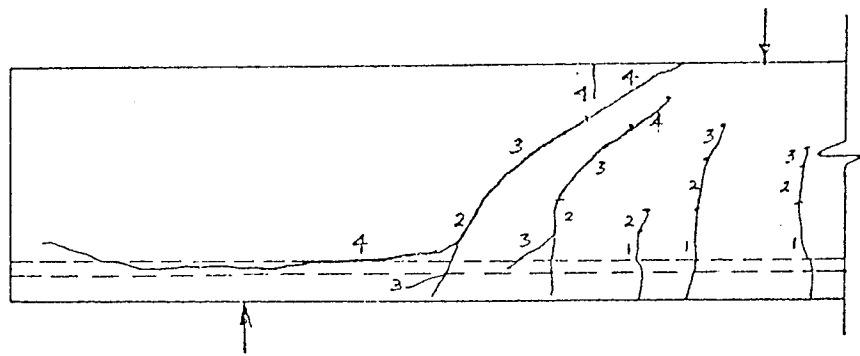
2.2. DEVELOPMENT OF CRACKS LEADING TO DIAGONAL FAILURE

Figure 2.1. shows the various stages of cracking in a reinforced concrete beam leading to the types of diagonal failure, considered in the present investigation.

Before any cracks form in the beam, it acts as a composite section, composed of uncracked concrete and steel reinforcement. When the limiting tensile strain in the concrete is reached, vertical flexural cracks form in the beam at regular intervals along the span according to the variation of the bending moment (Stage 1). These



(a) Shear Compression Failure



(b) Diagonal Tension Failure

FIG. 2.1 DEVELOPMENT OF CRACKING IN THE SHEAR SPAN OF BEAMS

cracks form at relatively low loads and generally extend to about $0.2d$ to $0.4d$, where d is the effective depth of the beam. As soon as this cracking occurs, the composite action of the beam is modified and a redistribution of stresses occurs in the regions adjacent to the cracked sections.

With increasing loads, more cracks appear and existing cracks progress upwards and where shear is present in addition to bending, becoming curved in the process (Stage 2). The cracks farthest away from the load points start curving as soon as they extend only a short distance upwards of the longitudinal reinforcement. Further increments of load result in only negligible propagation of cracks (Stage 3). At this stage, some back-cracking may also be seen from existing cracks. This frequently occurs in beams which ultimately show a diagonal tension failure. This back-cracking normally extends from above the level of the reinforcement, stopping at or slightly below the level of longitudinal reinforcement.

In beams failing in diagonal tension, failure occurs very suddenly (Stage 4) when one of the cracks, generally the one closest towards the load point, or a new crack joining the top ends of adjacent cracks, extends through the compression zone of the beam. The split may be sharp and thin or wide and destructive, depending upon the M/Vd ratio. The crack also extends along the reinforcement at failure, resulting in complete separation of the reinforcement from the concrete. Generally a crack is seen to extend from the top of the beam downwards above the diagonal crack at reduced depth

of the beam as the failure crack extends to the top surface.

This section of the beam may also be lifted upwards.

If the M/Vd ratio is low, the failure is of the shear-compression type. The first three stages of cracking proceed as described above. However, with further loading, the critical diagonal crack proceeds very slowly through the compression zone of the beam with a flatter trajectory, sometimes going into the constant-moment zone with an almost horizontal trajectory. The beam continues taking more load until reaching final failure (Stage 5), which is similar to the diagonal tension failure except that the ultimate diagonal failure does not follow the flatter trajectory, but rather the failure crack extends straight (at almost 45°) to the load point. The portion of concrete between the two cracks close to the load point may crush. A simultaneous split occurs along the reinforcement as an extension of the failure crack.

2.3. PROPAGATION OF CRACKS IN CONCRETE

KAPLAN (1961) showed that micro-cracks exist in concrete at loads considerably less than those causing fracture. BLACKMAN and SMITH (1958) concluded that imperfections in concrete consist of microscopic voids in the paste, imperfect bond of the paste and aggregate, microscopic voids in the mortar and imperfections in the aggregate. Their results suggest that concrete can be expected to resist failure more efficiently under a loading condition where

a relatively small area of the section is stressed to a point at or near its ultimate strength. HSU, SLATE, STURMAN and WINTER (1963) reported that microcracks exist at the interface between the coarse aggregate and mortar even before any load is applied, thus highlighting the fact that bond is the weakest link. Studies by MEYER, SLATE and WINTER (1969) indicate that bond cracking in concrete is increased by creep and shrinkage and the part of creep deformation associated with microcracking is non-recoverable. ROMUALDI and BATSON (1963) concluded that the low tensile strength of concrete is not inherent to the material but can be significantly improved if the spacing of thinly distributed wire reinforcement is reduced to 0.5 inches or less. HSU and SLATE (1963) showed that moisture content of the specimen during testing and water-cement ratios have opposite effects on the tensile and compressive strengths of paste, mortar and concrete, indicating a strong possibility that the tensile strength of concrete is a property different in nature from the compressive strength.

It is clear from above that a very careful interpretation of test results, especially of the strain gauge data, is needed when dealing with cracking in concrete. Problems of microcracking, creep and shrinkage must be kept in mind in any analysis.

2.4. BEAM AND ARCH ACTION IN R.C. BEAMS

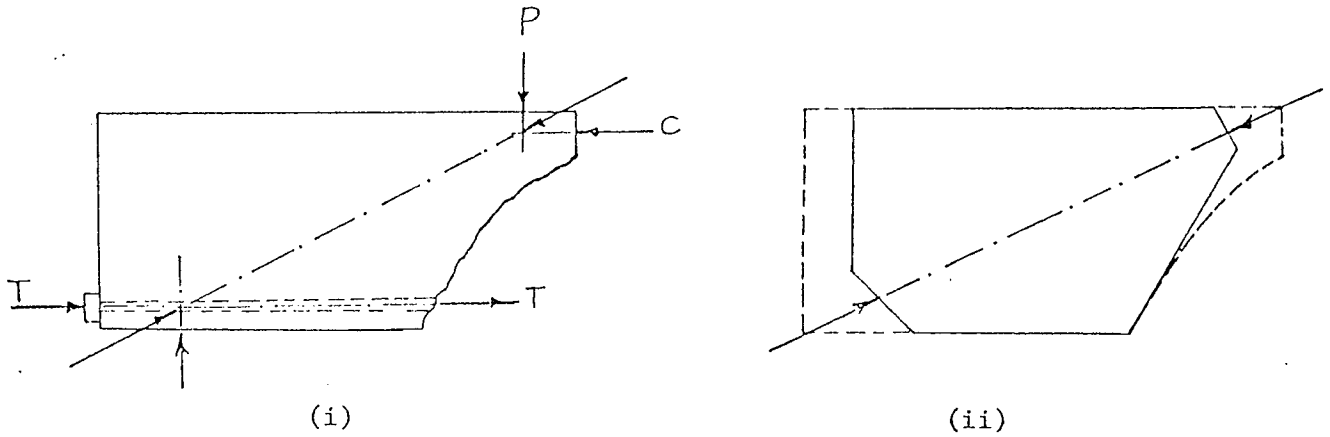
In beams without bonded reinforcement, the tension force

in the reinforcement is constant from one end of the beam to the other. The entire tension force is transferred to the concrete at the anchor plates (Figure 2.2a). From the equilibrium of the forces, it can be seen that the concrete body is under diagonal compression and, for four point loading, the thrust line is a straight diagonal line. The behaviour of such a beam is, thus, essentially that of a tied arch.

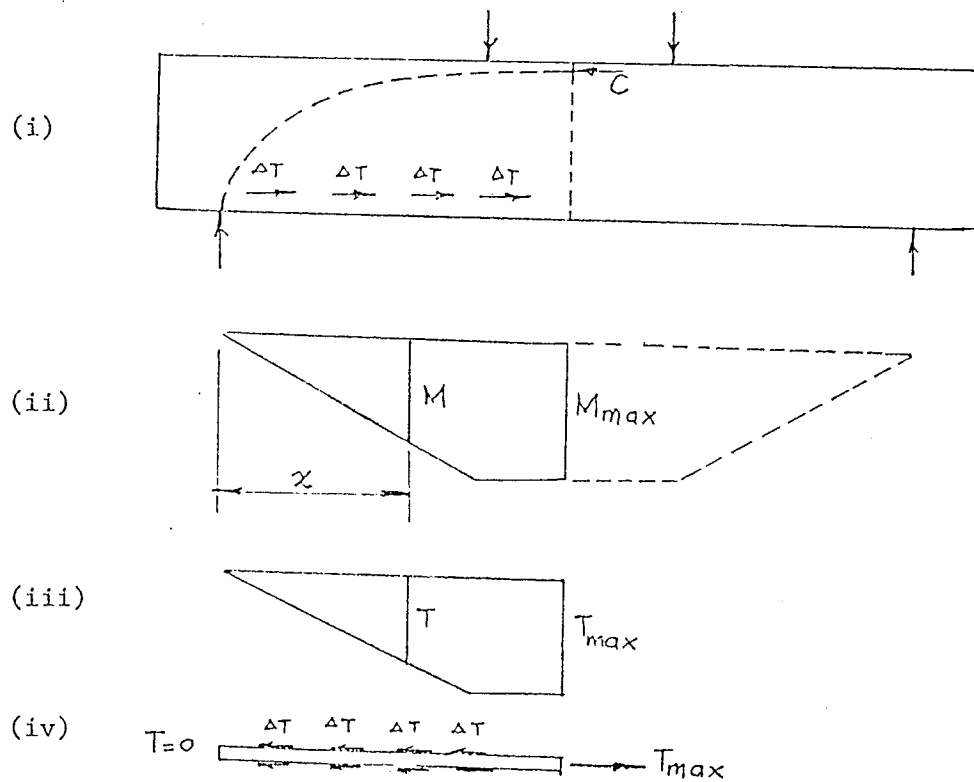
In a reinforced concrete beam with bonded reinforcement, the tensile force is distributed along the reinforcing bars (Figure 2.2b). The shape of the thrust line depends upon the distribution of the tensile force but is no longer a straight line as in the case of unbonded beam. The thrust line curves from the supports to the load point, remaining above the diagonal straight line for the unbonded beam as the horizontal tension force gradually increases from the supports towards the midsection.

The concrete block between two adjacent flexural cracks could be regarded as a short cantilever, spanning from the level of the flexural reinforcement to a point in the compression zone of the beam. These concrete cantilevers are acted on by the bond forces that develop as a result of bond between the concrete and the reinforcement. The resultant force acting on each cantilever is the difference of the tension force on either side of the cantilever.

KANI (1964) considered that when the resistance of the concrete cantilevers is exceeded, the bond forces cannot exist and conditions of beam without bond are obtained. The active



(a) Reinforced concrete beams without bond



(b) Reinforced concrete beam with bond

FIG. 2.2 INTERNAL FORCES OF REINFORCED CONCRETE BEAMS
KANI (1964)

cross-section that remains is that of a tied arch as the tension force in the reinforcement is constant. At this stage the compression line in shear spans becomes inclined and the highest compressive strain is found at the bottom fiber along the diagonal crack. As the flexural cracks form and extend in the compressive zone of the beam, the flow of tensile stresses between the concrete cantilevers and the rest of the beam is stopped until the last crack when an unyielding support of the beam is available. The transformation into an arch therefore results from a gradual process through which the resistance of the concrete blocks is lost.

Arching in unbonded beams is caused by a slip of the reinforcement while for bonded beams, displacements of vertical segments take place at the cracked segments. Arch action comes into play when the compressive force becomes inclined so that the lever arm changes along the span. On the other hand, beam action is caused by the bond forces in the reinforcement. However, if the compression force becomes inclined above the tops of the flexural cracks, it is possible for a beam to resist the external loads by both beam and arch actions.

The occurrence of arching action in beams with bonded reinforcement must result in the development of translational displacements (relative movement between steel and concrete) in the shear span of the beam, and in a decrease in the depth of the neutral axis in the centre of the beam. By examining the compatibility requirements of the concrete and steel in the shear span of a beam,

FENWICK (1966) concluded that arching occurs to different extents in different parts of the beam. The relative movements between steel and concrete result from the bending of the concrete cantilevers and internal rotations of the compression zone. He also showed that a change in the ratio of the spacing of cracks at the level of the reinforcement and at their top causes a change in the location of the centroid of compression zone and is responsible for the compression force to become inclined.

FENWICK (1966) found that arch action could develop to an appreciable extent in only two regions of a beam, i.e., above a diagonal crack and near the load point. For complete arching to occur over the entire span, these two regions should merge and this can happen only when the diagonal crack reaches the vicinity of a load point, the load being applied directly over the compression face.

2.5. FLEXURAL RESISTANCE OF THE CONCRETE CANTILEVERS

The bond forces acting on the concrete cantilevers produce a bending moment at the roots of the cantilevers and horizontal shear stresses in the tension zone of the beam. Since the spacing between the cracks near their tops reduces, the intensity of the shear stresses is slightly higher closer to the neutral axis. If this small reduction in the crack spacing is neglected, the average shear stress is given by $v_n = \frac{(\Delta T)}{(\Delta X)b}$, where v_n is the nominal shear

stress; ΔT is the bond force; ΔX is the crack spacing at reinforcement level and b is the width of the beam (Figure 2.3).

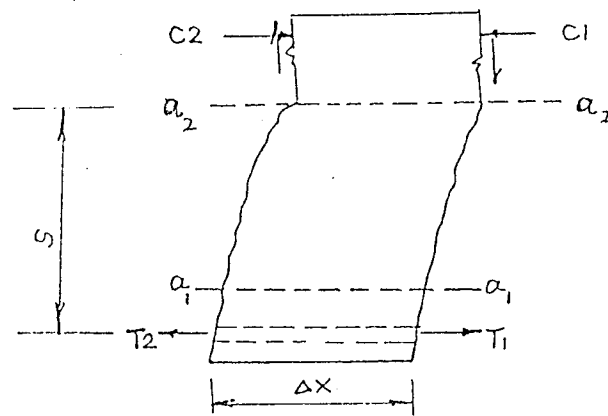
Several factors influence the stress distribution at the top of the concrete cantilevers, which may be quite complex. Some of the important factors are the bending moment and the shear sustained by the cantilever and the differential curvature of the compression and the tension zones of the beam between adjacent flexural cracks. The distribution of these stresses is shown in Figure 2.3.

The bending moment at the top of the concrete cantilevers can be resisted by:

- (a) the flexural resistance of the concrete between cracks.
- (b) shear transfer across cracks by aggregate interlock,
and
- (c) dowel action of the reinforcement.

KANI (1964) ignored the contributions of aggregate interlock and dowel action of the reinforcement and assumed that the strength of the concrete cantilevers was governed by the flexural strength of the section.

His expression for the bond force that could be carried by the concrete cantilevers was based on a linear strain distribution across the critical horizontal section of each concrete cantilever. This assumption violates the compatibility condition immediately above the crack which requires that the vertical flexural strain at this

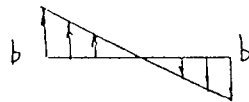


$$\begin{aligned} \text{Bond force} &= (\Delta T) = T_1 - T_2 \\ &= (\Delta C) = C_1 - C_2 \end{aligned}$$

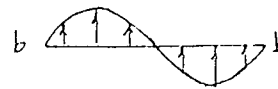
$$(i) \text{ horizontal shear at } a_1 - a_1 V_h = \frac{(\Delta T)}{(\Delta x) b}$$

(ii) Stress at the root of the cantilever (section a-a)

(a) Flexural stresses



(KANI - 1964)



(FENWICK - 1966)

(b) Shear stresses



(c) Direct stresses



FIG. 2.3 STRESS DISTRIBUTION IN A CONCRETE CANTILEVER

location must be zero. Stress distribution suggested by FENWICK (1966) seems to be more realistic. (Figure 2.3.)

Further, the shear stresses and the stresses due to the differential curvature of the tension and compression zones of the beam at the section considered are likely to modify the strength of the section. Section $a - a$ (Figure 2.3.), which forms the basis of Kani's equation, does not fail but the cracks propagate into the beam in an inclined direction. This shows that the roots of these concrete cantilevers are not the weakest link in the chain reaction ultimately leading to failure. From above it is clear that Kani's method is likely to over-estimate the flexural strength of the concrete cantilevers.

2.6. SHEAR TRANSFER ACROSS CRACKS BY AGGREGATE INTERLOCK

A detailed experimental study on the contribution of shear transfer across cracks by aggregate interlock has been reported by FENWICK (1966). It is suggested that a very large proportion of the bond force moment is resisted by shear transfer across cracks, both by aggregate interlock and by the dowel action of the longitudinal reinforcement.

When a crack forms, relative displacements of segments across the crack take place. These displacements can be described by a component normal to the direction of the crack (crack width, ' c'_w '), and a component parallel to the crack (shear displacement, ' δ'_s ').

This latter component, shear displacement, causes the larger aggregate particles embedded on one side of the crack to bear against the concrete across the crack. The larger aggregate particles behaving as small dowels, therefore, make it possible to transmit tangential forces across the crack.

The shear transfer across cracks by aggregate interlock would depend primarily on the area of contact of the aggregate particles projecting across the crack and the deformation characteristics of the aggregates.

The width of the crack, the shear displacements, the shape of the aggregate and its grading all influence the area of contact. On the other hand, load-deformation characteristics of the aggregates may vary in different directions due to water gain which in turn may be described as a soft layer of concrete on the underside of the reinforcement or on the underside of large aggregate particles. Further, the concrete strength, its water and air content and bond properties of the aggregate are some of the other factors that influence the load-deformation characteristics of concrete.

Tests of FENWICK (1966) indicate that the shear stress-shear displacement relationship is linear between limiting values of shear displacement ranging from 12% of crack width to 55%. Further, the shear transfer across cracks by aggregate interlock increases with higher compressive strength of concrete and smaller width of cracks. Fenwick concluded that where beam action predominates,

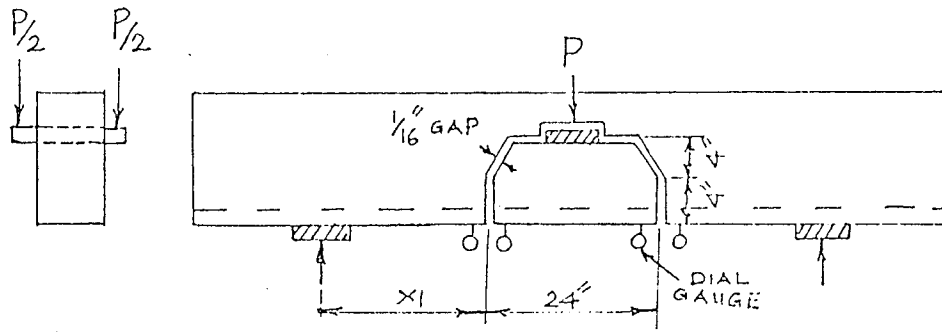
shear transfer across the cracks by aggregate interlock action is of major importance, accounting for about 60% of the resistance. The tests conducted by him were, however, limited in number and had preformed cracks and extensive instrumentation. It is doubtful whether the quantitative values found by Fenwick are applicable to normal reinforced beams. It is conceivable that the preformed cracks and instrumentation may have affected the behaviour of the beams. Also only a limited number of variables were investigated in the study. The work of Fenwick, however, highlighted the important contribution of aggregate interlock action.

2.7. DOWEL ACTION OF THE LONGITUDINAL REINFORCEMENT

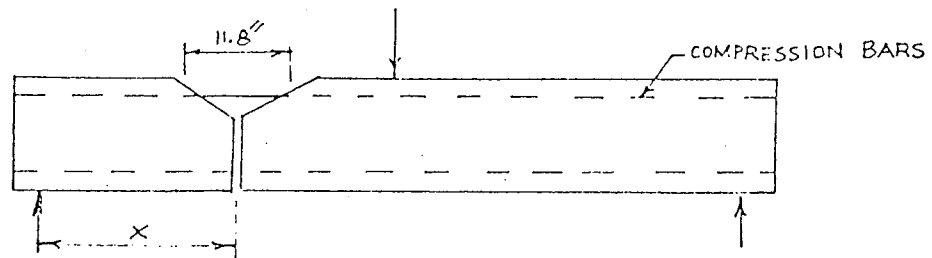
Dowel action of the longitudinal reinforcement has long been recognized and its contribution included in many of the expressions for the resistance of beams to diagonal cracking.

Several investigators have tried to establish dowel shear through the use of specially designed beam tests. Test arrangements of some of these research workers are shown in Figure 2.4.

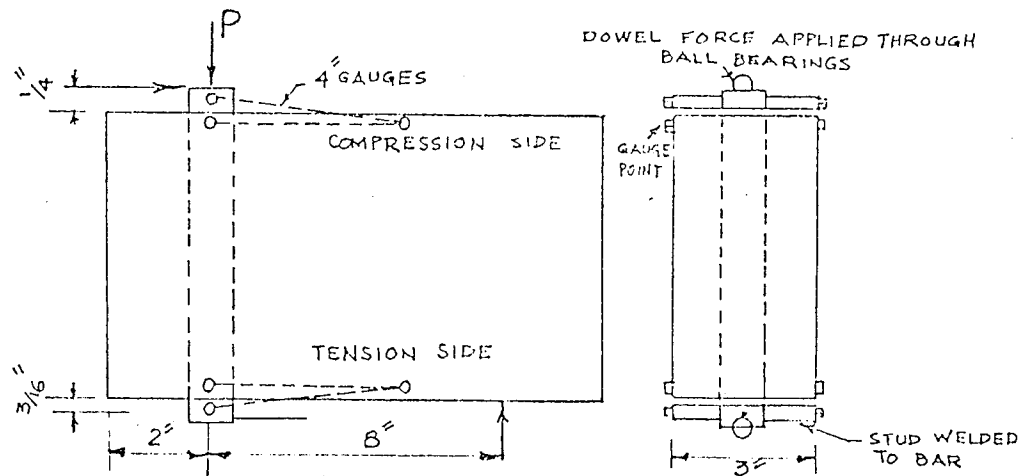
JONES (1956-August) found that quite high dowel forces develop in the reinforcement. He assumed that the longitudinal reinforcement along with the concrete cover below it was equivalent to a beam supported on an elastic foundation. This foundation could be used to reproduce the actions of the concrete above the reinforcement, assuming it to be equivalent to a set of independently acting springs.



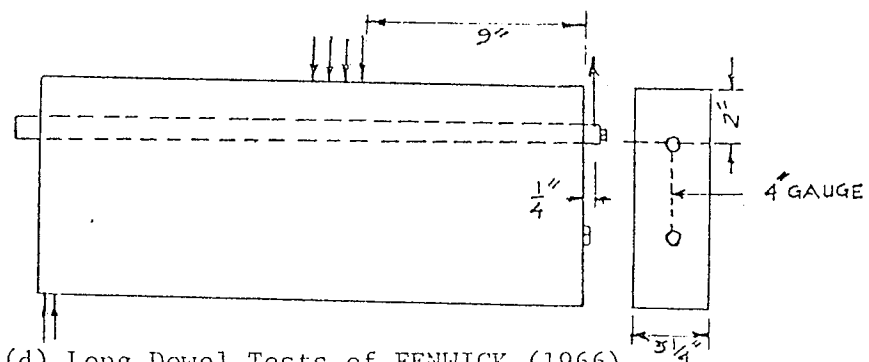
(a) Dowel Tests of KREFELD and THURSTON (1966)



(b) Dowel Tests of LORENTSEN (1965)



(c) Short Dowel Tests of FENWICK (1966)



(d) Long Dowel Tests of FENWICK (1966)

FIG. 2.4 DOWEL TEST ARRANGEMENT OF VARIOUS RESEARCH WORKERS

The deflected shape of the reinforcing bar could thus be found from a solution of the differential equation:

$$EI \frac{d^4 y}{dx^4} = Ky, \text{ where } K \text{ is the equivalent spring constant,}$$

EI is the flexural rigidity of the equivalent beam consisting of the reinforcing bars and the concrete below them, y is the distance measured from the neutral axis and x is the distance measured along the beam from support point.

WATSTEIN and MATHEY (1958) assumed that the centroid of the compression zone was located at the midpoint of the concrete section above the diagonal crack. Equilibrium of the moment was considered about this point, the shear transfer across cracks by aggregate interlock being neglected completely.

The dowel test arrangement of KERFELD and THURSTON (1966) is shown in Figure 2.4(a). Shear displacements were measured by dial gauges on either side of the crack on the tension side of the beam. It is conceivable that these gauges measured not only shear displacements but also the displacements due to the flexural rotation of the beam and also that of the concrete below the dowel crack as the gauges were located some distance away from the cracks on the tension surface of the beam.

Using a few simplifying assumptions, the authors developed the following expression for the dowel shear force.

$$V_1 = b \sqrt{f'_c} \left[1.3 \left(1 + \frac{180p}{\sqrt{f'_c}} \right) c + d \right] \frac{1}{\sqrt{x_1/d}} \dots (6.1.)$$

where c = depth of the concrete cover below the underside of the reinforcement, x , is the distance of the crack from the support point, and b is the width of the beam.

LORENTSEN (1965) made direct measurements of the dowel action (Figure 2.4b) and suggested the expression

$$K_r = 0.95 b H \sqrt{f'_c} \quad \dots (6.2.)$$

where K_r is the dowel shear force and H the depth of the beam.

FENWICK (1966) conducted a detailed test programme to investigate the shear transmitted across the cracks between the concrete cantilevers and that across the last crack in the shear span. Tests were conducted to find out the influence of the water content of the concrete mix, the position of the reinforcing bar in the concrete, the length of the dowel and the bond properties of the reinforcing bar. Test arrangement for his short and long dowel tests is shown in Figures 2.4(c) and (d) respectively.

It was found that the increase in the bond performance of the reinforcement results in an increase in the dowel shear capacity due to the increased effective stiffness of the reinforcing bars and the concrete acting with it. Further, significant differences were recorded in the performance of the bars located at the top and the bottom positions of the moulds. This was explained on the basis of water gain, i.e., the formation of a soft spongy layer of concrete on the lower surface of the horizontally positioned

reinforcing bars. Concrete strength, the spacing of cracks and position of the reinforcing bar as also the size and number of bars all affected the dowel capacity.

Fenwick concluded from the experimental results that the load remained approximately proportional to the displacement until the dowel cracks formed. With the formation of the dowel cracks, there was a reduction of about 10% of the dowel force and any further increase in displacement did not result in any further improvement in the load carried. The maximum possible proportion of the bond force moment that may be resisted by dowel action varied from 26% for bottom bars to 15% for top bars in Fenwick's experiments.

Most of the work prior to Fenwick's investigation was directed towards finding out the shear that can be transmitted across a single crack. The results of such work cannot therefore be applied to a beam containing a series of cracks.

It can be seen that the quantitative estimation of dowel resistance can at best be approximate. The analysis and calculation is based on a number of assumptions and cannot be expected to give very accurate results. The deflected shape of a reinforcing bar embedded in concrete is related to the transverse loading by the equation:

$$\frac{d^4 y}{dx^4} = \frac{p_x}{EI} \dots (6.3.), \text{ where } p_x \text{ is the load intensity}$$

on the bar at the point x and (EI) represents the flexural rigidity

of the reinforcing bar and the concrete acting with it.

Most of the investigators have replaced the loading function by the term " K_y " assuming that the loading function is proportional to the deflection of the bar. This in effect means that the reinforcing bar and the concrete acting with it is considered as a beam supported on an elastic foundation. The concrete foundation is thus assumed to respond in the manner of a set of independently acting springs. This in reality is not entirely true since one fiber of concrete cannot be displaced independently of the adjoining fibers.

The magnitude of the flexural rigidity (EI) is modified by the composite action of the reinforcing bar and the concrete as the bar bends and tangential displacements develop between the concrete and the steel, thus inducing bond stresses. In the solution to the differential equation, the term representing the flexural rigidity is assumed constant along the bar. Further, any predictions of maximum dowel resistance based on elastic state of stresses in the concrete and the reinforcement are not valid as the stress conditions close to dowel cracking are definitely not within the elastic range.

Dowel resistance is calculated from the shear displacements in a beam which arise from the flexural rotation of the concrete cantilevers and the rotation of the compressive zone of the beam. Any accurate estimate of the dowel resistance must, therefore, take into account both of the above contributing factors. Further,

the dowel action is influenced by several factors, some of which are:

- (1) variable concrete strength
- (2) the distance of the crack from the support
- (3) effects of combined stresses
- (4) the elastic response of the concrete, which itself depends on several factors
- (5) the depth of concrete cover below the reinforcement
- (6) the length of the concrete block in which the reinforcing bar is embedded
- (7) the size and number of reinforcing bars
- (8) the bond properties of the reinforcement, and
- (9) the bond properties of the concrete.

Some of these factors depend on the orientation of the reinforcing bars and the care exercised in avoiding segregation and water gain. It is thus obvious that dowel action is a very involved phenomenon and all these factors have to be kept in mind while evaluating its contribution to the resistance to diagonal failure.

C H A P T E R T H R E E

A CONCEPTUAL MODEL OF THE DIAGONAL FAILURE OF A R.C. BEAM

3.1. GENERAL

In this chapter a conceptual model of the diagonal failure of a reinforced concrete beam is developed. It is suggested that beam bending and arching action exist simultaneously in the shear span of a reinforced concrete beam for all types of diagonal failures identified previously, regardless of the manner or the type of loading. Flexural cracks divide the concrete into a number of blocks which can be considered to be concrete cantilevers loaded by the bond forces of the reinforcement and anchored in the compression zone of the beam. With progressive flexural cracking, it is suggested that arching develops from the inner portion of the beam outwards. Thus arch action is present over the entire range of diagonal failures, i.e., in short beams as well as in long beams. The extent of arch action is determined by the degree of cracking. When the resistance of the concrete cantilevers is exceeded, a critical diagonal crack appears. If the internal rotations necessary to stabilize the crack can take place without causing collapse of the member, arching develops over the entire span, accompanied by a modified beam action. Final failure may result from a failure of the arch, a compression failure of the modified beam or a flexural-tensile failure at a load level higher than that causing critical diagonal cracking.

3.2. THE CONCEPTUAL MODEL

When a beam is loaded and before any cracks form in the concrete, the beam behaves as a composite section consisting of concrete and the reinforcement. Under increasing loads, when the limiting tensile strain in the concrete is reached, vertical flexural cracks form from the tension surface of the beam and a redistribution of stresses takes place at the cracked sections. Due to the bond between concrete and steel, the tensile force in the reinforcement varies along the reinforcing bars. The flexural tension cracks in the beam divide the tension zone into a number of cantilevers. These concrete cantilevers are acted upon by the incremental tension forces (bond forces) in the reinforcement, which are shown in Figure 3.1 as " ΔT " forces. The function of each concrete block may be compared to that of a short cantilever embedded in the compression zone of the beam and loaded by the bond forces at the level of the reinforcement.

Equilibrium of forces in the shear span of the beam is shown in Figure 3.2 (a). Tension force T acts at the level of the reinforcement while the compression force C is acting in the compression

zone of the beam, jd being the lever arm between these two forces. Shear forces V_c and V_d are carried by the compression zone of the beam and the dowel action of the reinforcement respectively. As the cracks become inclined, shear displacements across the two faces of the crack give rise to the interlocking forces, shown by their resultant horizontal and vertical components, H_{ai} and V_{ai} . Since the flexural cracks are only slightly inclined at this stage, the resultant forces of aggregate interlock may be neglected and in simplified form the moment equation may be written as

$$M_x = V_x = Tjd = Cjd$$

or

$$V = T \frac{d(jd)}{dx} + jd \frac{dT}{dx} \dots\dots(3.1)$$

An isolated concrete cantilever is shown in Figure 3.2(b). The bond force, ΔT , at the level of the reinforcement induces a bending moment, M_b , and a horizontal shear force, V_h , at the root of this cantilever. The bond force moment is resisted by the flexural resistance of the cantilever, the aggregate interlock and the dowel action of the reinforcement, and the imbalance of aggregate interlock forces induces an axial force, P .

An examination of equation 3.1 shows that the external shear can be resisted by beam action as well as by the arch action. $\frac{dT}{dx}$ represents the effective bond force. With a constant lever arm jd , the term $jd \frac{dT}{dx}$ gives the contribution of the beam action. If the lever

arm changes along the span of the beam, the compression force in the beam becomes inclined and the term $T \frac{d(jd)}{dx}$ gives the contribution of the arch action. In case no arching develops, this term would be zero and external shear would be carried entirely by beam action. Thus,

$$V = jd \left(\frac{dT}{dx} \right)$$

or

$$\frac{dT}{dx} = \frac{V}{jd} \quad \dots\dots(3.2)$$

Since

$\frac{dT}{dx}$ is the bond force per unit length,

$v_h = (\frac{dT}{dx})/b$, where b is the width of the beam and v_h is the horizontal shear stress induced by the bond force. Substituting the value of $(\frac{dT}{dx})$ from equation 3.2, we obtain the familiar

$$v_h = \frac{V}{bjd} \quad \dots\dots(3.3)$$

The above equation shows that if the lever arm remains constant, there is no arching and the horizontal shear stress induced by the bond force is equal to the nominal shear stress, v_n , for the beam. When beam and arch action are present simultaneously, the horizontal shear stress is lower than the nominal shear stress for the beam.

Figure 3.3 shows how beam and arch action can exist simultaneously in the shear span of a beam. In this case, the

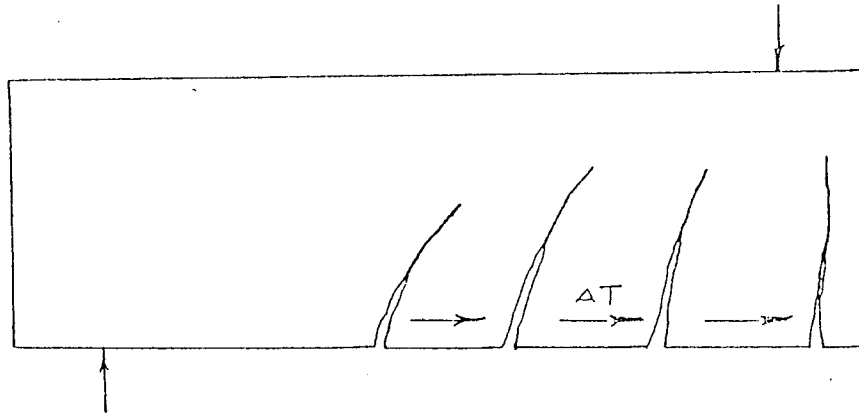


FIG. 3.1 FLEXURAL CRACKING DUE TO BOND FORCES AND ACTION OF CONCRETE CANTILEVERS

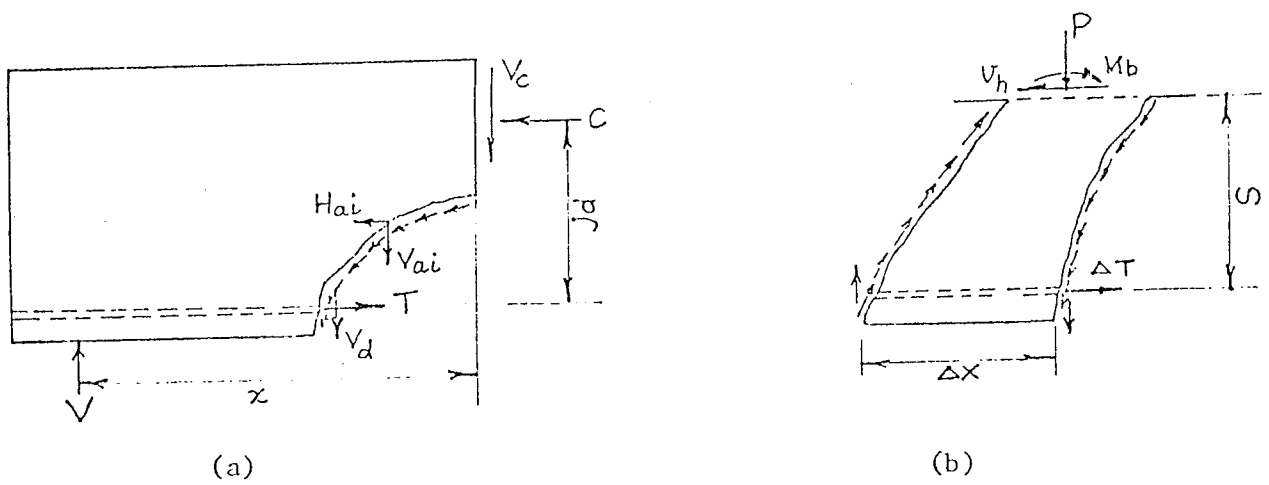


FIG. 3.2 EQUILIBRIUM OF FORCES BEFORE CRITICAL DIAGONAL CRACKING

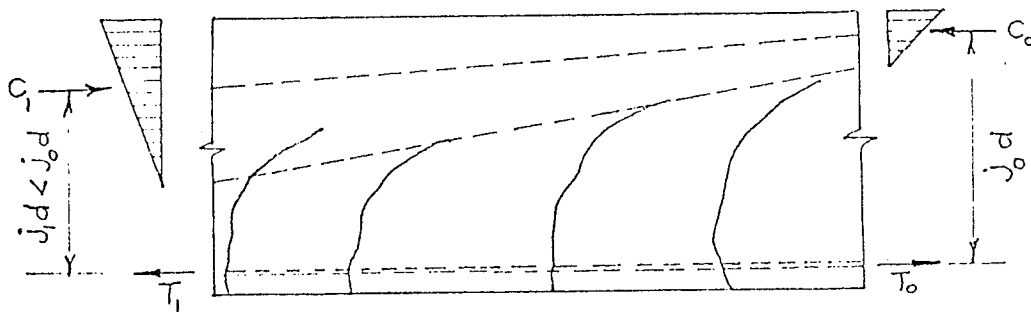


FIG. 3.3 BEAM AND ARCH ACTION IN SHEAR SPAN

compression force inclines above the flexural cracks with the result that bond forces are still active within the concrete cantilevers. The lever arm, from its maximum value in the midspan region, reduces towards the supports. With this distribution of forces, the external load is carried partly by beam action and partly by arch action.

As flexural cracks form in the shear span of the beam, a portion of the beam in the immediate vicinity of the cracked section starts behaving as an arch. With increased loading and progressive flexural cracking in the outer regions of the shear span, the zone of internal arching also proceeds outwards. Figure 3.4 shows the progressive development of internal arching. These internal arches develop in conjunction with the action of the concrete cantilevers which is associated with the bond forces. In other words, these internal arches do not produce a physical segregation of the beam into two separate regions of beam and arch action. The compressive forces associated with the internal arches are very small compared to those in the compression zone of the beam in the vicinity of the load point.

The actual stress distribution at the top of the flexural cracks is complex. The high tensile stresses associated with the cracks are likely to be limited to the area in close proximity of the crack. Since concrete is relatively strong in resisting high local stress intensities, the tensile failure of concrete is more likely to result from a lower average stress over a larger area than a high stress intensity over a small area. Bond forces in the concrete

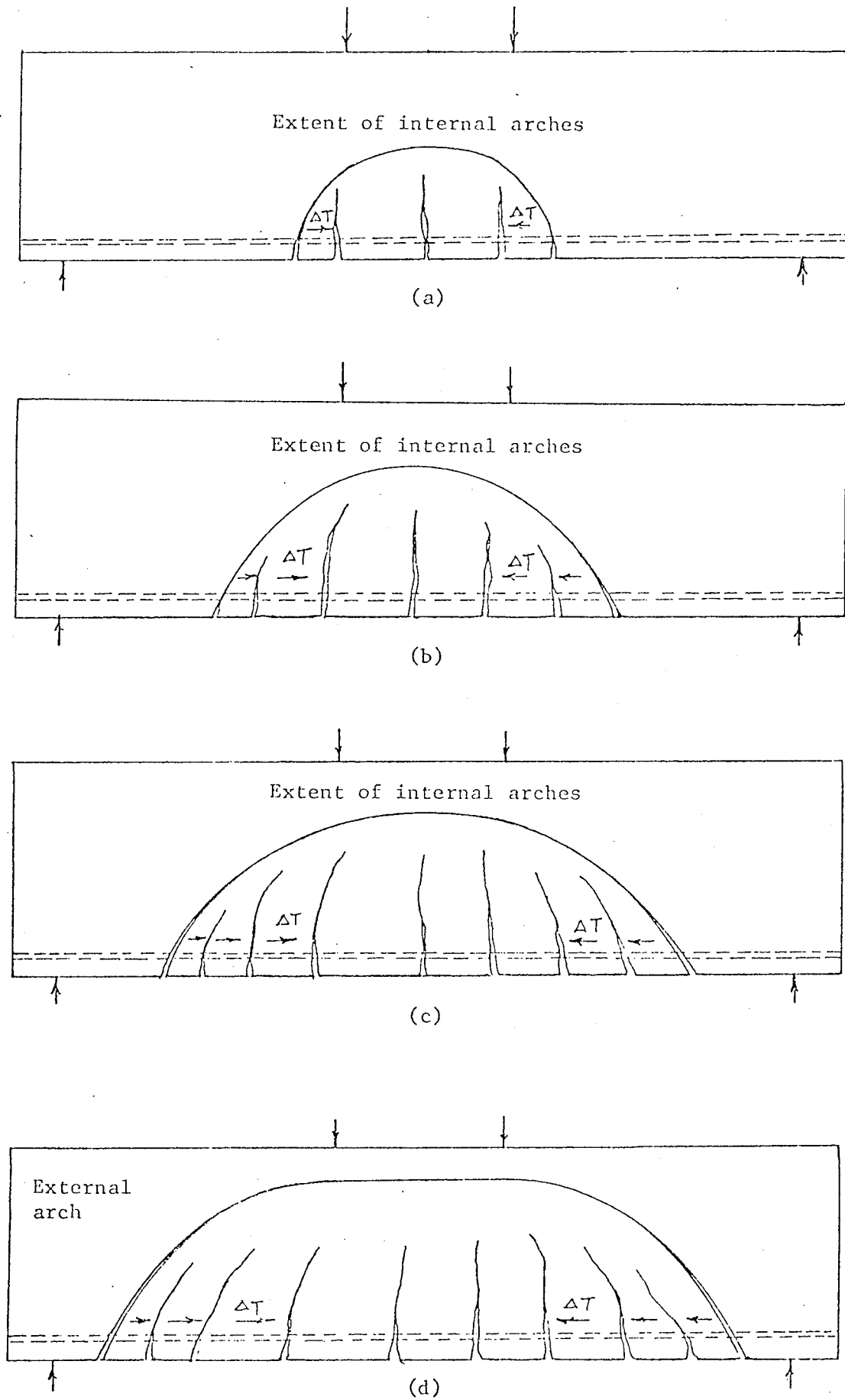


FIG. 3.4 PROGRESSIVE DEVELOPMENT OF INTERNAL ARCHING

cantilevers cause transverse flexural and shear stresses which are resisted by the flexural resistance of the concrete cantilevers, by aggregate interlock and by the dowel action of the reinforcement. So long as the flexural cracks in the beam remain vertical, all the bond force moment is resisted by the flexural resistance of the concrete cantilevers. When a flexural crack becomes inclined, aggregate interlock and dowel action of the reinforcement also become important modes of carrying the bond force moment. Thus the proportion of resistance of each mode is a variable depending upon the stage of loading, and the extent and nature of cracking.

At a critical stage of loading, the bond force moment that can be carried by the concrete cantilevers exceeds their strength. This results in the extension of a critical diagonal crack from an outer flexural crack or from within its vicinity. This may be preceded by the appearance of some back-cracking above the level of the reinforcement at outer locations of flexural cracks caused by a local tensile failure of concrete. As such diagonal cracks form, the portion of concrete below them is lost and the crack extends into compression zone of the beam in order to mobilize additional resistance.

The critical diagonal crack extends from an external flexural crack since the maximum bond force moment exists in the outer concrete cantilevers. This is so because with internal arching, the bond forces within the inner regions of concrete cantilevers are reduced and the most critical section is located at the outermost flexural crack.

The reader's attention is now drawn to the internal forces at critical diagonal cracking. These are shown in Figure 3.5.

As the critical diagonal crack extends into the compression zone of the beam, the compression zone is separated into two parts. Part of the total compressive force is carried above the diagonal crack and part of it is carried below the diagonal crack. The relative magnitude of these two forces depends upon the distribution of compressive strains over the compression zone near the tip of the diagonal crack in the vicinity of the load point. At this location, the maximum compressive strains exist at the compression face of the beam and diminish as the depth of the beam decreases.

V_1 and V_2 are the shear forces above and below the diagonal crack while C_1 and C_2 are the corresponding compressive forces above and below the diagonal crack. The tension force in the reinforcement changes from T_1 , where the diagonal crack crosses the reinforcement, to its maximum value, T_{\max} , at midspan. Dowel shear V_d is acting at the reinforcement level under the load point while dowel shear V_{d1} exists at the point the diagonal crack crosses the reinforcement. The resultants of forces above and below the top tip of diagonal crack are represented by R_1 and R_2 respectively. Though the diagonal crack divides the beam into two portions, part of the shear can still be carried by the interlocking action of the aggregates. The contribution of aggregate interlock, however, reduces significantly as the diagonal crack opens up.

Figure 3.6 shows internal force distributions and diagonal

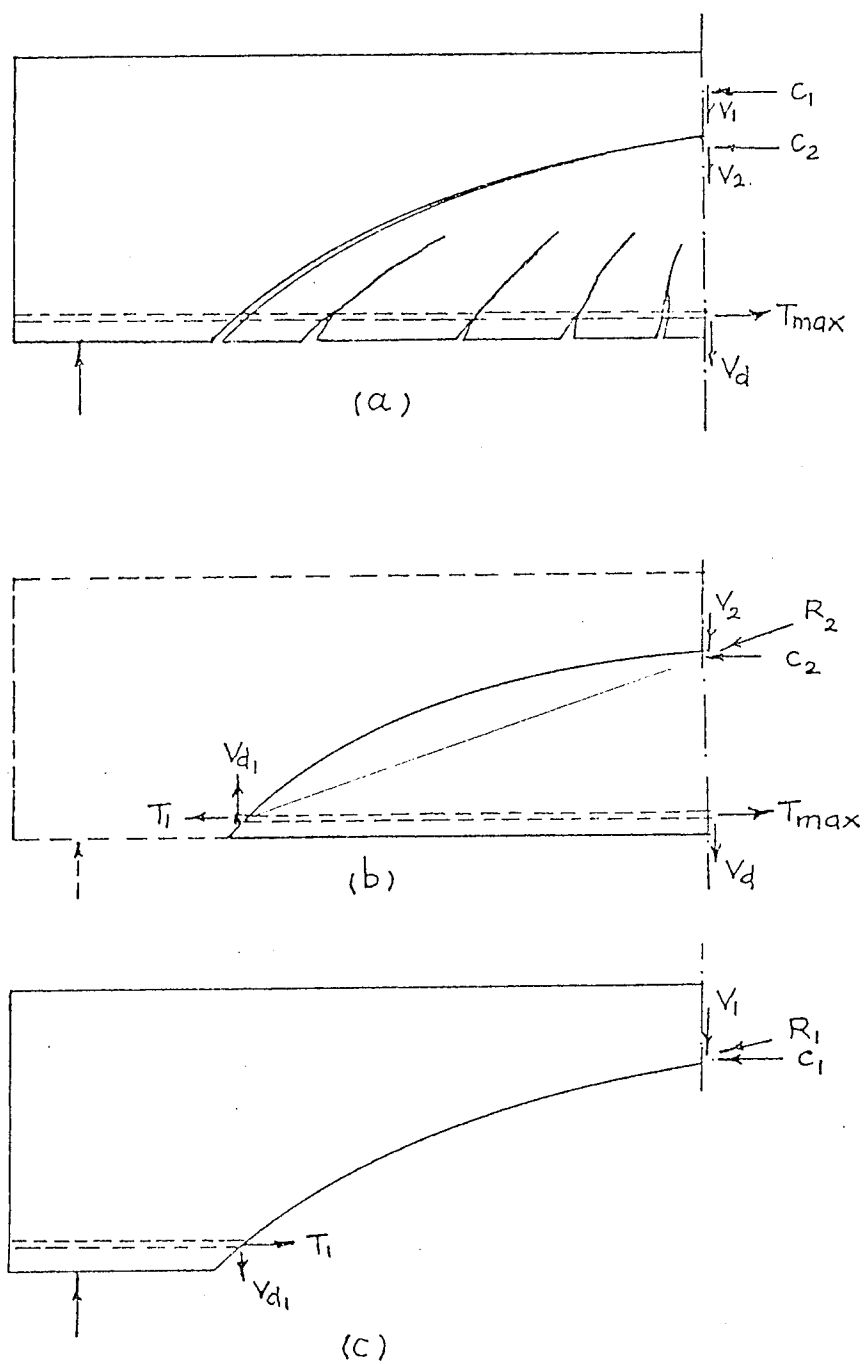
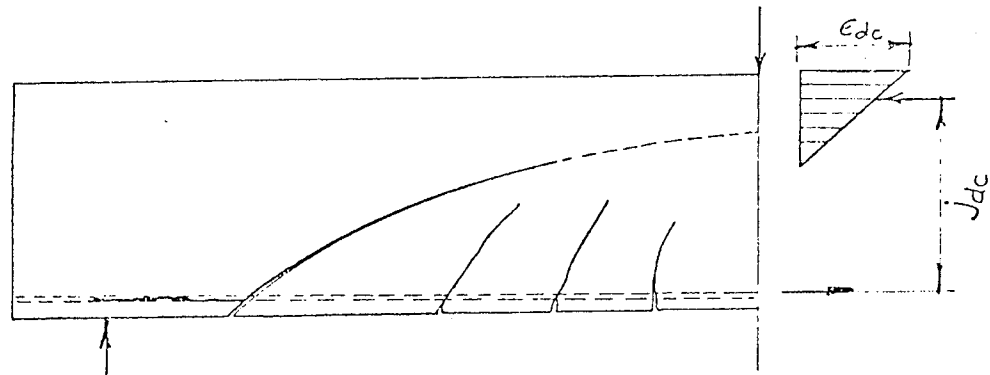
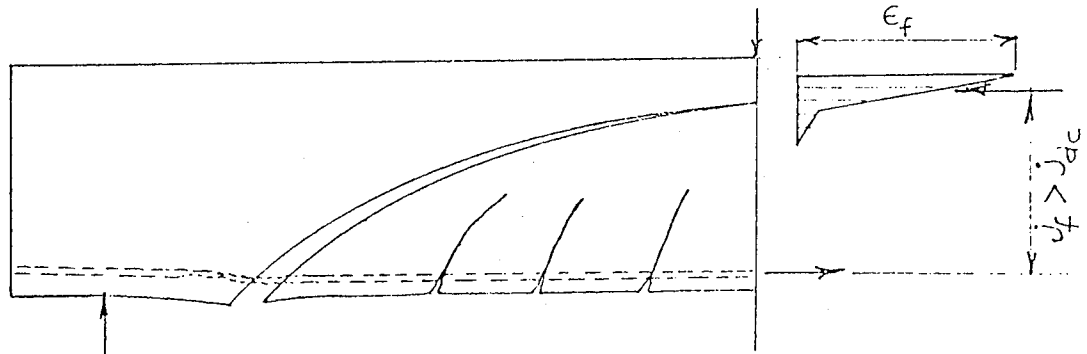


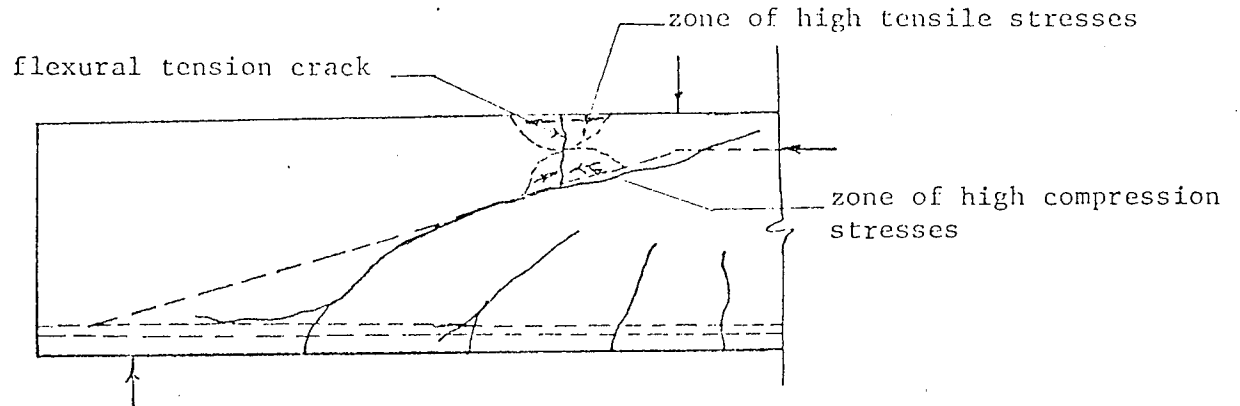
FIG. 3.5 INTERNAL FORCES AT CRITICAL DIAGONAL CRACKING



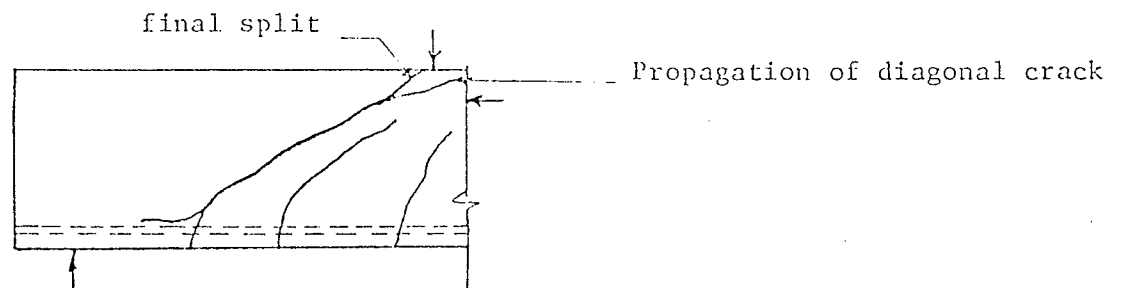
(a) Distribution of forces at critical diagonal cracking



(b) Distribution of forces after internal rotations



(c) Flexural tension failure



(d) Shear compression failure

FIG. 3.6 INTERNAL FORCE DISTRIBUTIONS AND DIAGONAL FAILURES

failures of beams. From the compressive strain distribution, it is clear that if the diagonal crack is located at the midpoint of the compression zone, the compressive force carried above the crack will be higher than that below it.

Extension of the diagonal crack in the compression zone of the beam results in significant internal rotations. The centre of rotation is located in the vicinity of the load point close to the tip of the diagonal crack. These internal rotations cause the diagonal crack to widen progressively as the distance from the centre of rotation increases.

Let us now examine the effect of these internal rotations on the internal force system. Figure 3.6(a) shows the distribution of forces at critical diagonal cracking. The maximum compressive strain at the compression face under the load point is ϵ_{dc} and the internal lever arm is j_{dc} . After internal rotation takes place, the maximum compressive strain increases to a final value of ϵ_f at ultimate failure (Figure 3.6(b)). This value is considerably higher than that at diagonal cracking. Further, the distribution of compressive strain over the compression face at this location also changes, resulting in a shift of the resultant compressive force upwards and an increase in the final lever arm to j_f from its value at diagonal cracking.

The critical diagonal crack opens up considerably at the reinforcement level due to internal rotations. This results in splitting of the reinforcement from the lower tip of the diagonal

crack towards the supports, which in turn causes a second redistribution of the internal forces with further rotations of the compression zone. The net effect of the internal rotations is that the proportion of the compressive force above the diagonal crack increases substantially while that below it decreases. Furthermore, the resultant of the compressive force and the shear force above the diagonal crack now lies in the direction of the critical diagonal crack. High diagonal compressive stresses exist just above the diagonal crack (Figure 3.6(c)), which are caused by the inclination of the resultant compression. Since the area of intact concrete above the diagonal crack is small, these high compressive stresses can result in high tensile stresses at the compression face above the location where the diagonal crack is at some distance from the compression face. When the limiting tensile stress at the compression face exceeds the tensile strength of the concrete, a crack extends from the compression face of the beam downwards to the diagonal crack, resulting in the failure of the beam due to flexural-tensile stresses. Such failures have been defined as diagonal tension failures.

In relatively short beams, the resultant thrust line in the compression zone is more steeply inclined due to heavy external shear and there is a greater effective area of concrete available above the diagonal crack where tensile stresses can develop so that tensile cracks do not form above the diagonal crack. In such cases, the diagonal crack is stabilized. This permits internal rotation to take place with the result that the neutral axis progressively shifts

upwards until a limiting location is reached. During such rotation, the tip of the diagonal crack progresses very little, if at all.

When the critical diagonal crack appears, internal arching extends along the crack. As the diagonal crack is stabilized well into the compression zone of the beam, this outermost of the internal arches lies in the region where the bulk of the resultant compressive force is located. Since the diagonal crack is not far removed from the external supports, the outermost of the internal arches is supported by a stiff or almost non-yielding support at the beam ends. This results in an effective external arch, composed of the intact portion of concrete above the diagonal cracks, being supported on the beam ends. At this stage, the compressive force above the diagonal crack becomes significantly inclined and can be transferred to the supports directly through the external arch. With the opening of cracks at the reinforcement level, horizontal displacements take place at the cracked segments resulting in a progressive reduction of the bond forces in the reinforcement and the external arch approaches more closely the conditions of a tied arch.

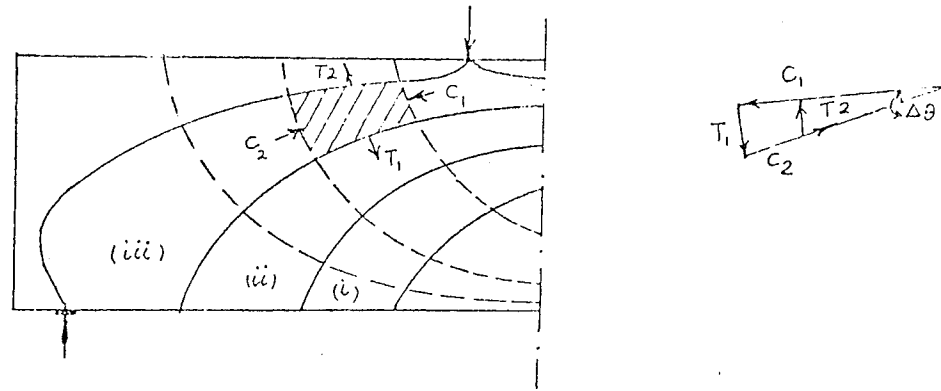
As arching develops over the entire span with the stabilization of the critical diagonal crack, a modified beam action, also exists as internal rotations take place. Any increase in the capacity of this beam action at this stage is more a result of the shift of the centre of compression upwards rather than an increase in the tension or the compression force. The capacity of the beam action can be calculated in a manner similar to that used for flexural-

compression failures.

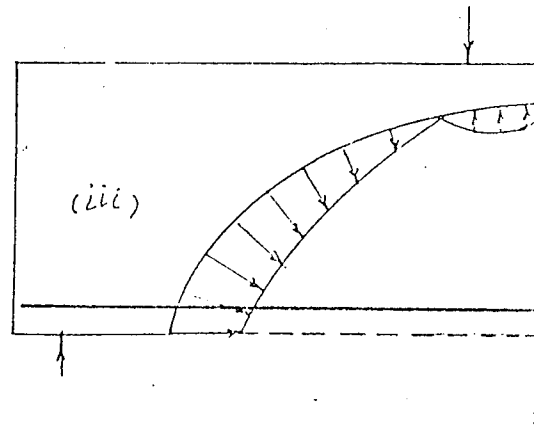
Consider the stress distribution along an internal arch. Internal arches develop along the flexural cracks which follow the compressive stress trajectories. These trajectories are normally shown as two systems of orthogonal trajectories, one system representing the direction of maximum principal stresses, the other representing the direction of minimum principal stresses. As concrete is weak in tension, cracks form normal to the direction of the principal tensile stress or, by definition, follow the shape of the compressive stress trajectories. Since the tension force in the reinforcement in beams with bond changes from zero value at supports to its maximum value at midspan, the resultant of the external reaction and the tension force in the reinforcement, i.e., the thrust line, flattens out gradually towards the midspan.

It is instructive to examine the condition of the stress trajectories of a reinforced concrete beam before cracking. These are shown in Figure 3.7. Compressive (minimum) stress trajectories are shown with full lines while tensile (maximum) stress trajectories are shown with dotted lines. The change in the direction of compressive force, i.e., the change in the direction of the compressive stress trajectory arises from the difference in the tensile forces normal to the compressive stress trajectory (Figure 3.7(a)). By definition, only normal forces are acting over the stress trajectories (Figures 3.7(b) and (c))* . The strips between consecutive compressive stress trajectories carry external loads by transferring their internal

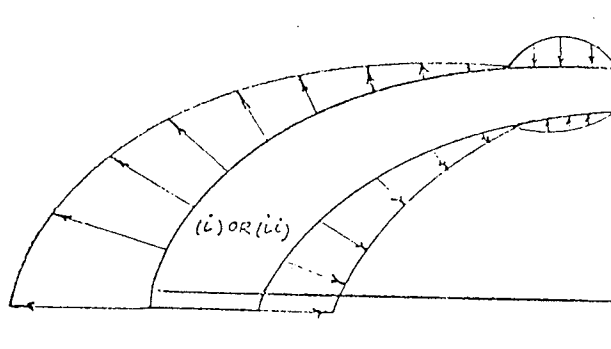
* KANI (1969)



(a) Internal forces and stress trajectories before cracking



(b) Stress distribution along external compressive stress trajectory



(c) Stress distribution along internal compressive stress trajectories

FIG. 3.7 COMPRESSIVE STRESS TRAJECTORIES AND STRESS DISTRIBUTIONS BEFORE CRACKING

support forces to the external support.

With the development of flexural cracks, a strip of concrete along the flexural cracks starts acting as an internal arch. Stress distribution on an internal arch is shown in Figure 3.8. No internal support forces can develop over the cracked area of the internal arch. As the cracks propagate further and become inclined, the support forces are further reduced. The bond forces are still effective within the concrete cantilevers.

The progressive development of internal arching is shown in Figure 3.9. Numbers 1, 2, 3, 4 represent the loading stages and the extent and location of flexural cracks. As these cracks form, there is a redistribution of internal forces. The stress trajectories at various stages of loading after cracking will have different profiles. Internal arching extends outwards along the profile of flexural cracks. Figure 3.9 also shows the compression force distribution over the compression face of the beam at diagonal cracking and after significant internal rotations. After internal rotations, the neutral axis shifts upwards as also does the location of the resultant compressive force. It is apparent that the internal arches closer to the centre of the beam carry no part of the compression force.

Consider one of the internal arches which carries a part of the compression force (Figure 3.10). The normal stresses over the internal arch give rise to internal reaction, R_i , which can be resolved into its vertical and horizontal components, V_i and H_i .

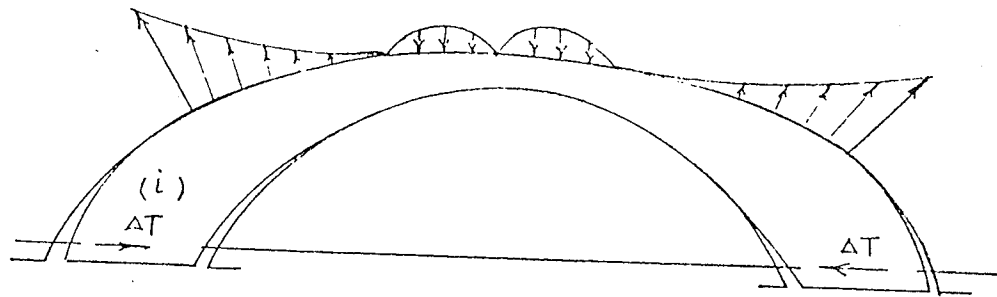


FIG. 3.8 STRESS DISTRIBUTION ALONG AN INTERNAL ARCH

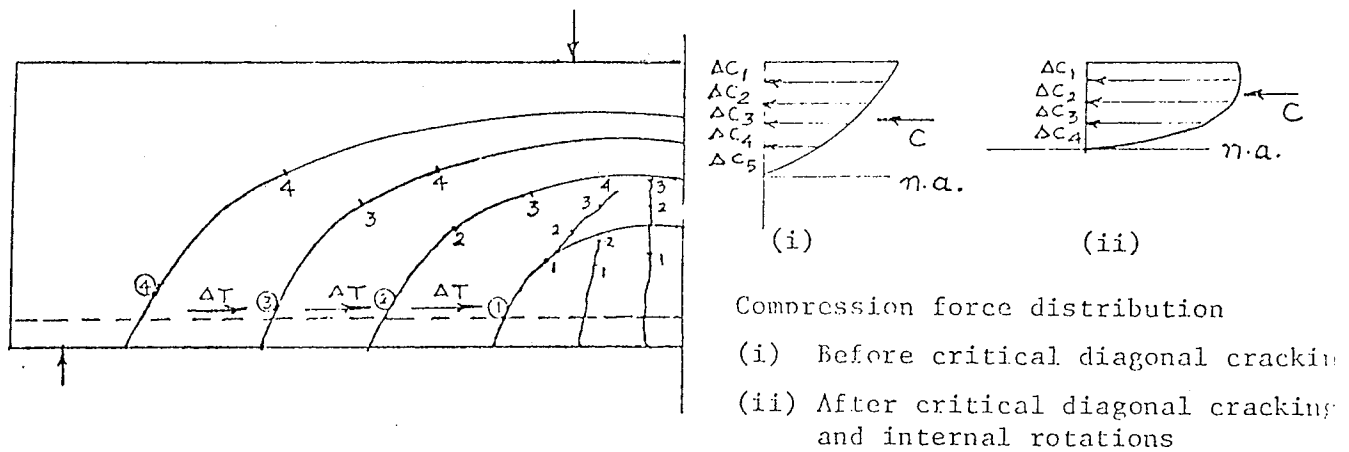


FIG. 3.9 DEVELOPMENT OF INTERNAL ARCHING AND COMPRESSIVE FORCE DISTRIBUTION

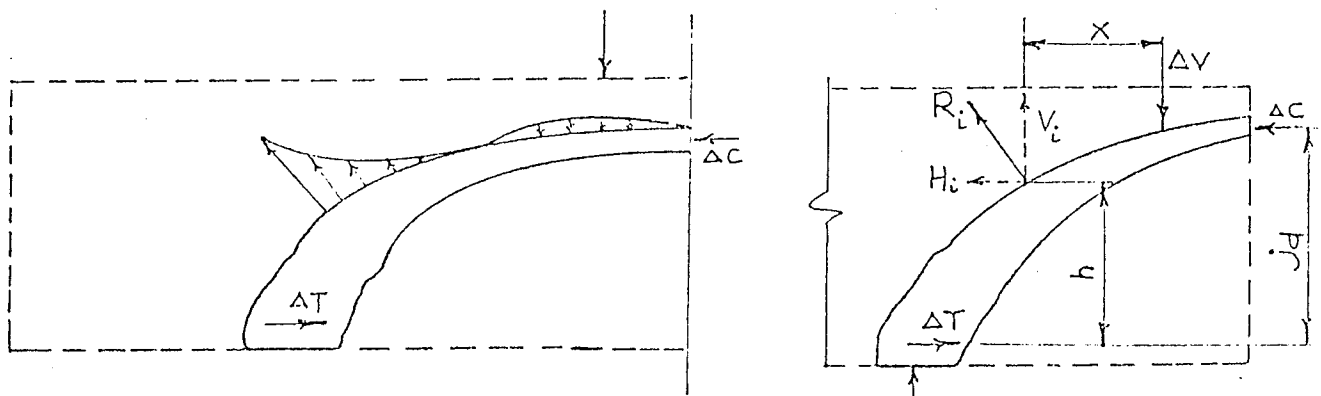


FIG. 3.10 FORCES ON AN INTERNAL ARCH

The horizontal component of internal reaction is generally small. Bond force, ΔT , is acting at the level of the reinforcement and a force ΔC acts within this arch in the compression zone of the beam. Part of the external shear, ΔV , is also acting over the arch at its point of application. As the flexural cracks propagate further, the resultant internal reaction moves closer to the external shear and is reduced in magnitude. Maintenance of equilibrium of the forces in turn requires a progressive reduction of the component of the compression force that can be carried by the internal arch. As the components of resultant compressive force that are carried by each arch are reduced, the capacity of the beam decreases. However, if the portion of the compressive forces within the internal arches can somehow be transferred to the external arch, much of this lost capacity can be regained. This occurs at the extension of a critical diagonal crack and its stabilization. Internal rotations take place in the compression zone of the beam and the resultant compressive force shifts upwards. If, however, the critical diagonal crack is not fully stabilized, failure takes place at a reduced capacity compared to the flexural resistance of the section.

It is now appropriate to consider the internal force system after critical diagonal cracking has taken place and has been stabilized and to consider the manner of ultimate collapse of the beam.

As already pointed out, internal arching extends over the entire span at this stage and an external arch, resting on the beam supports develops. As internal rotations develop, the bulk of

compression force is transferred to the external arch which is under diagonal compression. The resultant compression force inclines appreciably above the critical diagonal crack and can be transferred to the supports directly through the external arch.

The ultimate failure of the beam may result when either of the following happens.

- (i) the capacity of the external arch is exceeded.
- (ii) the flexural-tensile stresses above the diagonal crack reach the tensile strength of concrete at a load level higher than that causing critical diagonal cracking.
- (iii) the compressive stresses on the compression face directly under the load point exceed the compressive strength of concrete.

These failures have been defined as shear compression failures.

As internal rotations of the compression zone take place, the neutral axis shifts upwards until a limiting position is reached. During these stages the shape of the stress trajectories changes due to the propagation of cracks. The cracks straighten out more and more due to a gradual reduction of the bond forces, and in some cases, the eventual elimination of these forces. Most of the web of the beam is thus under diagonal compressive stresses. As the diagonal compressive stresses increase, they give rise to higher tensile stresses above the diagonal crack which may result in flexural-tension cracks. Further, as the internal rotations continue, the compressive strain at the compression face increases rapidly and the concrete at the

compression face may crush. It is evident that an interaction exists between arch action and a modified beam action even after critical diagonal cracking. The ultimate failure of the beam and the possibility of either type of failure discussed above depends primarily on the slenderness of the beam and the manner and the type of loading.

The simultaneous existence of the beam and arch action in the shear span of a reinforced concrete beam after flexural cracking may be considered in the following regions of loading.

- (1) From the appearance of first flexural cracks to critical diagonal cracking.
- (2) From the point of stabilization of the critical diagonal crack to ultimate collapse.

From the point of flexural cracking to the critical diagonal cracking, the action of concrete cantilevers controls the strength of the mechanism since the internal arches carry only a small part of the resultant compressive force. A diagonal crack occurs as the bond force moment exceeds the strength of the concrete cantilevers. If this diagonal crack is not stabilized, failure of the beam results from a flexural-tensile failure of concrete. However, if this crack is stabilized, internal arching extends over the entire span. With internal rotations, an interaction exists between the beam action of the flexural-compression type and the arch action. The ultimate failure may result from either of the two depending upon the slenderness of the beam and conditions of restraint on the

propagation of cracks. This interaction may cause a significant spread of collapse loads within the range it is effective.

3.3. THE INFLUENCE OF VARIOUS FACTORS ON PROPOSED FAILURE MODEL

3.3.1. Rotations in the Compression Zone

Horizontal displacements at the reinforcement level are caused by the bond forces applied to the concrete cantilevers and internal rotations of the compression zone. As a critical diagonal crack appears, the resultant of the forces at the point it crosses the reinforcement causes some splitting along the reinforcement. This results in increased internal rotations with an increase in the compression force carried above the diagonal crack. The resultant compressive force becomes inclined above the diagonal crack with the result that a zone of high tensile stresses exists above the diagonal crack. When such tensile stresses reach the tensile strength of concrete, a crack extends from the compression face of the beam downwards which may cause the flexural-tensile failure of the beam. The possibility of such a failure will increase with the slenderness of the beam. The internal rotations required to stabilize the diagonal crack will depend on the dowel force that can develop in the flexural tensile reinforcement. With dowel cracking, the dowel force will reduce and greater internal rotations will be required to prevent the failure of the beam.

As the internal rotations take place, the width of the diagonal crack increases with an increase in distance from the centre of rotation. Crack width at any point is defined as the distance between two sides of the crack in the direction of crack propagation. So long as the cracks are vertical, the only component of movement is the crack width. As the cracks become inclined, both longitudinal and transverse movements (δ_h and δ_v) take place across the crack due to the internal rotation of the compression zone (Figure 3.11). The following relations can be established from the figure.

$$\tan [\theta_1 + (90 - \theta)] = \frac{\delta_v}{\delta_h}, \text{ where } \theta \text{ is the crack angle at the point considered}$$

or

$$\left. \begin{aligned} \theta_1 &= \tan^{-1} \left(\frac{\delta_v}{\delta_h} \right) - (90 - \theta)^\circ \\ c_w &= \sqrt{\delta_h^2 + \delta_v^2} \cos \theta, \\ \delta_s &= \sqrt{\delta_h^2 + \delta_v^2} \sin \theta, \\ \text{and } \Delta &= \sqrt{\delta_h^2 + \delta_v^2}, \end{aligned} \right\} \dots\dots(3.4)$$

Δ being the total displacement of the

point.

The angle θ_1 , between the direction of movement of a particle and the perpendicular to the direction of crack, is generally small so that δ_s , the shear displacement would be substantially smaller than crack width, c_w .

Consider the diagonal crack shown in Figure 3.12. Point B on the crack moves to B'. The total displacement of the point is thus BB'.

$$\begin{aligned} c_w &= BB' \cos \theta_1 \\ &= \Delta \cos \theta_1 \end{aligned}$$

If Point A (Figure 3.12) represents the centre of rotation and l_{AB} the distance of point B from it,

$$\left. \begin{aligned} \Delta &= l_{AB} \theta_c \\ \text{and} \\ c_w &= l_{AB} \theta_c \cos \theta_1 \end{aligned} \right\} \dots\dots(3.5)$$

where θ_c is the angle of internal rotation. The internal rotation depends on the location of the diagonal crack within the compression zone of the beam. This rotation results in an increase of the compressive strain at the compression face of the beam and a shift of the neutral axis upwards. When the limiting position of the neutral axis is reached, i.e., when the neutral axis shifts upwards to the top tip of the diagonal crack, a failure of the beam may result from crushing of the concrete located above the diagonal crack in a manner similar to flexural-compression failures.

It has been shown that the width of diagonal crack increases with the distance from the centre of rotation which is located in the compression zone of the beam close to the tip of the diagonal crack. As internal rotations take place, the width of the diagonal crack increases considerably at the reinforcement level. As this width increases, the shear force that can be carried by the dowel

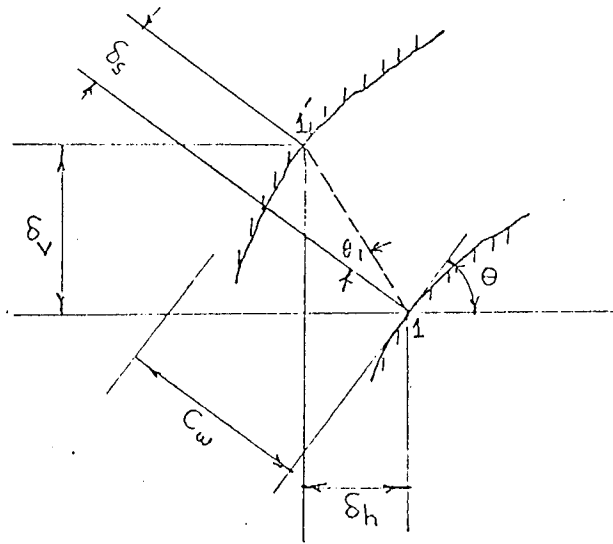


FIG. 3.11 DISPLACEMENTS ACROSS A CRACK

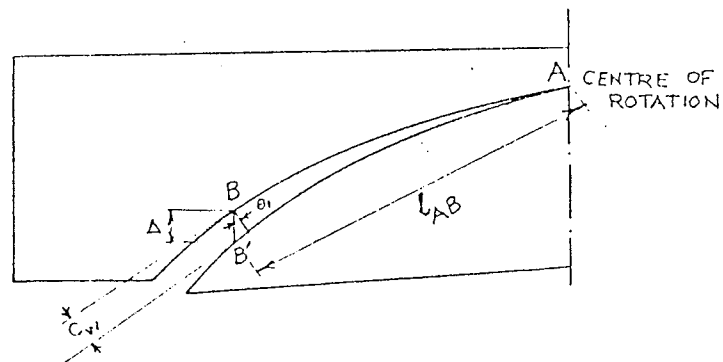


FIG. 3.12 INTERNAL ROTATIONS AND DIAGONAL CRACK WIDTH

action of the reinforcement reduces further and leads to further internal rotations. At the same time, considerable translational displacements occur at the reinforcement level at the cracked segments. Such translational displacements are essential for the slip of the reinforcement which progressively reduces the bond forces in the concrete cantilevers. Therefore, as the width of the diagonal cracks increases, the external arch approaches the conditions of a tied arch with only a small change in the tension force in the reinforcement along the span of the beam. As the resultant compressive force becomes inclined and higher diagonal compressive stresses exist above the diagonal crack, failure may also occur due to a flexural-tensile failure at a higher load.

3.3.2. The Method of Loading

It has been suggested that diagonal tension failure of a beam results from flexural tensile stresses that exist above the diagonal crack. If such stresses can be suppressed, the diagonal crack can be stabilized and the capacity of the beam increased.

If the beam is loaded directly over the compression face of the beam, high vertical compressive stresses exist in the region under the load point. These local stresses and the corresponding values of principal stresses have been calculated for the case of a load on a strip of infinite length and a constant width from the theory of elasticity.* These principal stresses for a given loading

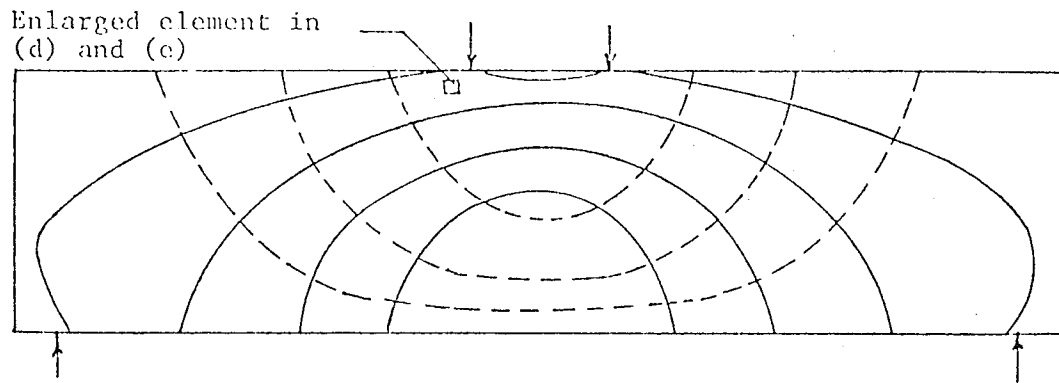
* For example, "Theoretical Soil Mechanics" by TERZAGHI, K., Figure 119, p. 377, John Wiley and Sons, New York, 1966 edition.

intensity depend solely on the location of the point considered relative to the point of application of the load.

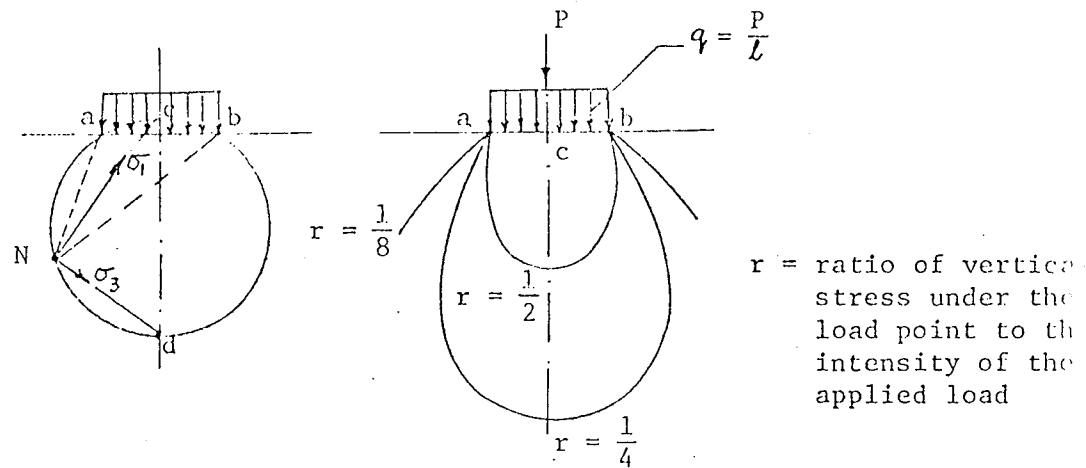
Figure 3.13(b) shows the orientation of principal stresses at a point due to a strip load. For every point on a circle through a, b, and N, the principal stresses have the same intensity. The directions of the principal stresses in every point on the circle abN pass through points c and d respectively. These points are located at the intersection between the circle and the plane of symmetry of the loaded strip. Furthermore, all points with equal vertical compressive stress are located on curves (Figure 3.13(c)) which resemble sections through the boundaries between the individual layers of a plant bulb. In fact, the space below the loaded area is called the pressure bulb. Pressure bulbs for $1/2$, $1/4$ and $1/8$ of the unit load intensity are shown on Figure 3.13(c). It shows that high vertical compressive stresses exist in the immediate vicinity of the load point.

Figure 3.13(a) shows a beam loaded through point loads directly over the compression zone of the beam. An element in the vicinity of the load points is shown in Figure 3.13(d) and (e), without local vertical loading and including the effect of the local vertical loading.

Let us now consider the relevance of pressure bulbs for beams directly loaded over the compression face of the beam. In relatively slender beams, the critical section above the tip of the diagonal crack where vertical tensile stresses exist, is

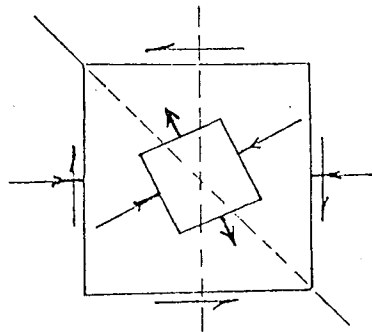


(a) Beam loaded through point loads directly above the compression face of the beam and stress trajectories.

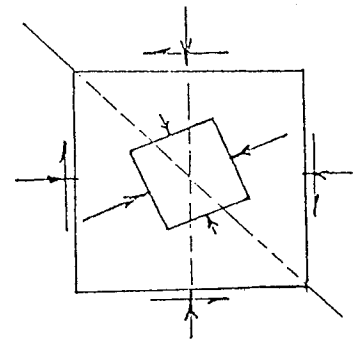


(b) Orientation of principal stresses at a point due to strip load.

(c) Curves of equal ratio between vertical pressure and unit load on strip with infinite length (pressure bulbs)



(d) Enlarged element without vertical loading



(e) Enlarged element with vertical loading

FIG. 3.13 EFFECT OF DIRECT LOADING ON THE COMPRESSION FACE OF THE BEAM

considerably removed from the point where the load is applied. In such cases sudden diagonal tension failure occurs regardless of the manner of loading as the diagonal crack extends into the compression zone of the beam. However, for shorter beams, the point of loading is closer to the diagonal crack and as the diagonal crack extends into the compression zone of the beam, it enters the zone influenced by the pressure bulbs under the load point. This results in suppression of the vertical tensile stresses above the diagonal crack. Thus the diagonal crack is stabilized and the flexural tensile failure of the beam does not take place. Furthermore, as the beam continues taking further load, the vertical compressive stresses under the load increase proportionately. Therefore, at no stage of loading after the stabilization of diagonal cracks, can a flexural tensile failure of the concrete take place in the immediate vicinity of the load point. At higher load levels, tensile cracks may appear from the compression face of the beam at sections relatively removed from the load point. At these points, the depth of the intact zone of concrete above the diagonal crack is deeper and the possibility of the tensile cracks extending to the diagonal cracks is remote. Most of the concrete is in diagonal compression at this stage and the full capacity of an external arch can develop. In such a case, ultimate failure may result from the failure of the arch or the compression failure of concrete at the compression face under the load point.

It can be seen that the intensity of vertical compressive

stresses will be higher for beams loaded through one or two concentrated loads. Such beams can, therefore, arrest the diagonal crack growth more effectively if the critical section is located close to the load point. When the beam is loaded through a multiple loading arrangement there are pressure bulbs under each strip load. The intensity of vertical pressure at such bulbs is lower than the previous case. However, since the vertical compressive stresses are distributed over the compressive face of the beam, such loading can stabilize the diagonal crack growth even for relatively slender beams. Furthermore, the failure of a beam at the appearance of diagonal cracks will not be as sudden as in the case of single or two-point loads. However, since the intensity of vertical compressive stresses is low, a flexural-tensile failure can take place at a delayed stage.

When a beam is loaded through secondary beams, the zone of local high vertical compressive stresses is removed from the main beam. In such a case, the vertical tensile stresses above the diagonal crack cannot be effectively suppressed. In beams of moderate length, the diagonal crack leads directly to the failure of the beam. When the beam is relatively short, it can generate the internal rotations necessary to stabilize the diagonal crack even when the load is applied through secondary beams and failure does not result at the appearance of the diagonal crack. However, the propagation of diagonal cracks is relatively unrestrained near the load points due to the absence of the restraining influence of the

pressure bulbs as the diagonal crack propagates in the compression zone. In such short beams arching develops over the entire span at the appearance of a critical diagonal crack but the full capacity of the arch cannot be mobilized due to premature failure due to unrestrained propagation of diagonal cracks and a flexural-tensile failure at a higher load level.

It is therefore concluded that for all failures that have been defined as diagonal tension failures the effect of the method of loading is not significant. However, for failures that have been defined as shear-compression, the method of load application will have considerable influence on the mechanism of failure and its strength.

3.3.3. Compressive and Tensile Strengths of Concrete and the Area of Concrete in the Compression Zone of the Beam

It was suggested that back-cracking at some of the outer flexural cracks in the shear span of the beam takes place due to a local tensile failure of the concrete. This can occur before the appearance of a critical diagonal crack. Such back-cracking may precipitate a diagonal crack as the area of concrete below the crack is then lost when considering the capacity of the concrete cantilevers. This behavior indicates that improvements in the tensile strength of concrete would result in some increase in the capacity of concrete cantilevers. However, since crack widths would also

be increased, the contribution of aggregate interlock would be reduced and the gain in strength would be rather small. It is, therefore, concluded that an increase in the strength of concrete would raise the strength of beams failing in diagonal tension only by a small amount.

In beams where an initial diagonal crack is stabilized, the compressive strength of concrete plays a significant role. Where failure takes place due to crushing of concrete, the ultimate capacity of the modified beam action would be proportional to the compressive strength of concrete. The capacity of the arch would also be raised with an increase of compressive strength due to a delayed flexural-tension failure and a greater capacity for carrying inclined compressive forces. However, the improvement in the strength of the arch would not be as significant as that of the modified beam.

The cross-sectional area of concrete in the compression zone of the beam is likely to have considerable influence on the strength of beams failing in shear compression. As discussed previously, beam failure occurs due to a failure within the compression zone above the diagonal crack in compression or in flexural-tension. Any increase in the area of the compression zone in such cases would therefore increase the capacity of the beam.

3.3.4. The a/d or $\frac{M}{Vd}$ Ratio

The type of diagonal failure that occurs in a beam is very closely associated with the beam's slenderness ratio. As the slenderness of the beam increases, there is an increase in the eccentricity of the resultant of external shear and compressive forces above the diagonal crack. Failure of the beam then takes place at the appearance of a critical diagonal crack due to instability. Therefore diagonal tension failures are expected to occur for all beams beyond a certain critical value of the a/d or $\frac{M}{Vd}$ ratio. As the slenderness increases further, a point is reached where bending failure precedes a diagonal failure and the full flexural capacity of the section is achieved. In these diagonal failures, an increase in the shear-span/depth ratio results in an increase in the magnitude of the bending moment and a corresponding increase in the width of cracks. As the cracks widen, the contribution of aggregate interlock decreases and the diagonal cracking load at which failure takes place is reduced.

When the shear-span/depth ratio of a beam is lower than a certain critical value, the diagonal crack is stabilized and arching develops over the entire span. At this stage the resultant compressive force can be transferred directly to the supports through the external arch. As the a/d ratio decreases, the capacity of the section increases with an increase of the intact area of concrete above the diagonal crack. Most of the web of the beam is in diagonal compression

in such cases. The external loads and the compressive forces can be transferred to the supports without damaging the web of the beam. It is, therefore, reasonable to assume that the capacity of the beam in shear-compression failures will improve with decreasing shear-span/depth ratios.

3.3.5. The Percentage of Longitudinal Reinforcement and its Bond Characteristics

An increase in longitudinal reinforcement reduces crack widths for a given loading and therefore results in an improvement in the critical diagonal cracking load. Furthermore, with a higher percentage of longitudinal reinforcement, the profile of the critical diagonal crack is likely to follow a lower trajectory. In other words, the diagonal crack will be located lower in the web of the beam than it would be with less longitudinal reinforcement. In beams where the diagonal crack is stabilized and arching develops over the entire span, the strength of the arch would be increased due to an increase in the area of concrete intact above the diagonal crack.

With an increase in the percentage of longitudinal reinforcement, the flexural capacity of the section increases. This increase is more than the corresponding increase in the diagonal cracking load. It is to be expected, therefore, that an increase in the percentage of longitudinal reinforcement will increase the

range of shear-span/depth ratios where diagonal tension failures can take place.

The bond characteristics of the longitudinal reinforcement are also an important factor in the mechanism of failure, as well as its strength. As the bond performance of the reinforcement improves, the spacing of cracks is reduced, as is their width. This in turn will increase the diagonal cracking load. However, in beams where the critical diagonal crack is stabilized, there will be a smaller cross-sectional area of concrete intact above the diagonal crack and the capacity of the external arch will be lower. With smooth polished bars, the tension force in the reinforcement will remain constant throughout its length and a true tied arch can develop when the diagonal crack becomes stabilized.

3.4. THE ROLE OF WEB REINFORCEMENT

Although admittedly beyond the scope of this thesis, a few remarks about the role of web reinforcement are in order here. The role of web reinforcement may be visualized from the conceptual model of diagonal failure described in section 3.2.

The whole problem of diagonal failure is basically a question of transferring the resultant of the external shear force and the horizontal compression force to the supports. The internal arches support the compression zone of the beam and each arch carries a portion of the compression force. However, as cracking proceeds

along the line of the compressive stress trajectories, the support forces for these arches cannot be fully mobilized. As a result, the capacity of such arches is reduced, causing premature failure. Thus, the function of the web reinforcement can be visualized as providing supports to the internal arches and as carrying these support forces to the external support.

When the a/d ratio of a beam is small, (that is when the beam is "deep") the resultant of shear and compression forces can be transferred directly to the supports from its location in the external arch. As the a/d ratio increases, the shear force that can be applied to the beam decreases, so that the resultant of shear and compressive forces also decreases. This resultant does not flow directly to the external support but some part of it is carried by each internal arch. Thus if the web reinforcement is added in such a way as to transfer the resultant forces within each arch to a point in the external arch from which point the concrete alone can transfer it to the external support, the shear capacity of the beam can be raised to that for very short beams. Figure 3.14 shows how bent up bars and stirrups can transfer the resultant forces into the external arch and to a point from which they can flow to the support. It can be seen that the bent up bars are to be expected to be more effective than vertical stirrups, since they carry the support forces directly to a region of the external arch

where the concrete alone can transfer them to the support. Stirrups perform this function in a series of steps.

The internal arches close to the midspan region carry no part of the resultant force, hence no web reinforcement is needed in this zone. Thus the effective zone of web reinforcement is only l_e , as shown in Figure 3.14. Close to external supports and near the midspan region, no reduction of strength exists due to arch behavior and concrete alone can develop the full capacity.

In the analogy of the concrete cantilevers, the total bond force on the cantilever is resisted as a tension force in the web reinforcement as well as by the cantilever bending action. There is also an inclined compression force in the concrete cantilever. The force system is thus similar to that in the familiar "truss analogy" with the difference that only part of the bond force is carried by the web reinforcement. The inclined compression forces in the concrete cantilevers suppress the flexural tensile stresses in the concrete and delay the cracks associated with high aggregate interlock stresses. Furthermore, dowel action of the reinforcement is enhanced by the web reinforcement due to a reduction of the splitting at the level of the dowels.

The opening of cracks at later stages of loading, which is responsible for failure, is suppressed by the web reinforcement and a measure of continuity across the cracks is provided. Transverse displacements due to internal rotations and bending of the concrete cantilevers stress the web reinforcement, the distribution of this

stress clearly depending upon the relative position of the web reinforcement and the cracks.

The addition of web reinforcement in a beam enhances the capacity of the concrete cantilevers. The failure of these cantilevers leading to critical diagonal cracking is delayed. After development of such cracking, complete arching may develop in a manner similar to that described for beams without web reinforcement.

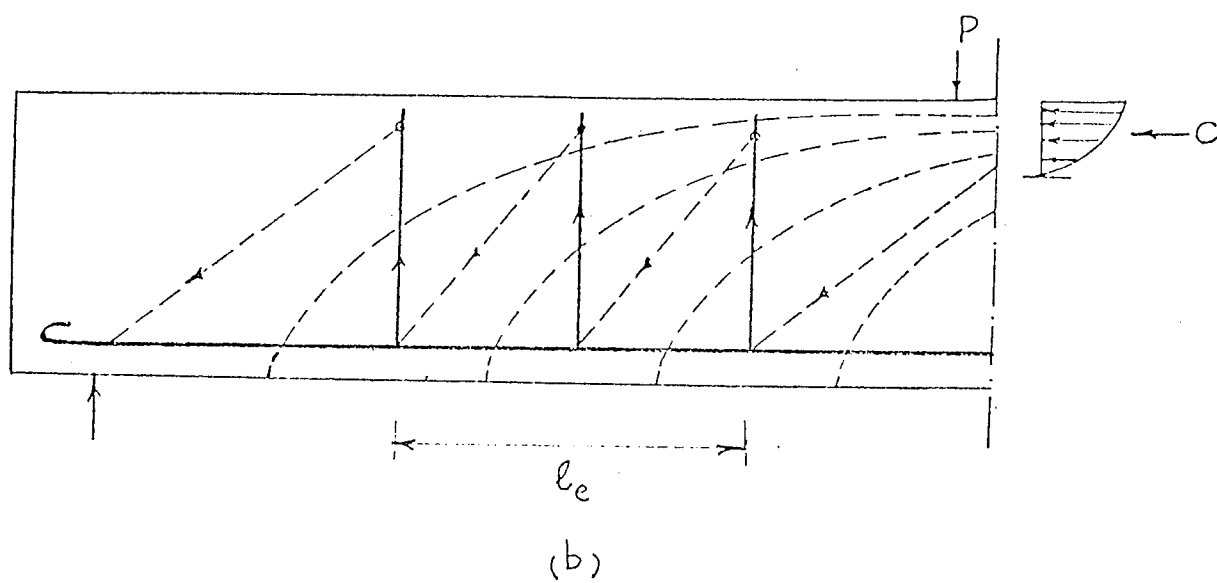
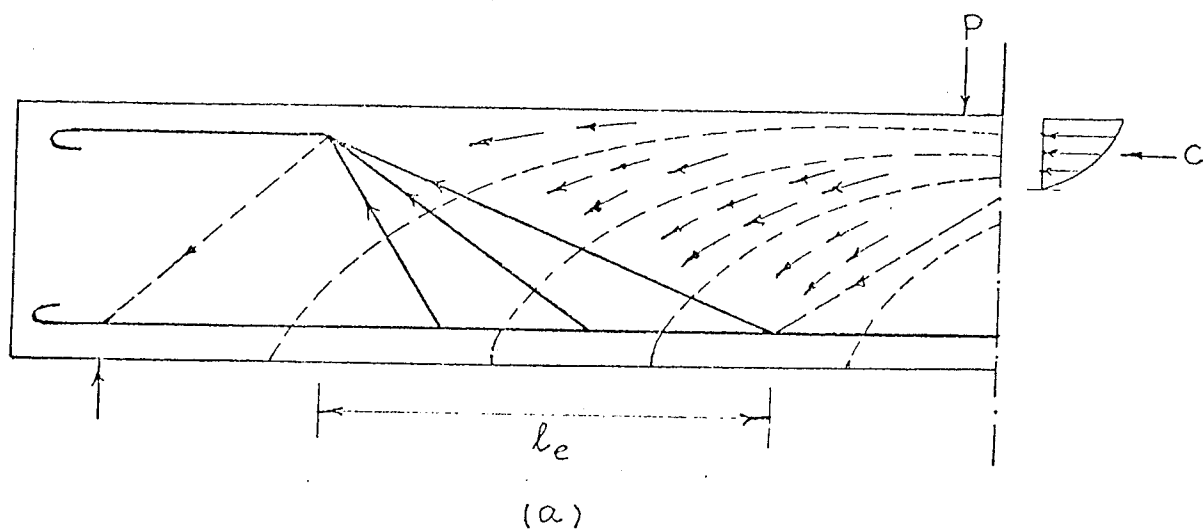


FIG. 3.14 FUNCTION OF WEB REINFORCEMENT

C H A P T E R F O U R

TEST PROGRAMME

4.1. GENERAL

This chapter describes the development of the test programme which consisted of a preliminary, followed by a more detailed, series of experiments.

Details of experimental work and the instrumentation employed are given in Appendix I.

4.2. PRELIMINARY SERIES OF TESTS

Two beams with a/d ratios of 2.5 and 3 and a longitudinal reinforcement of 1.41% were cast and tested with two point loads. The nominal compressive strength of concrete was 4,000 psi. These beams were instrumented with electrical resistance strain gauges both on the reinforcement and on the surface of concrete. Gauges on steel were applied on both sides of the reinforcing bar; for two reasons: to check on the accuracy of the readings, and to obtain at least one reading at a section if one of the two gauges at a section was broken while the cracks propagated.

Further, a portion of concrete in the compression zone of the beam in the shear span close to the load point was covered

with photoelastic coatings. These coatings are primarily meant for homogeneous, isotropic materials within the elastic range of stresses. However, it was considered that even a very approximate indication of the flow of internal stresses within the beam at various stages of loading prior to failure can be of significant importance. Considerable data was obtained for both beams for isoclinic and isochromatic fringe patterns both for normal and oblique incidence. Difficulties in both the recording of meaningful photoelastic data and in its interpretation as well as poor quality pictures resulted in discontinuing its use in the remaining test programme.

Considerable time was also spent on studying the suitability of various electrical resistance strain gauges for application on concrete and steel. Various aspects regarding their size, water-proofing, zero drift, etc. were looked into in detail for standardizing procedures for the remaining test series.

The beam with a/d ratio of 3.0 was retested on a shorter span ($a/d = 1.5$), using the cracked portion as an overhang. Thus a total of three tests was conducted in the preliminary series of tests.

4.3. INFERENCES DRAWN FROM PRELIMINARY TESTS

During the testing of the first three beams, it was seen

that as soon as a crack passed through the electrical resistance strain gauge, the gauge was broken and was lost for subsequent stages of loading. It was decided to use demountable mechanical (DEMEC) strain gauges in addition to the electrical resistance strain gauges. As cracking proceeds and crosses a set of DEMEC gauges, useful information can be obtained on the crack widths and shear displacements. Further, the two independent sets of strain gauges - DEMEC and electrical resistance - could be used to ascertain the changes in distributions of strains at various locations in the shear span. Plots of strain gauge data of the preliminary set of beams had shown that with the development of flexural cracking, compressive longitudinal flexural strains developed in the lower half of the beam at certain locations. Such strains were clearly not in line with the normal bending process associated with increased loading. It was considered that use of DEMEC and electrical resistance strain gauges in two halves of the beam would be useful in determining the accuracy of such strain distributions. Further, horizontal and inclined DEMEC gauge lines were also established for determining the bending of the concrete cantilevers, internal rotations of the compression zone and arching in the shear span of the beam. Details of instrumentation are given in Appendix I and instrumentation for each beam is given in Appendix II along with test results of the beams. Strain gauge data has been compiled into a separate report*. The data obtained from the tests of beams is summarized graphically in Appendix III.

*See p. 91 , Chapter 5.

4.4. MAIN TEST PROGRAMME

The primary variables selected for study were the shear span-depth ratio (or M/Vd in case of uniform loads) and the percentage of longitudinal reinforcement. Nominal compressive strength of concrete was 5,000 psi and the nominal yield strength of the reinforcement was 50,000 psi.

A total of 22 beams, including those of the preliminary series, was tested. Three different percentages of reinforcement, 1.87%, 1.41% and 1.03% were used in combination with a/d ratios varying from 1 to 6. The secondary variables selected for investigation consisted of load applied through the secondary beams and uniform loading. All beams were rectangular, 8 in. x 18 in. in cross-section, span length varying with a/d or l/d ratio. An overhang of 18 inches was used at either support. The overall length of the beams varied from 8 feet 8 inches to 22 feet.

The beams were divided into series A, B or C depending upon the percentage of reinforcement. Further, the series were divided into I, II or III depending upon whether the load was applied as concentrated loads over the compression face of the beam, through the secondary beams or uniformly distributed over the compression face of the beam.

Details of the series are as follows:

- (1) Series IA (8 beams) $p = 1.87\%$

This series comprised beams IA-1 to IA-8, with a/d ratios of 1, 1.5, 2, 2.5, 3, 4, 5 and 6 respectively.

(2) Series IB (4 beams, including 3 of the preliminary series)

$$p = 1.41\%$$

This series comprised beams IB-2, IB-4, IB-5 and IB-6 with a/d ratios of 1.5, 2.5, 3 and 4, respectively.

(3) Series IC (3 beams) $p = 1.03\%$

This series comprised beams IC-2, IC-5 and IC-6, with a/d ratios of 1.5, 3 and 4, respectively.

The loading in series I (A, B and C) consisted of two point loads, 3 feet apart, applied directly over the compression face of the beam.

(4) Series IIA (4 beams) $p = 1.87\%$

This series comprised beams IIA-2, IIA-2(b), IIA-4 and IIA-6, with a/d ratios of 1.5, 1.5, 2.5 and 4.0, respectively.

The load was applied as concentrated loads through secondary beams framing into the main beam. Originally only three beams were planned. Beam IIA-2(b) was only added after premature failure of beam IIA-2 occurred at the junction of the secondary beam to the main beam. Top reinforcing bars were added in the secondary beams framing into beam IIA-2(b) to avoid premature shearing at the junction of the main and secondary beams.

(5) Series IIIA (3 beams) $p = 1.87\%$

This series comprised beams IIIA-3, IIIA-6 and IIIA-8, having l/d ratios of 6.25, 10.25 and 14.25 respectively.

Uniform loading over the beam was simulated by 8 equally spaced loads directly applied over the compression face of the beam.

Beam numbers in any series signify the same a/d ratio except for series IIIA where they show the same overall length. For example, beams IA-2, IB-2, IC-2 and IIA-2 all have a/d ratios of 1.5.

The series of beams indicated above were so chosen as to demonstrate the various stages of development of the failure pattern of reinforced concrete beams where shear loading was significant. The range of series was chosen to demonstrate similarities and differences between the failure mechanisms of beams of different percentages of longitudinal reinforcement, manner of load application and type of loading. Since the primary objective of the experimental work was to demonstrate the mechanisms of diagonal resistance, the beams were extensively instrumented as described in Appendix I, in order to determine the internal force system at various stages of loading prior to failure. It was the function of these observations to indicate, in a quasi-quantitative manner, the reliability of the model of failure proposed in Chapter 3, when applied to beams having the wide range of characteristics and loadings discussed above.

CHAPTER FIVE

EXPERIMENTAL RESULTS

5.1 GENERAL

Extensive test results on the internal force distribution at various stages of loading prior to collapse were obtained from the tests of the beams described in Chapter 4. For the sake of discussion of the internal stress distribution, one beam has been selected as typical. The results of this beam, IIIA-3, are described in this chapter. Results obtained from each individual beam are summarized graphically in Appendix III.

Some of the experimental results are tabulated in Appendix II. However, due to the large volume of strain gauge data, the results of DEMEC rosettes, electrical resistance strain gauges, horizontal gauge line readings, horizontal displacements and inclined gauge line readings have been compiled into a separate report*.

The primary objective of the tests, the results of which are presented in this chapter, was to verify the various aspects of diagonal failures of beams developed in Chapter 3. Beam IIIA-3 was selected as typical as it failed in shear compression. The internal force system in this beam could therefore be studied both before the appearance of the critical diagonal crack and after it

* SHAH, A.A., "Strain Gauge Data - Some Aspects of the Diagonal Failure of Reinforced Concrete Beams," Report No. CE-3/73, Department of Civil Engineering, University of Manitoba, June 1973, pp.158

was stabilized. Besides, only a few gauge lines were affected by cracks in this beam and a rather complete set of strain gauge data was obtained. However, since all aspects of the diagonal failures could not be verified from the results of one typical beam, supplementary remarks are included, stemming from the results of other beams, details of which are given in Appendix III.

From the distribution of longitudinal flexural strains in the concrete and in the reinforcement, it is shown that with the onset of flexural cracking, longitudinal compressive strains develop in the "tension zone" of the beam in the vicinity of the cracked sections. As flexural cracking proceeds outwards, from the centre of the beam, these compressive strains also develop progressively outwards. However, such compressive strains develop in the region of the beam closer to the supports and directly over the supports only after the appearance of a critical diagonal crack and its stabilization. These observations are consistent with the progressive development of internal arching described in Chapter 3.

From the results of the distribution of longitudinal flexural strains in the reinforcement, it is shown that bond forces were reduced within the region where longitudinal compressive strains developed in the "tension zone" of the beam. The tension force in the reinforcement over the supports remained negligible until critical diagonal cracking took place. At this stage, the tension

force in the reinforcement directly over the supports increased significantly if the diagonal crack became stable. During subsequent stages, the bond forces continued to decline in magnitude and in some cases disappeared totally near collapse.

In many cases, high tensile strains were recorded at the compression face of the beam above the diagonal crack as it propagated into the compression zone of the beam. In relatively slender beams which failed suddenly at the appearance of a diagonal crack, failure was generally accompanied by a tension crack from the compression face of the beam downwards. This also was consistent with the presence of high tensile stresses above diagonal cracks and with the flexural-tensile failure described in Chapter 3.

The observations of the development of compressive strains in the lower half of the beam closer to the supports in beams of low a/d ratios after diagonal cracking are substantiated by the results of the distribution of concrete strains over inclined gauge lines. The results indicate that after critical diagonal cracking, the compressive force became inclined at a considerable angle between the load point and the supports. These observations are also consistent with the development of complete arching after diagonal cracking.

Horizontal displacements at the reinforcement level have been plotted from the horizontal gauge line readings to show the effect of bond forces and internal rotations. After diagonal cracking, the horizontal displacements increased considerably.

From the calculations of crack widths at various load levels, it is shown that the diagonal cracks opened up significantly after diagonal cracking, due to internal rotations in the compression zone. The width of diagonal cracks at the reinforcement level increased many times from their initial value at first diagonal cracking. This permitted translational displacements to occur at the cracked sections resulting in a progressive reduction of the bond forces. In some cases the tension force in the reinforcement was almost constant along its length at conditions nearing collapse. Such observations further support the development of complete arching after the stabilization of the diagonal crack. Longitudinal flexural strains in such cases showed a shift of the neutral axis upwards at midspan sections. Calculations of internal rotations from diagonal crack widths showed that internal rotations increased considerably after the appearance of diagonal cracks. At the same time longitudinal compressive strains increased considerably on the compression face of the beam under the load point, resulting in a shift of the resultant compression force upwards. These observations are consistent with the simultaneous presence of beam and arch action.

Results of the various beam tests showed that beam and arch behaviour were both present in the shear span of all beams regardless of the shear-span depth ratio, the percentage of reinforcement or the manner and the type of loading. The test results were then analyzed to determine the influence of these variables on the type of diagonal failure and on the ultimate capacity of the beams.

For concentrated loads, diagonal tension failures took place for a/d ratios of 2.5 and above until an a/d ratio was reached that was high enough to permit the flexural capacity of the section to be attained. For a/d ratios between 1.0 and 2.5, the failure was of the shear compression type. The point of minimum beam strength (expressed as a ratio of actual bending strength to full flexural strength) was observed to be at an a/d ratio of 2.5, regardless of the percentage of longitudinal reinforcement. With an increase in the longitudinal reinforcement, the range of diagonal tension failures increased, as would be expected.

It was found that the diagonal tension strength of beams uniformly loaded was higher than those loaded through concentrated loads. Loading through secondary beams did not reduce the diagonal cracking load but reduced the ultimate strength of beams failing in shear compression.

The above observations are fully in agreement with the conceptual model of diagonal failure described in Chapter 3.

5.2 DISTRIBUTION OF LONGITUDINAL FLEXURAL STRAINS IN CONCRETE

The test results for beam IIIA-3 are summarized in Figures 5.1(a) and (b). Details of the propagation of cracks and the locations of various sections and gauge points are shown on Figure 20, Appendix II.

Only a limited number of loading stages are plotted in

Figure 5.1(b). However, electrical resistance strain gauge readings for this beam were taken at 2,500 pound intervals. Details for intermediate readings are provided during the discussion wherever necessary. Strain readings have been plotted at each vertical section at 0, 4, 8 and 12 inch depths. In Figure 5.1(b), strain readings at 16 inch depth are the average strains in the reinforcement. Wherever a reading was not available at an intermediate point, the strains at two points have been joined by a dotted line. Also, when a reading was affected by a crack passing under the electrical resistance strain gauges or through the DEMEC measuring points, it has been joined by a broken chain line, signifying the presence of cracking.

5.2.1. DEMEC Data (Figure 5.1a)

The first flexural cracks appeared at a load of 20 kips and the first DEMEC readings were taken at a load of 30 kips. At this stage, compressive strains had already developed at $e'(12)^*$. Observations of crack pattern for this beam (Figure 20, Appendix II), show that the middle portion of the beam upto and including section e' had shown some flexural cracking at a load of 30 kips. All other gauges at the 12-inch level at sections a' , b' , c' and d' showed tensile strains at a load of 30 kips. At the compression face,

* Letter signifies a particular vertical section while the figures within the parenthesis represent the depth of the beam where the gauge point is located (Figure I.6, Appendix I)

compressive strains existed at all sections except directly over the support where the strain remained zero.

The second set of DEMEC readings was taken at a load of 50 kips. At this stage, flexural cracking had extended to section c'. However, a flexural crack had crossed gauge c'(12) and therefore the reading of this gauge was affected by the crack. The gauges at the 12-inch level at sections e' and d' both showed compressive strains while those at a' and b' continued showing tensile strains. It was further observed that the compressive strain at the compression face generally increased with load except at sections close to the support. Tensile strains developed directly over the support on the compression face.

A critical diagonal crack appeared at a load of 60 kips and became stable 4 1/2 inches below the compression face of the beam. At a load of 70 kips, another major diagonal crack developed in the other end of the beam while the previous crack extended to within 2 inches of the compression face of the beam. DEMEC readings were taken at a load of 75 kips. It was observed that there was a very sharp increase of the compressive strain at the compression face at section e'. While the compressive strain at sections d' and c' either remained constant or decreased, strains on the compression face directly over the support remained tensile. Further, in the lower half of the beam, at the 12-inch level, compressive strains were recorded at all sections from the supports towards the mid-section. It can be seen that the centre of compressive force

at section e' shifted upwards while it shifted progressively downward at sections d', c', b' and a', towards the support. If the locations of the resultant compressive forces at the various sections are joined, the profile of an arch is obtained.

The beam continued taking further load as the critical diagonal cracks widened. Another DEMEC reading was taken at a load of 90 kips. At this stage, compressive strains at sections c' and d' at the compression face diminished significantly while maximum compressive strains appeared at a depth of about 4 inches. The trend at the 12-inch level was exactly the same as it had been at the previous set of readings. Large compressive strains at the compression face at section e', close to the tip of the diagonal crack, show a shift of the resultant compressive force upwards and significant internal rotations within the compression zone after diagonal cracking.

5.2.2. Electrical Resistance Strain Gauge Data (Figure 5.1b)

Examination of the data from the gauges located at the 12-inch level showed that tensile strains developed initially at all sections. Gauges e(12), d(12), b(12) and a(12) recorded maximum tensile strains at 17.5, 32.5, 57.5 and 57.5 kips respectively. However, after recording a maximum value, these strains dropped consistently, ultimately becoming compressive at 27.5, 40, 65 and 72.5 kips, respectively, for the above gauges. Cracking interfered with strain readings at c(12). This gauge showed high tensile

strains before it finally broke at a load of 60 kips. Evidently the large tensile strains, before the gauge broke, do not represent the actual strain distribution at this location but rather are more an indication of the crack width. Similarly, gauge f(12) at midspan broke early as a flexural crack crossed the gauge.

From the above can be seen the progressive development of compressive strains in the lower half of the beam after flexural cracking, starting at the midspan and developing towards the supports. These results are quite consistent with data from the DEMEC end of the beam.

An examination of the strain distribution at the compression face shows that after the appearance of the critical diagonal crack, tensile strains developed at section c. As the load was further increased, tensile strains developed at section d as well. This indicated the presence of high flexural-tensile stress above the diagonal crack.

At sections e and f, the compressive strains at the compression face continued increasing with increasing load. After critical diagonal cracking, the location of the neutral axis at these sections shifted upwards as did the resultant compressive force.

5.2.3. Results of Other Beams

As already indicated, detailed results of individual beam tests are presented in Appendix III. It was observed that in beams

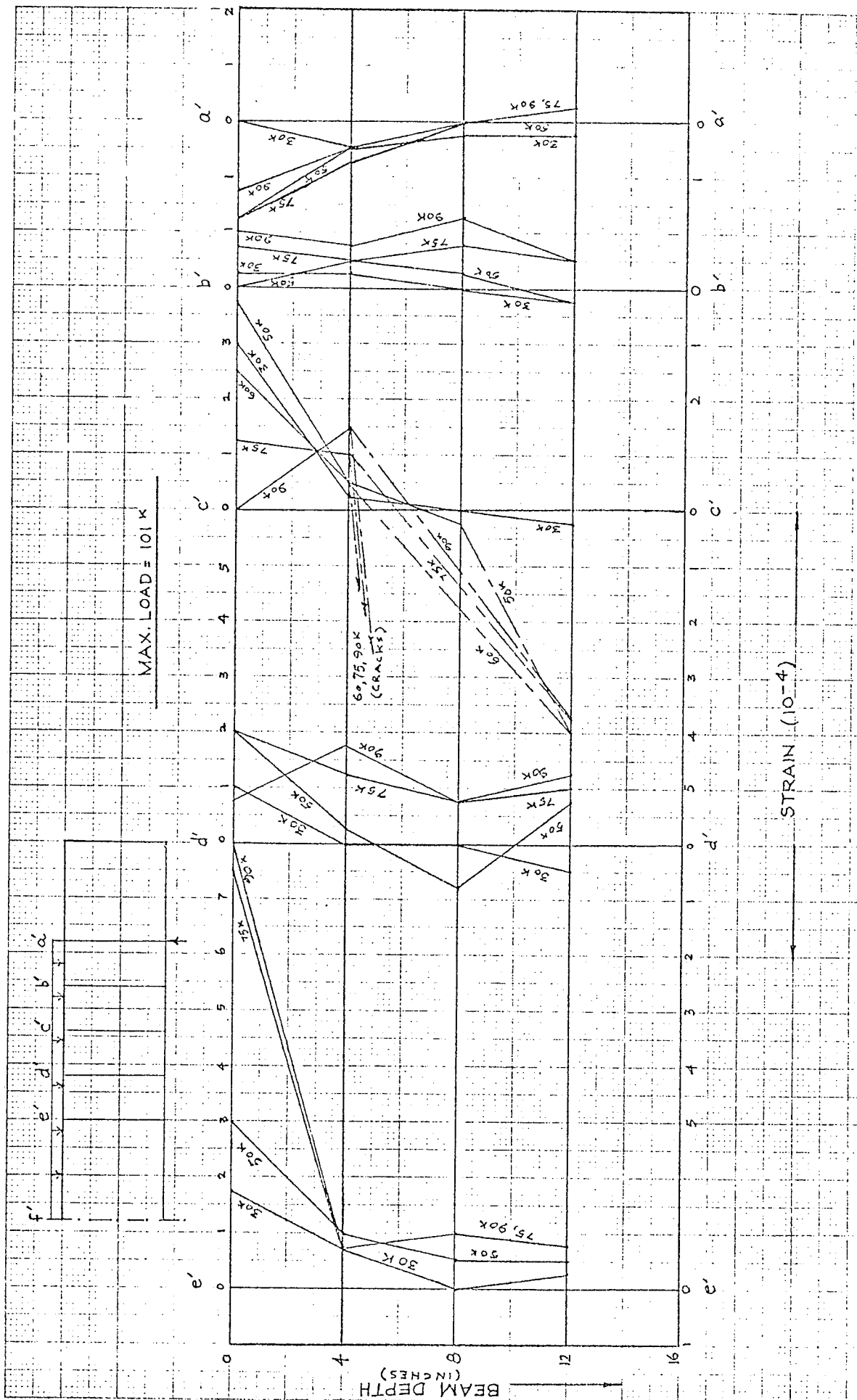


FIG. 5.1(a) LONGITUDINAL STRAIN — DEMEC DATA

BEAM III A-3

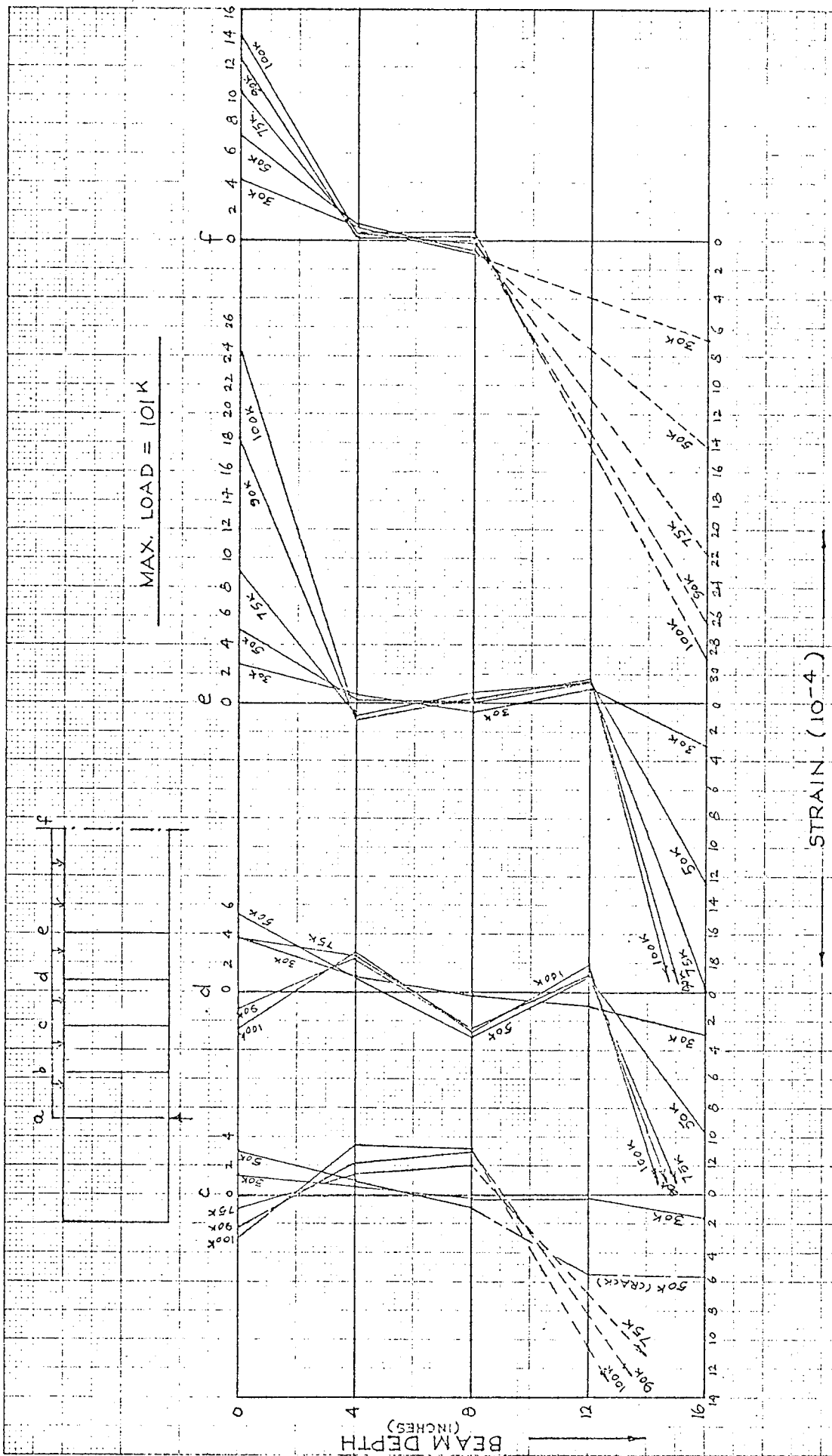


FIG. 5.1 (b) LONGITUDINAL STRAIN — Electrical Resistance Strain Gauge Data

BEAM III A - 3

that failed at the first appearance of a critical diagonal crack, the initial tensile strains at the 12 inch level changed into compressive strains in the region of the beam from the centre line to the midshear span. However, strains in the lower half near the supports of the beam remained tensile up to failure. Furthermore, maximum compressive strains were recorded at the compression face and the compressive force was not lowered up to failure. These results suggest that internal arching remained incomplete in such cases and failure was governed by the strength of the concrete cantilevers. A good example of such behaviour, that of beam IC-5, is shown on Figures III.14(a) and (b) in Appendix III.

5.3 DISTRIBUTION OF LONGITUDINAL FLEXURAL STRAIN IN THE REINFORCEMENT

The distribution of the longitudinal flexural strain in the reinforcement for beam IIIA-3 is shown in Figure 5.2. The nominal yield stress of the reinforcement was 50 kips per square inch, which gives a strain in the reinforcement of 16.67×10^{-4} at yielding, assuming a modulus of elasticity of 30×10^6 pounds per square inch. When the stress in the reinforcement is below the yield stress, the tension force in the reinforcement can be obtained from the strain reading and from the proportionality of stress and strain. However, when the strain exceeds that at yielding of the reinforcement, any increase in tension force results from strain hardening of the reinforcement, and the force must be obtained from

the stress-strain characteristics of the steel.

The bond force transferred to the reinforcement is the difference of the tension force in the reinforcement at opposite sides of the concrete cantilevers. Since the longitudinal flexural strain in the reinforcement is proportional to the tension force in the reinforcement, the distribution of this strain is a measure of the distribution of the tension force in the reinforcement. However, when a portion of the reinforcement has yielded, even relatively large differences in strain amount to only a small difference in the tension force in the reinforcement. The longitudinal strain distribution can thus be used for determining the bond forces in the reinforcement.

The longitudinal strain in the reinforcement in beam IIIA-3 varied according to the variation of the bending moment diagram at earlier stages of loading. Strains in the reinforcement at the support remained negligible upto the time the critical diagonal cracking was observed at a load of 60 kips. However, as flexural cracking proceeded from the midspan region of the beam outwards, the sections within this range showed higher strains than those compatible with the bending moment variation.

A major change was observed in the distribution of longitudinal flexural strains in the reinforcement after diagonal cracking. Whereas the reinforcement had not yielded anywhere before diagonal cracking, a portion of the reinforcement in the midspan region yielded at critical diagonal cracking. Furthermore, Figure 5.2

shows that significant strains developed over the supports and sections close to the supports at a load of 75 kips. As the loading was increased further, the strains at sections close to the supports continued increasing at a faster rate than those in the midspan region. This beam failed at a load of 101 kips. Just prior to failure, the reinforcement in the entire span length was beginning to yield. At this stage the tension force in the reinforcement was virtually constant throughout the span length.

It can be observed that with the appearance of flexural cracking, the bond forces in the midspan region of the beam were generally smaller than in the outer regions of the beam. The possibility of a sudden diagonal failure was, therefore, greater at the outermost flexural crack where the bond forces were more than those in the inner portions of the beam. When the critical diagonal crack became stabilized, the bond forces were reduced considerably. However, they were not entirely eliminated and disappeared only near ultimate failure. In the previous section, it was observed that compressive concrete strains developed in the regions of flexural cracking in the lower half of the beam. Longitudinal strain diagrams in the reinforcement showed that bond forces were still in existence within this zone. However, as these bond forces were smaller in the inner regions of the beam, internal arching was accompanied by the action of the concrete cantilevers. In slender beams, when the capacity of these cantilevers was exceeded, failure took place at the appearance of a critical diagonal

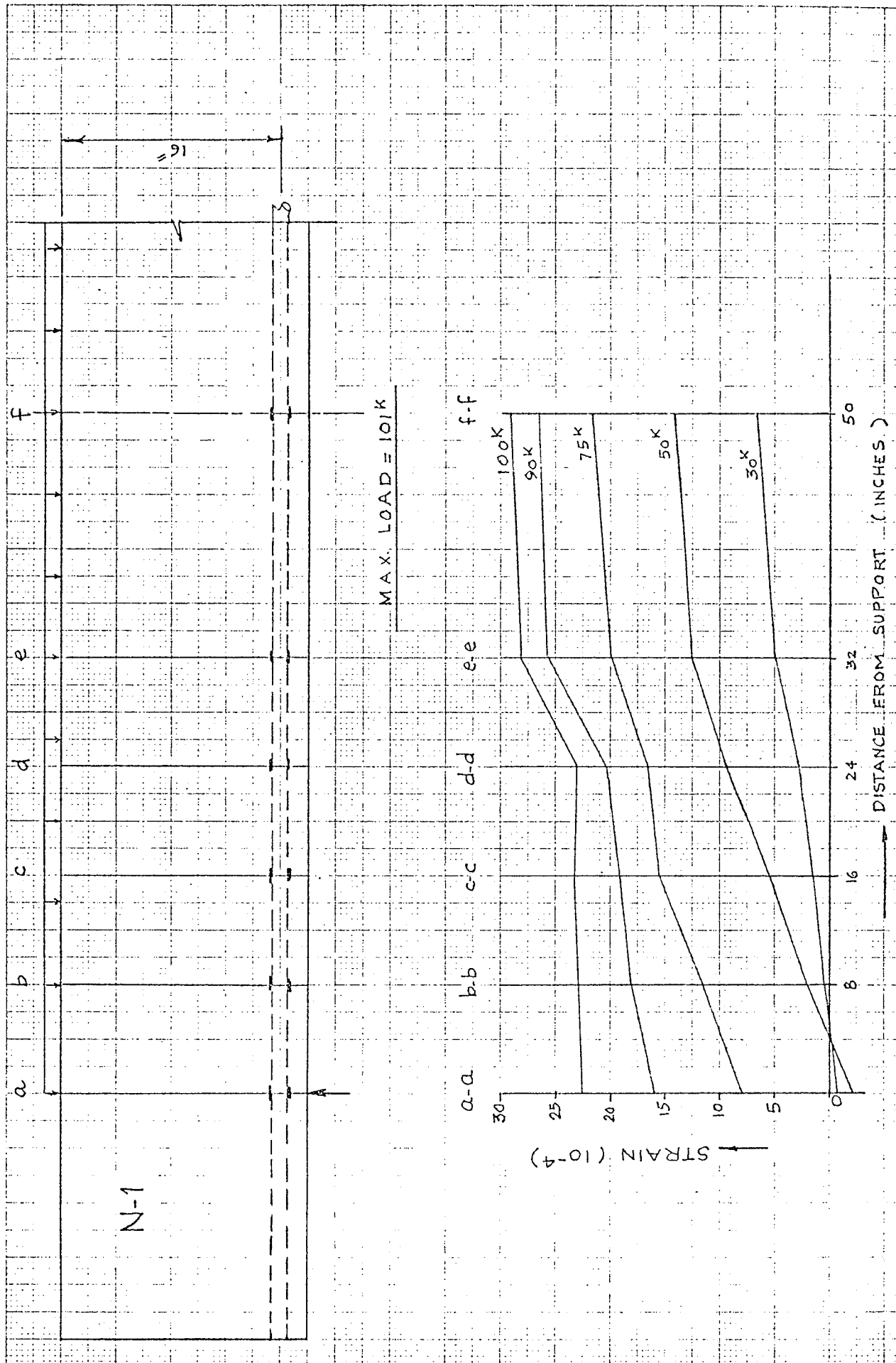


FIG.5.2 — BEAM III A-3: LONGITUDINAL STRAIN IN THE REINFORCEMENT

crack.

Values of longitudinal flexural strains in the reinforcement are plotted for individual beam tests in Appendix III. In these results, it is shown that in beams failing by diagonal tension at the appearance of a critical diagonal crack, the strains in the reinforcement at the supports remained negligible up to failure.

Failure generally took place at the outermost locations of the flexural cracks where the bond forces were a maximum. Beam IA-5 shown on Figure III.27 of Appendix III is a good example of this behaviour. On the other hand, in case of beams failing by shear-compression, the bond forces were reduced considerably after diagonal cracking.

5.4 DISTRIBUTION OF CONCRETE STRAINS OVER INCLINED GAUGE LINES

The distribution of concrete strains over inclined gauge lines along with the location of the gauge lines is shown for beam IIIA-3 in Figure 5.3. The Figure shows that before critical diagonal cracking at a load of 60 kips, the maximum compressive strains existed at the compression face. However, a significant redistribution of stresses occurred at critical diagonal cracking and subsequent stages prior to ultimate failure of the beam. Maximum compressive strains shifted downwards almost to the location where the original neutral axis was located. A comparison of the magnitudes of the compressions at c' on Figure 5.1(a) and Figure 5.3

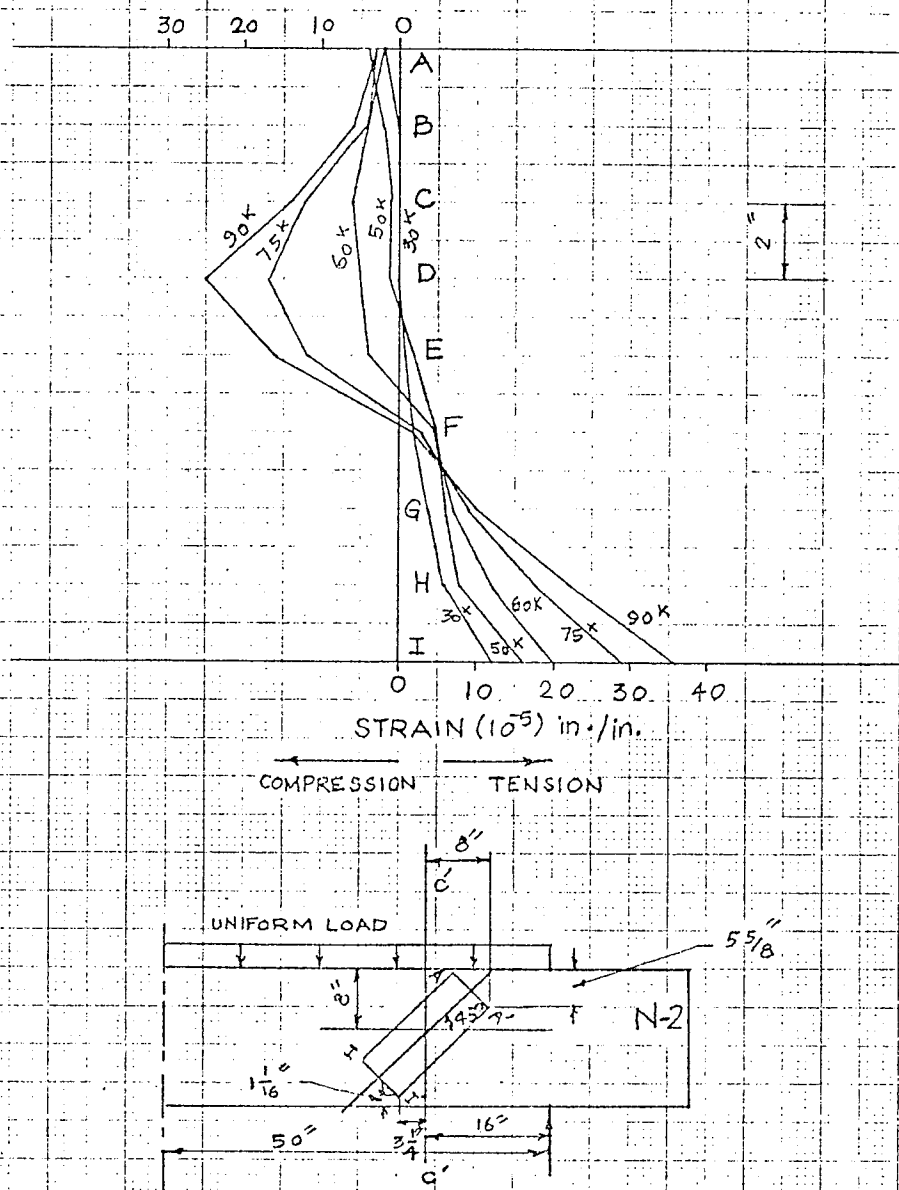


FIG. 5.3 — BEAM IIIA-3: CONCRETE STRAIN DISTRIBUTION
AT INCLINED GAUGE LINES

indicates that the compressive force became significantly inclined.

Diagrams representing the results of inclined gauge line readings are shown for individual beam tests in Appendix III.

5.5 DISPLACEMENTS RESULTING FROM BENDING OF CONCRETE CANTILEVERS AND ROTATION OF THE COMPRESSION ZONE

It has already been explained in Chapter 2 how displacements can occur due to the bending of concrete cantilevers and the rotations of the compressive zone. Horizontal displacements of the vertical sections were measured as follows.

Three horizontal gauge lines A, B and C at depths 2 in., 5 in., and 16 inches were run from the vertical axis of symmetry at midspan. The gauge points of each level were a continuous measuring line starting from the midspan, at 8 in. intervals. At various loading stages, strain readings were converted to length differences for 8 in. measuring intervals. The total horizontal displacements of a point is the sum of all measured length differences between this particular point and the midspan. If plane cross sections were to remain plane, the displacements of points at level C (reinforcement level) could be worked out from a line joining the displacements at levels A and B in the compression zone of the beam. The difference between the projected displacements of points at level C and those measured at this point, gives the total horizontal displacement of the points at the reinforcement level due to the bending of concrete

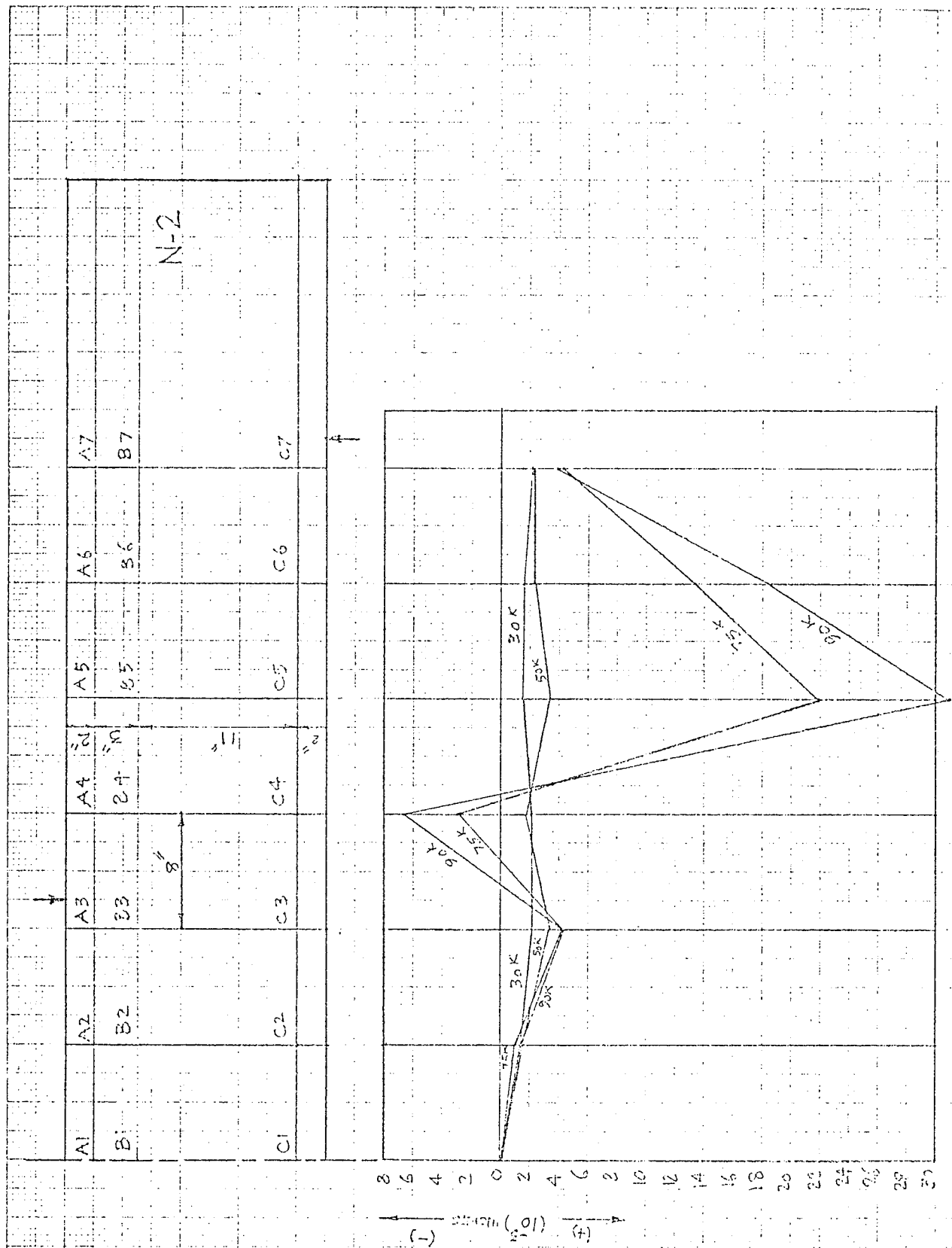


FIG. 5.4 — SERIES IIIA: Horizontal Displacement of Concrete Cantilevers

BEAM IIIA-3

cantilevers and the internal rotations.

Results of the horizontal displacement measurements of concrete cantilevers for beam IIIA-3 are shown on Figure 5.4. The maximum displacement at 50 kips was only 3.33×10^{-3} inches. However, after critical diagonal cracking at 60 kips, there was a significant increase of the horizontal displacement at the reinforcement level and a maximum value of 30.83×10^{-3} inches was recorded at 90 kips.

Values of horizontal displacement at the reinforcement level are shown graphically in Appendix III for individual beam tests. It was observed that for all beams failing at the appearance of a critical diagonal crack, the horizontal displacements were generally 3 to 4 times smaller than such displacements near collapse in beams failing by shear compression. Substantial increases in the displacements at the reinforcement level invariably occurred after critical diagonal cracking. Since the action of the bond forces is not so important at this stage, the results clearly point towards large internal rotations after the formation of a major diagonal crack.

5.6 CRACK WIDTHS AND INTERNAL ROTATIONS

Crack widths and internal rotations are calculated from equations 3.4 and 3.5 presented in Chapter 3. Electrical resistance strain gauge data is of no particular use in calculating crack widths as such a gauge breaks at a limiting tensile strain due to cracking.

Crack widths are calculated from results of DEMEC gauges. DEMEC gauge points were placed at fixed locations and so there was no control on the location of the gauge points relative to the cracks. It was, therefore, entirely coincidental if the inclined crack crossed the DEMEC rosettes. However, in quite a few cases, especially in beams failing by shear-compression, the cracks did cross the rosettes. Measurements were also taken on 8-inch inclined gauge lines and on 2-in. gauge lines, perpendicular to the 8-inch gauge lines. In some cases, the cracks crossed the inclined gauge lines perpendicular to the measuring line and the crack width could be calculated directly from the reading.

The location of the crack within a DEMEC rosette had to be noted carefully. Sometimes a crack crossed all the measuring lines within a rosette while at other times the crack crossed only one or two of the measuring lines. A careful observation of the angle at which the crack crossed the gauge points was required, and these angles were measured directly from the beams.

Significant opening of cracks was observed after stabilization of diagonal cracks. In such cases the strain due to cracking was much higher than the normal strain distribution. Crack widths and internal rotations were calculated from the total strain reading at each load level, assuming all deformation was due to the crack. However, the error associated in calculation of crack widths neglecting normal strains is small and since the relative magnitudes of crack widths and internal rotations were required, the calculations were

considered to be sufficiently accurate. Using this method, it was found that in shear-compression failures, the width of diagonal cracks at sections removed from the tip of the crack increased many times from their value at diagonal cracking.

Crack widths and rotations of the compression zone for two typical beams failing in shear compression are now discussed. Crack widths and internal rotations for individual beam tests are given in Appendix III.

5.6.1 Beam IA-1

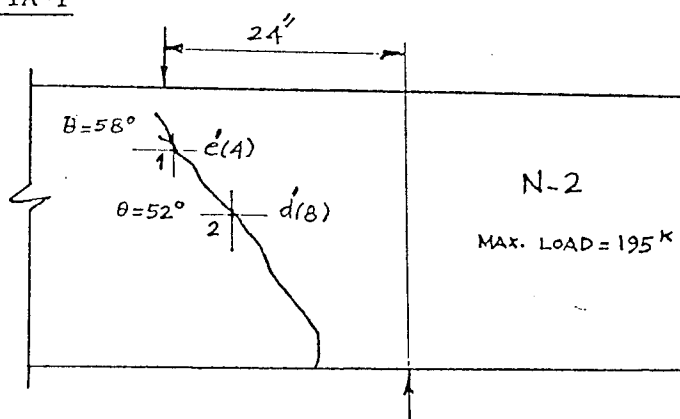


FIG. 5.5 DEMEC ROSETTES AND DIAGONAL CRACK: BEAM IA-1

Figure 5.5, shows the critical diagonal crack crossing two DEMEC rosettes at $e'(4)$ and $d'(8)$ respectively. These points are marked 1 and 2 and crack angles at these locations are also shown on the figure. Equations 3.4 are used to determine crack widths.

Point (I) $\theta = 58^\circ$

Load (Kips)	80	100	120	150	180
$\epsilon_h^* (10^{-3})$ in.	1.046	1.694	2.142	2.590	2.938
$\epsilon_v^* (10^{-3})$ in.	1.096	1.792	2.590	2.540	4.532
$\Delta^* (10^{-3})$ in.	1.516	2.468	3.360	3.630	5.400
θ_1^*	$14^\circ 30'$	$14^\circ 40'$	$18^\circ 20'$	$12^\circ 40'$	$25^\circ 10'$
$c_w^* (10^{-3})$ in.	1.465	2.390	3.190	3.540	4.880

*Figs. 3.11 and 3.12

Point 2 $\theta = 52^\circ$

Load (Kips)	50	80	100	120	150	180
$\epsilon_h (10^{-3})$ in.	2.440	5.674	7.320	8.764	9.612	12.300
$\epsilon_v (10^{-3})$ in.	2.192	6.674	9.362	12.350	17.330	22.410
$\Delta (10^{-3})$ in.	2.265	8.760	11.890	15.130	19.800	25.600
θ_1	$3^\circ 50'$	$11^\circ 40'$	$14^\circ 0'$	$16^\circ 30'$	$23^\circ 0'$	$23^\circ 20'$
$c_w (10^{-3})$ in.	3.26	8.58	11.50	14.50	18.22	23.50

The maximum crack width at point 2 was 23.50×10^{-3} in. at a load of 180 kips. At point 1, the width of crack remained small throughout and was only 4.88×10^{-3} in. at 180 kips. Point 1 was located quite close to the tip of the diagonal crack. If the centre of rotation is assumed to be near the tip of the crack, it is reasonable to find that the width of crack at points close to the centre of rotation remains small. The location of the centre of rotation can

be found at any load level by applying equations 3.5 to points 1 and 2. For example, the distance between points 1 and 2 along the line of the diagonal crack was found by measurement to be 5.66 inches. If ℓ_{01} represents the length from the centre of rotation to point 1, the following relations can be derived at a load of 80 kips.

$$\Delta = 1.516 \times 10^{-3} = \ell_{01} \theta_c \quad (\text{Point 1})$$

and

$$\Delta = 8.76 \times 10^{-3} = (\ell_{01} + 5.66) \theta_c, \quad (\text{Point 2})$$

Solving the above equations, $\ell_{01} = 1.19$ in. Using this value, $\theta_c = 1.28 \times 10^{-3}$ radians.

If ℓ_{01} values are calculated for other load levels, they remain similar, varying from 1.20 to 1.62 inches. However, exact ℓ_{01} values for each load may be used for finding the internal rotations. It is found that the internal rotations keep increasing with increasing loads and at 180 kips, $\theta_c = 3.56 \times 10^{-3}$ radians. Large compressive longitudinal strains were observed under the load point during these stages.

Readings of the inclined gauge lines between points FG* and E'F'* (where cracks cross these lines) also show a rapid increase in the width of the diagonal cracks after diagonal cracking.

* Appendix II shows photographs of beams and Appendix III shows plots of inclined gauge lines.

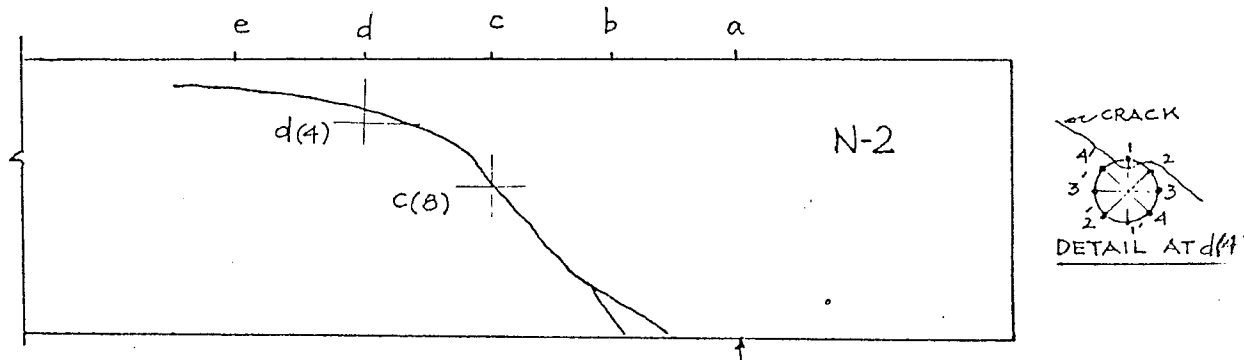
5.6.2. Beam IIIA-3

Fig. 5.6 DEMEC ROSETTES AND DIAGONAL CRACK: BEAM IIIA-3

Though the final failure occurred on end N1, a major diagonal crack existed on end N2, where DEMEC readings were taken. This crack crossed the DEMEC rosettes at c(8) and d(4). At d(4), this crack crossed the DEMEC rosette in a rather peculiar fashion (Figure 5.6). While the general slope of the crack profile at d(4) was around 20° , the crack bent horizontally to pass through the vertical gauge points of the rosette only. Since the crack was horizontal while passing the vertical gauge line, this reading was taken directly as the crack width. The width so calculated varied from 19.920×10^{-3} in. at 75 kips to 49.054×10^{-3} at 90 kips.

Following crack widths were recorded at c(8).

$$\theta = 55^\circ$$

Load (Kips)	60	75	90
$c_w (10^{-3})$ in.	4.33	25.00	55.00

If the centre of rotation is considered to be located at the tip of the diagonal crack, an internal rotation of 1.59×10^{-3} and 3.92×10^{-3} radians at a load of 75 and 90 kips respectively is obtained

from crack widths at d(4). Consideration of crack widths at c(8) at the same loads gives the rotations as 1.16×10^{-3} and 2.56×10^{-3} respectively at the same load levels. It seems that the crack width at d(4), which is only 12 1/2 inches from the tip of the crack, is not compatible with the centre of rotation located at the tip of the crack. If the two crack widths are to be compatible with each other, the centre of rotation should be located about 35 inches away from d(4), i.e. somewhere in the midspan region. If the centre of rotation is considered to be so located, the respective rotations at d(4) and c(8) at 90 kips are reduced to 1.4×10^{-3} radians. There is no doubt that significant rotations did develop, though there may be a question about the location of the centre of rotation or whether the width of crack at d(4) was abnormally high. Maximum width of diagonal crack on inclined gauge lines between D'E' was recorded as 61×10^{-3} inches.

5.6.3 Results of Other Tests*

It was found that diagonal cracks widened significantly in all beams eventually failing in shear compression. In some cases, the width of the diagonal cracks was nearly 0.07 inches at locations removed from their tips. On the other hand, the width of cracks in beams failing suddenly at the appearance of a diagonal crack remained small up to failure. The average width of cracks before failure was about 3.5×10^{-3} inches and in no case did the width exceed 6.2×10^{-3} inches. This shows the wide difference in the width of cracks for beams failing by diagonal

* See Appendix III.

tension and shear compression and clearly points out towards significant rotations of the compression zone after diagonal cracking. These results are consistent with the conceptual model of diagonal failure presented in Chapter 3.

5.7 INFLUENCE OF DIFFERENT VARIABLES ON BEAM STRENGTH AND THE MECHANISM OF FAILURE

A number of factors arising from the results of the beam tests are tabulated in Tables 5.1 to 5.6.

The ultimate moment, M_u , for each beam was calculated on the basis of the maximum loads. Flexural capacity of each beam was calculated using both the actual yield strength of the reinforcement (M_{f1}) and with the nominal value of 50 ksi used for the entire test series (\bar{M}_{f1}). Dimensionless indicators of comparative beam strength, M_u/M_{f1} and M_u/\bar{M}_{f1} are plotted as functions of a/d or the l/d ratio for each series and shown in Figures 5.7 and 5.8. For uniformly distributed loads, the ultimate moments are calculated both for the definition of shear span equal to one-fourth of the span length of the beam and for the actual critical cross-section of failure as observed in the tests. The comparative moment values obtained using the actual observed cross-section of failure are shown with dotted lines on the plots.

A problem arises in the interpretation of the dimensionless indicator of beam strength, M_u/M_{f1} , because it varies with any changes in the value of flexural moment. The flexural moment, M_{f1} , is calculated for the actual yield strength of the reinforcement of each beam. But when diagonal failure occurs before yielding of the reinforcement, M_u is almost totally unaffected by the yield strength of the reinforcement. Thus beams with different f_y values

TABLE 5.1
TEST RESULTS - SERIES IA

BEAM NO.	a/d	f'_c (test) (psi)	f'_t (test) (psi)	P_c Kips	P_u Kips	Type of Failure	$\frac{P_c}{P_u}$	$M_u = \frac{a \cdot P_u}{2}$ (K-in.)	f_y (ksi)	M_{fl} (K-in.)	\bar{M}_{fl} (K-in.)	$\frac{M_u}{M_{fl}}$ %	$\frac{M_u}{\bar{M}_{fl}}$ %
IA-1*	1.0	4992	511	60.00	*Load- ed to 195 Kips	----	---	-----	49.915	1705.0	1705.0	97.0*	97.0*
IA-2	1.5	4992	511	50.00	94.75	S.C.	0.528	1137.0	50.158	1713.0	1705.0	66.3	66.5
IA-3	2.0	4992	511	45.00	72.00	S.C.	0.625	1152.0	50.447	1725.0	1705.0	66.8	67.7
IA-4	2.5	4992	511	37.50	39.70	D.T.	0.945	794.0	50.034	1710.0	1705.0	46.5	46.5
IA-5	3.0	4375	415	37.50	37.50	D.T.	1.000	900.0	50.556	1730.0	1705.0	52.0	52.8
IA-6	4.0	5860	566	37.50	40.50	D.T.	0.925	1296.0	50.255	1719.0	1705.0	75.5	76.0

Table Continued

TABLE 5.1(Continued)

BEAM NO.	a/d	f'_c (test) (psi)	f'_t (test) (psi)	P_c Kips	P_u Kips	Type of Failure	$\frac{P_c}{P_u}$	$M_u = \frac{a \cdot P_u}{2}$ (K-in.)	f_y (ksi)	M_{fl} (K-in.)	\bar{M}_{fl} (K-in.)	$\frac{M_u}{M_{fl}}$ %	$\frac{M_u}{\bar{M}_{fl}}$ %
IA-7	5.0	5860	566	37.50	39.00	D.T.	0.962	1560.0	50.229	1718.0	1705.0	91.0	91.6
IA-8	6.0	5860	566	30.00	34.40	D.T.	0.926	1652.0	50.187	1716.0	1705.0	96.5	97.0

D.T. = Diagonal Tension; S.C. = Shear Compression; $p = 1.85\%$; $M_{fl} = f_y \cdot A_s \cdot d(1-0.4K)$;

$\bar{M}_{fl} = \bar{f}_y A_s d(1-0.4\bar{K})$.

$K = p f_y(\text{test})/0.75 f'_c(\text{test})$; $\bar{K} = p \cdot \bar{f}_y/0.75 f'_c(\text{nominal})$; $\bar{f}_y = 50$ ksi; f'_c (nominal) = 5 ksi;

* This beam was not loaded to failure and results used are one of Kani's similar tests. (KANI - 1966)

TABLE 5.2

TEST RESULTS - SERIES IB

BEAM NO.	a/d	f'_c (test) (psi)	f'_t (test) (psi)	P_c Kips	P_u Kips	Type of Failure	$\frac{P_c}{P_u}$	$M_u = \frac{a \cdot P_u}{2}$ (K-in.)	f_y (ksi)	M_{f1} (K-in.)	\bar{M}_{f1} (K-in.)	$\frac{M_u}{M_{f1}}$ %	$\frac{M_u}{\bar{M}_{f1}}$ %
IB-2	1.5	4198	493	42.5	122.5	S.C.	0.345	1470.0	74.967	1870.0	1268.0	78.6	100.0*
IB-4	2.5	4198	493	37.5	38.3	D.T.	0.935	766.0	74.967	1870.0	1268.0	41.0	60.5
IB-5	3.0	4198	493	35.0	37.5	D.T.	0.980	900.0	74.967	1870.0	1268.0	48.1	71.0
IB-6	4.0	4992	511	37.5	39.0	D.T.	0.962	1248.0	47.944	1243.0	1299.0	100.3	96.0

D.T. = Diagonal Tension; S.C. = Shear Compression; $p = 1.41\%$ $M_{f1} = f_y \cdot A_s d (1 - 0.4K)$ $\bar{M}_{f1} = \bar{f}_y \cdot A_s \cdot d (1 - 0.4K)$ $K = p \cdot f_y (\text{test}) / 0.75 f'_c (\text{test})$ $\bar{K} = p \cdot \bar{f}_y / 0.75 f'_c (\text{nominal})$ $f'_c (\text{nominal}) = 4 \text{ ksi for beams IB-2, IB-4 and IB-5; } 5 \text{ ksi for beam IB-6; } \bar{f}_y = 50 \text{ ksi}$

* Rectified

TABLE 5.3

TEST RESULTS - SERIES IC

BEAM NO.	a/d	$f'_c(\text{test})$ (psi)	$f'_t(\text{test})$ (psi)	P_c Kips	P_u Kips	Type of Failure	$\frac{P_c}{P_u}$	$M_u = \frac{a \cdot P_u}{2}$ (K-in.)	f_y (ksi)	M_{fl} (K-in.)	\bar{M}_{fl} (K-in.)	$\frac{M_u}{M_{fl}}$ %	$\frac{M_u}{\bar{M}_{fl}}$ %
IC-2	1.5	5357	525	50.0	87.7	S.C.	0.570	1052.4	49.091	965.5	981.0	109.0	107.4
IC-5	3.0	5357	525	36.0	40.2	D.T.	0.897	964.8	48.902	964.0	981.0	100.1	98.3
IC-6	4.0	5357	525	31.4	31.4	F.	1.000	1004.8	48.864	963.0	981.0	104.4	102.5

D.T. = Diagonal Tension; S.C. = Shear Compression; $p = 1.03\%$;

$M_{fl} = f_y A_s d(1-0.4K)$; $\bar{M}_{fl} = \bar{f}_y A_s d(1-0.4\bar{K})$; $K = p f_y(\text{test})/0.75 f'_c(\text{test})$;

$\bar{K} = p \bar{f}_y/0.75 f'_c(\text{nominal})$; $f'_c(\text{nominal}) = 5 \text{ ksi}$; $\bar{f}_y = 50 \text{ ksi}$

TABLE 5.4
TEST RESULTS - SERIES II A
 (SECONDARY BEAM LOADING)

BEAM NO.	a/d	f'_c (test) (psi)	f'_t (test) (psi)	P_c Kips	P_u Kips	Type of Failure	$\frac{P_c}{P_u}$	$M_u = \frac{a \cdot P_u}{2}$ (K-in.)	f_y (ksi)	M_{f1} (K-in.)	\bar{M}_{f1} (K-in.)	$\frac{M_u}{M_{f1}}$ %	$\frac{M_u}{\bar{M}_{f1}}$ %
IIA-2	1.5	5152	547.0	50.0	55.0	Cross beam sheared off	0.910	660.0	52.212	1780.0	1705.0	37.05	38.70
IIA-2(b)	1.5	7334	741.5	60.0	81.0	S.C.	0.740	972.0	51.825	1828.0	1705.0	53.20	57.00
IIA-4	2.5	5152	547.0	37.5	39.6	D.T.	0.947	792.0	52.076	1775.0	1705.0	44.55	46.50
IIA-6	4.0	5152	547.0	37.5	37.5	D.T.	1.000	1200.0	51.711	1761.0	1705.0	68.00	70.40

D.T. = Diagonal Tension; S.C. = Shear Compression; $p = 1.85\%$

$M_{f1} = f_y A_s d(1-0.4K)$; $\bar{M}_{f1} = \bar{f}_y A_s d(1-0.4\bar{K})$; $K = pf_y(\text{test})/0.75 f'_c(\text{test})$; $\bar{K} = p\bar{f}_y/f'_c(\text{nominal})$;
 $f'_c(\text{nominal}) = 5 \text{ ksi}$; $\bar{f}_y = 50 \text{ ksi}$.

TABLE 5.5
TEST RESULTS - SERIES III A (using a=1/4)
 (UNIFORM LOAD)

BEAM NO.	[*] a/d	f' _c (test) (psi)	f' _t (test) (psi)	P _c Kips	P _u Kips	Type of Failure	$\frac{P_c}{P_u}$	[*] $M_u = \frac{a \cdot P_u}{2}$ (K-in.)	f _y (ksi)	M _{f1} (K-in.)	\bar{M}_{f1} (K-in.)	$\frac{M_u}{M_{f1}}$ %	$\frac{M_u}{\bar{M}_{f1}}$ %
IIIA-3	1.56	5820	546	60.0	101.0	S.C.	0.585	1262.0	51.482	1780.0	1705.0	71.0	73.0
IIIA-6	2.56	5820	546	50.0	66.5	S.C.	0.752	1363.0	51.711	1790.0	1705.0	76.2	80.0
IIIA-8	3.56	5820	546	50.0	52.5	D.T.	0.953	1498.0	51.943	1798.0	1705.0	83.4	87.9

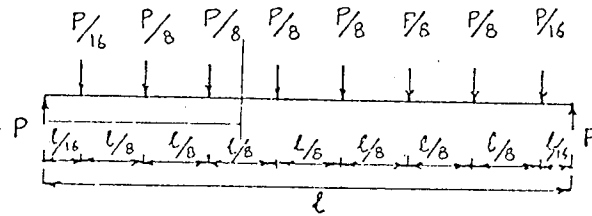
D.T. = Diagonal Tension; S.C. = Shear Compression; p = 1.85%;

$M_{f1} = f_y A_s d(1-0.4K)$; $\bar{M}_{f1} = \bar{f}_y A_s d(1-0.4\bar{K})$;

$K = pf_y(\text{test})/0.75 f'_c(\text{test})$; $\bar{K} = p\bar{f}_y/f'_c(\text{nominal})$; $f'_c(\text{nominal}) = 5 \text{ ksi}$; $\bar{f}_y = 50 \text{ ksi}$.

* Shear arm is defined as one-fourth of the span length (beams IIIA-3, IIIA-6 and IIIA-8 have l/d ratios of 6.25, 10.25 and 14.25 respectively.)

TABLE 5.6
COMPARATIVE MOMENTS - SERIES III A
(UNIFORM LOAD)
(Using Actual Cross Sections of Failure)



x = Distance of the cross-section of failure from support.

BEAM NO.	x (observed) in.	l in.	x/l	$(M_u)_x$ (K-in.)	M_{f1} (K-in.)	\bar{M}_{f1} (K-in.)	$(M_u)_x/M_{f1}$ %	$(M_u)_x/\bar{M}_{f1}$ %
IIIA-3	36	100	0.360	1166	1780	1705	65.5	68.5
IIIA-6	41	164	0.250	1020	1790	1705	57.0	59.8
IIIA-8	50	228	0.220	1034	1798	1705	57.7	60.7

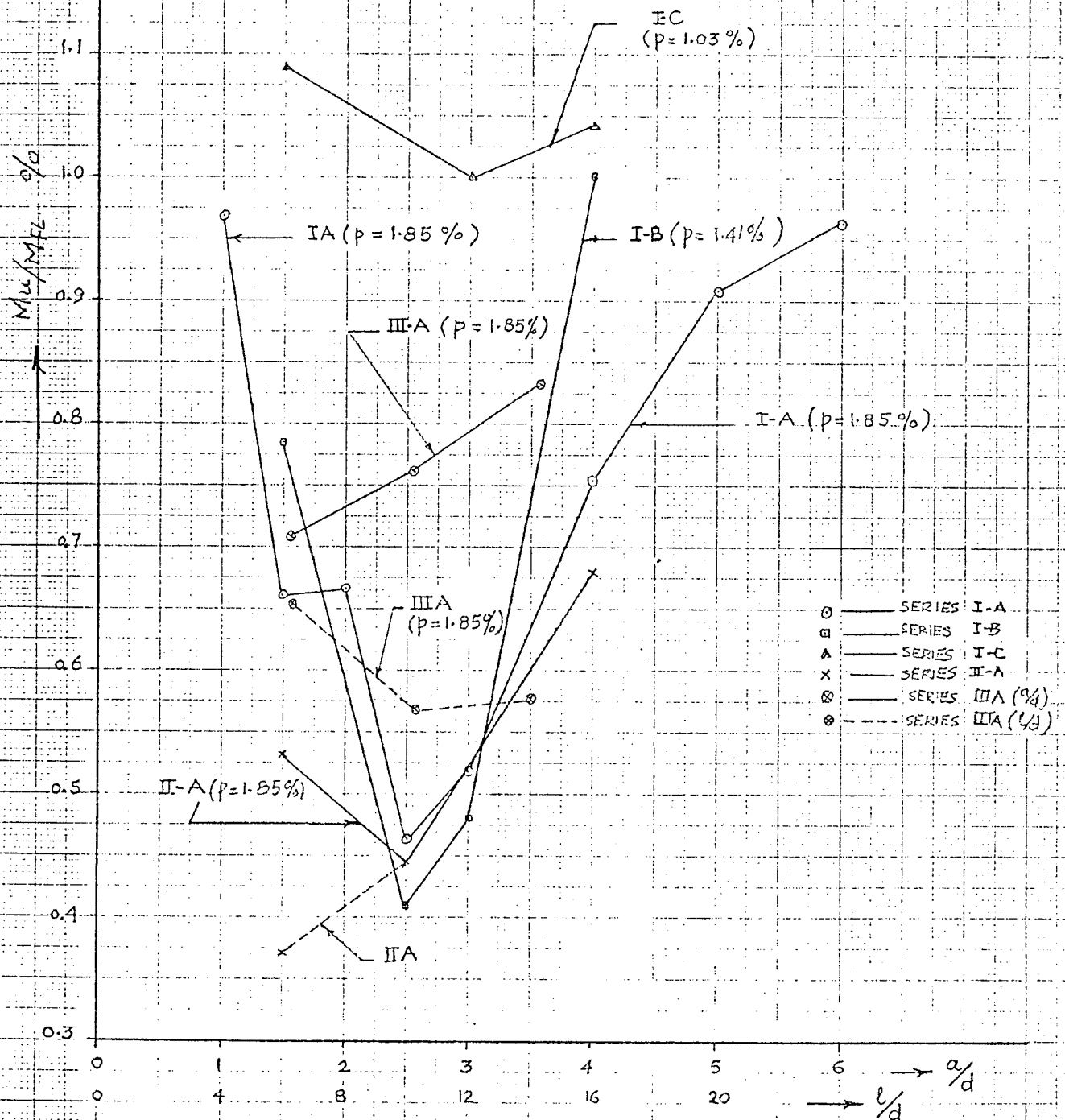


FIG. 5.7 COMPARATIVE MOMENT M_u/M_{FL} Vs a/d

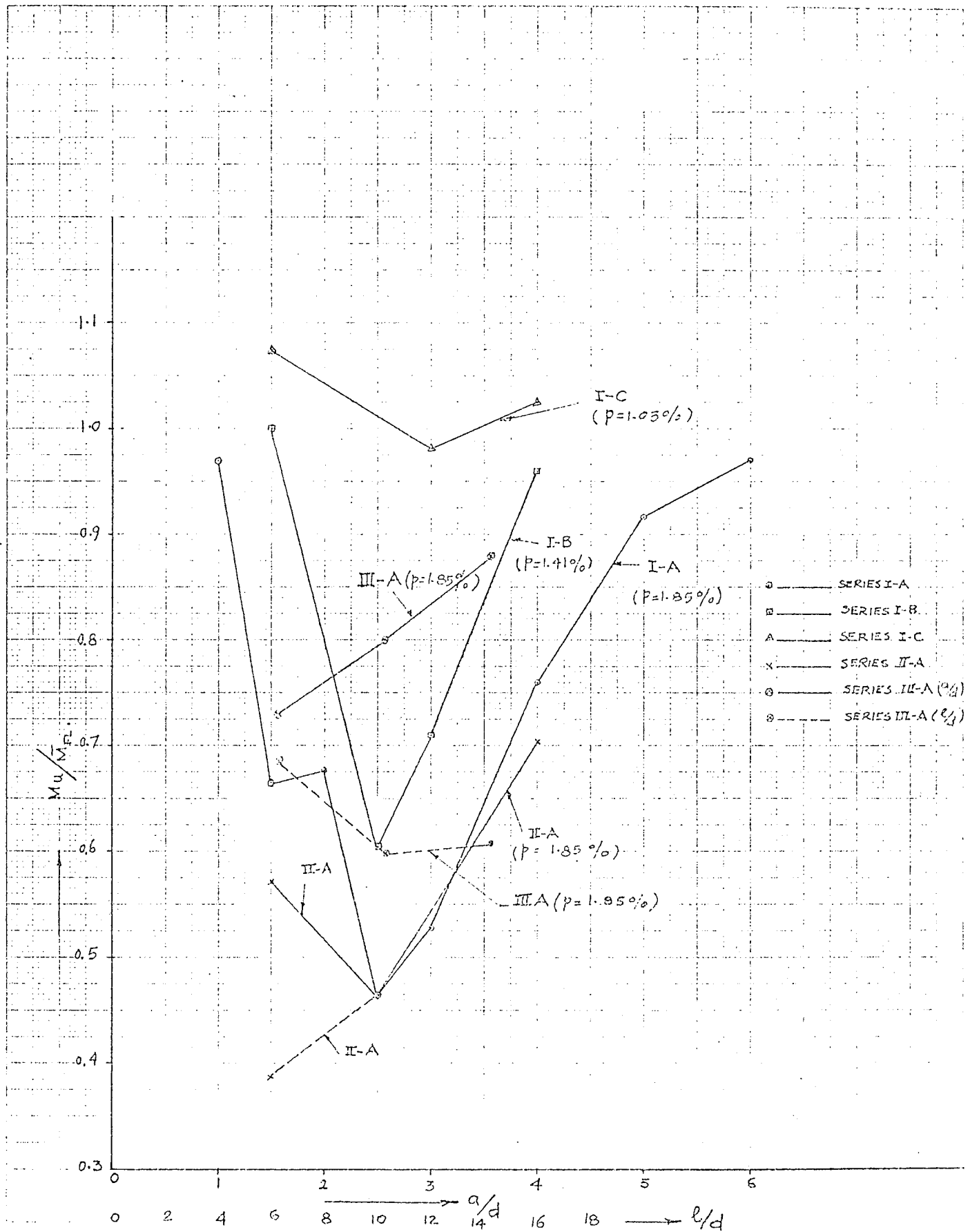


FIG. 5.8—COMPARATIVE MOMENT M_u/\bar{M}_{FL} VS a/d OR l/d

but, otherwise identical, would yield different values of M_u/M_{f1} .

To remove this problem in this test series, \bar{M}_{f1} is calculated on the basis of the nominal yield strength which is the same for the entire series of tests. If the actual steel stress at failure is greater than the nominal value used, values of M_u/\bar{M}_{f1} are greater than 100% and these values are rectified by \bar{F}_y/f_y , using 100% as a lower value for M_u/\bar{M}_{f1} after rectification.

The nominal yield strength for the series was 50 Ksi which was used for calculations of comparative moments. The variation of the yield strength of the reinforcement was within 4% of the nominal value for all tests except for the preliminary series of tests. The calculated values for both M_u/M_{f1} and M_u/\bar{M}_{f1} in this investigation are therefore close to each other and quite consistent for the series. The only large difference lies in case of preliminary beams IB-2, IB-4 and IB-5. Rectification was required for only one beam, IB-2, where M_u/\bar{M}_{f1} is reported as 100%.

Following observations are made on the influence of different variables in the study on the strength of beams and the mechanism of failure.

5.7.1. The a/d Ratio

The parameter a/d (or l/d for uniform loads), was found to have a very significant influence on the diagonal strength of reinforced concrete beams. The point of minimum beam strength

was observed to be at an a/d ratio of 2.5 for beams loaded by concentrated loads regardless of the percentage of longitudinal reinforcement. On both sides of this point of minimum strength the capacity of the beam increased. Further, the beams between a/d ratios of 1.0 and 2.5 failed in shear-compression while those between a/d ratios of 2.5 and higher until the flexural capacity of the section was attained, showed diagonal tension failures. For all diagonal tension failures, failure occurred suddenly at the appearance of the critical diagonal crack. Within the range of shear-compression failures, the beam capacity increased with a decrease in the shear-span/depth ratio.

The above observations are consistent with the conceptual model of diagonal failure presented in Chapter 3. For short beams (a/d ratios between 1.0 and 2.5), the critical diagonal crack was stabilized before failure while for more slender beams, failure occurred suddenly due to the lack of such stabilization.

5.7.2. The Percentage of Longitudinal Reinforcement

The amount of longitudinal flexural reinforcement was found to have considerable influence on the relative beam strength. For low values of the longitudinal reinforcement*, the beam capacity almost always approached the flexural capacity of the section. As

* $p = 1.03$ (Series IC)

the percentage of longitudinal reinforcement increased, the range of a/d ratios where a reduced strength existed increased. This is consistent with the conclusions drawn in Chapter 3.

5.7.3 Loading Through Secondary Beams

For diagonal tension failures, the effect of loading through secondary beams was negligible as the diagonal cracking loads remained almost unaffected. Beams with an a/d ratio of 2.5 showed the same comparative moment value whether they were loaded directly over the compression face of the beam or through the secondary beams. The beam with an a/d ratio of 4.0 loaded through secondary beams showed a reduction in strength of 7.1% compared to the equivalent beam which was directly loaded over the compression face of the beam. This small reduction in strength is well within the limits of experimental error to be expected, and therefore cannot be considered significant.

Beam IIA-2 with an a/d ratio of 1.5 failed prematurely due to the shearing of the secondary beam at its junction to the main beam as the critical diagonal crack entered the secondary beam. This beam was neglected in the analysis. Another similar beam, IIA-2(b), with the same a/d ratio was tested with top reinforcing bars through the secondary beams to avoid premature shearing. This beam did not fail at the appearance of the critical diagonal crack but continued taking further load. The propagation of critical

diagonal cracks was faster at this stage than in the comparable beam loaded directly over the compression face of the beam.

Diagonal cracks from either end of the beam propagated from the shear spans into the zone of constant moment in the midspan region of the beam. Failure was caused by an unrestrained propagation of cracks. These cracks from both ends joined in the midspan and a diagonal split occurred in one shear span accompanied by splitting along the reinforcement. However, in the case of beam IA-2, which was exactly the same as beam IIA-2(b) except that it was loaded directly over the compression face of the beam, it can be seen that the diagonal cracks almost stopped propagating after they were stabilized. Evidence of the restraining effect of pressure bulbs under direct loads is clear from these two comparable test beams.

The strength of beam IIA-2(b) was only 53.2% of its flexural strength while that of beam IA-2 was 66.3% of the flexural strength. The difference in yield strength of the reinforcement for these two beams was 4.5%.

If M_u/M_{fl} values are considered, it is found that a reduction of 19.7% occurred in strength due to secondary beam loading. On the other hand, if M_u/\bar{M}_{fl} values are taken into account, the reduction of strength is 14.3%.

The results of loading through secondary beams are consistent with the conceptual model of diagonal failure presented in Chapter 3. It is pertinent to note that longitudinal flexural strain distribution for beam IIA-2(b), loaded through secondary beams, had shown

the development of complete arching over the entire span of the beam after critical diagonal cracking (Appendix III). However, the full strength of external arch could not be attained due to an unrestrained propagation of diagonal cracks in the vicinity of the load points, and loss of stability of the arch.

5.7.4. Uniform Loads

(a) Assuming $a = \ell/4$

Assuming shear span as one-fourth of the span length for three beams tested with ℓ/d ratios of 6.25, 10.25 and 14.25, gives the equivalent a/d ratios of 1.56, 2.56 and 3.56 respectively. The beam capacity of these three beams varied as 71.0%, 76.2% and 83.4% of their flexural capacities, respectively. These values were consistently higher than comparable beams where concentrated loads were applied.

Beams with ℓ/d ratios of 6.25 and 10.25 continued taking further load after critical diagonal cracking and ultimately showed shear-compression failures. The beam with ℓ/d ratio of 14.25 showed a diagonal tension failure. It is apparent from Figures 5.7 and 5.8 that the reduction in strength due to diagonal failures is not as sharply defined in case of uniform loads as in concentrated loads.

(b) Using Critical Cross-Section of Failure

Beam capacities were worked out by calculating the ultimate

moment for each beam at the critical cross-section of failure, using the actual loading pattern employed for the beams (Table 5.6). The comparative moment values so obtained were lower than those obtained by using $a = \ell/4$. However, the minimum strength was still considerably higher than for point loads. The results are in agreement with the failure model discussed in Chapter 3, where it was suggested that distribution of load over the compression face of the beam creates a more favourable condition to suppress the flexural-tensile stresses above the diagonal crack, especially for relatively slender beams where point loads are removed from the critical cross-section of failure.

5.7.5 The Compressive Strength of Concrete

The compressive strength of concrete was not one of the variables in the experimental work. However, in case of beam IIA-2(b), the compressive strength of concrete was more than 7000 psi whereas the nominal strength was 5,000 psi. Beam IA-2, having a compressive strength of 5,000 psi, otherwise the same and loaded over the compression face of the beam, showed critical diagonal cracking at 50 kips, the same as beam IIA-2, loaded through secondary beams. Beam IIA-2(b), on the other hand developed critical diagonal cracking at 60 kips. The tensile splitting strength of all these beams was about 10% of their compressive strength. These results suggest that the diagonal cracking load was improved by an increase

in the strength of concrete.

Beams failing by crushing of concrete had almost the same compressive strength in all cases and so the effect of compressive strength on such failures could not be examined.

5.8 DEFLECTIONS OF BEAMS

In the opinion of the writer, there is a close connection between the deflection of a beam and the crack development in it. The smaller the beam deflection, the later the first crack forms and the slower is its progress. Further, the deflection of a beam depends not only on its moment of inertia but also on the shape of the bending moment curve.

In all beam tests, deflection readings were generally taken at midspan and under load points at various stages of loading prior to collapse. These deflections are given in Appendix II and shown graphically in Appendix III.

It was observed that in all beams with higher a/d ratios, the first flexural cracks appeared at relatively low loads (ranging from 5 kips to 7.5 kips) while such cracks were delayed for shorter beams and appeared as late as 20 to 25 kips. The first cracks, however, generally appeared at comparable deflections. In many cases, there was a significant fall of load at critical diagonal cracking while deflections either increased or remained constant. In beams with lower percentage of flexural reinforcement, the final

diagonal failure was a relatively slow failure, with large deflections immediately preceding failure.

C H A P T E R S I X

EXISTING RESEARCH AND PRESENT INVESTIGATION

6.1. GENERAL

Extensive test data and empirical equations are now available to determine the diagonal resistance of reinforced concrete beams without web reinforcement. However, there has not been general agreement on the internal mechanisms of diagonal resistance and the internal force system at collapse. ACI-ASCE COMMITTEE (1962) observed that the problems of shear and diagonal tension have not been fundamentally and conclusively solved. The committee suggested further work "not only to explore other areas of the problem but to establish a basically rational theory for effects of shear and diagonal tension on the behaviour of reinforced concrete members". Since then considerable effort has been spent on this aspect of the problem. In this chapter, the conceptual model of diagonal failure as presented in Chapter 3, is discussed in the light of existing research. The work of previous research workers is also examined to compare the effect of shear-span/depth ratio, the percentage of longitudinal reinforcement and the manner and type of loading on the diagonal strength of beams as observed in the present investigation.

Kani's method of analysis [KANI (1964)] is used to determine ultimate beam capacities. It is shown that his equations for beam action underestimate the capacity of the beams while those for arch action may sometimes overestimate the strength.

6.2. CONCEPTUAL MODEL OF DIAGONAL FAILURE AND EXISTING RESEARCH

Some of the research workers who have investigated diagonal failures of reinforced concrete beams have concluded that after flexural cracking and up until final collapse of the beam occurs, the beam continues behaving as a beam, regardless of whether a stabilized critical diagonal crack has developed or not. Others have concluded that after diagonal cracking occurs, a cracked reinforced member behaves as a two-hinged tied arch.

SWAMY, ANDRIOPOULOS and ADEPEGBA (1970) presented test data to show that there exist, up to the point of complete collapse, distinct tensile and compressive zones over the entire span of the beam and a beam continues behaving essentially as a beam until failure, for all cases of diagonal failures. BROMS (1969) suggested that internal rotations take place in the compression zone of the beam after critical diagonal cracking. He postulated that if such a crack was stabilized, then failure would result from a failure of the compression zone of the concrete due to crushing of concrete above the diagonal crack. Thus if the location of the diagonal crack within the compression zone as well as the stress distribution over the compression zone were to be known, the ultimate strength may be found in a manner similar to that used for flexural compression failures.

FENWICK and PAULAY (1968) concluded that shear could be resisted either by beam action or by arch action. They considered

arch action to be confined to areas near a load point and in the vicinity of the supports. KANI (1964) concluded that after the resistance of the concrete cantilevers was destroyed, the active cross-section was reduced to that of a tied arch.

The most significant conclusion drawn from the present investigation is that beam and arch action exist simultaneously in the shear span of all reinforced concrete beams regardless of the shear-span/depth ratio, the percentage of longitudinal reinforcement and the manner and type of loading. Before critical diagonal cracking develops, the action of concrete cantilevers predominates and internal arches are not significant from the beam strength point of view. This is perhaps why the presence of such internal arches was ignored by many of the research workers. After a critical diagonal crack has formed and has been stabilized, the compression force becomes significantly inclined while internal rotations take place. KANI (1964) considered only the inclination of the compression force and concluded that the beam was converted into a tied arch. On the other hand, BROMS (1969) considered internal rotations alone and the failure to be due to the crushing of the concrete. The present investigation highlights the fact that both of these actions are present simultaneously. This, in effect, means that there are two critical sections where failure can take place. One is located at the tip of the diagonal crack under the load point which can fail in a manner similar to a flexural-compression failure. The other type of failure can result from the inclination of the compression

force and the presence of flexural-tensile stresses above it near the compression face which can cause a delayed flexural-tensile failure. An interaction, therefore, exists between the beam and arch actions. The writer is convinced that a significant spread of results of short beams reported by various investigators is primarily because of the interaction of this beam and arch action.

The conclusions of the writer on the existence of flexural-tensile stresses above a diagonal crack and failure due to instability in diagonal tension failures are compatible with the work of FENWICK (1968) and BROMS (1969). Further, the conclusion that the critical diagonal crack extends when the capacity of concrete cantilevers is exceeded is similar to that of KANI (1964) and FENWICK (1968). Kani, however, considered only the flexural resistance of the concrete cantilevers and neglected aggregate interlock and dowel action of the reinforcement. Besides, Kani considered the strength of an average hypothetical cantilever. The writer believes that the diagonal crack extends when the bond force moment that can be carried by the most critical cantilever is exceeded.

Another aspect of the internal arching suggested by the writer is that these arches are not simply the theoretical compressive stress trajectories in a reinforced concrete beam. It is shown from the longitudinal flexural strain diagrams that after flexural cracking, these internal arches are real arches. The compressive force within these internal arches is, however, very small compared to the high compression that exists at the compression face of the

beam directly under the load point. Thus, these arches carry only a small portion of the resultant compressive force.

6.3. SHEAR STRESS AT DIAGONAL CRACKING AND COLLAPSE

Shear stress at diagonal cracking and collapse is computed in Table 6.1. For comparison purposes, A.C.I. code values have also been computed both for nominal and experimental values of compressive strength of concrete, with and without a capacity reduction of 0.85. These shear stress values are shown graphically in Figures 6.1 to 6.6.

The ultimate shear stress at failure showed a very large variation over the entire range of diagonal failures. It was also affected significantly by the manner of load application. Thus it cannot be considered to be a very reliable property of the material or a suitable indicator of beam strength. The A.C.I. code stipulates that the diagonal cracking load should be considered as the end of the useful capacity of a beam. A considerable reserve of strength in short beams is therefore, ignored. Even if diagonal cracking loads are considered, the A.C.I. code values are generally on the conservative side except for low percentages of reinforcement. Tests of series IC show that shear stress at failure is considerably reduced by a decrease in the percentage of reinforcement. A.C.I. code values for shear stress for this series are higher than those actually observed for diagonal tension failures.

It clearly points out that in the A.C.I. code equation,

$$v_c = 1.9 \sqrt{f'_c} + 2500 P_w \frac{V_u d}{M_u} \dots\dots(6.1)$$

the effect of compressive strength of concrete is over-estimated at the expense of the percentage of longitudinal reinforcement.

Tests of several research workers* have also shown the unreliable value of the shear stress at failure. Furthermore, as pointed out in the conceptual model of diagonal failure, the problem of the diagonal behaviour of the beam is to transfer the resultant of shear force and compressive force to the beam supports. By considering shear stress values, the larger of the two components, i.e., the compressive force, is ignored. Besides, the internal arches transfer a portion of the resultant compressive force by transferring their support forces to the external arch and then to the beam supports. Thus it may be concluded that shear stress at failure is not a good indicator of beam strength. The relative beam strength in the tests reported in this investigation varied from 46.5% of the flexural moment to full flexural capacity. This relative beam strength, showing a smaller variation than that shown by the use of a "shear stress", is, therefore, a better indicator of beam capacity. This is in agreement with results of KANI (1966).

* FERGUSON (1956), KANI (1966)

TABLE 6.1
SHEAR STRESS AT DIAGONAL CRACKING AND COLLAPSE

BEAM	a/d	$v_u = \frac{1}{2} \frac{P_u}{bd}$ psi	$v_c = \frac{1}{2} \frac{P_c}{bd}$ psi	v_c (ACI) psi			
				1971		1963	
				f'_c (test)	f'_c (nominal)	f'_c (test)	f'_c (nominal)
IA-1	1.0	807.0	234.5	180.3	180.3	153.3	153.3
IA-2	1.5	370.0	195.2	164.9	164.9	140.0	140.0
IA-3	2.0	281.5	175.8	157.2	157.2	133.8	133.8
IA-4	2.5	152.8	146.5	152.6	152.6	129.8	129.8
IA-5	3.0	146.5	146.5	141.2	149.5	120.0	127.0
IA-6	4.0	156.0	146.5	157.2	145.6	133.8	123.7
IA-7	5.0	150.1	146.5	154.9	143.3	131.5	121.9
IA-8	6.0	134.5	117.2	153.4	141.8	130.4	120.2
IB-2	1.5	479.0	166.0	153.2	150.2	130.2	127.8
IB-4	2.5	150.0	146.5	141.2	138.2	120.1	117.7
IB-5	3.0	146.5	136.8	138.1	135.2	117.6	115.0
IB-6	4.0	152.3	146.5	145.4	145.4	123.6	123.6

Table Continued

TABLE 6.1 (Continued)

BEAM	a/d	$v_u = \frac{1}{2} \frac{P_u}{bd}$ psi	$v_c = \frac{1}{2} \frac{P_c}{bd}$ psi	v_c (ACI) psi			
				1971		1963	
				f'_c (test)	f'_c (nominal)	f'_c (test)	f'_c (nominal)
IC-2	1.5	342.0	195.2	151.4	156.2	128.8	132.9
IC-5	3.0	157.0	140.6	142.8	147.6	121.2	125.5
IC-6	4.0	122.8	122.8	140.7	145.5	119.6	123.8
IIA-2	1.5	214.7	195.2	167.6	164.9	142.3	140.0
IIA-2(b)	1.5	316.5	234.5	194.0	164.9	164.9	140.0
IIA-4	2.5	154.8	146.5	155.1	152.6	131.9	129.8
IIA-6	4.0	146.5	146.5	148.1	145.6	126.0	123.7
IIIA-3	1.56*	394.5	234.5	174.7	157.2	148.5	133.8
IIIA-6	2.56*	260.0	195.2	163.1	145.6	138.8	123.7
IIIA-8	3.56*	205.0	195.2	158.0	141.8	134.2	120.2

$$v_c \text{ (A.C.I.) } 1971 = 1.9 \sqrt{f'_c} + 2500 p_w \frac{v_u d}{M_u}$$

$$v_c \text{ (A.C.I.) } 1963 = \phi (1.9 \sqrt{f'_c} + 2500 p_w \frac{v_u d}{M_u}) ; \quad \phi = 0.85$$

* using $a = 1/4$

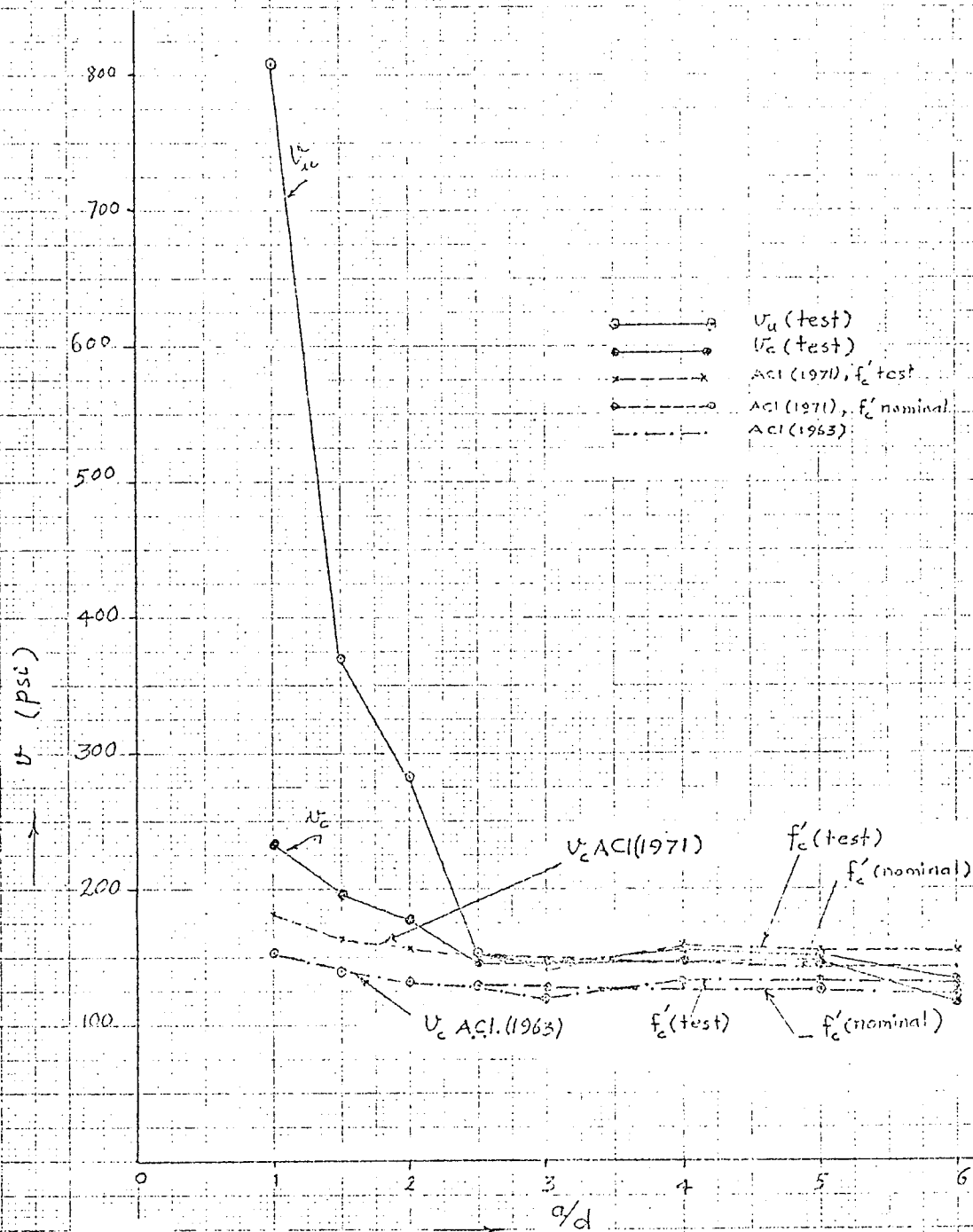


FIG. 6.1-SERIES IA: SHEAR STRESS VS. SHEAR SPAN-DEPTH RATIO

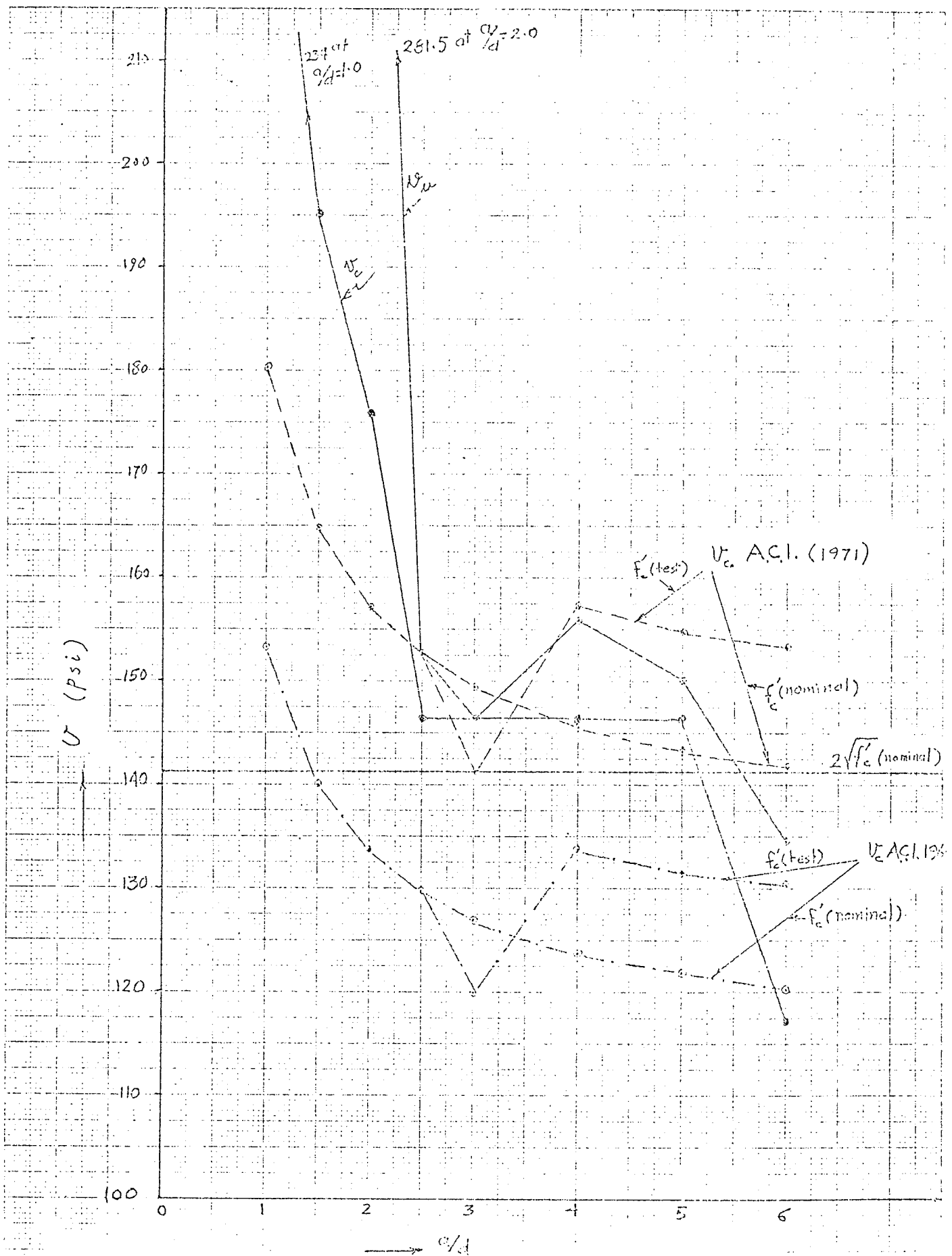


FIG. 6.2—SERIES IA ——— SHEAR STRESS V vs. SHEAR SPAN-DEPTH RATIO

NOTE: This is a magnification of Fig. 6.1

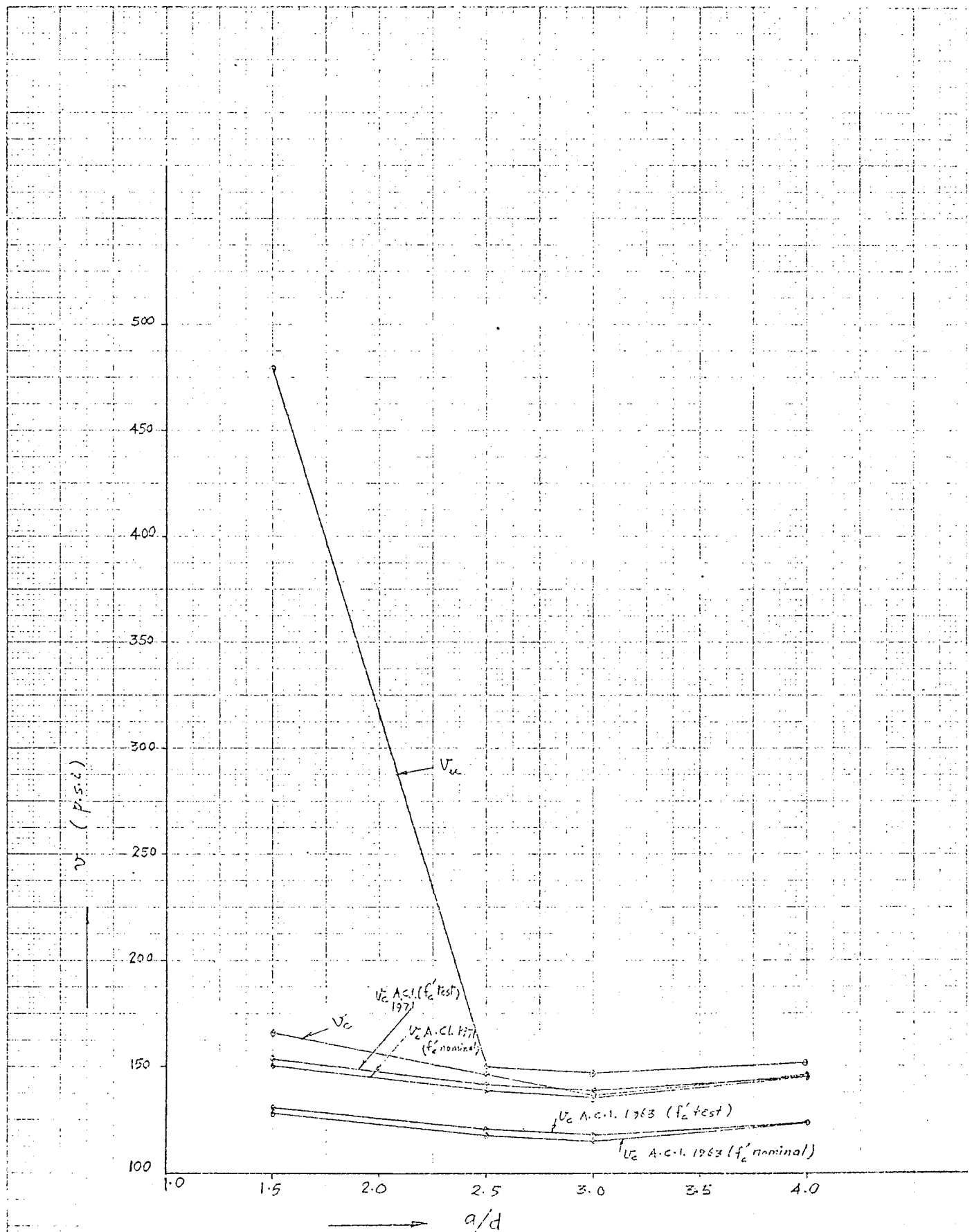


FIG.6.3-SERIES I-B — SHEAR STRESS V VS SHEAR SPAN-DEPTH RATIO

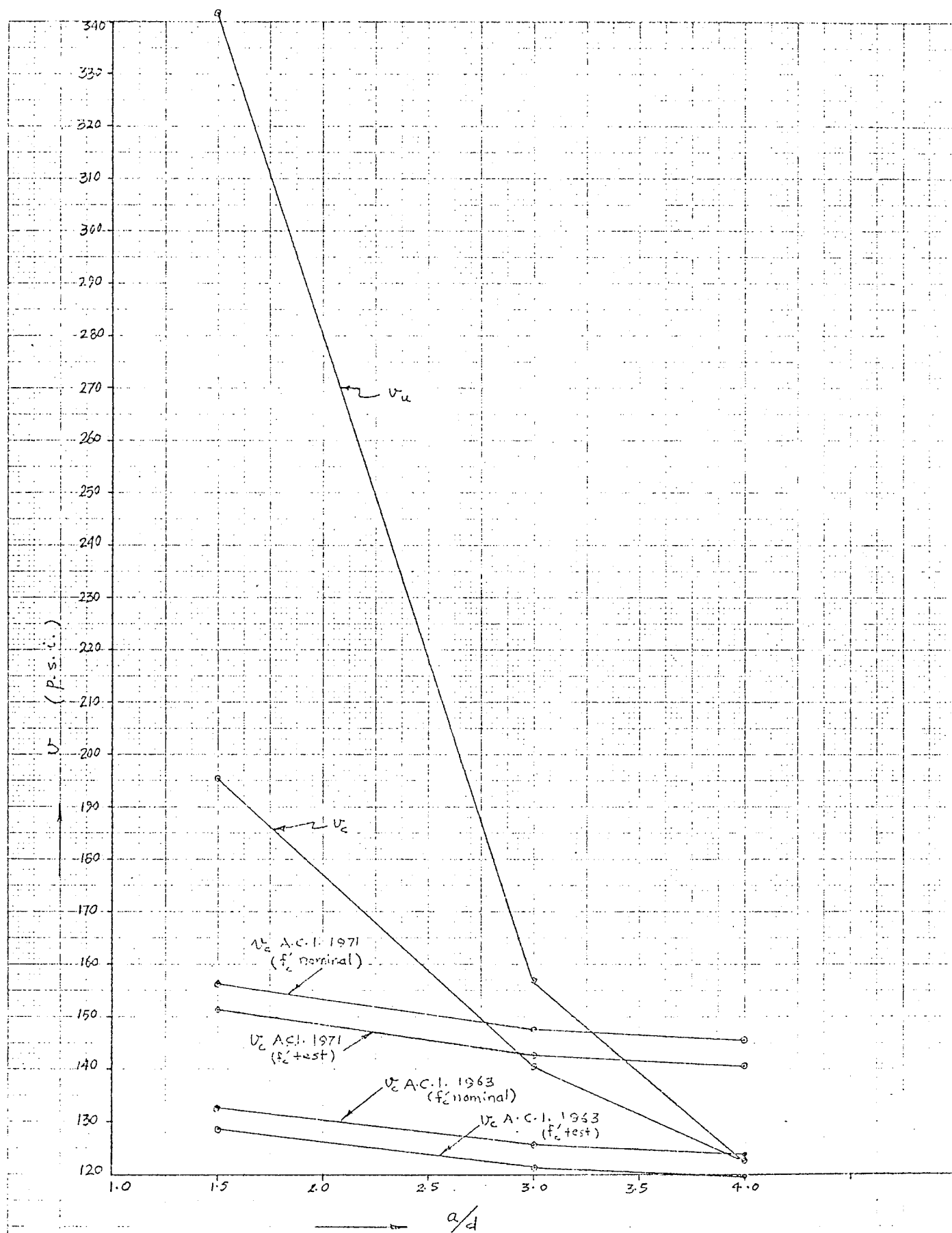


FIG. 6.4 — SERIES I-C — SHEAR STRESS V vs. SHEAR SPAN-DEPTH RATIO

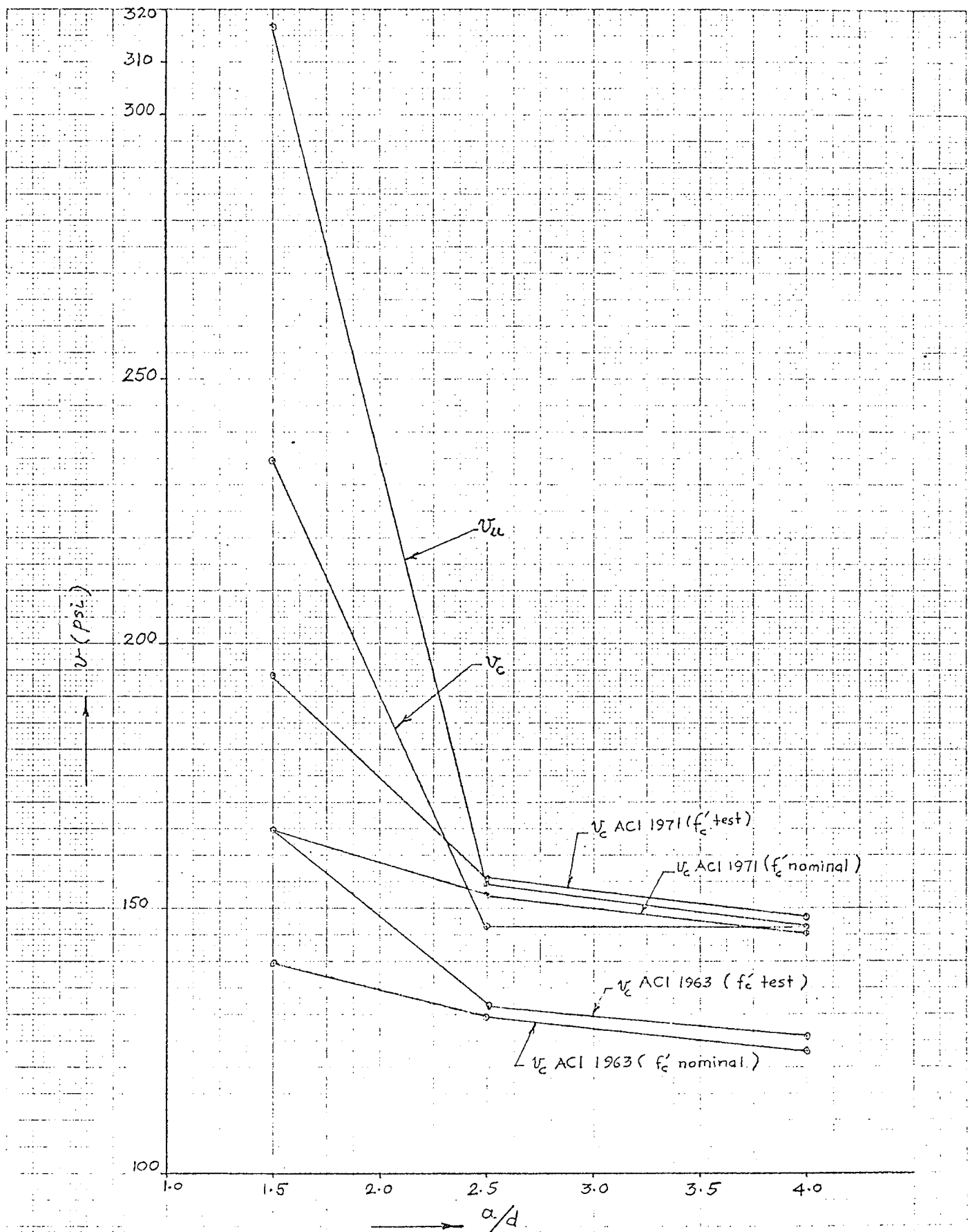


FIG. 6.5- SERIES IIA — SHEAR STRESS V_s SHEAR SPAN-DEPTH RATIO

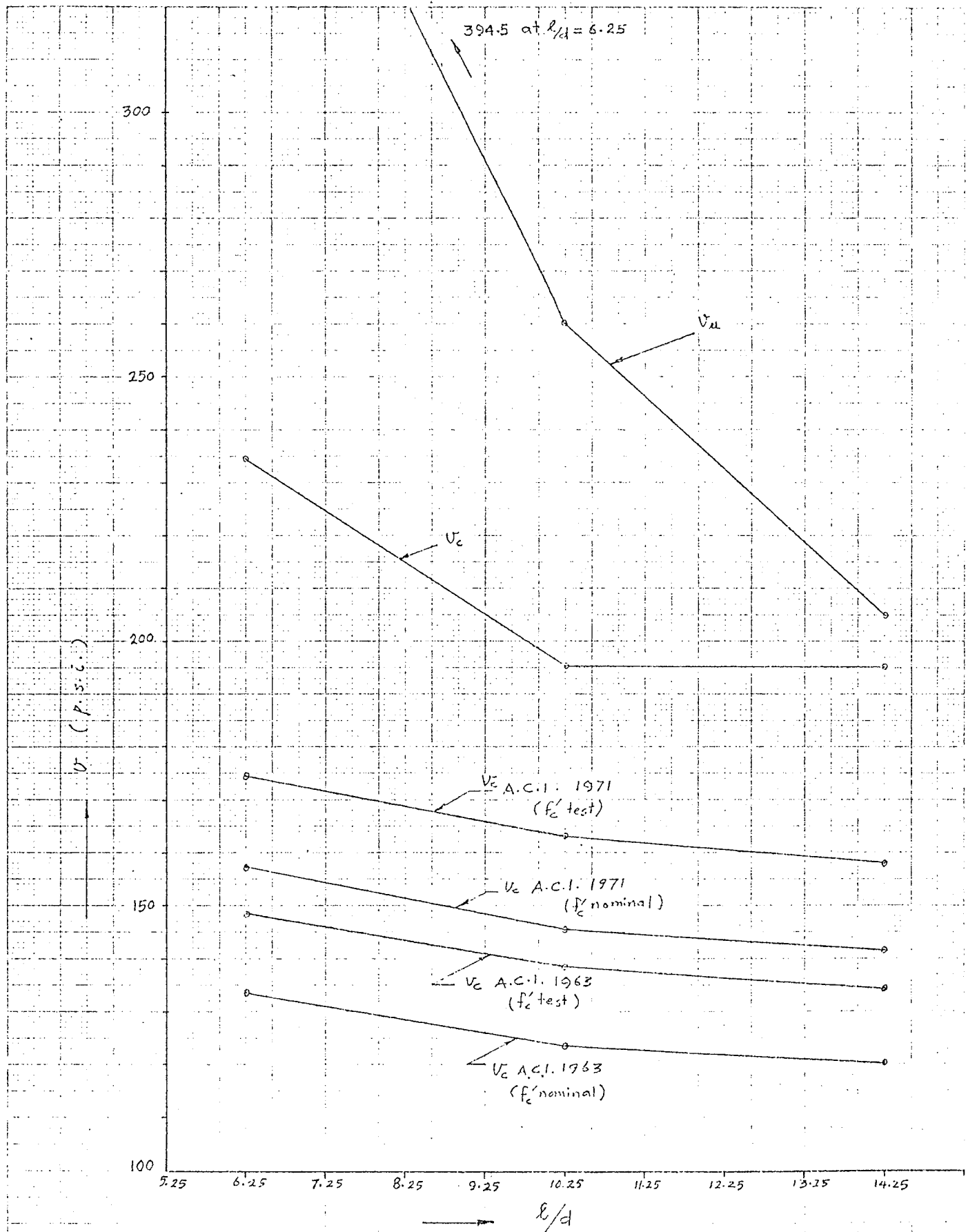


FIG. 6.6 — SERIES III-A — SHEAR STRESS V vs l/d RATIO

6.4. EFFECT OF DIFFERENT VARIABLES ON DIAGONAL STRENGTH OF BEAMS

6.4.1. The Compressive Strength of Concrete

KANI (1966) concluded that the compressive strength of concrete did not affect the diagonal strength of beams within the entire range of his tests. Tests of MOODY (1953), MORROW and VIEST (1957) and TAUB and NEVILLE (1960), however, suggest a significant influence on the diagonal strength of beams. Though the compressive strength of concrete was not one of the variables in the study, any variations of compressive strength from the nominal values did not seem to have any significant influence on the strength of beams. In one case*, however, where the compressive strength of concrete was appreciably higher than the nominal strength, there was definite evidence of some improvement of strength. In the conceptual model of diagonal failure presented by the writer, the compressive strength of concrete would be more significant in beams where failure resulted from a crushing of concrete.

The linear relationship between $\frac{V_u}{bd\sqrt{f'_c}}$ and

$\frac{P_w V_u d}{M_{uv}\sqrt{f'_c}}$ assumed by the A.C.I. equation seems to be somewhat over-

simplified. It is probable that the relationship of the above two variables is a curve giving a smaller contribution of the compressive strength.

* Beam IIA-2(b)

6.4.2. The a/d Ratio

The minimum point of strength on the comparative moment diagram was found to be at an a/d ratio of 2.5 for point loads. This is in agreement with results of MORROW and VIEST (1957), LEONHARD and WALTHER (1961) and KANI (1964). These results are shown in Figure 6.7. The general trend of results of the writer on the comparative moments diagrams was also similar to the results shown in Figure 6.7.

Only three tests were conducted by the writer on beams with uniform loads. It was found that using a definition of $a = \ell/4$, the concept of a minimum point on the diagram was not applicable to beams uniformly loaded. For equivalent a/d ratios of 1.56, 2.56 and 3.56, consistently higher values of comparative moments were obtained. The first two beams failed at a delayed stage after critical diagonal cracking. KANI (1966) derived the behaviour of beams with uniformly distributed loads with a similar definition of shear span ($a = \ell/4$) from the results of LEONHART and WALTHER (1962). These results show a considerable scatter of comparative beam strengths and the point of minimum strength is not sharply defined. In fact, the lowest and the highest points of the comparative moment diagrams between a/d ratios of 1.25 and 3.75 differ only by about 10%.

If the shear-arm ratio of beams loaded uniformly is taken as $\ell/4$, it represents the ratio of $\frac{M_{\max}}{V_{\max}}$ and not $\frac{M}{V}$ at the critical

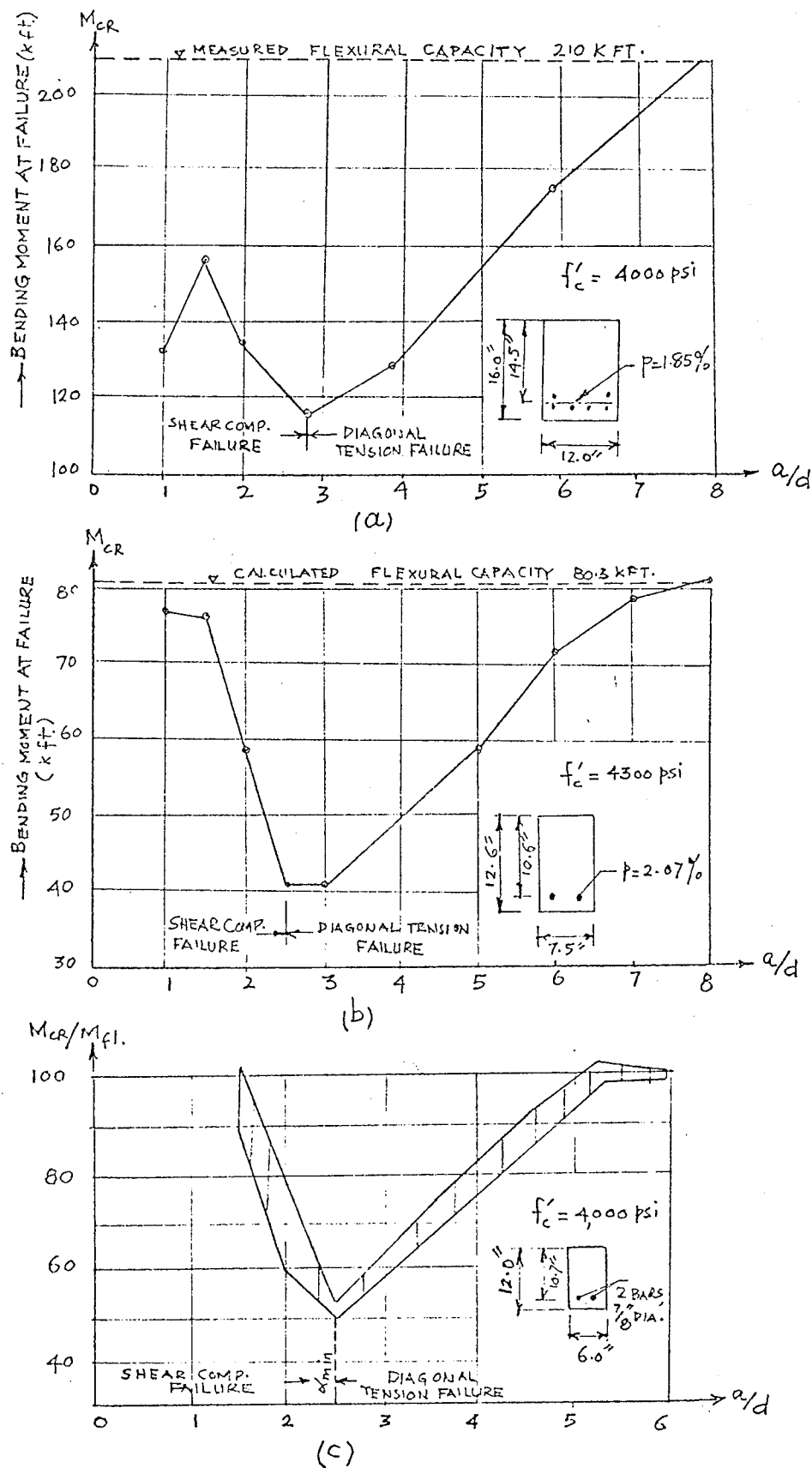


FIG. 6.7 BENDING MOMENT AT FAILURE VS a/d RATIO
 (a) MORROW and VIEST (1957) (b) LEONHARDT and WALTHER (1961) (c) KANI (1964)

section. The critical cross-section of failure calculated with the above definition gives the distance of the failure section from the support as $x = 0.19 \ell$, where ℓ is the span length. The ratio $\frac{x}{\ell}$ thus remains constant for any variation of ℓ/d ratio. Results of KREFELD and THURSTON (1966 - April) and IYENGAR and RANGAN (1967) suggest that the distance between the support and the critical cross-section of failure varies inversely with ℓ/d ratios. Krefeld and Thurston proposed the following equations for general use in calculating the critical cross-sections of failure.

$$\left. \begin{aligned} & \text{and} \\ & \left[\frac{M}{Vd} \right]_x = 0.267 \ell/d \text{ for } 4 \leq \ell/d \leq 10 \\ & \left[\frac{M}{Vd} \right]_x = \frac{(2 \ell/d) - 4}{\left(\frac{\ell}{d} - 4 \right)} \text{ for } 10 \leq \ell/d \end{aligned} \right\} \dots\dots(6.2)$$

The $\frac{x}{\ell}$ values for each beam uniformly loaded in the present investigation were computed from the actual cross-sections of failure. It was found that the values of $\frac{x}{\ell}$ decreased with an increase in the length of span (or ℓ/d ratio since the effective depth of all beams was constant). This observation is similar to the conclusions of KREFELD and THURSTON (1966 - April). The ultimate beam capacities were computed from the actual cross-sections of failure* and plotted on the comparative moment diagrams. It was found that the point of

* Table 5.6, Chapter 5.

minimum strength occurred at l/d ratio of 10.25 out of three beams with l/d ratios of 6.25, 10.25 and 14.25. Since beams with l/d ratios of 6.25 and 10.25 continued taking considerable load after diagonal cracking, it is probable that the exact point of minimum strength was somewhere between l/d ratios of 10.25 and 14.25. In any event, the difference in comparative moment values of all these three beams was very small. Even this approach shows that the point of minimum strength is not sharply defined. Since critical cross-sections cannot be determined very precisely, this approach has its own limitations. However, it can be concluded that in beams uniformly loaded, a sharp reduction of strength does not occur. This observation is in agreement with the conceptual model of diagonal failure proposed in Chapter 3. It was suggested that where multiple loads are applied on the compression face of the beam, diagonal cracks can be stabilized in relatively more slender beams due to vertical compressive stresses under each point load which suppress the tensile stresses above the diagonal crack.

6.4.3. The Percentage of Longitudinal Reinforcement

The effect of the percentage of longitudinal reinforcement on beam strength is shown in Figure 6.8 for tests of KANI (1966). These results show that the range of diagonal failures increased with an increase of the longitudinal reinforcement while the point of minimum beam strength was usually obtained at an a/d ratio of

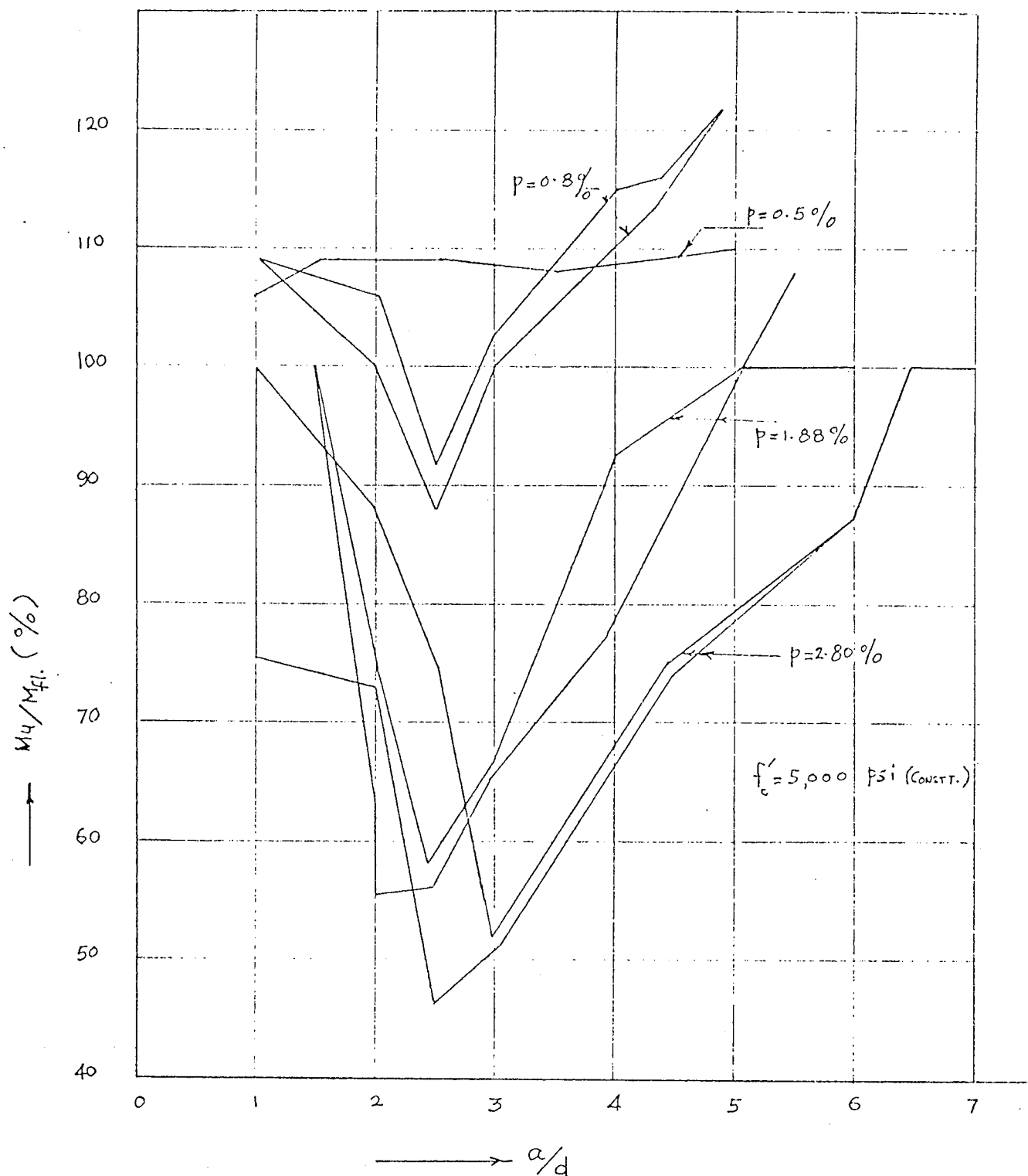


FIG. 6.8 EFFECT OF PERCENTAGE OF LONGITUDINAL REINFORCEMENT ON BEAM STRENGTH
(KANI — 1966)

2.5 regardless of the amount of longitudinal reinforcement.

These conclusions are in agreement with the tests of the writer on beams loaded with point loads. For low percentages of reinforcement, the beam strength approached the flexural capacity.

6.4.4. The Method of Loading

(a) Uniform Loads

The strength of beams with uniform loads was generally higher than comparable beams where point loads were applied. Tests of FERGUSON (1956) and LEONHARDT and WALTHER (1961) with uniform loads show the same trend.

(b) Secondary Beam Loading

FERGUSON (1956) showed that much of the increased capacity of the beams with small a/d ratios is lost if the beam is loaded through secondary beams framing into the main beam.

Results of FERGUSON (1956) are tabulated in Table 6.2. The a/d ratio in all cases was 1.35. Loading arrangement shows various combinations of loading through secondary beams and supports. Ferguson found that when the load was applied through cross members the failure shear was only 39% as large as with loads applied directly to the top of the beam. Further, when the load was

applied through cross members entirely within the lower half of the beam, the load was even further lowered to 29% of the value. Ferguson had explained that diagonal cracks have vertical tensile stresses at their top tips and since high vertical compressive stresses exist directly under the load point, the propagation of cracks is delayed or retarded. Failure only resulted when concrete above the crack crushed. When such vertical compressive stresses were removed from the vicinity of the diagonal crack, either by loading through secondary beams, or when the a/d ratio was fairly high, the diagonal crack propagated unrestrained and caused failure.

Results of TAUB and NEVILLE (1960) are shown in Table 6.3. They found that there was only a very slight reduction in the ultimate load and considerable reserve in strength beyond diagonal cracking even in beams loaded through secondary beams. However, Taub and Neville used stirrups in addition to the longitudinal reinforcement in the secondary beams. It is probable that a diagonal crack from the main beam crossed the line of these stirrups. This can again conceivably set up the vertical compressive forces in the main beam similar to those under directly loaded beams.

There is no doubt that vertical compressive stresses under the load point arrest the propagation of diagonal crack in the compression zone of the beam. However, tests of the writer suggest that even in the absence of such stresses, beams with small a/d ratios can sustain the stress conditions generated by a critical diagonal crack. Beam IIA-2(b) did not have any stirrup at all in

TABLE 6.2
THE EFFECT OF MANNER OF LOADING
ON DIAGONAL STRENGTH OF BEAMS
FERGUSON (1956)

DETAILS OF BEAMS:

Beam Size: 4" x 10" x 42" long
 A_s = 2 No. 5
 l = 39 in. (simple span)
 a/d = 1.35 (symmetrical loading)

When load is applied through cross beams, it is applied $7\frac{1}{2}$ in. on either side of the axis of main beam.

TEST RESULTS


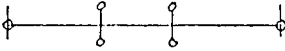
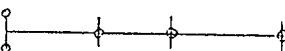
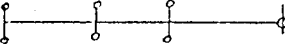
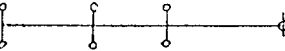
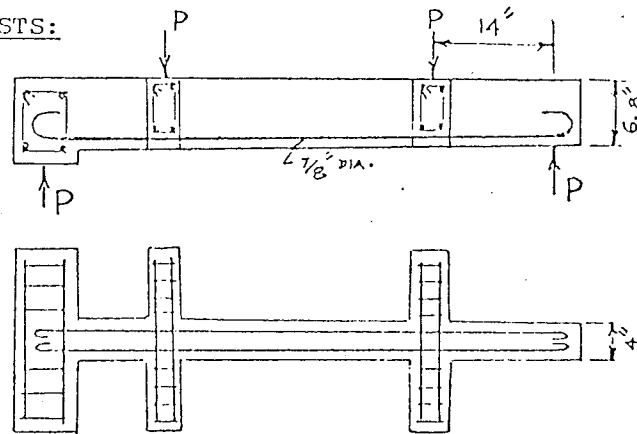
BEAM NO.	LOADING ARRANGEMENT	UNIT SHEAR v psi	f'_c psi	$\frac{v}{f'_c}$
S1		635	3420	0.186
F4		602	3070	0.196
S2		250	3400	0.0735
S4		250	3440	0.0727
S3		203	3400	0.0596
F6	 Cross members entirely within lower half depth of beam	181	3880	0.0554

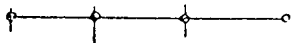
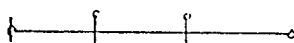
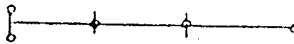
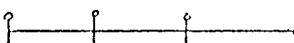
TABLE 6.3
THE INFLUENCE OF MANNER OF LOADING
ON DIAGONAL STRENGTH OF BEAMS

TAUB AND NEVILLE (1960)

DETAILS OF BEAM TESTS:



TEST RESULTS

LOADING ARRANGEMENT	DIAGONAL CRACKING v_n / f_{cu}	ULTIMATE LOAD v_u / f_{cu}
	0.156	0.210
	0.144	0.194
	0.116	0.189
	0.116	0.189

the zone where a diagonal crack could have crossed it. Still it carried further load after critical diagonal cracking. Due to the absence of vertical compressive stresses under the load point, the propagation of cracks was faster than that associated with direct loading over the compression face and it failed also at a lower load. Failure resulted from an unrestrained propagation of diagonal cracks in the midspan region of the beam.

6.5. COMPARISON OF TEST RESULTS WITH KANI'S ANALYTICAL SOLUTIONS*

Reference has been made to the work of Kani in Chapters 1 and 2. Kani considered that the magnitude of the bond forces on the concrete cantilevers was limited by the flexural capacity of the roots of these cantilevers (Figure 6.9a). Flexural failure of the concrete cantilevers caused the cracks to extend in an inclined direction. Resistance of the concrete cantilevers was thus given by $\frac{\Delta T}{\Delta X} = \frac{f'_t}{6} \cdot \frac{\Delta X}{s} \cdot b$ (6.3)

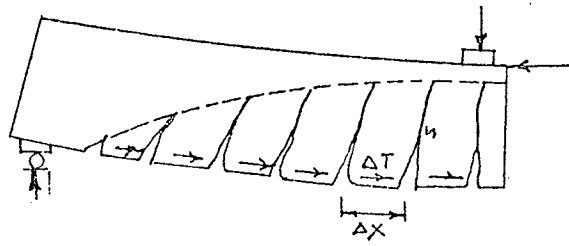
The cracking moment at the time the resistance of concrete cantilevers was broken was shown to be

$$M_{CR} = M_o \cdot \frac{\Delta X}{s} \cdot a/d \quad \text{.....(6.4)}$$

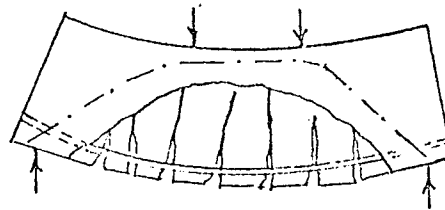
where

$$M_o = 7/8 \cdot \frac{bd^2}{6} f'_c$$

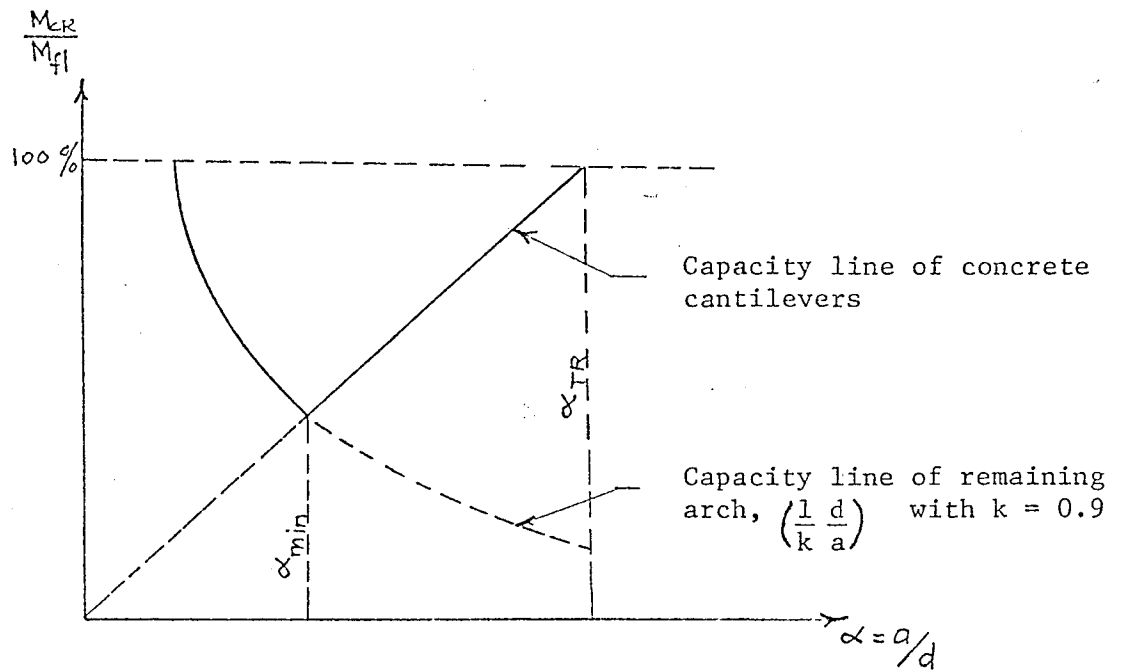
* KANI (1964)



(a) Function of Concrete Cantilevers



(b) Remaining Concrete Arch



(c) Capacity Lines of Concrete Cantilevers and Remaining Arch

FIG. 6.9 FUNCTION OF CONCRETE CANTILEVERS AND THE REMAINING CONCRETE ARCH — KANI (1964).

Equation 6.4 indicated that the cracking moment was a linear function of shear-span/depth ratio until the full flexural capacity of the beam was attained.

Kani further assumed that once the resistance of concrete cantilevers was broken, the active cross section was reduced and only a tied arch remained (Figure 6.9b). The strength of such a tied arch was given by

$$M_{CR} = \frac{M_{f\ell}}{K} \frac{d}{a} \quad \dots\dots(6.5)$$

Beam capacity lines for concrete cantilevers and the remaining arch are shown in Figure 6.9(c). If the a/d ratio where the full flexural capacity is attained is defined as α_{TR} and the minimum point of strength (at the intersection of capacity lines of concrete cantilevers and remaining arch) as α_{min} , the following conclusions were derived:

(a) For a/d values less than α_{min} , the capacity of the remaining arch is more than that of concrete cantilevers and failure only results when the capacity of the arch is destroyed.

(b) Between α_{min} and α_{TR} , the capacity of concrete cantilevers governs the beam strength and transformation into an arch cannot take place. This results in sudden diagonal failure.

(c) Beyond α_{TR} only flexural failures occur.

Kani further showed that the value of α_{TR} could be determined from the relation:

$$\alpha_{TR} = 6p \frac{f_y}{f'_t} \frac{s}{\Delta X} \quad \dots\dots(6.6)$$

In this expression average values of crack spacing and crack height were used.

Also, α_{min} could be determined from the expression,

$\alpha_{min} = \sqrt{\frac{\alpha_{TR}}{K}}$, where K represents the coefficient of biaxiality, directly under the concentrated applied load.

In the region of (a/d) values lower than α_{min} , the capacity of tied arch governed so that the ultimate moment could be calculated by the equation

$$M_u = \frac{M_{fl}}{K} \cdot \frac{d}{a}$$

For (a/d) ratios higher than α_{min} within the region of diagonal failure, the ultimate capacity was governed by flexural strength of concrete cantilevers, given by

$$M_u = \frac{M_{fl}}{\alpha_{TR}} \cdot \frac{a}{d} \quad \dots\dots(5.7)$$

In the development of his basic equations for beam action, Kani ignored the contributions of dowel action and aggregate interlock. He also neglected the internal rotations of the compression zone. It is reasonable to assume that any analysis based on the flexural strength of the roots of the concrete cantilevers alone is

perhaps an oversimplification of the actual conditions at collapse. Further, the bond force, ΔT , induces shear stresses in addition to the flexural stresses at the roots of the concrete cantilevers, and axial tension or compression also exist, complicating the stress field at the roots of the concrete cantilevers. These are very likely to reduce the flexural capacity of the roots of the concrete cantilevers below that calculated in simple bending. Furthermore, the linear strain distribution assumed at the roots of the cantilevers contravenes the requirements of compatibility for that zone of concrete. It is thus apparent that Kani's equations are likely to overestimate the flexural strength of the concrete cantilevers. As already pointed out, Kani has also ignored any second redistribution of moments at advanced stages of cracking when rotations of the compression zone take place. Thus, moment-rotation characteristics of the beams subjected to both moment and varying shear, such as those in the zone of a plastic hinge in a rigid frame have been ignored. Whether concrete fails by breaking away of the roots of the cantilevers, by a failure of the arch or by crushing of the compression zone is thus dependent on a number of factors. However, in shear compression failures, continued internal rotations and very large increases of the compressive strain at the compression face in the vicinity of the tip of the diagonal crack definitely point towards an interaction between various modes of resistance near collapse.

From the above discussion, it can be seen that Kani's approach while ignoring the contributions of aggregate interlock and the dowel

action of the reinforcement, overestimates the flexural strength of the roots of the concrete cantilevers. If the net result is that the analytical expressions give reasonably close results to the observed data, it may be useful in predicting ultimate beam capacities. It was therefore considered reasonable to compare the experimental results with those obtained from Kani's analytical expressions. Two different approaches were used - first, using all experimental values in Kani's expressions; and second, using nominal values for f'_c , f'_t and f_y alongwith analytical values for crack height and experimental values for crack spacing. In the opinion of the writer, use of all experimental values is more realistic, and more reliable.

Results of comparison of test results with Kani's equations are shown on Table 6.4. They may be summarized as follows.

(1) Wide variations in the interpretation of results are possible if the computations are based on nominal or test values.

(2) The point where the computed results are closer to the test results lies at the point of minimum strength on M_u/M_{f1} plots. As the a/d ratio increases above α_{min} , wide differences exist between the computed beam strength and that observed. The strength of concrete cantilevers is generally underestimated by about 30%. This percentage reduces to about 20% for beams where load is applied through secondary beams and increases to between 40 to 50% for uniformly loaded beams.

(3) Strength of the tied arch is considerably overestimated when the load is applied through the secondary beams. For beams

loaded directly over the compression face failing in shear-compression, considerable scatter exists in the results. In some cases, it is possible to overestimate the strength of the arch action. This is due to the fact that a true tied arch with a constant tensile force in the reinforcement does not develop in all such cases. However, for uniform loads, the computed strength of the tied arch is closer to test results for shear-compression failures.

TABLE 6.4

KANI'S EQUATIONS AND TEST RESULTS

(USING α_{TR} FOR EACH SERIES - EXPERIMENTAL VALUES)

SERIES	BEAM NO.	a/d	M_{Fl} (K-in.)	α_{TR}	α_{min}	(A) M_u (calc.) (K-in.)	(B) M_u (test) (K-in.)	% Difference $\frac{B-A}{A} \times 100$
I-A	1	1.0	1705.0	8.10	3.00	1894	-----	-----
	2	1.5	1713.0	8.10	3.00	1270	1137	-11.7
	3	2.0	1725.0	8.10	3.00	958	1152	+16.8
	4	2.5	1710.0	8.10	3.00	760	794	+ 4.3
	5	3.0	1730.0	8.10	3.00	641	900	+28.8
	6	4.0	1719.0	8.10	3.00	849	1296	+34.4
	7	5.0	1718.0	8.10	3.00	1060	1560	+32.1
	8	6.0	1716.0	8.10	3.00	1250	1652	+24.9
I-B	2	1.5	1870.0	8.87	3.14	1385	1470	+ 5.8
	4	2.5	1870.0	8.87	3.14	831	766	- 8.5
	5	3.0	1870.0	8.87	3.14	683	900	+24.1
	6	4.0	1243.0	8.87	3.14	843	1248	+32.5

Table Continued

TABLE 6.4 (Continued)

SERIES	BEAM NO.	a/d	M_{Fl} (K-in.)	TR	min	(A) M_u (calc.) (K-in.)	(B) M_u (test) (K-in.)	%Difference $\frac{B-A}{B} \times 100$
I-C	2	1.5	965.5	5.35	2.44	715	1052.4	+32.1
	5	3.0	964.0	5.35	2.44	542	964.8	+43.9
	6	4.0	963.0	5.35	2.44	723	1004.8	+28.0
II-A	2	1.5	1780.0	7.80	2.79	1318	660.0	-99.7*
	2(b)	1.5	1828.0	7.80	2.79	1355	972.0	-39.4
	4	2.5	1775.0	7.80	2.79	789	792.0	+ 0.4
	6	4.0	1761.0	7.80	2.79	904	1200.0	+24.6
III-A	3	1.56	1780.0	9.10	3.18	1296	1262.0	- 0.5
	6	2.56	1790.0	9.10	3.18	778	1363.0	+42.9
	8	3.56	1798.0	9.10	3.18	704	1498.0	+53.0

* Failed Prematurely

C H A P T E R S E V E N
CONCLUSIONS AND SUGGESTIONS FOR
FURTHER WORK

7.1 CONCLUSIONS

This investigation was primarily directed towards an understanding of the internal mechanisms of diagonal resistance of reinforced concrete beams without web reinforcement. Variables examined were the shear-span/depth ratio, the percentage of longitudinal reinforcement and the manner and the type of loading. A total of 22 beams were tested with extensive strain gauge instrumentation to determine the internal force system at various levels of loading prior to collapse. The results included observations of longitudinal flexural strains for concrete and the reinforcement, strains on inclined gauge lines, horizontal displacements, opening of cracks and internal rotations.

The following conclusions were derived.

- (1) It was found that beam and arch actions exist simultaneously in all types of diagonal failures discussed, regardless of the shear-span/depth ratio, the percentage of longitudinal reinforcement and the manner and type of loading.
- (2) With the appearance of flexural cracks, the "tension side" of the beam is divided into a number of blocks, which can be con-

sidered to be concrete cantilevers loaded by the bond forces at the level of the reinforcement. As flexural cracks appear, internal arching takes place in the cracked region of the beam. Further, with an increase in load, these internal arches extend outwards as flexural cracks appear in the outer regions of the beam.

(3) Prior to the formation of a critical diagonal crack, the action of concrete cantilevers predominates. The capacity of the concrete cantilevers is governed by

- (a) the flexural resistance of the concrete blocks
- (b) the shear transfer across cracks by interlocking action of the aggregates, and
- (c) the shear transfer across cracks by the dowel action of the reinforcement

(4) At a critical stage of loading, the resistance of concrete cantilevers is exceeded and a diagonal crack extends in the compression zone of the beam to mobilize additional resistance. The critical diagonal crack may be preceded by some back-cracking above the level of the reinforcement from outer locations of the flexural cracks, signifying a local tensile failure of concrete. When this happens, the resistance of the concrete block below the new crack is lost and this precipitates the formation of the critical diagonal crack.

- (5) As the critical diagonal crack extends in the compression zone of the beam, there exist high tensile stresses above the diagonal crack. Depending upon the direction of the resultant of shear force and the compressive force above the diagonal crack, a flexural-tensile failure may occur if the beam is relatively slender. If the beam is short, the diagonal crack is stabilized.
- (6) The internal arches contribute to the load carrying capacity by transferring the resultant compressive forces located within such arches to the external supports. At low levels of load when flexural cracking is limited, these arches exist in regions where no significant compression forces lie and thus their contribution is limited.
- (7) At the appearance of a critical diagonal crack, the internal arching extends over the entire span of the beam. If the diagonal crack is stabilized, the outermost of these internal arches then receives a non-yielding support at the beam ends. Internal rotations take place in the vicinity of the load point close to the tip of the diagonal crack which result in an increase of diagonal crack widths, a shift of the neutral axis at midspan upwards and a reduction of the bond forces within the concrete cantilevers. Further, the compression force between the load point and the beam supports becomes

significantly inclined and can be transferred to the supports directly through the external arch. Failure may ultimately result from a crushing of concrete at the compression face, the capacity of which may be determined in a manner similar to that used for flexural-compression failures, or it may result from higher flexural-tensile stresses above the diagonal crack at a delayed stage.

Though beam and arch actions exist simultaneously in a cracked reinforced beam, their resistance to diagonal failures is not additive.

- (8) Experimental results showed that the minimum point of beam strength on the comparative moment plots always occurred at an a/d ratio of 2.5 for point loads. In beams with a/d ratios of 2.5 or higher, the failure was of the diagonal tension type and the capacity of concrete cantilevers increased with an increase of a/d ratios. Between a/d ratios of 1 and 2.5, the critical diagonal crack was stabilized and the failure ultimately occurred due to crushing of concrete or a flexural-tensile failure above the diagonal crack. In beams with uniformly distributed loads and those loaded through secondary beams, complete arching developed after diagonal cracking similar to beams where point loads were applied. It was found that the point of minimum strength for uniformly loaded beams was not sharply defined.

- (9) The amount of longitudinal flexural reinforcement had considerable influence on the relative beam strength. The range of diagonal tension failures increased with an increase in the amount of longitudinal reinforcement. The point of minimum beam strength, however, remained unaffected by the amount of the longitudinal reinforcement. Further, with low values of longitudinal reinforcement, the beam strength approached the flexural capacity of the section and diagonal failures were preceded by large deflections.
- (10) The method of loading did not have any influence on the strength of beams showing diagonal tension failures. However, in beams loaded through secondary beams, where a critical diagonal crack did not cause failure, the ultimate beam capacity was lower than those directly loaded over the compression face of the beam due to an unrestrained propagation of diagonal cracks in the vicinity of the load points. The strength of beams uniformly loaded was generally higher than those where point loads were applied.
- (11) The ultimate shear stress at failure showed large variations and cannot be considered to be a reliable property of the material in a concrete beam. Relative beam strength, showing lesser variations, appears to be a better indicator of the beam strength. It is shown that A.C.I. code equations overestimate

the contribution of the compressive strength of concrete at the expense of the amount of longitudinal reinforcement.

- (12) From a description of the internal arches, it is shown that such arches transfer their support forces to the external arch from where they can be directly transferred to the beam supports. As cracking proceeds, the internal arches cannot develop the full amount of their support forces and the capacity of the beam is reduced unless the compression force shifts upwards due to internal rotations that take place at diagonal cracking. It is concluded that the function of the web reinforcement is to provide supports to the internal arches which are lost due to propagation of cracks and eventually to transfer these forces in the external arch to a point from where concrete alone can transfer them to the beam supports. Also, it is suggested that the web reinforcement carries part of the bond forces in the concrete cantilevers and suppresses the excessive opening of cracks.
- (13) It is shown that KANI (1964) neglects the contributions of aggregate interlock and the dowel action of the reinforcement in the strength of concrete cantilevers while overestimating their flexural resistance. Kani's analytical solutions for strength of concrete cantilevers and the remaining arch are used to determine beam capacities. It is concluded that his

equations for the strength of concrete cantilevers underestimate the beam strength by about 20% to 50% depending primarily upon the a/d ratio and the method of loading. It is also shown that Kani's equations for strength of the remaining arch may sometimes over estimate the beam strength.

7.2 SUGGESTIONS FOR FURTHER WORK

One of the reasons for the difficulties associated with the problem of diagonal failure has been the great number of parameters influencing the beam strength. Some of these parameters were outlined in Chapter 1. In order to draw any significant conclusions from a limited number of tests, only a limited number of variables can be studied.

The primary variables in this investigation consisted of the shear-span/depth ratio and the percentage of longitudinal reinforcement. Type of loading and the manner of loading were the secondary variables. Out of a total of 22 beams, only 3 beams were tested with uniform loads and 4 beams were tested with loading through secondary beams. The whole investigation was confined to beams without web reinforcement. The tests were conducted to examine the validity of the conceptual model of diagonal failure presented in Chapter 3. Sufficient test data is available in the literature on some aspects of the conceptual model of diagonal failure. However, certain aspects of the conceptual model need extensive strain gauge instrumentation to determine the internal force distribution at various levels of loading. In examining the test results available, the writer finds that the majority of other research workers have employed a minimum of instrumentation and have concentrated on failure loads and

failure conditions generally. More particularly, sufficient information on the behaviour of a cracked beam from the point of flexural cracking to critical diagonal cracking is not available.

Since the validity of a hypothesis can only be judged by extensive test results, the writer feels that additional experimental work is required to clarify the problem even further and to test the validity of the conceptual model of diagonal failure presented in this investigation. It is felt that not only is the number of tests an important factor but also the instrumentation employed. In order to determine the distribution of the compression force, extensive instrumentation is required on the compression face and over vertical sections from the point of application of the load to the midshear span. This would be useful in determining the location of the neutral axis more accurately and the zone in which internal rotations after critical diagonal cracking result in large increases of the compressive strain at the compression face of the beam. Furthermore, sufficient instrumentation is required in the lower half of the beam throughout its span to verify the development of internal arching.

Any further work may be divided into:

- (a) beams without web reinforcement
- (b) beams with web reinforcement

(a) Beams Without Web Reinforcement

(1) The writer feels that the compressive strength of concrete is an important factor especially in shear compression failures. Since the effect of this parameter was not considered in the present investigation, it would be useful to test beams for an entire range of diagonal failures

for two or three different **grades** of concrete.

(2) Sufficient number of tests were not conducted with uniform loads in the present investigation. It is suggested that tests be conducted for the entire range of ℓ/d values for which diagonal failures take place alongwith different percentages of the reinforcement. A typical scheme of experimental work may consist of $\frac{\ell}{d}$ ratios varying as 4, 6, 8, 10, 12, 15 and 18 with there different percentages of reinforcement varying as 1.0%, 1.5% and 2.0%.

(3) It is suggested that tests with secondary beam loading be confined to a/d ratios between 1.0 and 2.5 only. Since only limited information was obtained from results of test with secondary beam loading within the above range in the present investigation, a typical test series may consist of beams with a/d ratios of 1.0, 1.5, 2.0 and 2.5 with three different percentage of longitudinal reinforcement varying as 1.0%, 1.5% and 2.0%.

(4) Only one beam of each type was tested in the present investigation. It is suggested that further similar specimens may be tested to verify the various aspects of the conceptual model of diagonal failure outlined in this thesis.

(b) Beams With Web Reinforcement

The present work was limited to beams without web reinforcement only. However, the function of web reinforcement was described from the conceptual model. It is suggested that beams with different types of web reinforcement (vertical stirrups, inclined stirrups, and bent-up bars) be tested with similar other beams without web reinforcement to

verify conclusions on the function of the web reinforcement and to determine the zone in which the web reinforcement is more effective.

Bibliography

- (1) Alami, Z. Y., and Ferguson, P. M., "Accuracy of Models Used in Research on Reinforced Concrete," ACI Journal, Proceedings Volume 60, November, 1963, pp. 1643-1663.
- (2) Al-Alusi, A. F., "Diagonal Tension Strength of Reinforced Concrete T-Beams with Varying Shear Span," ACI Journal, Proceedings Volume 53, No. 11, May, 1957, pp. 1067-1077.
- (3) ACI Committee 318, "Building Code Requirements for Reinforced Concrete," i) ACI (318-63), ACI, Detroit 1963, Chapters 12 and 17.
ii) ACI (318-71), ACI, Detroit 1971, Chapter 11.
- (4) ACI Committee 318, "Commentary on Building Code Requirements for Reinforced Concrete (ACI 318-71)," ACI, Detroit 1971, Chapter 11.
- (5) ACI-ASCE Committee 426(326), "Shear and Diagonal Tension," ACI Journal, Proceedings Volume 59, No. 1-3, January; February and March, 1962, pp. 1-30, 227-333 and 353-395.
- (6) ACI-ASCE Committee 326, "Shear, Diagonal Tension and Torsion in Structural Concrete," Bibliography No. 4, ACI, Detroit 1962, 121 pp.
- (7) Base, G. D., "Further Notes on the Demec - a Demountable Mechanical Strain Gauge for Concrete Structures," Magazine of Concrete Research, Volume 7, March, 1955, pp. 35-38.
- (8) Binns, R. D., and Mygind, H. S., "The Use of Electrical Resistance Strain Gauge and the Effect of Aggregate Size on Gauge Length in Connection with Testing Concrete," Magazine of Concrete Research, Volume 1, January, 1949, pp. 35-39.
- (9) Bjuggren, U., Discussion of "Bond and Anchorage," by T. D. Mylrea, ACI Journal, Proceedings Volume 44, No. 4, Part 2, December, 1948, pp. 551-552.
- (10) Blackman, J. S., Smith, G. M., and Young, L. E., "Stress Distribution Affects Ultimate Tensile Strength," ACI Journal, Proceedings Volume 55, No. 12, 1958, pp. 679-694.
- (11) Bresler, B., and Pister, K. S., "Strength of Concrete Under Combined Stresses," ACI Journal, Proceedings Volume 55, No. 3, 1958, pp. 321-345.

- (12) Bresler, B., and Scordelis, A. C., "Shear Strength of Reinforced Concrete Beams," ACI Journal, Proceedings Volume 60, January, 1963, pp. 51-74.
- (13) Broms, B. B., "Stress Distribution, Crack Patterns and Failure Mechanisms of Reinforced Concrete Members," ACI Journal, Proceedings Volume 61, No. 12, December, 1964, pp. 1535-1551, and Volume 62, September, 1965, pp. 1095-1108.
- (14) Broms, B. B., "Shear Strength of Reinforced Concrete Beams," Journal of the Structural Division, Proceedings of ASCE, Volume 95, No. ST. 6, June, 1969, pp. 1339-1358.
- (15) Brook, G., Discussion of "The Riddle of Shear and Its Solution" ACI Journal, Proceedings Volume 61, December, 1964, pp. 1587-1590.
- (16) Chang, T. S., and Kesler, C. E., "Static and Fatigue Strength in Shear of Beams with Tensile Reinforcements," ACI Journal, Proceedings Volume 54, June, 1958, pp. 1033-1057.
- (17) Clark, A. P., "Diagonal Tension in Reinforced Concrete Beams," ACI Journal, Proceedings Volume 48, October, 1951, pp. 145-156.
- (18) Cooke, R. W., and Seddon, A. E., "The Laboratory Use of Bonded Wire Electrical Resistance Strain Gauges on Concrete at the Building Research Station," Magazine of Concrete Research, Volume 8, March, 1956, pp. 31-38.
- (19) Diaz de Cossio, R., Discussion of "Shear and Diagonal Tension" Report by ACI-ASCE Committee 326, ACI Journal, Proceedings Volume 59, September, 1962, pp. 1323-1332.
- (20) Diaz de Cossio, R., and Loera, S., Discussion of "Basic Facts Concerning Shear Failure," by G. N. J. Kani, ACI Journal, Proceedings Volume 63, No. 12, December, 1966, pp. 1511-1514.
- (21) Faber, O., "Reinforced Concrete Beams in Bending Shear," Concrete Publications, London, 1916.
- (22) Fenwick, R. C., and Paulay, T., Discussion of "The Riddle of Shear Failure and Its Solution," ACI Journal, Proceedings Volume 61, No. 12, December, 1964, pp. 1590-1595.
- (23) Fenwick, R. C., "The Shear Strength of Reinforced Concrete Beams," Ph.D. Thesis, University of Canterbury, Christchurch, 1966.
- (24) Fenwick, R. C., and Paulay, T., "Mechanisms of Shear Resistance of Concrete Beams," Journal of the Structural Division, Proceedings of ASCE, Volume 94, No. ST 10, October, 1968, pp. 2325-2350.

- (25) Ferguson, P. M., Discussion of "Diagonal Tension in Reinforced Concrete Beams" by Clark, ACI Journal, Proceedings Volume 48, October, 1951, pp. 1561-1563.
- (26) Ferguson, P. M., "Some Implications of Recent Diagonal Tension Tests," ACI Journal, Proceedings Volume 53, No. 2, August, 1956, pp. 157-172.
- (27) Friberg, B. F., "Design of Dowels in Transverse Joints of Concrete Pavements," Transactions, ASCE, Volume 105, 1940, pp. 1076-1116.
- (28) Guralnick, S. A., "Strength of Reinforced Concrete Beams," Journal of the Structural Division, Proceedings of ASCE, Volume 85, ST. 1, 1959, pp. 1-42.
- (29) Guralnick, S. A., "Strength of Reinforced Concrete Beams," Transactions, ASCE, Volume 125, 1960, pp. 603-653.
- (30) Guralnick, S. A., "High Strength Steel Bars for Concrete Reinforcement," ACI Journal, Proceedings Volume 57, No. 3, September, 1960, pp. 241-282.
- (31) Hetényi, M., "Beams on Elastic Foundations," University of Michigan Studies - Scientific Series, No. XVI, 1946.
- (32) Hognestad, E., and Viest, I. M., "Some Applications of Electrical Resistance SR-4 Gauges in Reinforced Concrete Research," ACI Journal, Proceedings Volume 46, February, 1950, pp. 445-454.
- (33) Hognestad, E., "What Do We Know About Diagonal Tension and Web Reinforcement," Circular Series No. 64, University of Illinois Engineering Experiment Station, 1952.
- (34) Hsu, T., Slate, F., Sturman, G., and Winter, G., "Microcracking of Plain Concrete and the Shape of Stress Strain Curve," ACI Journal, Proceedings Volume 60, February, 1963, pp. 209-224.
- (35) Hsu, T., "Mathematical Analysis of Shrinkage Stresses in a Model of Hardened Concrete," ACI Journal, Proceedings Volume 60, March, 1963, pp. 371-390.
- (36) Hsu, T., and Slate, F., "Tensile Bond Strength Between Aggregate And Cement Paste or Mortar," ACI Journal, Proceedings Volume 60, April 1963, pp. 465-486.
- (37) Iyengar, K. T. S. R., and Rangan, B. V., "A New Theory for the Shear Strength of Reinforced Concrete Beams," Indian Concrete Journal, March, 1967, pp. 102-109.

- (38) Jones, R., "The Ultimate Strength of Reinforced Concrete Beams in Shear," Magazine of Concrete Research (London), Volume 8, No. 23, August, 1956, pp. 69-84.
- (39) Kani, G. N. J., "The Mechanism of the So-Called Shear Failure," Transactions, Engineering Institute of Canada, Volume 6, No. A-3, April, 1963.
- (40) Kani, G. N. J., "The Riddle of Shear Failure and Its Solution," ACI Journal, Proceedings Volume 61, No. 4, April, 1964, pp. 441-467.
- (41) Kani, G. N. J., "Basic Facts Concerning Shear Failure," ACI Journal, Proceedings Volume 63, No. 6, June, 1966, Part 1, pp. 675-692; Part 2, Supplement.
- (42) Kani, G. N. J., "How Safe Are Our Large Reinforced Concrete Beams?" ACI Journal, Proceedings Volume 64, No. 3, March, 1967, pp. 128-141.
- (43) Kani, G. N. J., "A Rational Theory for the Function of Web Reinforcement," ACI Journal, Proceedings Volume 66, No. 3, March, 1969, pp. 185-197.
- (44) Kaplan, M. F., "Crack Propagation and the Fracture of Concrete," ACI Journal, Proceedings Volume 58, November, 1961, pp. 591-610.
- (45) Krefeld, W. J., and Thruston, C. W., "Contribution of Longitudinal Steel to Shear Resistance of Reinforced Concrete Beams," ACI Journal, Proceedings Volume 63, No. 3, March, 1966, pp. 325-344.
- (46) Krefeld, W. J., and Thruston, C. W., "Studies of Shear and Diagonal Tension Strength of Simply Supported Reinforced Concrete Beams," ACI Journal, Proceedings Volume 63, No. 4, April, 1966, pp. 451-476.
- (47) Laupa, A., Siess, C. P., and Newmark, N. M., "Strength in Shear of Reinforced Concrete Beams," Bulletin No. 428, University of Illinois Engineering Experiment Station, 1955 (73 pp.).
- (48) Leonhardt, F., and Walther, R., "Contributions to the Treatment of the Problems of Shear in Reinforced Concrete Construction," Translation No. 111, Cement and Concrete Association, London, 1964. (Published in German in December, 1961).
- (49) Leonhardt, F., and Walther, R., "Schuberversuche an einfeldrigen Stablbetonbalken mit und Ohne Schubbewehrung," Bulletin 151, Deutscher Ausschuss für Stahlbeton, Berlin, 1962, pp. 25-30.

- (50) Leonhardt, F., "Reducing the Shear Reinforcement in Reinforced Concrete Beams and Slabs," Magazine of Concrete Research Volume 17, December, 1965, pp. 187-198.
- (51) Lorentsen, M., "Theory for the Combined Action of Bending Moment and Shear in Reinforced and Prestressed Concrete Beams," ACI Journal, Proceedings Volume 62, No. 4, April, 1965, pp. 403-420.
- (52) MacGregor, J. G., Discussion of "The Riddle of Shear Failure and Its Solution" by G. N. J. Kani, ACI Journal, Proceedings Volume 61, No. 12, December, 1964, pp. 1590-1595.
- (53) MacGregor, J. G., Discussion of "How Safe Are Our Large Reinforced Concrete Beams?" by G. N. J. Kani, ACI Journal Proceedings Volume 64, No. 9, September, 1967, pp. 603-604.
- (54) Mathey, R. G. and Watstein, D. "Effect of Tensile Properties of Reinforcement on the Flexural Characteristics of Beams," ACI Journal, Proceedings Volume 56, No. 12, June, 1960, pp. 1253-1273.
- (55) Mathey, R. G., and Watstein, D., "Shear Strength of Beams Without Web Reinforcement Containing Deformed Bars of Different Yield Strengths," ACI Journal, Proceedings Volume 60, February, 1963, pp. 183-208.
- (56) Meyers, B., Slate, F., Winter, G., "Relationship Between Time-Dependent Deformation and Micro-Cracking of Plain Concrete," ACI Journal, Proceedings Volume 66, January, 1969, pp. 60-68.
- (57) Moe, J., Discussion of "Shear and Diagonal Tension" by ACI-ASCE Committee 426(326), ACI Journal, Proceedings Volume 59, No. 9, September, 1962, pp. 1334-1339.
- (58) Moody, K. G., "An Investigation of Reinforced Concrete Beams Failing in Shear," University of Illinois, Department of Theoretical and Applied Mechanics, June, 1953.
- (59) Moody, K. G., Viest, I. M., Elstner, R. C., and Hognestad, E., "Shear Strength of Reinforced Concrete Beams," Part I, II, III, IV, ACI Journal, Proceedings Volume 51, Nos. 4-7, December, 1954, January, February, March, 1955, pp. 317-332, 417-434, 525-539 and 697-730.
- (60) Moretto, O., "An Investigation of the Strength of Welded Stirrups in Reinforced Concrete Beams," ACI Journal, Proceedings Volume 42, No. 5, November, 1945, pp. 141-162.

- (61) Morice, P. B., "The Design and Use of a Demountable Mechanical Gauge for Concrete Structures," Magazine of Concrete Research, Volume 5, August, 1953, pp. 37-42.
- (62) Morrow, J., and Viest, I. M., "Shear Strength of Reinforced Frame Member Without Web Reinforcement," ACI Journal, Proceedings Volume 53, March, 1957, pp. 833-869.
- (63) Mörsch, E., "Tests of Shearing Stresses in Reinforced Concrete Beams," (Versuche Über Schubspannungen in Betoneisenträgern), Beton Und Eisen (Berlin), Volume 2, No. 4, October, 1903, pp. 269-274 (in German).
- (64) Mörsch, E., "Tests of Shear Action of Reinforced Concrete Girders," (Versuche Über die Schubwirkungen bei Eisenbetoutragern) Deutsche Bauzeitung, (Berlin), Volume 41, Nos. 30, 32, 35, April-May, 1907, pp. 207-212, 223-228, 241-243 (in German).
- (65) Mörsch, E., "Concrete Steel Construction," Translation of the 3rd Company Edition, Engineering News Publishing Company, New York, 1909, 368 pp.
- (66) Neville, A. M., and Lord, E., "Some Factors in the Shear Strength of Reinforced Concrete Beams," Structural Engineer (London) Volume 38, July, 1960, pp. 213-223.
- (67) Neville, A. M., and Taub, J., "Resistance to Shear of Reinforced Concrete Beams," Parts 1, 2, 3 and 4, ACI Journal, Proceedings Volume 57, No. 2-5, August, September, October, and November, 1960, pp. 193-220, 315-336, 443-463, and 517-532.
- (68) Rensaa, E. M., "Shear, Diagonal Tension, Anchorage in Beams," ACI Journal, Proceedings Volume 55, No. 6, December 1958, pp. 695-716.
- (69) Richart, F. E., "An Investigation of Web Stresses in Reinforced Concrete Beams," University of Illinois Bulletin No. 166, Engineering Experimental Station, 1927.
- (70) Ritter, W., "The Hennebique Design Method," (Die Bauweise Hennebique), Schweizerische Bauzeitung (Zurich), Volume 33, No. 7, February, 1899, pp. 59-61 (in German).
- (71) Romualdi, J. P., and Batson, G. B., "Mechanics of Crack Arrest in Concrete," Journal of the Structural Division, Proceedings of ASCE, Volume 89, No. EM3, June, 1963, pp. 147-168.
- (72) Sewell, J. S., "A Neglected Point in the Theory of Concrete-Steel," Engineering News, Volume 49, No. 5, January, 1903, pp. 112-113.

- (73) Slate, F. O., and Olsefski, S., "X-Rays for Study of Internal Structure and Microcracking of Concrete," ACI Journal, Proceedings Volume 60, No. 5, May, 1963, pp. 575-588.
- (74) Smith, R. B. L., "Interaction of Moment and Shear on the Failure of R. C. Beams Without Web Reinforcement," Civil Engineering and Public Works Review (London), Volume 61, Part 1, No. 719, June, 1966, pp. 723-725, Part 2, No. 720, July, 1966, pp. 869-872, and Part 3, No. 721, August, 1966, pp. 967-970.
- (75) Sozen, M. A., Zwoyer, E. M., and Siess, C. P., "Strength in Shear of Beams Without Web Reinforcement," Bulletin 452, Engineering Experiment Station, University of Illinois, Urbana, 1959.
- (76) Swamy, R. N., "Moment-Shear Interaction in Reinforced Concrete Beams," paper presented to the International Conference on Shear, Torsion and Bond in Reinforced and Prestressed Concrete, India, January, 1969.
- (77) Swamy, R. N., Andriopoulos, A., and Adepegba, D., "Arch Action and Bond in Concrete Shear Failures," Proceedings of ASCE, Volume 96, No. ST6, June, 1970, pp. 1069-1091.
- (78) Talbot, A. N., "Tests of Concrete: I Shear; II Bond," Bulletin No. 8, University of Illinois Engineering Experiment Station, September, 1906, pp. 1-34.
- (79) Talbot, A. N., "Tests on Reinforced Concrete Beams," Bulletin No. 14, University of Illinois Engineering Experiment Station, 1907.
- (80) Talbot, A. N., "Tests of Reinforced Concrete Beams," Resistance to Web Stresses, Series of 1907 and 1908," Bulletin No. 29, University of Illinois Engineering Experiment Station, January, 1909, pp. 1-85.
- (81) Taub, J., Discussion of "Some Implications of Recent Diagonal Tension Tests" by Phil M. Ferguson, ACI Journal, Proceedings Volume 53, No. 12, June, 1957, pp. 1185-1190.
- (82) Taub, J., and Neville, A. M., Discussion of "Strains in Beams Having Diagonal Cracks," ACI Journal, Proceedings Volume 55, June, 1959, pp. 1454-1457.
- (83) Taub, J., and Neville, A. M., "Resistance to Shear of Reinforced Concrete Beams, Parts I and II," ACI Journal, Proceedings Volume 57, No. 2, August, 1960, pp. 193-220, No. 3, September, 1960, pp. 315-336.

- (84) Taylor, R., "Some Shear Tests on Reinforced Concrete Beams Without Web Reinforcement," Magazine of Concrete Research (London), Volume 12, No. 36, November, 1960, pp. 145-154.
- (85) Taylor, R., "Some Aspects of the Problem of Shear in Reinforced Concrete Beams (Parts 1 and 2)," Civil Engineering and Public Works Review (London) Volume 58, No. 682, May, 1963, pp. 629-632, No. 683, June, 1963, pp. 768-770.
- (86) Van der Berg, F. J., "Shear Strength of Reinforced Concrete Beams Without Web Reinforcement, Part I - Distribution of Stresses Over Beam Cross Section," ACI Journal, Proceedings Volume 59, No. 10, October, 1962, pp. 1467-1478. "Part 2 - Factors Affecting Load at Diagonal Cracking," ACI Journal, Proceedings Volume 59, No. 11, November, 1962, pp. 1587-1600.
- (87) Walther, R., "The Ultimate Strength of Prestressed and Conventionally Reinforced Concrete Under the Action of Moment and Shear," Ph.D. Thesis, Lehigh University, Civil Engineering, 1957.
- (88) Walther, R., "Calculation of the Shear Strength of Reinforced and Prestressed Concrete Beams by Shear Failure Theory," Beton-und Stahlbetonbau (Berlin - Wilmersdorf), Volume 57, No. 11, November, 1962, pp. 261-271.
- (89) Watstein, D., and Mathey, R. G., "Strains in Beams Having Diagonal Cracks," ACI Journal, Proceedings Volume 55, No. 6, 1958, pp. 717-728.
- (90) Zwoyer, E. M., and Siess, C. P., "Ultimate Strength in Shear of Simply Supported Prestressed Concrete Beams Without Web Reinforcement," ACI Journal, Proceedings Volume 51, No. 8, October, 1954, pp. 181-200.

APPENDIX I

EXPERIMENTAL WORK

TABLE OF CONTENTS

APPENDIX I

	Page
I.1 THE SIZE OF BEAMS	192
I.2 FORMS FOR BEAMS	194
I.3 CONCRETE MATERIALS	195
I.4 MIXING, CASTING AND CURING OF CONCRETE	197
I.5 DETAILS OF THE REINFORCEMENT	198
I.6 PROPERTIES OF THE REINFORCING STEEL	201
I.7 TESTS OF CONCRETE CYLINDERS	213
I.8 DEFLECTION AND STRAIN MEASUREMENTS	213
I.8.1. Deflection Measurements	213
I.8.2. Strain Measurements	218
(a) Electrical Resistance Strain Gauges on Steel	218
(b) Electrical Resistance Strain Gauges on Concrete	219
(c) Strain Readings with Electrical Resistance Strain Gauges	221
(d) Locations of the Electrical Re- sistance Strain Gauges	224
(e) DEMEC Gauges	227
(f) Measurements with DEMEC Gauges	230
(g) Comparison of Longitudinal Strain Readings from Electrical Resistance Strain Gauges and DEMEC Gauges	232
(h) Summary of Instrumentation on Beams	233

	Page
I.9 TEST ARRANGEMENT AND PROCEDURE	237
I.9.1. Test Arrangement for Beams of Series IA, IB and IC	237
I.9.2. Test Arrangement for Beams of Series IIA	240
I.9.3. Test Arrangement for Beams of Series IIIA	241
I.9.4. Preparation of Beams before Test	241
I.9.5. Test Procedure	244

LIST OF FIGURES

APPENDIX I

Figure		Page
I.1	Secondary Beams of Series IIA	194
I.2	Details of Forms	196
I.3	Typical Stress-Strain Relationships of the Reinforcement (1 inch dia. bars)	210
I.4	Typical Stress-Strain Relationships of the Reinforcement (7/8 inch dia. bars - Beam IB-6)	211
I.5	Typical Stress-Strain Relationships of the Reinforcement (3/4 inch dia. bars)	212
I.6	Standard Gauge Locations	226
I.7 I.8	Loading Arrangement for Series IA, IB and IC	238, 239
I.9	Loading Arrangement for Series IIA - Secondary Beam Loading	242
I.10	Loading Arrangement for Series IIIA - Uniform Load	242
I.11	Loading Pattern for Uniform Load	243

LIST OF TABLES

APPENDIX I

		Page
I.1	The Size of Beams and Beams in Each Series	192
I.2	Details of Reinforcing Bars	200
I.3	Properties of the Reinforcing Steel - Series IA	202
I.4	Properties of the Reinforcing Steel - Series IB	205
I.5	Properties of the Reinforcing Steel - Series IC	206
I.6	Properties of the Reinforcing Steel - Series IIA	207
I.7	Properties of the Reinforcing Steel - Series III A	209
I.8	Compression Test of Concrete Cylinders	214
I.9	Tensile Splitting Test of Concrete Cylinders	215
I.10	Comparison of Compressive and Tensile-Splitting Strengths of Concrete Cylinders	216
I.11	Details of Instrumentation on Beams	234
I.12	Details of Loading Arrangement - Series III A	241

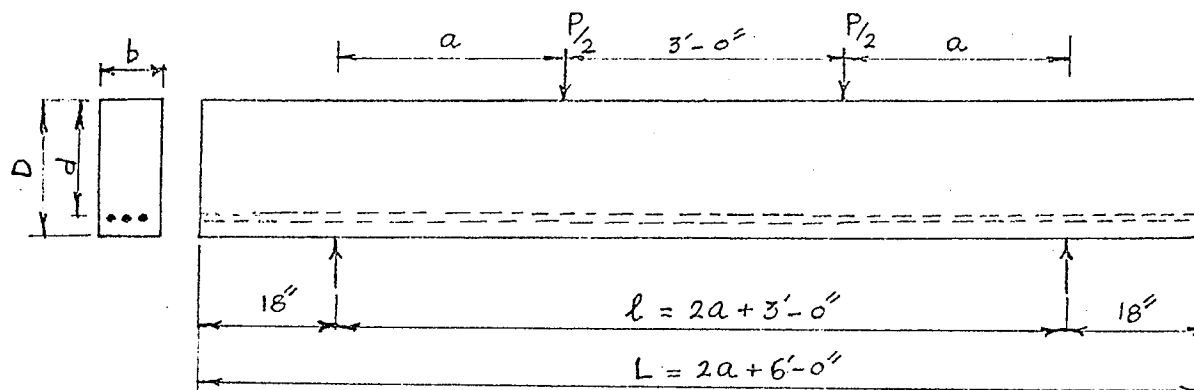
I.1 THE SIZE OF BEAMS

All beams in the test programme were 8 in. x 18 in. in cross-section, with an effective depth of 16 in. to the centre of the reinforcement. The length of the beam varied according to the a/d or l/d ratio. Table I.1 shows the size of the beams. Basically, there were 8 different lengths of the beams, varying from 8 feet 8 in. long to 22 feet long. Series IA comprised of beams of all 8 different lengths as shown in the table. Series IB, IC, and IIIA each comprised a fewer number of beams. These are also shown in Table I.1.

The sizes of the beams in Series IIA were similar to the comparable ones of Series I, except that the beams of this series had secondary beams cast monolithically with the main beam, through which loading was applied.

TABLE I.1

THE SIZE OF BEAMS AND BEAMS IN EACH SERIES



(a) THE SIZE OF BEAMS

$D = 18$ in., $d = 16$ in. and $b = 8$ in. for all beams

BEAM NO.	a/d	a	ℓ	L	REMARKS
1	1.0	1'-4"	5'-8"	8'-8"	Beams with same numbers in different series are of same overall length.
2	1.5	2'-0"	7'-0"	10'-0"	
3	2.0	2'-8"	8'-4"	11'-4"	
4	2.5	3'-4"	9'-8"	12'-8"	
5	3.0	4'-0"	11'-0"	14'-0"	
6	4.0	5'-4"	13'-8"	16'-8"	
7	5.0	6'-8"	16'-4"	19'-4"	
8	6.0	8'-0"	19'-0"	22'-0"	

(b) BEAMS IN EACH SERIES

a/d	ℓ/d	SERIES NO.				
		IA	IB	IC	IIA	
1.0	-	IA-1				
1.5	-	IA-2	IB-2	IC-2	IIA-2, IIA-2(b)	
2.0	-	IA-3				
2.5	-	IA-4	IB-4		IIA-4	
3.0	-	IA-5	IB-5	IC-5		
4.0	-	IA-6	IB-6	IC-6	IIA-6	
5.0	-	IA-7				
6.0	-	IA-8				
-	6.25					IIIA-3
-	10.25					IIIA-6
-	14.25					IIIA-8

The centre lines of the secondary beams were 3 ft. apart (Figure I.1) and they were cast symmetrically about the centre line of the main beam, as shown.

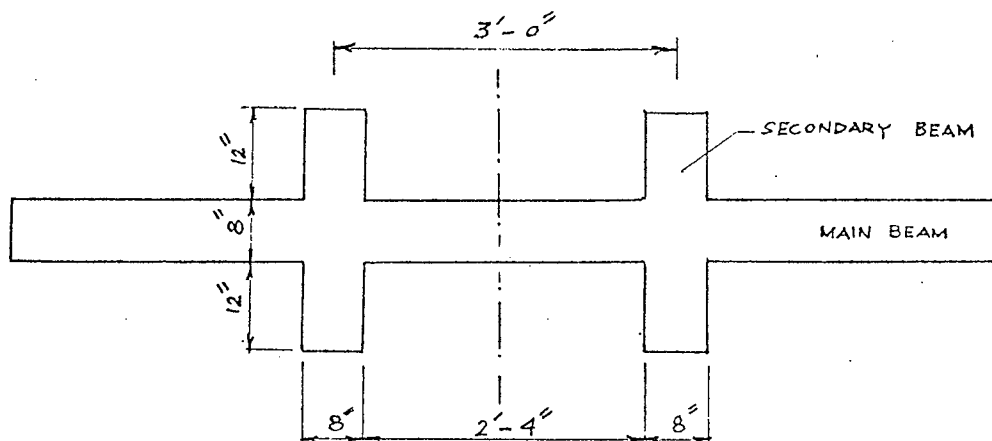


FIGURE I.1 SECONDARY BEAMS OF SERIES IIA

These secondary beams consisted of extensions from the main beam, 8 inches wide, 12 inches long, and of the same depth as the main beam.

I.2 FORMS FOR BEAMS

Eight different forms were required for the whole series. Some of these were reused for similar sizes in different series. Some modifications of the formwork was also necessary for the secondary beams in Series IIA.

Since steel forms were not readily available for the cross-section and lengths required, plywood forms were designed for the

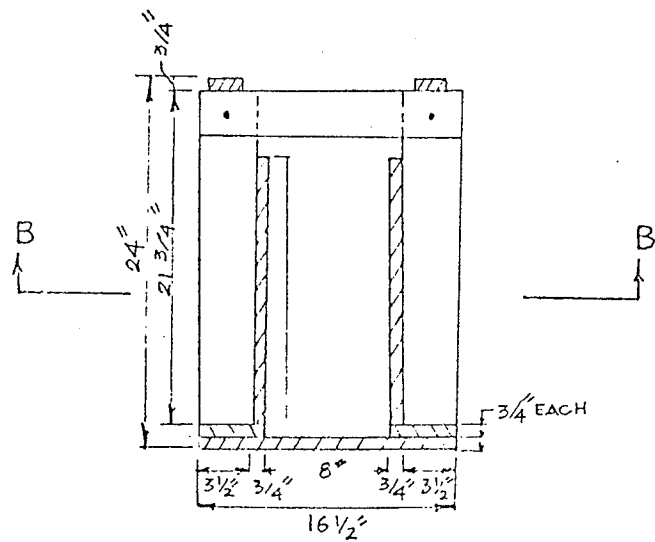
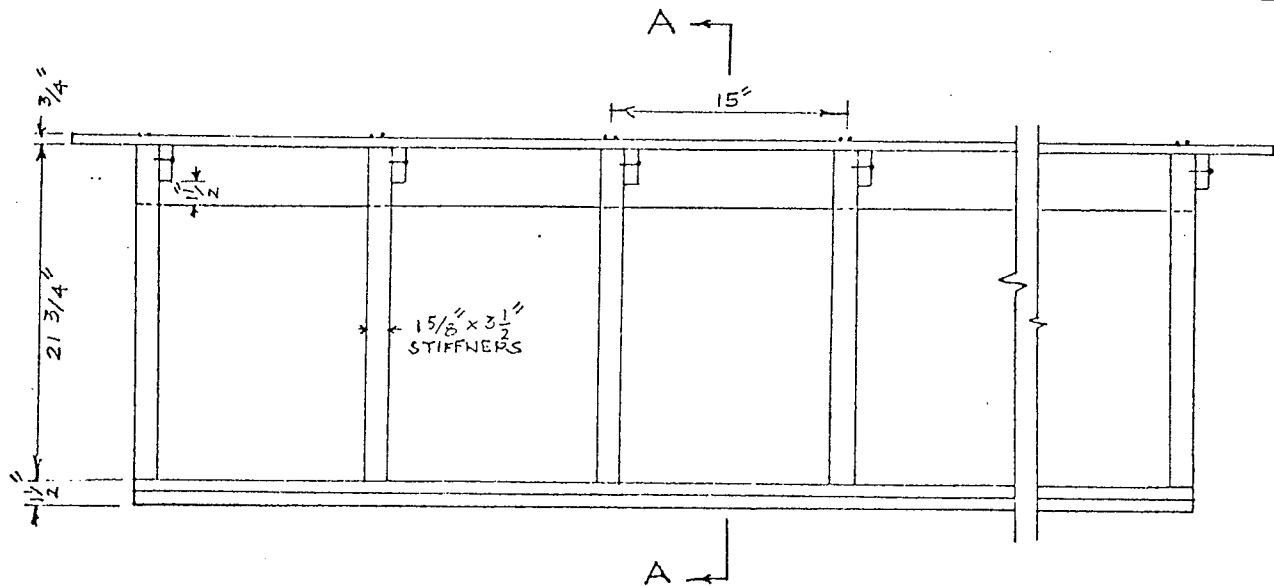
test series. Previous experience of the writer had indicated that a very careful handling of external stiffeners is required for these plywood forms so that the pressures exerted by the concrete during pouring and hardening process do not result in large deformations of the form sides during casting and a lack of uniform width of the final beam along its length.

A detailed sketch of the forms is shown in Figure I.2. The forms were designed for concrete pressures on the sides, taking into account the effect of the use of electrical vibrators during casting. They were also checked for excessive deflections at the time of casting. Three-quarter inch plywood was used both for the base and the sides of the beam with stiffeners spaced at 15 inch intervals.

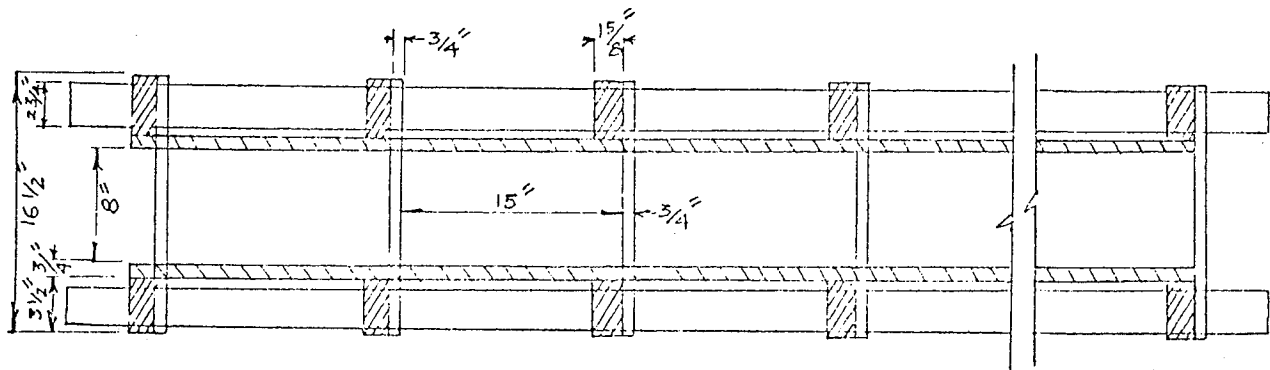
The arrangement shown worked out well for vibrating concrete during pouring, and for screeding the top surface. The widths of the beams measured afterwards were fairly uniform and very close to the required 8 inch width, the average deviation being no more than one-sixteenth of an inch.

I.3 CONCRETE MATERIALS

The cement used throughout the entire series (except for beam IIA-2b), was normal portland cement. Beam IIA-2(b) was cast with high early strength portland cement, obtained from a local supplier. The specific gravity of the cement was 3.13.



SECTION A-A



SECTION BB

FIG. I.2 - DETAILS OF FORMS

The aggregate used in the beams was 3/4 inch maximum size and was generally well rounded. The specific gravity of coarse and fine aggregate was 2.70. The aggregate was quite strong and an examination of the surface of failure in the concrete beams showed that few of these aggregate particles were broken.

The specific gravity of sand and its average fineness modulus were 2.66 and 3.28 respectively.

I.4 MIXING, CASTING AND CURING OF CONCRETE

All concrete was obtained from a ready-mix plant in Winnipeg, with the exception of beam IIA-2(b), which was cast at the laboratory at the end of all other tests. The decision to use ready-mixed concrete was influenced by the fact that rotary mixer in the University concrete laboratory has a capacity of only 3 1/2 cubic feet.

Beam IIA-2(b), which was one of the smallest in length, required about 4 Laboratory batches. This beam was cast with a water-cement ratio of 0.48. The proportions of aggregate, cement and water were weighed out for each mix.

Six inch dia. by twelve inch long control cylinders were cast with each set of beams that were cast at any one time. The specified slump was 2 inches. In actual practice it varied from 1 inch to 3 inches and in one case it reached 5 inches. A slump test was performed for each mix. Before pouring the concrete, the forms were lubricated with oil and the joints closed by two coats of shellac. Concrete was vibrated with an electric vibrator. Care was

taken to see that no segregation took place. The electrical resistance strain gauges on the reinforcement necessitated further care in vibrating the fresh concrete. Though the gauges were rather elaborately protected, there was always the possibility that some of them might be damaged or the leads broken. Even with utmost care, it was found later that 18 of the 244 gauges in the concrete had open connections. Since these gauges could not be replaced, they were lost for the purposes of the test.

As soon as the beams were cast, they were placed under wet burlap at room temperature and covered with a thin plastic cover. They were taken out of the forms about 3 days after casting and were kept covered by wet burlap for about one month. They were then dried and the electrical resistance and DEMEC gauges were placed on them. From this point onwards to the time they were tested (which was from about 75 days to 135 days after casting), they were stored dry at room temperature. The date of casting and the date of test was recorded for each beam. The cylinders were also tested the same day as the beam, both for compressive strength and tensile strength. Standard compressive and split-cylinder tests were used.

I.5 DETAILS OF THE REINFORCEMENT

The longitudinal reinforcement was so placed in the forms that the depth to the centre of the reinforcement for all cases was

16 inches. The reinforcing bars were supported on commercial plastic chairs of 1 1/2 inch height. The sizes of bars used in different series were 1, 7/8 and 3/4 inch dia. respectively. For one inch dia. bars, the chairs gave a 16-inch effective depth directly. For other sizes of bars, small strips were placed below the supporting chairs to get the same effective depth. The chairs were spaced about 3 feet apart to prevent the bars' sagging.

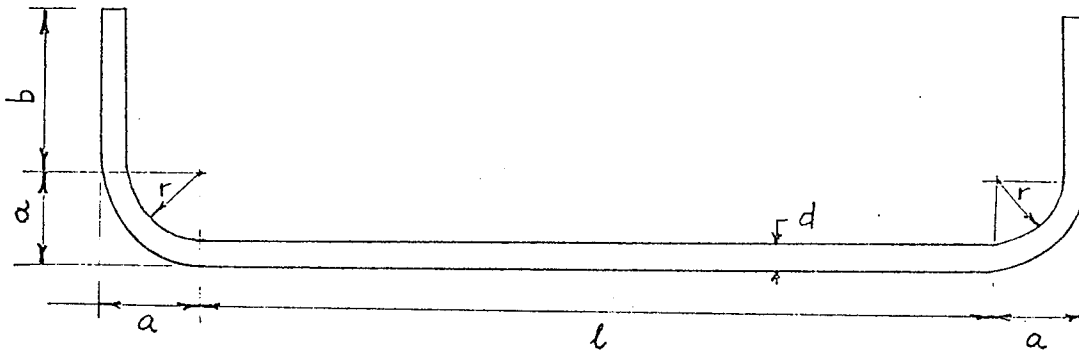
All bars were bent in accordance with the A.C.I. code*. Details of reinforcement are shown in Table I.2. These bars were bent cold and coupons, 2 ft. 6 inches long, from each bar were tested for the strength of steel.

Three reinforcing bars were used in each beam. These bars were placed in one layer, being so spaced across the width as to give a cover of 1 1/2 inches on either side and enough space in between for vibrating the concrete properly.

This main reinforcement was the only reinforcement used in each of the beams except beam IIA-2(b). This beam had additional reinforcement consisting of three one-inch dia. bars in the secondary beams at the top and two 3/8 inch dia. bars at the bottom, supported by one stirrup (3/8 inch dia.) each at the extreme end in the secondary beams. This assured that the short secondary beams would not be sheared off as the diagonal crack entered the secondary beam (as occurred in Beam IIA-2).

* A.C.I. code 1971, clause 7.1.

TABLE I.2
DETAILS OF REINFORCING BARS



BAR DIA. (d) in.	a in.	b in.	r in.	L in.
1	4.0	11.5	3.00	$\ell + 34$
7/8	3.5	10.5	2.50	$\ell + 31$
3/4	3.0	9.0	2.25	$\ell + 26$

NOTE: (1) 'L' is the total length of the bar whereas ' ℓ ' is the length of the straight portion.

(2) $(\ell + 2a)$ was always 4 in. less than the overall length of the beam, giving 2 inch cover on either end.

I.6 PROPERTIES OF THE REINFORCING STEEL

The nominal yield strength of the reinforcement specified for the test series was 50,000 psi.

Details of the physical properties of the reinforcement are given in Tables I.3 to I.7. Except for the beams of the preliminary series of tests (IB-2, 4 and 5), the test results show the yield strength of the reinforcement varying from approximately 49,000 psi to 53,000 psi. Precise values for each beam were obtained by testing coupons of each bar used in the beams. The percentage elongation for an 8 inch gauge length varied from 22 to 25% for the steel used in these beams, showing quite ductile failure. Typical stress-strain relations for 1, 7/8 and 3/4 inch dia. bars are shown in Figures I.3, I.4 and I.5.

The average yield stress for the preliminary series was about 75,000 psi and the elongation only 14% to 15%. It seemed that the supplier had made some mistake in not supplying intermediate grade steel as specified.

TABLE I.3
PROPERTIES OF THE REINFORCING STEEL - SERIES IA
 (1 INCH DIA. BARS)

BEAM NO.	SPECI- MEN NO.	YIELD		ULTIMATE		% Elong- ation	Remarks
		LOAD lbs	STRESS f_y psi	LOAD lbs	STRESS f_u psi		
IA-1	1	39,220	49,962	62,080	79,083	26.0	
	2	39,100	49,809	62,080	79,083	25.0	
	3	39,230	49,974	61,880	78,828	24.0	
	AVERAGE		49,915		78,998	25.0	
IA-2	1	39,430	50,219	62,820	80,025	24.0	
	2	39,360	50,140	62,660	79,822	24.0	
	3	39,340	50,115	62,810	80,013	22.0	
	AVERAGE		50,158		79,953	23.3	
IA-3	1	39,610	50,459	63,020	82,280	25.0	
	2	39,550	50,382	62,930	80,166	24.0	
	3	39,650	50,501	63,030	80,293	24.0	
	AVERAGE		50,447		80,246	24.3	

Table Continued

TABLE I.3 (Continued)

BEAM NO.	SPECI-MEN NO.	YIELD		ULTIMATE		% Elong-ation	Remarks
		LOAD lbs	STRESS f_y psi	LOAD lbs	STRESS f_u psi		
IA-4	1	39,270	50,025	62,670	79,834	22.0	
	2	39,210	49,949	62,820	80,025	24.0	
	3	39,350	50,127	62,920	80,153	24.0	
	AVERAGE		50,034		80,004	23.3	
IA-5	1	39,710	50,586	62,890	80,115	23.0	
	2	39,600	50,446	62,870	80,089	24.0	
	3	39,750	50,637	63,010	80,267	24.0	
	AVERAGE		50,556		80,157	23.7	
IA-6	1	39,580	50,420	63,100	80,382	23.0	
	2	39,560	50,395	63,090	80,369	22.0	
	3	39,210	49,949	62,790	79,987	24.0	
	AVERAGE		50,255		80,246	23.0	

Table Continued

TABLE I.3 (Continued)

BEAM NO.	SPECI-MEN NO.	YIELD		ULTIMATE		% Elong-	Remarks
		LOAD lbs	STRESS f_y psi	LOAD lbs	STRESS f_u psi		
IA-7	1	39,790	50,688	63,080	80,357	22.5	
	2	39,220	49,962	62,970	80,217	22.0	
	3	39,280	50,038	63,060	80,331	24.0	
	AVERAGE		50,229		80,306	22.8	
IA-8	1	39,470	50,280	62,970	80,217	23.0	
	2	39,400	50,191	63,010	80,267	----	The bar broke outside gauge length.
	3	39,320	50,089	62,770	79,962	22.0	
	AVERAGE		50,187		80,149	22.5	

AVERAGE FOR ENTIRE SERIES:

$$f_y = 50,223 \text{ psi}; \quad f_u = 80,007 \text{ psi}.$$

TABLE I.4

PROPERTIES OF THE REINFORCING STEEL - SERIES IB

(7/8 INCH DIA. BARS)

(a) Beams IB-2, IB-4, IB-5 (Preliminary Tests)

SPECIMEN NO.	YIELD		ULTIMATE		% Elongation	Remarks
	LOAD lbs	STRESS f_y psi	LOAD lbs	STRESS f_u psi		
1	44,500	74,167	67,080	111,800	14.0	
2	44,930	74,883	67,020	111,700	15.0	
3	45,720	76,200	67,210	112,017	14.2	
4	44,880	74,800	67,000	111,667	14.0	
5	44,870	74,783	67,110	111,850	15.0	
AVERAGE	$f_y(\text{av.}) = 74,967$		$f_u(\text{av.}) = 111,807$		14.4	

(b) Beam IB-6

TEST NO.	YIELD		ULTIMATE		% Elongation	Remarks
	LOAD lbs	STRESS psi	LOAD lbs	STRESS psi		
1	28,700	47,833	46,300	77,167	22.0	
2	28,800	48,000	46,100	76,833	22.0	
3	28,800	48,000	46,600	77,667	21.0	
AVERAGE	$f_y(\text{av.}) = 47,944$		$f_u(\text{av.}) = 77,222$		21.7	

TABLE I.5
 PROPERTIES OF THE REINFORCING STEEL - SERIES IC
 (3/4 INCH DIA. BARS)

BEAM NO.	SPECIMEN NO.	YIELD		ULTIMATE		% Elong- ation	Remarks
		LOAD lbs	STRESS f_y psi	LOAD lbs	STRESS f_u psi		
IC-2	1	21,600	49,091	34,500	78,409	23.0	
	2	21,600	49,091	34,450	78,295	22.0	
	3	21,600	49,091	34,500	78,409	24.0	
	AVERAGE		49,091		78,371	23.0	
IC-5	1	21,600	49,091	34,050	77,386	22.0	
	2	21,450	48,750	34,000	77,273	22.0	
	3	21,500	48,864	33,950	77,159	24.0	
	AVERAGE		48,902		77,273	22.7	
IC-6	1	21,600	49,091	34,100	77,500	25.0	
	2	21,400	48,636	34,200	77,727	22.0	
	3	21,500	48,864	34,100	77,500	23.0	
	AVERAGE		48,864		77,576	23.3	

AVERAGE FOR ENTIRE SERIES:

$$f_y = 48,952 \quad \text{psi}; f_u = 77,740 \quad \text{psi}$$

TABLE I.6
PROPERTIES OF THE REINFORCING STEEL - SERIES II A
 (1 INCH DIA. BARS)

BEAM NO.	SPECIMEN NO.	YIELD		ULTIMATE		% Elong- ation
		LOAD lbs	STRESS f_y psi	LOAD lbs	STRESS f_u psi	
II A-2	1	40,960	52,178	63,180	80,484	23.0
	2	40,900	52,102	62,950	80,191	24.0
	3	41,100	52,357	62,970	80,217	23.0
	AVERAGE		52,212		80,297	23.3
II A-2(b)	1	40,940	52,153	62,870	80,089	24.0
	2	40,540	51,643	62,660	79,822	23.0
	3	40,570	51,679	63,020	80,280	22.0
	AVERAGE		51,825		80,067	23.0
II A-4	1	40,740	51,898	62,730	80,548	23.0
	2	40,960	52,178	62,840	80,051	23.0
	3	40,940	52,153	62,870	80,089	24.0
	AVERAGE		52,076		80,229	23.3

(Table Cont'd)

TABLE I.6 (CONT'D)

BEAM	SPECIMEN NO.	YIELD		ULTIMATE		%Elong- ation
		LOAD lbs	STRESS f_y psi	LOAD lbs	STRESS f_u psi	
II A-6	1	40,610	51,732	62,360	79,440	24.0
	2	40,630	51,758	62,620	79,771	23.0
	3	40,540	51,643	62,660	79,822	24.0
	AVERAGE		51,711		79,678	23.7

AVERAGE FOR ENTIRE SERIES:

$$f_y = 51,706 \text{ psi}; \quad f_u = 80,068 \text{ psi.}$$

TABLE I.7
PROPERTIES OF REINFORCING STEEL - SERIES III A

(1 INCH DIA. BARS)

BEAM NO.	SPECIMEN NO.	YIELD		ULTIMATE		% Elong- ation
		LOAD lbs	STRESS f_y psi	LOAD lbs	STRESS f_u psi	
III A-3	1	40,530	51,631	62,140	79,159	25.0
	2	40,390	51,452	62,100	79,108	24.0
	3	40,320	51,363	62,260	79,312	24.0
	AVERAGE		51,482		79,193	24.3
III A-6	1	40,610	51,732	62,360	79,440	24.0
	2	40,630	51,758	62,620	79,771	23.0
	3	40,540	51,643	62,660	79,822	24.0
	AVERAGE		51,711		79,678	23.7
III A-8	1	41,230	52,522	62,810	80,013	24.0
	2	41,250	52,548	62,530	79,656	24.0
	3	41,480	52,841	62,870	80,089	23.0
	AVERAGE		52,637		79,919	23.7

AVERAGE FOR ENTIRE SERIES:

$$f_y = 51,943 \text{ psi}; \quad f_u = 79,597 \text{ psi.}$$

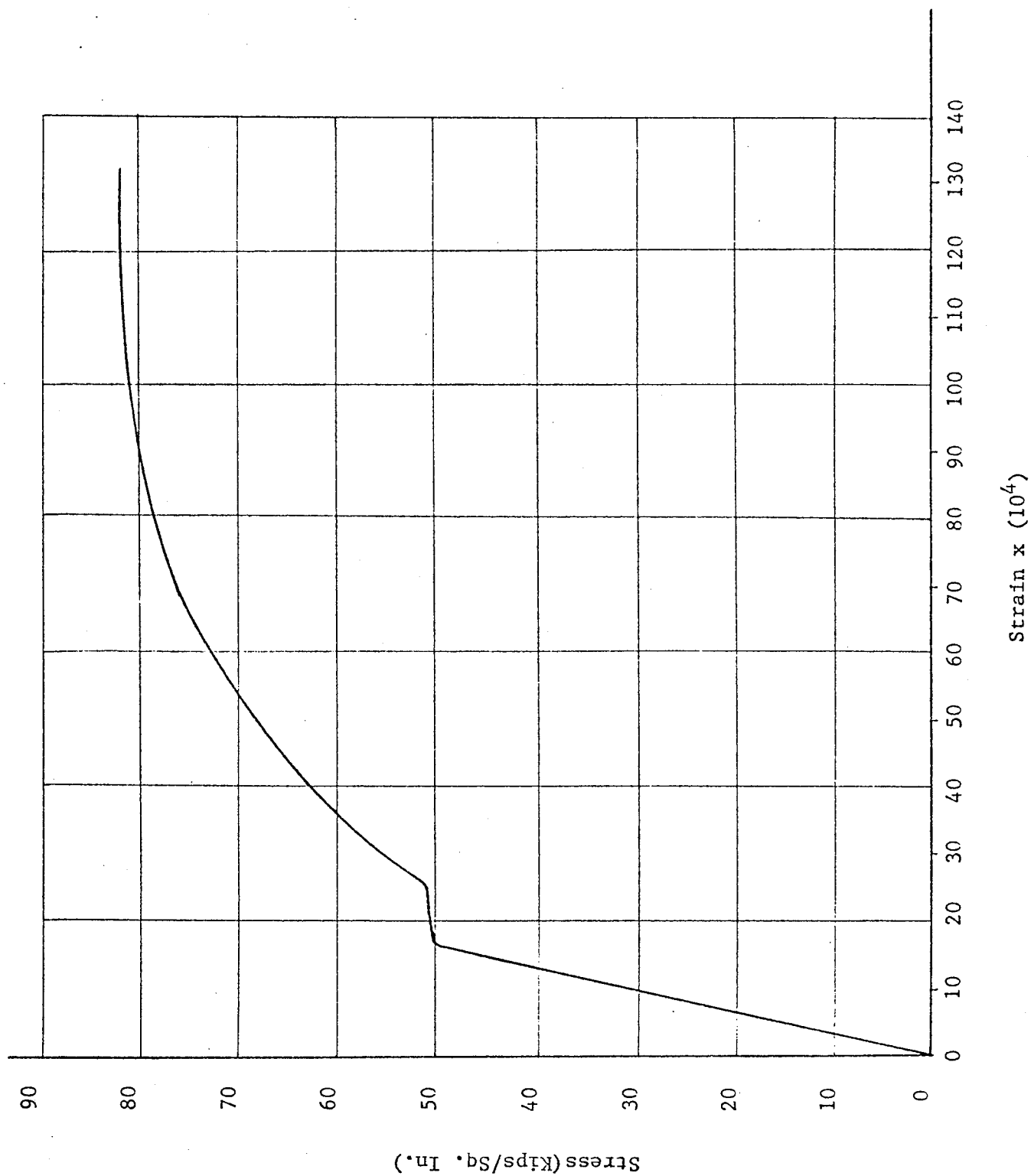


FIG. I.3 TYPICAL STRESS-STRAIN RELATIONSHIPS OF THE REINFORCEMENT (1 INCH DIA. BAPS)

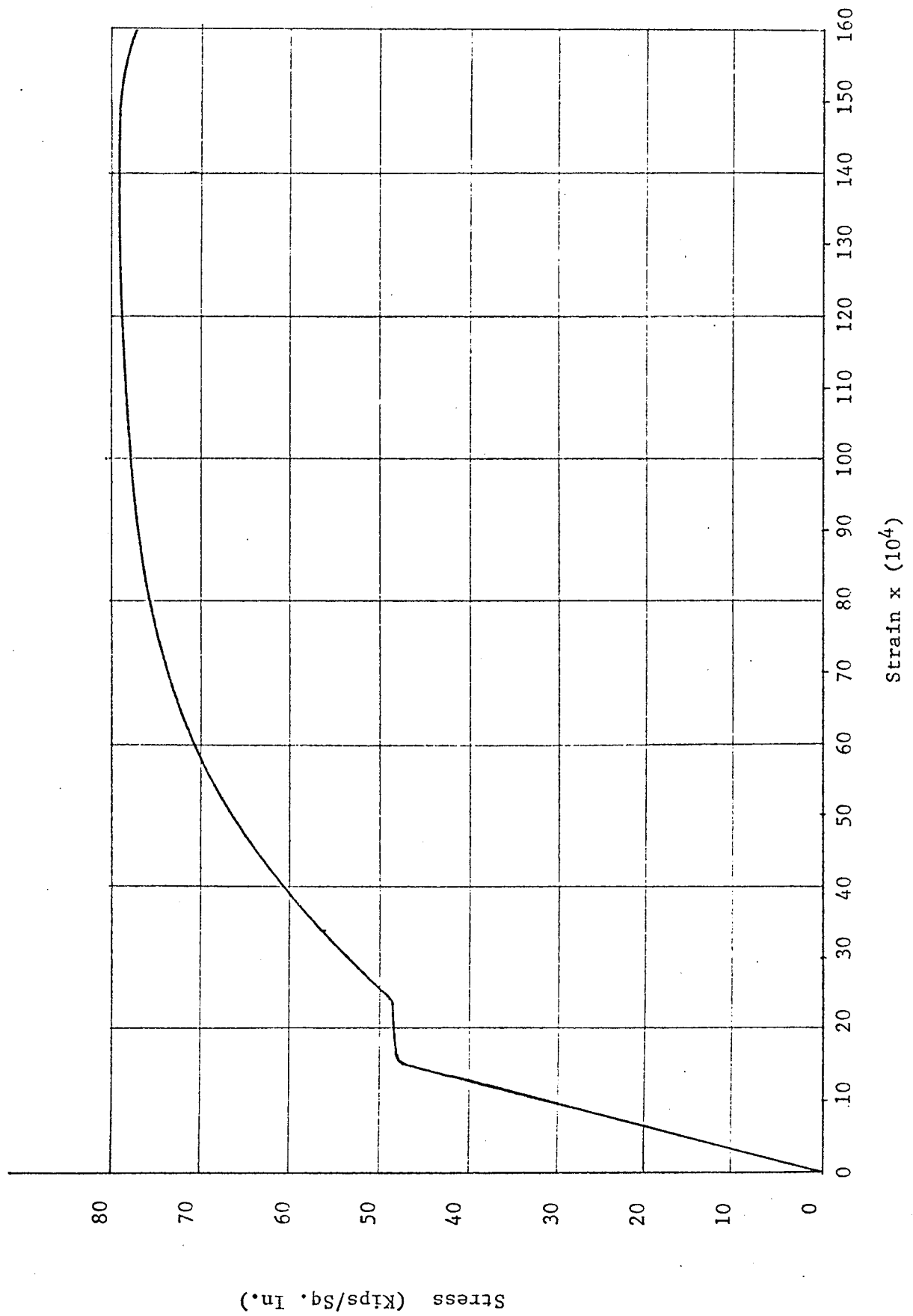


FIG. I.4 TYPICAL STRESS-STRAIN RELATIONSHIPS OF THE REINFORCEMENT (7/8 INCH DIA. BARS - BEAM IB-6)

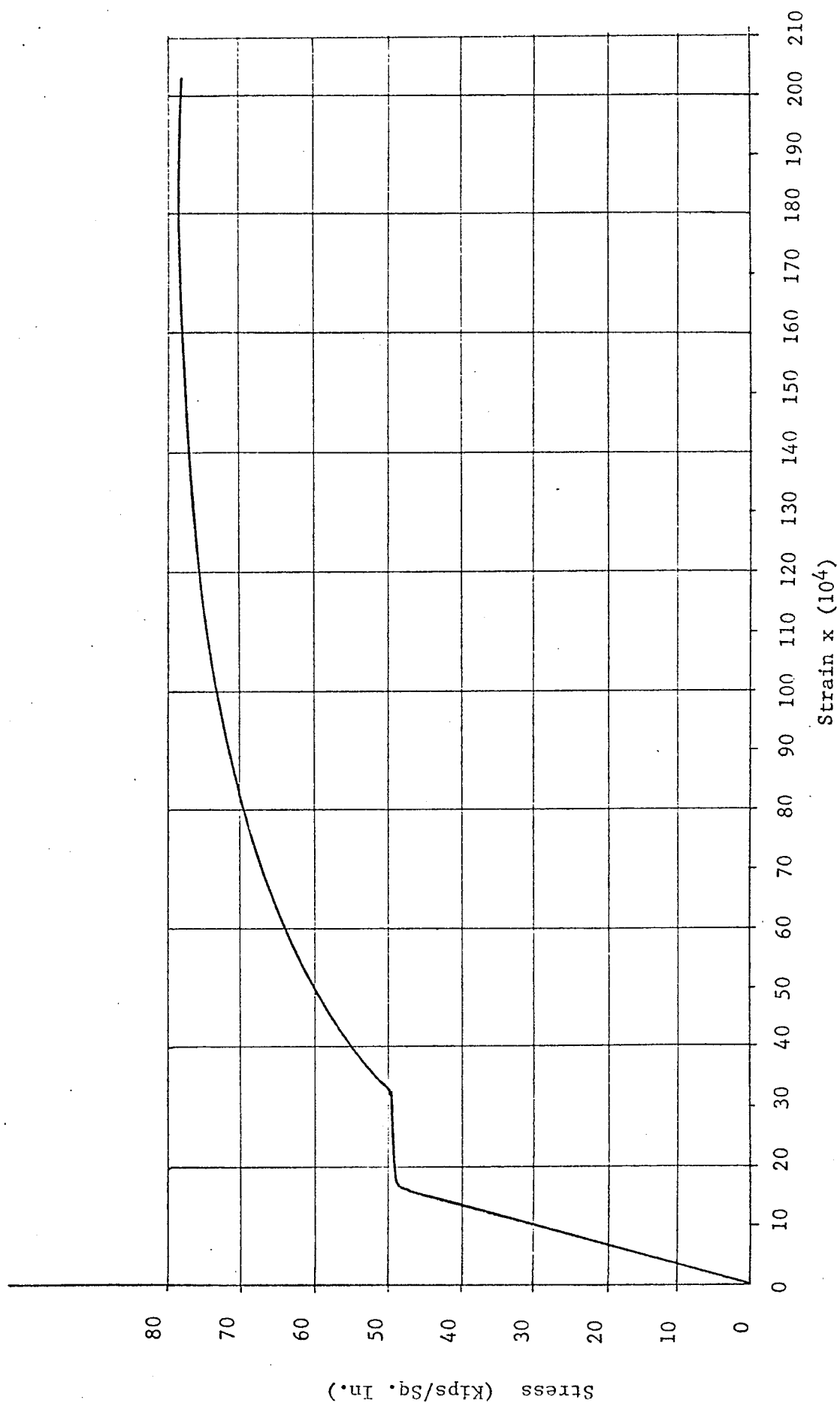


FIG. I.5 TYPICAL STRESS-STRAIN RELATIONSHIPS OF THE REINFORCEMENT (3/4 INCH DIA. BARS)

I.7 TESTS OF CONCRETE CYLINDERS

Test cylinders, six inch dia. by twelve inch long, were cast with all the beams and tested at the same time as the beams. Two tests, uniaxial compression and tensile splitting were performed and an average for each beam was recorded.

Results of these tests are given in Tables I.8 and I.9. The nominal compressive strength for preliminary tests (Beams IB-2, IB-4 and IB-5) was 4,000 psi whereas that for the remaining series was 5,000 psi.

The results show that the compressive strength was generally higher than the nominal values, with only one exception. Cylinders cast with beam IIA-2(b), showed a very high average of 7,334 psi. All the remaining values were within 15% of the nominal strength.

Table I.16 shows that the ratio (f'_t/f'_c) was fairly constant over the entire test programme, the tensile splitting strength being generally around 10% of the compressive strength.

I.8 DEFLECTION AND STRAIN MEASUREMENTS

I.8.1 Deflection Measurement

Deflection readings were taken for most beams both at midspan and under one of the load points. In some beams deflections at midspan only were recorded. These readings were taken with

TABLE I.8
COMPRESSION TEST OF CONCRETE CYLINDERS

BEAMS	NO. OF TESTS	AGE (days)	SLUMP (in.)	COMPRESSIVE STRENGTH (f'_c) psi		
				MAX. f'_c	MIN. f'_c	AVG. f'_c
IA-1, IA-2, IA-3, LA-4 and IB-6	3	92	2.5	5,160	4,920	4,992
	3	93	2.5	4,950	4,850	
	3	94	2.5	5,380	4,810	
	3	102	2.5	4,995	4,850	
IA-5	4	85	2.0	4,645	4,105	4,375
IA-6, IA-7 and IA-8	6	95	1.0	6,155	5,660	5,860
IB-2, IB-4 and IB-5	6	75	5.0	4,350	4,030	4,198
IC-2, IC-5 and IC-6	9	111	2.5	5,525	4,850	5,357
IIA-2, IIA-4 and IIA-6	5	133	2.0	5,245	4,920	5,152
	3	135	2.0	5,595	5,135	
IIA-2(b)	2	15	2.0	7,720	7,610	7,334
	2	16	2.0	7,105	6,900	
IIIA-3, IIIA-6 and IIIA-8	8	126	2.0	5,980	5,635	5,820

TABLE I.9

TENSILE SPLITTING TEST OF CONCRETE CYLINDERS

BEAMS	NO. OF TESTS	AGE (days)	TENSILE SPLITTING STRENGTH (f'_t) psi		
			MAX. f'_t	MIN. f'_t	AVG. f'_t
IA-1, IA-2, IA-3, IA-4 and IB-6	3	92	570	500	511
	3	102	493	485	
IA-5	3	85	442	388	415
IA-6, IA-7 and IA-8	4	95	542	630	566
IB-2, IB-4 and IB-5	3	75	511	480	493
IC-2, IC-5 and IC-6	3	111	529	519	525
IIA-2, IIA-4 and IIA-6	4	133	576	524	547
IIA-2(b)	3	15	750	734	742
IIIA-3, IIIA-6 and IIIA-8	4	126	571	530	546

TABLE I. 10
COMPARISON OF COMPRESSIVE AND TESILE-SPLITTING
STRENGTH OF CONCRETE CYLINDERS

MIX NO.	BEAM NO.	f'_c psi	f'_t psi	f'_t/f'_c %
1	IA-1, 2, 3, 4 ; IB-6	4,992	511	10.4
2	IA-5	4,375	415	9.5
3	IA-6, 7, 8	5,860	566	9.6
4	IB-2, 4, 5	4,198	493	11.7
5	IC-2, 5, 6	5,357	525	9.8
6	II A-2, 4, 6	5,152	547	10.6
7	II A-2 (b)	7,334	742	10.1
8	III A-3, 6, 8	5,820	546	9.4

$$(f'_t/f'_c) \text{ av.} = 10.1\%$$

either a one inch or a two inch deflection gauge, reading to 0.001 in.

The normal procedure adopted for these readings was as follows.

- (1) One reading was taken as soon as the load was increased to the required level. At this stage, strain gauge readings were taken or cracks were marked. Load was not maintained during this period, but decreased slightly.
- (2) The second reading was recorded before the load was increased to the next level. The time period between the two readings as well as the load at the end of the reading was recorded.

The main purpose of the above procedure was to keep the deflection almost constant at each level of loading, even though a small drop in applied load was experienced. This procedure seemed to be desirable because DEMEC gauge readings took considerable time, and it was felt preferable to hold the geometric quantities as constant as possible during reading.

In the preliminary series of tests, no DEMEC gauges were employed. Electrical resistance gauges were read by an automatic digital voltmeter data logger. Since the time period between readings was small, in those preliminary tests the load rather than the deflection was held constant. It was assumed that very little deformation would take place during the automatic reading of the strain gauges.

I.8.2 Strain Measurements

In the preliminary series of tests, only electrical resistance strain gauges were used over one-half span length both on steel and concrete. In the main series of tests demountable mechanical strain gauges (DEMEC) were used in addition to the electrical resistance strain gauges. These were used only on the concrete and over one half of the span, on the same side of the beams as the electrical gauges, but at the opposite end.

(a) Electrical Resistance Strain Gauges on Steel

The strain gauges used on the reinforcing bars of the tests were KYOWA foil strain gauges* of the type KFC-5-C1-11, having a gauge length of 5 m.m. and a gauge factor of 2.11.

At each gauge location, both top and bottom of the reinforcing bar, a length of 10 to 15 m.m. was filed to a completely smooth finish, eliminating the deformations.

The smooth surface was then cleaned with acetone and the gauges were glued on with the recommended gauge cement and held in place until the adhesive had cured. Strain gauge terminal points were then affixed, allowed to cure for 12 hours and the output leads from the strain gauge to the terminal points soldered into position. The gauges and leads were then carefully waterproofed with synthetic

* KYOWA (JAPAN)

rubber and silicone sealant.

After the gauges were waterproofed, their leakage resistance was checked. A minimum gauge resistance of 120×10^6 ohms was considered to be adequate.

The bars, with gauges affixed, were then immersed in water for two days and checked for resistance again to see whether the waterproofing was satisfactory. Faulty gauges were removed and replaced.

Despite all the above precautions, only about 80% of these gauges functioned satisfactorily. Some of these gauges had open connections after casting, the lead wires having been broken probably during the vibration of concrete. Others had insufficient resistance or showed erratic, unstable readings. These gauge-readings were not considered in analysis. As might be expected, the percentage of gauges that worked well increased in the latter part of the work, indicating the effect of the experience gained.

(b) Electrical Resistance Strain Gauges on Concrete

Due to the heterogeneous nature of concrete and presence of large aggregate particles, it is not possible to obtain accurate or reliable strain values with a small gauge length. It becomes necessary to use larger gauge lengths and to consider the average strains at the points.

Several investigations* have suggested that the gauge

* BINNS and MYGIND (1949); HOGNESTAD and VIEST (1950) and COOKE and SEDDON (1956).

length should be at least 3-4 times the maximum size of the aggregate used. The maximum size of the aggregates in this test series was three-quarter inch or about 19 m.m. Thus the appropriate size of the electrical resistance gauges for concrete becomes from 57 m.m. to 76 m.m. For the entire test programme, 67 m.m. foil gauges manufactured by KYOWA (Japan) (type KC-70-A1-11), having a gauge factor of 2.13, were used. These gauges are especially recommended for applications on concrete and appeared to give reasonably good results.

Two to five rosettes of these gauges were also used on each beam except beams of the preliminary series. These rosettes were made out from the 67 m.m. gauges by placing one gauge horizontal at the point, one vertical and a third one at 45° angle between the previous two gauges.

The gauges were applied on the surface of concrete in the following manner.

After the surface of concrete was smoothened with sand paper around the area the gauges were to be applied, the area was washed with acetone to clean out all the dust particles, and remove any traces of grease or oil. A layer of adhesive was applied to the concrete to fill any surface voids, allowed to cure, and then the gauges affixed carefully. Air bubbles were rolled out from under the gauge using gentle pressure from the thumb, and then the gauge was held in position until the adhesive had cured. Terminal points were then affixed, and the leads from the gauges connected.

(c) Strain Readings with Electrical Resistance Strain Gauges

The strains were measured through the Scanner Unit of the Department's Hewlett Packard Data Acquisition System. This unit can accommodate 300 pair input through 25 connectors, each having a 12 wire cable. This data acquisition system works automatically (or manually), switching on one line after the other, thus giving one reading at a time. The data system, includes a voltmeter which converts the "out of balance" voltage of each strain gauge bridge into digital form. These readings have then to be converted to appropriate readings of strain.

Two terminal boxes, each accommodating 24 active and dummy gauge wires, were especially constructed for the test series. These boxes could accommodate the maximum number of gauges that were used on any beam through the entire series. A dummy or temperature compensating gauge was connected into each box for every active gauge. Since, ideally, dummy gauges should be under exactly the same thermal conditions as the active gauges, the gauges on another beam were used as dummy gauges for the beam under test. For gauges on the reinforcing bars, dummy gauges were placed on a separate steel plate.

Some studies were also made to check zero drift and to determine the most stable resistors to be used in the permanent arms of the electrical bridge used. The best resistors that could be obtained locally

indicated an unacceptably high drift over a period of a few hours (the duration of the tests) and over a period of two weeks. It was finally decided to use Japanese resistors (KYOWA), which performed very well over a four-hour period and a one week period. These resistors were mounted in the gauge box on a piece of steel, and covered with styrofoam insulation.

All connections were checked before the start of the test and it was ascertained that there were no "cold" or "short" connections (either in the soldering at the terminal points or in the gauge boxes) and that the connections were made to the correct gauge number. This last factor was checked by checking each gauge on the digital voltmeter by noticing change of voltage reading as each gauge was pressed carefully with the thumb. Those gauges which had open connections on steel as well as those which had large zero drifts were noted for future reference before the start of the test.

A six-volt battery was used to apply the circuit voltage. The battery was charged for 4 to 5 hours the day preceding each test. The scanner unit of the Hewlett Packard data acquisition system was also warmed up for a period of half an hour before each test.

Strain readings were recorded at 2,500 pound load intervals for most of the beams. In some cases readings at 2,000 or 5,000 pound intervals were also made, depending upon the expected ultimate load. In a few cases, the reading interval was reduced to 1,000 pounds at critical stages of loadings.

As already mentioned, the data acquisition system gave readings of voltage at each load level and they were converted to direct strain by the relationship,

$$\text{Strain} = \frac{\Delta V}{V} \cdot \frac{4}{GF}, \text{ where}$$

ΔV = Voltage difference between load reading and the zero load reading of the same gauge.

V = Battery voltage.

GF = Gauge factor, 2.11 for steel and 2.13 for concrete.

Ideally the value of battery voltage should be constant. However there was usually a difference of a few micro-volts between its readings at the beginning and end of the test. In the conversion equation, the value of V was that actually recorded at each load level.

When a crack passes through an electrical resistance strain gauge, the gauge usually breaks and is lost for the remaining part of the test. However, when the crack passes very close to the gauge or the crack passes through the gauge but is so small that the gauge does not break, the reading obtained gives very large strains compared to the strains at the previous load level. This reading was not interpreted as the average strain at that point, but rather as a measure of the crack width and very localized strains. This interpretation is further supported by results which showed that in many cases the gauge gave a large strain reading before breaking at the next load level. Such high strain readings must therefore be interpreted with extreme caution.

Despite all the precautions, and care taken in preparing the specimens and taking the readings, a few of the readings were out of line with the general trend, due to undetected loose connection problems, drift in gauge resistances, etc. Such readings were ignored in the interpretation of test results.

In beams of series IA, IC, and beam IB-6, electrical resistance strain gauges on the compression face of the beam at all locations except under the load point were applied over the top surface of the beam, whereas in all other cases the gauges were on the side of the beam, very close to the top edge. Since the top surface was rough, a layer of epoxy was applied at each gauge location, allowed to dry, and then the gauges were placed with the gauge cement over the epoxy surface. It was found, however, during the tests that all gauges in such a location gave erratic results. It is suspected that the laitance on the concrete surface became loose under load, and the gauges affixed to this laitance were not capable of giving meaningful results. The results obtained from these poorly affixed gauges were also discarded.

(d) Locations of the Electrical Resistance Strain Gauges

In the preliminary series of tests, the locations of the gauges differed slightly from the rest of the series. Gauge numbers and precise gauge locations for each of these beams are indicated along with the material on experimental results in Appendix II.

The following points may be noted, about the general location of the electrical resistance strain gauges (excluding the preliminary series of tests).

(1) Electrical resistance strain gauges were placed on only one half span of the beams, at six different vertical sections, a, b, c, d, e, and f, respectively (Figure I.6a);

(a) Section a was directly over the support, while section f was at midspan;

(b) Section c was at the "midshear" span and section e under the load point for beams with concentrated loads,

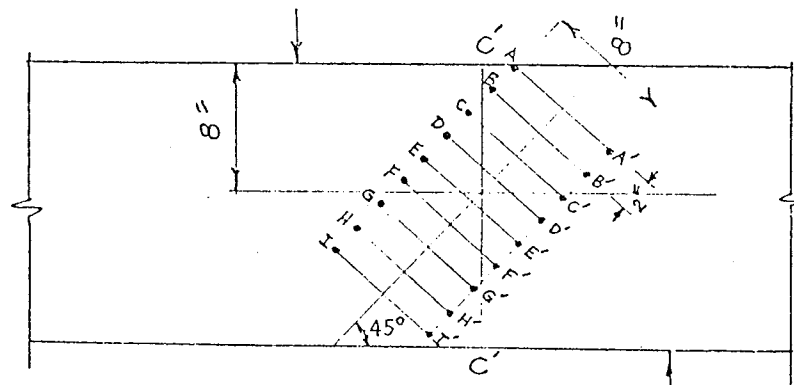
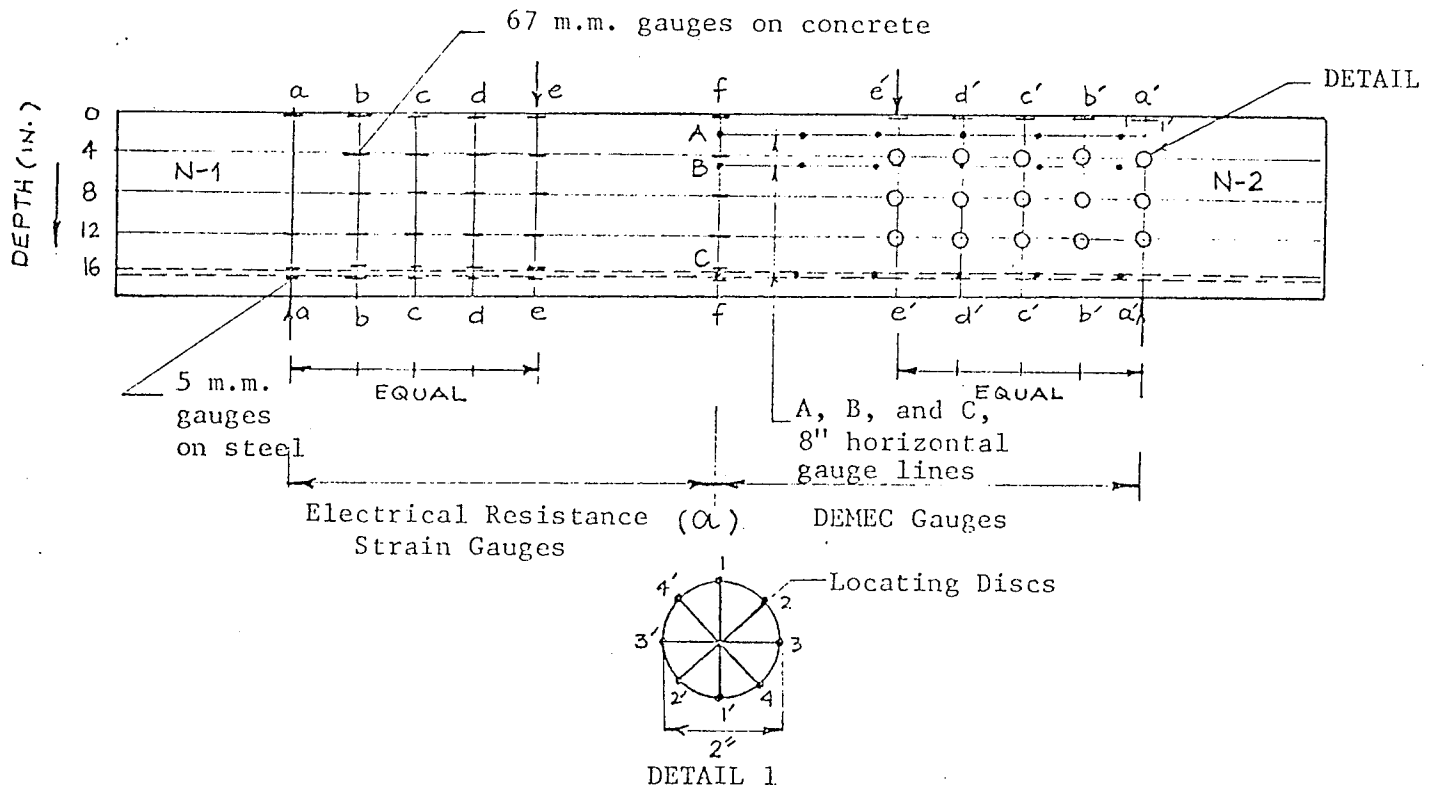
(c) Section b was at midpoint between sections a and c. Similarly section d was at midpoint between sections c and e;

(d) Sections b, c, d and e for uniformly distributed loads were the corresponding equivalent locations;

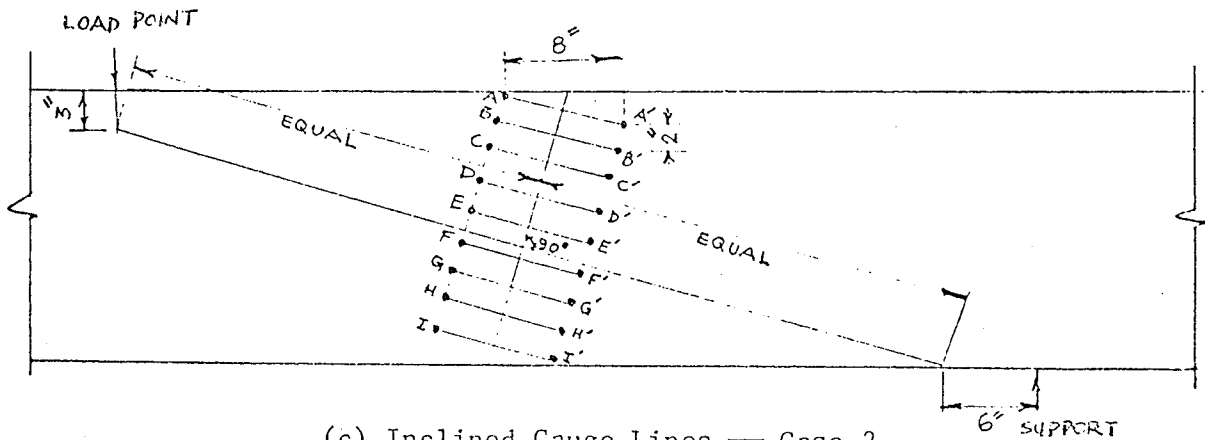
(2) On the concrete surface gauges were placed at 0 in., 4 in., 8 in., and 12 in. (or 0, $d/4$, $d/2$, and $3d/4$ inches, where d is the effective depth of the beam) below the top surface of the beam.

As mentioned before, gauges on the steel reinforcement were placed on one of the three reinforcing bars only, at both the top and the bottom surfaces of the bar.

In beams of Series IIA, which included secondary beams, gauges on the concrete at section e could not be placed on the main beam. For these beams, gauges were placed at special sections e_1 and e_2 , the details of which can be seen from the data of individual beam tests in Appendix II.



(b) Inclined Gauge Lines — Case 1.



(c) Inclined Gauge Lines — Case 2.

FIG. I-6 STANDARD GAUGE LOCATIONS

(e) DEMEC Gauges*

DEMEC gauges were used only on concrete surfaces and on all of the beams of the series except the preliminary set of beams. They were used on the second half of the beam, on the same side as the electrical resistance gauges. This side was called N1 - N2, and the electrical gauges were placed on the end N1 and the DEMEC gauges on the end N2 of the beam. (The only exception was beam IIIA-8, where the gauges were placed on side S1 - S2 of the beam, the electrical resistance strain gauges being on the end S1 and the DEMEC gauges on end S2).

Three types of measurements were made with DEMEC gauges.

(i) Horizontal Gauge Line Measurements (Figure I.6a)

At vertical locations 2 in., 5 in., and 16 in. below the top of the beams, (signified by letters A, B, and C) and from the vertical section of symmetry at midspan to the beam supports, measurements were made on 8 in. gauge lines. For beams of Series IIA these measurements were not made due to the presence of the secondary beams. Location of these gauges are shown on plots of each beam in Appendix III.

(ii) Inclined Gauge Line Measurements (Figure I.6b and c)

Inclined gauge lines for an 8 in. gauge length were

* Refer to the work of MORICE (1953) and BASE (1955).

established as follows:

CASE 1 For short beams (a/d upto 2.5), the centre line of gauge length was marked at 45° at the point of intersection of midshear span and mid-depth of the beam. 8 in. gauge lines were then laid out at 2 in. intervals from the top (Figure I.6b).

CASE 2 For longer beams, a point was marked six inches from the support and another 3 inches below the load point. These two were joined by a line. A line perpendicular to this line at its centre was taken as the centre line of the gauge lines which extended from the top to the bottom of the beam (Figure I.6c).

For beams with a/d ratio of 5 or 6, these measurements were not made.

Corresponding locations were used for beams with uniformly distributed loads. Locations of inclined gauge lines for individual beams are shown with plots of inclined gauge line data in Appendix III.

(iii) DEMEC Rosettes and Longitudinal Strain Readings at the Compression Face of the Beams (Figure I.6a)

The locations of these sections corresponded exactly with those for the electrical resistance strain gauges. The locations were distinguished by using a' , b' , etc. for vertical sections instead of a , b , etc. as for the electrical resistance strain gauges. The only difference was that readings at midspan were not taken

with DEMEC gauges. A 2 in. gauge length was used for these readings. At the compression face, readings were taken of the longitudinal strain only (See Figure I-6a). The reading is labelled 1-1' (at zero depth from top) in the experimental results of beams. At all other locations, four readings in a rosette, 1-1', 2-2', 3-3' and 4-4', were taken to give a complete strain field. Reading 3-3' at each rosette location and 1-1' at compression face only give the longitudinal strains directly.

Two inch and eight inch DEMEC gauges were used in the investigation. The gauge factors for each were 2.49×10^{-5} and 1.00×10^{-5} respectively.

Strain was calculated from the DEMEC readings using the expression:

$$\epsilon = GF (Rdg_i - Rdg_o)$$

where GF is the gauge factor,

Rdg_i is the gauge reading at the i th increment

and Rdg_o is the initial gauge reading.

The locating discs required for these gauges were attached to the concrete surface using polymethylene thacrylate resin and hardner in specified proportions. The discs were pressed firmly on the surface of the concrete and the exact gauge distance between points was set with the standard measuring points on an invar setting bar.

(f) Measurements with DEMEC Gauges

Various factors influenced the accuracy of readings made with DEMEC gauges and are discussed in this section.

(1) Importance of Zero Load Readings

In calculating strains, the readings at all load levels were subtracted from the zero load readings, as discussed above. Thus, if an inaccuracy were to exist in the zero load reading at any point, the entire set of results for that point would be affected. Particular care in recording zero load readings was therefore necessary. In many cases, the zero load reading was taken twice and the average of the two was recorded as the reading. It was observed that it was quite possible for readings to differ by one division of the scale (equivalent to a strain of 0.25×10^{-4}), if the same reading were taken by different persons or at different times.

(2) Temperature Effects

The influence of the temperature change on the gauge was found by taking readings periodically on the standard invar bar. In most of the cases no corrections were required for temperature within the range of precision attainable with the gauges.

A second problem associated with temperature is that of the thermal expansion of the concrete during the period of the test. Tests lasted from 4 to 5 hours and although the temperature of the lab where the testing was done was not thermostatically controlled, no temperature corrections due to this effect have been made to the results, as it was

estimated that minor temperature changes within a period of 4 to 5 hours would not be significant.

(3) Non-Uniformity of Concrete Strains

The work of COOK and SEDDON (1956) indicated that local variations in the strains due to the difference in the elastic properties of the material within the concrete may cause some error. This is particularly applicable to concrete where larger aggregate particles are embedded in the matrix of mortar. The error has been estimated to be as high as 10 per cent with a 2 in. DEMEC gauge. No systematic correction is possible in this case.

(4) Positioning of Locating Discs

The effective gauge length during measurements is the distance between the centroid of the area of the adhesive attaching the locating discs to the specimen. This effective length may be different from that set-out with the standard invar bar. However, the error associated with it is estimated to be very small. It is also an error which cannot be compensated for in a systematic manner.

(5) Location of the Gauge Points

Horizontal, vertical and inclined gauge readings were taken, as mentioned earlier, and it was observed that an accurate reading requires the instrument to be truly normal to the gauge points being read. Further, it was found that if the observer rested his hands on the beam he was in a position to hold the gauge more steadily. Since the strains measured remained small compared to the gauge's

minimum resolution, small variations of readings were rather significant. It was generally observed that greater reliance could be placed on the horizontal gauge readings rather than those in a vertical or inclined position. A further problem stemmed from the fact that the vertical strains were generally quite small and sometimes they remained almost zero throughout the loading range.

(6) Effect of Crack Locations

Location of cracks significantly influenced the strain readings, either when the crack passed very close to the measuring points or between them. It was therefore important that crack locations were recorded, in order that crack widths could be separated from the genuine strains, in interpreting raw strain data.

(7) Errors of Reading the Gauges

If the gauge readings were read by different observers during the test, there was a possibility of observational error. This difference between observers was eliminated by having readings taken by the same observer throughout any one test. All zero load readings were taken at the start of the test and therefore include the self weight of the beams and that of the loading-arrangement. This total weight remained less than 1000 pounds in all cases.

(g) Comparison of Longitudinal Strain Readings from Electrical Resistance Strain Gauges and DEMEC Gauges

The electrical resistance strain gauges and the DEMEC gauges were placed at symmetrical locations on the two halves of the beam. Some differences in comparative readings are to be expected since concrete is not a homogeneous material like steel or glass and the strain

distribution on both halves cannot be expected to be identical. Besides, one of the very important aspects in the strain reading of a particular gauge in this study was the location of the major and minor cracks relative to the gauge location. The profile of the cracks on the two halves of the beams were generally similar, but contained important local differences. It was anticipated therefore that DEMEC and electric resistance strain gauge readings could be compared qualitatively, but not quantitatively.

Flexural cracks on the two halves of the beams were relatively more uniform in distribution than diagonal cracks. Therefore, in diagonal tension failures, the comparative gauge readings might be expected to be closer to one another. Detailed crack profiles for each beam along with the gauge locations are given in Appendix II.

(h) Summary of Instrumentation on Beams

A summary of the instrumentation on beams is given in Table I.11. In Appendix II, the detailed location of gauges on each beam is shown along with their results. The precise location of horizontal and inclined gauge lines are shown in Appendix III on the plots of results from these gauge lines.

TABLE I.11

DETAILS OF INSTRUMENTATION ON BEAMS

SERIES	BEAM NO.	ELECTRICAL RESISTANCE STRAIN GAUGES ON:		DEMEC GAUGES		
		CONCRETE (1) (Gauge Nos.)	STEEL (1) (Gauge Nos.)	HORIZONTAL GAUGE LINE (2)	INCLINED GAUGE LINE (2)	ROSETTES AND GAUGES ON COMPRESSION FACE (3)
IA	1	1-20	21-28	S ⁽³⁾	CASE A ⁽⁴⁾	S ⁽³⁾
	2	1-28	29-40	S	CASE A	S
	3	1-26	27-38	S	CASE A	S
	4	1-28	29-40	S	CASE A	S
	5	1-31	32-43	S	CASE B	S
	6	1-27	28-39	S	CASE B	S
	7	1-25	26-37	S	-----	S
	8	1-25	26-37	S	-----	S

Table Continued

TABLE I.11 (Continued)

SERIES	BEAM NO.	ELECTRICAL RESISTANCE STRAIN GAUGES ON:		DEMEC GAUGES		
		CONCRETE (1) (Gauge Nos.)	STEEL (1) (Gauge Nos.)	HORIZONTAL GAUGE LINE	INCLINED (2) GAUGE LINE	ROSETTES AND GAUGES ON COMPRESSION FACE
IB	2	1-5	-----	--	-----	--
	4	1-25	26-35	--	-----	--
	5	1-25	26-35	--	-----	--
	6	1-29	30-41	S	CASE B	S
IC	2	1-20	21-32	S	CASE A	S
	5	1-28	29-40	S	CASE B	S
	6	1-27	28-39	S	CASE B	S
	2	1-26	27-38	--	CASE A	*(5)
II A	2 (b)	1-26	27-38	--	-----	*
	4	1-28	29-40	--	CASE A	*
	6	1-31	32-43	--	CASE B	*

Table Continued

TABLE I.11 (Continued)

SERIES	BEAM NO.	ELECTRICAL RESISTANCE STRAIN GAUGES ON:		DEMEC GAUGES		
		CONCRETE (1) (Gauge Nos.)	STEEL (1) (Gauge Nos.)	HORIZONTAL GAUGE LINE	INCLINED (2) GAUGE LINE	ROSETTES AND GAUGES ON COMPRESSION FACE
III A	3	1-28	29-40	S	CASE A	S
	6	1-27	28-39	S	CASE B	S
	8	1-25	26-37	S	-----	S

- (1) Locations of electrical resistance strain gauges are given in Appendix II.
- (2) Horizontal and inclined gauge lines are shown on plots of individual beams in Appendix III.
- (3) S = Standard Location as shown on Fig. I.6.
- (4) CASE A and CASE B as shown on Fig. I.6(b) and (c).
- (5) * See Appendix II.

I.9 TEST ARRANGEMENT AND PROCEDURE

The beams were loaded by a 200,000 - pound maximum capacity hydraulic jack in a 200-ton Universal test frame. The jack was calibrated before the test programme and also checked again during the testing programme.

I.9.1 Test Arrangement for Beams of Series IA, IB and IC

The test arrangement for beams of series IA, IB, and IC is shown in Figure I-7 and Figure I-8.

On one side, the beam was supported on a roller to allow rotational movement with longitudinal restraint. On the other end of the beam an additional set of rollers were used so that both longitudinal and rotational movements could take place. The beam was supported by plates at both supports and was centred carefully over the loading head of the frame.

Load was applied at two points, three feet apart. The centre lines of these points were carefully marked and a 1/4 in. layer of plaster of paris was applied over the area to be covered by loading plates to ensure uniform contact. The plates and rollers were then placed as shown in Figure I-7 with a short, stiffened I-beam over the top of the rollers. The short beam distributed the load which was applied through an 8 in. load cell placed directly under the loading head of the jack. Rollers were also placed under the load cell. The test beam, the load cell and the loading head of the jack were aligned carefully. The loading scheme

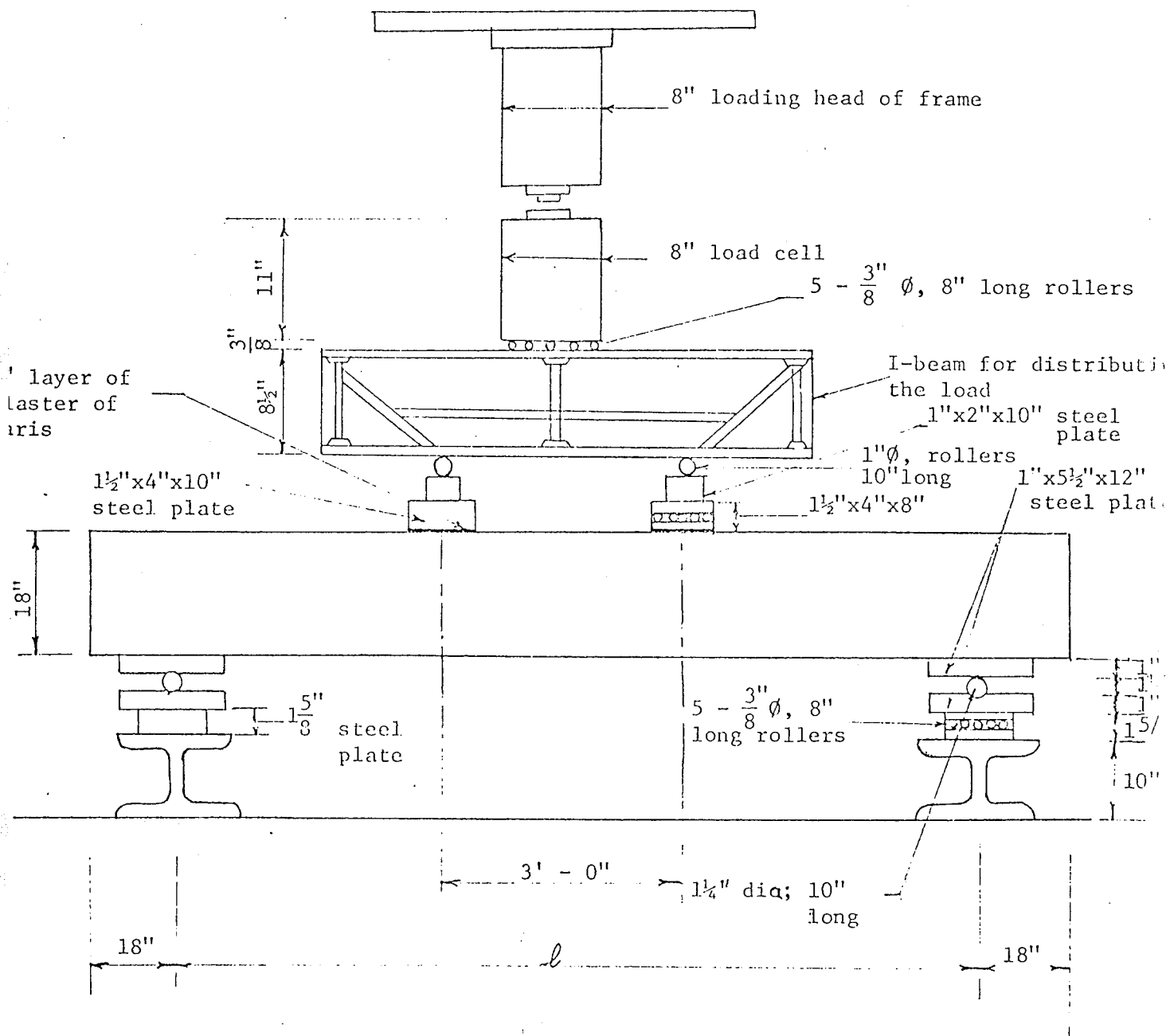


FIG. 1.7 LOADING ARRANGEMENT FOR SERIES IA, IB AND IC

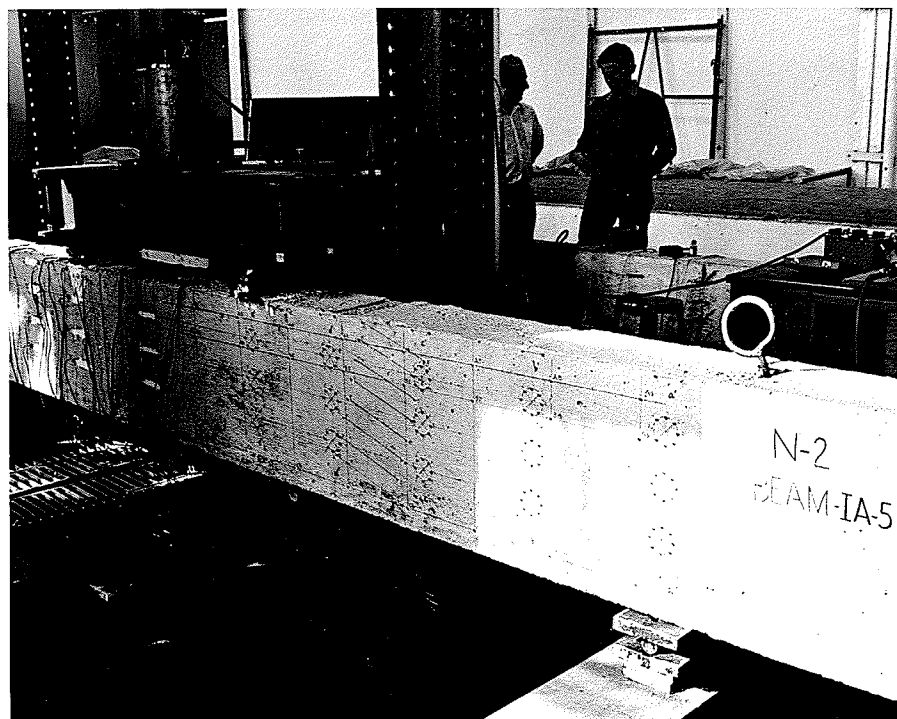


FIG. I-8 LOADING ARRANGEMENT FOR SERIES IA, IB AND IC

chosen was assumed to provide negligible parasitic restraint.

I.9.2 Test Arrangement for Beams of Series IIA

The test arrangement for series IIA, where the main beam was loaded through the secondary beams, is shown in Figure I-9. The arrangement of the support plates and rollers was similar to that described in the preceding section for the beams of series IA, IB and IC. The load was applied at the centre of the secondary beams, which projected 12 inches from the main beam. The transverse centre lines of the half-loads at each longitudinal loading section were therefore 20 inches apart, since the main beam itself was 8 inches wide. Parasitic restraints on this secondary beam were minimized by the use of appropriate rollers.

I.9.3 Test Arrangement for Beams of Series III A

Uniformly distributed loads in this series were simulated by eight equally spaced concentrated loads, since the bending moment diagram for a uniform load and eight concentrated loads is very similar in shape. The general arrangement for the tests of this series is shown in Figure I-10 and a diagram of the loading arrangement used is shown in Figure I-11. The dimensional details are given in Table I-12.

TABLE I-12 DETAILS OF LOADING ARRANGEMENT - SERIES III A

BEAM NO.	SPAN LENGTH	DISTANCE " b "	PLATES			I-BEAM		TOP I-BEAM	
			Level 1	Level 2		Level 3		c/c of rollers 4a+4b	Length 5a+5b
			Length=a	c/c of rollers =a+b	Length 1.5a+b	c/c of rollers 2a+2b	Length 3a+3b		
IIA-3	8'-4"	1"	11 1/2"	12 1/2"	18 1/4"	25"	37 1/2"	50	62 1/2"
IIIA-6	13'-8"	9"	11 1/2"	20 1/2"	26 1/4"	41"	61 1/2"	82	102 1/2"
IIIA-8	19'-0"	17"	11 1/2"	28 1/2"	34 1/4"	57"	85 1/2"	114	142 1/2"

The half-rollers were required to increase the overall stability of the set-up. In all other respects the test arrangements were the same as for the previous series.

I.9.4 Preparation of Beams Before Test

As already described, one side of the beam was instrumented both with the electrical resistance and the DEMEC strain gauges. The

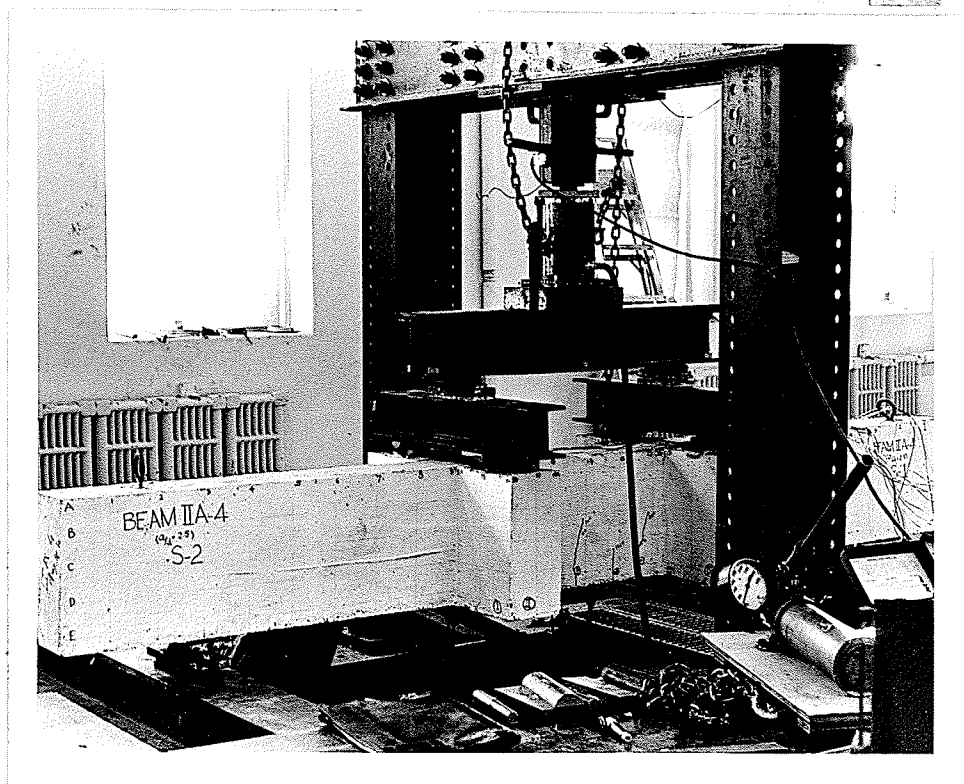


FIG. I-9 LOADING ARRANGEMENT FOR SERIES IIA
(SECONDARY BEAM LOADING)

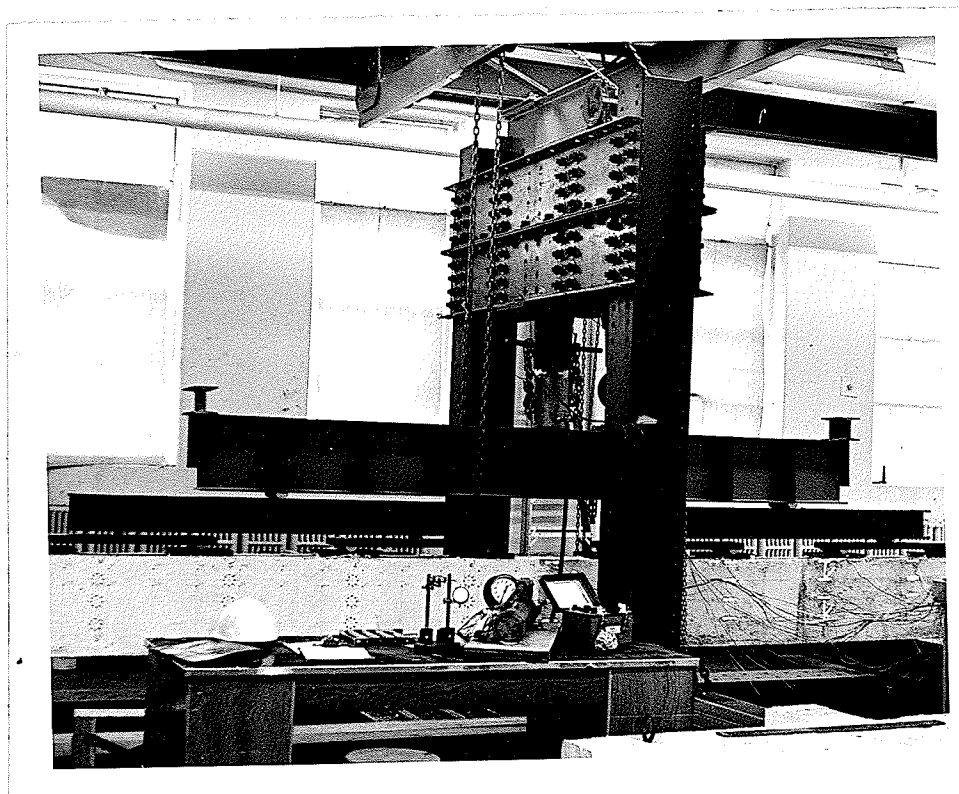


FIG. I-10 LOADING ARRANGEMENT FOR SERIES IIIA
(UNIFORM LOAD)

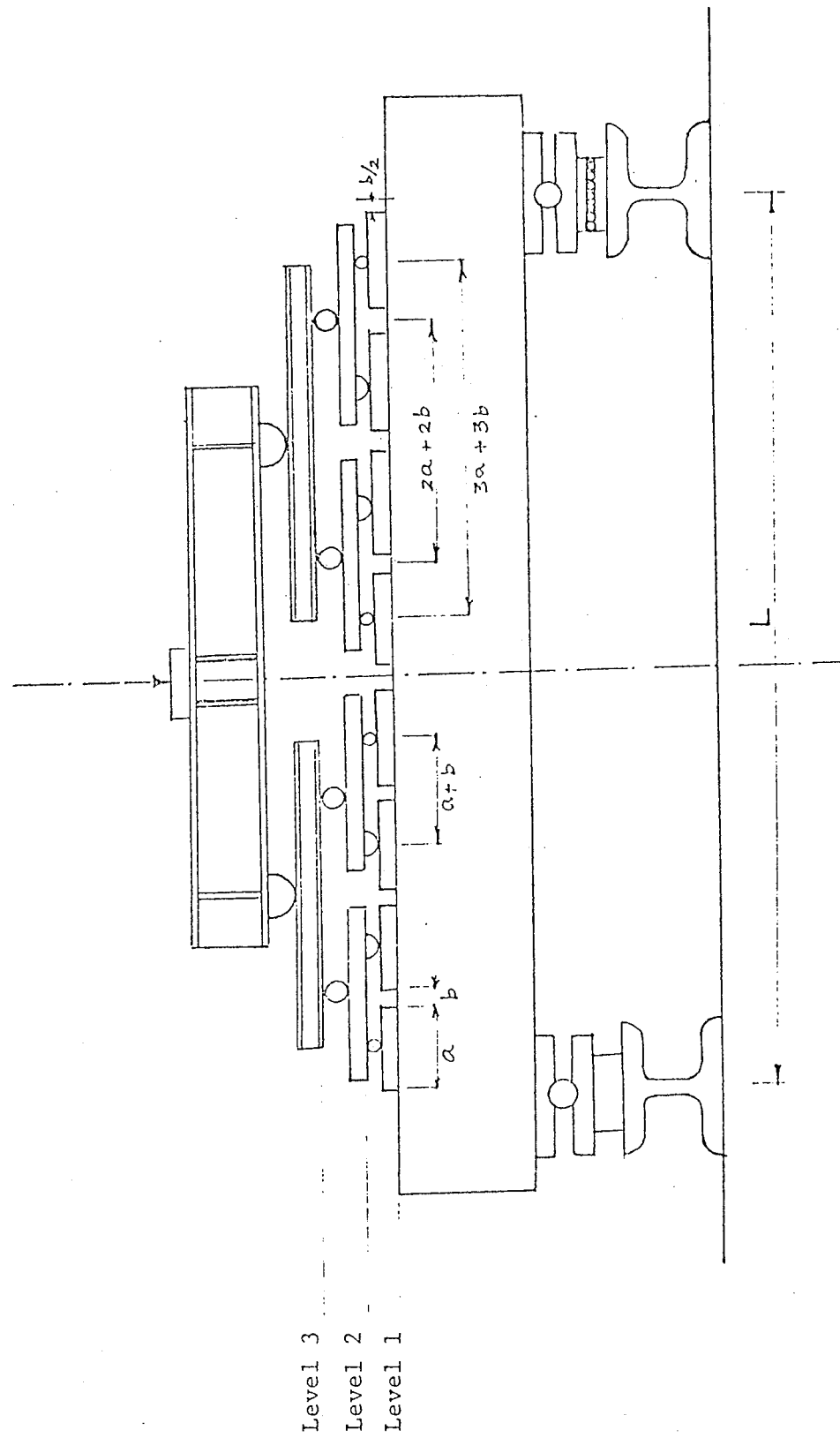


FIG. I.11 LOADING PATTERN FOR UNIFORM LOAD

other side of the beam, S1-S2, was painted white with latex paint and a grid-work of lines at 6 in. horizontal and 4 in. vertical intervals was laid out, as can be seen faintly in Figure I-9. Each end of the beam was marked N1, N2, S1 or S2 alongwith beam number to identify the various photographs to be taken. The date of casting and that of testing was also noted on end N1 for reference. End N1 on which electrical resistance strain gauges were placed was unpainted. However, the other half N2, was painted white before the locating discs for DEMEC gauges were placed. The various types of DEMEC gauge measuring lines were distinguished by using different colours joining lines to the DEMEC points. The gauge points, and the half-painted beam is visible in Figure I-10.

The purpose of painting the beam was to assist in the detection of cracks as they formed and progressed at various load levels. The grid work was laid out to help in recording the detailed location of cracks at various load levels. On side N1-N2, no grid work was laid out since the location of the gauge lines provided adequate reference points for determining the crack locations. Also, this side was already crowded with strain gauge instrumentation, and further grid lines would only add an element of confusion to the pattern.

I.9.5 Test Procedure

After all the readings at zero load were taken, the beam was loaded in regular increments of 2 to 5 kips, depending upon the maximum

load anticipated. In some cases the increments were reduced near failure. At each load increment, a full set of electrical resistance strain gauge readings was taken by the automatic data unit. DEMEC gauge readings were only taken at specified load levels, 3 to 7 sets of readings being taken for various tests. Sometimes an entire set of DEMEC readings was taken and sometimes only a partial set was recorded, depending upon the data already accumulated, the time taken for recording the readings and the anticipated importance of a particular reading. DEMEC readings at low loads were not taken, the first reading being recorded after some flexural cracking had taken place in the midspan area or in the shear span. Subsequent reading intervals were usually equally spaced to failure, though in some cases the interval between the last two sets of readings was closer. Further, since the failure load could not be anticipated very closely, the reading interval near failure could not be pre-assigned.

Deflections were recorded at each load interval along with details of the propagation of cracks, the time taken at each reading and whether a DEMEC reading set - complete or partial - was taken at that load level.

While the loading was interrupted at each increment to record deflections and strains and to mark the cracks, no attempt was made to maintain the load. Cracks were usually identified according to the order of formation, and the ends of cracks were marked with corresponding loads in kips. A separate table was made and completed during the test giving crack numbers, the load at which they originated, the crack height and their distance from either support at important

load levels until failure. This elaborate record in tabular form was kept only for side S1-S2, since it was found more convenient to locate and follow the cracks on the white painted surface. On side N1-N2, it was sometimes difficult to see the propagation of the cracks in detail, especially on the end on which the electrical resistance strain gauges were placed, as this end was not painted. Besides marking the crack numbers and recording the height of cracks, the horizontal distance between the cracks at the reinforcement level was also recorded. This extensive record of the cracks was used to draw detailed cracking patterns to scale on graph paper for both sides of the beams, to be used in later investigation of beam behaviour and analytical studies.

Photographs of the beams during loading and of various important details at failure were also taken, to supplement the cracking pattern record. Colour slides of the failed specimens of the entire test programme were also made, before the beams were physically removed as insurance against loss of key data after the tests had been completed.

APPENDIX II

EXPERIMENTAL RESULTS

APPENDIX II

EXPERIMENTAL RESULTS

II.1 GENERAL

In this Appendix, gauge locations for individual beams and crack pattern on both sides of the beams are shown. Loading stages, deflections and crack formation for the entire test series are tabulated and comments made on the failure of beams.

Results of the strain gauge data, however, were very extensive. Due to the large volume of strain gauge data, the results of DEMEC rosettes, electrical resistance strain gauges, horizontal gauge line readings, horizontal displacements and inclined gauge line readings have been compiled into a separate report.*

II.2 LOADING STAGES, DEFLECTIONS AND CRACK FORMATION

Results of all beam tests are tabulated in this section accompanied by figures showing gauge locations and crack patterns on both sides of the beam.

* See p. 91

TABLE II.1

BEAM IA-1 - LOADING STAGES, DEFLECTIONS AND CRACK FORMATION

LOADING STAGE	LOAD (KIPS)		DEFLECTION (10^{-3}) in.		READING TIME (MINUTES)	REMARKS
	START OF READING	END OF READING	AT MIDSPAN A \rightarrow B	UNDER LOAD PT. A \rightarrow B		
1	5	4.85	16.0 \rightarrow 16.0	20.0 \rightarrow 20.0	3	Formation of first flexural cracks, and their vertical extension. (These cracks later became inclined.)
2	10	9.90	26.0 \rightarrow 26.5	32.0 \rightarrow 32.0	2	
3	15	14.60	36.0 \rightarrow 36.5	41.5 \rightarrow 41.5	2	
4	20	19.50	44.0 \rightarrow 45.0	50.5 \rightarrow 50.5	2	
5	25	24.50	51.0 \rightarrow 52.5	59.0 \rightarrow 59.0	3	
6	30	29.00	59.0 \rightarrow 60.5	67.0 \rightarrow 67.0	6	
7	35	34.05	67.0 \rightarrow 68.5	76.0 \rightarrow 76.5	10	Formation of first diagonal crack and its extension into the compression zone.
8	40	39.00	75.0 \rightarrow 77.5	84.0 \rightarrow 85.0	9	
9	45	44.25	84.5 \rightarrow 85.5	93.0 \rightarrow 94.0	2	
10*	50	48.30	93.0 \rightarrow 97.0	102.0 \rightarrow 103.5	31	
11	55	54.40	103.5 \rightarrow 104.0	111.5 \rightarrow 112.0	3	Appearance of a new major diagonal crack and its propagation through the compression zone of the beam.
12	60	58.55	111.0 \rightarrow 113.0	119.5 \rightarrow 120.5	9	
13	65	63.85	120.0 \rightarrow 121.0	128.0 \rightarrow 129.5	5	
14	70	68.95	128.0 \rightarrow 130.0	136.0 \rightarrow 137.0	5	
15	75	74.00	137.0 \rightarrow 137.5	144.0 \rightarrow 145.0	3	Extension of the diagonal crack to within $2\frac{1}{4}$ in. of the compression zone of the beam.
16*	80	76.80	144.5 \rightarrow 144.5	152.5 \rightarrow 151.5	83	

TABLE BEAM 1A-1 (CONTINUED)

LOADING STAGE	LOAD (KIPS)		DEFLECTION (10^{-3}) in.		READING TIME (MINUTES)	REMARKS
	START OF READING	END OF READING	AT MIDSPAN A \rightarrow B	UNDER LOAD PT. A \rightarrow B		
17	85	84.45	153.0 \rightarrow 153.0	160.0 \rightarrow 160.0	4	Extension of flexural cracks almost stopped. Diagonal cracks propagating very slowly.
18	90	88.85	159.0 \rightarrow 160.0	166.0 \rightarrow 166.5	6	
19	95	94.15	167.0 \rightarrow 167.5	173.5 \rightarrow 174.0	3	
20*	100	97.25	173.0 \rightarrow 175.0	181.0 \rightarrow 181.0	26	
21	105	104.25	183.0 \rightarrow 183.0	189.5 \rightarrow 189.5	2	Diagonal cracks have extended in the vicinity of load point and have become stabilized.
22	110	108.80	189.0 \rightarrow 189.0	196.0 \rightarrow 196.0	2	
23	115	113.70	196.0 \rightarrow 196.0	203.0 \rightarrow 203.0	2	
24*	120	116.55	203.5 \rightarrow 207.0	210.0 \rightarrow 212.0	29	
25	125	123.80	211.0 \rightarrow 211.0	222.0 \rightarrow 222.0	33	
26	130	128.15	222.0 \rightarrow 222.0	229.0 \rightarrow 228.0	2	
27	135	132.50	228.5 \rightarrow 228.0	235.0 \rightarrow 234.5	2	
28	140	136.55	235.0 \rightarrow 235.0	242.0 \rightarrow 241.0	3	
29	145	142.50	244.0 \rightarrow 244.0	250.5 \rightarrow 250.5	3	
30*	150	143.60	252.0 \rightarrow 251.0	258.0 \rightarrow 256.0	37	
31	155	152.45	263.5 \rightarrow 262.5	268.0 \rightarrow 267.0	3	The critical diagonal crack has extended to within 1 3/8 in. of the compression face of the beam.
32	160	156.85	268.5 \rightarrow 268.0	274.0 \rightarrow 273.0	4	
33	165	162.00	276.0 \rightarrow 274.5	282.0 \rightarrow 280.5	2	
34	170	166.60	283.0 \rightarrow 281.0	289.0 \rightarrow 287.0	2	

TABLE BEAM IA-1 (CONTINUED)

LOADING STAGE	LOAD (KIPS)		DEFLECTION (10^{-3}) in.		READING TIME (MINUTES)	REMARKS
	START OF READING	END OF READING	AT MIDSPAN A \rightarrow B	UNDER LOAD PT. A \rightarrow B		
35	175	170.75	290.0 \rightarrow 289.0	296.0 \rightarrow 295.0	2	No further propagation of cracks, since a load of 150 kips was applied.
36*	180	171.80	298.5 \rightarrow 297.0	304.5 \rightarrow 302.5	30	
37	185	179.85	309.5 \rightarrow 307.5	316.0 \rightarrow 313.5	4	Test discontinued as the capacity of loading jack was reached.
38	190	184.10	315.0 \rightarrow 314.0	321.5 \rightarrow 320.0	2	
39	195	188.90	322	328	6	

* DEMEC gauge readings were taken

A \rightarrow B A = deflection at start of reading
 B = deflection at end of reading

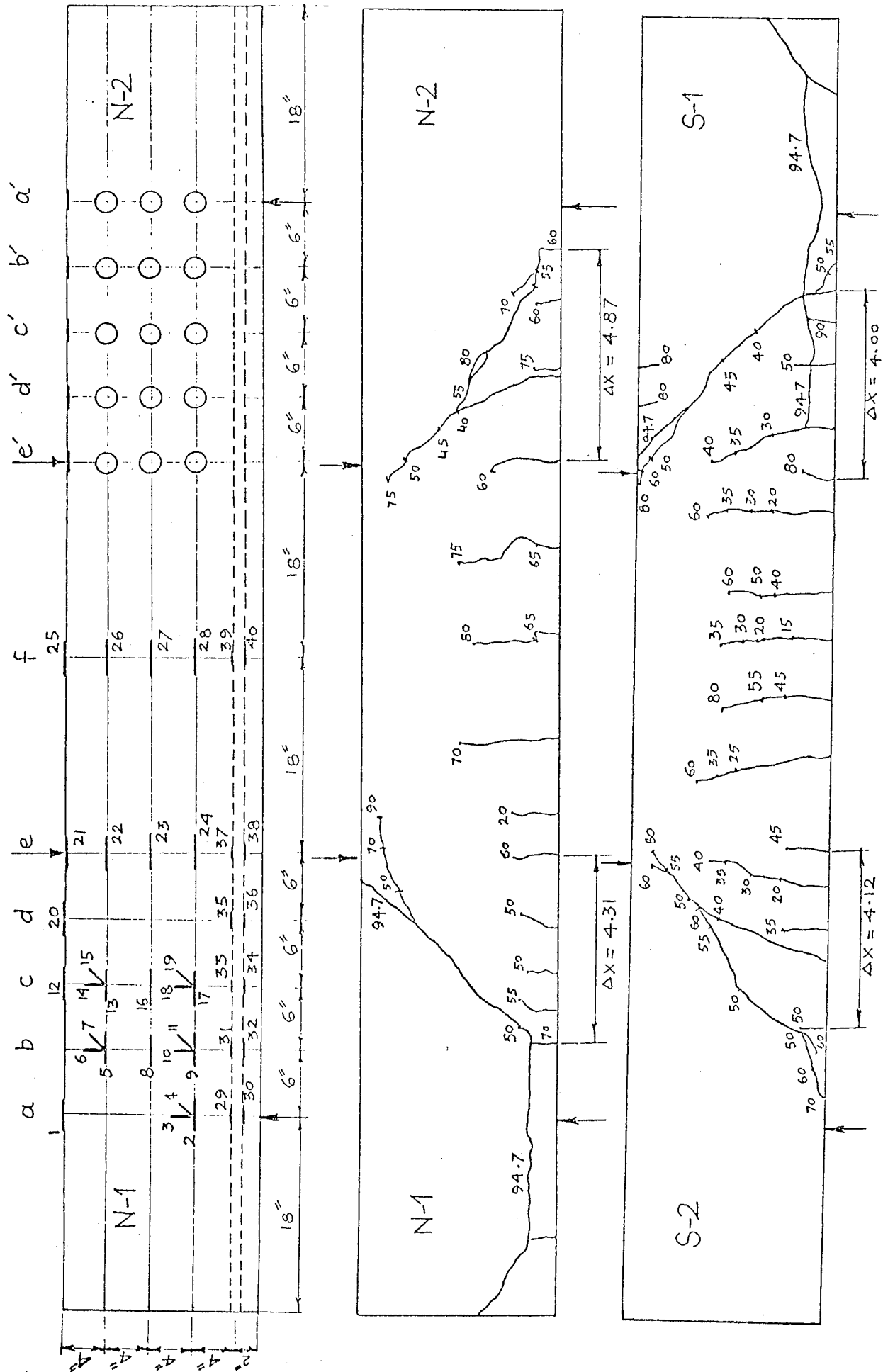


FIG. II.2 - BEAM IA-2 - LOCATION OF STRAIN GAUGES AND CRACK PATTERNS ON BOTH SIDES OF THE BEAM

TABLE II.2

BEAM IA-2 - LOADING STAGES, DEFLECTIONS AND CRACK FORMATION

LOADING STAGE	LOAD (KIPS)		DEFLECTION (10^{-3}) in.		READING TIME (MINUTES)	REMARKS
	START OF READING	END OF READING	AT MIDSPAN A \rightarrow B	UNDER LOAD PT. A \rightarrow B		
1	5	4.80	15.0 \rightarrow 15.5	20.0 \rightarrow 19.5	3	
2	10	9.80	30.0 \rightarrow 30.5	32.0 \rightarrow 32.5	3	
3	15	14.60	43.0 \rightarrow 44.0	44.0 \rightarrow 44.0	4	Appearance of first flexural crack.
4	20	19.45	56.0 \rightarrow 57.0	54.5 \rightarrow 55.0	5	Appearance of more flexural cracks and their vertical extension.
5	25	24.15	67.5 \rightarrow 68.0	64.5 \rightarrow 65.5	5	
6	30	29.00	79.5 \rightarrow 81.0	75.5 \rightarrow 77.0	6	Appearance of first crack in the shear span and its extension 6 in. vertically.
7	35	33.90	91.5 \rightarrow 93.5	87.0 \rightarrow 88.5	6	
8*	40	37.85	105.5 \rightarrow 106.5	99.0 \rightarrow 99.5	60	Observation of first diagonal cracking
9	45	44.00	121.0 \rightarrow 122.0	112.0 \rightarrow 113.0	22	Further extension of diagonal cracks.
10	50	48.20	140.0 \rightarrow 143.0	128.5 \rightarrow 131.5	10	Observation of a major extension of diagonal cracks, the end of crack being only 1 1/8 in. from the compres- sion face of the beam. This crack branching back- wards as well, crossing the reinforcement.
11	55	53.60	157.0 \rightarrow 159.0	145.0 \rightarrow 147.0	9	

TABLE BEAM IA-2 (CONTINUED)

LOADING STAGE	LOAD (KIPS)		DEFLECTION (10^{-3}) in.		READING TIME (MINUTES)	REMARKS
	START OF READING	END OF READING	AT MIDSPAN A \rightarrow B	UNDER LOAD PT. A \rightarrow B		
12*	60	57.70	174.0 \rightarrow 177.0	163.0 \rightarrow 165.0	31	Diagonal cracks in the vicinity of the load point.
13	65	64.10	191.0 \rightarrow 192.0	179.5 \rightarrow 180.0	4	Stabilization of diagonal cracks. The beam continues taking further load.
14	70	68.70	205.0 \rightarrow 207.5	193.5 \rightarrow 194.5	3	Stabilization of diagonal cracks. The beam continues taking further load.
15	75	73.65	221.0 \rightarrow 223.0	208.0 \rightarrow 209.0	3	Stabilization of diagonal cracks. The beam continues taking further load.
16*	80	76.75	238.0 \rightarrow 242.0	223.5 \rightarrow 226.0	28	Extension downward of vertical cracks from compression face above diagonal cracks.
17	85	83.90	261.0 \rightarrow 261.0	243.0 \rightarrow 243.0	5	Midspan deflection exceeding 0.3 in. as the beam failed along critical diagonal crack. Typical shear compression failure occurred with a split along the reinforcement.
18	90	87.60	277.0 \rightarrow 280.0	257.0 \rightarrow 258.5	6	
19	94.75	--	--	--	--	

* DEMEC gauge readings were taken

A \rightarrow B A = deflection at start of reading

B = deflection at end of reading

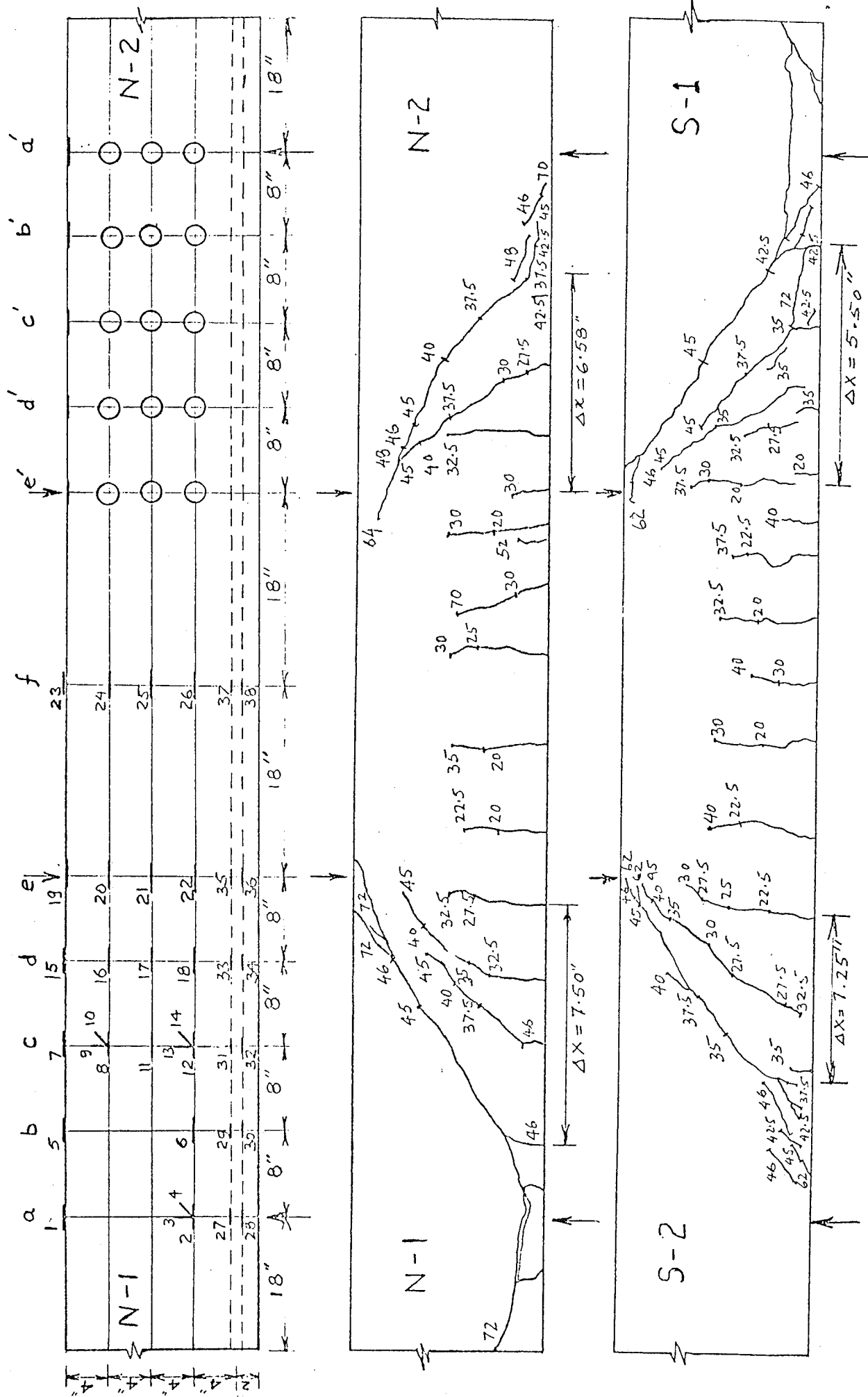


FIG. II.3 - BEAM IA-3 - LOCATION OF STRAIN GAUGES AND CRACK PATTERNS ON BOTH SIDES OF THE BEAM

TABLE II.3

BEAM IA-3 - LOADING STAGES, DEFLECTIONS AND CRACK FORMATION

LOADING STAGE	LOAD (KIPS)		DEFLECTION (10^{-3}) in.		READING TIME (MINUTES)	REMARKS
	START OF READING	END OF READING	AT MIDSPAN A \rightarrow B	UNDER LOAD PT. A \rightarrow B		
1	2.5	2.35	11.5 \rightarrow 11.5	13.0 \rightarrow 13.0	2	
2	5.0	4.95	24.5 \rightarrow 24.5	24.5 \rightarrow 24.0	2	
3	7.5	7.35	34.0 \rightarrow 35.5	33.0 \rightarrow 33.0	2	
4	10.0	9.85	44.0 \rightarrow 44.5	40.5 \rightarrow 40.5	2	
5	12.5	12.25	52.5 \rightarrow 53.0	46.5 \rightarrow 47.0	2	
6	15.0	14.65	59.5 \rightarrow 60.0	52.5 \rightarrow 53.0	2	
7	17.5	17.10	67.5 \rightarrow 68.0	58.5 \rightarrow 59.0	2	
8	20.0	19.25	76.5 \rightarrow 78.0	66.0 \rightarrow 68.5	4	
9	22.5	21.80	86.0 \rightarrow 87.0	74.5 \rightarrow 76.0	5	Observation of first flexural crack and its extension to a height of 6 in.
10	25.0	24.20	94.0 \rightarrow 96.0	82.0 \rightarrow 84.0	3	Appearance of first flexural cracks in shear span close to the load point.
11	27.5	26.45	104.5 \rightarrow 106.0	91.0 \rightarrow 93.0	12	Vertical propagation of flexural cracks -- later inclined propagation.
12*	30.0	28.65	114.0 \rightarrow 115.5	99.5 \rightarrow 101.5	26	
13	32.5	31.85	124.5 \rightarrow 124.5	108.0 \rightarrow 109.0	5	
14	35.0	33.70	133.5 \rightarrow 135.0	116.0 \rightarrow 119.0	7	
15	37.5	36.50	145.0 \rightarrow 146.0	127.0 \rightarrow 130.0	5	Appearance of new diagonal cracks and extension in inclined direction

TABLE BEAM IA-3 (CONTINUED)

LOADING STAGE	LOAD (KIPS)		DEFLECTION (10^{-3}) in.		READING TIME (MINUTES)	REMARKS
	START OF READING	END OF READING	AT MIDSPAN A \rightarrow B	UNDER LOAD PT. A \rightarrow B		
16*	40.0	38.50	156.0 \rightarrow 157.5	138.0 \rightarrow 140.0	21	Extension of a diagonal crack close to the load point to within $3\frac{1}{2}$ in. of the compression face.
17	42.5	41.90	167.5 \rightarrow 168.0	148.0 \rightarrow 149.0	4	
18*	45.0	41.50	178.0 \rightarrow 183.5	158.0 \rightarrow 164.0	26	
						Observation of a major extension of diagonal cracks, significant fall in load and observation of splitting along reinforcement at lower ends of diagonal cracks. Extension of critical crack to within $1\frac{1}{2}$ in. of the compression face.
19	42.5	42.50	186.0 \rightarrow 187.0	166.0 \rightarrow 167.0	5	
20	45.0	44.00	204.0 \rightarrow 205.0	178.0 \rightarrow 178.5	3	
21*	46.0	44.50	210.0 \rightarrow 212.0	184.0 \rightarrow 187.0	12	
22*	47.0	46.45	218.0 \rightarrow 220.0	192.0 \rightarrow 194.0	10	Extension of critical diagonal crack to within $\frac{1}{2}$ in. of the compression face.
23*	48.0	47.20	228.0 \rightarrow 229.0	202.0 \rightarrow 202.5	22	
						Visible widening of diagonal cracks. No further propagation of cracks.
24	49.0	48.85	234.0 \rightarrow 234.0	206.5 \rightarrow 206.5	2	
25	50.0	49.70	237.5 \rightarrow 237.5	209.0 \rightarrow 209.0	2	

TABLE BEAM IA-3 (CONTINUED)

LOADING STAGE	LOAD (KIPS)		DEFLECTION (10^{-3}) in.		READING TIME (MINUTES)	REMARKS
	START OF READING	END OF READING	AT MIDSPAN A \rightarrow B	UNDER LOAD PT. A \rightarrow B		
26	51.0	50.70	241.5 \rightarrow 241.5	213.0 \rightarrow 213.0	3	
27*	52.0	51.15	246.0 \rightarrow 246.5	217.0 \rightarrow 218.5	8	
28	53.0	52.65	252.0 \rightarrow 252.5	223.0 \rightarrow 223.5	3	
29*	54.0	53.10	257.0 \rightarrow 258.0	227.0 \rightarrow 229.0	12	
30	55.0	54.70	263.0 \rightarrow 263.0	232.0 \rightarrow 234.0	2	
31	56.0	55.65	267.5 \rightarrow 268.0	237.0 \rightarrow 238.0	2	
32	58.0	57.45	276.0 \rightarrow 277.0	245.0 \rightarrow 246.0	2	
33*	60.0	57.85	283.0 \rightarrow 283.0	254.0 \rightarrow 259.0	24	
34	62.0	61.30	302.0 \rightarrow 302.0	270.0 \rightarrow 271.5	4	
35	64.0	63.30	312.0 \rightarrow 312.0	279.0 \rightarrow 279.0	2	Extension of diagonal cracks into the zone of pure flexure with reduced slopes.
36	66.0	65.30	322.0 \rightarrow 322.0	288.0 \rightarrow 289.0	2	Further widening of critical diagonal cracks.
37	68.0	67.00	333.0 \rightarrow 334.0	298.0 \rightarrow 300.0	2	Further widening of critical diagonal cracks.
38*	70.0	66.20	347.0 \rightarrow 353.0	311.0 \rightarrow 317.0	23	Further widening of critical diagonal cracks.
39	72.0	--	370	332	--	Beam failed in shear compression after maintaining the load momentar- ily accompanied by a split along the reinforcement.

* DEMEC gauge readings were taken

A \rightarrow B A = deflection at start of reading

B = deflection at end of reading

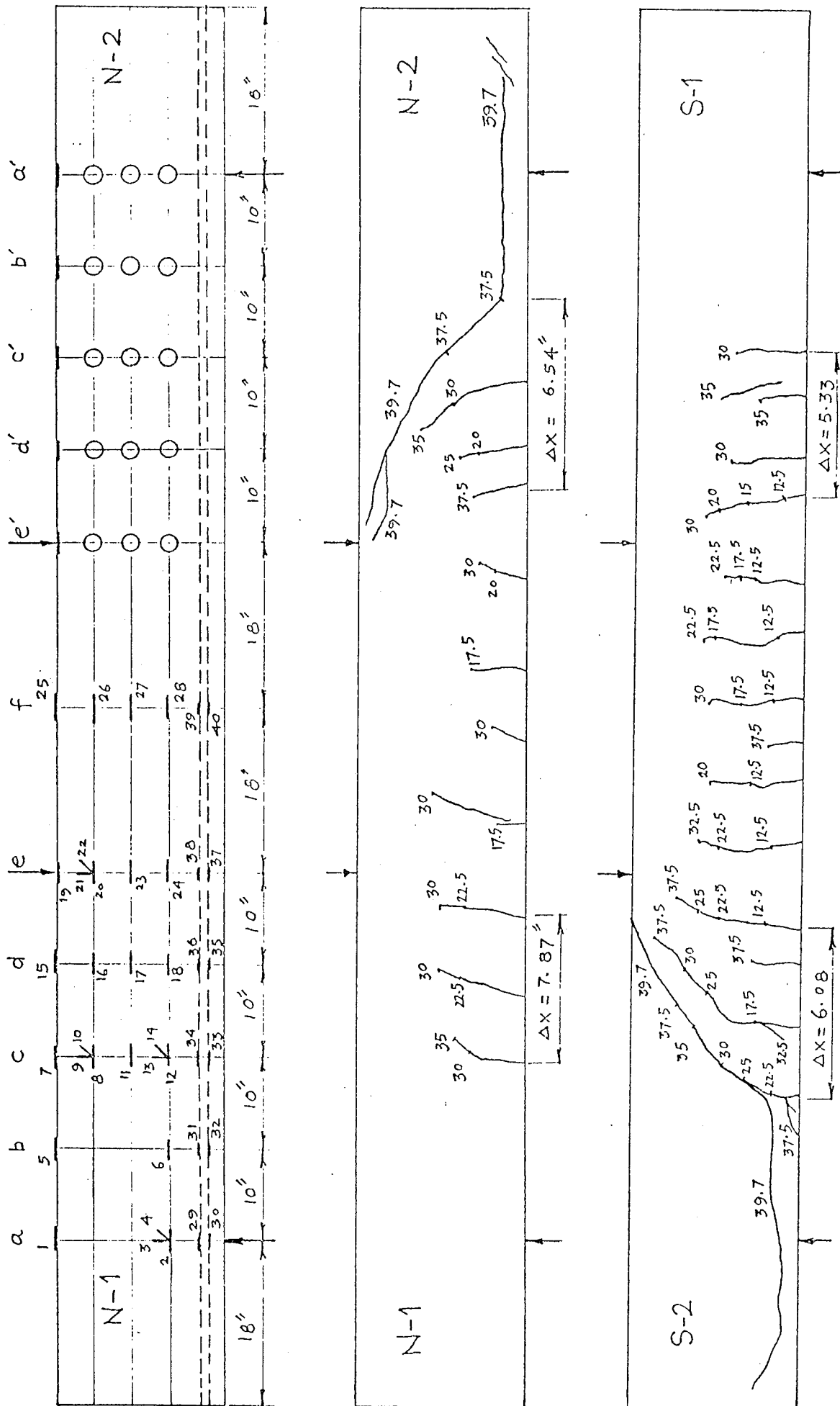


FIG. II.4 -- BEAM IA-4 - LOCATION OF STRAIN GAUGES AND CRACK PATTERNS ON BOTH SIDES OF THE BEAM

TABLE II.4

BEAM IA-4 - LOADING STAGES, DEFLECTIONS AND CRACK FORMATION

LOADING STAGE	LOAD (KIPS)		DEFLECTION (10^{-3}) in.		READING TIME (MINUTES)	REMARKS
	START OF READING	END OF READING	AT MIDSPAN A \rightarrow B	UNDER LOAD PT. A \rightarrow B		
1	2.5	2.25	11.0 \rightarrow 11.0	11.0 \rightarrow 11.0	2	
2	5.0	4.90	22.5 \rightarrow 23.0	21.0 \rightarrow 21.0	2	
3	7.5	7.45	32.0 \rightarrow 32.5	27.5 \rightarrow 27.5	2	
4	10.0	9.90	41.0 \rightarrow 41.0	35.0 \rightarrow 36.0	2	
5	12.5	12.10	51.5 \rightarrow 53.0	43.0 \rightarrow 45.0	5	Appearance of first flexural cracks.
6	15.0	14.45	65.0 \rightarrow 66.5	54.5 \rightarrow 56.5	4	Observation of more flexural cracks and their extension vertically upwards.
7	17.5	16.75	80.5 \rightarrow 82.0	69.0 \rightarrow 70.5	9	Observation of more flexural cracks and their extension vertically upwards.
8*	20.0	18.90	95.0 \rightarrow 96.0	82.0 \rightarrow 83.0	28	Observation of more flexural cracks and their extension vertically upwards.
9	22.5	21.90	109.0 \rightarrow 110.0	95.0 \rightarrow 96.0	9	Observation of more flexural cracks and their extension vertically upwards.
10	25.0	24.25	212.5 \rightarrow 123.0	106.5 \rightarrow 108.0	6	Extension of flexural cracks in inclined directions in the shear span.
11	27.5	26.50	135.5 \rightarrow 138.0	120.0 \rightarrow 122.0	10	
12*	30.0	28.60	151.0 \rightarrow 152.0	133.5 \rightarrow 135.5	33	

TABLE BEAM IA-4 (CONTINUED)

LOADING STAGE	LOAD (KIPS)		DEFLECTION (10^{-3}) in.		READING TIME (MINUTES)	REMARKS
	START OF READING	END OF READING	AT MIDSPAN A \rightarrow B	UNDER LOAD PT. A \rightarrow B		
13	32.5	31.70	166.0 \rightarrow 166.5	148.0—148.5	6	Backwards branching-off of some cracks above reinforcement level in the shear span, while propagating into the compression zone at the same time.
14*	35.0	33.55	178.5 \rightarrow 180.0	160.0—162.0	23	
15*	37.5	36.15	194.5 \rightarrow 195.5	176.0—178.0	18	
16	39.7	--	--	--	--	Sudden diagonal tension failure occurred by extension of the last diagonal crack through the compression zone and a fine split along the reinforcement from the lower end of the crack.

* DEMEC gauge readings were taken

A \rightarrow B A = deflection at start of reading

B = deflection at end of reading

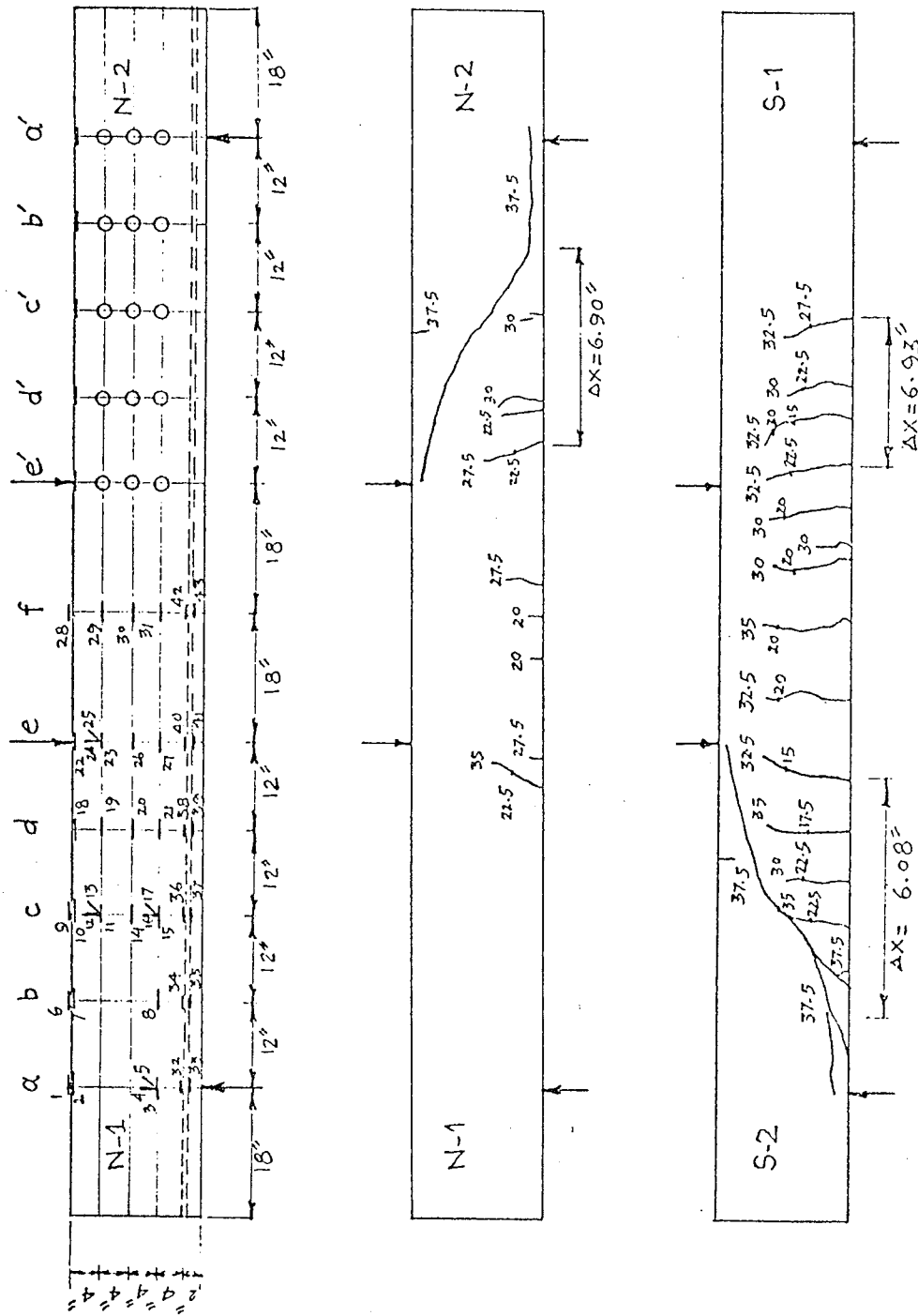


FIG. 11.5 - BEAM IA-5 - LOCATION OF STRAIN GAUGES AND CRACK PATTERNS ON BOTH SIDES OF THE BEAM

TABLE II.5

BEAM IA-5 - LOADING STAGES, DEFLECTIONS AND CRACK FORMATION

LOADING STAGE	LOAD (KIPS)		DEFLECTION (10^{-3}) in.		READING TIME (MINUTES)	REMARKS
	START OF READING	END OF READING	AT MIDSPAN A \rightarrow B	UNDER LOAD PT. A \rightarrow B		
1	2.5	2.5	15.5 \rightarrow 15.5	13.0 \rightarrow 13.0	2	
2	5.0	5.0	31.0 \rightarrow 31.0	26.0 \rightarrow 26.0	2	
3	7.5	7.5	46.0 \rightarrow 47.0	40.0 \rightarrow 41.0	2	
4	10.0	10.0	63.0 \rightarrow 66.0	55.0 \rightarrow 56.0	2	
5	12.5	12.5	79.0 \rightarrow 82.5	69.0 \rightarrow 71.0	2	
6*	15.0	15.0	100.0 \rightarrow 107.0	86.0 \rightarrow 98.0	22	Observation of first flexural cracks.
7	17.5	17.5	121.5 \rightarrow 126.0	111.5 \rightarrow 115.0	5	
8*	20.0	20.0	141.0 \rightarrow 149.0	129.0 \rightarrow 136.0	28	Appearance of more flexural cracks and their slow upwards propagation.
9	22.5	22.5	161.5 \rightarrow 168.0	148.0 \rightarrow 153.0	20	
10	25.0	25.0	180.0 \rightarrow 181.5	164.0 \rightarrow 165.5	2	Extension of cracks in inclined directions in shear span.
11	27.5	26.95	198.0 \rightarrow 199.0	180.0 \rightarrow 182.0	10	
12*	30.0	28.85	216.0 \rightarrow 218.0	195.0 \rightarrow 198.0	21	
13	32.5	31.90	237.0 \rightarrow 238.0	214.0 \rightarrow 214.5	5	
14	35.0	34.05	256.0 \rightarrow 257.0	230.0 \rightarrow 231.0	5	Critical diagonal crack remaining well below the compression face.

TABLE BEAM IA-5 (CONTINUED)

LOADING STAGE	LOAD (KIPS)		DEFLECTION (10^{-3}) in.		READING TIME (MINUTES)	REMARKS
	START OF READING	END OF READING	AT MIDSPAN A \rightarrow B	UNDER LOAD PT. A \rightarrow B		
15	37.5	--	--	--	--	Failure occurred suddenly when a new diagonal crack extended through the compression zone of the beam. A small crack at the compression face above the diagonal crack was seen to extend downwards at failure. Failure was accompanied by a limited split along the reinforcement.

Load maintained constant at each stage up to 25 kips.

*DEMEC gauge readings were taken

A \rightarrow B A = deflection at start of reading

B = deflection at end of reading.

TABLE II.6

BEAM IA-6 - LOADING STAGES, DEFLECTIONS AND CRACK FORMATION

LOADING STAGE	LOAD (KIPS)		DEFLECTION (10^{-3}) in.		READING TIME (MINUTES)	REMARKS
	START OF READING	END OF READING	AT MIDSPAN A \rightarrow B	UNDER LOAD PT. A \rightarrow B		
1	2.5	2.50	18 \rightarrow 18	17 \rightarrow 17	2	
2	5.0	4.85	39 \rightarrow 40	36 \rightarrow 37	2	
3	7.5	7.30	66 \rightarrow 67	56 \rightarrow 57	2	
4	10.0	9.70	91 \rightarrow 92	80 \rightarrow 81	2	
5	12.5	12.00	122 \rightarrow 123	107 \rightarrow 109	7	Appearance of first flexural cracks.
6*	15.0	13.90	158 \rightarrow 159	141 \rightarrow 141	78	Observation of flexural cracks in the shear spans.
7	17.5	17.00	190 \rightarrow 191	170 \rightarrow 171	5	
8*	20.0	19.00	225 \rightarrow 226	201 \rightarrow 203	25	Vertical exten- sion of cracks.
9	22.5	21.85	259 \rightarrow 260	233 \rightarrow 234	6	
10*	25.0	24.15	294 \rightarrow 296	266 \rightarrow 268	11	
11	27.5	27.05	328 \rightarrow 328	297 \rightarrow 297	3	
12*	30.0	28.85	361 \rightarrow 362	327 \rightarrow 328	25	Appearance of inclined cracks in shear spans in the vicinity of applied loads.
13	32.5	32.00	395 \rightarrow 396	360 \rightarrow 360	5	
14*	35.0	33.85	427 \rightarrow 428	389 \rightarrow 390	30	Backwards branch- ing-off of some cracks while extending upwards at the same time.
15	37.5	36.75	464 \rightarrow 464	424 \rightarrow 424	5	Observation of a critical diagonal extension of some cracks.
16*	40.0	38.55	499 \rightarrow 501	458 \rightarrow 458	20	

TABLE BEAM IA-6 (CONTINUED)

LOADING STAGE	LOAD (KIPS)		DEFLECTION (10^{-3}) in.		READING TIME (MINUTES)	REMARKS
	START OF READING	END OF READING	AT MIDSPAN A \rightarrow B	UNDER LOAD PT. A \rightarrow B		
17	40.5	--	--	--	--	Failure occurred by a sudden extension of the critical diagonal crack through the compression zone of the beam to the load point and a split along the reinforcement.

* DEMEC gauge readings were taken.

A \rightarrow B A = deflection at start of reading
 B = deflection at end of reading

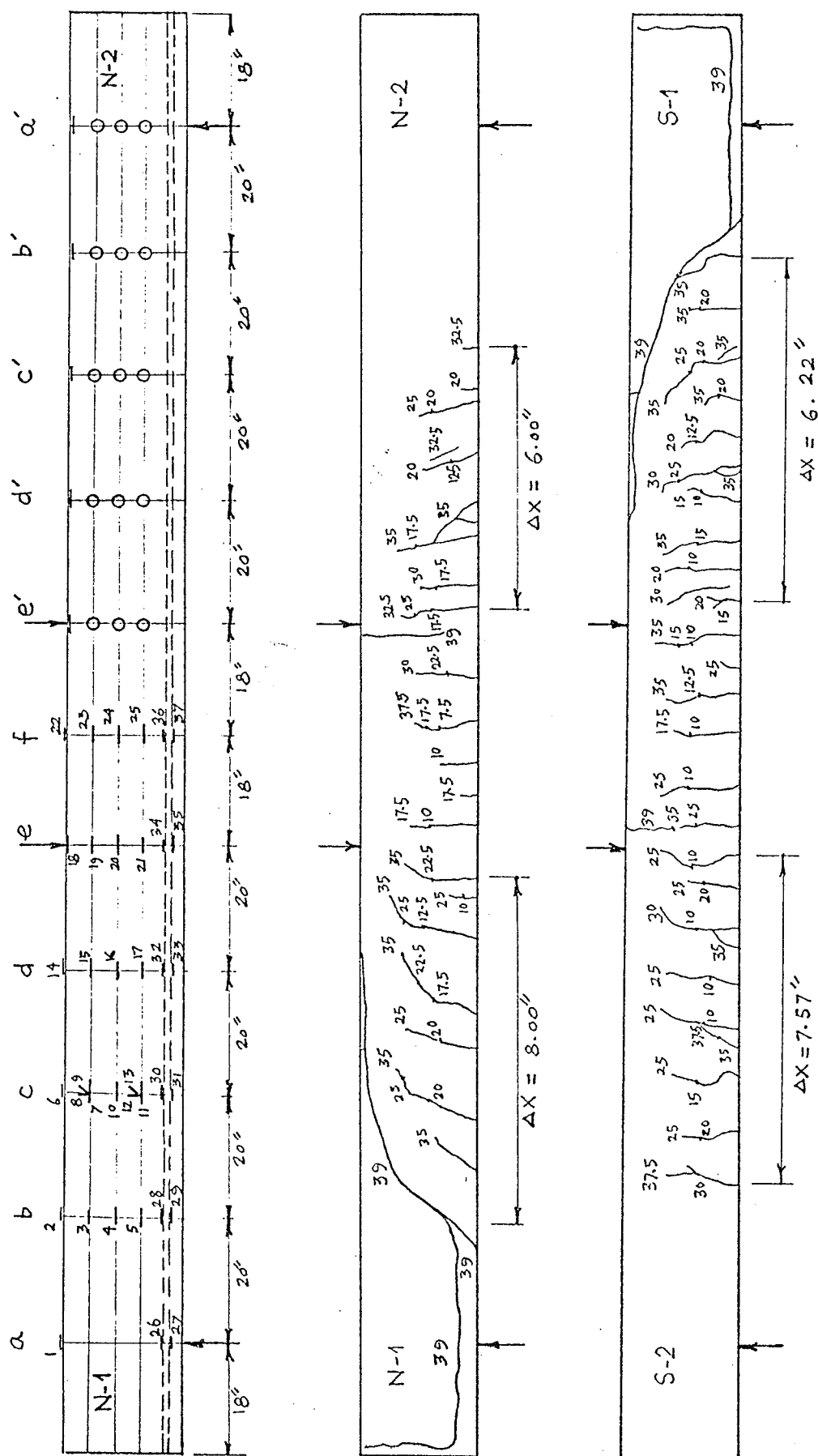


FIG. II.7 - BEAM IA-7 - LOCATION OF STRAIN GAUGES AND CRACK PATTERNS ON BOTH SIDES OF THE BEAM

BEAM IA-7 - LOADING STAGES, DEFLECTIONS AND CRACK FORMATION

LOADING STAGE	LOAD (KIPS)		DEFLECTION (10^{-3}) in.		READING TIME (MINUTES)	REMARKS
	START OF READING	END OF READING	AT MIDSPAN A \rightarrow B	UNDER LOAD PT. A \rightarrow B		
1	2.5	2.40	29 \rightarrow 29	27 \rightarrow 27	2	Observation of first flexural cracks in midspan and shear spans close to the load points and their vertical extension.
2	5.0	4.85	63 \rightarrow 63	62 \rightarrow 62	2	
3	7.5	7.20	103 \rightarrow 103	101 \rightarrow 101	2	
4	10.0	9.25	153 \rightarrow 153	149 \rightarrow 149	11	
5	12.5	11.95	206 \rightarrow 206	199 \rightarrow 200	5	" "
6*	15.0	14.05	258 \rightarrow 257	249 \rightarrow 250	31	" "
7	17.5	17.00	310 \rightarrow 311	301 \rightarrow 303	6	" "
8	20.0	19.50	363 \rightarrow 363	353 \rightarrow 354	12	Extension of cracks in the shear spans in inclined directions.
9	22.5	22.15	414 \rightarrow 414	401 \rightarrow 403	14	Backwards branching off of some cracks above the level of the reinforcement.
10*	25.0	23.65	466 \rightarrow 466	452 \rightarrow 452	78	
11	27.5	27.30	525 \rightarrow 525	508 \rightarrow 508	2	
12*	30.0	29.10	572 \rightarrow 572	553 \rightarrow 553	20	
13	32.5	32.15	626 \rightarrow 626	604 \rightarrow 603	3	
14*	35.0	33.75	679 \rightarrow 680	654 \rightarrow 655	28	
15*	37.5	36.60	743 \rightarrow 744	714 \rightarrow 716	6	

TABLE BEAM IA-7 (CONTINUED)

LOADING STAGE	LOAD (KIPS)		DEFLECTION (10^{-3}) in.		READING TIME (MINUTES)	REMARKS
	START OF READING	END OF READING	AT MIDSPAN A \rightarrow B	UNDER LOAD PT. A \rightarrow B		
16	39.0	--	--	--	--	Failure occurred when the last crack extended diagonally through the compression zone resulting in complete split. Failure crack was considerably removed from the load point. A complete split occurred along the reinforcement from the lower end of the crack towards the anchorage zone.

* DEMEC gauge readings were taken

A \rightarrow B A = deflection at start of reading
 B = deflection at end of reading

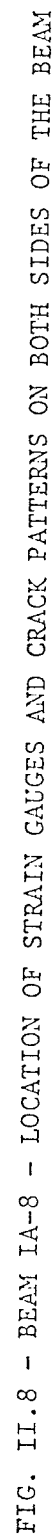


TABLE II.8

BEAM IA-8 - LOADING STAGES, DEFLECTIONS AND CRACK FORMATION

LOADING STAGE	LOAD (KIPS)		DEFLECTION (10^{-3}) in.		READING TIME (MINUTES)	REMARKS
	START OF READING	END OF READING	AT MIDSPAN A \rightarrow B	UNDER LOAD PT. A \rightarrow B		
1	2.5	2.45	40 \rightarrow 41	31 \rightarrow 33	2	Appearance of first flexural cracks both in the midspan region and in the shear spans.
2	5.0	4.70	94 \rightarrow 95	90 \rightarrow 92	2	
3	7.5	7.15	178 \rightarrow 179	166 \rightarrow 167	5	
4	10.0	9.60	263 \rightarrow 264	247 \rightarrow 248	7	Vertical extension of flexural cracks
5	12.5	12.05	341 \rightarrow 341	326 \rightarrow 328	5	Further propagation of cracks in shear spans in inclined directions.
6*	15.0	14.05	421 \rightarrow 421	405 \rightarrow 405	72	Extension of cracks in more inclined directions.
7	17.5	17.25	505 \rightarrow 506	490 \rightarrow 492	4	
8	20.0	19.65	585 \rightarrow 586	568 \rightarrow 570	6	
9	22.5	22.05	662 \rightarrow 664	642 \rightarrow 643	7	Failure occurred by a diagonal extension of critical crack to the load point resulting in complete split. A crack extended downwards from the compression face (in the midspan region) at failure. Extensive split along the reinforcement was observed in the entire shear span.
10*	25.0	24.10	742 \rightarrow 743	720 \rightarrow 722	26	
11	27.5	27.15	827 \rightarrow 828	806 \rightarrow 806	7	
12*	30.0	29.00	903 \rightarrow 905	879 \rightarrow 881	26	
13	34.4	--	--	--	--	

* DEMEC gauge readings were taken

A \rightarrow B A = deflection at start of reading

B = deflection at end of reading

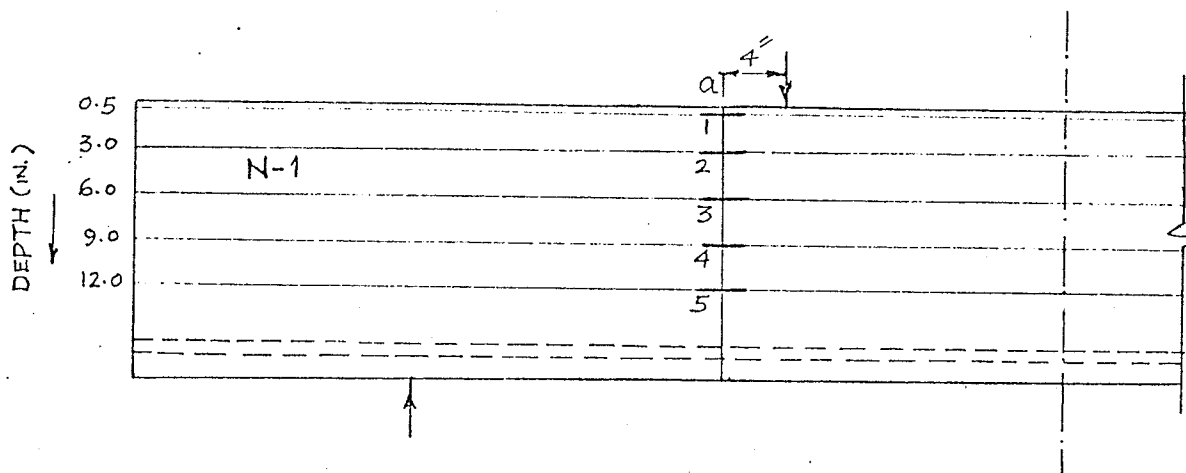


FIG. II.9 GAUGE LOCATIONS ON BEAM IB-2

TABLE II.9

BEAM IB-2 - LOADING STAGES, DEFLECTIONS AND CRACK FORMATION

LOADING STAGE	LOAD (KIPS)	DEFLECTION (10^{-3}) IN.		REMARKS
		AT MIDSPAN	UNDER LOAD PT.	
1	5.0	15	8	
2	7.5	23	13	
3	10.0	32	20	
4	12.5	42	27	
5	15.0	51	34	
6	17.5	58	40	
7	20.0	65	47	
8	22.5	72	53	
9	25.0	78	60	Observation of first flexural crack.
10	27.5	84	66	Vertical extension of flexural cracks,
11	30.0	90	72	later becoming inclined.
12	32.5	96	78	
13	35.0	101	83	
14	37.5	106	88	

TABLE BEAM IB-2 (CONTINUED)

LOADING STAGE	LOAD (KIPS)	DEFLECTION (10^{-3}) IN.		REMARKS
		AT MIDSPAN	UNDER LOAD PT.	
15	40.0	112	93	Observation of a major diagonal crack on one end of the beam.
16	42.5	120	100	
17	45.0	129	107	
18	47.5	135	113	
19	50.0	141	118	
20	52.5	148	124	Extension of the critical diagonal crack upwards and its stabilization.
21	55.0	156	130	
22	57.5	164	140	Development of a major diagonal crack on the other end of the beam.
23	60.0	170	145	
24	62.5	177	150	Slow propagation of diagonal cracks with reduced slopes.
25	65.0	184→187	162→164	
26	67.5	195	170	
27	70.0	202	177	
28	72.5	208	184	
29	75.0	215	190	Diagonal cracks in the vicinity of the compression face.
30	77.5	224	198	
31	80.0	232	205	No further propagation of cracks.
32	82.5	240	212	Widening of diagonal cracks with further application of load and their slow extension into the region of pure flexure with almost a horizontal trajectory.
				" "

TABLE BEAM IB-2 (CONTINUED)

LOADING STAGE	LOAD (KIPS)	DEFLECTION (10^{-3}) IN.		REMARKS
		AT MIDSPAN	UNDER LOAD PT.	
33	85.0	248	220	Widening of diagonal cracks with further application of load and their slow extension into the region of pure flexure with almost a horizontal trajectory.
34	87.5	256	227	" "
35	90.0	264	236	" "
36	92.5	273	245	" "
37	95.0	280	253	" "
38	97.5	290	261	" "
39	100.0	299	272	" "
40	102.5	308	282	" "
41	105.0	218	292	" "
42	107.5	327	300	" "
43	110.0	340	313	" "
44	112.5	350	323	" "
45	115.0	360	335	" "
46	117.5	374	348	" "
47	120.0	386	364	" "
48	122.5	—	—	Failure occurred by shear compression as the diagonal crack caused a split, the two portions of the beam jumped apart and load fell off completely. A split also occurred along the reinforcement.

This beam was part of the preliminary set of beams. Load was kept constant at every loading stage. No DEMEC gauges were used.

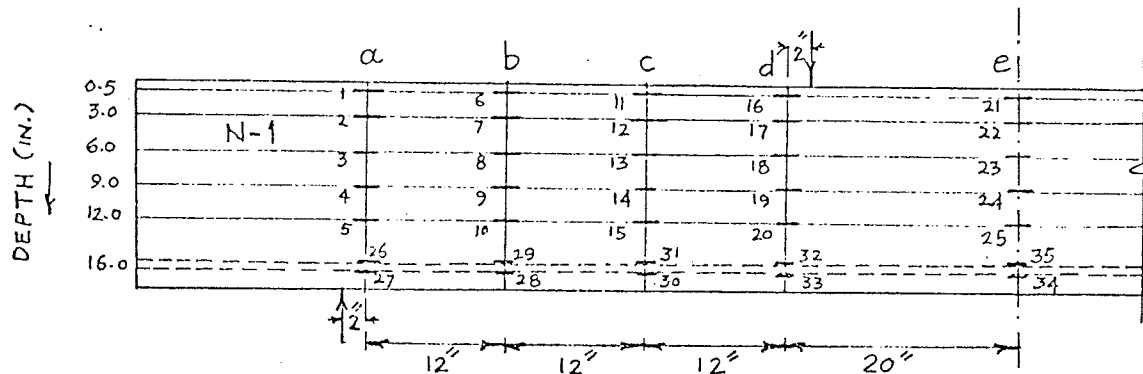


FIG. II.10 GAUGE LOCATIONS ON BEAM IB-4

TABLE II.10

BEAM IB-4 - LOADING STAGES, DEFLECTIONS AND CRACK FORMATION

LOADING STAGE	LOAD (KIPS)	MIDSPAN DEFLECTION (10^{-3}) IN.	REMARKS
1	5.0	21	
2	10.0	46	
3	15.0	76	
4	20.0	111	Appearance of first flexural cracks,
5	25.0	144	and their vertical propagation,
6	30.0	173	later becoming in-
7	35.0	205	clined.
8	37.5	296	Occurrence of critical diagonal cracking, the crack almost causing failure by going through the compression zone.

TABLE BEAM IB-4 (CONTINUED)

LOADING STAGE	LOAD (KIPS)	MIDSPAN DEFLECTION (10^{-3}) IN.	REMARKS
9	38.3	324	The critical diagonal crack resulted in failure. A crack extended from the compression face downwards above the diagonal crack. A split along the reinforcement was also observed.

This beam was part of the preliminary set of beams. Load was kept constant at every loading stage. No DEMEC gauges were used.

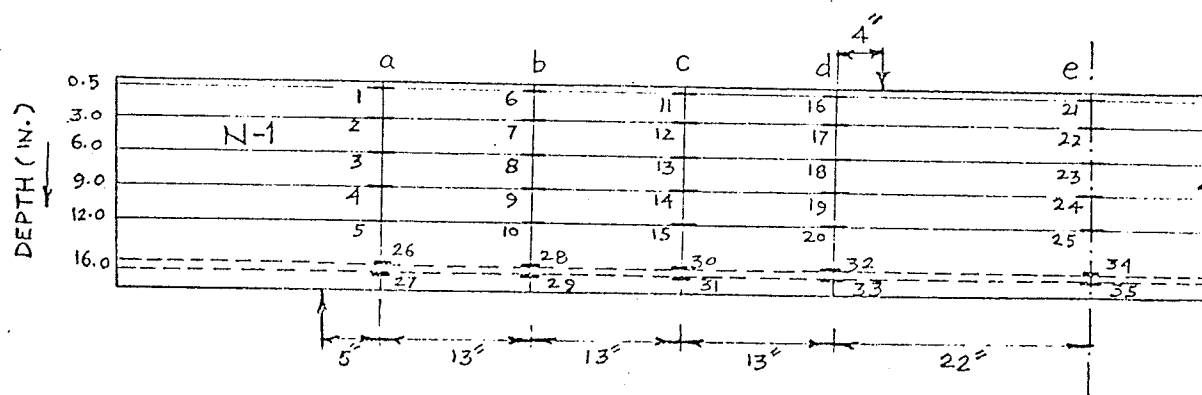


FIG. II.11 GAUGE LOCATIONS ON BEAM IB-5

TABLE

BEAM IB-5 - LOADING STAGES, DEFLECTIONS AND CRACK FORMATION

LOADING STAGE	LOAD (KIPS)	MIDSPAN DEFLECTION (10^{-3}) IN. A \rightarrow B	REMARKS
1	5.0	30	
2	10.0	64	
3	15.0	116	
4	17.5	138	
5	20.0	158	Observation of first flexural cracks.
6	22.5	183 \rightarrow 189	Vertical extension of flexural cracks,
7	25.0	204 \rightarrow 213	later becoming inclined in the shear spans.
8	27.5	228 \rightarrow 237	" "
9	30.0	250 \rightarrow 257	" "
10	32.5	273 \rightarrow 277	" "
11	35.0	298 \rightarrow 302	Observation of critical diagonal cracking.

TABLE BEAM IB-5 (CONTINUED)

LOADING STAGE	LOAD (KIPS)	MIDSPAN DEFLECTION (10^{-3}) IN. A \rightarrow B	REMARKS
12	37.5	321	Failure occurred by extension of diagonal crack suddenly through the compression zone of the beam, and a split along the reinforcement from the lower end of the crack.

This beam was part of the preliminary set of beams. Load was kept constant at every loading stage. No DEMEC gauges were used.

A \rightarrow B A = deflection at start of reading
 B = deflection at end of reading

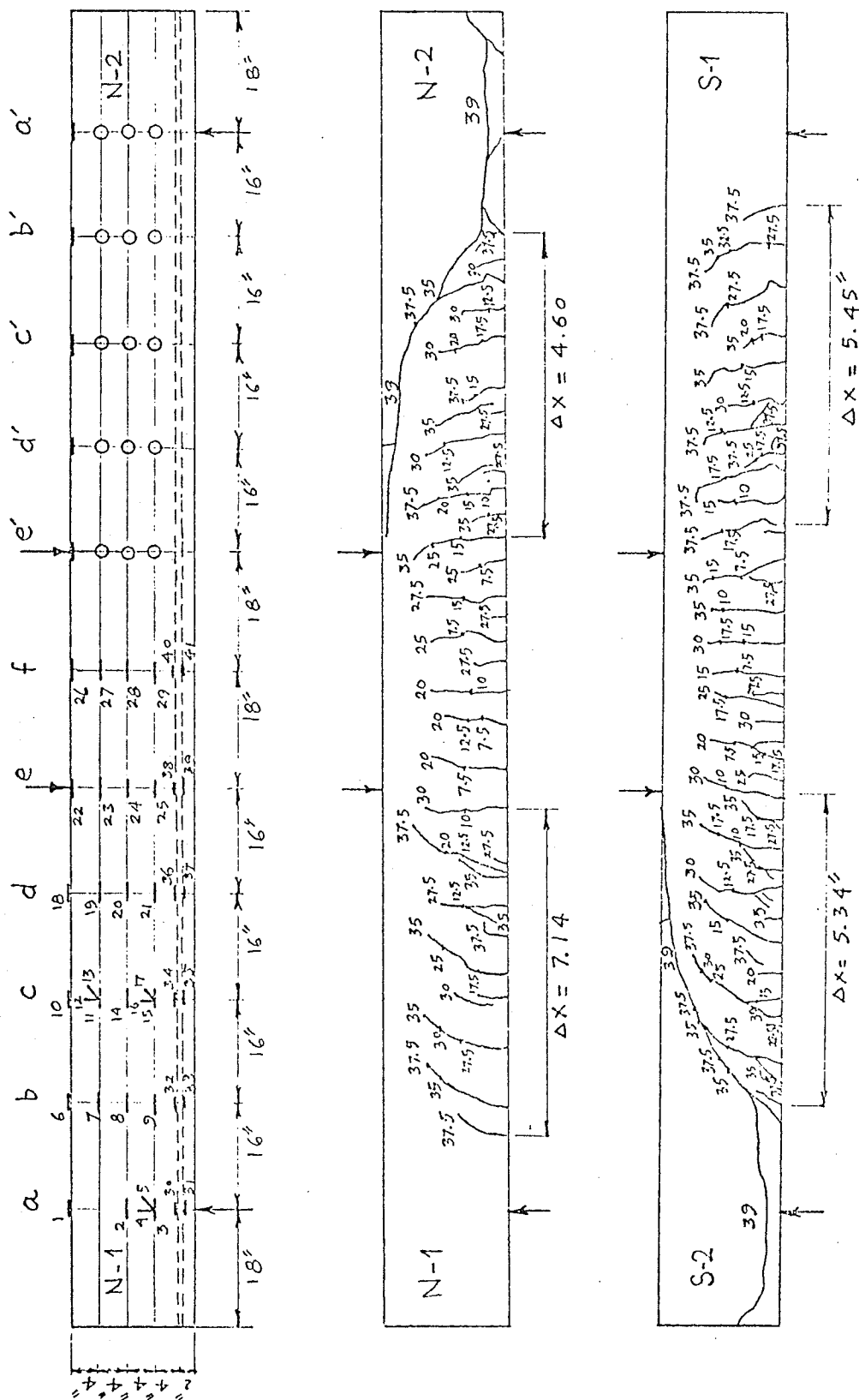


FIG. II.12 - BEAM IB-6 - LOCATION OF STRAIN GAUGES AND CRACK PATTERNS ON BOTH SIDES OF THE BEAM

TABLE II.12

BEAM IB-6 - LOADING STAGES, DEFLECTIONS AND CRACK FORMATION

LOADING STAGE	LOAD (KIPS)		DEFLECTION (10^{-3}) in.		READING TIME (MINUTES)	REMARKS
	START OF READING	END OF READING	AT MIDSPAN A \rightarrow B	UNDER LOAD PT. A \rightarrow B		
1	2.5	2.45	16 \rightarrow 16	14 \rightarrow 16	2	Observation of first flexural cracks in the zone of pure flexure.
2	5.0	4.85	36 \rightarrow 36	34 \rightarrow 35	2	
3	7.5	7.00	64 \rightarrow 64	61 \rightarrow 62	5	
4	10.0	9.35	107 \rightarrow 109	104 \rightarrow 105	8	Appearance of first flexural cracks in shear spans, and their propagation vertically, later becoming inclined.
5	12.5	11.70	149 \rightarrow 151	143 \rightarrow 145	9	
6	15.0	14.30	195 \rightarrow 196	187 \rightarrow 188	10	
7	17.5	16.75	233 \rightarrow 234	223 \rightarrow 226	10	
8*	20.0	18.70	273 \rightarrow 274	261 \rightarrow 264	80	
9	22.5	22.10	310 \rightarrow 312	303 \rightarrow 305	3	
10	25.0	23.90	350 \rightarrow 352	337 \rightarrow 338	15	
11	27.5	26.65	392 \rightarrow 393	376 \rightarrow 378	14	Some cracks in the shear spans, while propagating further, also branching off backwards at the level of the reinforcement.
12*	30.0	28.80	429 \rightarrow 430	413 \rightarrow 415	26	
13	32.5	32.10	472 \rightarrow 473	454 \rightarrow 456	4	
14*	35.0	33.45	506 \rightarrow 513	494 \rightarrow 496	25	

TABLE BEAM IB-6 (CONTINUED)

LOADING STAGE	LOAD (KIPS)		DEFLECTION (10^{-3}) in.		READING TIME (MINUTES)	REMARKS
	START OF READING	END OF READING	AT MIDSPAN A \rightarrow B	UNDER LOAD PT. A \rightarrow B		
15*	37.5	36.40	560 \rightarrow 562	540 \rightarrow 542	18	No observation of splitting along the reinforcement upto this stage.
16	39.0	--	--	--	--	Beam failed suddenly as a diagonal crack joining the tips of two outermost cracks went completely through the compression zone of the beam, terminating near the load point. This was accompanied by a split along the reinforcement.

*DEMEC gauge readings were taken

A \rightarrow B A = deflection at start of reading

B = deflection at end of reading

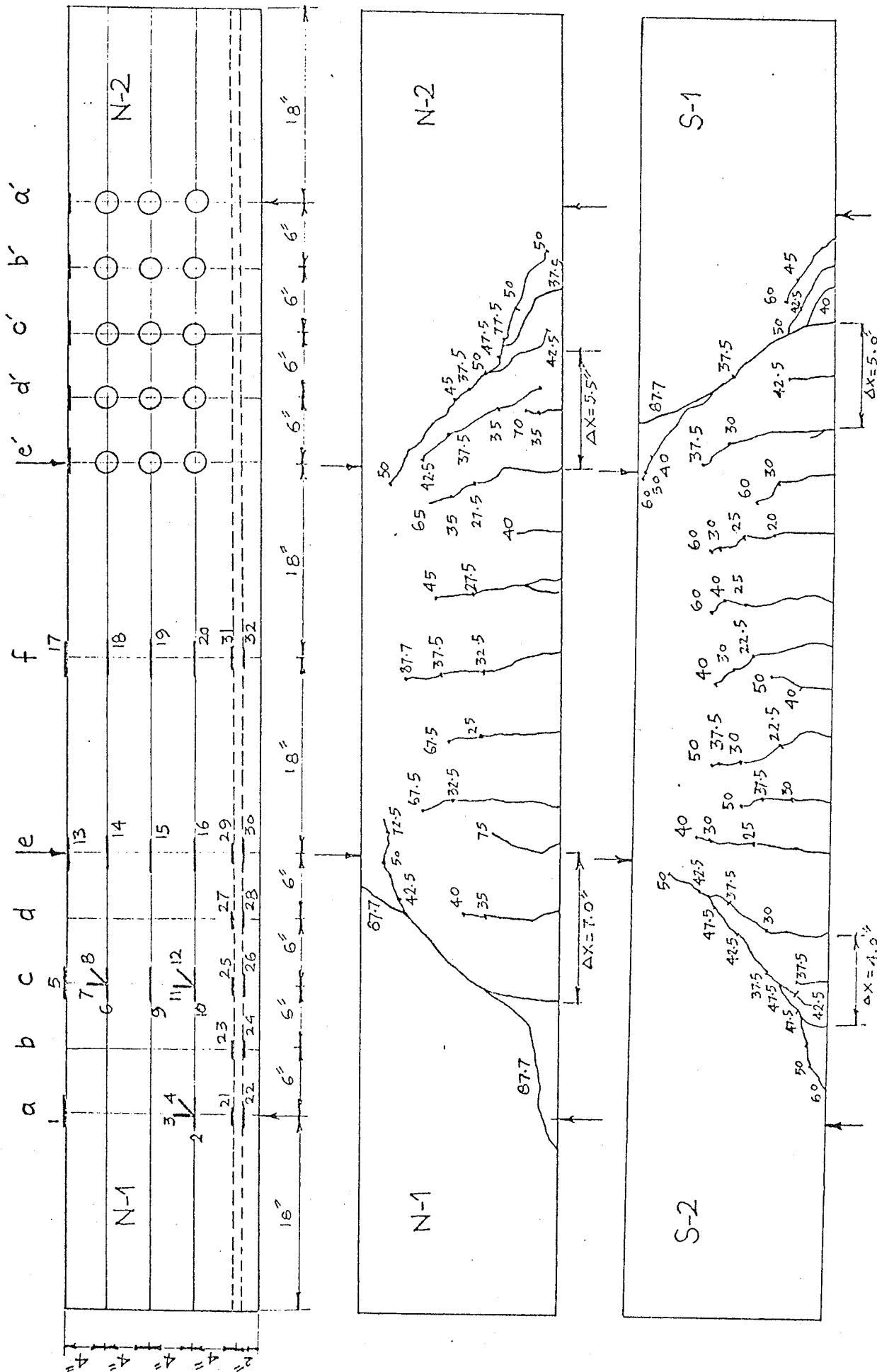


FIG. II.13 - BEAM IC-2 - LOCATION OF STRAIN GAUGES AND CRACK PATTERNS ON BOTH SIDES OF THE BEAM

TABLE II.13

BEAM IC-2 - LOADING STAGES, DEFLECTIONS AND CRACK FORMATION

LOADING STAGE	LOAD (KIPS)		DEFLECTION (10^{-3}) in.		READING TIME (MINUTES)	REMARKS
	START OF READING	END OF READING	AT MIDSPAN A \rightarrow B	UNDER LOAD PT. A \rightarrow B		
1	2.5	2.40	10 \rightarrow 10	9 \rightarrow 9	2	Observation of first flexural cracks in the region of pure flexure.
2	5.0	4.85	19 \rightarrow 19	18 \rightarrow 18	2	
3	7.5	7.30	27 \rightarrow 27	26 \rightarrow 26	2	
4	10.0	9.85	34 \rightarrow 34	31 \rightarrow 31	2	
5	12.5	12.35	41 \rightarrow 41	36 \rightarrow 38	2	
6	15.0	14.75	48 \rightarrow 48	41 \rightarrow 42	2	
7	17.5	17.25	52 \rightarrow 53	46 \rightarrow 47	2	
8	20.0	19.45	57 \rightarrow 58	51 \rightarrow 52	2	
9	22.5	21.75	65 \rightarrow 66	57 \rightarrow 58	2	Appearance of first flexural cracks in the shear spans.
10	25.0	23.90	73 \rightarrow 74	65 \rightarrow 68	6	
11	27.5	26.60	82 \rightarrow 83	73 \rightarrow 75	2	
12*	30.0	27.70	92 \rightarrow 94	83 \rightarrow 86	76	
13	32.5	32.05	103 \rightarrow 104	93 \rightarrow 94	4	Appearance of significant diagonal cracks in the shear spans and their propagation into the compression zone.
14	35.0	34.15	106 \rightarrow 107	99 \rightarrow 101	4	
15	37.5	36.10	117 \rightarrow 119	107 \rightarrow 110	6	
16*	40.0	36.80	131 \rightarrow 133	117 \rightarrow 120	29	Appearance of cracks near the supports.
17	42.5	41.55	145 \rightarrow 147	130 \rightarrow 133	6	

TABLE BEAM IC-2 (CONTINUED)

LOADING STAGE	LOAD (KIPS)		DEFLECTION (10^{-3}) in.		READING TIME (MINUTES)	REMARKS
	START OF READING	END OF READING	AT MIDSPAN A \rightarrow B	UNDER LOAD PT. A \rightarrow B		
18	45.0	44.25	154 \rightarrow 155	139 \rightarrow 141	3	Occurrence of a major extension of diagonal cracks. At this stage the diagonal cracks have extended to within 2 in. of the compression face.
19	47.5	45.40	162 \rightarrow 166	149 \rightarrow 155	3	
20*	50.0	47.65	178 \rightarrow 181	167 \rightarrow 169	34	
21	52.5	52.15	191 \rightarrow 191	179 \rightarrow 180	2	Occurrence of a very imperceptible propagation of cracks and a visible widening.
22	55.0	54.15	201 \rightarrow 201	188 \rightarrow 190	2	
23	57.5	57.00	207 \rightarrow 208	195 \rightarrow 196	2	
24*	60.0	57.65	216 \rightarrow 218	204 \rightarrow 206	25	
25	62.5	61.90	228 \rightarrow 229	215 \rightarrow 216	2	
26	65.0	64.40	236 \rightarrow 242	223 \rightarrow 225	3	Slow extension of diagonal cracks into the zone of pure flexure, almost parallel to the axis of the beam.
27	67.5	66.70	249 \rightarrow 250	232 \rightarrow 234	3	
28*	70.0	67.65	259 \rightarrow 260	242 \rightarrow 244	23	
29	72.5	71.60	271 \rightarrow 272	254 \rightarrow 255	2	
30*	75.0	73.50	280 \rightarrow 281	262 \rightarrow 264	8	
31	77.5	76.65	289 \rightarrow 290	273 \rightarrow 274	6	Continued widening of diagonal cracks.
32*	80.0	77.55	298 \rightarrow 306	282 \rightarrow 283	16	

TABLE BEAM IC-2 (CONTINUED)

LOADING STAGE	LOAD (KIPS)		DEFLECTION (10^{-3}) in.		READING TIME (MINUTES)	REMARKS
	START OF READING	END OF READING	AT MIDSPAN A \rightarrow B	UNDER LOAD PT. A \rightarrow B		
33	82.5	81.20	323 \rightarrow 325	294 \rightarrow 295	3	A very slow widening of cracks continued near failure and beam ultimately failed along the diagonal crack with a split along the reinforcement extending to the support.
34	85.5	82.35	379 \rightarrow 381	327 \rightarrow 329	2	
35	87.5	81.80	471 \rightarrow 473	393 \rightarrow 397	2	
36	87.7	--	--	--	--	

* DEMEC gauge readings were taken

A \rightarrow B A = deflection at start of reading
 B = deflection at end of reading

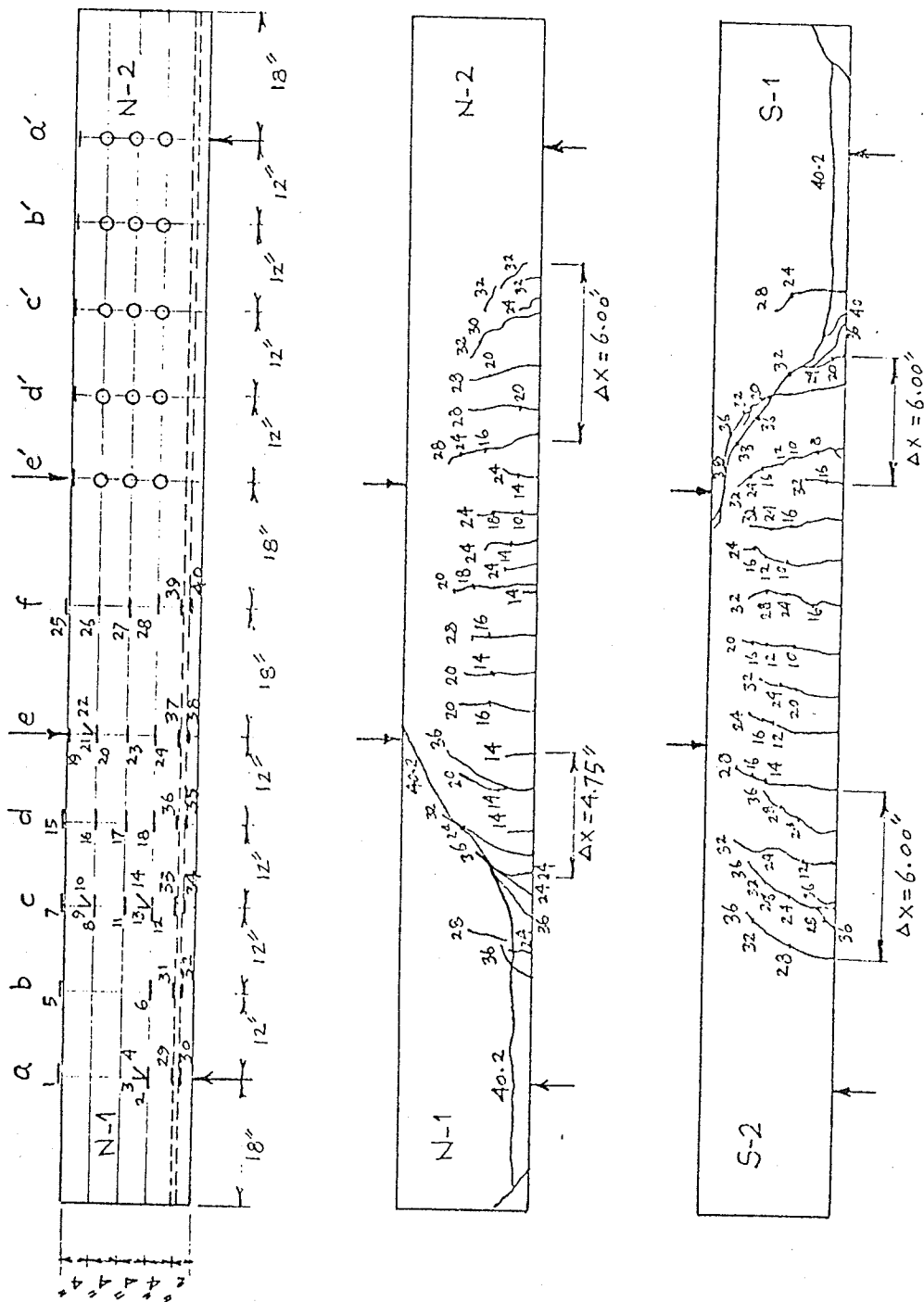


FIG. II.14 - BEAM IC-5 - LOCATION OF STRAIN GAUGES AND CRACK PATTERNS ON BOTH SIDES OF THE BEAM

BEAM IC-5 - LOADING STAGES, DEFLECTIONS AND CRACK FORMATION

LOADING STAGE	LOAD (KIPS)		DEFLECTION (10^{-3}) in.		READING TIME (MINUTES)	REMARKS
	START OF READING	END OF READING	AT MIDSPAN A \rightarrow B	UNDER LOAD PT. A \rightarrow B		
1	2.0	1.90	10 \rightarrow 10	10 \rightarrow 10	2	Appearance of flexural cracks and their vertical extension both in the region of pure flexure and the shear spans.
2	4.0	3.85	20 \rightarrow 20	24 \rightarrow 24	2	
3	6.0	5.85	30 \rightarrow 30	35 \rightarrow 35	2	
4	8.0	7.85	42 \rightarrow 42	45 \rightarrow 46	3	
5	10.0	9.60	55 \rightarrow 58	57 \rightarrow 62	3	Extension of flexural cracks in inclined direction in the shear spans as they proceeded upwards.
6	12.0	11.00	80 \rightarrow 82	83 \rightarrow 86	32	
7	14.0	13.55	105 \rightarrow 107	111 \rightarrow 112	3	
8*	16.0	14.80	129 \rightarrow 132	132 \rightarrow 136	27	
9	18.0	17.40	153 \rightarrow 155	156 \rightarrow 159	3	
10*	20.0	18.85	177 \rightarrow 181	178 \rightarrow 181	27	
11	22.0	21.55	202 \rightarrow 203	202 \rightarrow 203	3	
12*	24.0	22.25	223 \rightarrow 227	220 \rightarrow 224	32	
13	26.0	25.60	253 \rightarrow 254	247 \rightarrow 250	2	
14*	28.0	26.75	273 \rightarrow 276	268 \rightarrow 272	30	
15*	30.0	29.25	298 \rightarrow 299	292 \rightarrow 296	13	Observation of a major extension of critical diagonal crack, the diagonal crack extending to within $2\frac{1}{2}$ in. of the compression face.
16*	32.0	30.70	320 \rightarrow 321	315 \rightarrow 316	33	
17	34.0	33.45	346 \rightarrow 347	342 \rightarrow 344	4	
18*	36.0	34.45	377 \rightarrow 379	372 \rightarrow 373	32	

TABLE BEAM IC-5 (CONTINUED)

LOADING STAGE	LOAD (KIPS)		DEFLECTION (10^{-3}) in.		READING TIME (MINUTES)	REMARKS
	START OF READING	END OF READING	AT MIDSPAN A \rightarrow B	UNDER LOAD PT. A \rightarrow B		
19	38.0	37.30	411	403	4	Beam recorded a maximum load of 38.35 kips and then the load dropped. However, the beam again started taking more load as large deflections continued. Final failure occurred by the extension of the diagonal crack through the compression zone of the beam and a simultaneous split along the reinforcement.
20	40.2	--	--	--	--	

* DEMEC gauge readings were taken

A \rightarrow B A = deflection at start of reading
 B = deflection at end of reading

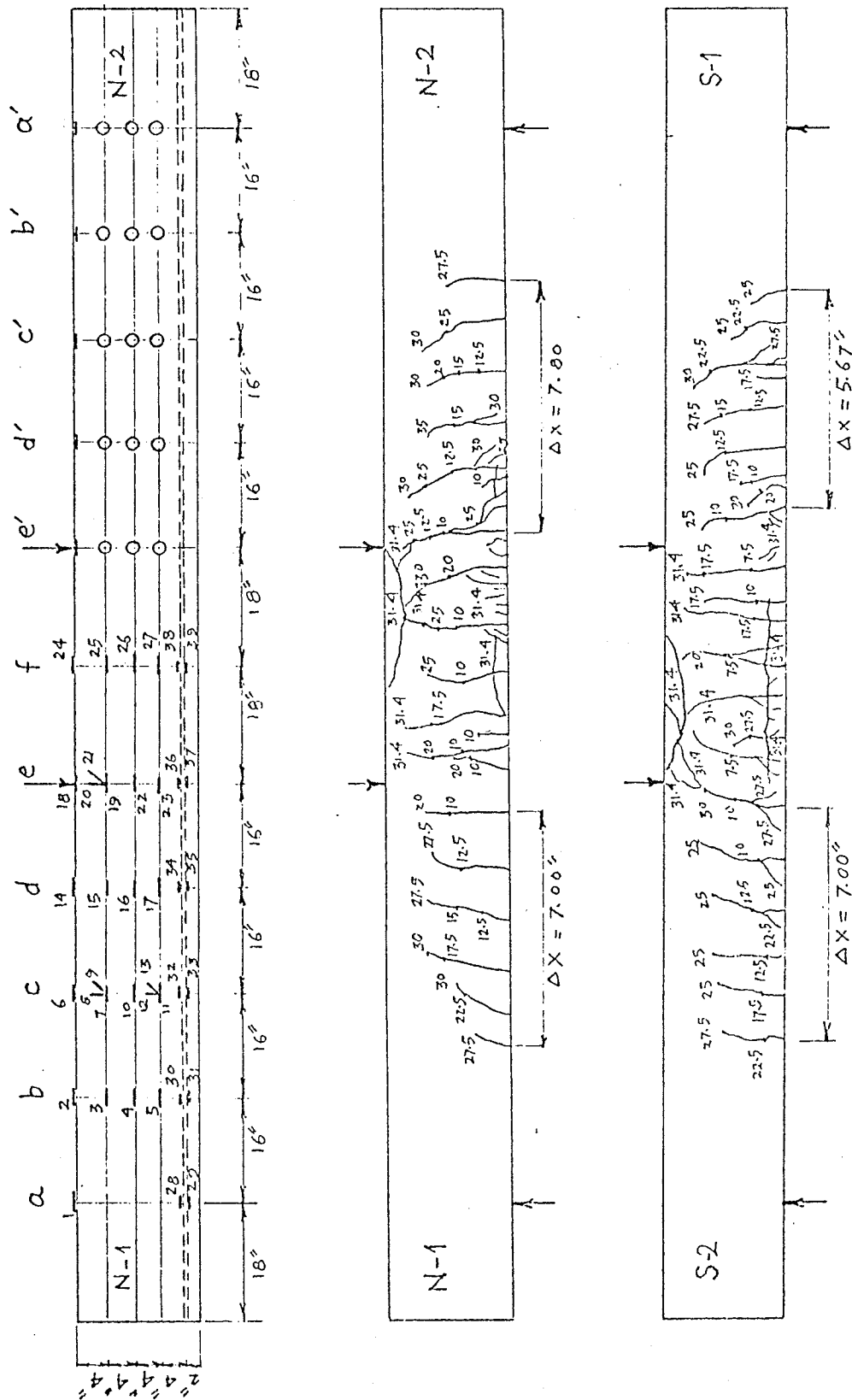


FIG. II.15 - BEAM IC-6 - LOCATION OF STRAIN GAUGES AND CRACK PATTERNS ON BOTH SIDES OF THE BEAM

BEAM IC-6 - LOADING STAGES, DEFLECTIONS AND CRACK FORMATION

LOADING STAGE	LOAD (KIPS)		DEFLECTION (10^{-3}) in.		READING TIME (MINUTES)	REMARKS
	START OF READING	END OF READING	AT MIDSPAN A \rightarrow B	UNDER LOAD PT. A \rightarrow B		
1	2.5	2.45	20 \rightarrow 20	17 \rightarrow 17	2	
2	5.0	4.85	40 \rightarrow 40	37 \rightarrow 38	2	
3	7.5	7.00	64 \rightarrow 66	60 \rightarrow 61	3	Appearance of first flexural cracks in the region of pure flexure.
4	10.0	9.20	119 \rightarrow 122	113 \rightarrow 116	10	Appearance of first flexural cracks in shear span.
5	12.5	11.65	174 \rightarrow 176	166 \rightarrow 168	12	Vertical propagation of flexural cracks, later becoming inclined in the shear spans.
6	15.0	14.15	230 \rightarrow 231	219 \rightarrow 221	10	
7	17.5	16.75	281 \rightarrow 282	268 \rightarrow 269	8	
8*	20.0	19.00	332 \rightarrow 334	317 \rightarrow 319	21	
9	22.5	22.00	382 \rightarrow 385	365 \rightarrow 367	4	
10	25.0	24.15	433 \rightarrow 434	413 \rightarrow 415	8	
11	27.5	26.80	482 \rightarrow 482	463 \rightarrow 464	6	
12*	20.0	27.35	549 \rightarrow 555	523 \rightarrow 531	28	
13	31.4	--	--	--	--	Beam failed in flexure in the midspan region after very large deflections. a portion of concrete at the compression face chipped off. Splitting along the reinforcement occurred in the zone of pure flexure.

* DEMEC gauge readings were taken.

A \rightarrow B A = deflection at start of reading

B = deflection at end of reading

BEAM IIA-2 - LOADING STAGES, DEFLECTIONS AND CRACK FORMATION

LOADING STAGE	LOAD (KIPS)		DEFLECTION (10^{-3}) in.		READING TIME (MINUTES)	REMARKS
	START OF READING	END OF READING	AT MIDSPAN A \rightarrow B	UNDER LOAD PT. A \rightarrow B		
1	2.5	2.45	11 \rightarrow 11	11 \rightarrow 11	2	Appearance of flexural cracks, and their propa- gation vertically, later becoming inclined in shear spans.
2	5.0	4.90	21 \rightarrow 21	21 \rightarrow 21	2	
3	7.5	7.35	29 \rightarrow 29	30 \rightarrow 30	2	
4	10.0	9.80	38 \rightarrow 38	38 \rightarrow 38	2	
5	12.5	12.30	45 \rightarrow 45	45 \rightarrow 45	2	
6	15.0	14.75	52 \rightarrow 52	53 \rightarrow 53	2	
7	17.5	17.25	59 \rightarrow 59	59 \rightarrow 59	2	
8	20.0	19.60	64 \rightarrow 65	65 \rightarrow 65	2	
9	22.5	22.15	71 \rightarrow 71	71 \rightarrow 71	2	
10	25.0	24.55	77 \rightarrow 78	77 \rightarrow 78	2	
11	27.5	26.95	85 \rightarrow 86	85 \rightarrow 86	2	
12*	30.0	28.75	92 \rightarrow 93	92 \rightarrow 92	18	Appearance of new diagonal cracks in the shear spans.
13	32.5	31.95	100 \rightarrow 101	100 \rightarrow 100	2	
14	35.0	34.15	107 \rightarrow 108	106 \rightarrow 107	3	
15	37.5	36.90	115 \rightarrow 116	114 \rightarrow 114	3	
16*	40.0	37.70	122 \rightarrow 122	120 \rightarrow 119	81	
17	42.5	42.15	131 \rightarrow 131	128 \rightarrow 128	2	
18	45.0	44.20	136 \rightarrow 136	133 \rightarrow 133	6	
19	47.5	46.90	142 \rightarrow 142	139 \rightarrow 139	3	
20*	50.0	48.00	148 \rightarrow 149	144 \rightarrow 144	26	
21	52.5	51.85	156 \rightarrow 156	152 \rightarrow 152	3	

TABLE BEAM IIA-2 (CONTINUED)

LOADING STAGE	LOAD (KIPS)		DEFLECTION (10^{-3}) in.		READING TIME (MINUTES)	REMARKS
	START OF READING	END OF READING	AT MIDSPAN A \rightarrow B	UNDER LOAD PT. A \rightarrow B		
22*	55.0	50.15	163 \rightarrow 167	157 \rightarrow 164	32	A completely new diagonal crack appeared in the shear span of the beam, propagated through the compression zone of the beam and after crossing the secondary beam, appeared in the zone of pure flexure. Load dropped by about 5 kips. As the load was increased to 55 kips again, failure occurred when the secondary beam sheared off at its junction to the main beam.

*DEMEC gauge readings were taken

A \rightarrow B A = deflection at start of reading

 B = deflection at end of reading

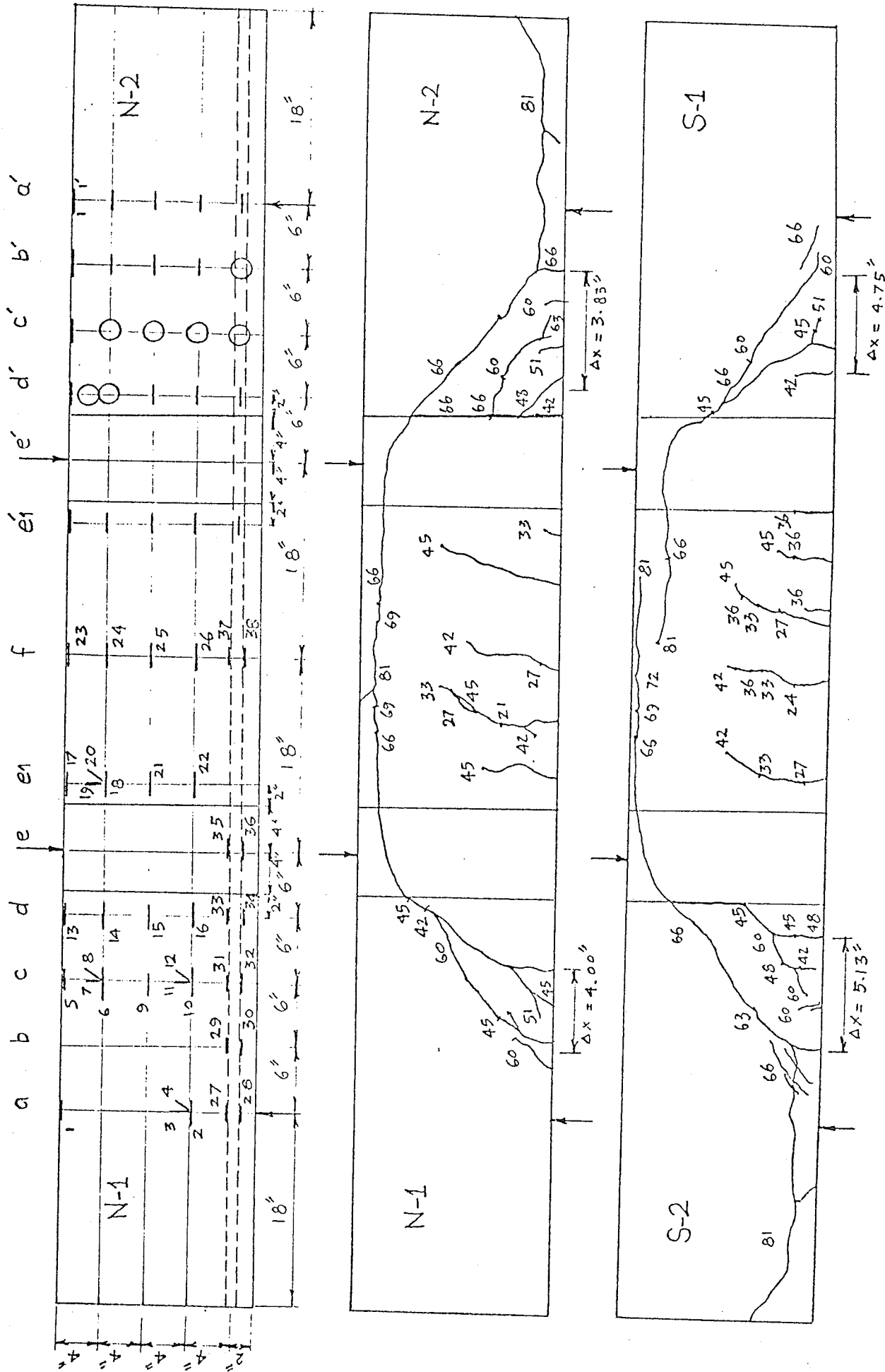


FIG. II.17 - BEAM IIA-2(b) - LOCATION OF STRAIN GAUGES AND CRACK PATTERNS ON BOTH SIDES OF THE BEAM

TABLE II.17

BEAM IIA-2(b) - LOADING STAGES, DEFLECTIONS AND CRACK FORMATION

LOADING STAGE	LOAD (KIPS)		MIDSPAN DEFLECTION (10^{-3}) IN. A \rightarrow B	READING TIME (MINUTES)	REMARKS
	START OF READING	END OF READING			
1	3.0	2.90	11 \rightarrow 11	2	Observation of first flexural cracks in the zone of pure flexure.
2	6.0	5.80	20 \rightarrow 20	2	
3	9.0	8.80	30 \rightarrow 30	2	
4	12.0	11.80	39 \rightarrow 39	2	
5	15.0	14.70	46 \rightarrow 46	2	
6	18.0	17.70	50 \rightarrow 51	2	
7	21.0	20.70	56 \rightarrow 57	2	
8	24.0	23.60	63 \rightarrow 64	2	Appearance of flexural cracks in the shear spans, their propagation vertically, later be- coming inclined.
9	27.0	26.60	69 \rightarrow 70	10	
10*	30.0	28.75	75 \rightarrow 76	28	
11	33.0	32.60	85 \rightarrow 87	4	
12	36.0	35.20	90 \rightarrow 91	7	
13	39.0	38.70	97 \rightarrow 98	2	
14*	42.0	39.80	104 \rightarrow 105	23	
15	45.0	43.50	114 \rightarrow 116	10	Load and deflection dropping while detailed strain readings are taken and cracks on the beam are marked.
16	48.0	47.25	124 \rightarrow 125	11	
17*	51.0	42.00	133 \rightarrow 115	97	
18	54.0	53.40	142 \rightarrow 143	5	
19	57.0	56.25	149 \rightarrow 151	5	

TABLE BEAM IIA-2(b) (CONTINUED)

LOADING STAGE	LOAD (KIPS)		MIDSPAN DEFLECTION (10 ⁻³) IN. A — B	READING TIME (MINUTES)	REMARKS
	START OF READING	END OF READING			
20*	60.0	57.00	164→164	12	Observation of a major diagonal crack in one of the shear spans.
21	63.0	62.50	178→179	8	
22*	66.0	51.00	190→184	60	
					Occurrence of critical diagonal cracking in both shear spans. Diagonal cracks crossing the secondary beams and appearing in the zone of pure flexure almost parallel to the axis of the member and close to the compression face. Load dropping by 6 kips instantly and further dropping while strain readings are taken.
23	69.0	68.50	231→233	2	Extension of diagonal cracks in the zone of pure flexure, approaching the midsection of the beam.
24	72.0	71.25	243→244	3	
25*	75.0	72.00	256→257	7	The beam failed suddenly (after taking the load momentarily) by the propagation of the diagonal crack in the zone of flexure. A portion of concrete above the crack chipped off while a simultaneous split occurred along the reinforcement
26	78.0	76.00	273→274	5	
27	81.0	--	--	--	

* DEMEC gauge readings were taken

A → B A = deflection at start of reading
 B = deflection at end of reading

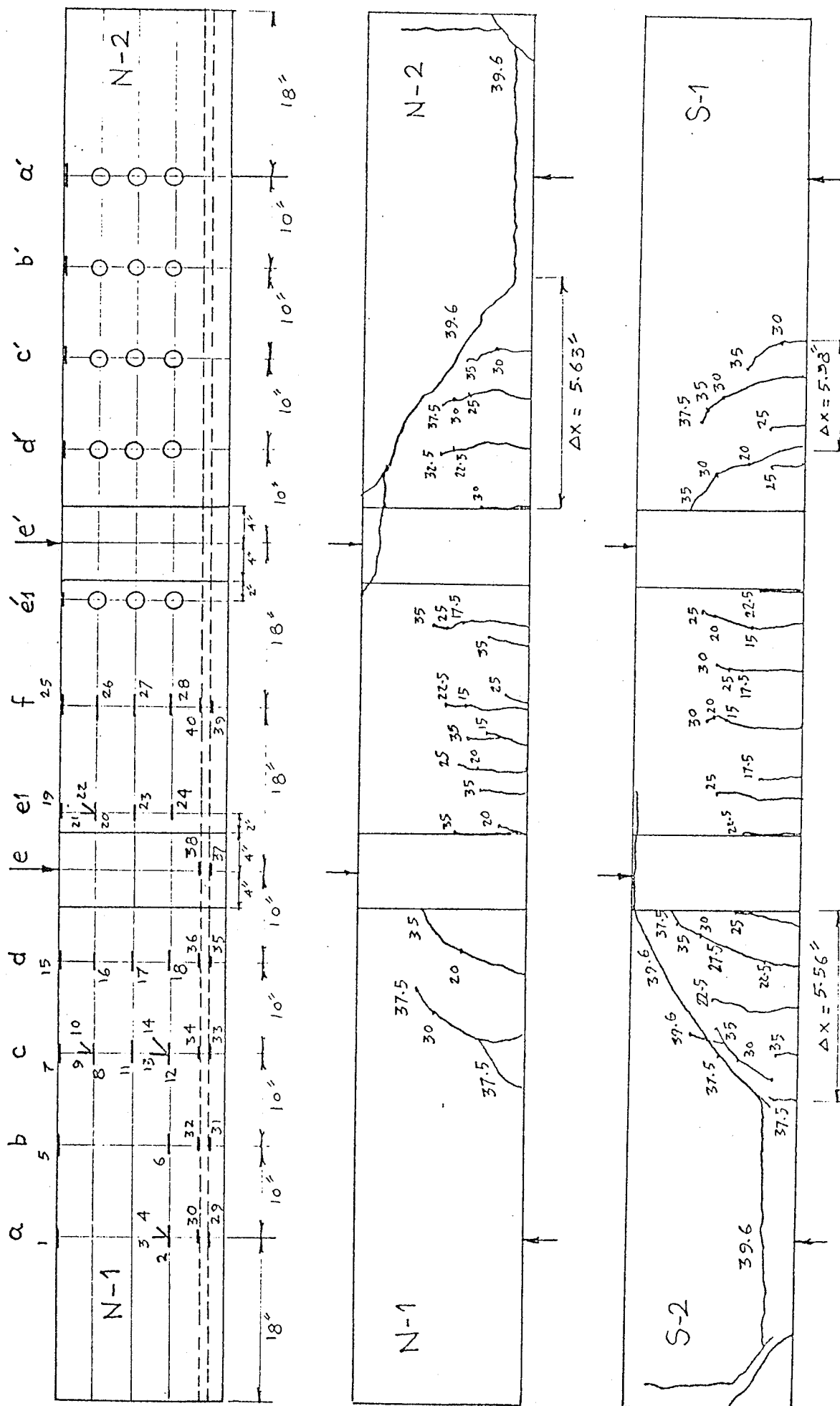


FIG. II.18 - BEAM IIA-4 - LOCATION OF STRAIN GAUGES AND CRACK PATTERNS ON BOTH SIDES OF THE BEAM

TABLE II.18

BEAM IIA-4- LOADING STAGES, DEFLECTIONS AND CRACK FORMATION

LOADING STAGE	LOAD (KIPS)		DEFLECTION (10^{-3}) in.		READING TIME (MINUTES)	REMARKS
	START OF READING	END OF READING	AT MIDSPAN A \rightarrow B	UNDER LOAD PT. A \rightarrow B		
1	2.5	2.40	12 \rightarrow 12	15 \rightarrow 15	2	Appearance of flexural cracks in the zone of pure flexure.
2	5.0	4.85	25 \rightarrow 25	29 \rightarrow 29	2	
3	7.5	7.20	37 \rightarrow 37	37 \rightarrow 38	2	
4	10.0	9.55	50 \rightarrow 53	48 \rightarrow 48	5	
5	12.5	12.05	66 \rightarrow 67	59 \rightarrow 60	2	
6	15.0	14.10	80 \rightarrow 81	72 \rightarrow 73	6	
7	17.5	16.70	94 \rightarrow 95	86 \rightarrow 87	4	Observation of flexural cracks in the shear spans and their propagation vertically, later becoming inclined.
8*	20.0	18.70	108 \rightarrow 110	100 \rightarrow 101	20	
9	22.5	21.70	125 \rightarrow 126	116 \rightarrow 116	8	
10*	25.0	23.90	139 \rightarrow 141	129 \rightarrow 130	20	
11	27.5	26.95	155 \rightarrow 156	144 \rightarrow 145	2	
12*	30.0	28.85	171 \rightarrow 173	157 \rightarrow 158	23	
13	32.5	32.10	187 \rightarrow 187	171 \rightarrow 172	2	Appearance of a major diagonal crack in the shear span.
14*	35.0	33.75	200 \rightarrow 202	184 \rightarrow 184	20	
15	37.5	36.75	217 \rightarrow 219	199 \rightarrow 200	6	
16	39.6	--	--	--	--	Sudden failure of the beam was caused by an extremely rapid propagation of the diagonal crack through the compression zone of the beam accompanied by a split along the reinforcement.

* DEMEC gauge readings were taken.

A \rightarrow B A = deflection at start of reading

B = deflection at end of reading

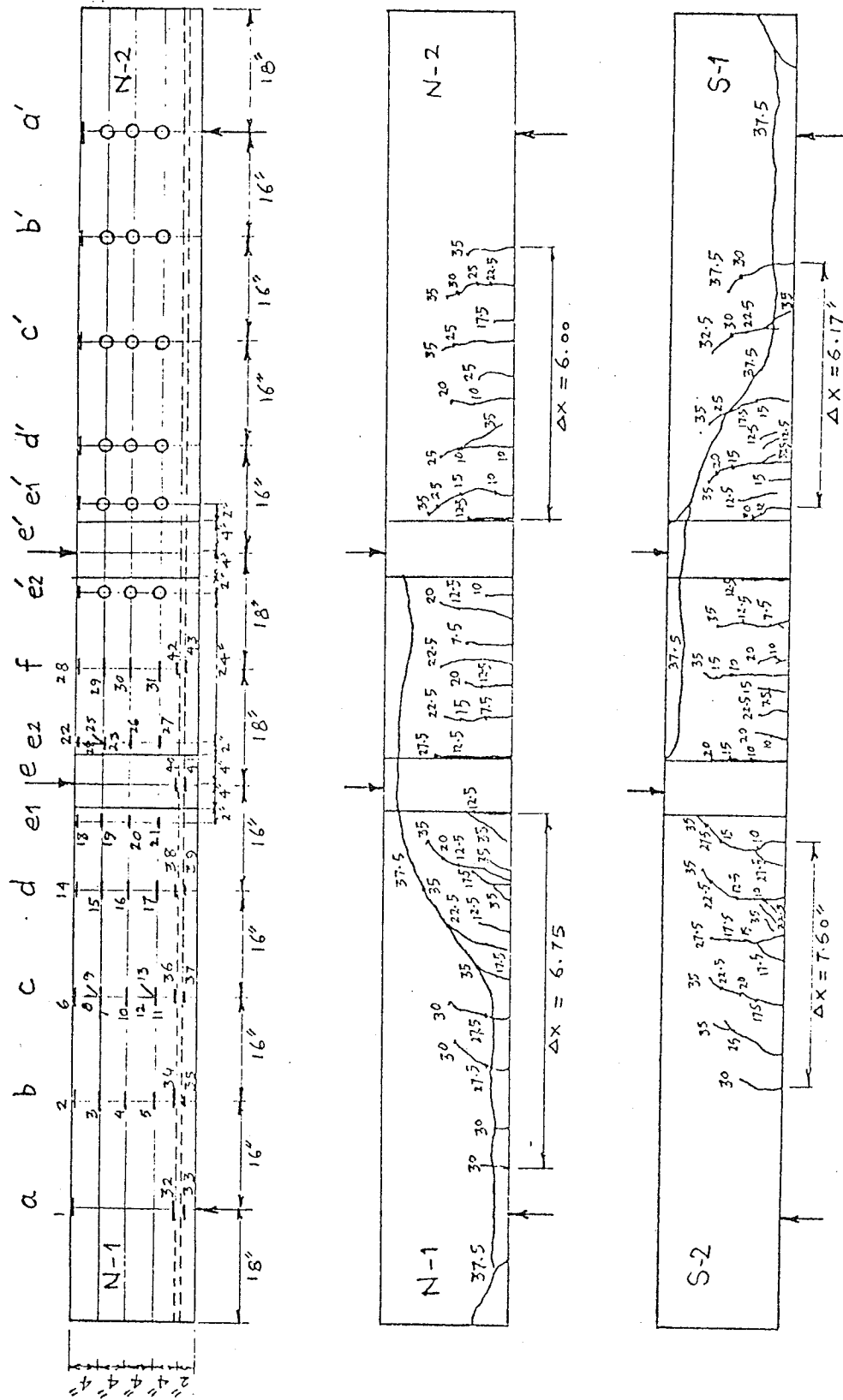


FIG. II.19 - BEAM IIA-6 - LOCATION OF STRAIN GAUGES AND CRACK PATTERNS ON BOTH SIDES OF THE BEAM

BEAM IIA-6 - LOADING STAGES, DEFLECTIONS AND CRACK FORMATION

LOADING STAGE	LOAD (KIPS)		DEFLECTION (10^{-3}) in.		READING TIME (MINUTES)	REMARKS
	START OF READING	END OF READING	AT MIDSPAN A \rightarrow B	UNDER LOAD PT. A \rightarrow B		
1	2.5	2.35	18 \rightarrow 18	20 \rightarrow 20	2	
2	5.0	4.85	42 \rightarrow 42	45 \rightarrow 45	2	
3	7.5	7.10	69 \rightarrow 69	70 \rightarrow 70	2	Appearance of flexural cracks in the zone of pure flexure.
4	10.0	9.40	102 \rightarrow 104	102 \rightarrow 104	6	Observation of flexural cracks in the shear spans.
5	12.5	11.85	138 \rightarrow 140	138 \rightarrow 140	8	Vertical propagation of cracks, later becoming inclined in the shear spans.
6	15.0	14.25	173 \rightarrow 175	171 \rightarrow 173	6	
7	17.5	16.80	208 \rightarrow 210	204 \rightarrow 205	5	
8*	20.0	18.75	241 \rightarrow 245	237 \rightarrow 237	48	
9	22.5	22.05	279 \rightarrow 281	271 \rightarrow 271	5	
10*	25.0	24.15	310 \rightarrow 311	300 \rightarrow 301	12	
11	27.5	26.90	344 \rightarrow 344	333 \rightarrow 333	5	Backwards branching-off of some cracks at the level of the reinforcement while propagating further into the compression zone.
12	30.0	28.85	376 \rightarrow 377	363 \rightarrow 364	20	
13	32.5	32.00	412 \rightarrow 413	398 \rightarrow 399	4	
14*	35.0	33.55	455 \rightarrow 446	430 \rightarrow 431	26	Inclined cracks remain significantly below the compression face of the beam.

TABLE BEAM IIA-6 (CONTINUED)

LOADING STAGE	LOAD (KIPS)		DEFLECTION (10^{-3}) in.		READING TIME (MINUTES)	REMARKS
	START OF READING	END OF READING	AT MIDSPAN A \rightarrow B	UNDER LOAD PT. A \rightarrow B		
15	37.5	--	48.5	462	--	The beam sustained the load for about 3 minutes. Failure occurred by a sudden propagation of a diagonal crack (joining the top tips of two pre-existing cracks) through the compression zone of the beam. The failure crack propagated horizontally in the zone of pure flexure. A split along the reinforcement was also observed.

* DEMEC gauge readings were taken

A \rightarrow B A = deflection at start of reading

 B = deflection at end of reading

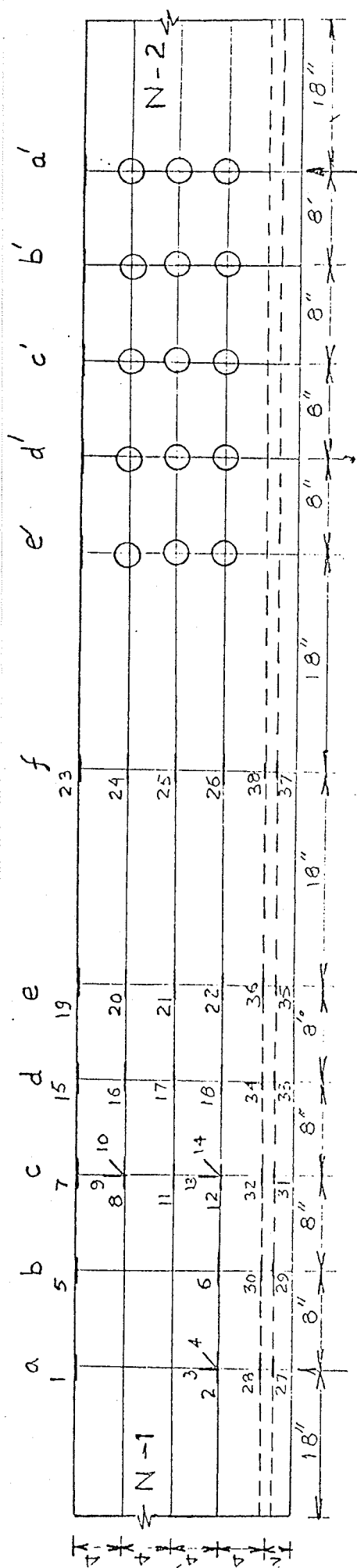


FIG. II.20 - BEAM IIIA-3 - LOCATION OF STRAIN GAUGES AND CRACK PATTERNS ON BOTH SIDES OF THE BEAM

TABLE II.20

BEAM IIIA-3 - LOADING STAGES, DEFLECTIONS AND CRACK FORMATION

LOADING STAGE	LOAD (KIPS)		MIDSPAN DEFLECTION (10 ⁻³) IN. A → B	READING TIME (MINUTES)	REMARKS
	START OF READING	END OF READING			
1	2.5	2.50	12→12	2	Appearance of flexural cracks and their vertical propagation, later becoming inclined
2	5.0	4.95	24→24	2	
3	7.5	7.35	34→34	2	
4	10.0	9.85	43→44	2	
5	12.5	12.35	52→53	2	
6	15.0	14.75	62→62	2	
7	17.5	17.35	71→72	2	
8	20.0	19.50	79→80	4	
9	22.5	21.95	87→89	4	With increasing load, appearance of cracks in the outer regions of the beam.
10	25.0	24.50	96→98	4	
11	27.5	26.75	105→107	11	
12*	30.0	28.90	114→117	18	
13	32.5	32.15	125→125	2	
14	35.0	34.35	133→134	3	
15	37.5	37.00	142→142	2	
16	40.0	39.20	151→153	9	
17	42.5	42.00	161→161	3	
18	45.0	44.25	168→169	4	
19	47.5	47.10	176→177	2	
20*	50.0	48.80	183→185	23	
21	52.5	52.10	193→193	2	
22	55.0	54.35	200→201	2	
23	57.5	56.65	208→209	2	

TABLE BEAM IIIA-3 (CONTINUED)

LOADING STAGE	LOAD (KIPS)		MIDSPAN DEFLECTION (10 ⁻³) IN. A → B	READING TIME (MINUTES)	REMARKS
	START OF READING	END OF READING			
24*	60.0	58.40	217→220	20	Appearance of a major diagonal crack on one end of the beam and its propagation to within 4½ in. of the compression face.
25	62.5	62.00	229→230	2	
26	65.0	64.05	237→239	2	
27	67.5	66.65	248→249	6	
28	70.0	68.20	258→262	9	Development of another major diagonal crack in the other end of the beam, the previous crack penetrating to within 2 in. of the compression face.
29	72.5	71.95	274→274	2	
30*	75.0	72.25	293→299	21	Slow propagation of diagonal cracks almost parallel to the axis of the members.
31	77.5	77.00	309→316	2	
32	80.0	79.20	325→325	2	
33	82.5	81.75	339→341	2	Visible widening of cracks.
34	85.0	84.20	355→357	2	
35	87.5	86.55	368→370	2	
36*	90.0	88.10	382→386	13	
37	92.5	91.85	399→400	2	
38	95.0	93.90	408→408	2	
39	97.5	96.50	421→424	2	
40	100.0	98.30	445→450	2	

TABLE BEAM IIIA-3 (CONTINUED)

LOADING STAGE	LOAD (KIPS)		MIDSPAN DEFLECTION (10^{-3}) IN. A \rightarrow B	READING TIME (MINUTES)	REMARKS
	START OF READING	END OF READING			
41	101.0	--	--	--	Failure occurred when two diagonal cracks joined together and a chunk of concrete above these cracks was broken. Splitting along the reinforcement occurred from the inner diagonal crack to the support and the whole block of concrete between the two diagonal cracks came apart from the beam.

* DEMEC gauge readings were taken

A \rightarrow B A = deflection at start of reading
 B = deflection at end of reading

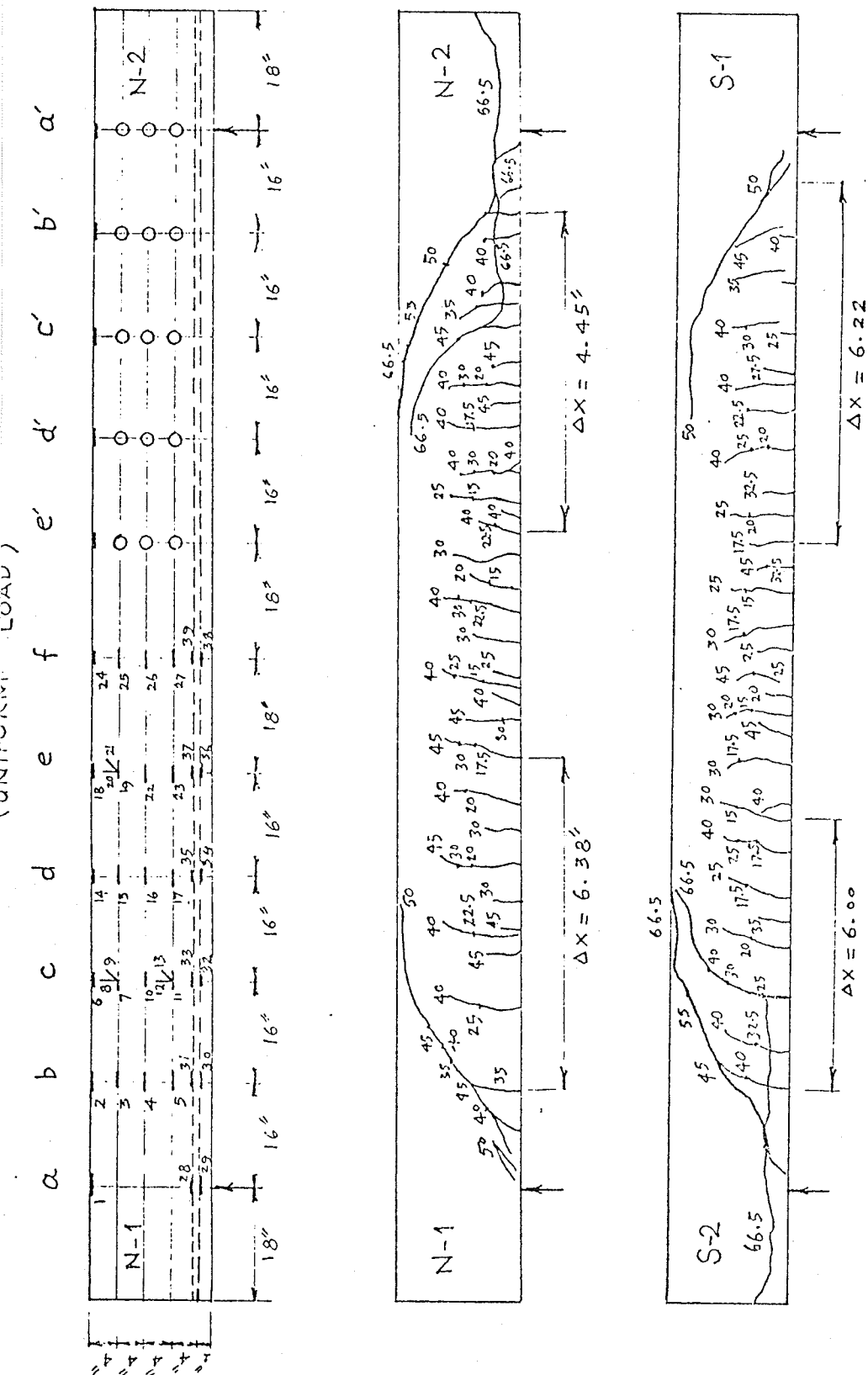


FIG. II.21 - BEAM IIIA-6 - LOCATION OF STRAIN GAUGES AND CRACK PATTERNS ON BOTH SIDES OF THE BEAM

TABLE II.21

BEAM IIIA-6 - LOADING STAGES, DEFLECTIONS AND CRACK FORMATION

LOADING STAGE	LOAD (KIPS)		MIDSPAN DEFLECTION (10^{-3}) IN. A \rightarrow B	READING TIME (MINUTES)	REMARKS
	START OF READING	END OF READING			
1	2.5	2.50	15 \rightarrow 15	2	Appearance of flexural cracks, and their propagation vertically upwards, later becoming inclined
2	5.0	4.90	29 \rightarrow 30	2	
3	7.5	7.35	45 \rightarrow 46	2	
4	10.0	9.90	64 \rightarrow 65	2	
5	12.5	12.10	84 \rightarrow 88	2	
6	15.0	14.45	110 \rightarrow 115	5	
7	17.5	16.90	139 \rightarrow 143	8	
8*	20.0	18.85	166 \rightarrow 174	104	
9	22.5	22.30	196 \rightarrow 197	5	
10	25.0	24.30	216 \rightarrow 219	7	
11	27.5	27.10	240 \rightarrow 243	3	
12*	30.0	29.00	264 \rightarrow 268	18	Cracking has extended to a large portion of the span.
13	32.5	32.20	290 \rightarrow 291	4	
14	35.0	34.40	310 \rightarrow 312	5	
15	37.5	37.05	334 \rightarrow 336	3	
16*	40.0	38.90	357 \rightarrow 361	24	
17	42.5	42.30	385 \rightarrow 385	3	
18	45.0	44.15	401 \rightarrow 405	8	
19	47.5	47.05	428 \rightarrow 429	3	

TABLE BEAM IIIA-6 (CONTINUED)

LOADING STAGE	LOAD (KIPS)		MIDSPAN DEFLECTION (10 ⁻³) IN. A → B	READING TIME (MINUTES)	REMARKS
	START OF READING	END OF READING			
20*	50.0	46.65	450→481	27	Penetration of a major diagonal crack on one end through the compression zone, becoming parallel to the axis of the beam near the compression face. Load dropping considerably.
21	50.0	49.50	500→502	3	
22	52.0	51.80	525→526	2	
23	55.0	51.00	593→594	2	
					Occurrence of a major extension of the diagonal crack on the other end of the beam; diagonal cracks on both ends being almost symmetrical and very close to the compression face. Load again dropping by 4 kips.
24	58.0	57.45	671→673	2	Stabilization of diagonal cracks and their visible widening.
25	60.0	59.60	693→693	2	" "
26	62.5	61.25	728→745	10	" "
27	65.0	64.40	775→778	2	" "
28	66.5	--	--	--	A very destructive diagonal failure occurred when two diagonal cracks on one end joined at the compression face and the block of concrete between them came completely apart from the beam. Horizontal splitting also occurred along the reinforcement from the inner crack to the end of the beam.

* DEMEC gauge readings were taken

A → B A = deflection at start of reading
 B = deflection at end of reading

(UNIFORM LOAD)

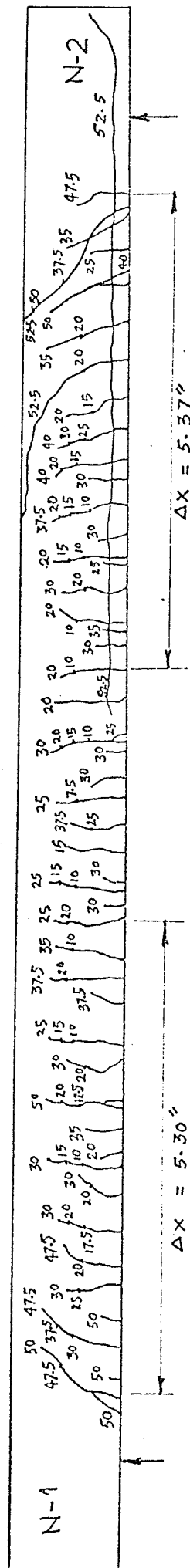
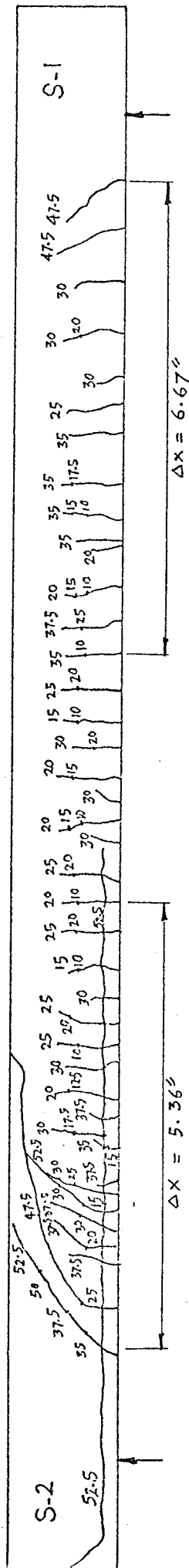
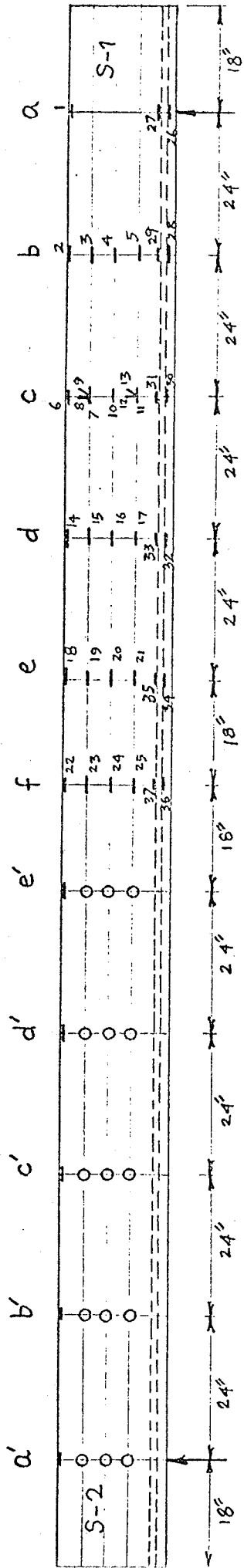


FIG. II.22 - BEAM IIIA-8 - LOCATION OF STRAIN GAUGES AND CRACK PATTERNS ON BOTH SIDES OF THE BEAM

TABLE II.22

BEAM IIIA-8 - LOADING STAGES, DEFLECTIONS AND CRACK FORMATION

LOADING STAGE	LOAD (KIPS)		MIDSPAN DEFLECTION (10 ⁻³) IN. A → B	READING TIME (MINUTES)	REMARKS
	START OF READING	END OF READING			
1	2.5	2.50	24→25	2	Appearance of flexural cracks and their propagation vertically.
2	5.0	4.85	57→60	3	
3	7.5	7.15	96→101	5	
4	10.0	9.60	159→166	11	
5	12.5	12.10	216→221	4	
6	15.0	14.45	272→278	7	
7	17.5	17.20	328→335	4	
8*	20.0	19.25	383→393	34	Flexural cracks have appeared over a large portion of the span.
9	22.5	22.30	443→446	3	
10*	25.0	24.45	491→498	16	
11	27.5	27.25	546→550	3	Flexural cracks becoming inclined in the outer regions of the beam.
12*	30.0	29.15	591→600	38	
13	32.5	32.10	651→655	3	
14*	35.0	34.35	702→710	28	No further propagation of cracks in the middle portion of the beam. Appearance of new cracks closer to the supports.
15	37.5	37.10	759→763	12	
16*	40.0	39.50	810→814	10	
17	42.5	42.30	864→866	4	
18	45.0	44.60	915→917	3	
19	47.5	46.80	967→972	3	

TABLE BEAM IIIA-8 (CONTINUED)

LOADING STAGE	LOAD (KIPS)		MIDSPAN DEFLECTION (10^{-3}) IN. A \rightarrow B	READING TIME (MINUTES)	REMARKS
	START OF READING	END OF READING			
20*	50.0	48.80	1024 \rightarrow 1036	22	Observation of a major extension of a diagonal crack, the crack being within 3 in. of the compression face.
21	52.5	--	--	--	The beam failed with a very destructive diagonal failure after sustaining the load momentarily. Two diagonal cracks extended to the compression zone and the whole block of concrete between them came apart. Splitting along the reinforcement extended from the midspan of the beam to the anchorage zone.

* DEMEC gauge readings were taken

A \rightarrow B A = deflection at start of reading

B = deflection at end of reading

II.3 COMMENTS ON THE FAILURE OF BEAMS

In this section, all beams of the entire test series are discussed individually. Crack formation at various important stages of loading is described and comments made on the failure of the beams, as observed during the tests. Descriptions of all beams are accompanied by photographs of the beams showing the instrumentation used and the progress of cracking until collapse.

II.3.1 Beam IA-1 (Figs. 23 to 26)

The first flexural cracks appeared in the beam at a load of 30 kips. These cracks developed into significant diagonal cracks at a load of about 50 kips and as the load was increased to 60 kips, a major diagonal crack developed on both ends of the beam. This crack propagated to within 5 inches of compression face of the beam. Further increments of load resulted in only small increases in the propagation of cracks and the beam continued taking considerable load. At a load of 80 kips, there were new diagonal cracks on different faces. Some back-cracking from pre-existing cracks was also seen. The location of the initial crack on end S1 at 150 kips was only $1 \frac{3}{4}$ inches from the compression face. However, as the loading was continued, there was little further propagation of cracks. The capacity of loading jack was 200,000 pounds and as the load reached 195,000 pounds there were no signs of ultimate failure in the beam. The test was discontinued at this stage.

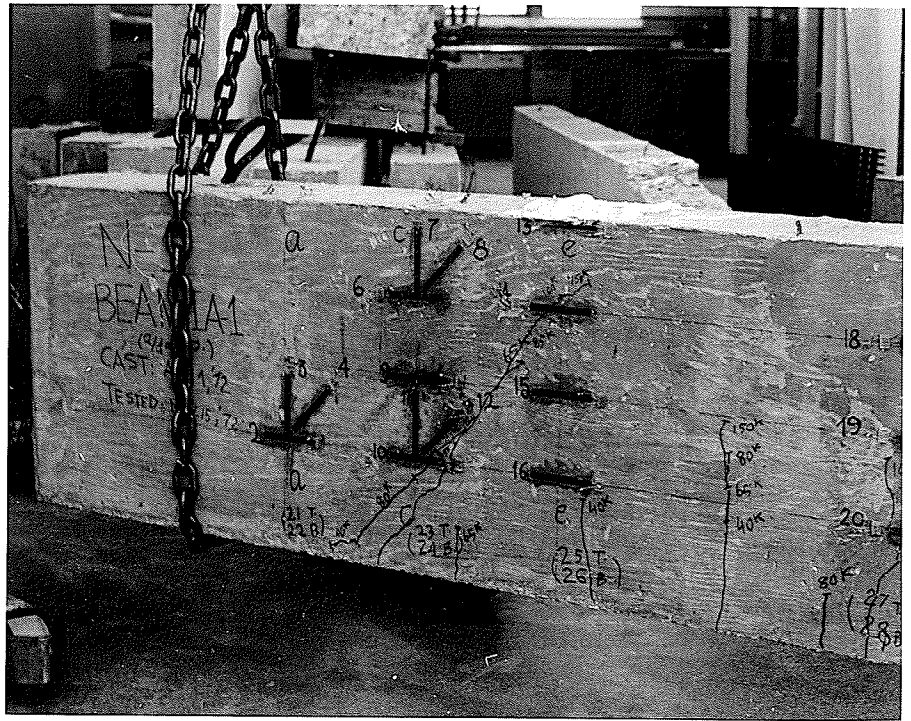


FIG. 23 BEAM IA-1 AT MAXIMUM LOADING - SIDE N1

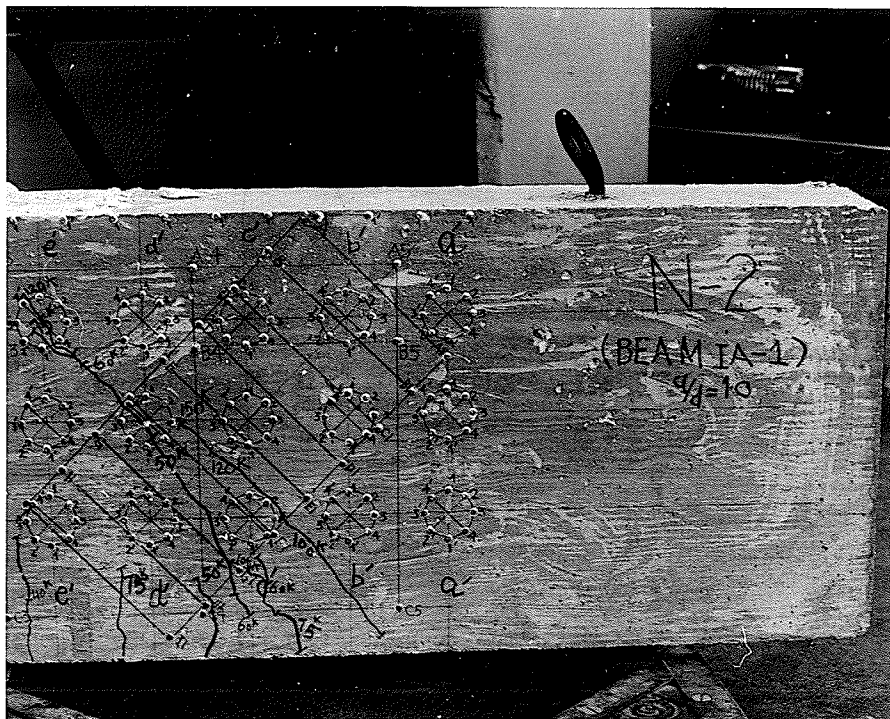


FIG. 24 BEAM IA-1 (SIDE N2) SHOWING DEMEC GAUGES
AND CRACK LOCATIONS

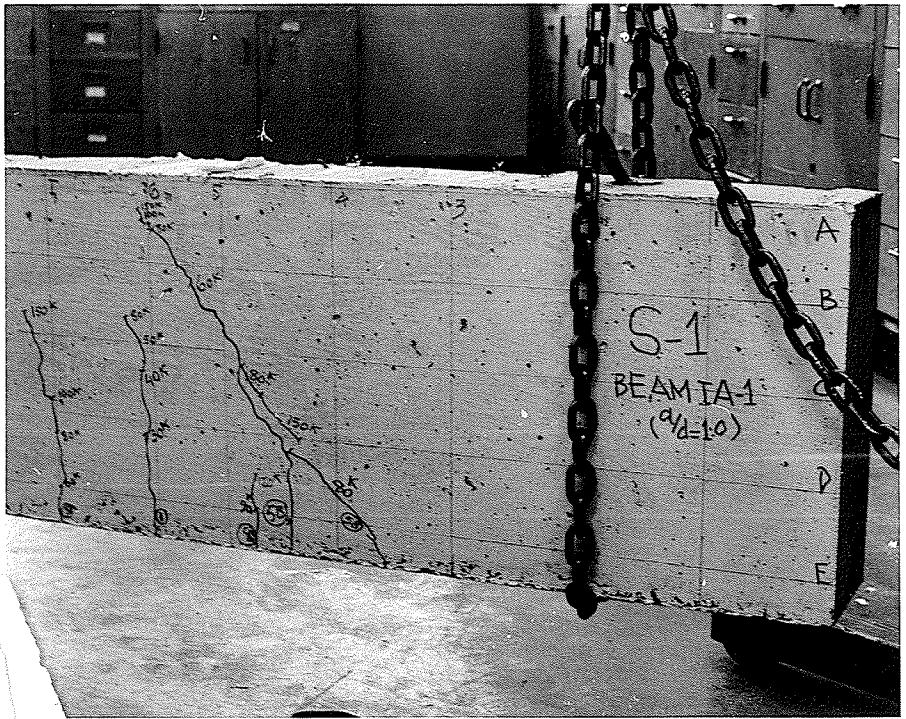


FIG. 25 CRACK LOCATIONS ON SIDE S1 OF BEAM IA-1

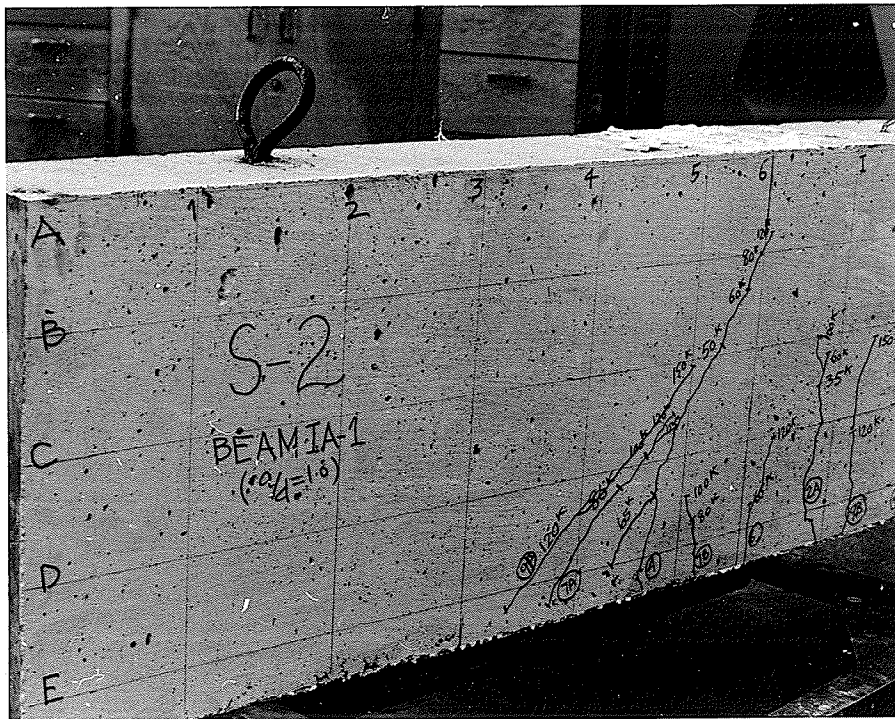


FIG. 26 CRACK LOCATIONS ON SIDE S2 OF BEAM IA-1

III.3.2 Beam IA-2 (Figs. 27 and 28)

The first flexural cracks in this beam developed on side S1-S2 at a load of 15 kips. First cracks in shear span appeared at a load of 30 kips. Significant diagonal cracking occurred at 40 kips and the cracks progressed to a height* of 10 inches. At 50 kips, a major diagonal cracking was observed while there was no appreciable movement of the flexural cracks in the constant moment zone. At 60 kips the diagonal cracks were well developed on all sides and especially on side S1, where the critical crack was only 1/2 in. below the top. Diagonal cracks, could also be seen going into the constant moment zone with a flatter trajectory.

With further loading, there was no perceptible propagation of cracks though a visible widening of critical diagonal cracks occurred.

At a load of 80 kips, while the critical diagonal crack on face S1 was just 1/4 inches from top, two cracks became visible at the top end of the beam, above the diagonal crack. These cracks travelled downwards a distance about 1 3/4 in.

Cracks on face S2 remained 2 inches below the compression face at this stage and subsequent stages of loading. The final failure was on end N1/S1 at a load of 94.7 kips. The two portions of the beam, separated by the diagonal crack, came apart with a sudden split, accompanied by a horizontal split all along the reinforcement from the lower end of the crack to the support and some chipping of concrete at the end.

* These heights are taken from beam bottom, which includes 2 in. of cover below the reinforcement.

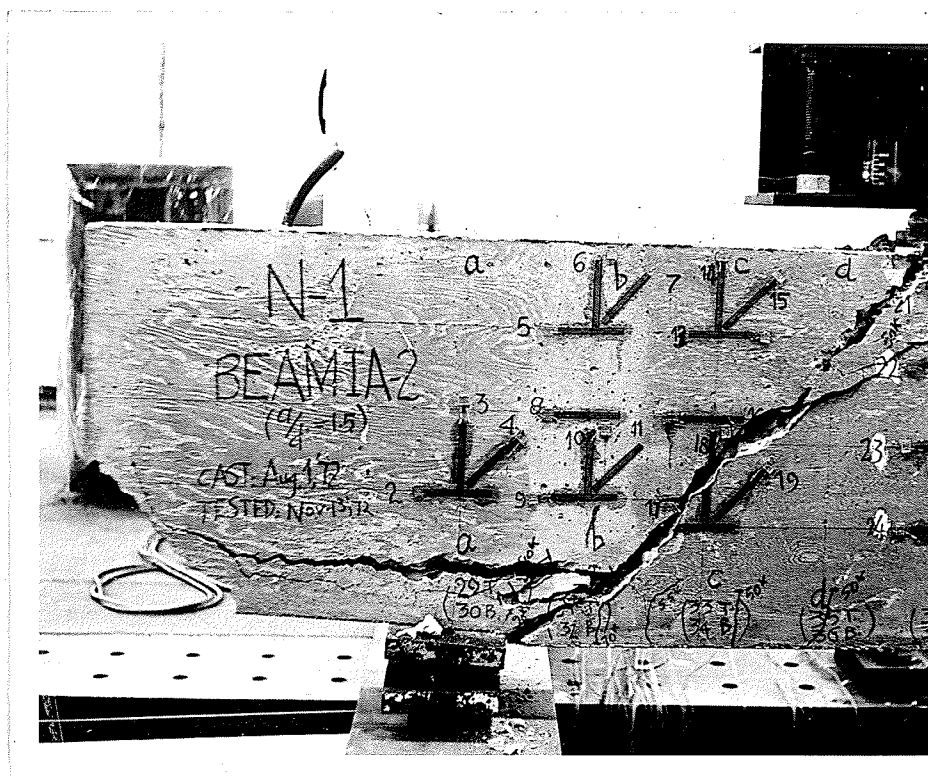


FIG. 27 FAILURE OF BEAM IA-2

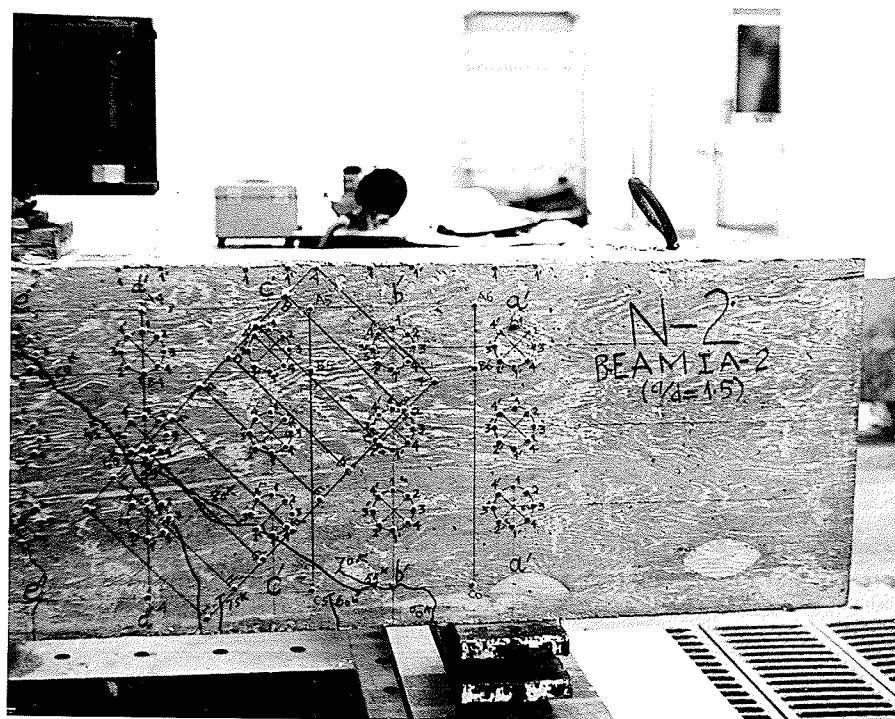


FIG. 28 CRACKING AND DEMEC GAUGE LOCATIONS ON BEAM IA-2

Towards the load point, the final split was almost straight at 45° , extending to the outer end of the load plate. The final split did not proceed into the zone of constant moment though the diagonal cracking had progressed into this zone at previous stages of loading with a flatter slope. From a load of 60 kips onwards, significant local cracking in the vicinity of the supports close to the major inclined cracks was also visible.

II.3.3 Beam IA-3 (Figs. 29 and 30)

The first flexural cracks appeared in the midspan region at 20 kips and in the shear span at 27.5 kips. Further cracking developed with increase of load. Significant diagonal cracking could be seen at a load of 35 kips and 40 kips. At a load of 45 kips, a major diagonal crack suddenly propagated through the shear span on end S1 and a similar crack on end S2 propagated to within 1 1/2 inches of the compression face. Failure seemed to be imminent. There was a significant drop in the load while the deflection increased slightly. Load was then increased in one thousand pound increments while numerous strain and deflection readings were taken. Despite a fully cracked section, the beam continued taking more load without any further diagonal cracking while these cracks widened. Cracking also occurred over the supports. After a load of 56 kips, the load increment interval was increased to 2000 pounds. At a load of 62 kips, the diagonal cracks proceeded into the constant moment zone with flatter slopes. The ultimate failure occurred at a load of 72 kips, the failure being very similar to that reported for beam IA-2. In both of these beams,

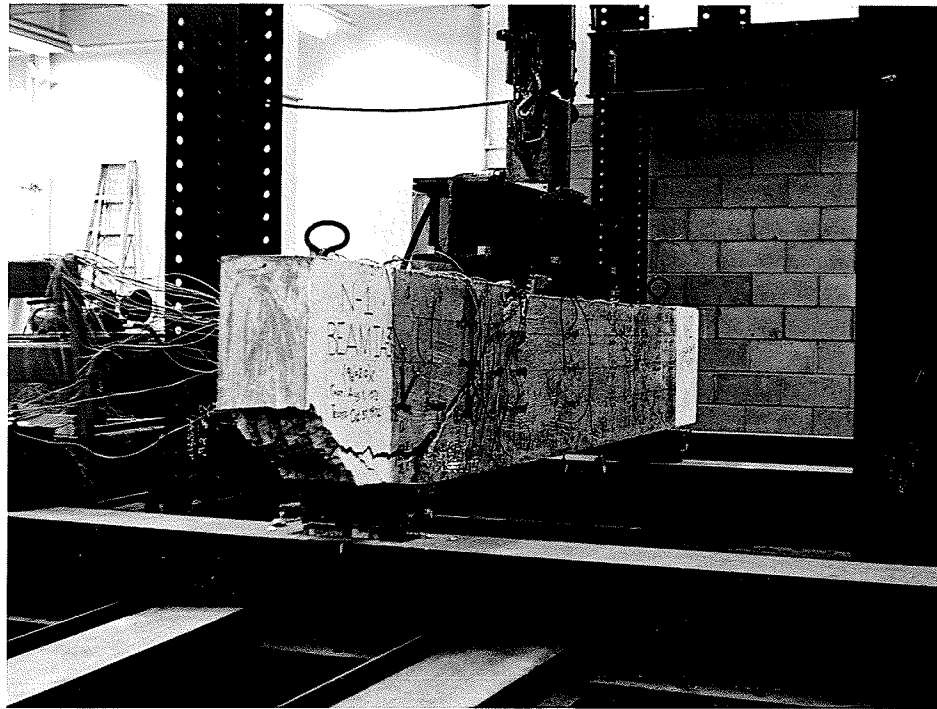


FIG. 29 BEAM IA-3 SHOWING FINAL FAILURE

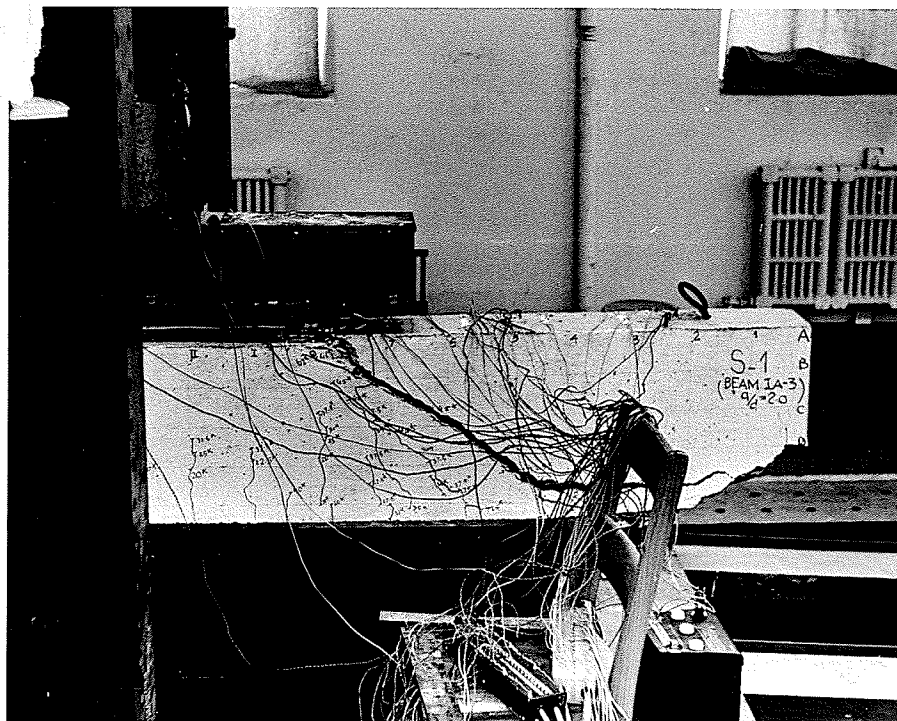


FIG. 30 BEAM IA-3 SHOWING CRACKING AND FINAL FAILURE ON END S1

fine particles of concrete along the final cracked surface could be seen.

II.3.4 Beam IA-4 (Fig. 31)

The first flexural cracks appeared at a load of 12.5 kips. As the load was increased there were further cracks. The cracks on end N1/S1 remained fewer and farther apart than those on end N2/S2. The flexural cracks in midspan progressed to a maximum height of 12 1/2 inches at 30 kips and stayed there while diagonal cracking developed at further loading. The critical diagonal crack on end N2/S2 became fairly well defined at 35 kips. A diagonal crack closer to the load point had progressed well into the compression zone when an entirely new inclined crack became visible at 37.5 kips on end N2 and a similar pre-existing crack on S2 progressed higher. These cracks, however, were very sharp and thin and the beam appeared fairly intact. As the load was increased for the next increment, the beam failed suddenly with an extension of the pre-existing crack closer to the supports, at 39.7 kips. The failure occurred on end N2/S2, failure crack remaining fairly thin. A split along the reinforcement also developed and this also remained quite sharp. The failure cracks remained entirely within the shear span. A close look at the failure surface showed clear split without any fine particles of concrete along the failure plane.

II.3.5 Beam IA-5 (Fig. 32 and 33)

The first flexural cracks appeared in this beam at a load of 15 kips. With further loading, more cracks appeared away from the load points and closer to the supports, but remained very sharp and fine. At

35 kips, the diagonal cracks were well below the compression face of the beam and had just started deviating from the original vertical cracks. The beam seemed to be fairly intact in appearance. At 37.5 kips, the beam failed suddenly, when an entirely new diagonal crack in shear span (end N2/S2) travelled right through the beam section to the load point. The failure crack passed above the top tip of an inclined crack on end S2 and branched off in three different directions backwards, one of these being a partial split along the reinforcement. Another crack originated from the compression face of the beam above the diagonal crack as it propagated to failure. The failure was a typical case of diagonal tension, the final split being extremely sudden. The failure crack remained relatively fine, though not as sharp as that of beam IA-4. At failure, there were only a few cracks on side S1 while side N1 appeared to be almost crack free. This latter may be due to the fact that this surface was not painted.

II.3.6 Beam IA-6 (Fig. 34)

At a load of 12.5 kips, first flexural cracks appeared both in the midspan and close to load points in the shear span.

This beam showed a different behaviour than beams IA-4 and IA-5, there being more cracks with slower propagation as the load was increased. The inclined cracking seemed to be more severe on end N2/S2.

At a load of 37.5 kips, a vertical crack in the shear span on end N2 extended significantly in an inclined direction, while cracks re-

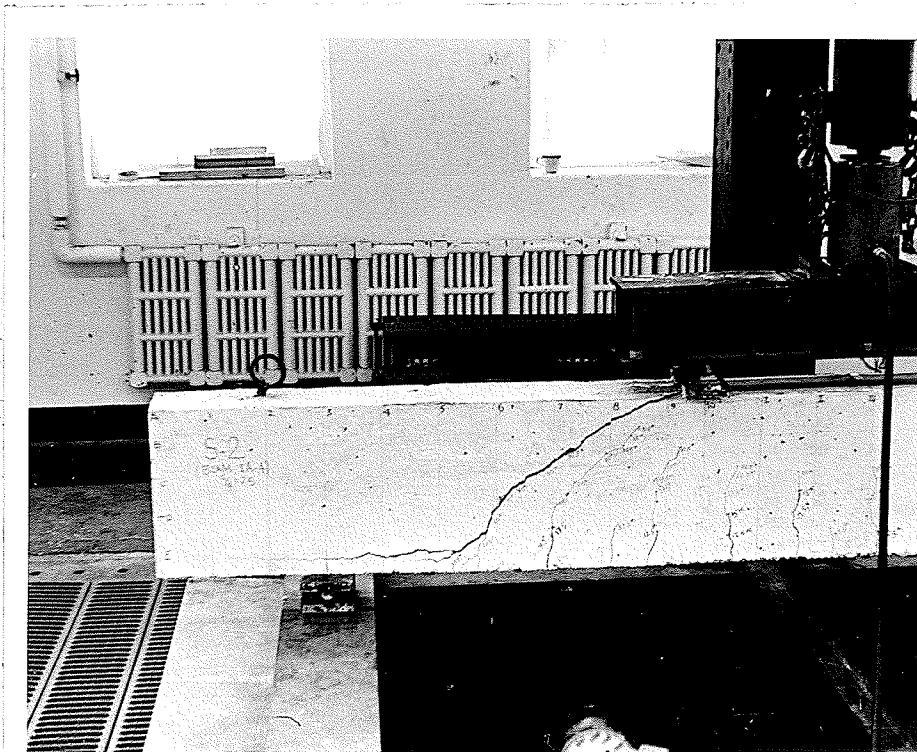


FIG. 31 DIAGONAL FAILURE OF BEAM IA-4

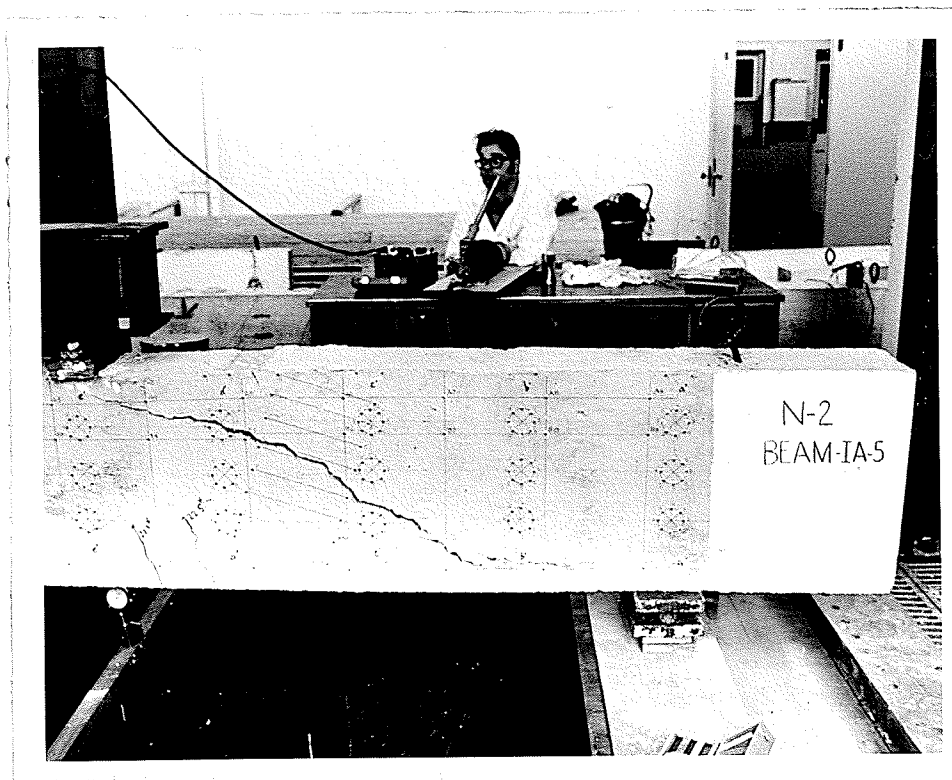


FIG. 32 DIAGONAL FAILURE OF BEAM IA-5

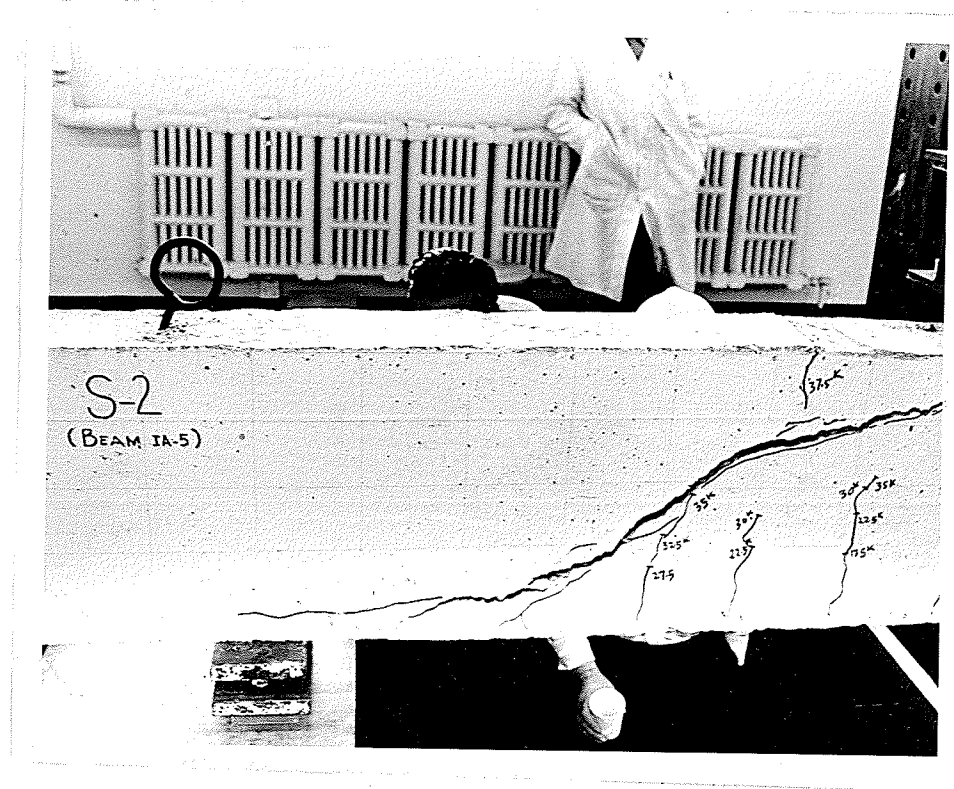


FIG. 33 FAILURE OF BEAM IA-5 ON END S-2

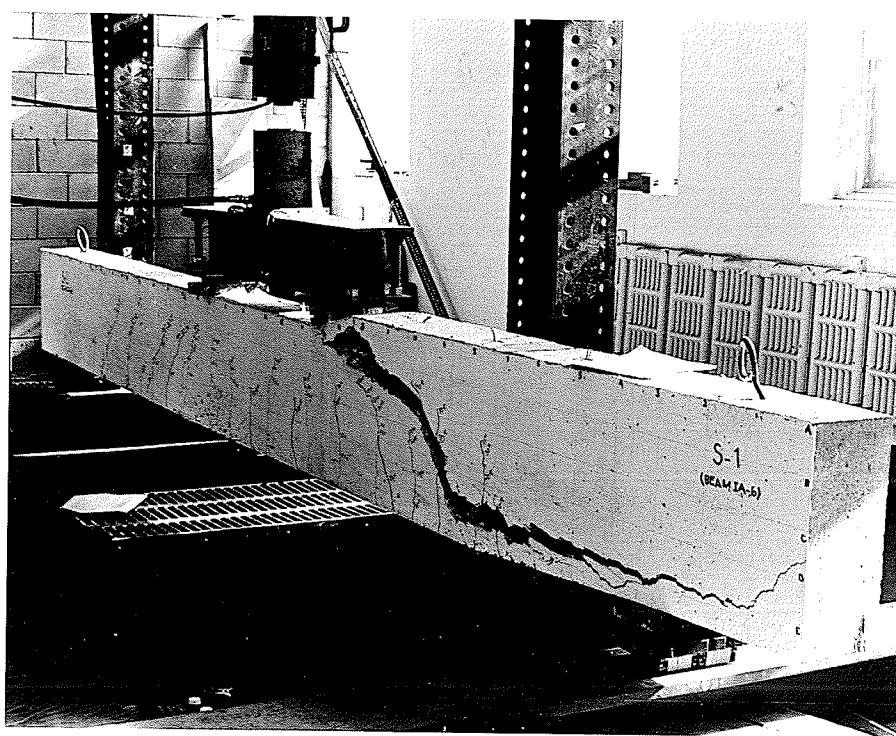


FIG. 34 CRACKING PATTERN AND FAILURE OF BEAM IA-6

mained vertical on end S2. At a load of 40 kips, a diagonal crack appeared on end S2 which crossed the existing cracks at a 45° angle and extended on both sides of the pre-existing cracks. The ultimate failure was triggered off from this crack on both ends N2 and S2, the failure crack diagonally crossing the shear span to load point. There was also a significant split of the concrete along the reinforcement which extended to the support. The two portions of the beam separated by the diagonal crack came apart and the end of the beam where failure occurred was lifted up.

II.3.7 Beam IA-7 (Fig. 35)

The first flexural cracks were observed at a load of 10 kips, both in the midsection and shear span close to load points. With an increase in load, more and more cracks appeared in the shear span and existing cracks became inclined. Cracking on ends N1/S1 was more pronounced. The diagonal cracks progressed slowly with an increase in load and at 35 kips, the max. height of these cracks was about 14 inches from the beam bottom. The beam failed at a load of 39 kips with a split, similar to, but more destructive than beam IA-6. The failure, which occurred on ends N1/S1, was unique in that it was very remote from the load point and the diagonal crack at its top was about 18 inches away from the load point. On the other hand, the lower end of the crack was much closer to the support, being only about 12 inches from it. There was an extensive split along the reinforcement so that all the concrete on the outer side of the reinforcement was chipped off and the reinforcing

bars were exposed not only at the bottom but also at the end cross-section. The cracked portion of the split beam section was lifted up.

It was observed before the test that there was some segregation of concrete at the beam bottom and some small cavities existed due to improper compaction. This may partly explain the different location of the failure section.

II.3.8 Beam IA-8 (Fig. 36)

The first flexural cracks were observed at a very low load of 5 kips. As the load increased, many more cracks appeared which were approximately the same distance apart as in beam IA-7. Cracks on ends N1/S1 were, however, fewer and a greater distance apart.

As the load was increased, flexural cracks appeared closer to the supports and by a load of about 30 kips, they were very close to section b. At higher loads, vertical cracks progressed in inclined directions as with other beams. Ultimate failure occurred at a load of 34.4 kips on ends N1/S1 when an inclined crack proceeded both backwards and forwards from an existing crack. The lower end of the crack then moved along the reinforcement, causing horizontal cracking to the support point. The upper end of the crack terminated at the loading plate. A crack extending from top downwards appeared at failure load in the midspan. The portion of the beam above the inclined crack was lifted upwards and the longitudinal reinforcement was exposed for some distance. This failure crack was quite close to the load point, as opposed to that of beam IA-7, the lower end of the crack being between sections c and d.

Considerable segregation of concrete existed in this beam from midspan towards the support on end N1/S1 on the underside of the beam. There seemed to have been insufficient compaction and some cavities existed in the concrete. The beam was patched-up at these locations before the test. Since the failure occurred in this section of the beam it



FIG. 35 DIAGONAL FAILURE OF BEAM IA-7

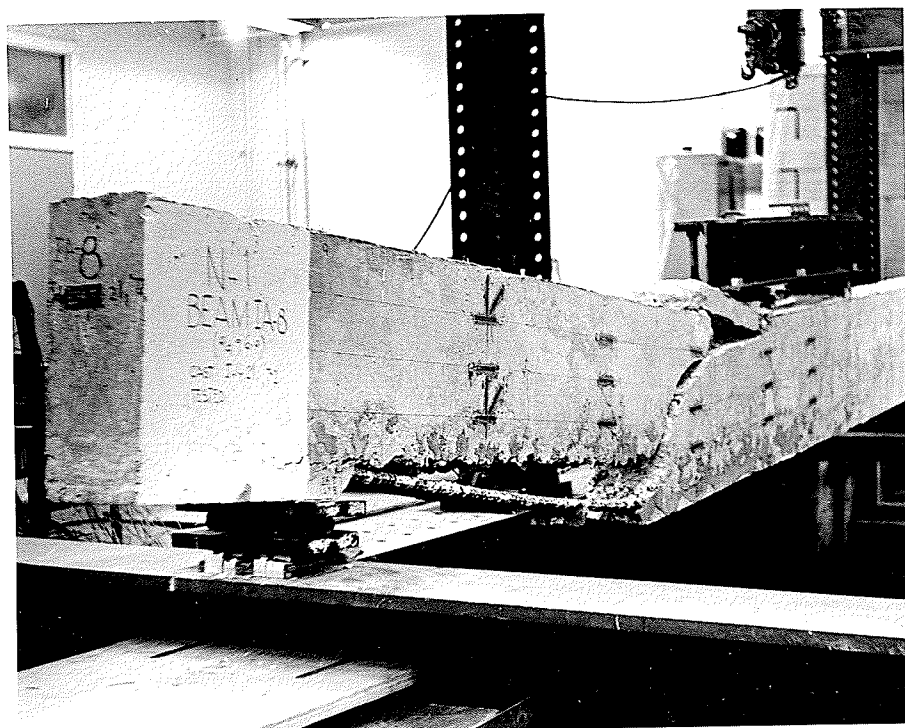


FIG. 36 DIAGONAL FAILURE OF BEAM IA-8

is possible that the beam may have taken slightly more load before failure if the compaction of the concrete in the beam had been more complete.

II.3.9 Beam IB-4 (Figs. 37 and 38)

The first flexural cracks were observed at a load of 20 kips and as the load was increased, only a few more cracks could be seen. At a load of 37.5 kips, a diagonal crack extended suddenly throughout the shear span of the beam and became flatter in slope as it progressed towards the load point. Another crack appeared from the compression face of the beam at reduced section above the diagonal crack. The beam section at this location was lifted up. This diagonal crack also caused a horizontal split along the reinforcement. With another increment of 0.8 kips, the beam split completely at 38.3 kips.

II.3.10 Beam IB-5 (Fig. 39)

The first flexural cracks occurred at a load of 20 kips. As the load was increased, the beam seemed fairly intact until a load of 35 kips when a critical diagonal crack extended appreciably. The final failure at a load of 37.5 kips resembled the failure of beam IB-4 except that the final split was more pronounced.

II.3.11 Beam IB-2 (Fig. 40)

The first flexural cracks appeared at a load of 20 kips. Critical diagonal cracking occurred at a load of 42.5 kips, the diagonal crack progressing considerably through the shear span of the

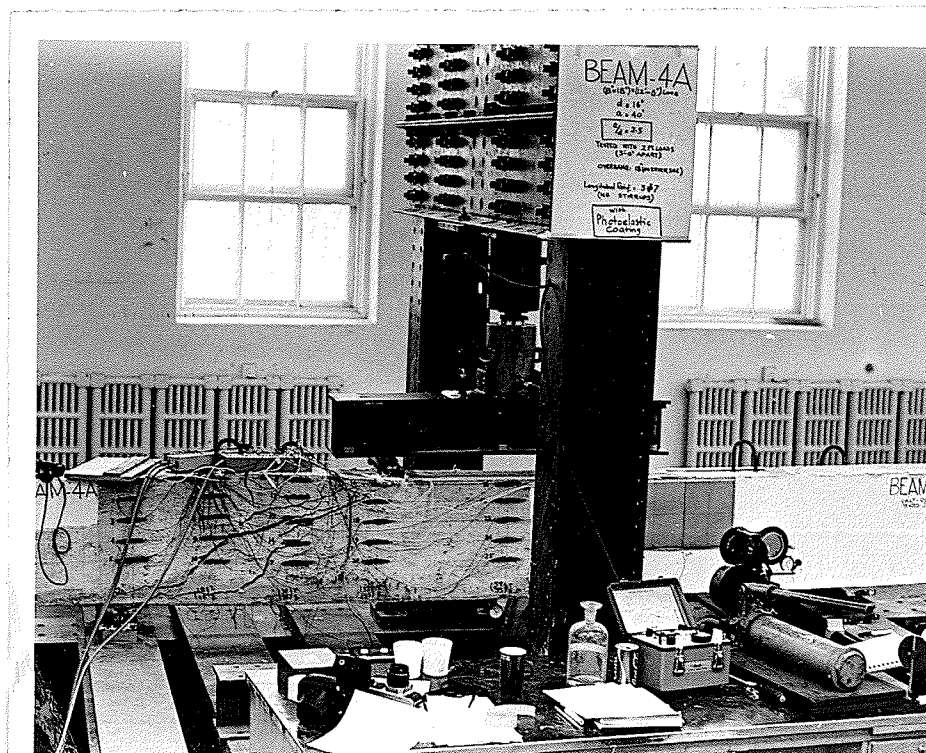


FIG. 37 FAILURE OF BEAM IB-4

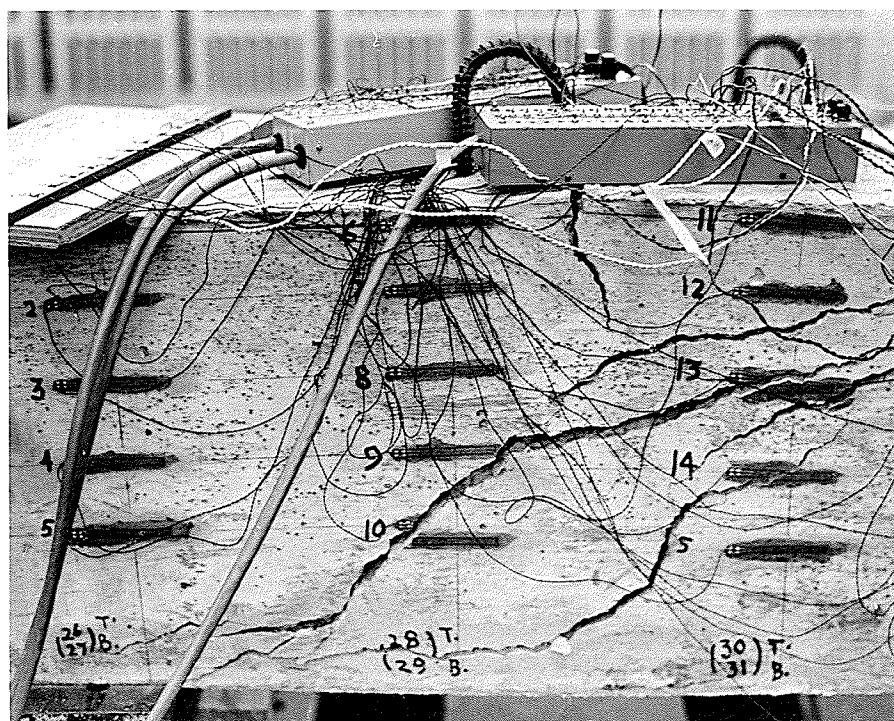


FIG. 38 A CLOSE VIEW OF FAILURE OF BEAM IB-4

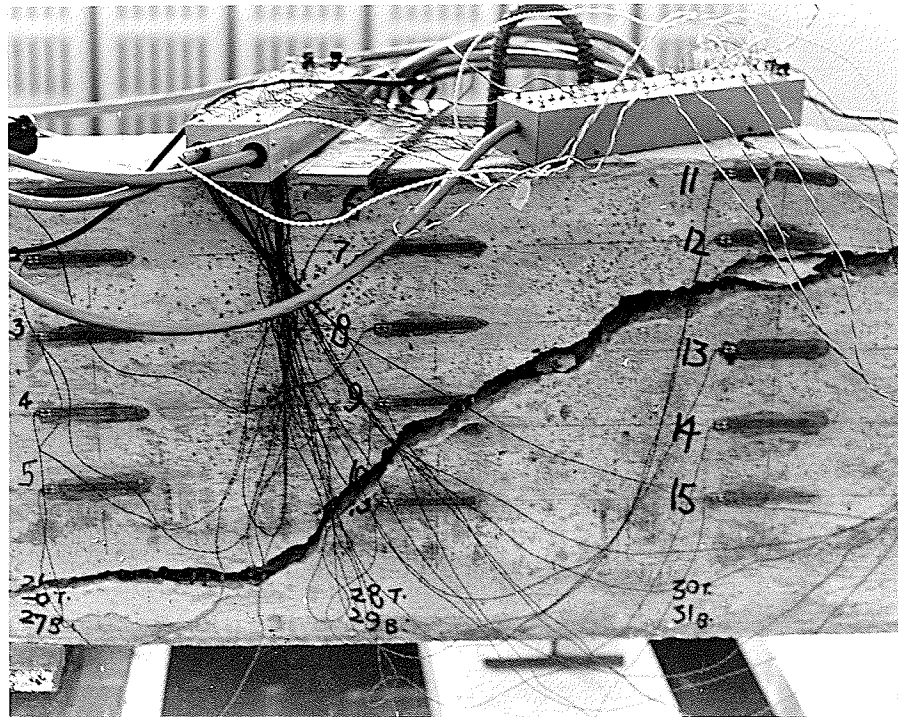


FIG. 39 FAILURE OF BEAM IB-5

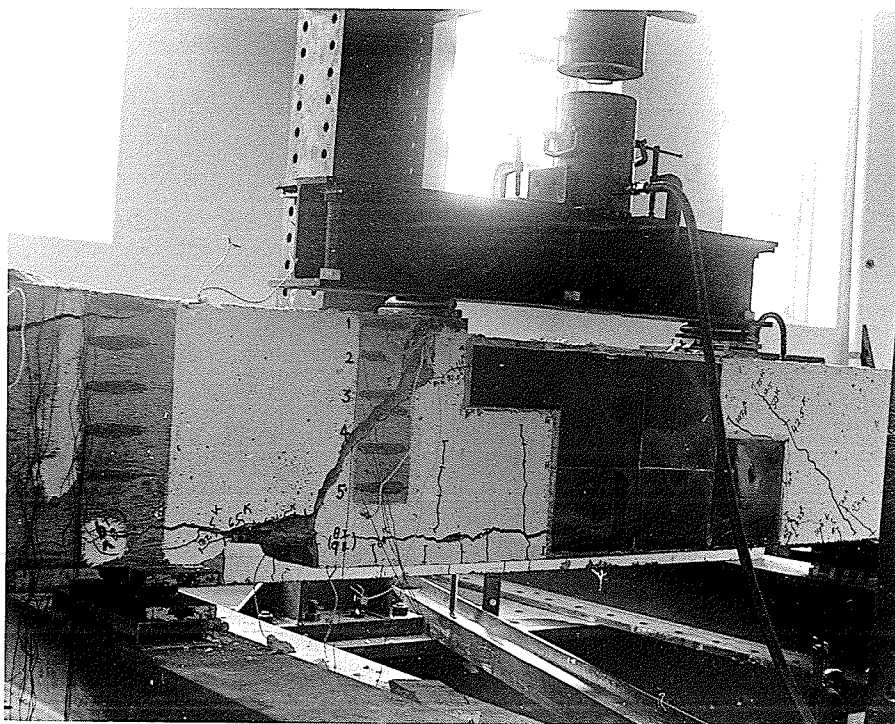


FIG. 40 FAILURE OF BEAM IB-2

beams. With further increments of load, the propagation of cracks was rather slow.

As the load was increased from 75 kips, there was little further propagation of cracks until a new crack formed at 107.5 kips and existing cracks extended into the midspan region. The beam finally failed at a load of 122.5 kips with a complete diagonal split between the support and the load point and a horizontal split all along the reinforcement.

From a load of 60 kips onwards, small local cracks appeared close to the supports and at a load of 82 kips a crack existed right over the support. However, further loading did not result in any more cracks over the supports, though the existing cracks widened.

The final diagonal failure did not follow the existing diagonal cracks at the top tip but proceeded directly to the loading plate. The two portions of the beam separated by the diagonal crack came completely apart, joined only by the reinforcement.

II.3.12 Beam IB-6 (Fig. 41 and 42)

The first flexural cracks were observed at a load of 7.5 kips and as the load was increased, numerous other cracks developed. The cracks later became inclined in the shear spans as they progressed higher or appeared closer towards the supports.

The ultimate diagonal failure occurred on ends N2/S2 at a load of 39 kips with the crack extending on both sides of a pre-existing crack which had just appeared at a load of 35 kips. The failure crack terminated close to the load point and proceeded as a split along the

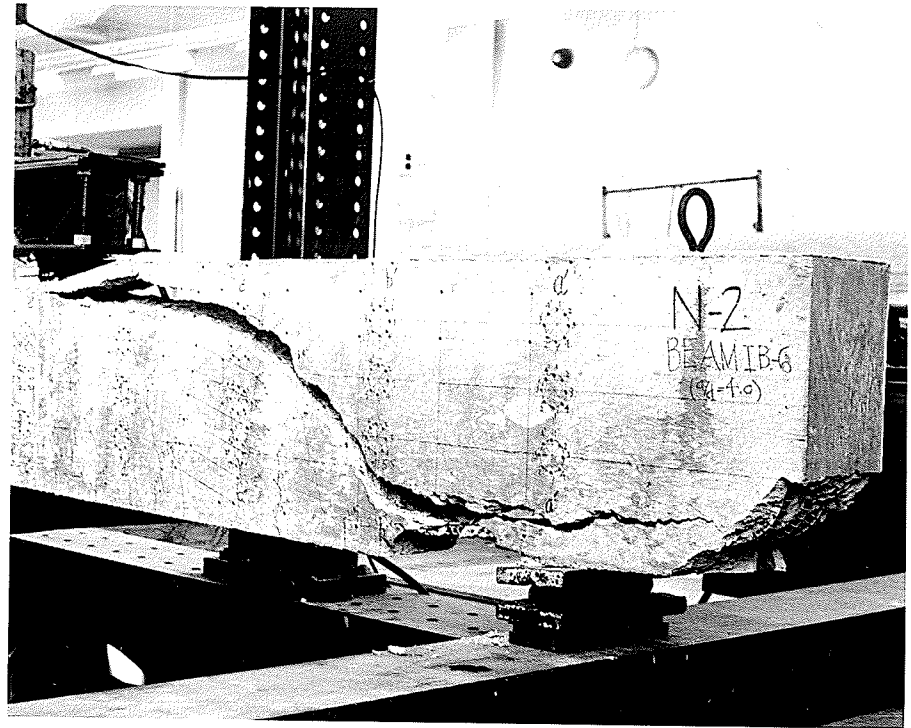


FIG. 41 DIAGONAL TENSION FAILURE OF BEAM IB-6
(END N-2)



FIG. 42 DIAGONAL TENSION FAILURE OF BEAM IB-6
(END S2)

reinforcement to the end of the beam. A section at reduced depth above the diagonal crack was lifted up at failure. The failure was a typical diagonal tension failure. The cracking remained fairly thin and sharp up to the final split and immediately before failure, the diagonal crack was still 5 inches below the top surface of the beam.

One observation of considerable interest was the rather frequent back-cracking, showing progressive and systematic destruction of the resistance of the concrete sections between the cracks.

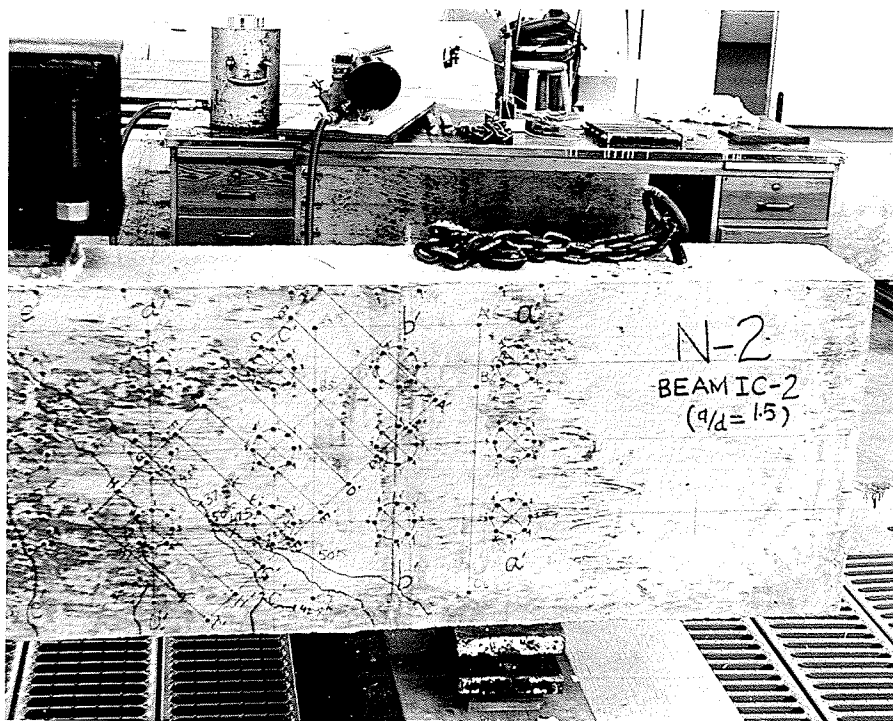
II.3.13 Beam IC-2 (Figs. 43 and 44)

The first flexural cracks appeared at a load of 20 kips and significant diagonal cracking had developed from 37.5 kips onwards on various faces of the beam. At a load of 50 kips, a major diagonal crack progressed to within 2 1/2 inches of the compression face on end N1 and 1 3/4 inches on end S1.

As the load was increased, extensions of this crack moved into midsection with flatter trajectories. This propagation was only very slight and stopped completely at about 72.5 kips. Multiple cracks also occurred at supports from 47.5 kips to 60 kips. Further increments of load resulted in widening of critical diagonal cracks only. As the load was increased from 80 kips to 82.5 kips, there were relatively larger deflections which increased further as the load was increased to 85 kips and then to 87.5 kips. During this loading, the deflection of the beam increased by about 0.17 inches. Slow diagonal failure and very ductile widening of cracking occurred during this period before the final split at 87.7 kips, which was sudden and similar to that for beam IA-2 except



FIG. 43 FAILURE OF BEAM IC-2

FIG. 44 BEAM IC-2 SHOWING DEMEC GAUGE LOCATIONS AND
CRACKING IN THE BEAM

that there was no significant split along the reinforcement.

II.3.14 Beam IC-5 (Fig. 45)

The first flexural cracks appeared at a load of 8 kips and progressed with an increase in load. The propagation of the cracks in the midsection became insignificant after about 20 kips, when the diagonal cracks extended in a typical fashion. The beam ends N1/S1 showed more pronounced cracking than the ends N2/S2. From 36 kips onwards there was no propagation of cracks at all on ends N2/S2. At 36 kips, major diagonal cracking occurred on N1/S1, the cracks extending to a height of 15 5/8 inches and propagating backwards as well.

As the load was increased from 38 kips, it seemed that the beam had finally failed at 38.35 kips as the critical crack proceeded to the load point with some horizontal splitting along the reinforcement. There were large deflections. However, the beam started taking some more load at this stage, there being much larger deflections. The diagonal failure finally occurred at a load of 40.2 kips resembling a flexural failure in the amount of deflections. At final failure the diagonal crack progressed about 4 to 5 inches into the midsection and an extensive horizontal split occurred along the reinforcement to the support.

II.3.15 Beam IC-6 (Fig. 46)

The first flexural cracks appeared at a load of 7.5 kips and numerous cracks developed on further loading. At a load of 30 kips, while

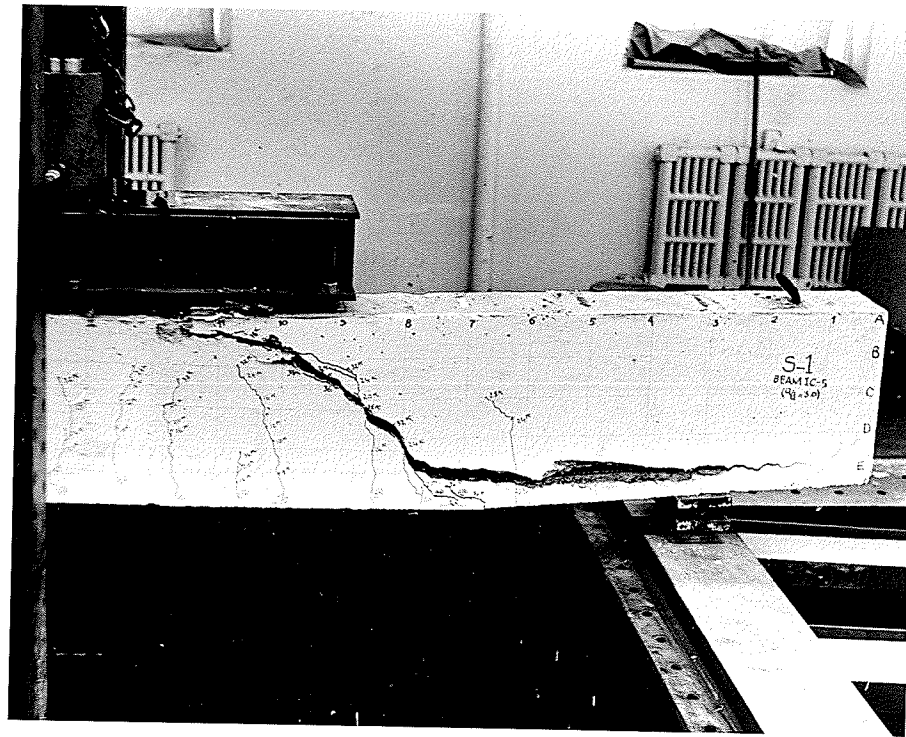


FIG. 45 DIAGONAL FAILURE OF BEAM IC-5

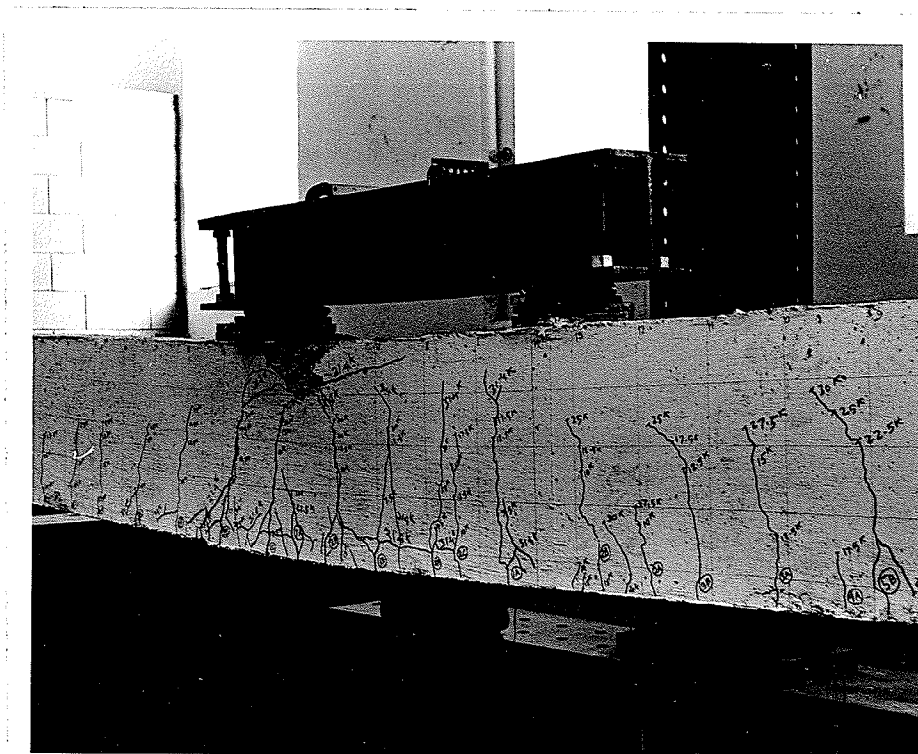


FIG. 46 CRACKING AND FINAL FLEXURAL FAILURE OF BEAM IC-6

there existed both diagonal cracks in the shear span and vertical cracks in the midsection, the beam started deflecting considerably, recording a maximum load of 31.4 kips. As the beam failed in flexure, the deflection exceeded 1 inch. A chunk of concrete at midspan was broken off at failure and a horizontal split occurred along the reinforcement in the midsection. This was the only beam in the entire test series which showed a flexural failure.

II.3.16 Beam IIA-2 (Figs. 47 and 48)

This beam remained remarkably sound as the loading was increased and it was not until a load of 27.5 kips that the first cracks developed. First significant diagonal cracking occurred at a load of 40 kips. With further loading there was a major propagation of a diagonal crack to a height of 8 1/2 inches at a load of 50 kips. At this stage the diagonal cracks had gone into the secondary beam on end S2 but the beam seemed to be fairly intact. At a load of 55 kips, there was a major extension of cracks on all sides. On side S1, a new diagonal crack formed. Another diagonal crack propagated significantly to a height of 14 inches, going into the secondary beam end, then continuing in the section of secondary beam, terminating at a height of 17 inches, about 3 inches away from the edge of the main beam. On side S2, three new cracks appeared, the most critical of these progressed to a height of 12 1/4 inches before entering the secondary beam and progressing further in it to a height of 17 1/2 inches (only 1/2 inch from top edge), 3 inches from the edge of the main beam. Similar cracking occurred on end N2. End N1, especially the secondary beam on this end, was fairly intact. In the meanwhile, the load

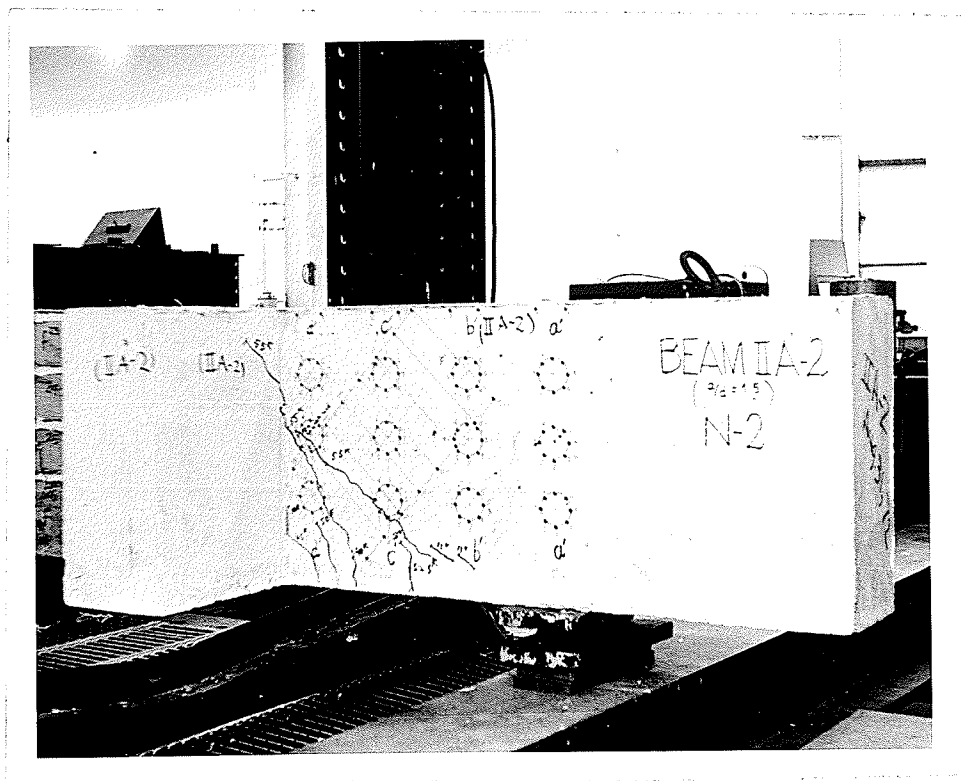


FIG. 47 BEAM IIA-2 SHOWING LOCATION OF DEMEC GAUGES AND CRACKS



FIG. 48 FAILURE OF BEAM IIA-2 AT THE JUNCTION OF SECONDARY BEAM TO THE MAIN BEAM

dropped by 5 kips. The load was again increased to 55 kips, but after sustaining this load momentarily the beam failed suddenly. The failure was at the junction of the secondary beam to the main beam at the end S2. This secondary beam sheared off completely, thus exposing the whole section including the longitudinal reinforcement. The main diagonal crack causing failure was clearly visible through the sheared surface. It seemed to be a premature failure. As the diagonal crack passed through the secondary beam, which was not rigidly connected to the main beam with top reinforcing, it resulted in a split of the secondary beam from the main beam, there being no restraint against it.

II.3.17 Beam IIA-2 (b) (Fig. 49 and 50)

The first flexural cracks developed in the midsection at a load of 21 kips. As the load was increased, the first cracks in the shear span were delayed and appeared only at a load of 42 kips. At 45 kips, first significant diagonal cracking was observed on the end N1, going through the shear span and into the cross beam at a height of 13 inches. At this stage, no diagonal cracks existed on end N2. On loading the beam further, the critical diagonal cracking was observed at a load of 60 kips on ends N1 and S1, progressing into the secondary beam. A major diagonal crack developed on end S2 at a load of 63 kips followed by the appearance of the same crack on end N2 at a load of 66 kips. At this load, the diagonal cracks on all faces of the beam crossed through the secondary beams and were visible in the midsection of the main beam, as they emerged from the secondary beams. This extensive cracking

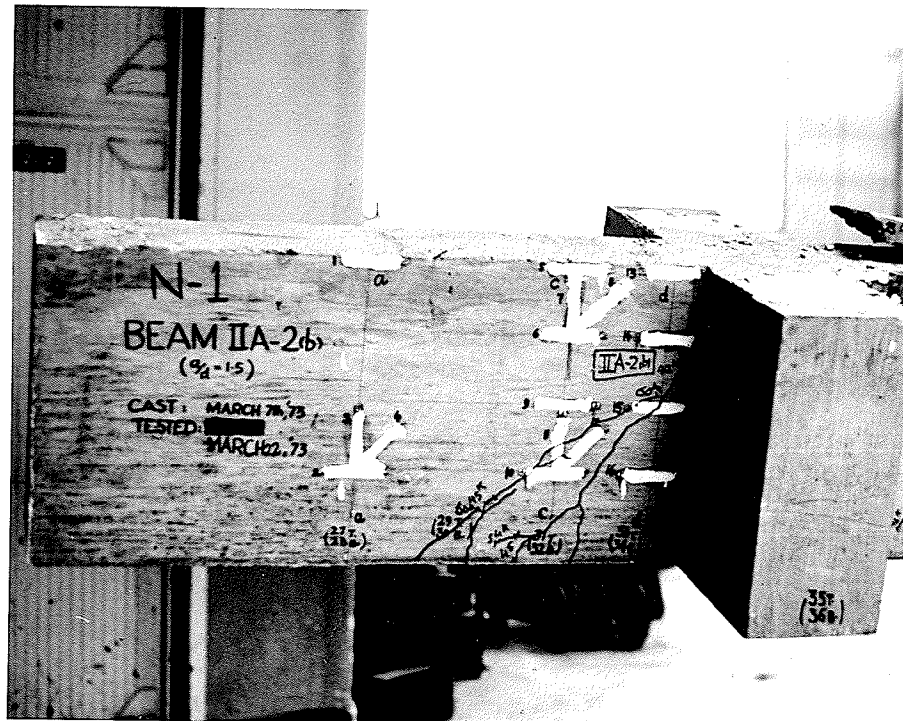


FIG. 49 - BEAM IIA-2 (b) AT FAILURE - END N1



FIG. 50 - BEAM IIA-2 (b) AT FAILURE - END N2

resulted in a sudden drop of the load by 6 kips and further dropped another 6 kips while an entire set of DEMEC readings was taken.

As the load was increased, the beam continued taking more load while the critical cracks progressed in the midsection on all ends of the beam. Failure occurred at 81 kips when cracks from opposite sides joined at about midspan. This resulted in, a sudden diagonal split on ends N2/S2, some chipping of concrete at top of the beam at midsection above the cracks, and horizontal splitting along the reinforcement. The top reinforcement in the secondary beam was exposed.

II.3.18 Beam IIA-4 (Figs 51 and 52)

The first flexural cracks appeared in midsection at a load of 15 kips. Cracks in the shear spans were observed from 20 to 25 kips. These cracks progressed vertically and later became inclined. The final failure occurred at a load of 39.6 kips on sides N2/S2 from a crack that had originated only at the previous load increment of 37.5 kips. The diagonal failure crack went through the secondary beam and was observed emerging out in the constant moment zone, about 3 inches beyond the junction of the secondary beams to the main beam. As the diagonal crack crossed the secondary beams, a portion of concrete at its top was broken off and a simultaneous split occurred along the reinforcement. It was observed that ultimate failure developed when the diagonal cracks were well below the top and the beam appeared to be able to carry more load.

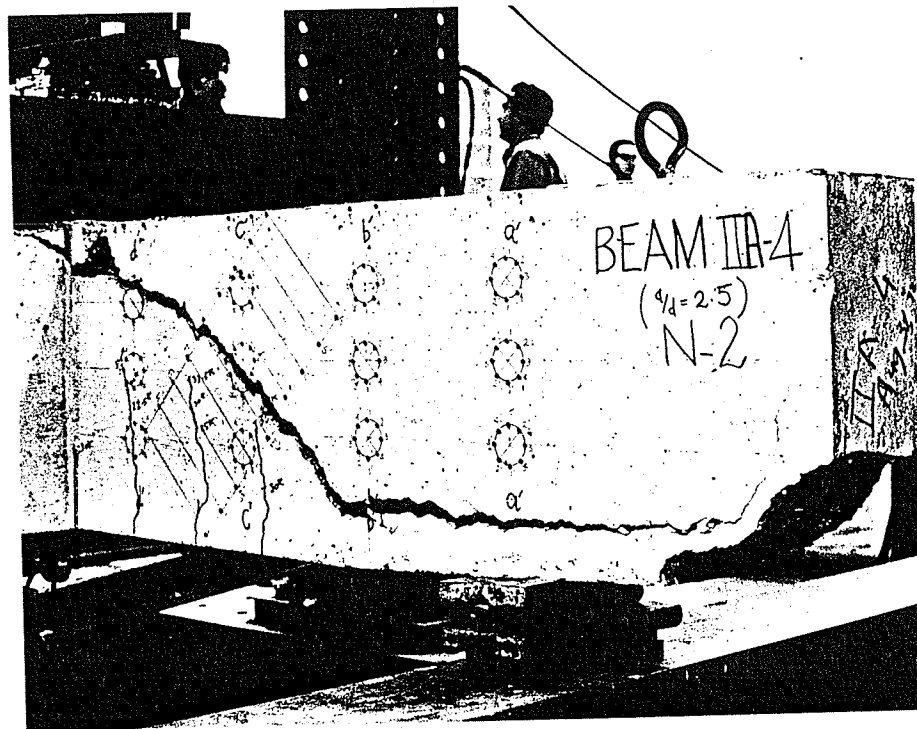


FIG. 51 DIAGONAL FAILURE OF BEAM IIA-4 (END N-2)

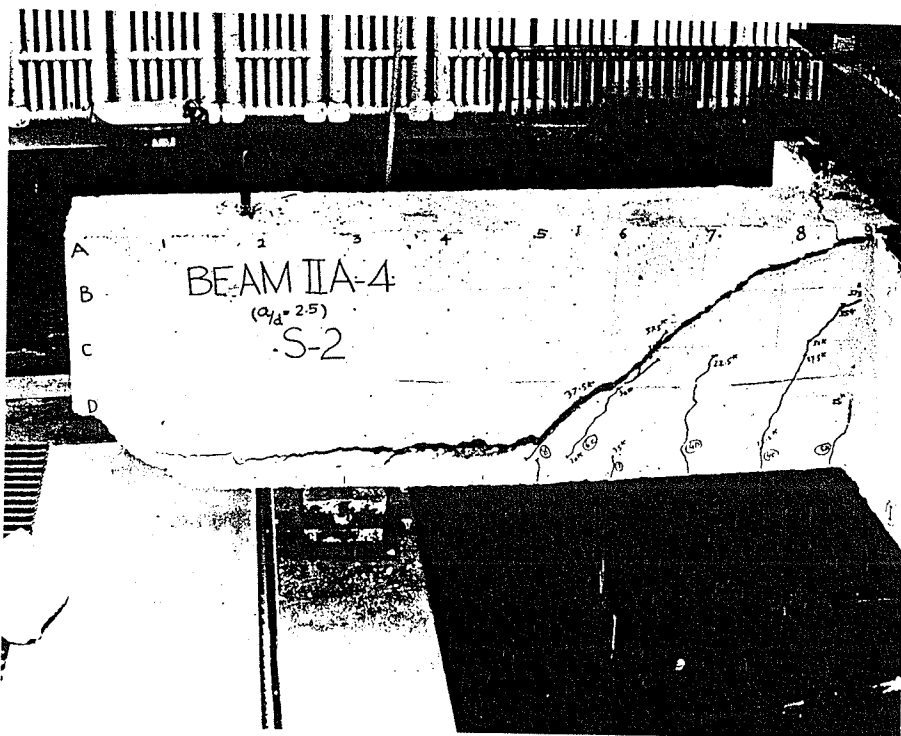


FIG. 52 - DIAGONAL FAILURE OF BEAM IIA-4 (END N-2)

II.3.19 Beam IIA-6 (Figs. 53 and 54)

The first flexural cracks were observed in mid-section at a load of 7.5 kips and cracks occurred in the shear spans at a load of 10 kips. A very balanced cracking developed on all faces of the beam as the load was increased. The cracks in shear spans became inclined as they progressed upwards and cracking extended towards the supports with increased loading. Some back-cracking was also observed at a load of 35 kips. The beam sustained a load of 37.5 kips for about three minutes when, suddenly, a destructive diagonal split occurred on ends N1/S1. The two portions of the beam jumped apart suddenly while the diagonal crack went through the entire shear span and the entire zone of constant moment. A split along the reinforcement also occurred. The diagonal crack causing failure crossed the existing cracks at about 45° angle and was entirely new in nature and developed suddenly at failure. It seemed that it originated from the extreme tips of two pre-existing cracks in the shear span of the beam.

II.3.20 Beam IIIA-3 (Figs. 55 to 58)

The first flexural cracks developed in the midspan region at a load of about 20 kips and shifted outwards as the load was increased. Flexural cracks in the shear spans became inclined at a load of 30 kips. A major diagonal crack was observed on ends N2/S2 at a load of 60 kips.

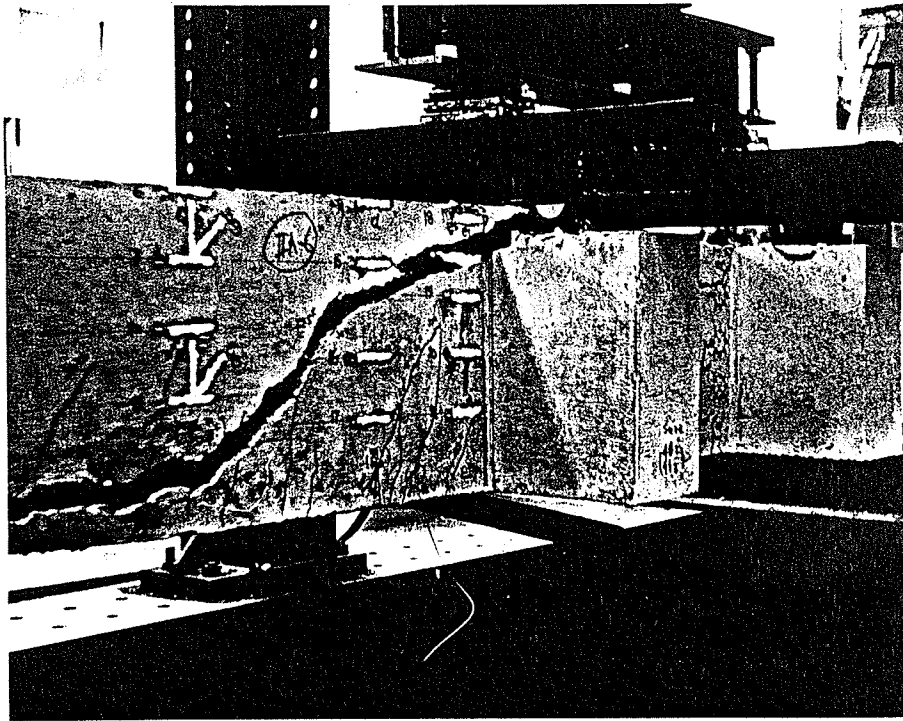


FIG. 53 DIAGONAL TENSION FAILURE OF BEAM IIA-6

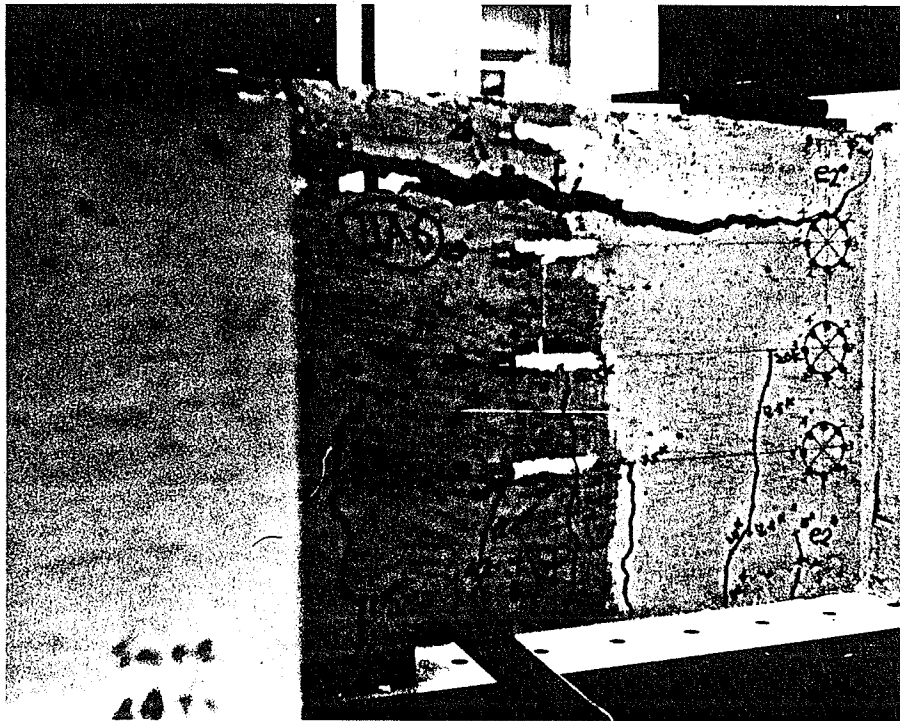


FIG. 54 BEAM IIA-6 SHOWING THE EXTENSION OF DIAGONAL
CRACK THROUGH MID-SECTION

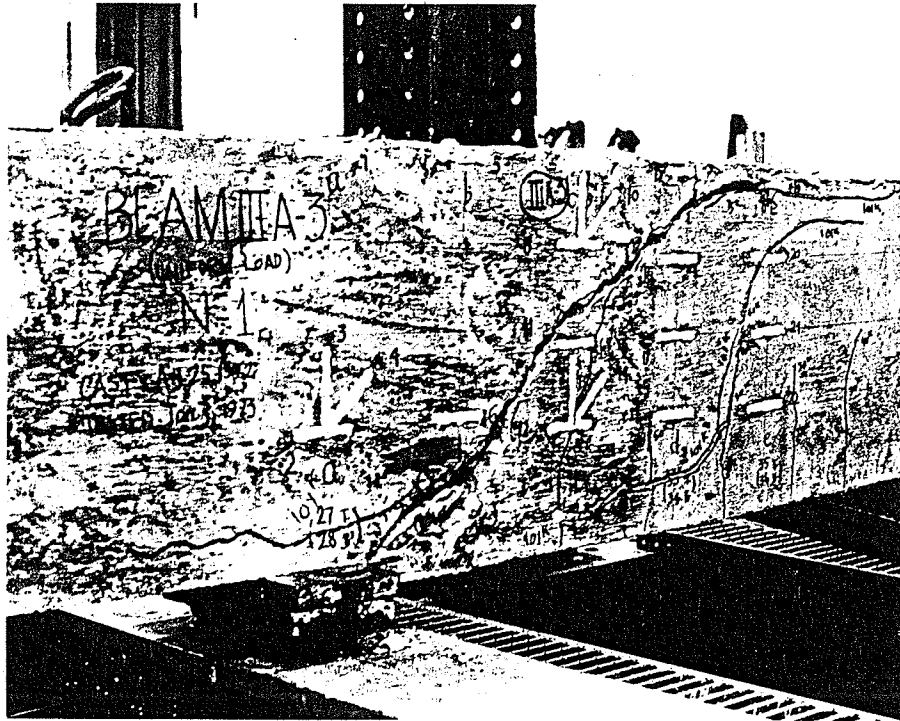


FIG. 55 FINAL FAILURE OF BEAM IIIA-3 (END N1)

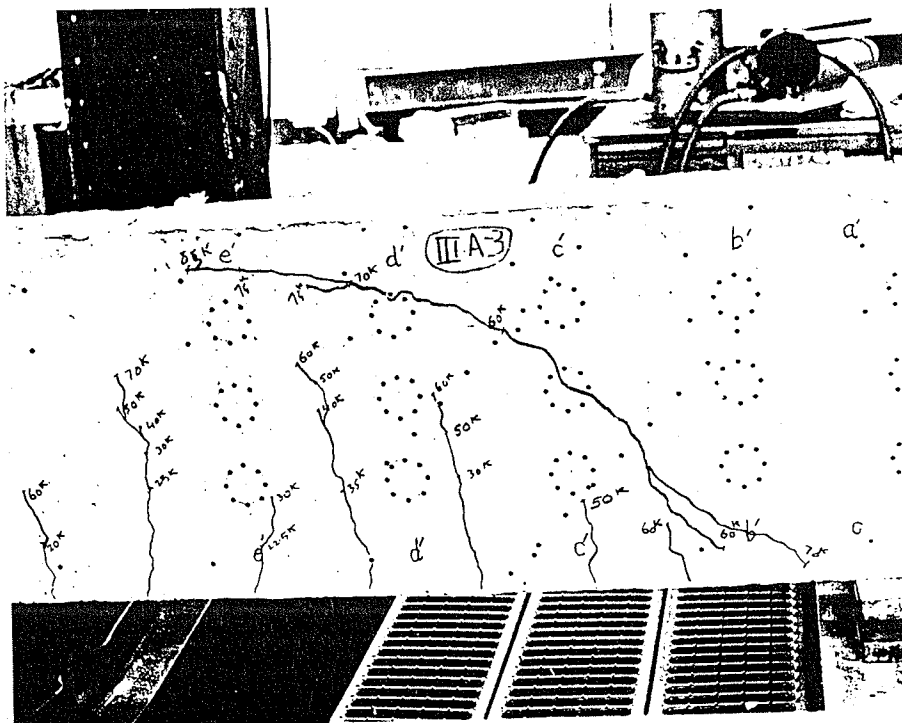


FIG. 56 CRACKING ON END N-2 OF BEAM IIIA-3
AS FAILURE OCCURRED ON END N-1

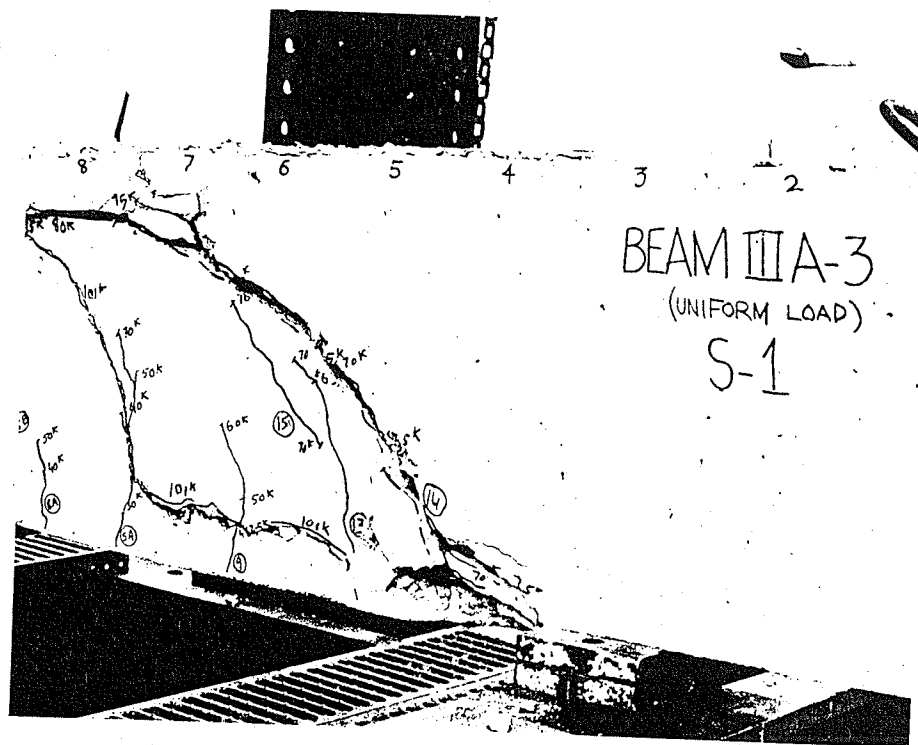


FIG. 57 FAILURE OF BEAM IIIA-3 (END S-1)

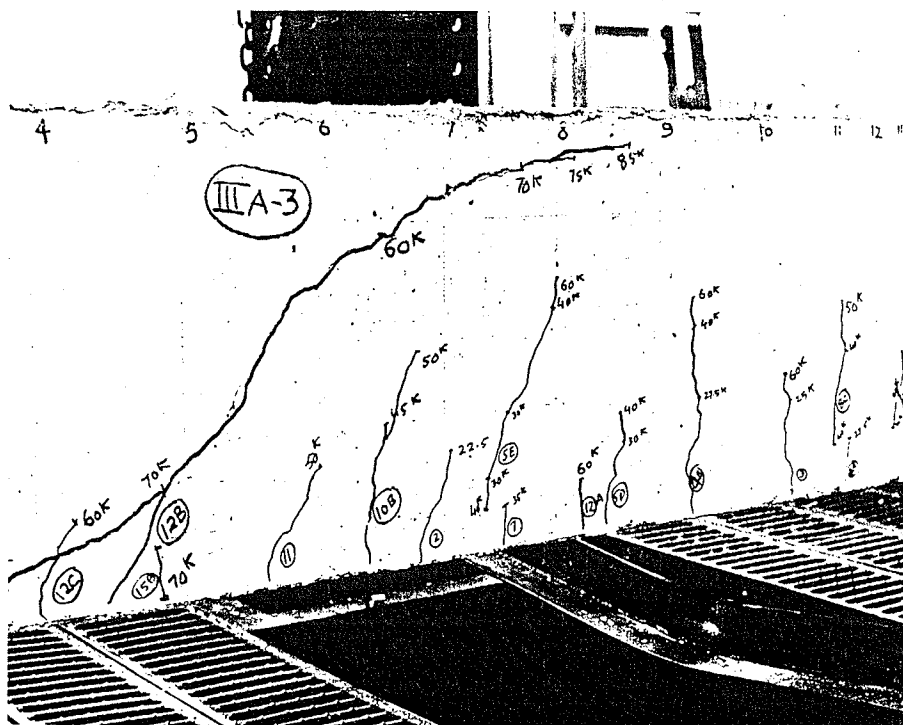


FIG. 58 CRACKS ON END S-2 AT FAILURE OF BEAM IIIA-3

At a load of 70 kips, new diagonal cracks appeared on ends N1/S1. At this stage, diagonal cracks had appeared on all ends of the beam. These critical cracks propagated further as the load was increased. The critical diagonal crack on ends N2/S2 progressed to within 1 1/4 inches of the compression face at a load of 85 kips while a similar crack on the other end became horizontal at a lower location.

As the load was further increased, the critical cracks widened without any propagation. The final failure occurred when the concrete above the top tip of the critical diagonal crack on ends N1/S1 chipped off as another diagonal crack extended to join it. Horizontal splitting along the reinforcement developed from the lower end of the inner diagonal crack towards the supports. At failure, the entire block of concrete between the two diagonal cracks came apart from the rest of the beam. This failure was different from the previous failures in that final failure was triggered off by two major diagonal cracks simultaneously.

II.3.21 Beam IIIA-6 (Figs. 59 and 60)

The first flexural cracks appeared at a load of 15 kips. As the load was increased, the cracks remained vertical in the midsection and inclined only slightly in the outer regions of the span. Significant diagonal cracking had developed at a load of 35 kips, the maximum height of diagonal cracks being 10 1/2 inches at this stage. At a load of 40 kips, diagonal cracks appeared on ends S1-S2, which were closer to the supports. At a load of 50 kips, there was a major failure on ends N1/S1, the crack touching the top surface of the beam on end N1 while it tapered off horizontally about 2 inches below on end S1. Cracking also extended on the

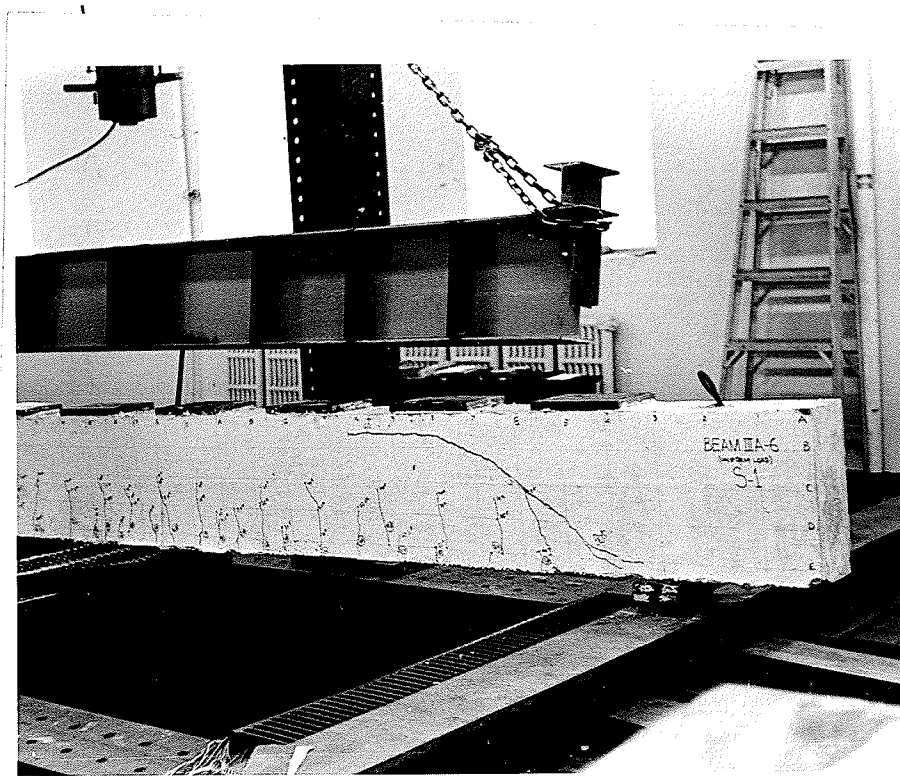


FIG. 59 CRACKING ON END S-1 OF BEAM IIIA-6 AT FAILURE



FIG. 60 FAILURE OF BEAM IIIA-6

other end. It seemed that the beam had failed completely, the load dropped significantly to 46.65 kips as the deflections continued increasing. The beam, however, started taking more load and a major failure developed on ends N2/S2 at a load of 55 kips, the diagonal cracks extending to within one inch of the compression face of the beam. At this stage all faces of the beam were almost completely cracked and a balanced pattern existed on all faces. The beam continued taking more load while the cracks on ends N2/S2 started widening appreciably. The ultimate failure occurred on ends N2/S2 at a load of 66.5 kips when two diagonal cracks caused a simultaneous diagonal split along with a split along the reinforcement. The portion of the beam above the outer diagonal crack was lifted up at failure. The block between the two critical diagonal cracks was completely separated from the rest of the beam, the split being similar to that for beam IIIA-3.

II.3.22 Beam IIIA-8 (Figs. 61 and 62)

The first flexural cracks developed in the beam at a load of 7.5 kips. Further cracking was very well distributed over the span as the load was increased. Diagonal cracks became more inclined closer to the supports. By a load of 30 kips, cracks had appeared over a large part of the span except for a very short distance near the supports.

From a load of 30 kips to a load of 45 kips, the existing diagonal cracks progressed higher but the propagation was very slow and many of the cracks did not move at all. At a load of 47.5 kips, diagonal cracks appeared close to the supports on all faces. At a load of 50 kips, critical shear cracks suddenly developed on ends N2/S2 and progressed

to within 3 inches of the compression face of the beam. At a load of 52.5 kips, sudden failure occurred on ends N2/S2 when two diagonal cracks joined together and split the beam completely. The failure was very destructive in nature. The block of concrete between the critical diagonal cracks came apart from the rest of the beam. In this case this split was 100% and the block had to be removed before the beam was lifted out of the frame. The portion of the beam above the outer diagonal crack was lifted up at failure. Large deformations of the longitudinal reinforcement below the cracks developed at failure. One unique feature of the accompanying horizontal split along the reinforcement was that it not only developed from the lower end of the crack towards the supports but also backwards from the inner crack to the midspan of the beam.



FIG. 61 FAILURE OF BEAM IIIA-8

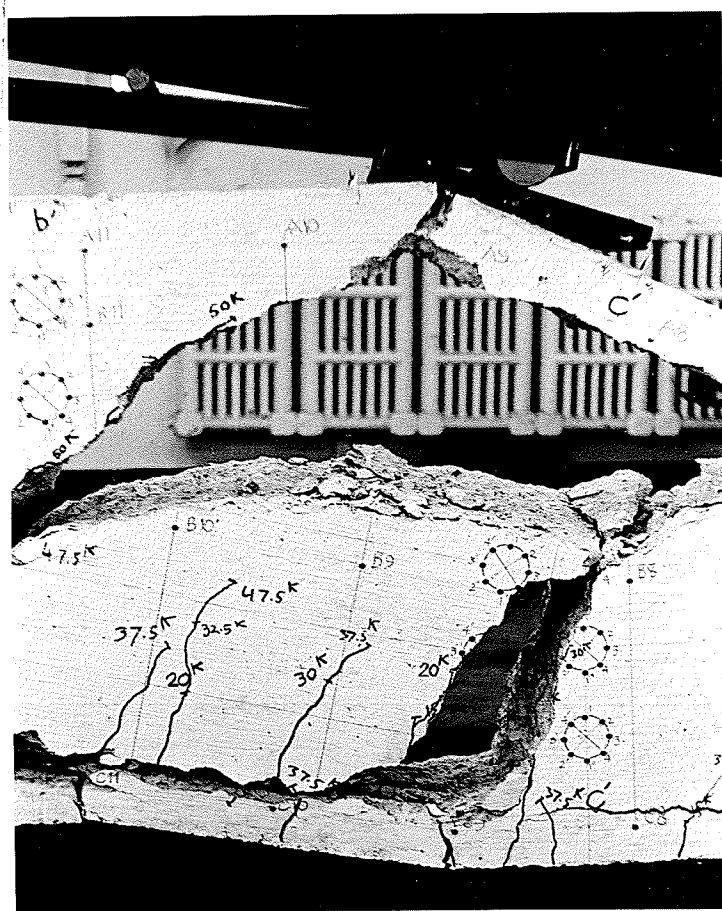


FIG. 62 A CLOSE VIEW OF THE FAILURE OF BEAM IIIA-8

APPENDIX III

PRESENTATION OF EXPERIMENTAL RESULTS

TABLE OF CONTENTS

APPENDIX III

	Page
III.1 DISTRIBUTION OF LONGITUDINAL FLEXURAL STRAINS IN CONCRETE	355
III.1.1 Tests of Series IA	356
III.1.2 Tests of Series IB	387
III.1.3 Tests of Series IC	395
III.1.4 Tests of Series IIA	406
III.1.5 Tests of Series IIIA	419
III.2 DISTRIBUTION OF LONGITUDINAL FLEXURAL STRAINS IN THE REINFORCEMENT	429
III.2.1 Beams of Series IA	431
III.2.2 Beams of Series IB	437
III.2.3 Beams of Series IC	440
III.2.4 Beams of Series IIA	443
III.2.5 Beams of Series IIIA	447
III.3 DISTRIBUTION OF CONCRETE STRAINS OVER INCLINED GAUGE LINES	450
III.4 DISPLACEMENTS RESULTING FROM BENDING OF CONCRETE CANTILEVERS AND ROTATION OF THE COMPRESSION ZONE	461
III.5 CRACK WIDTHS AND INTERNAL ROTATIONS	481
III.6 DEFLECTIONS OF BEAMS	491

III.1. DISTRIBUTION OF LONGITUDINAL FLEXURAL STRAINS IN CONCRETE

Test results of individual beams are summarized in this section. Details of the location of gauges, the propagation of cracks and data obtained in the tests of the beams are given alongwith other test results for each beam in appendix II. Since electrical resistance strain gauge readings were available at regular load intervals, ranging from 1000 pounds to 5000 pounds intervals, details for intermediate readings are filled in during the discussion whenever necessary.

Strain readings are plotted at each vertical section at 0, 4, 8 and 12 inch depth. In the plots of electrical resistance strain gauge data, average strains in the reinforcement are also shown. When reference is made to various gauge points, they are signified e(8), d(12), etc., the letters signifying the vertical section and the figures within parenthesis, the depth of the beam where the point is located.

Whenever a reading is not available at an intermediate point, the strains at two points are joined by a dotted line. Also, when a strain reading is affected by a crack passing under the electrical resistance strain gauges or through the DEMEC measuring points, it is joined by a broken chain line, showing the effect of cracking. This scheme is the same as that employed in Chapter 5.

III.1.1. TESTS OF SERIES IA

(i) BEAM IA-1 ($a/d = 1.0$)

The test results for beam IA-1 are summarized in Figs. III.1 (a) and (b).

DEMEC DATA (Fig. III.1a)

With increasing loads, tensile strains developed at the compression face over the support. These strains remained small in magnitude but generally increased with higher loads. Critical diagonal cracking was observed in this beam at a load of 60 kips. Above this load level, the centre of compression between the load point and midshear span showed a significant shift downwards. During this loading range, compressive strains at $a'(12)$, $b'(12)$ and $c'(12)$ kept on increasing. Cracks crossed the gauge lines at sections $d'(8)$ and $e'(4)$. These readings have not been plotted due to the large strains associated with cracking. At a load of 180 kips, the strain at $d'(8)$ was 6.15×10^{-3} . Compressive strains under the load point at the compression face steadily increased with load. Tensile strains also developed at the compression face at midshear span and increased after critical diagonal cracking.

ELECTRICAL RESISTANCE STRAIN GAUGE DATA (Fig. III.1b)

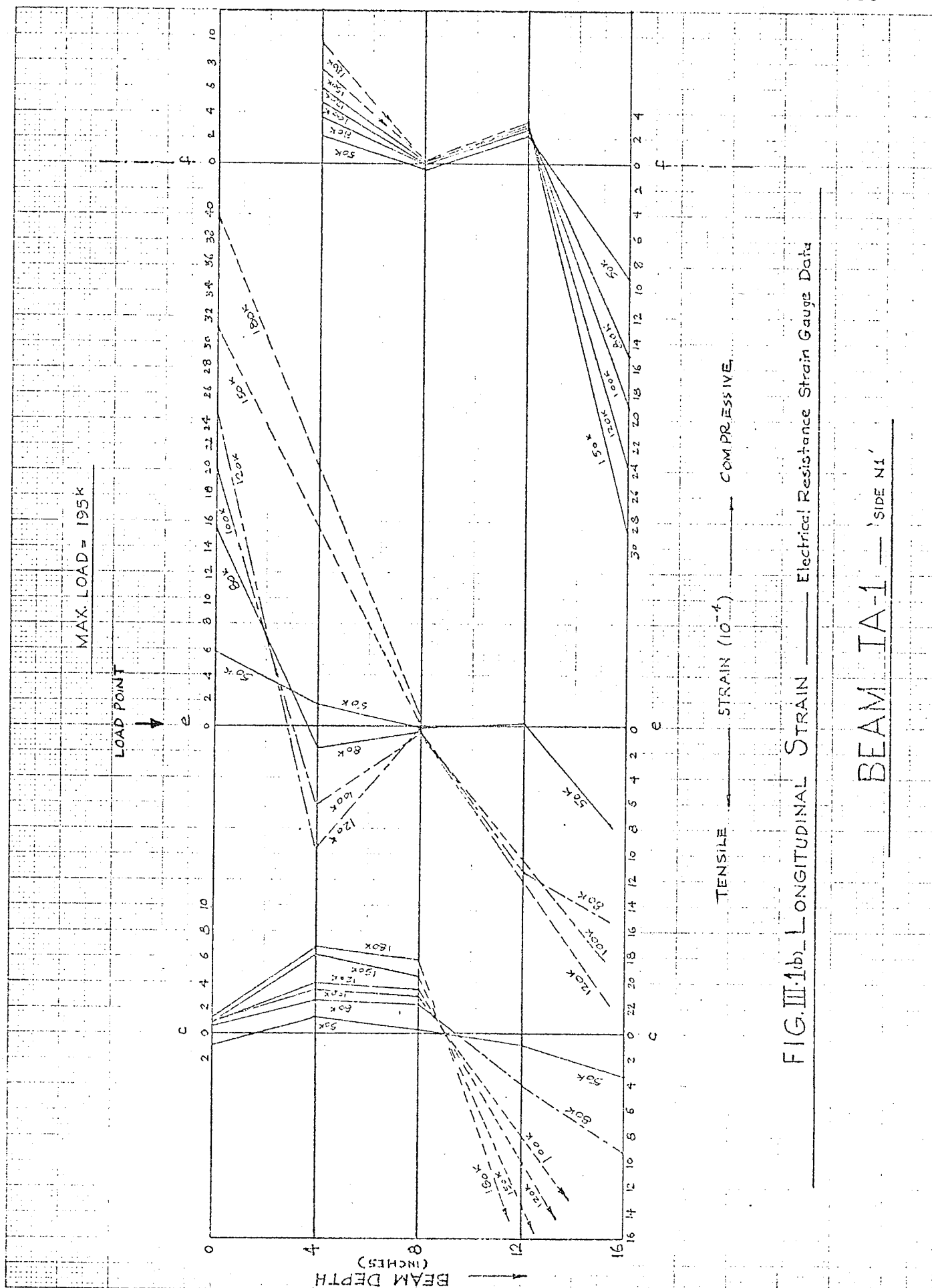
Tensile strains existed at the compression face over the support right from the beginning. Examination of the data from gauge $a(12)$ showed that tensile strains developed

initially and increased up to a load of 60 kips, at which load critical diagonal cracking occurred in the beam. With further loading, the tensile strains began to drop until the strains became compressive at a load of 75 kips and then remained so to failure. Gauge c(12) showed high tensile strains before it broke. It is probable that the readings of this gauge were affected by cracking. This may be established from the behaviour of gauge e(12). This gauge developed tensile strains initially, recording a maximum tensile strain of 0.30×10^{-4} at a load of 25 kips. Above this load, however, the tensile strain began to drop until it became compressive at a load of 35 kips. This compressive strain increased systematically up to a load of 50 kips when suddenly large tensile strains were recorded and the gauge eventually broke at a load of 100 kips, no doubt, due to cracking.

The behaviour of gauge f(12) at midspan also followed the typical pattern. It developed tensile strains initially, recording a maximum tensile strain of 0.64×10^{-4} at a load of 20 kips. Above this load level, the tensile strains began to drop until the strains became compressive at a load of 30 kips and remained so for the remaining part of the loading. This gauge eventually recorded a maximum compressive strain of 3.25×10^{-4} at a load of 180 kips.

Large compressive strains were observed on the compression face under the load point, especially after critical diagonal cracking.

The behaviour of gauges located at the 12-inch level ($3/4$ of the effective depth of the beam), showed that all gauges started with gradually increasing tensile strains. However, with flexural cracking, the pattern changed. First flexural cracks occurred in the midspan region of the beam and proceeded outwards. Similarly, the strains at the 12-inch level became compressive first at the midspan then at the load point and finally at the supports at load of 30 kips, 35 kips and 60 kips respectively. At the latter of these loads, critical diagonal cracking was observed. As the beam continued taking further load after diagonal cracking, the strain pattern remained unchanged except that larger compressive strains were recorded in the lower half of the beam at sections near the supports.



(ii) BEAM IA-2 ($a/d = 1.5$)

The test results for beam IA-2 are summarized in Figs. III.2 (a) and (b).

DEMEC DATA (Fig. III.2a)

Cracks crossed the gauge lines at $e'(4)$, $e'(12)$ and $d'(12)$. Small tensile strains developed at the compression face over the support and also at section b' . Compressive strains at sections c' and d' at the compression face remained small while those under the load point increased rapidly with load, especially after diagonal cracking. By the time a load of 50 kips had been reached, the critical diagonal crack was well into the compression zone of the beam. It was at this stage that the beam started taking more load without any significant propagation of cracks. The longitudinal strain diagram shows that at a load of 40 kips, $c'(12)$ had already developed compressive strains while compressive strains at $b'(12)$ and $a'(12)$ developed at a load of 60 kips. It is difficult to estimate the true strains at $d'(12)$ and $e'(12)$ due to cracking. However, it could be observed that compression centre shifted downwards over sections at support and close to it after critical diagonal cracking.

ELECTRICAL RESISTANCE STRAIN GAUGE DATA (Fig. III.2b)

An examination of the data from gauge $f(12)$ showed that tensile strains developed from the initial stages of loading, reaching a maximum of 0.89×10^{-4} at a load of 20 kips when

flexural cracks in the midspan region were observed. Above this load, the tensile strains at this gauge location began to drop until the strains became compressive at a load of 30 kips and remained so to failure. A maximum compressive strain of 1.46×10^{-4} was recorded at a load of 75 kips after which the compressive strain dropped slightly.

Large compressive strains were observed at the compression face under the load point. From the point of critical diagonal cracking at a load of 50 kips to collapse, the increase of the compressive strains was more rapid.

Gauge e(12) showed tensile strains as the load increased, reaching a maximum of 1.32×10^{-4} at a load of 25 kips. This value then reduced gradually until the strains became compressive at a load of 40 kips. Similar observations were recorded for gauges d(12), c(12), b(12) and a(12). All of these gauges developed tensile strains initially, showing maximum values at a load of 45, 35, 35 and 40 kips respectively. With further loading, tensile strains reduced gradually until compressive strains developed at a load of 50 kips at all these locations as the critical diagonal crack caused a significant split. Thereafter, all these gauges continued to show compressive strains to failure except for c(12). This gauge developed sudden tensile strains at a load of 65 kips and broke at the next load increment. This evidently resulted from an approaching crack interfering with the strain distribution at the point.

From the above, it can be seen that compressive strains at $3/4$ th of the effective depth of the beam developed at midspan at a load of 30 kips, under the load point at a load of 40 kips and at all other sections at a load of 50 kips. The development of these compressive strains, therefore, followed the progressive development of flexural cracking from midspan region outwards. Compressive strains at sections closer to the support at the 12-inch level only developed after critical diagonal cracking.

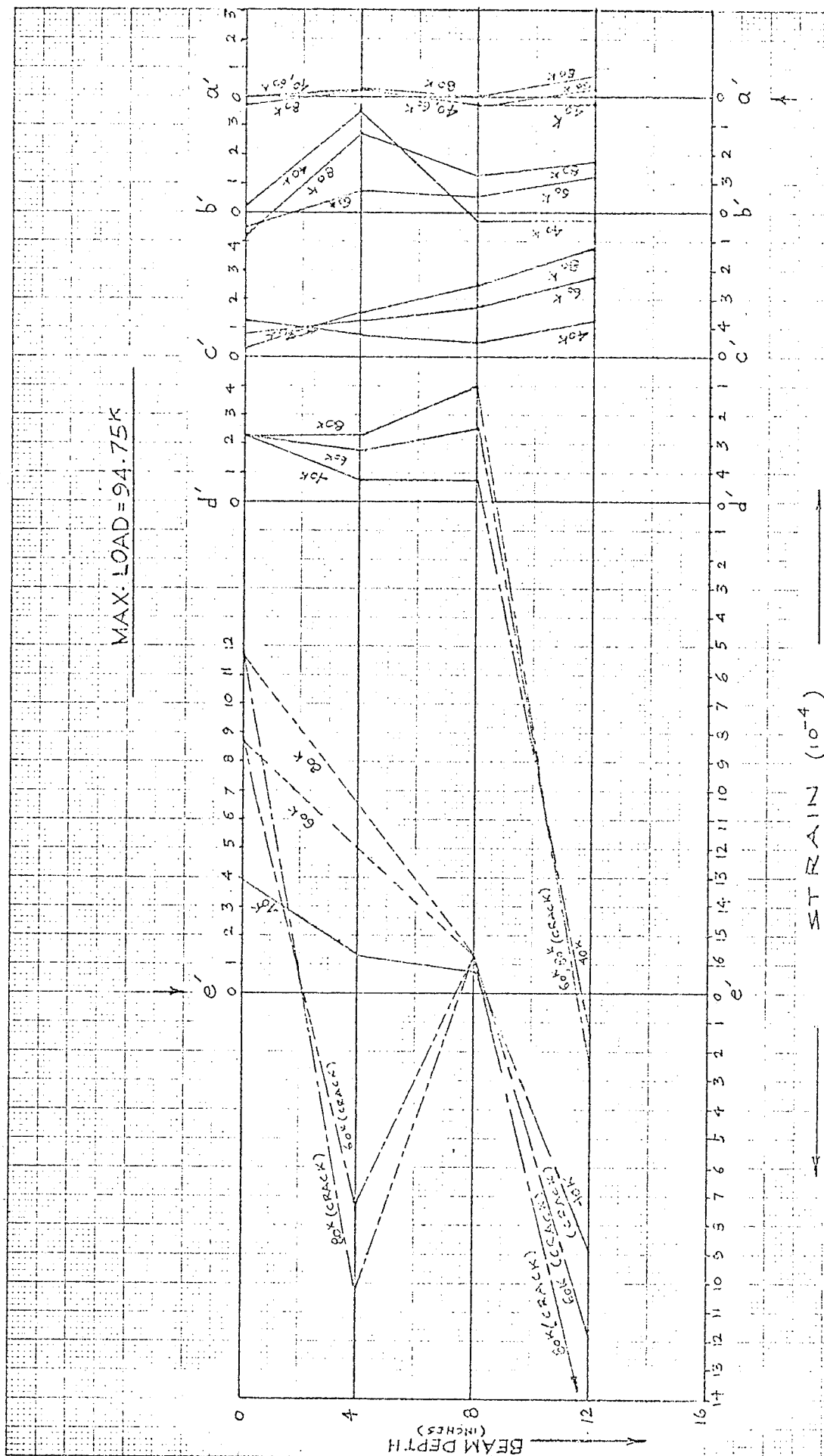


FIG. III-2(a) LONGITUDINAL STRAIN—DEMEC DATA

BEAM IA-2

MAX. LOAD = 94.75K

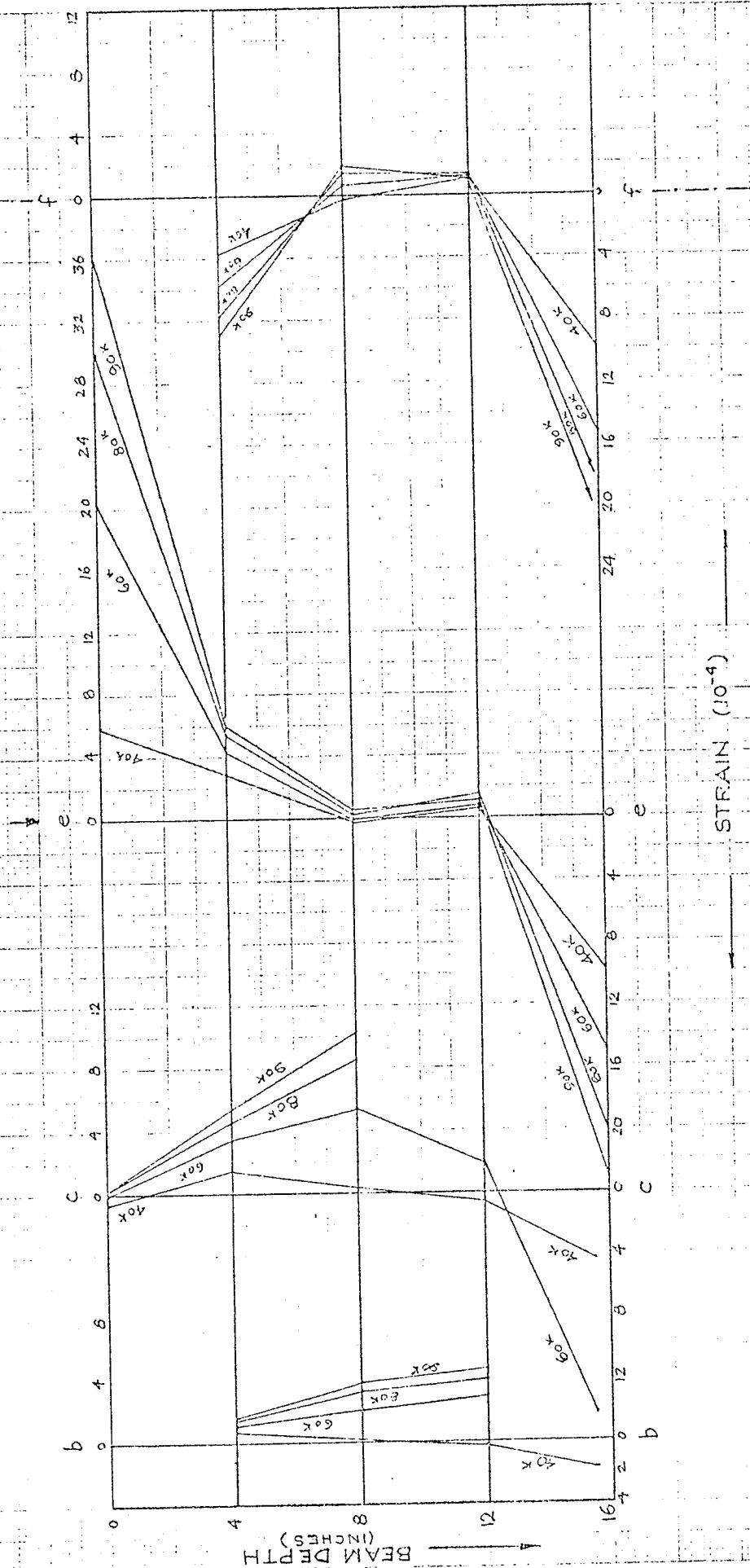
STRAIN (10^{-4})

FIG. III. 2(b) — LONGITUDINAL STRAIN ——— Electrical Resistance Strain Gauge Data

BEAM IA-2 — SIDE 'N'

(iii) BEAM IA-3 ($a/d = 2.0$)

The test results for beam IA-3 are summarized in Figs. III.3 (a) and (b).

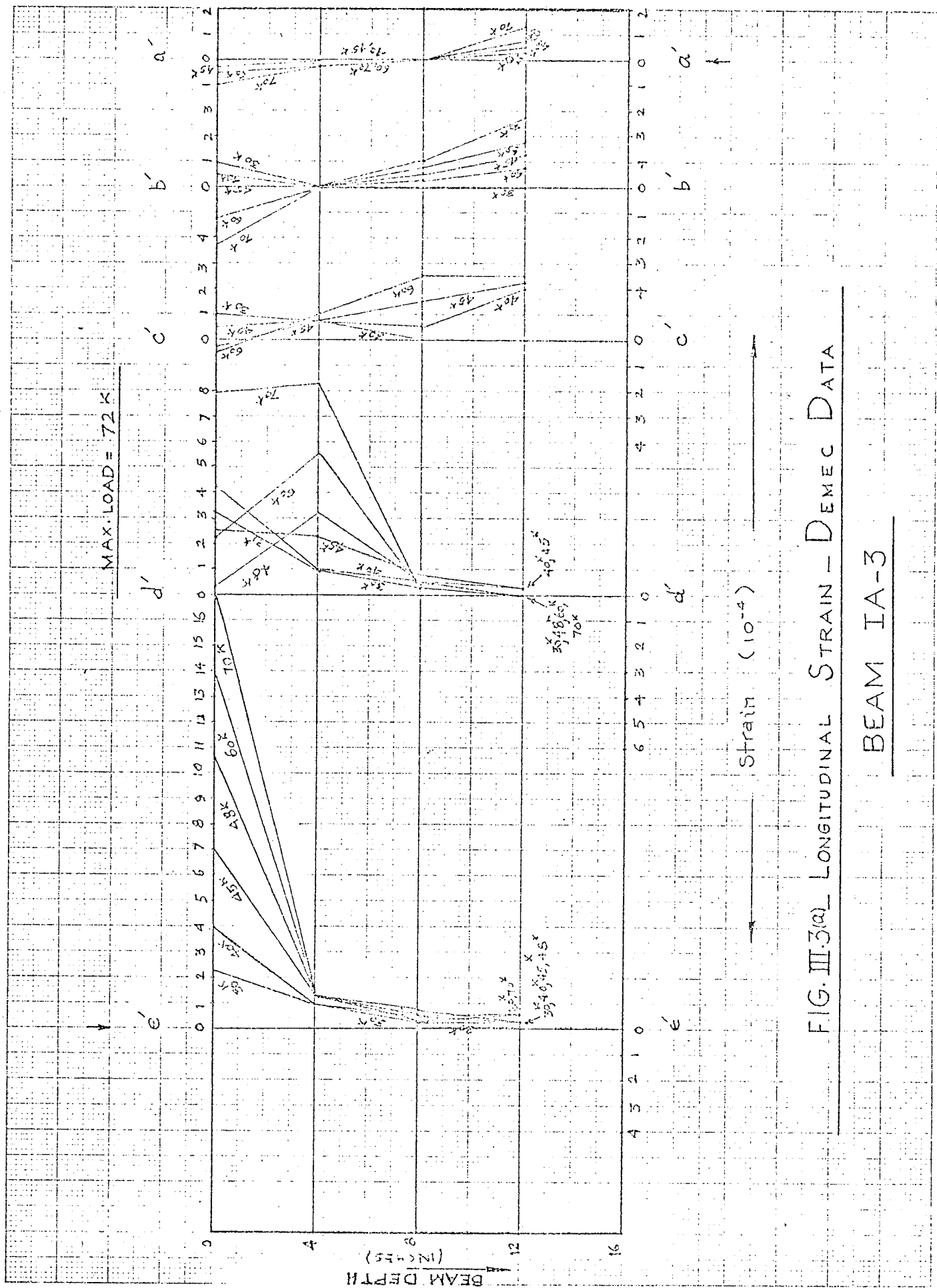
DEMEC DATA (Fig.III.3a)

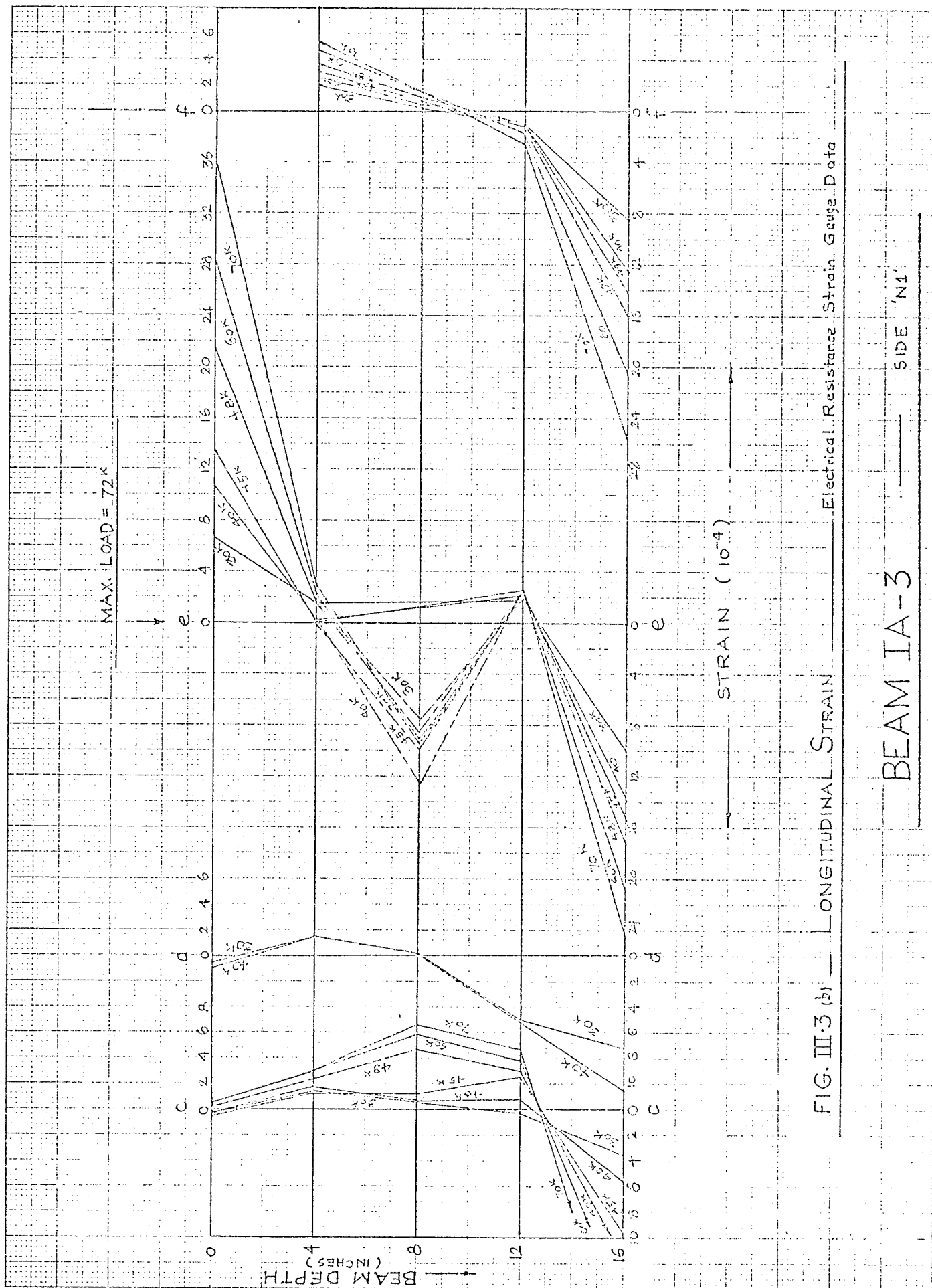
Compressive strains developed gradually from the midspan region outwards at the 12 inch level. After the appearance of a critical diagonal crack at a load of 45 kips, compressive strains developed at $a'(12)$, directly over the support. At subsequent loading stages, as the critical diagonal crack became stable, the compressive strains at 12 inch level near the supports increased. Furthermore, tensile strains developed at sections closer to supports at the compression face. However, large increases of compressive strain at the compression face directly under the load point were observed at critical diagonal cracking and prior to ultimate failure of the beam.

ELECTRICAL RESISTANCE STRAIN GAUGE DATA (Fig.III.3b)

An examination of all gauges at the 12 inch level showed that tensile strains developed initially. The readings of gauge $f(12)$ were erratic and could not be relied upon. Maximum tensile strains at $e(12)$, $d(12)$, $c(12)$, $b(12)$ and $a(12)$ were recorded at a load of 12.5, 12.5, 32.5, 32.5 and 42.5 kips respectively. All these gauges showed a reduction of tensile strains after reaching the maximum, ultimately reducing to compressive strains at a load of 17.5, 20, 37.5,

45 and 46 kips respectively. These compressive strains generally increased to failure except at d(12) where tensile strains developed due to cracking, recording a high tensile strain of 9.72×10^{-4} at a load of 32.5 kips before the gauge broke at a load of 35 kips. Compressive strains at b(12) and a(12) only developed when the beam was significantly cracked by the critical diagonal crack. Strain readings were taken at 1000 pound intervals at load levels near critical diagonal cracking and it was observed that the change of tensile strains to compressive strains at sections close to support at the 12 inch level took place rather abruptly, coinciding with critical diagonal cracking.





(iv) BEAM IA-4 ($a/d = 2.5$)

The test results for beam IA-4 are summarized in Fig.

III.4. Results of DEMEC data are not presented as there appears to have been some error in recording the zero load readings.

ELECTRICAL RESISTANCE STRAIN GAUGE DATA (Fig.III.4)

An examination of the data from gauge f(12) showed that tensile strains developed initially and increased to a value of 0.55×10^{-4} at a load of 10 kips. However, with further loading, the tensile strains began to drop, developing into compressive strains at a load of 15 kips. A maximum compressive strain of 1.37×10^{-4} was recorded at a load of 20 kips. Later a tensile strain of 3.34×10^{-4} developed suddenly at a load of 25 kips and increased rapidly, recording a maximum value of 19.80×10^{-4} at a load of 37.5 kips. It is evident that these large tensile strains are a result of cracking. Gauge f(8) was also affected by cracking from a load of 25 kips onwards. A close look at gauge f(0) shows that its readings were rather erratic and could not be relied upon.

Gauges e(8) and e(12) were also affected by cracking. Tensile strains at e(12) were only 1.24×10^{-4} at a load of 10 kips when a sudden jump occurred, strains reaching 11.9×10^{-4} at a load of 17.5 kips before the gauge broke at a load of 20 kips. Similarly, gauge e(8) showed rapid increases of tensile strain after a load of 17.5 kips with the onset

of cracking.

Cracking also affected gauge d(12). At a load of 10 kips, the tensile strain was only 0.48×10^{-4} but increased rapidly to 18.5×10^{-4} at a load of 25 kips before the gauge broke at the next load increment.

At c(12), maximum tensile strains were recorded at a load of 20 kips. Above this load, the tensile strains reduced until compressive strains developed at a load of 25 kips. These compressive strains, however, abruptly changed to tensile strain at 32.5 kips which increased rapidly as failure approached. A flexural crack was seen to pass under gauge c(12) at 32.5 kips. Tensile strains shown by gauge c(12) are, therefore, a result of cracking.

Gauges at 12 inch level at sections a and b showed consistent increase of tensile strains till failure. There were no cracks at these sections. This clearly shows that compressive strains at the 12 inch level did not extend to sections close to the support.

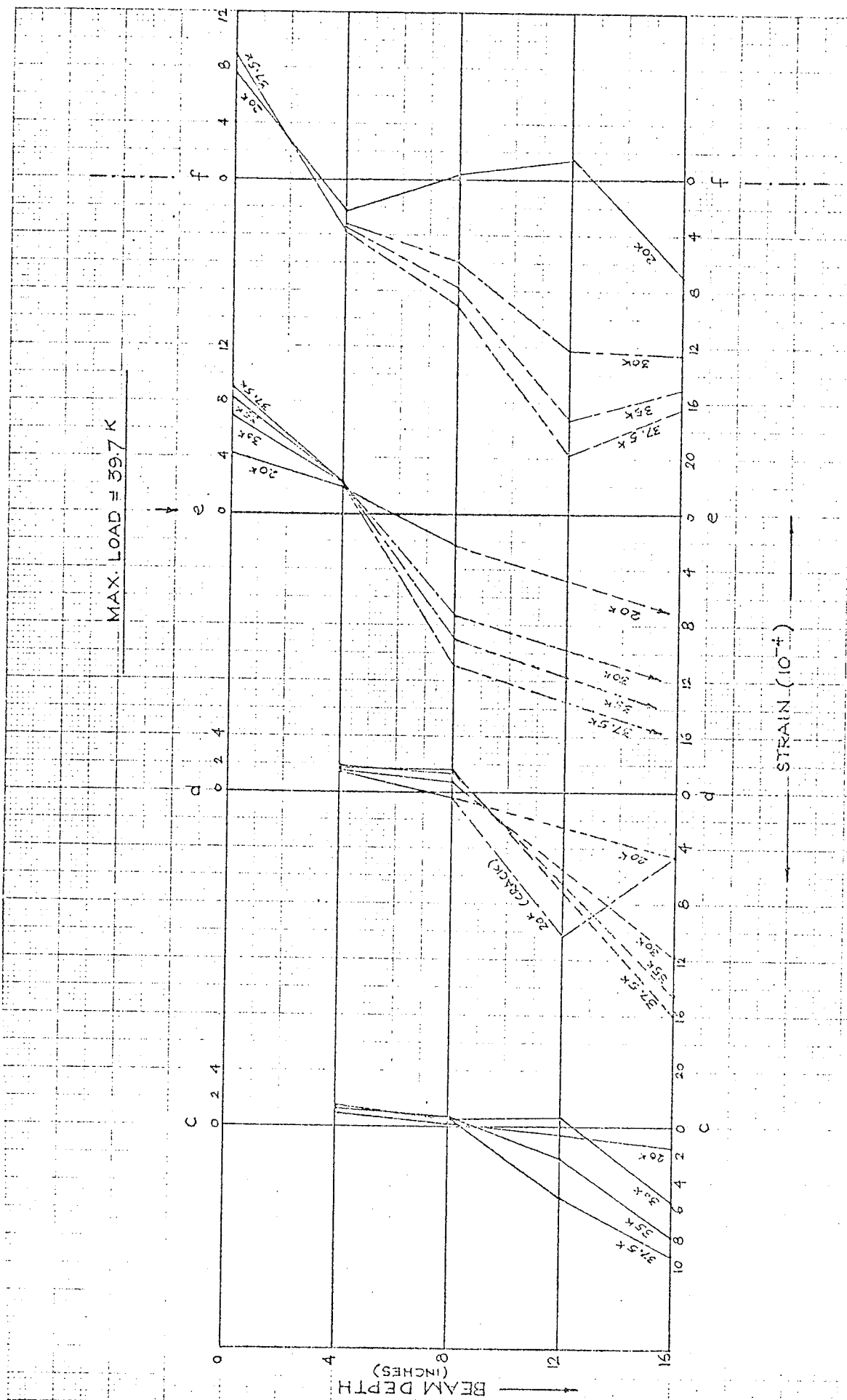


FIG. III.4—LONGITUDINAL STRAIN ——— Electrical Resistance Strain Gauge Data

BEAM IA-4 ——— SIDE 'N1'

(v) BEAM IA-5 ($a/d = 3.0$)

The test results for beam IA-5 are summarized in Figs. III.5 (a) and (b).

DEMEC DATA (Fig.III.5a)

Compressive strains under the load point on the compression face could not be recorded as the DEMEC points were not properly fixed to the concrete surface at this location while cracking interfered with strain distribution at e'(12). Compressive strains remained generally small on the compression face. Initial tensile strains at the 12-inch level at sections c' and d' changed to compressive strains at a load of 30 kips. Though small compressive strains were recorded over the supports at the 12-inch level from the beginning, it is quite probable that this may be due to an error in the initial DEMEC reading taken at zero load. This observation is supported by the fact that the gauge at the 12-inch level at section b' showed tensile strains over the whole load range.

ELECTRICAL RESISTANCE STRAIN GAUGE DATA (Fig.III.5b)

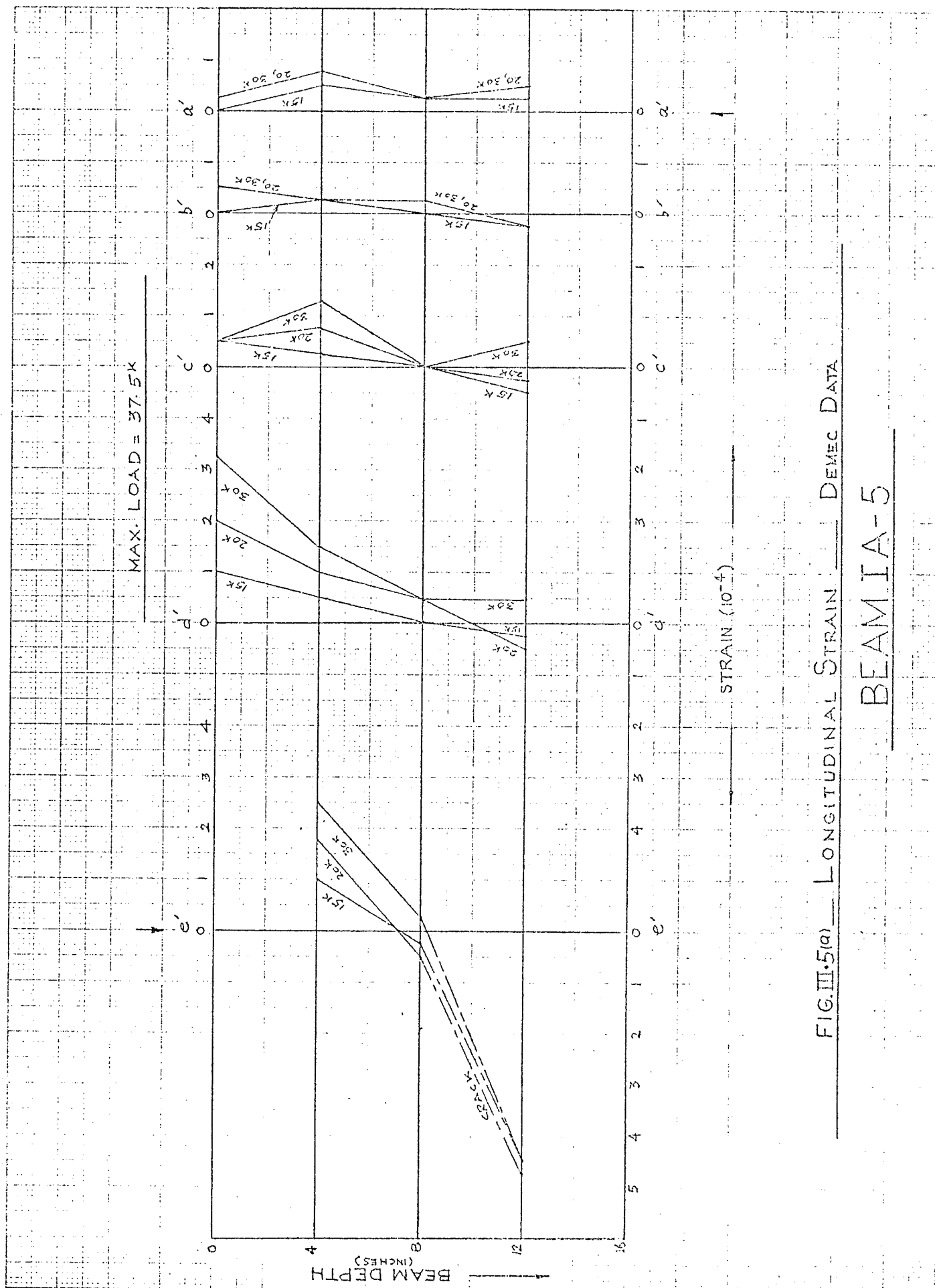
This data also shows that compressive strains at the compression face of the beam remained small upto failure. Sudden critical diagonal cracking caused the failure of the beam.

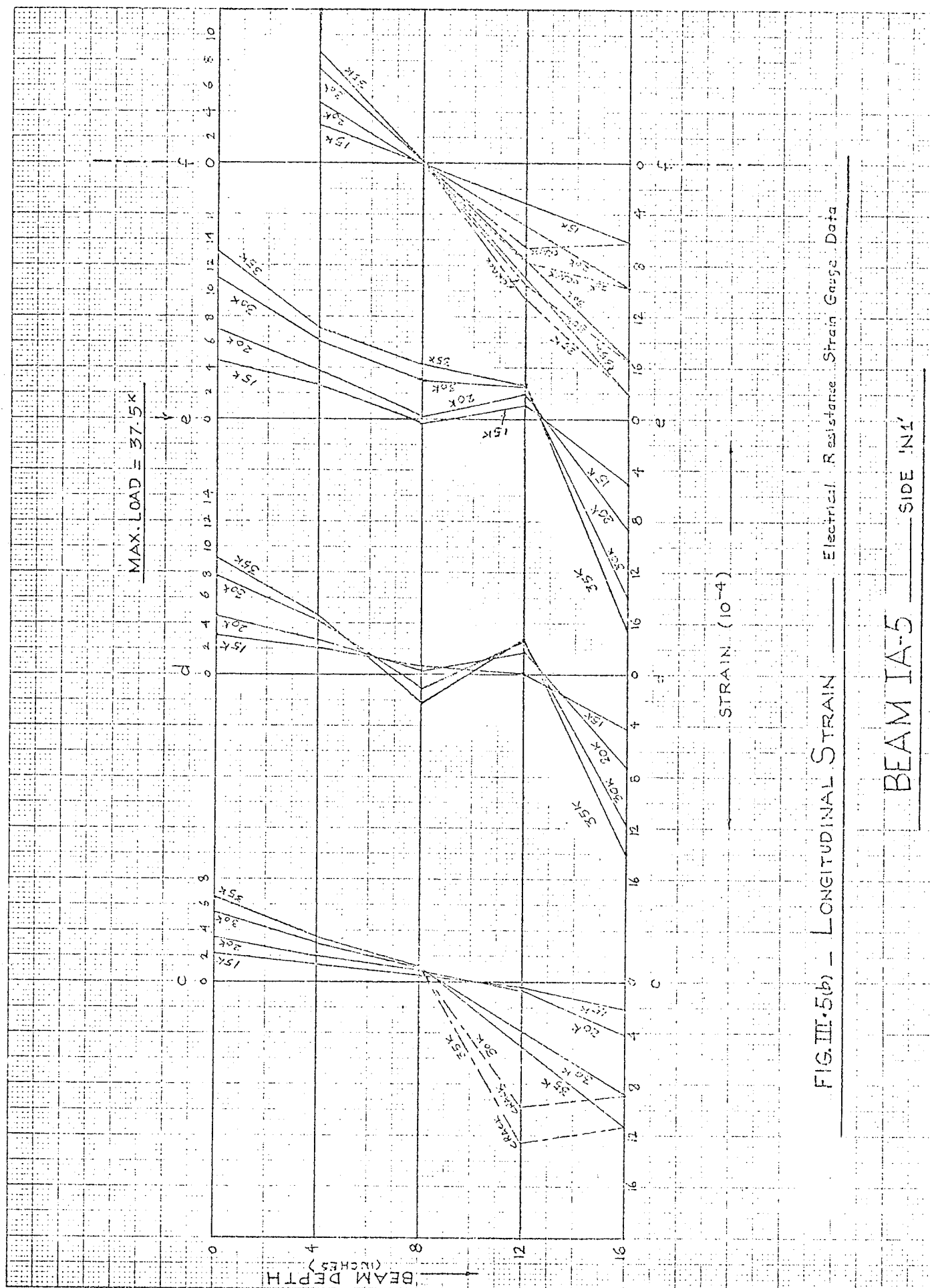
Gauge f(12) showed a gradual increase of tensile strains to a value of 0.45×10^{-4} at a load of 7.5 kips but suddenly

jumped to a value of 3.46×10^{-4} at a load of 10 kips. This gauge was affected by cracking.

Maximum tensile strains at e(12) and d(12) occurred at a load of 12.5 kips and then reduced to compressive strains at a load of 15 kips. These compressive strains then continued increasing gradually. Strains at c(12) remained tensile, with a sudden sharp increase due to cracking at 27.5 kips. It is possible that compressive strains may have been observed at this location at later stages of loading had cracking not interfered with the strain readings.

Strains at sections a(12) and b(12) remained tensile from the beginning upto failure of the beam.





(vi) BEAM IA-6 ($a/d = 4.0$)

The test results for beam IA-6 are summarized in Figs. III.6 (a) and (b).

DEMEC DATA (Fig. III.6a)

Compressive strains developed at the 12 inch level at sections e' and d' after flexural cracking. However, cracks interfered with strain distribution at c'(12). Strains remained generally small at a'(12) and b'(12). Initial reading at a'(12) seems to be somewhat erratic.

ELECTRICAL RESISTANCE STRAIN GAUGE DATA (III.6b)

Many of the gauges on this beam gave erratic results, no uniform trend of strain being observed. This may possibly have been due to improper soldering and "cold" connections, either at the terminal points or at the gauge box. Significant drifts were observed in the gauge readings and it is evident that not too much reliance can be placed on results from this beam. Gauges b(12), c(12) and d(12) were more consistent. At the 12 inch level, strains remained tensile throughout at sections b and c. At d(12), initial tensile strains reduced to compressive strains at 12.5 kips but suddenly reversed to tensile strains at 20 kips due to the onset of cracking as the gauge finally broke at 30 kips after recording high tensile strains.

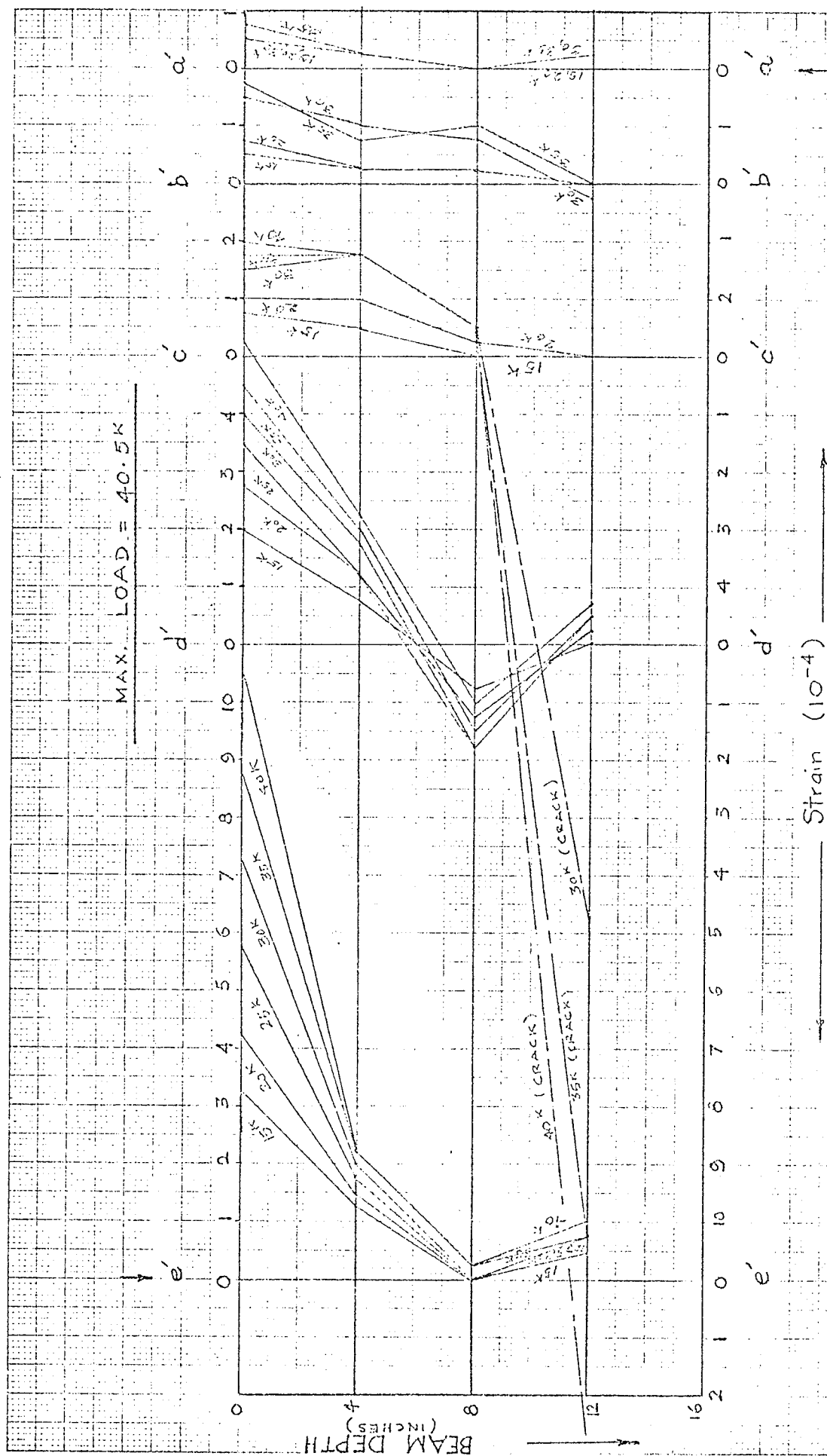
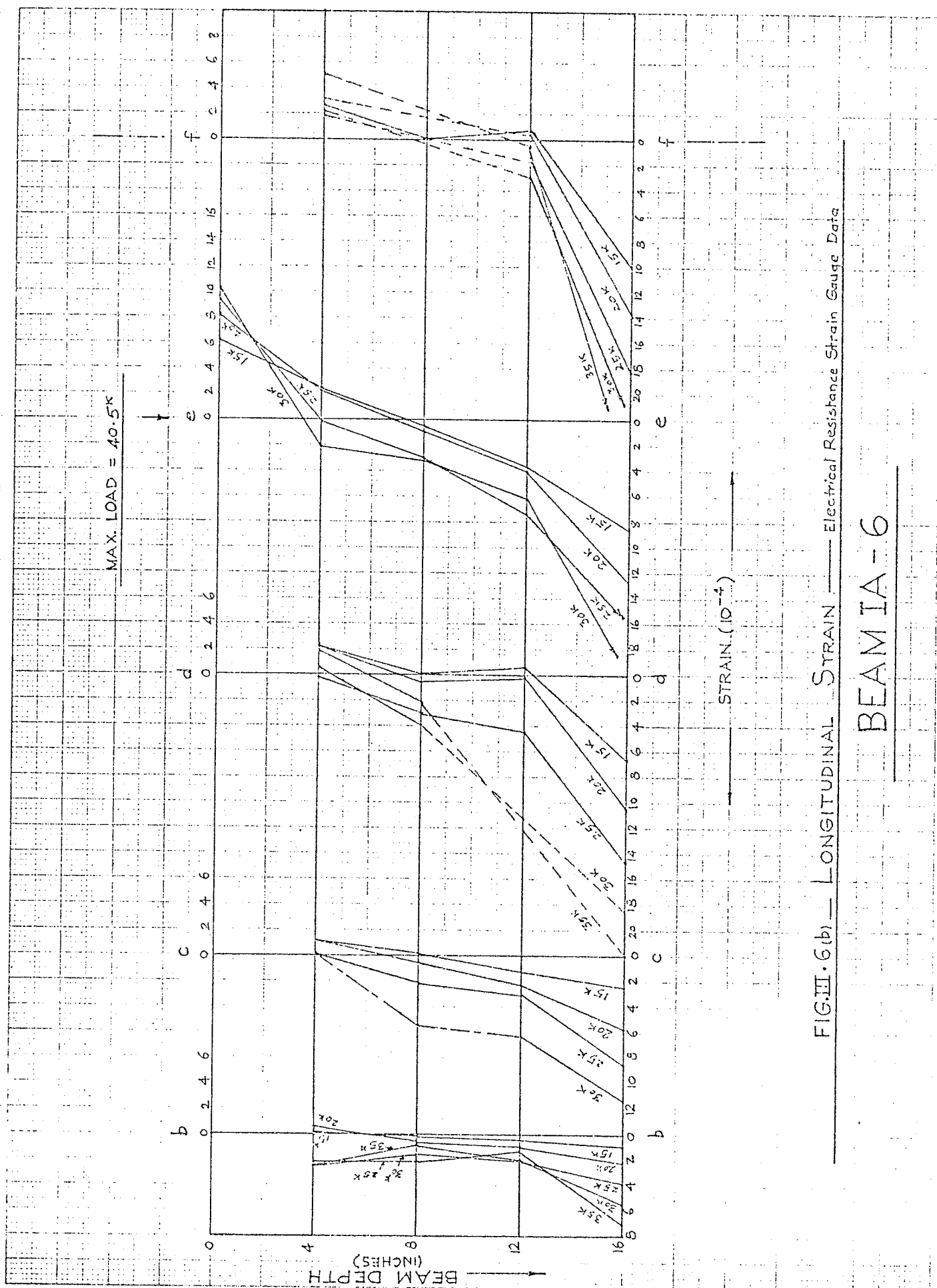


FIG. III-6(a) — LONGITUDINAL STRAIN — DEMEC DATA

BEAM IA-6



(vii) BEAM IA-7 ($a/d = 5.0$)

The test results for beam IA-7 are summarized in Figs. III.7(a) and (b).

DEMEC DATA (Fig.III.7a)

Initial tensile strains reduced to compressive strains at gauges $e'(12)$ and $c'(12)$ while cracking at gauge $d'(12)$ did not allow correct strains to be recorded. Initial tensile strains at gauges $a'(12)$ and $b'(12)$, however, kept on increasing steadily until sudden diagonal failure occurred at the appearance of a critical diagonal crack.

ELECTRICAL RESISTANCE STRAIN GAUGE DATA (Fig.III.7b)

Gauge $f(12)$ broke at a load of 10 kips as a flexural crack passed right through it. As this crack approached upwards, it also broke gauge $f(8)$ at a load of 35 kips.

Initial tensile strains at gauges $e(12)$ and $d(12)$ reduced to compressive strains at a load of 10 and 12.5 kips respectively and kept increasing steadily thereafter.

Gauges $c(12)$ and $b(12)$ showed highly erratic results throughout the test and their readings are of little value.

(viii) BEAM IA-8 ($a/d = 6.0$)

The test results for beam IA-8 are summarized in Figs. III.8 (a) and (b).

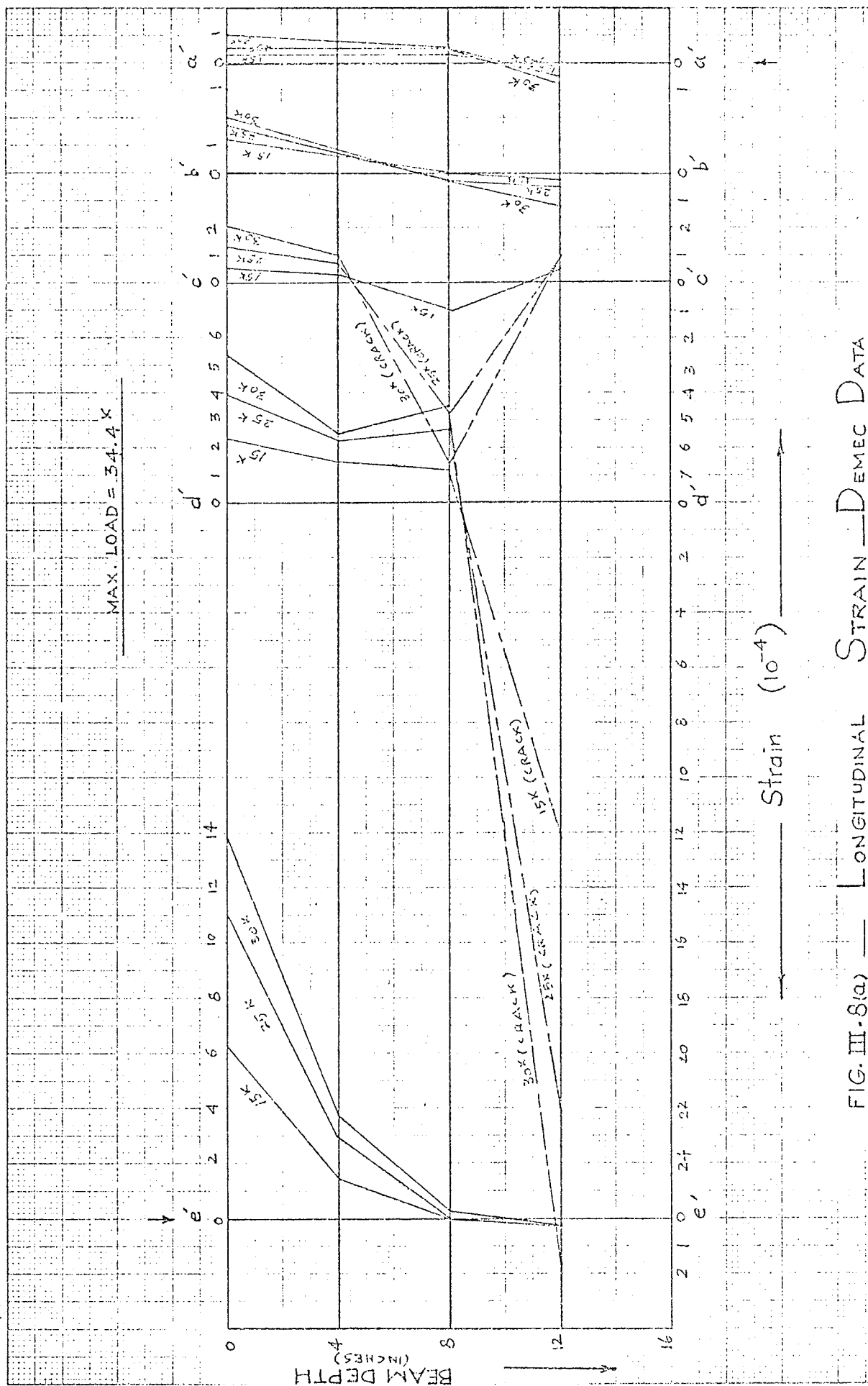
DEMEC DATA (Fig.III.8a)

Initial tensile strains at gauges $a'(12)$ and $b'(12)$ kept on increasing with load while small compressive strains developed at $c'(12)$. Cracking at $d'(12)$ interfered with the strain pattern. At $e'(12)$ very small tensile strains were observed and these remained so over the loading range. This, however, may possibly be due to a small error in the zero load reading.

ELECTRICAL RESISTANCE STRAIN GAUGE DATA (Fig.III.8b)

Gauges $b(12)$ and $c(12)$ gave erratic readings from the beginning and are of no practical use. Cracking interfered at $d(12)$ where sudden high tensile strains developed at a load of 7.5 kips, increasing rapidly till the gauge broke at a load of 25 kips. Strains at $e(12)$ remained very small. Initial tensile strains (1.09×10^{-4} at a load of 5 kips) reduced to small compressive strains at a load of 15 kips which remained almost constant throughout the remaining loading stages. The same pattern could be observed at $f(12)$, where initial tensile strains reduced to compressive strains of about 1.12×10^{-4} at a load of 15 kips and remained almost the same. The compressive strains at $f(4)$ kept on increasing with load showing that the neutral axis did not shift upwards at this

location. Appearance of diagonal crack resulted in failure of the beam.



BEAM IA-8

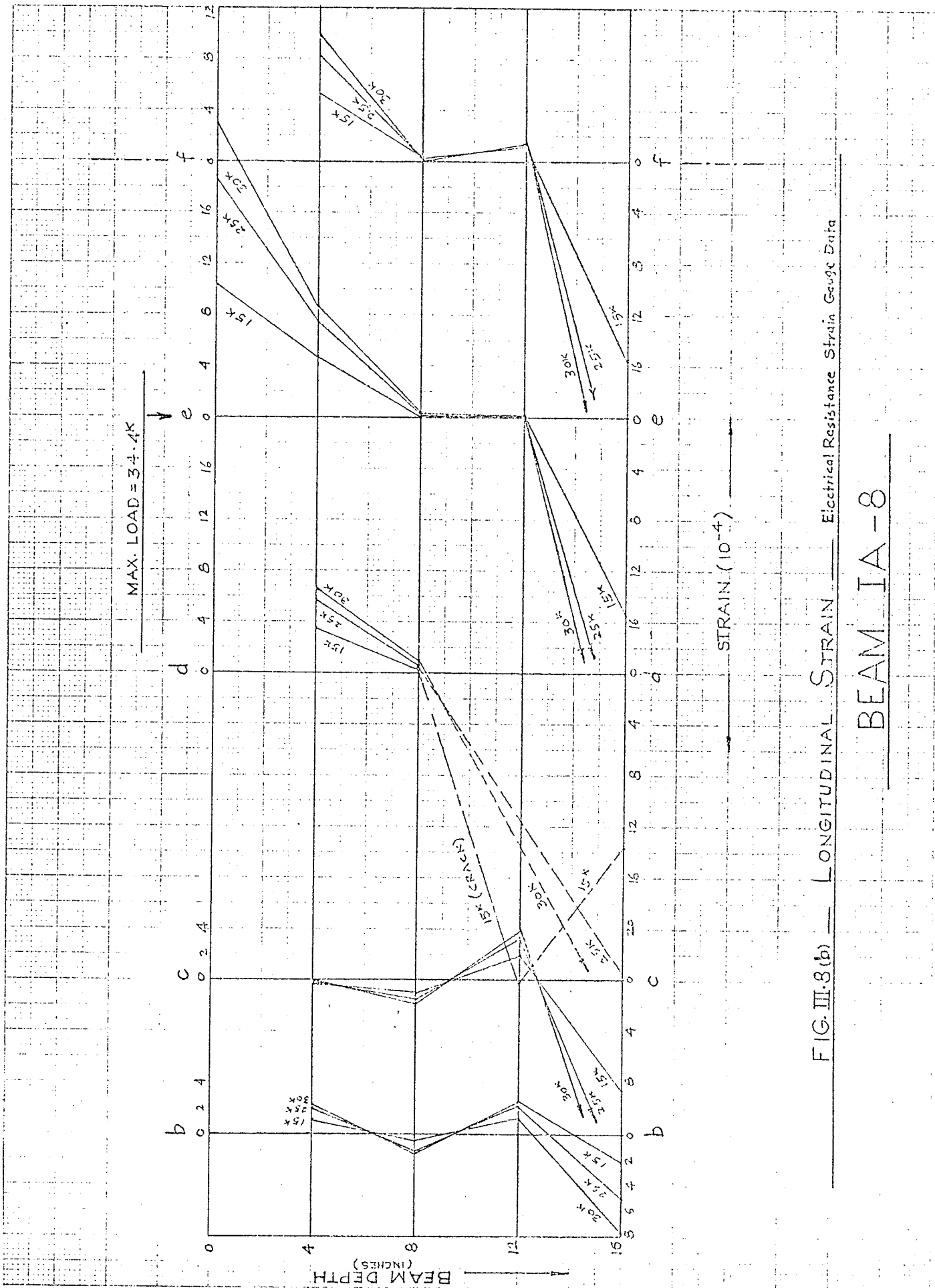


FIG. III-8(b) — LONGITUDINAL STRAIN — Electrical Resistance Strain Gauge Data

BEAM IA-8

III.1.2 TESTS OF SERIES IB

(i) BEAM IB-2 ($a/d = 1.5$)

The results for this beam are summarized in Fig.III.9. This beam was a retest of beam IB-5 over a shorter span, giving an a/d ratio of 1.5. No new gauge lines were added and the only gauge line on concrete was section a, located 4 inches away from the load point, in the shear span.

Until critical diagonal cracking occurred, the maximum compressive strains at section a were observed at the compressive face of the beam. However, after critical diagonal cracking, the maximum compressive strains shifted somewhat downwards. The beam carried considerable load after diagonal cracking. At conditions nearing ultimate failure, very large compressive strains were observed at section a, 3 inches below the compression face.

Strain readings from these gauges are not entirely reliable because the same gauges were used in an earlier test on beam IB-5 and it is possible that some of them might have been damaged. No DEMEC gauges were used on this beam.

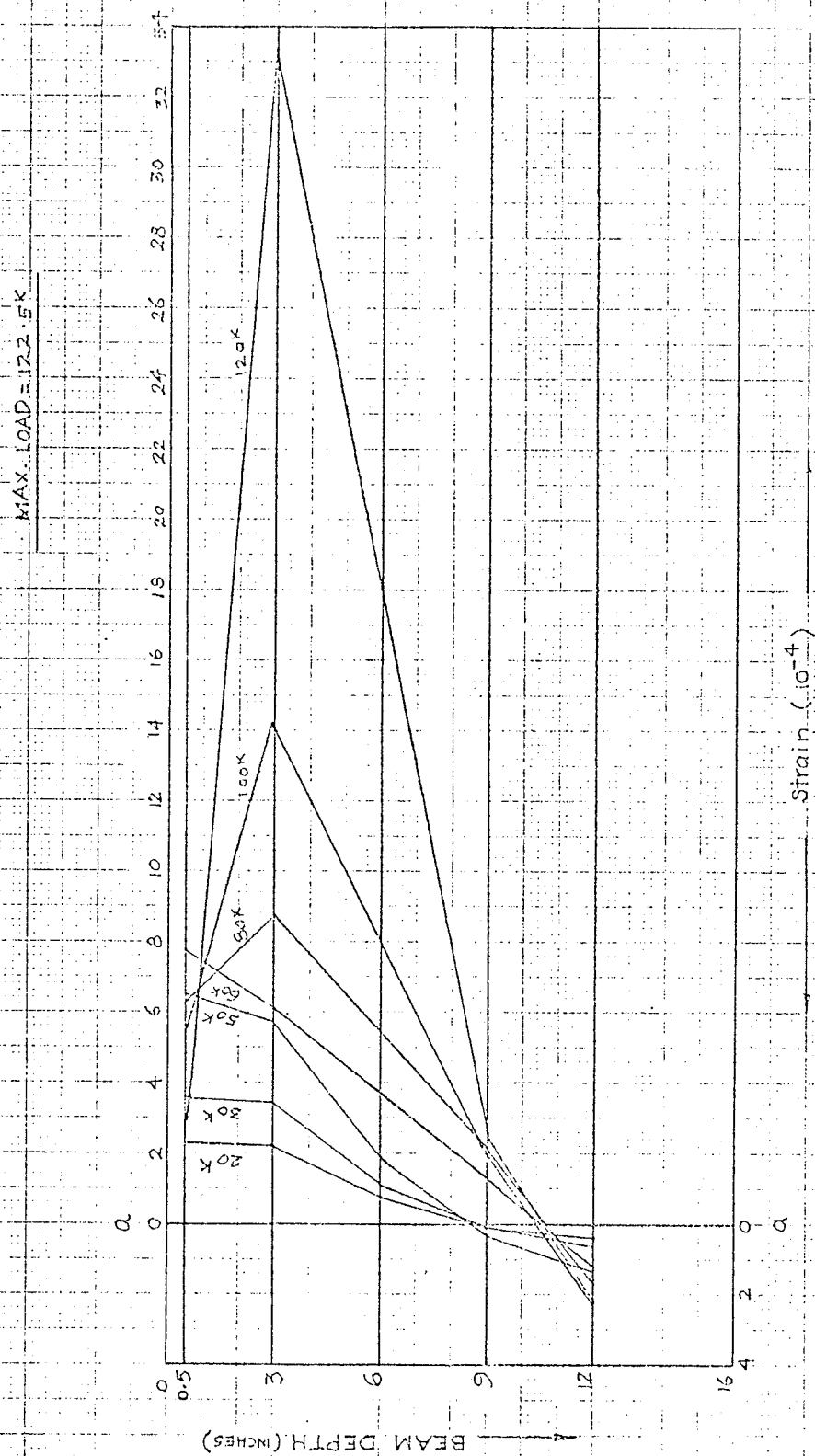


FIG. III-9 — LONGITUDINAL STRAIN — Electrical Resistance Strain Gauge Data

BEAM IB-2

NOTE — SECTION a-a IS 4" FROM LOAD POINT.

(ii) BEAM IB-4 ($a/d = 2.5$)

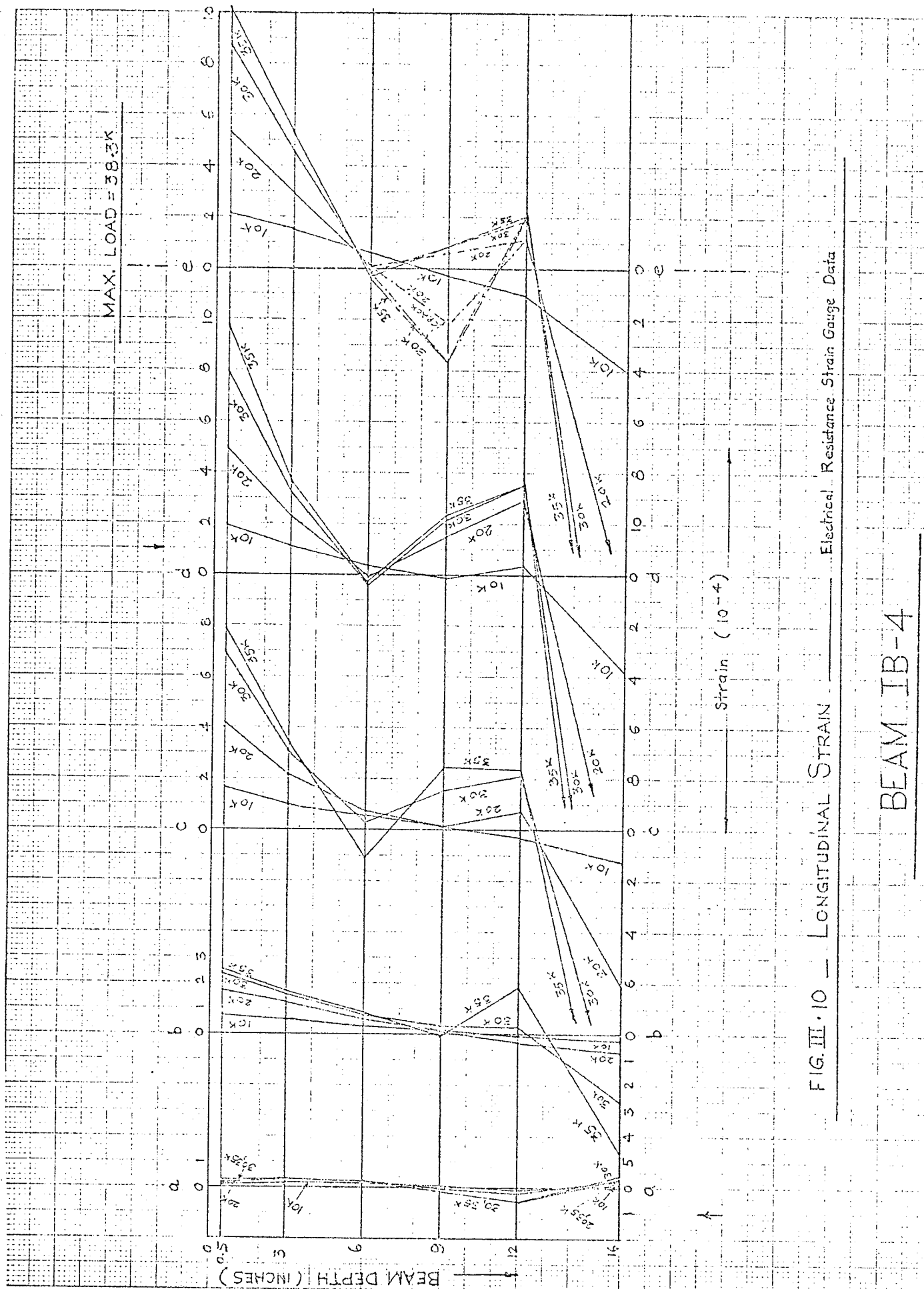
The test results for this beam are summarized in Fig.

III.10.

Since this beam was part of the preliminary tests, only electrical resistance strain gauges were used. Gauge locations on this beam were slightly different from the standard location used in most of the beams.

At early stages of loading, the variation of longitudinal strain was more or less a straight line variation on vertical sections throughout the span. However, with further loading and progressive cracking, compressive longitudinal strains were recorded at 12 inch level, from midspan outwards, until at failure all sections except a(12) showed compressive strains. Strains at compression face at all locations remained compressive throughout, and increased with higher loads.

This beam test was the first conducted during this investigation and the peculiar strain distribution after cracking seemed difficult to explain. It was only later, when extensive DEMEC strain gauges were also applied and the results of other beams also showed a consistently similar trend, that the development of internal arching within the beam was indicated. In this beam, sudden diagonal failure occurred at the appearance of a critical diagonal crack.

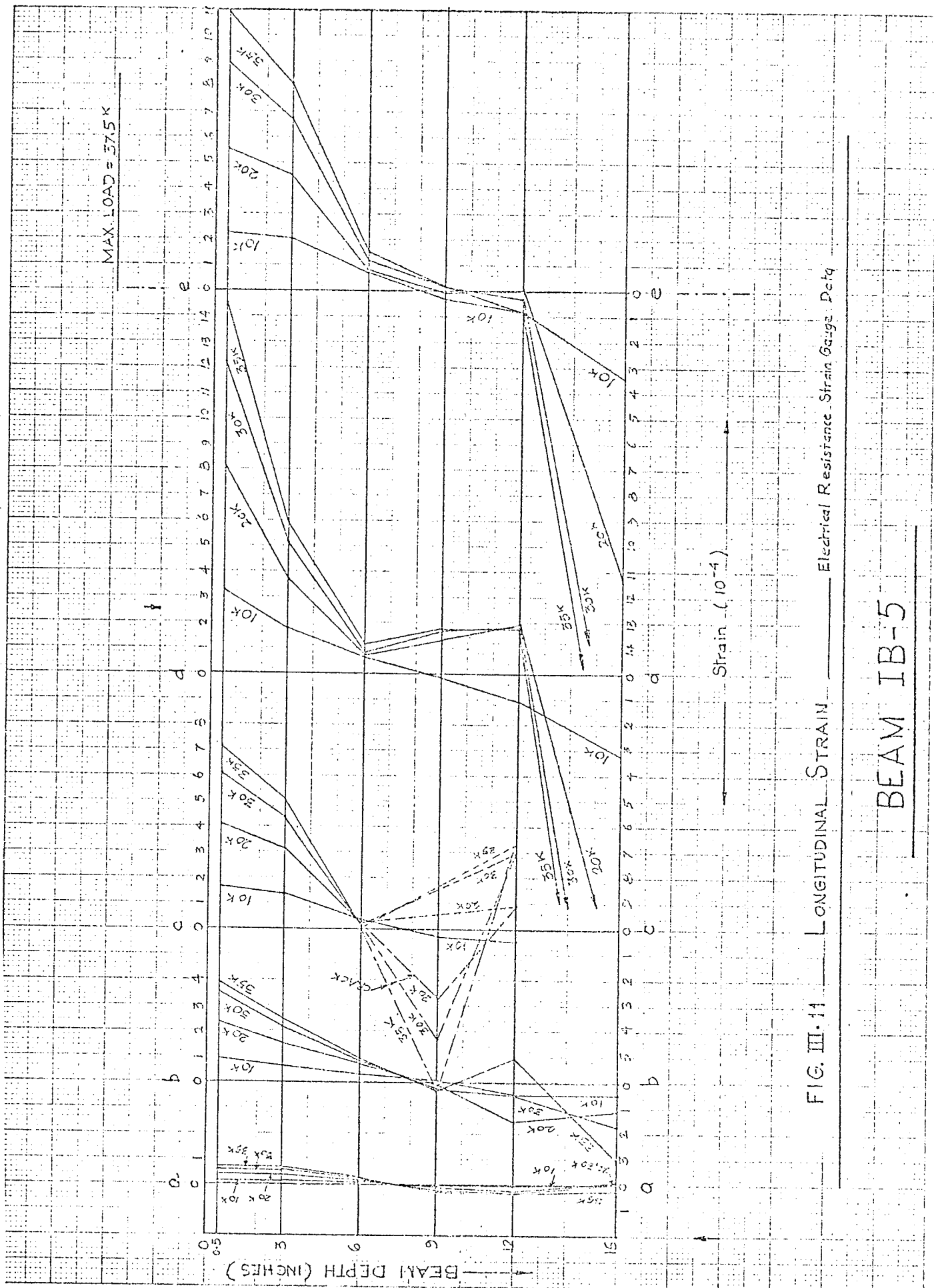


(iii) BEAM IB-5 ($a/d = 3.0$)

The test results for this beam are summarized in Fig.

III.11. This beam was also part of preliminary tests.

The general strain pattern for this beam is similar to that for beam IB-4. Compressive strains at compression face at all locations kept on increasing with higher loads. By a load of 20 kips, compressive strains at the 12 inch level had also developed upto the midshear span. At a load of 35 kips, compressive strains were recorded at b(12). Failure resulted at a load of 37.5 kips from a sudden extension of the diagonal crack. Strains at a(12), directly over the support remained tensile throughout the test.



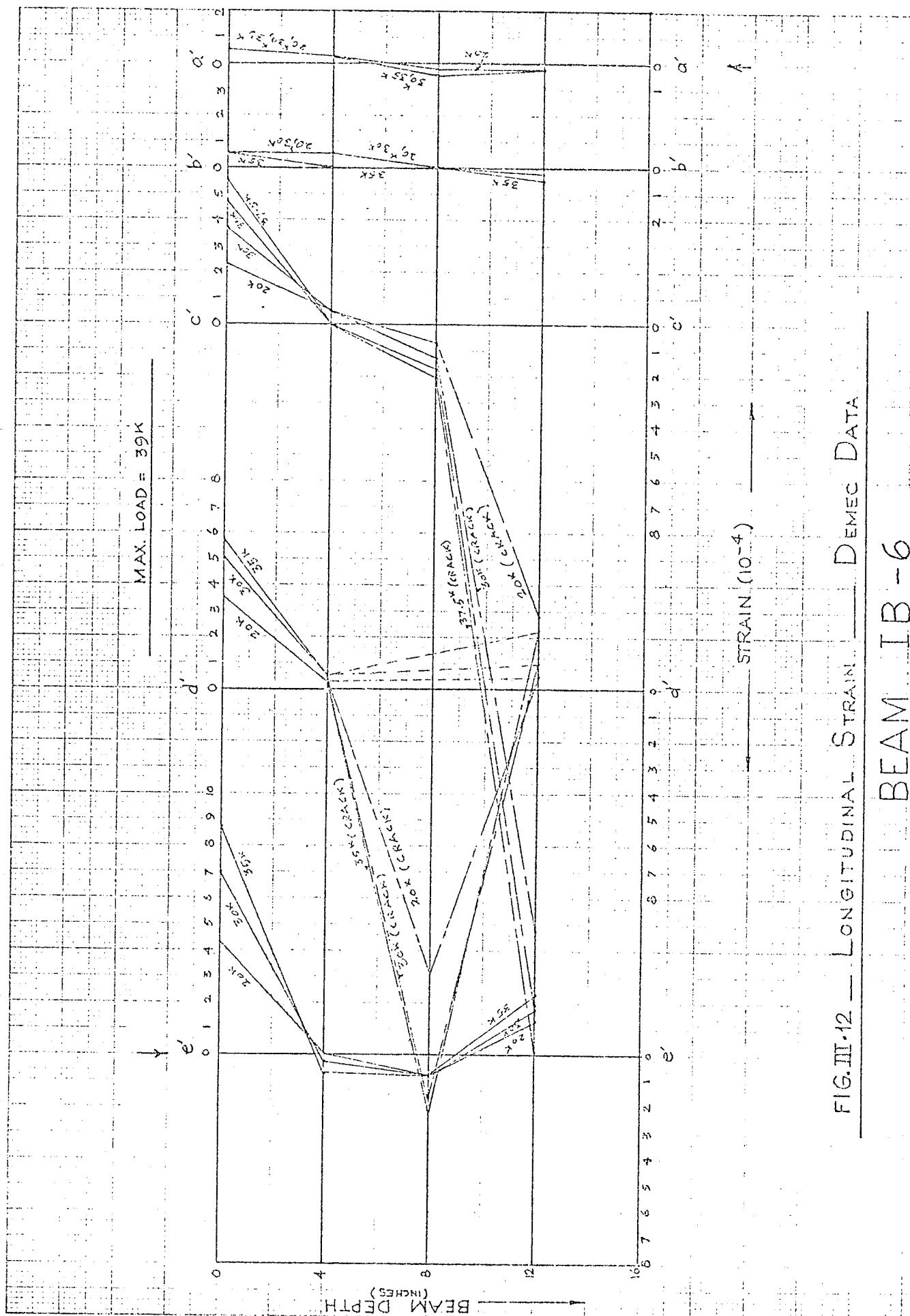
(iv) BEAM IB-6 ($a/d = 4.0$)

The test results for beam IB-6 are summarized in Fig. III.12.

The results from electrical resistance strains gauges were highly erratic with frequent drifts of significant magnitude. No consistent trend was observed in the gauges on concrete and it is probable that the soldering was not done properly and many of the connections had "cold" contacts. Due to unreliable nature of these readings, they have not been plotted.

Fig.III.12 shows the plot of DEMEC data. This beam was tested with the main test series.

Strains at the compression face of the beam remained compressive and generally small till failure. Gauges $a'(12)$ and $b'(12)$ continued showing tensile strains while cracking interfered with gauge $c'(12)$. Initial tensile strains reduced to compressive strains at gauges $e'(12)$ and $d'(12)$, which is consistent with the results of similar beams failing by diagonal tension.



III.1.3 TESTS OF SERIES IC

(i) BEAM IC-2 ($a/d = 1.5$)

The test results for beam IC-2 are summarized in Figs.

III.13 (a) and (b).

DEMEC DATA (Fig.III.13a)

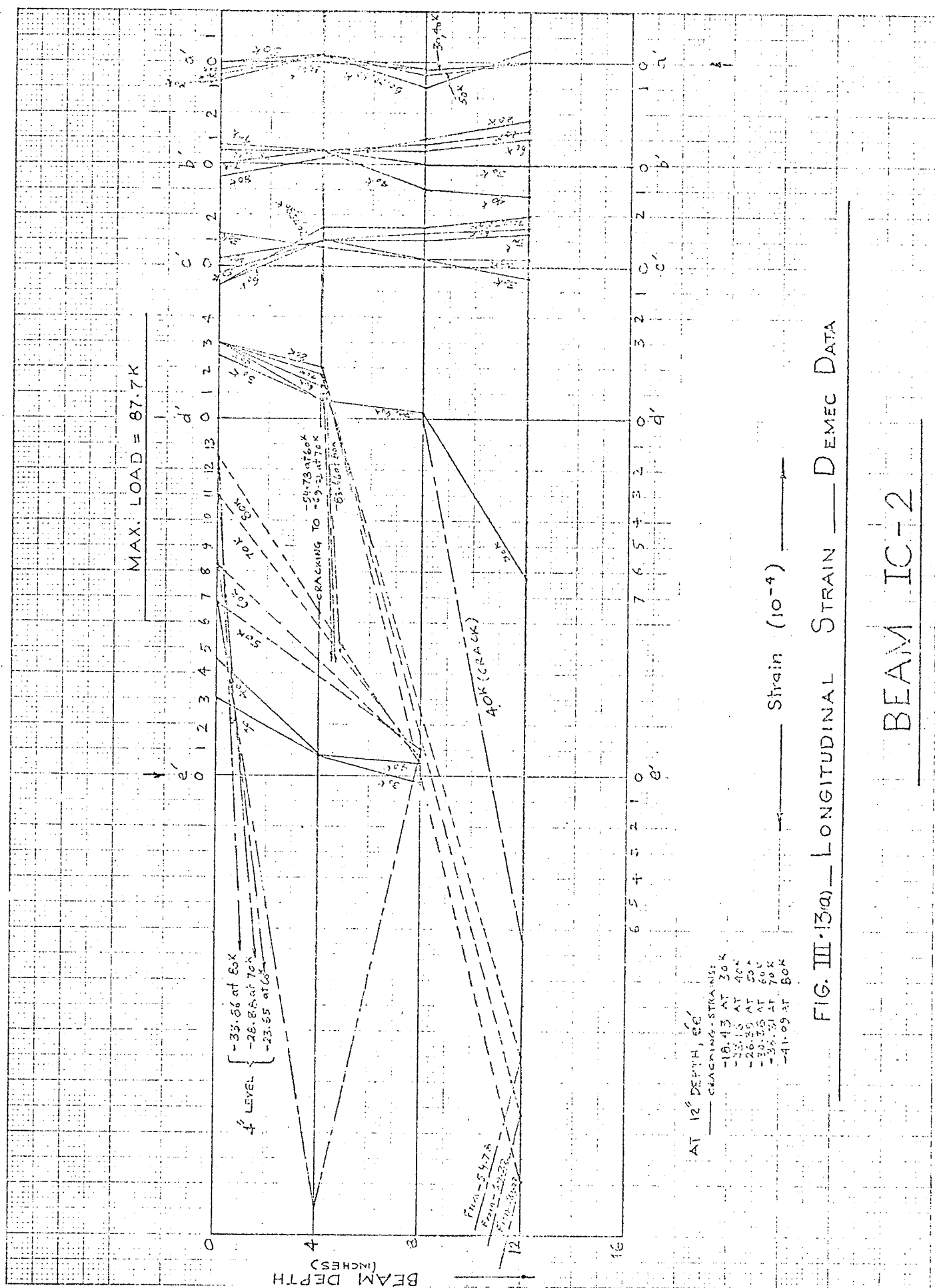
Cracks crossed gauges $d'(8)$, $d'(12)$ and $e'(12)$. Strains recorded at these locations are a measure of the crack width. Critical diagonal cracking occurred at a load of 50 kips and as the crack became stable, compressive strains were recorded at $a'(12)$ and $b'(12)$. Small tensile strains developed over the area close to the supports at the compression face while large compressive strains were recorded under the load point.

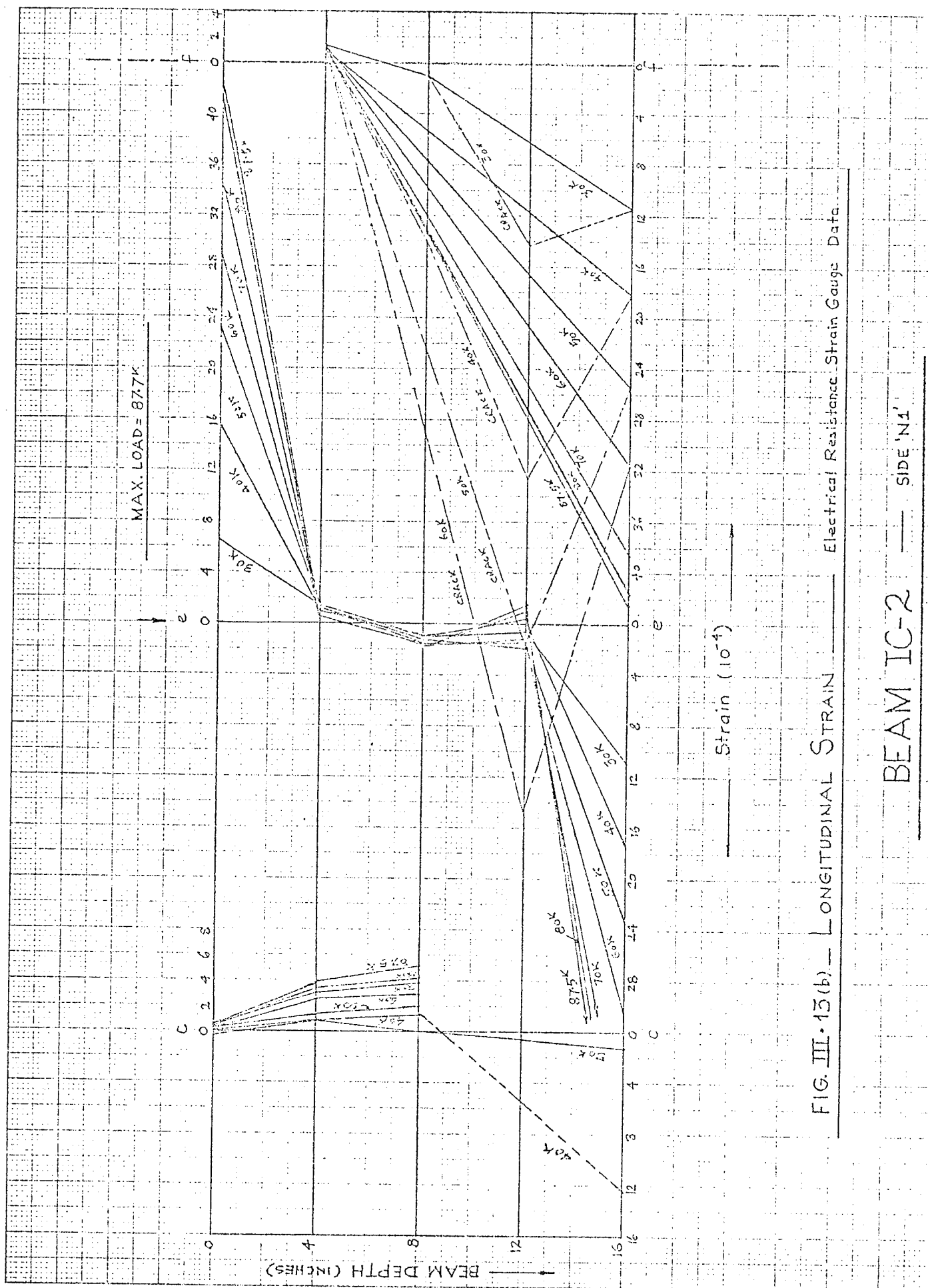
ELECTRICAL RESISTANCE STRAIN GAUGE DATA (Fig.III.13b)

High compressive strains, especially after critical diagonal cracking, under the load point show rotations taking place in the compressive zone. The compressive strain at the 4-inch level remained practically constant, thereby showing that the centre of rotation was almost at this location.

Gauges at 12-inch level all showed tensile strains during the early stages of loading. Maximum tensile strains at this level were recorded at sections f, e, c and a at loads of 20, 25, 25 and 35 kips respectively. With an increase in load, the tensile strains reduced until they became compressive, first at $e(12)$ and ultimately at $a(12)$. At $f(12)$ and $c(12)$, the

tensile strains reduced after recording a maximum value but jumped suddenly to high values as cracks passed under the gauges. At f(12), the tensile strain suddenly jumped to 9.12×10^{-4} at a load of 27.5 kips from 0.85×10^{-4} at a load of 25 kips and kept increasing rapidly. Similarly, gauge c(12) broke at 40 kips. Neglecting the results of f(12) and c(12), which are a measure of the crack width, it can be seen that compressive strains at the 12-inch level developed from the midspan region outwards. Furthermore, compressive strains at supports, at the 12-inch level, only developed after critical diagonal cracking and its stabilization.





(ii) BEAM IC-5 ($a/d = 3.0$)

The test results for beam IC-5 are summarized in Fig. III.14(a) and (b).

DEMEC DATA (Fig.III.14a)

Strains at the compression face remained compressive for all sections at all stages of loading and increased with the applied load. Initial tensile strains at sections e' and c' at 12-inch level reduced to compressive strains at a load of 20 and 28 kips respectively. A crack crossed the gauge points at section d' (12). The strains shown by this gauge are, therefore, only a measure of the crack width. Initial tensile strains at a' (12) and b' (12) remained so until failure of the beam. Significant load after major diagonal cracking was never developed though the failure was a relatively slow diagonal failure.

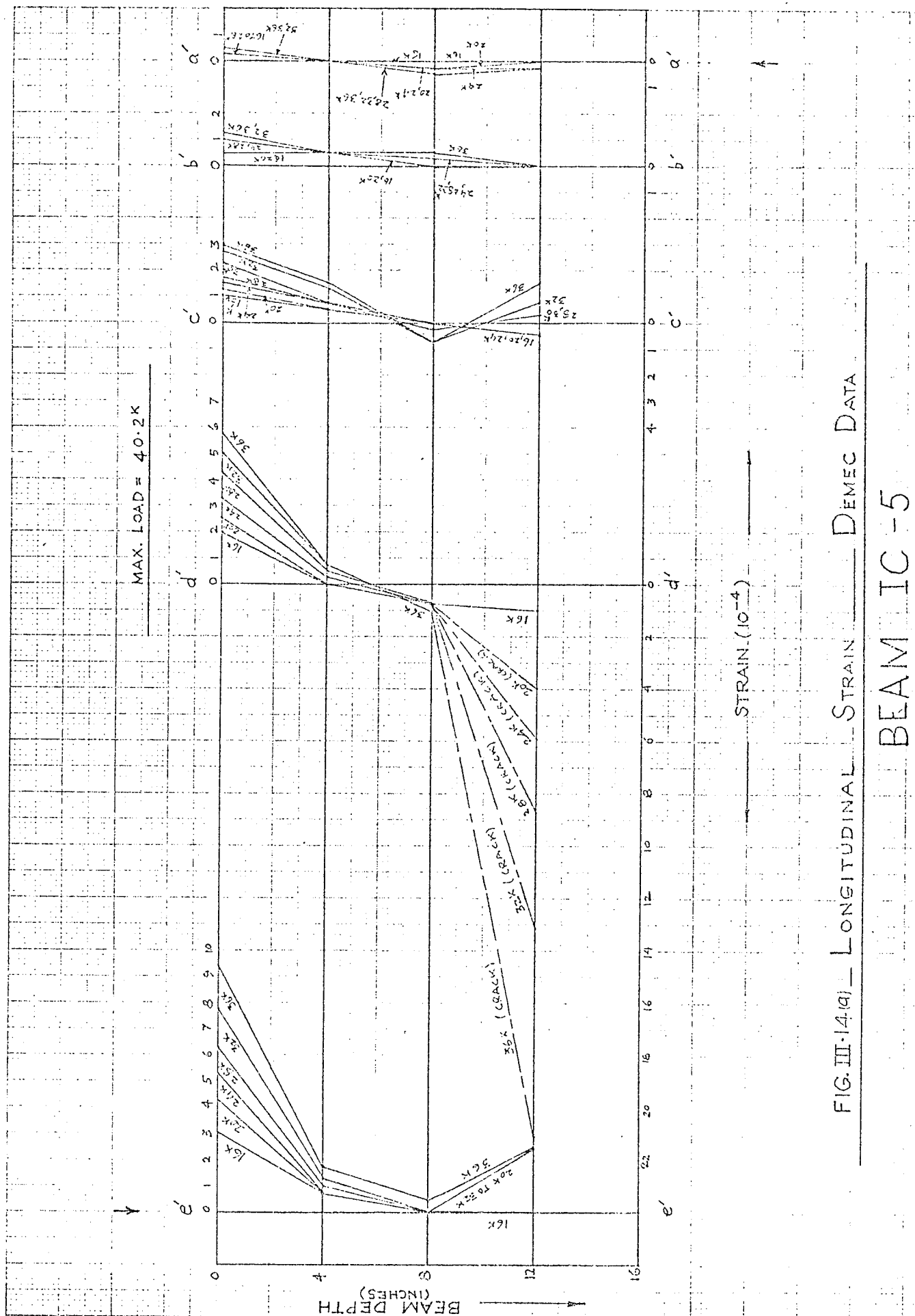
ELECTRICAL RESISTANCE STRAIN GAUGE DATA (Fig.III.14b)

From the crack pattern, it can be seen that gauges $f(4)$ and $d(8)$ were influenced by the cracks. Gauge $d(8)$ broke at a load of 26 kips after recording high tensile strains from 20 kips onwards, though till then it had all along been showing compressive strains. Gauge $f(4)$ did not break but recorded high tensile strains.

Gauges at the 12-inch level at all locations developed tensile strains during the initial stages of loading. At sections f , e , d and c they recorded maximum tensile strains

at a load of 10, 12, 16 and 26 kips respectively. These tensile strains remained small, the maximum being at c(12) at a load of 26 kips, which was only 1.7×10^{-4} . With further loading, the tensile strains reduced and ultimately compressive strains were observed at f(12), e(12) and d(12) at a load of 20 kips and at c(12) at a load of 34 kips. The gauges at these sections then continued showing compressive strains throughout the remaining part of the test until failure.

Strains at a(12) and b(12), however, remained tensile throughout and increased with loading.



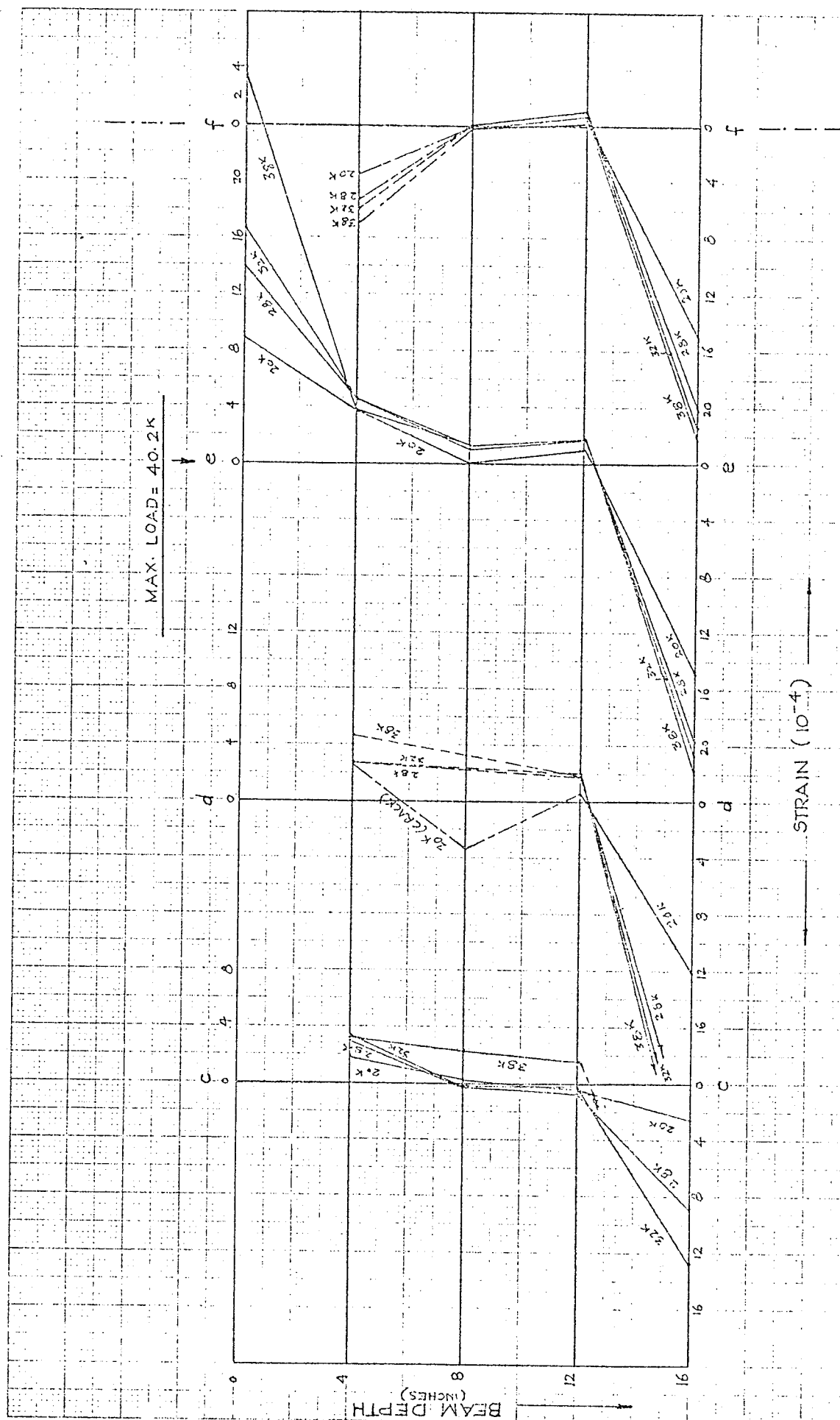


FIG. III-14(b) — LONGITUDINAL STRAIN — Electrical Resistance Strain Gauge Data

BEAM IC-5

(iii) BEAM IC-6

The test results of beam IC-6 are summarized in Figs. III.15 (a) and (b).

DEMEC DATA (Fig.III.15a)

Compressive strains at the compression face of the beam increased with loading while the initial tensile strains at the 12-inch level reduced to compressive strains at sections e', d' and c' at a load of 20, 20 and 30 kips respectively. At a'(12) and b'(12), the tensile strains remained so throughout the loading. Failure of the beam resulted from a flexural failure of the beam.

ELECTRICAL RESISTANCE STRAIN GAUGE DATA (Fig.III.15b)

Tensile strains were recorded at all gauges located at the 12-inch level during the initial stages of loading. Maximum tensile strains occurred at f(12), e(12) and d(12) at a load of 7.5 kips and at c(12) at a load of 12.5 kips. These strains then gradually reduced to compressive strains at gauges f(12), e(12) and d(12) at a load of 10, 12.5 and 12.5 kips respectively and remained so for the remaining stages of loading. The initial tensile strain at c(12) reduced but then jumped suddenly due to cracking as the gauge broke at a load of 25 kips. All the strains at the 12-inch level, whether tensile or compressive, remained low. The initial tensile strains at b(12) continued increasing until the failure of the beam.

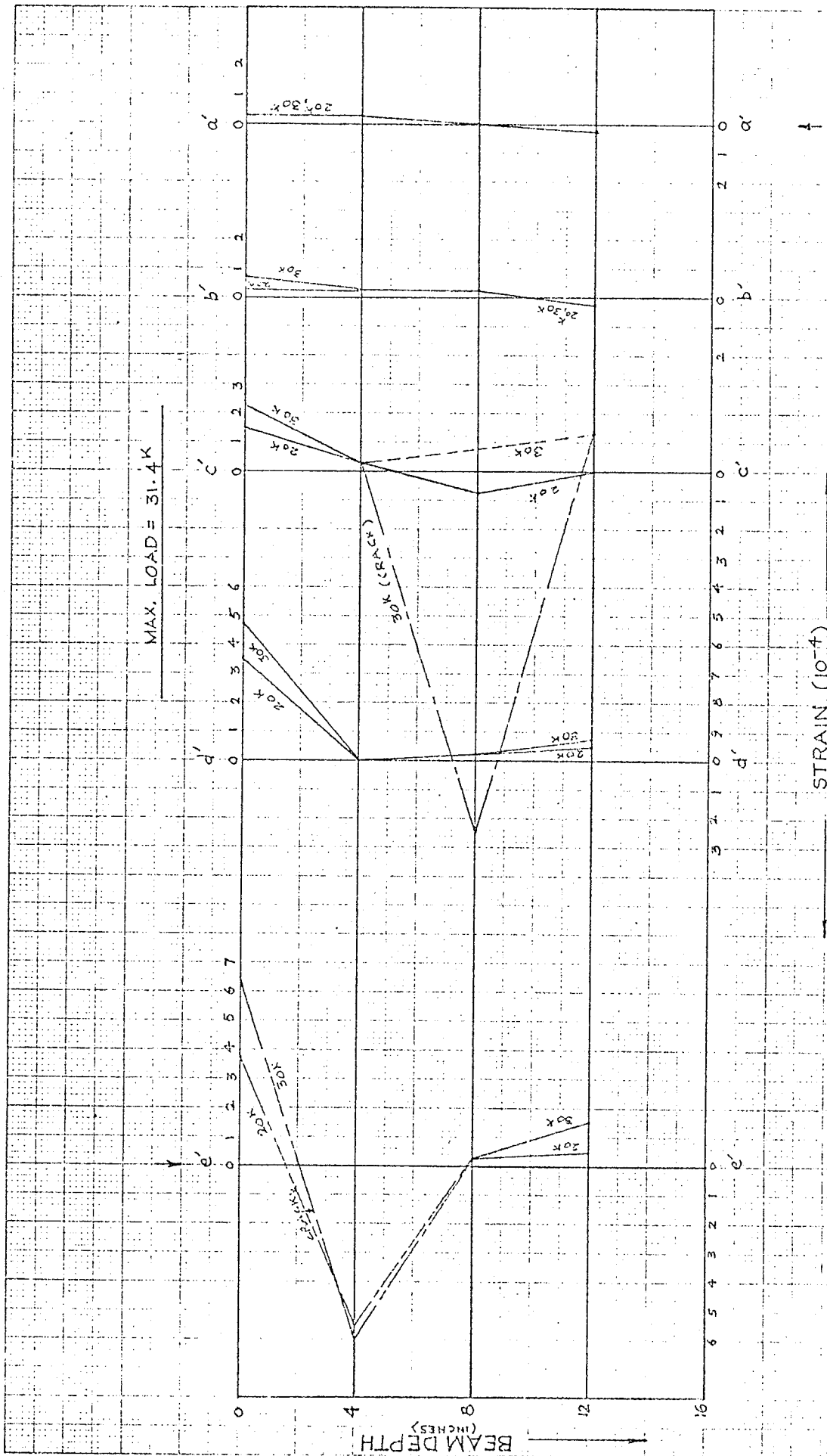
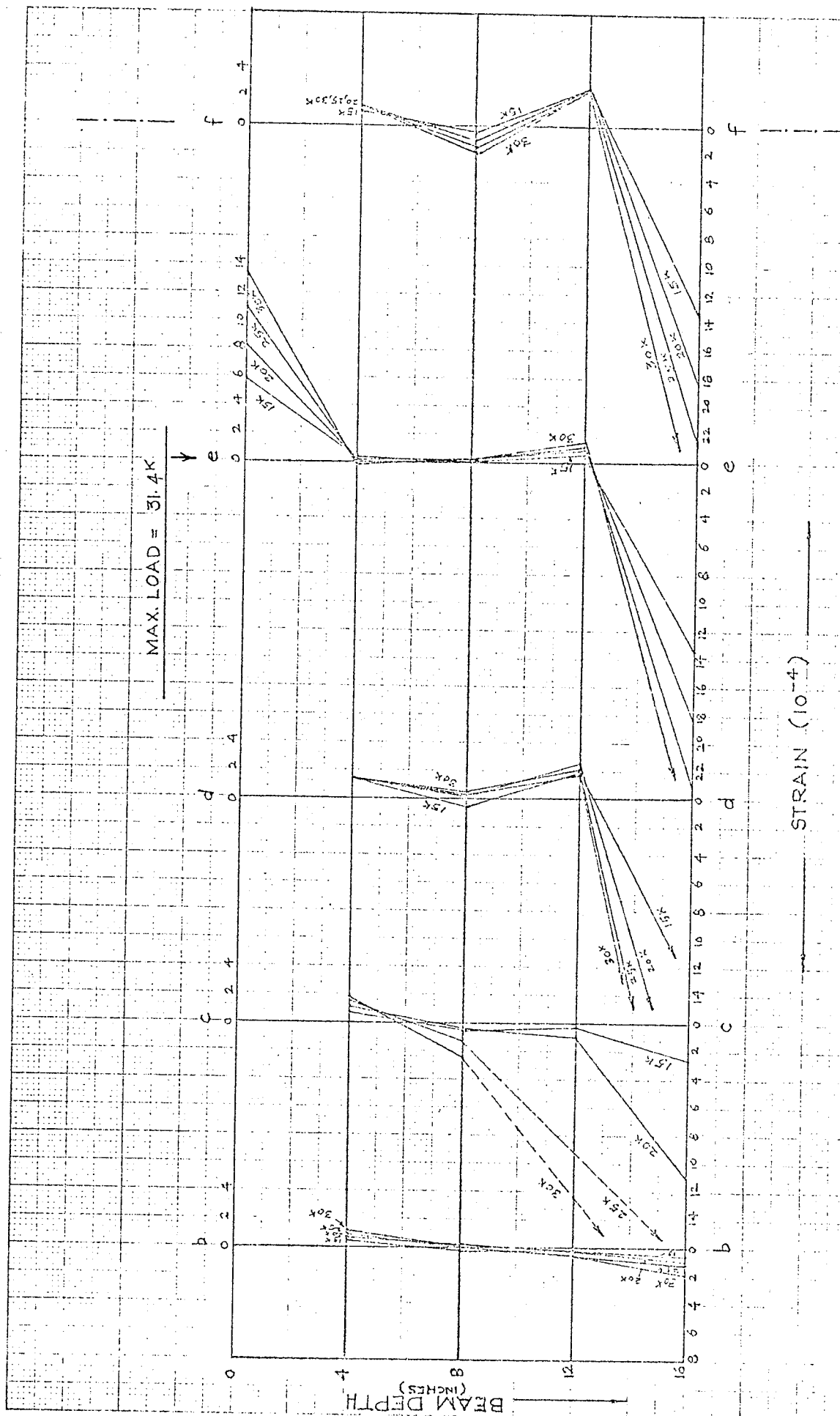


FIG. III.15(a) — LONGITUDINAL STRAIN — DEMEC DATA

BEAM IC-6



III.1.4 TESTS OF SERIES IIA

(i) BEAM IIA-2 ($a/d = 1.5$)

The results of electrical resistance strain gauge data are not presented, there being significant drifts in the gauge readings. Fig.III.16 summarizes the results of DEMEC data.

This beam had failed by shearing off of the secondary beam at its junction with the main beam at a load of 55 kips. Strains at the compression face remained compressive at all sections at all stages of loading except for the section directly over support at the last load level. Furthermore, at the last load increment, compressive strains had developed at the 12-inch level at section a', directly over the support and section b' close to the support when premature failure of the beam occurred. Strains at the 12-inch level remained very low throughout, especially at sections d' and e', where no strains could be recorded within the range of DEMEC gauge.

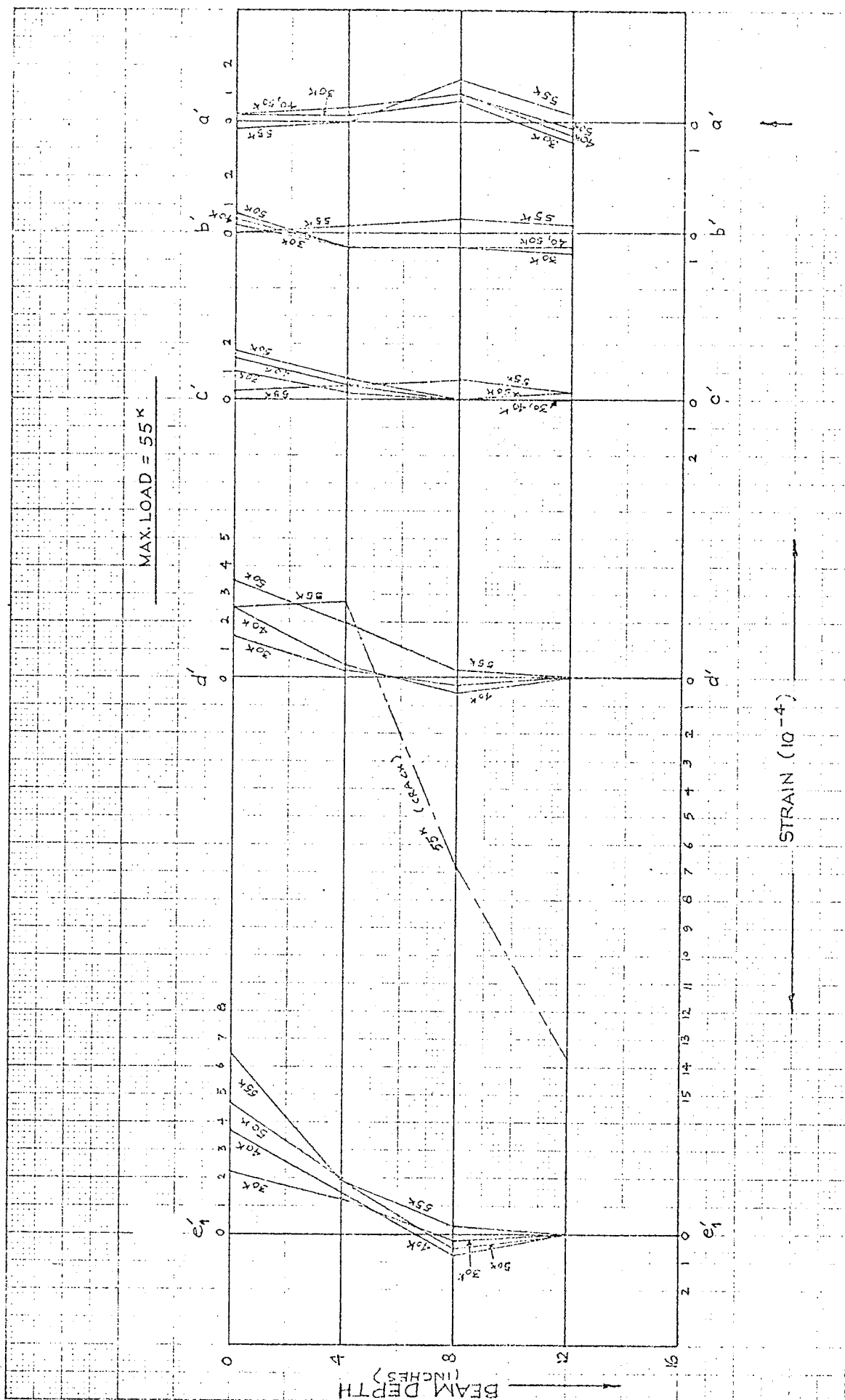


FIG. III-16 — LONGITUDINAL STRAIN — DEMEC DATA
BEAM IIA-2

(ii) BEAM IIA-2(b) ($a/d = 1.5$)

The only difference of this beam with beam IIA-2 was that top reinforcement was used in the secondary beam. The only stirrups used were at the secondary beam ends to support this reinforcement and there was no stirrup which could cross the line of a diagonal crack at advanced stages of cracking when cracks entered the secondary beams. The test results of this beam are summarized in Figs.III.17(a) and (b).

DEMEC DATA (Fig.III.17a)

Compressive strains at all sections at the compression face increased with load until major diagonal cracking at a load of 66 kips. Similar cracking had occurred in beam IIA-2 at a load of 55 kips. Beam IIA-2(b) continued taking more load as the diagonal cracks proceeded into the zone of pure flexure. Tensile strains developed at sections a', b' and c' at compression face after diagonal cracking. Further, the compressive strains at section d' at compression face reduced significantly.

For this beam only, DEMEC readings at reinforcement level were also taken on the concrete surface and are reported on Fig.III.17(a). Large tensile strains can be observed at this level.

DEMEC data from this beam test is very self-consistent. At the 12-inch level initial tensile strains reduced to compressive strains at sections e' and d' at a load of 21 kips and at section c' at a load of 42 kips. Tensile strains at sections b' and a' did not show any change until major diagonal cracking at 66 kips when both of them

reduced to compressive strains. At that and subsequent stages of loading, compressive strains existed at 12-inch level throughout the span. Further, it can be seen from sections a', b' and c', that the compression centre shifted downwards while tensile strains developed above the diagonal crack. Final failure at 81 kips was at a lower load than that for the corresponding beam of series IA, i.e., beam IA-2. Final failure in this beam was caused relatively early by the unrestrained movement of the diagonal cracks in the midspan region.

ELECTRICAL RESISTANCE STRAIN GAUGE DATA (Fig.III.17b)

In earlier tests, it had been observed that the compressive strains at midspan were generally lower than those under the load point. In this beam, however, the compressive strains at midspan were higher. Major differences could be seen from 66 kips onwards, i.e., after critical diagonal cracking. During these stages, compressive strains at midspan increased much more rapidly, clearly pointing out the effect of concentrated load, applied directly over the beam.

The gauge at section f on the 12-inch level broke due to cracking during early stages of loading. However, the results of other gauges at this level are very consistent. Compressive strains developed from midspan outwards. Further, compressive strains at a(12) developed only at major diagonal cracking. An examination of test data shows that compressive strains at c(12) had developed at a load of 51 kips before the gauge suddenly broke after recording high tensile strains.

The results of both electrical resistance strain gauges and the DEMEC gauges show that compressive strains developed in the lower half of the beam from midspan region towards the supports after flexural cracking.

MAX. LOAD = 81K

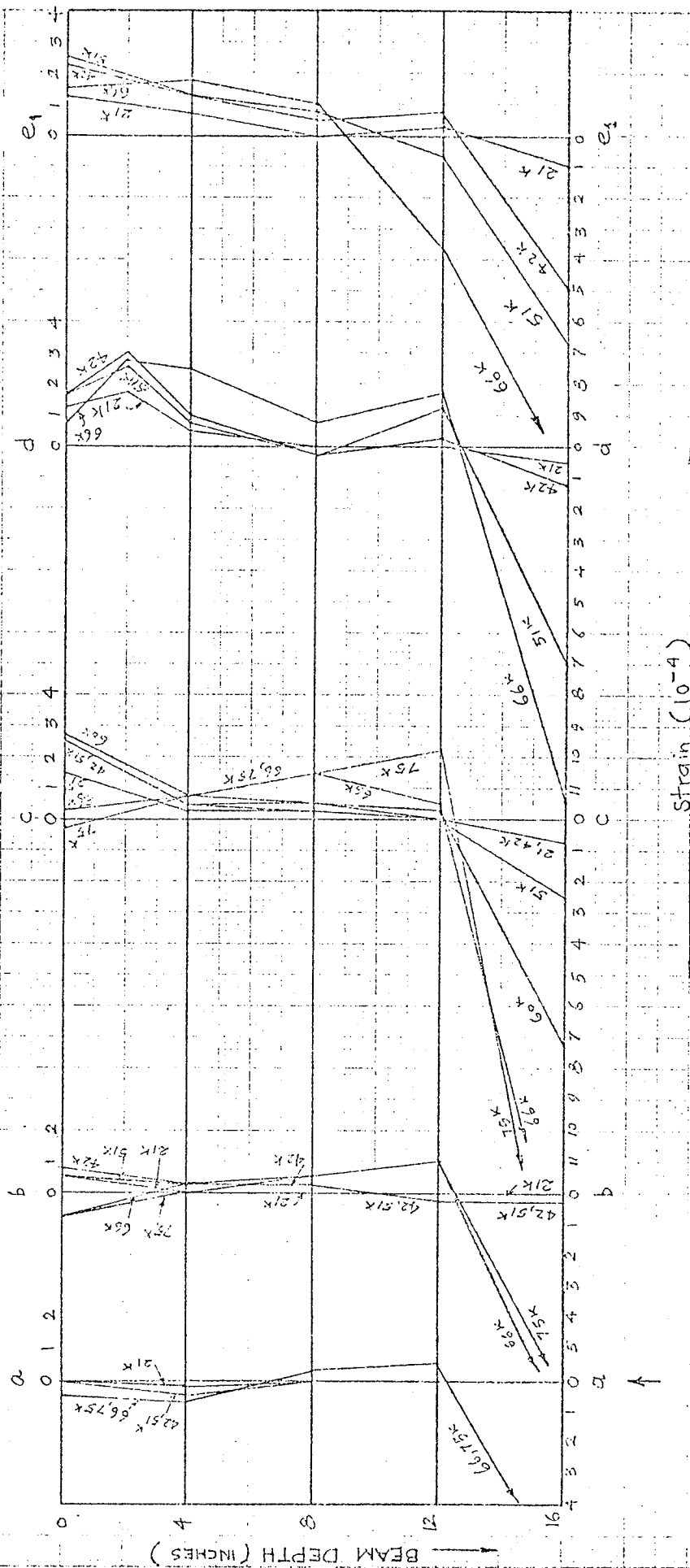
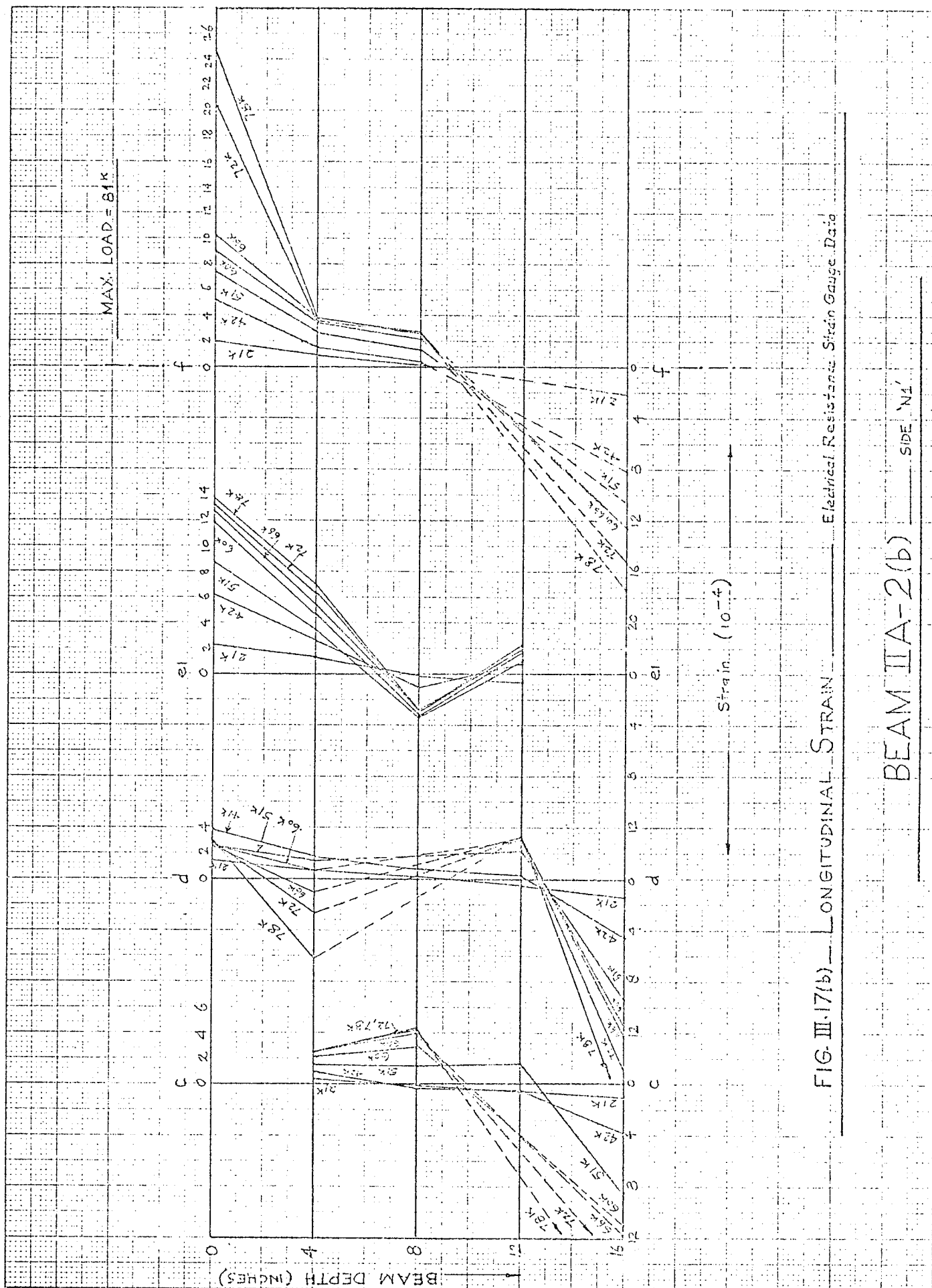


FIG. III-17(a) — LONGITUDINAL STRAIN — DEMEC DATA

BEAM IIA-2(b)

NOTE: STRAIN READINGS AT 16" FOR THIS BEAM ONLY ARE DEMEC READINGS AT THIS LEVEL.



(iii) BEAM IIA-4 ($a/d = 2.5$)

The test results of this beam are summarized in Figs. III.18(a) and (b).

DEMEC DATA (Fig.III.18a)

Cracking interfered with strain pattern at d' (12). However, compressive strains developed at e' (12) at a load of 20 kips and at c' (12) at a load of 25 kips. Gauge b' (12) did not show any tensile strains until failure approached. Gauge a' (12) showed some small compressive strains and it appears that the DEMEC gauge reading at zero load was somewhat erroneous.

Small tensile strains developed over the compression face of the beam directly over the support while elsewhere compressive strains increased with load to failure.

ELECTRICAL RESISTANCE STRAIN GAUGE DATA (Fig.III.18b)

Many of the electrical resistance strain gauges showed considerable drifts and cannot be relied upon. Considering the gauges at the 12-inch level, the gauges at sections b and a were erratic. However, gauge readings at c(12), d(12) and f(12) were consistent and reliable. Gauge f(12) broke early at a load of 20 kips but gauges at other sections showed that initial tensile strains recorded a maximum and then reduced to compressive strains at a load of 15, 15 and 27.5 kips respectively for gauges e(12), d(12) and c(12). Appearance of a diagonal crack caused the sudden diagonal tension failure of the beam.

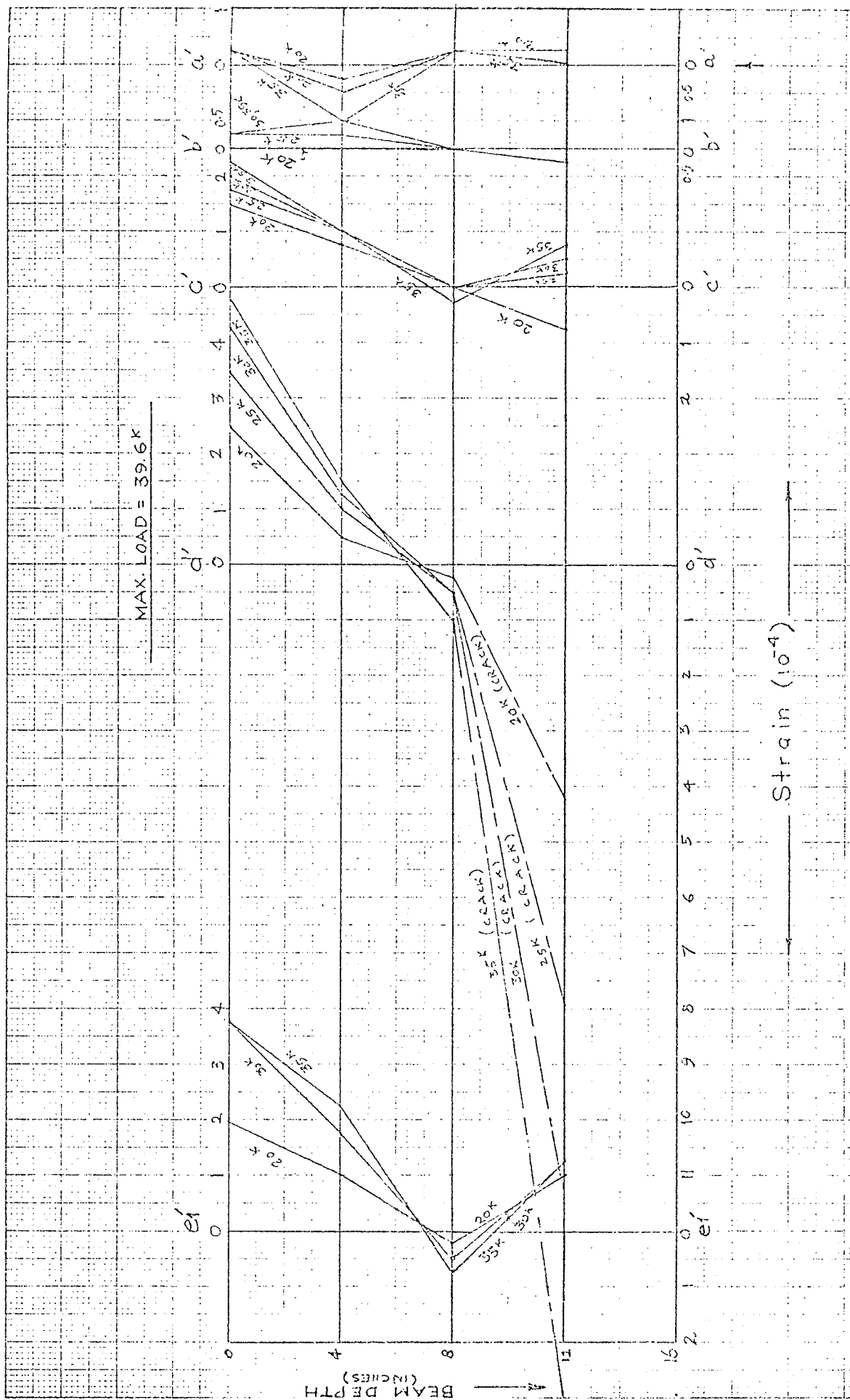


FIG. III.18(a) — LONGITUDINAL STRAIN — DEMEC DATA

BEAM IIA-4

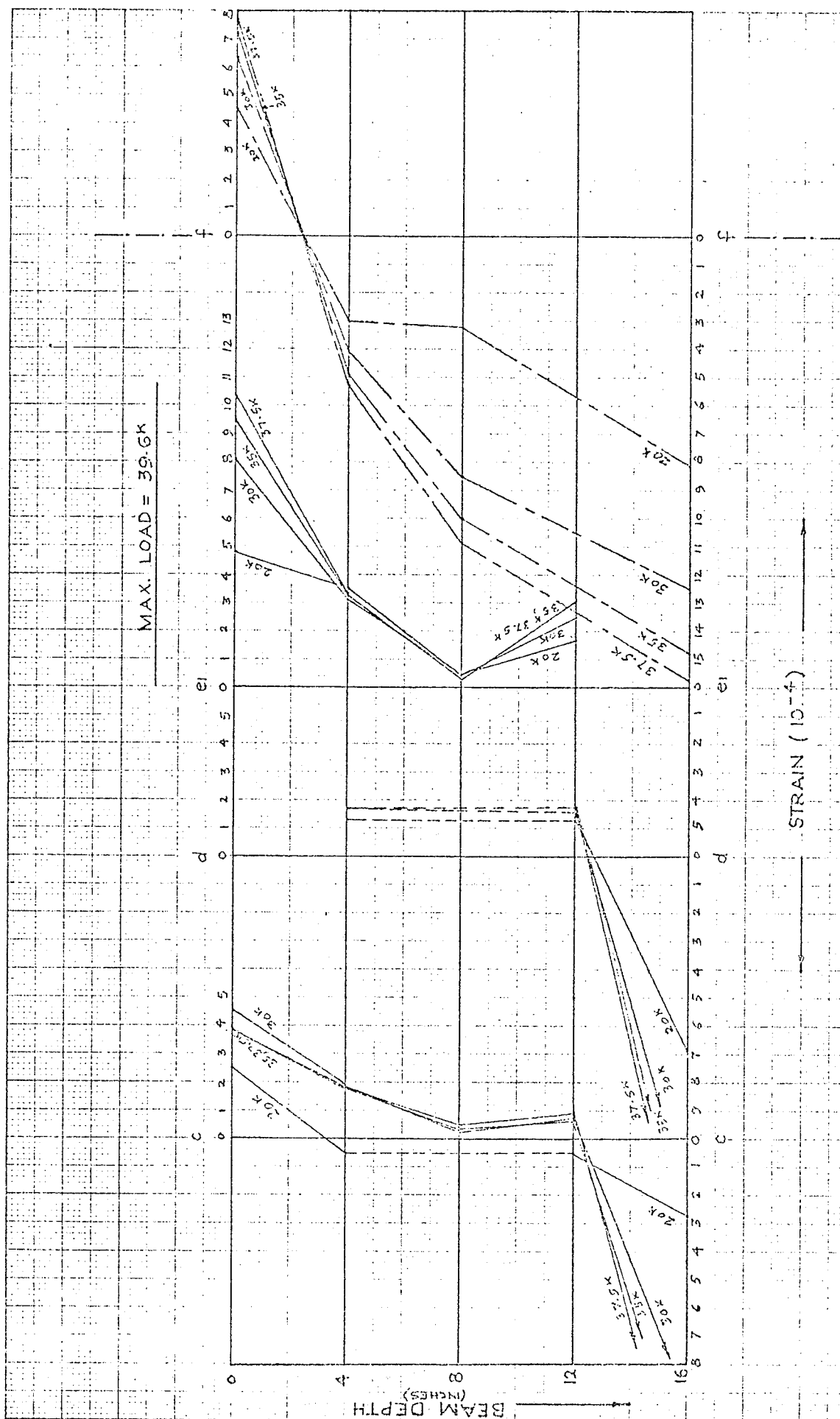


FIG. III-18(b) — LONGITUDINAL STRAIN — Electrical Resistance Strain Gauge Data
 BEAM IIA-4

(iv) BEAM IIA-6 ($a/d = 4.0$)

The test results for this beam are summarized in Figs. III.19 (a) and (b).

DEMEC DATA (Fig.III.19a)

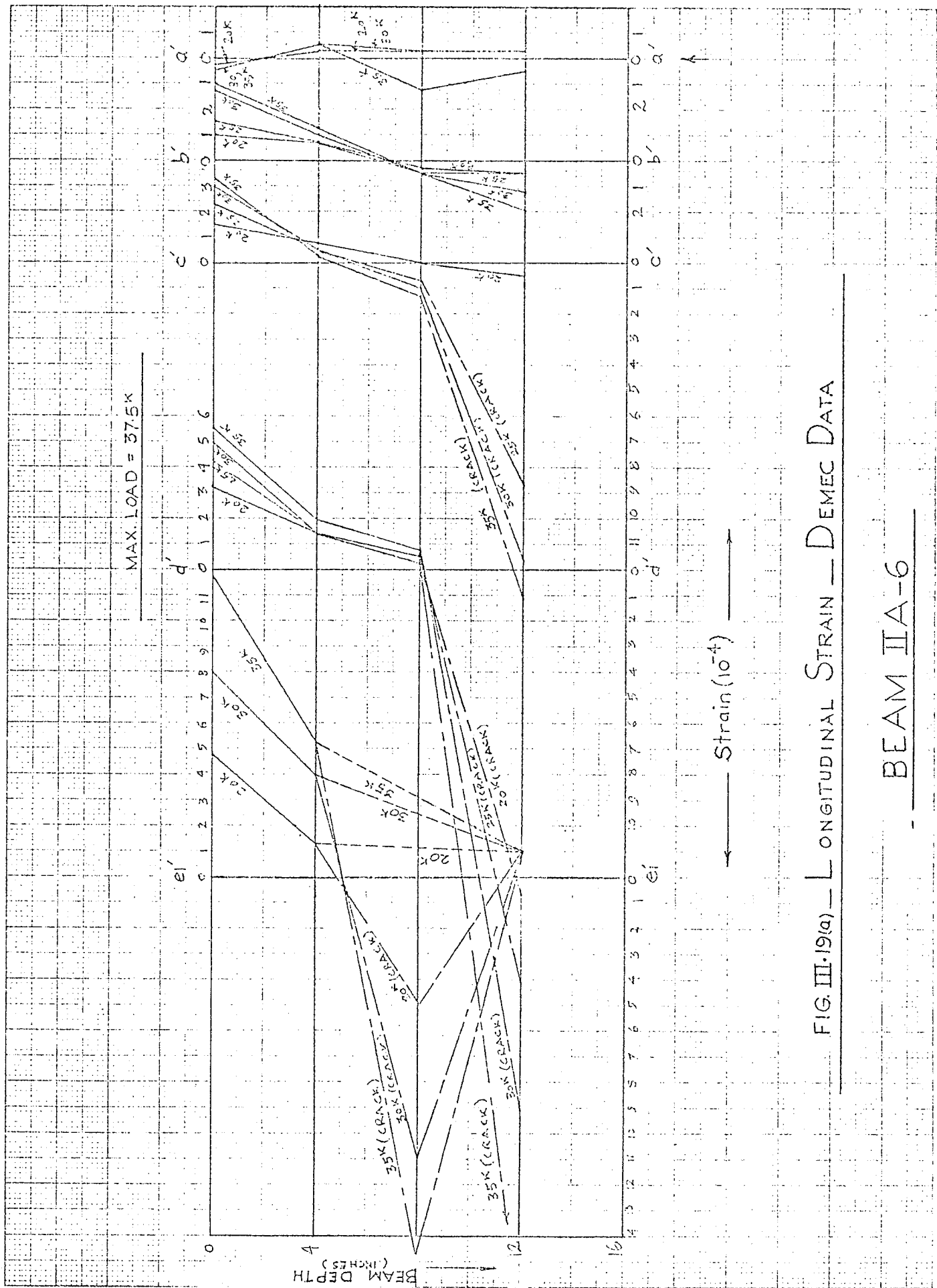
Cracks crossed the gauge lines at $c'(12)$, $d'(12)$ and $e_1'(8)$. Strains at these points are only a measure of the crack width. As the cracking proceeded, initial tensile strains reduced to compressive strains at gauge $e_1'(12)$. Tensile strains at $b'(12)$, however, continued increasing. Failure occurred at the appearance of a critical diagonal crack.

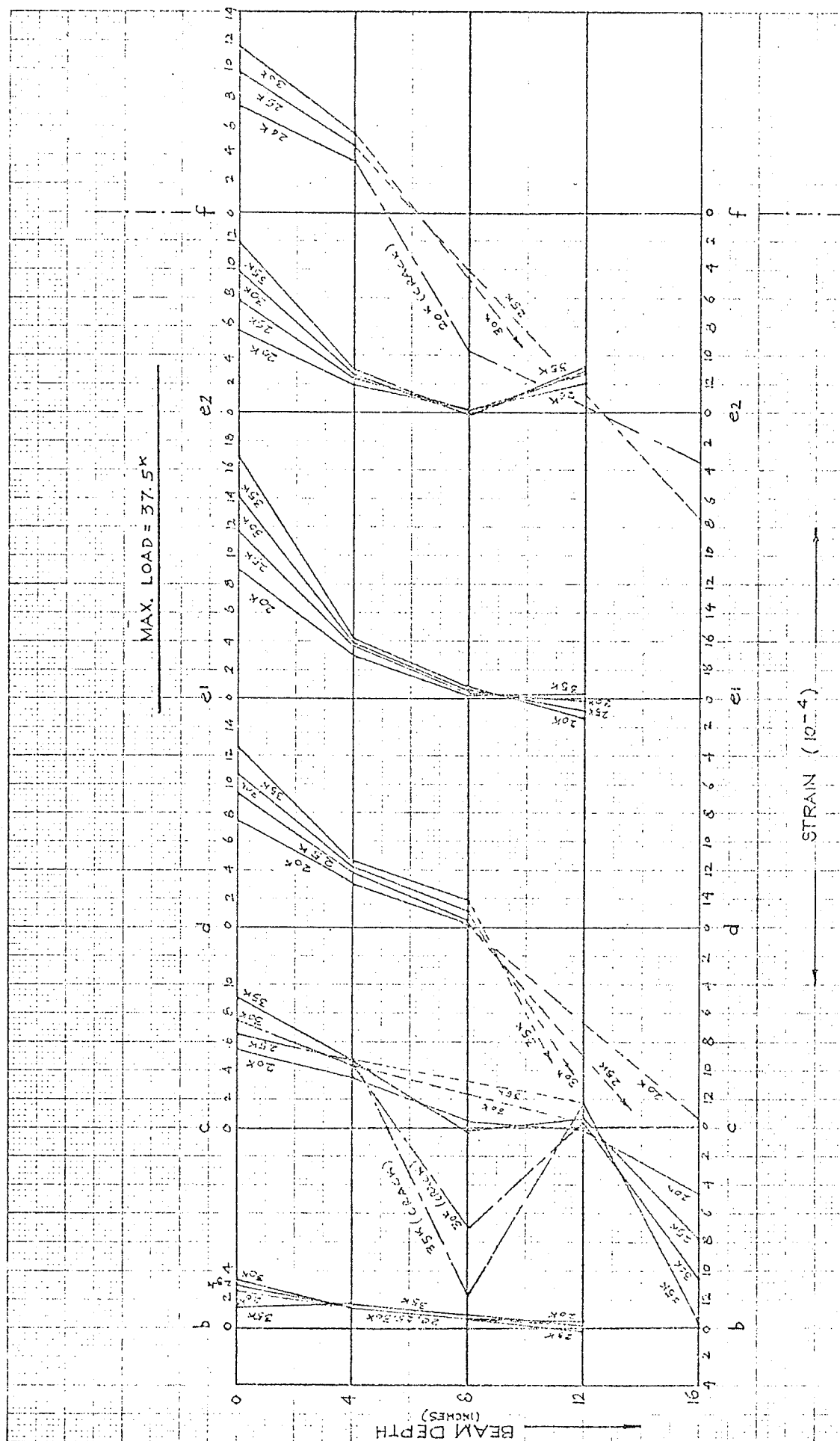
ELECTRICAL RESISTANCE STRAIN GAUGE DATA (Fig.III.19b)

Compressive strains on the compression face all generally increased with the load.

At the 12-inch level, gauge $d(12)$ did not function while gauge $b(12)$ showed considerable drifts. At $f(12)$, the initial tensile strains reduced to very small compressive strains at 7.5 kips, coinciding with the appearance of the first flexural cracks. However, as the flexural crack directly under this gauge moved upwards, large tensile strains were recorded before the gauge broke at 15 kips.

Initial tensile strains at $e(12)$ and $c(12)$ recorded a maximum value and then reduced to compressive strains at a load of 15 and 22.5 kips respectively. All strains at the 8-inch and 12-inch level generally remained low till collapse.





III.1.6 TESTS OF SERIES IIIA

(i) BEAM IIIA-3

Results of beam IIIA-3 have been discussed in Chapter 5, and plots of DEMEC and electrical resistance strain gauge data are reproduced in Figs. III.20 (a) and (b).

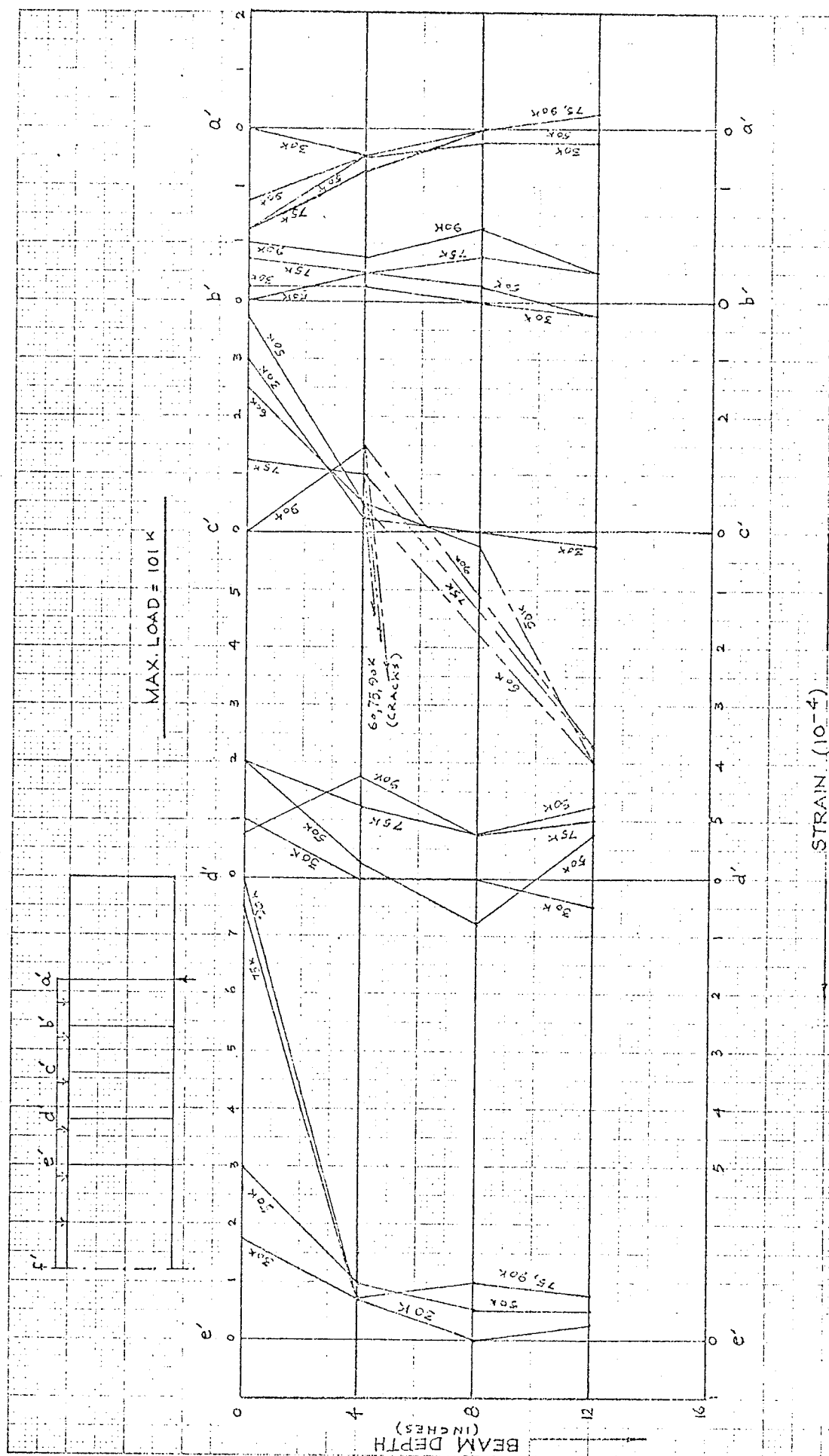


FIG. III.20(a) LONGITUDINAL STRAIN — DEMEC DATA

BEAM III A-3

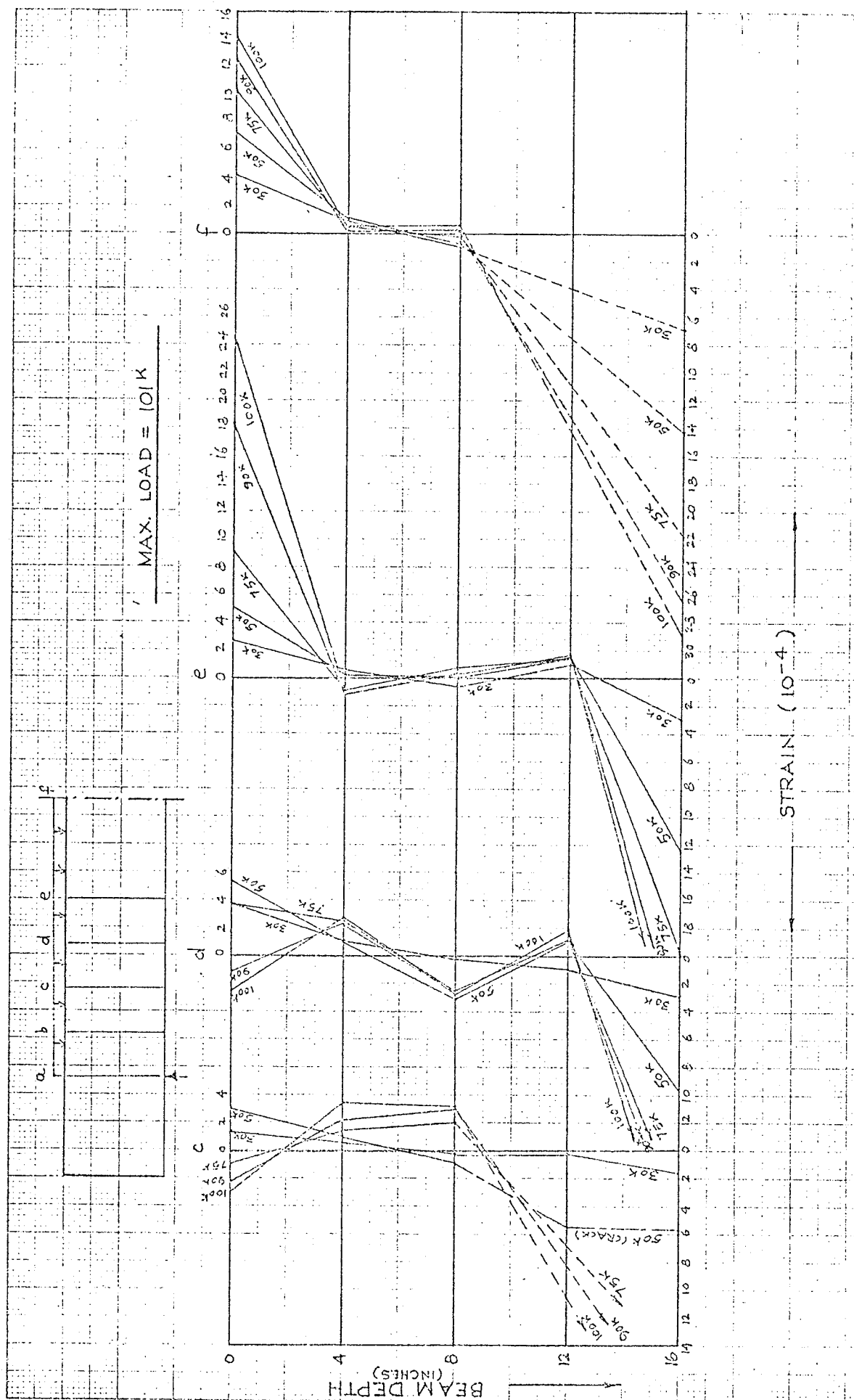


FIG. III.20 (b) LONGITUDINAL STRAIN — Electrical Resistance Strain Gauge Data

BEAM III A-3

(ii) BEAM IIIA-6 ($l/d = 10.25$)

The test results for this beam are summarized in Figs. III.21 (a) and (b).

DEMEC DATA (Fig.III.21a)

Compressive strains at all locations on the compression face increased until diagonal cracking occurred at a load of 50 kips. Gauge readings at section c' at compression face at a load of 62.5 kips suggest that some tension developed at this location. Tensile strains also developed at the compression face over the support. Initial tensile strains at gauges e' (12), d' (12) and c' (12) reduced progressively to compressive strains. However, cracking interfered with gauge b' (12) and correct strain distribution could not be recorded at this location at later stages of loading. No DEMEC readings were taken at a' (12) above a load of 50 kips. At this stage initial tensile strains had reduced to zero and it is probable that the gauge would have shown compressive strains above a load of 50 kips after critical cracking as in similar other tests. Since the beam was severely cracked at this stage and it was rather dangerous to stand under it, only one set of readings was taken at the midshear-span after diagonal cracking.

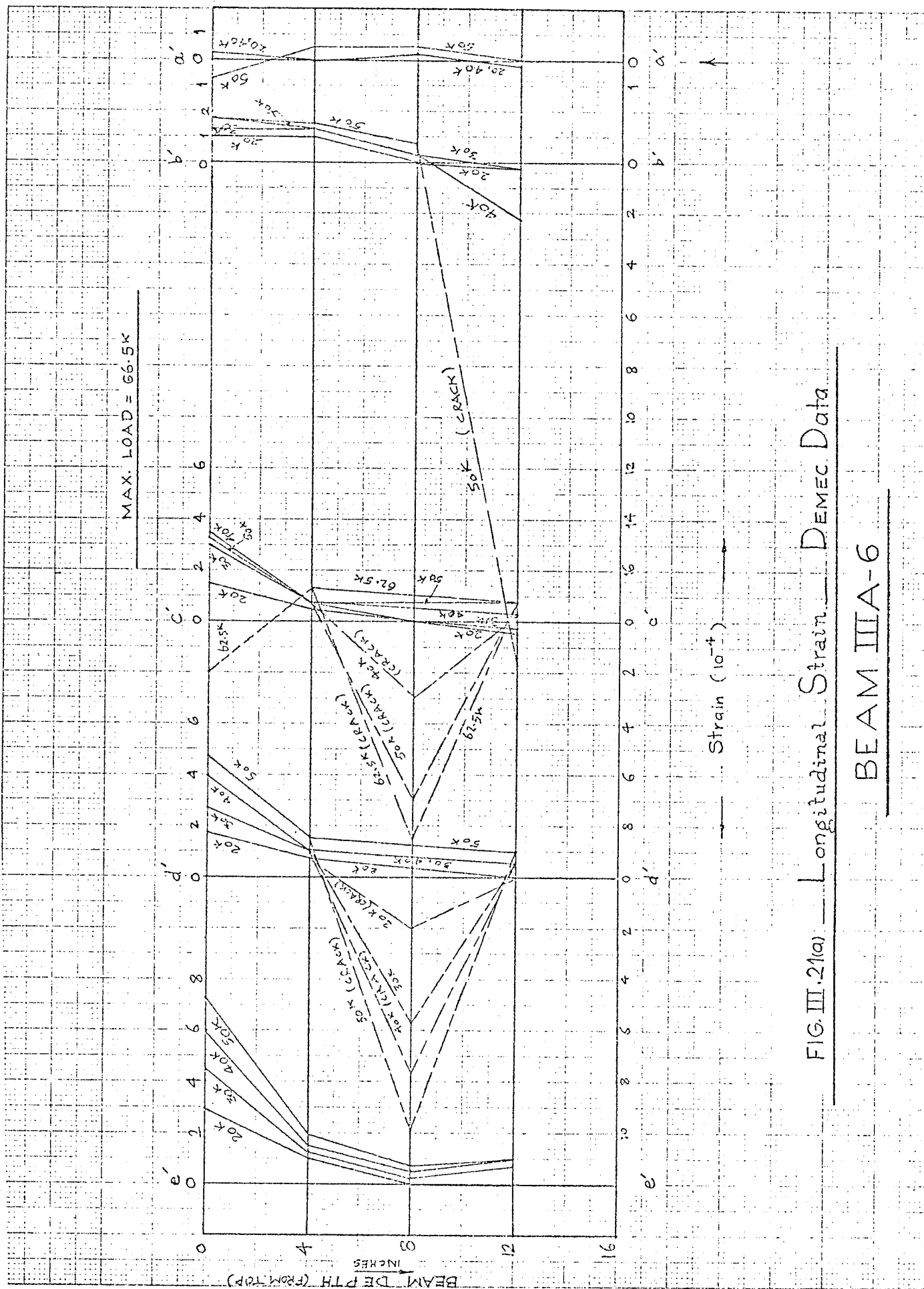
ELECTRICAL RESISTANCE STRAIN GAUGE DATA (Fig.III.21b)

Consider the gauges at the 12-inch level. Gauge b(12) broke at a load of 37.5 kips due to cracking. Gauge c(12) recorded tensile strains initially which increased to a certain load

level and then started reducing until the strains became compressive and remained so to failure.

An examination of the data from gauge d(12) shows that this gauge also developed tensile strains initially which increased to a load of 15 kips. However, these strains started reducing and became compressive at a load of 20 kips and remained compressive thereafter. Similarly, gauge e(12) and f(12) developed initial tensile strains which increased to a load of 10 kips. With further loading, these strains reduced to compressive strains which remained almost constant to failure.

There was no gauge at the 12-inch level at section a over the support. It was, therefore, not possible to record the strains at the 12-inch level upto the support. However, the data of this beam is consistent with other tests, showing progressive development of compressive strains in the lower half of the beam from midspan outwards after flexural cracking.



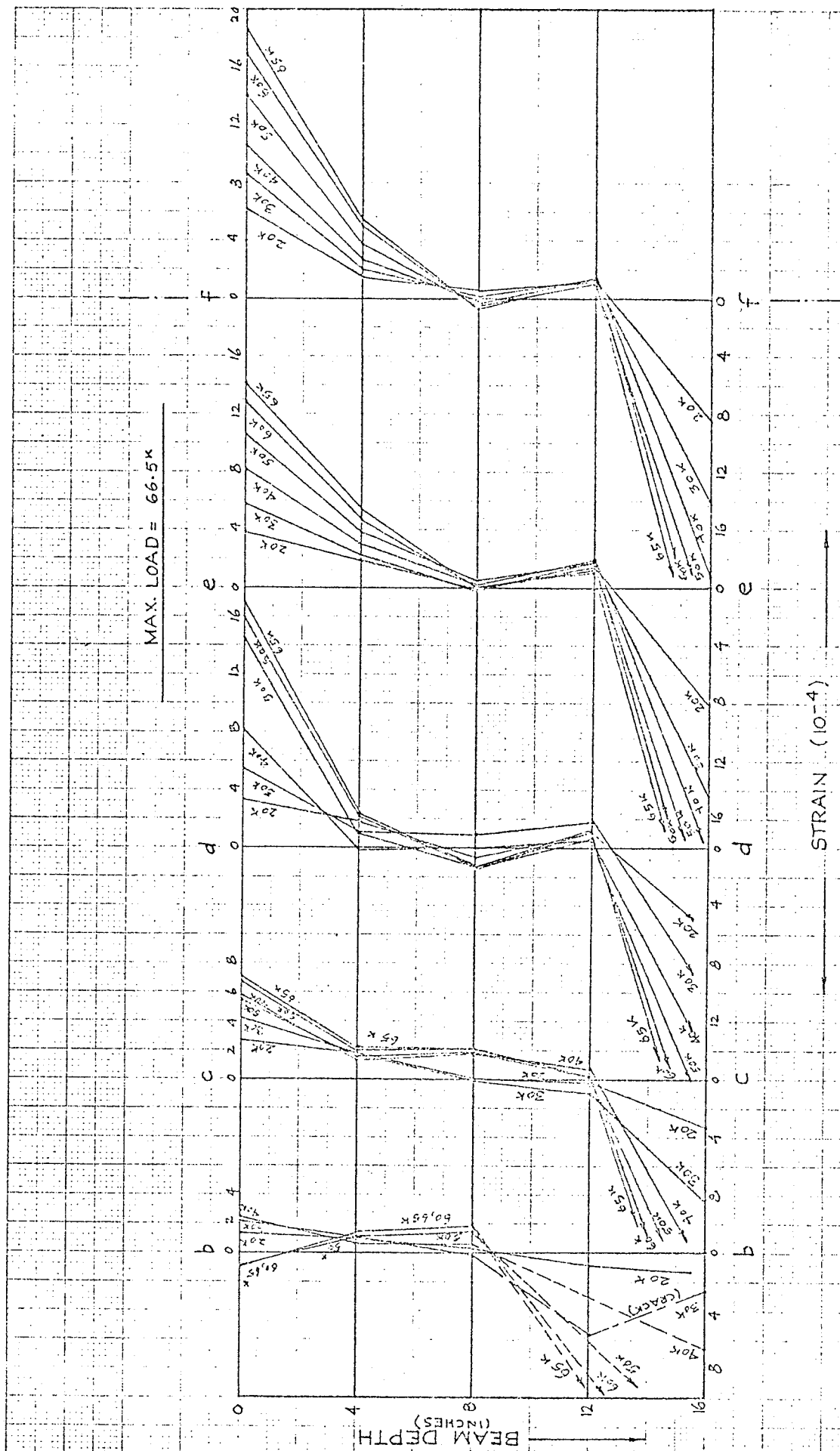


FIG. III-21(b) — LONGITUDINAL STRAIN — Electrical Resistance Strain Gauge Data

BEAM IIIA-6

(iii) BEAM IIIA-8 ($l/d = 14.25$)

The test results for this beam are summarized in Fig. III.22 (a) and (b).

DEMEC DATA (Fig.III.22a)

Strains at the compression face remained compressive and increased with load until failure of the beam at diagonal cracking. Strains at the 12-inch level generally remained small. At $e'(12)$ and $c'(12)$, no strains could be recorded within the least reading of the DEMEC gauge. Small compressive strains developed at $d'(12)$ after flexural cracking while strains at $b'(12)$ remained tensile till failure of the beam. Readings of gauge $a'(12)$ show that the strains remained tensile throughout the test.

ELECTRICAL RESISTANCE STRAIN GAUGE DATA (Fig.III.22b)

Cracks caused gauges $f(12)$ and $e(12)$ to break at a load of 20 and 22.5 kips respectively after recording very high tensile strains. Strains at gauge $d(12)$ were erratic from the beginning and are not plotted. Gauges $c(12)$ and $b(12)$, however, were quite consistent. They showed tensile strains initially and such strains kept on increasing until they reduced to compressive strains progressively at a load of 20 and 40 kips respectively. Gauge $c(12)$ was affected by cracks at later stages of loading and broke after recording tensile strains.

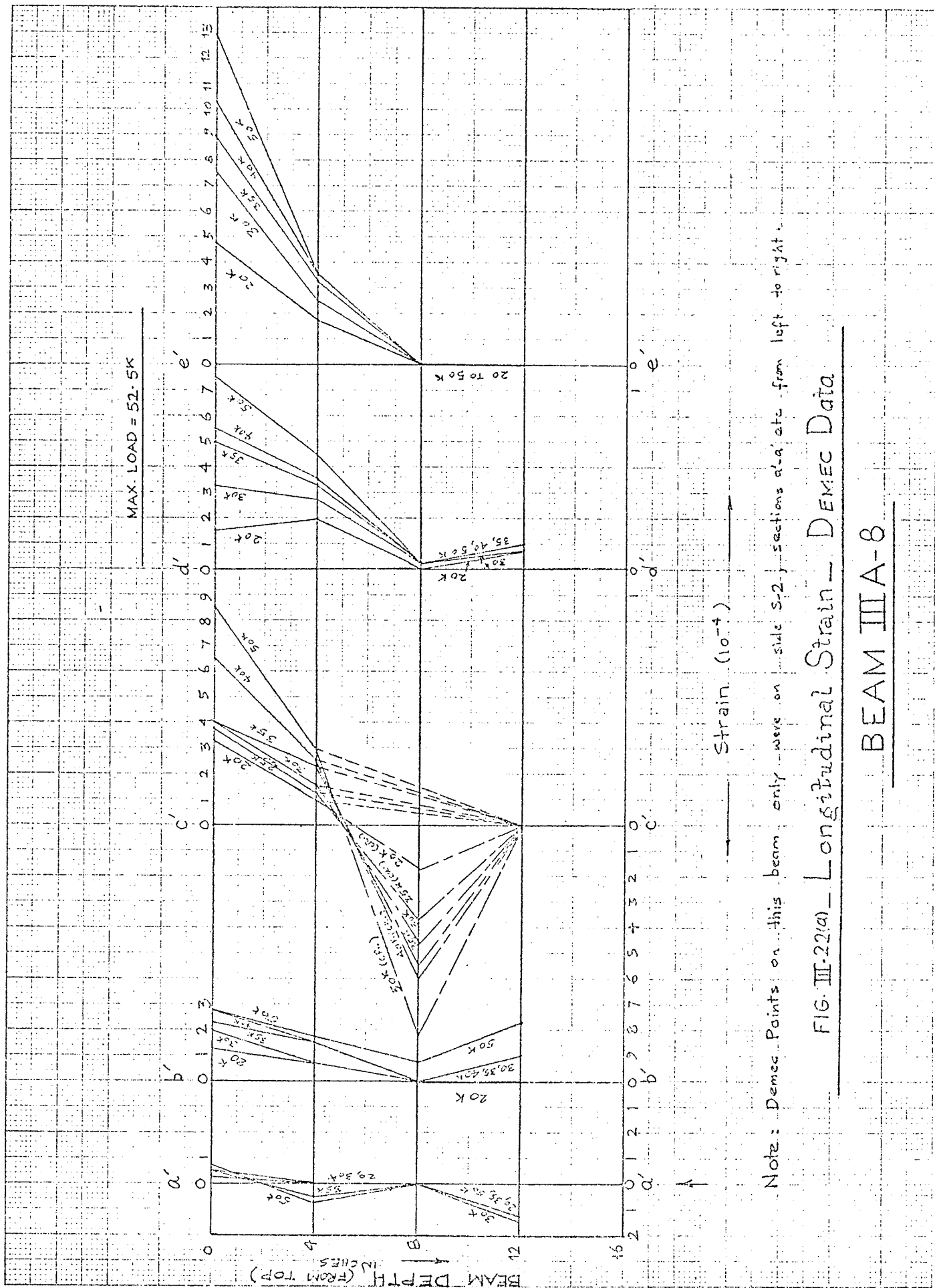


FIG. III-22(a) Longitudinal Strain - DEMEC Data

BEAM IIIA-8

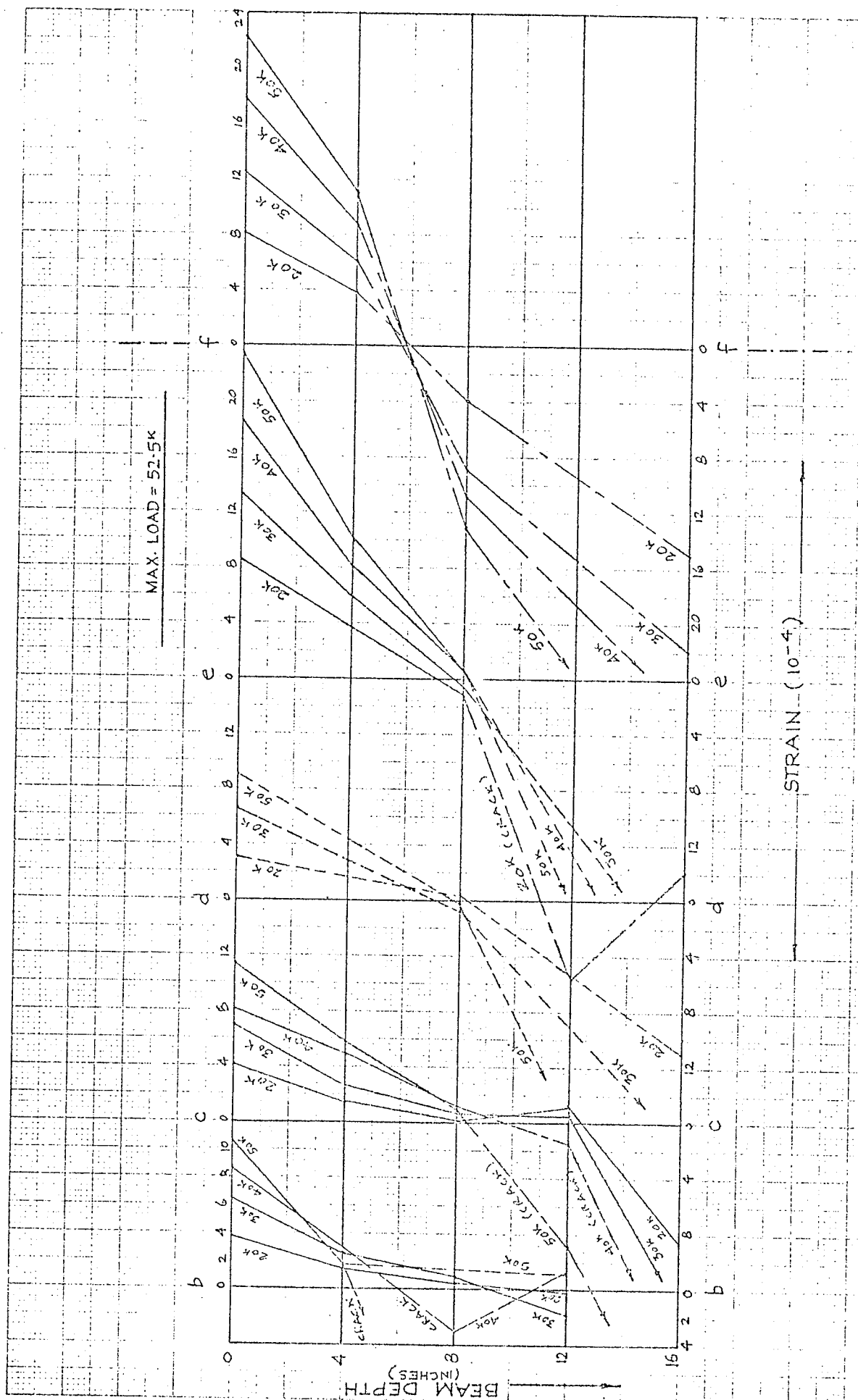


FIG. III-22(b) — LONGITUDINAL STRAIN — Electrical Resistance Strain Gauge Data

BEAM IIIA-8

III.2 DISTRIBUTION OF LONGITUDINAL FLEXURAL STRAINS IN THE REINFORCEMENT

In this section, the variation of longitudinal strains in the reinforcement is shown along one half of the span for individual beam tests. The nominal yield stress of the reinforcement was 50 ksi, which gives a strain in the reinforcement of 16.67×10^{-4} at yielding using a modulus of elasticity of 30×10^6 psi for steel. The actual yield stress of most of the beams was very close to the nominal value (Appendix I), the only significant differences arising in the beams of the preliminary series of tests. For these beams, if the actual yield stress of 75 ksi is used, the strain at yielding of the reinforcement works out to be 25×10^{-4} .

As long as the stress in the reinforcement remains below the yield stress, the tension force in the reinforcement can be calculated with a modulus of elasticity of 30×10^6 psi for steel. However, when the strain exceeds that at yielding, the stiffness of the reinforcement decreases many times and the only incremental increase in the tension force results from a strain hardening of steel. Therefore, when the strain in the reinforcement exceeds that at yielding, relatively large differences in strain amount only to a small difference in the tension force in the reinforcement.

The bond force in the reinforcement is the difference of the tension force in the reinforcement at the opposite sides of concrete cantilevers. The greater the bond force, the greater the bending moment generated. The distribution of longitudinal

flexural strain in the reinforcement is a measure of the distribution of the tension force and hence the bond forces in the reinforcement.

Test results summarized in this section show how these bond forces are affected by flexural and diagonal cracking and the mode of failure of the beam.

III.2.1 BEAMS OF SERIES IA (Figs.III.23 to III.30)

Considered first are the beams that failed by shear compression. Beam IA-1 was not loaded upto failure but the maximum load recorded was higher than the major diagonal cracking load. Beams IA-2 and IA-3 showed shear compression failures.

The longitudinal strain in the reinforcement varied according to the variation of the bending moment at earlier stages of loading. As cracking progressed, sections closer to the load point showed higher strains than those consistent with the bending moment variation. Strains in the reinforcement over supports remained negligible till the time critical diagonal cracking occurred. Before diagonal cracking, sections of the beam from the support to the midshear span showed much lower strains than those in the remaining part of the beam. With the development of a major diagonal crack, strains at sections over support and close to the support showed a sudden jump while the strains in the midsection increased slowly. At this stage no section of the reinforcement had yielded, though the reinforcement between the load points was fairly close to it.

Figs.III.23 to III.25, representing results of beams IA-1, IA-2 and IA-3 show that major increases in strains at sections a and b took place at a load of 80, 60 and 45 kips respectively. At these loads the concrete strain diagrams show that compressive strains in the lower half of the beam had already developed over the entire span. It can be seen from the diagrams that some

bond forces were still acting, especially between midshear span and supports even after diagonal cracking. However, the bond forces reduced significantly after diagonal cracking. As the loading proceeded, the reinforcement in the midspan region yielded. Strains closer to support continued rising faster than at other sections of the beam with the result that bond forces decreased further. As failure conditions approached, the reinforcement in the entire span had yielded and strains were substantially in excess of those compatible with yielding. In beam IA-2, the strain in the reinforcement was virtually constant from end to end.

Beams IA-4 to IA-8 failed by sudden diagonal tension failure. Longitudinal strain distribution in the reinforcement is shown for these beams in Figs.III.26 to III.30.

The strain diagrams of these beams are similar to the earlier beams up to the point major diagonal cracking occurred. In these beams, however, this cracking resulted in ultimate failure. Tensile strains in the reinforcement above the support remained negligible till failure while bond forces continued to exist. Bond forces at sections closer to the load point reduced with the progress of flexural cracking.

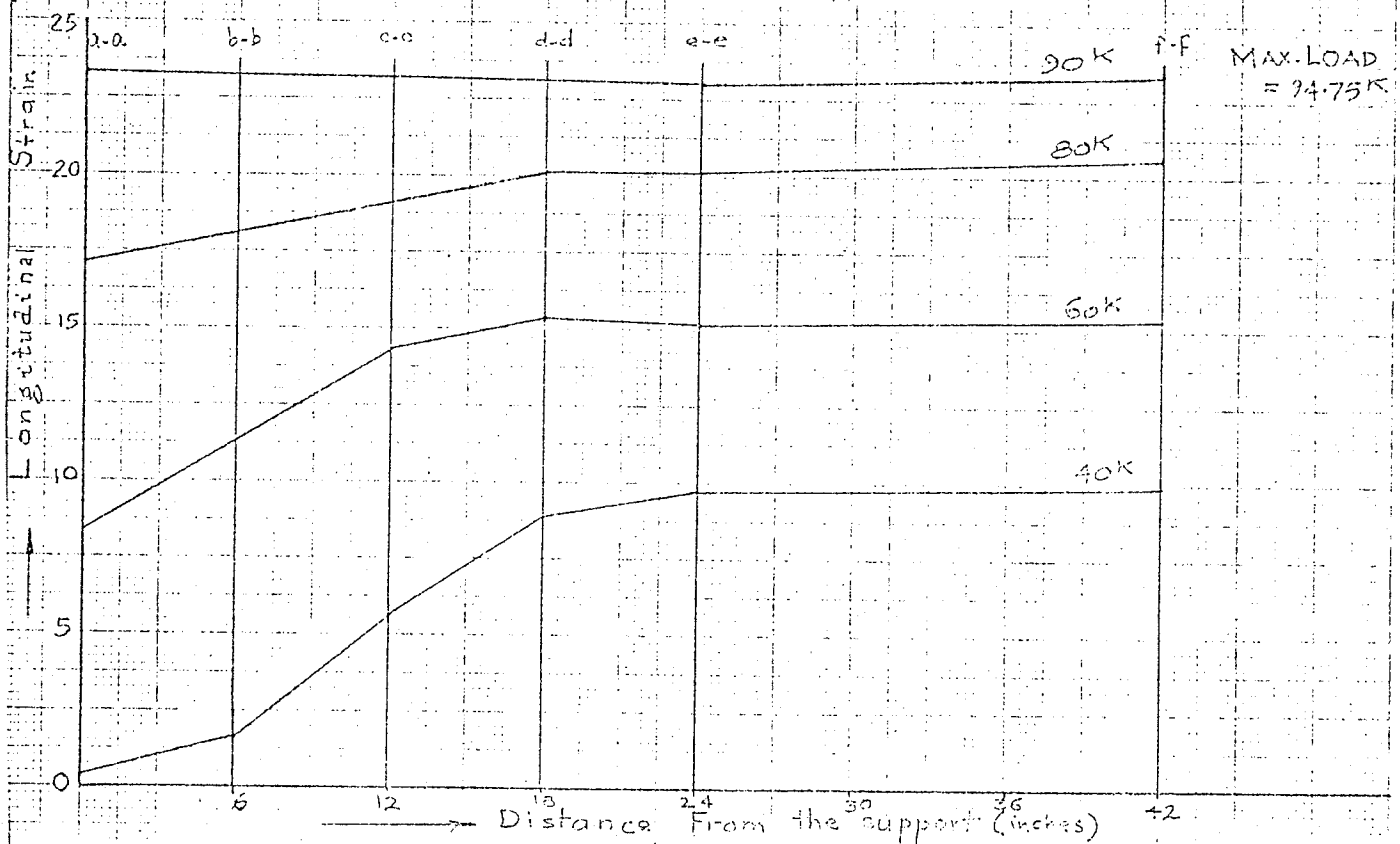
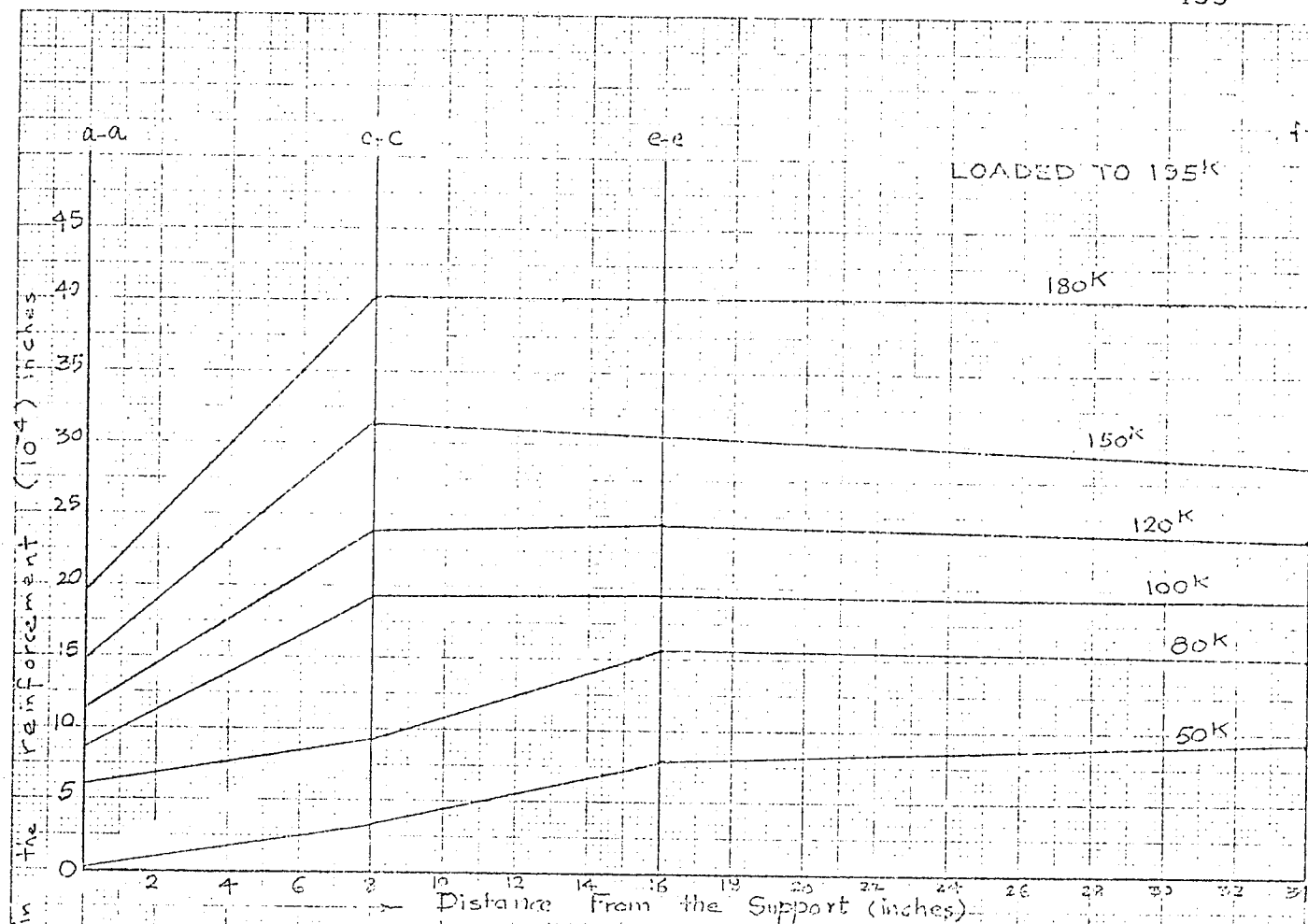
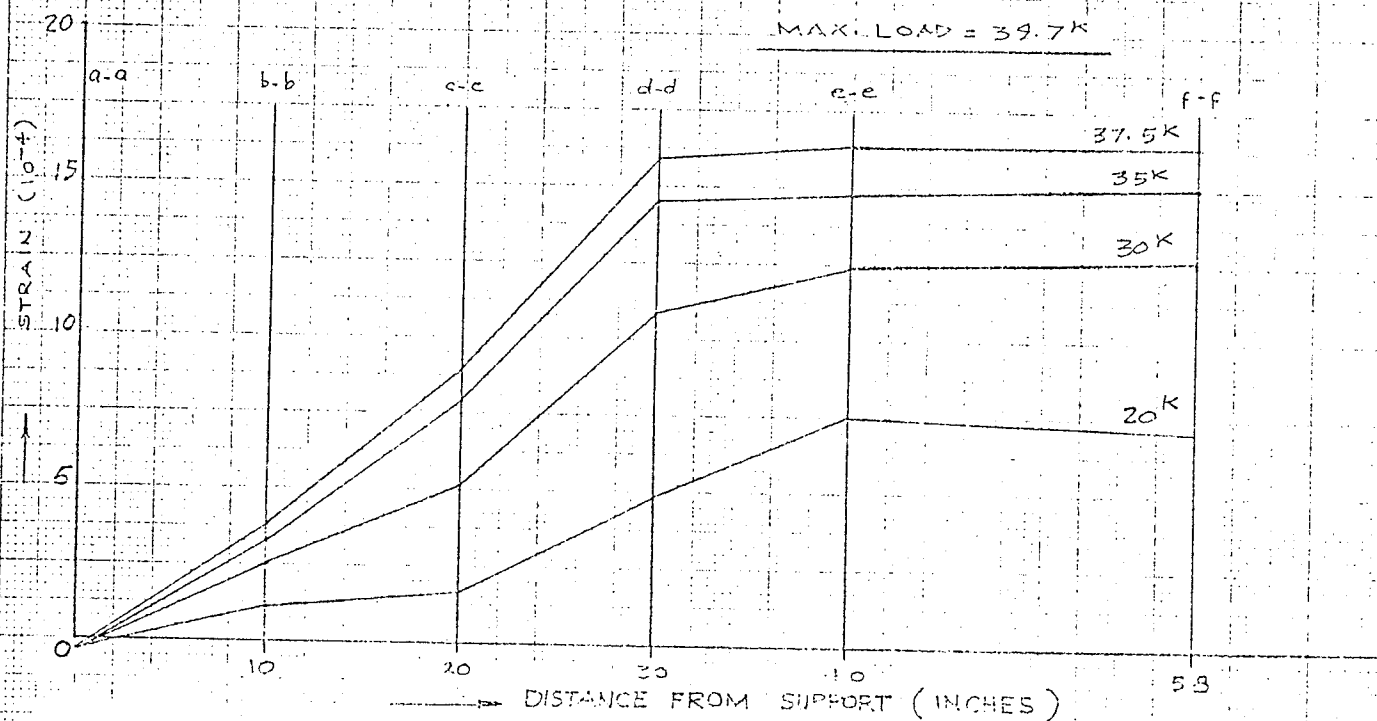
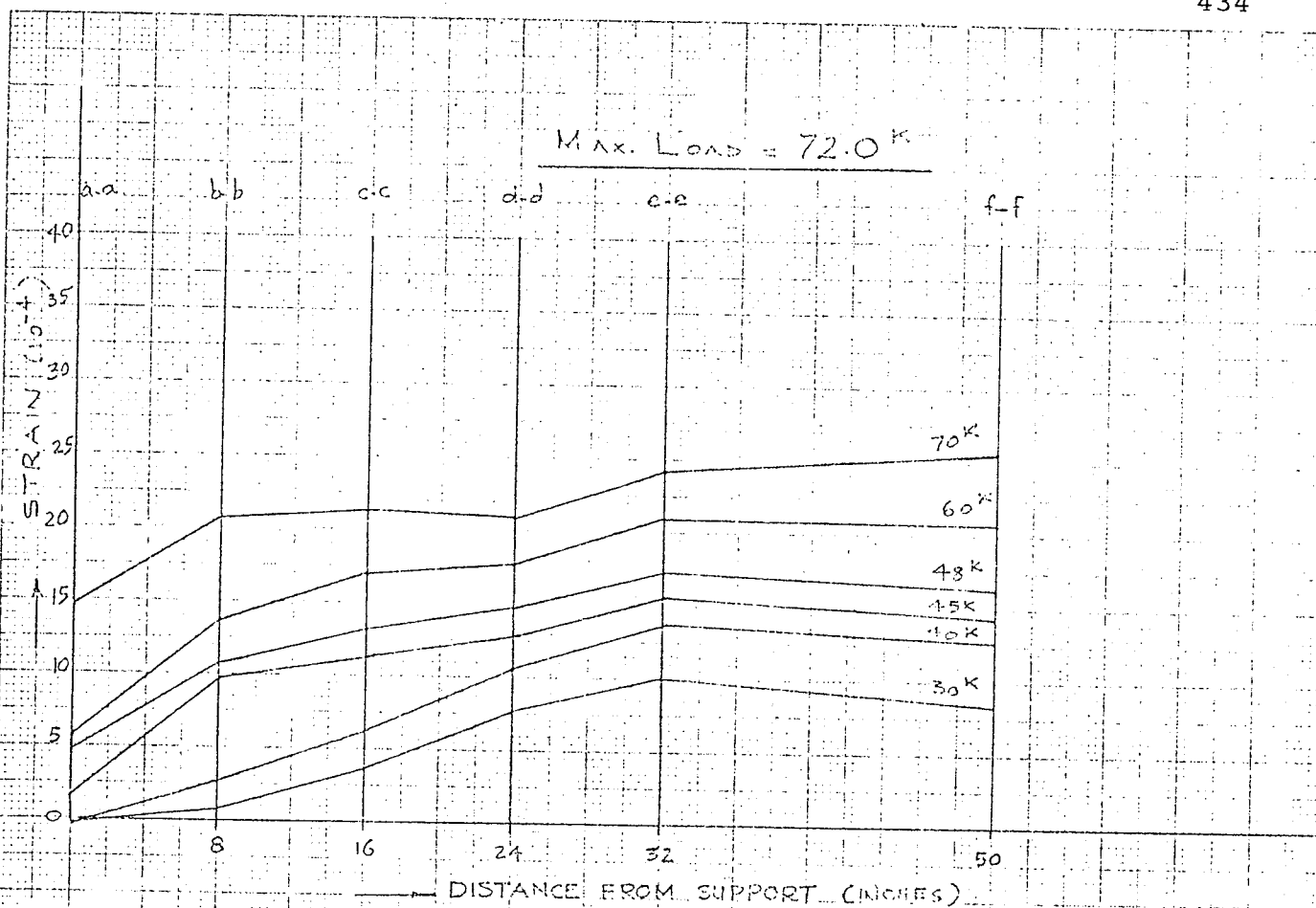


FIG. 23 TOP: BEAM IA-1

FIG. 24 BOTTOM: BEAM IA-2

LONGITUDINAL STRAIN IN THE REINFORCEMENT



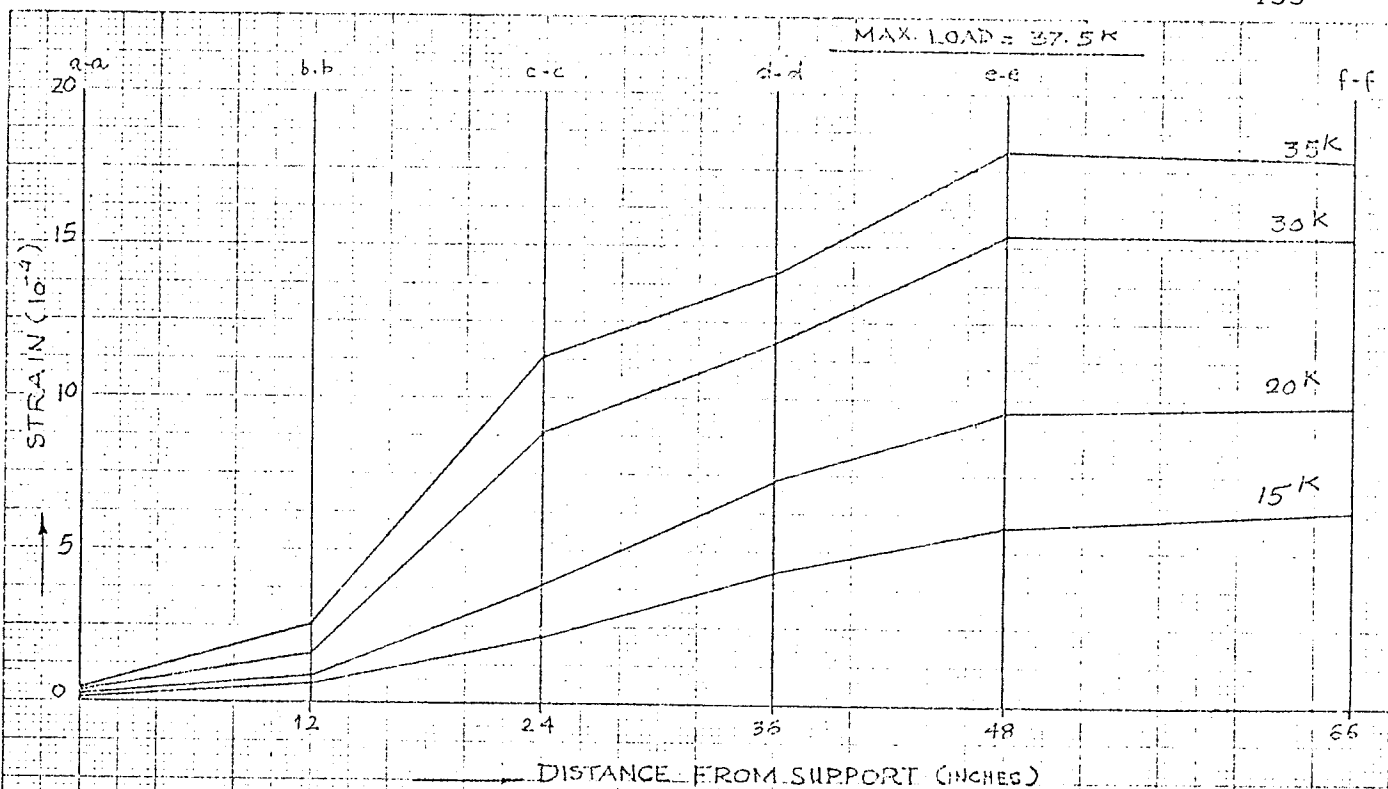


FIG. III.27 BEAM IA-5: LONGITUDINAL STRAIN IN THE REINFORCEMENT

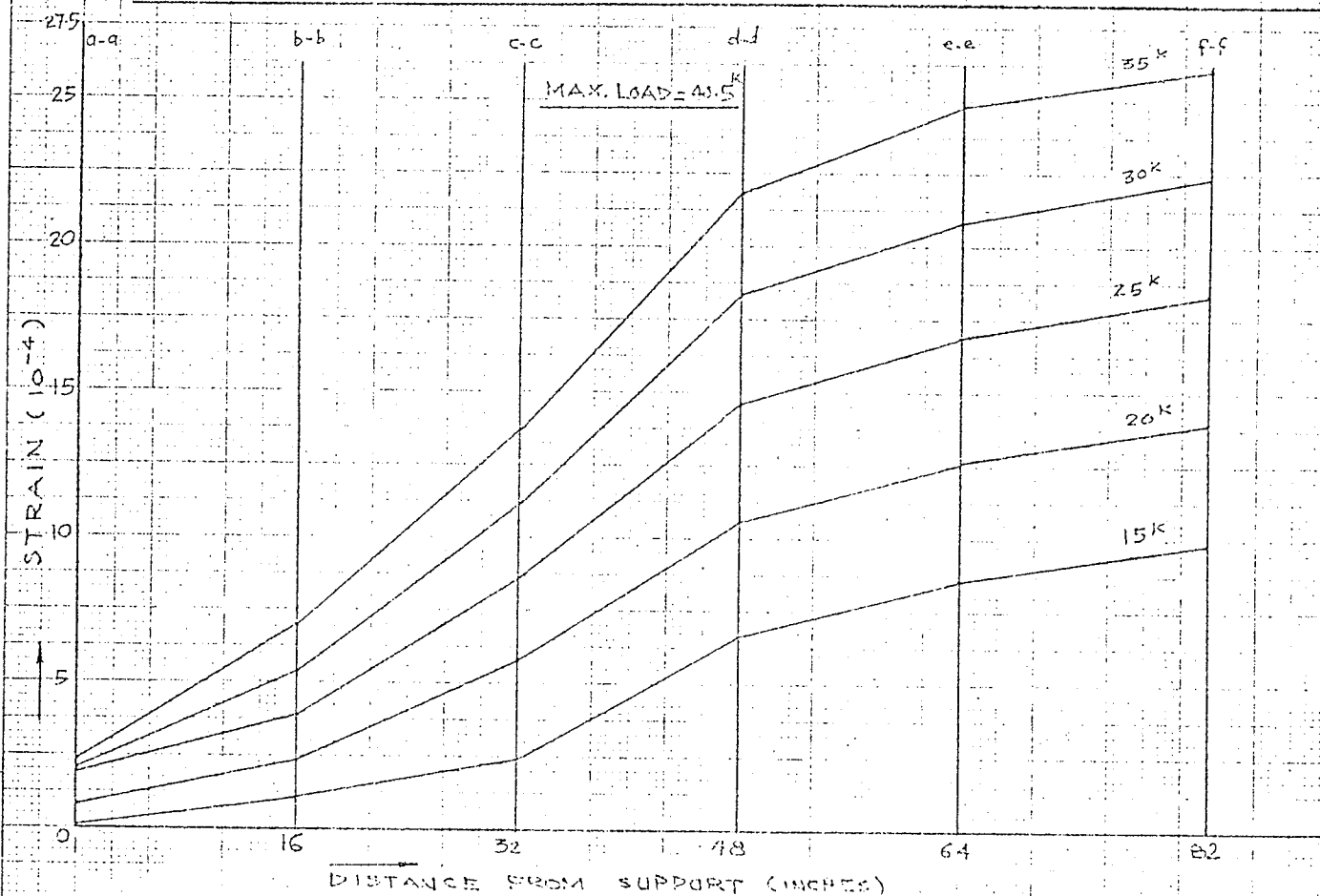


FIG. III.28 BEAM IA-6: LONGITUDINAL STRAIN IN THE REINFORCEMENT

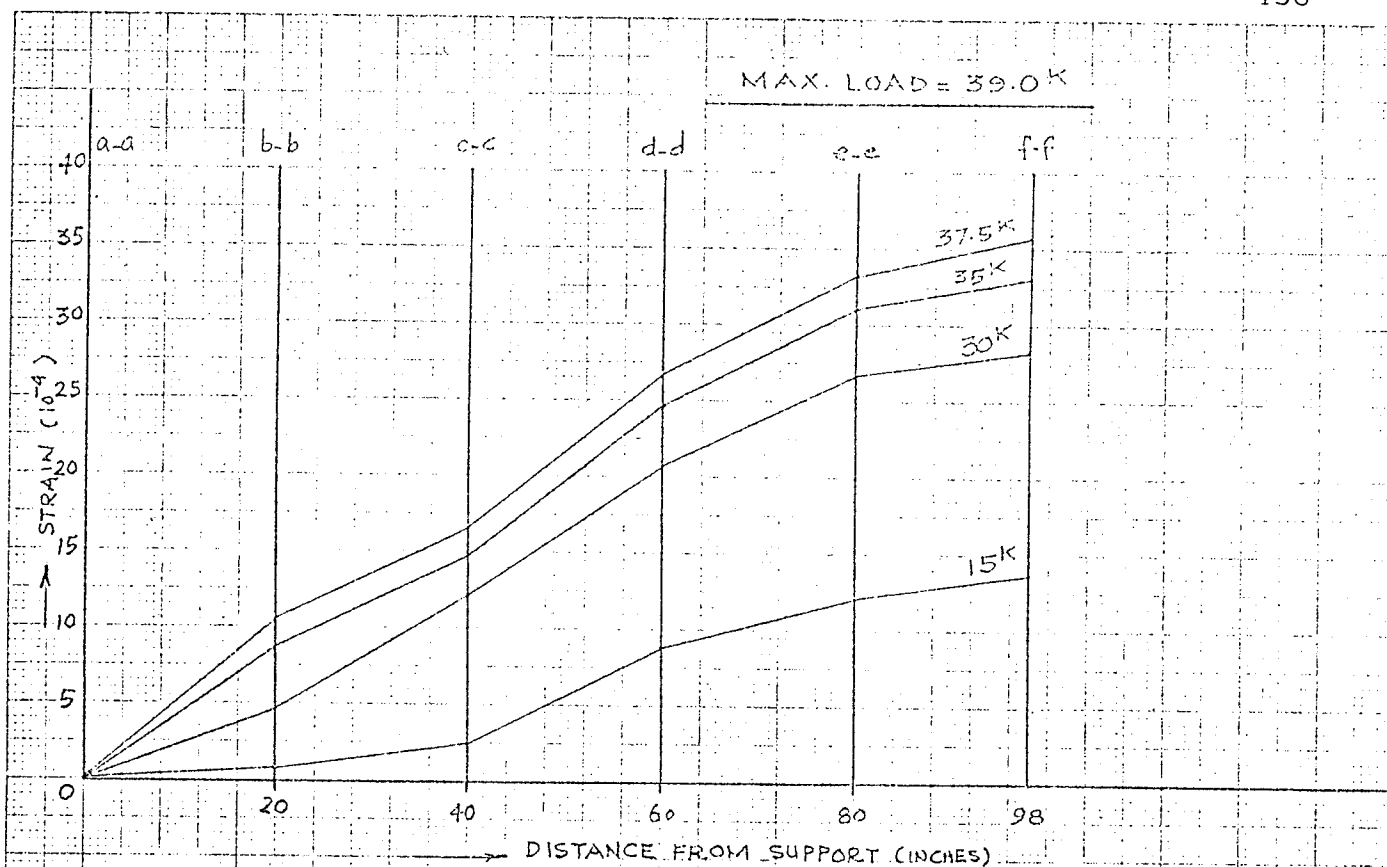


FIG. III.29 BEAM IA-7: LONGITUDINAL STRAIN IN THE REINFORCEMENT

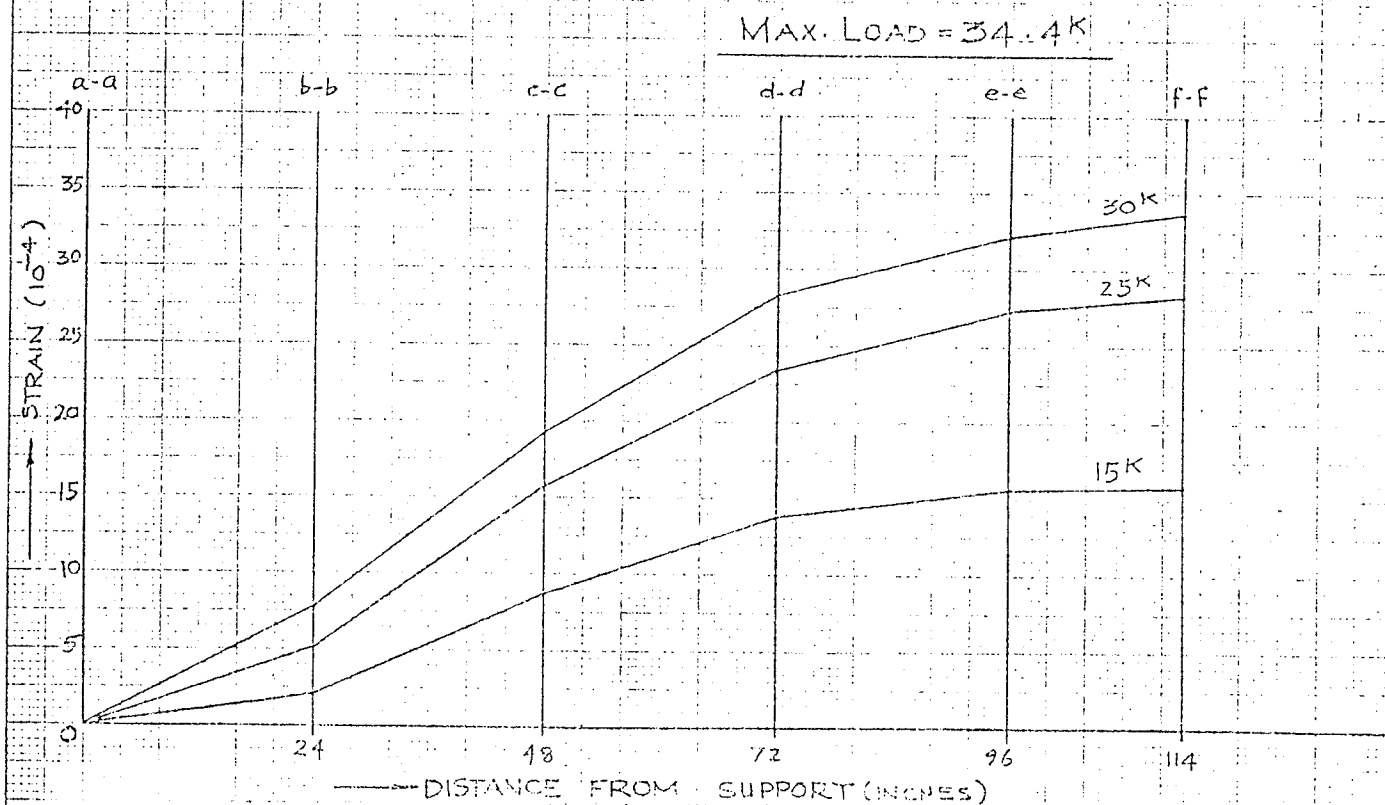


FIG. III.30 BEAM IA-8: LONGITUDINAL STRAIN IN THE REINFORCEMENT

III.2.2 BEAMS OF SERIES IB (Figs.III.31 to III.33)

Beam IB-2 was a retest of beam IB-5 on a shorter span and it did not have any regular series of gauges on the reinforcement. Results of beam IB-4, IB-5 and IB-6 are reported in Figs.III.31 to III.33. All these beams failed by diagonal tension. Results show that longitudinal flexural strains in the reinforcement remained negligible over the supports or close to the supports until failure. Strains at section c for beam IB-5 could not be recorded as both of the gauges on the reinforcement at this location did not function. Continued presence of bond forces can be seen in all beams.

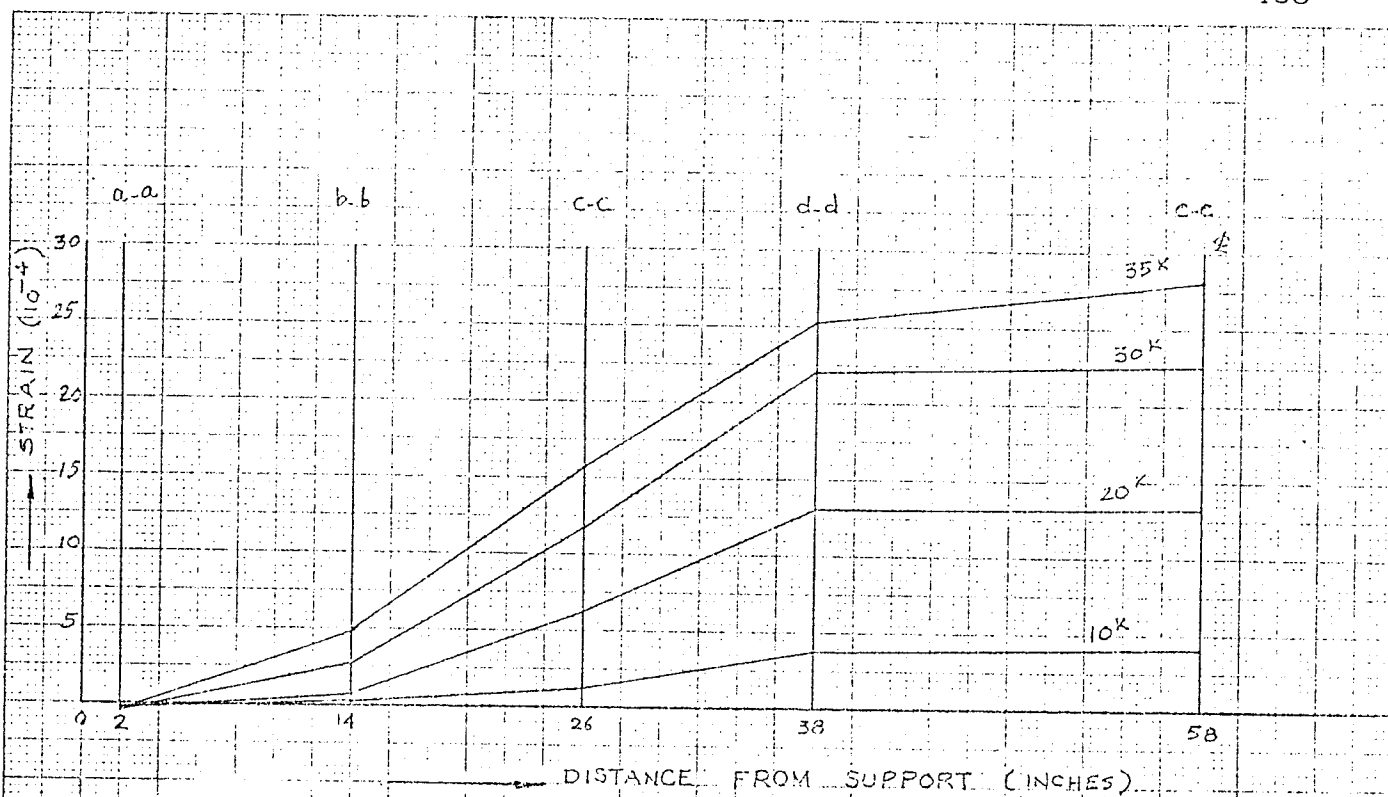


FIG. III.31 — BEAM IB-4: LONGITUDINAL STRAIN IN THE REINFORCEMENT

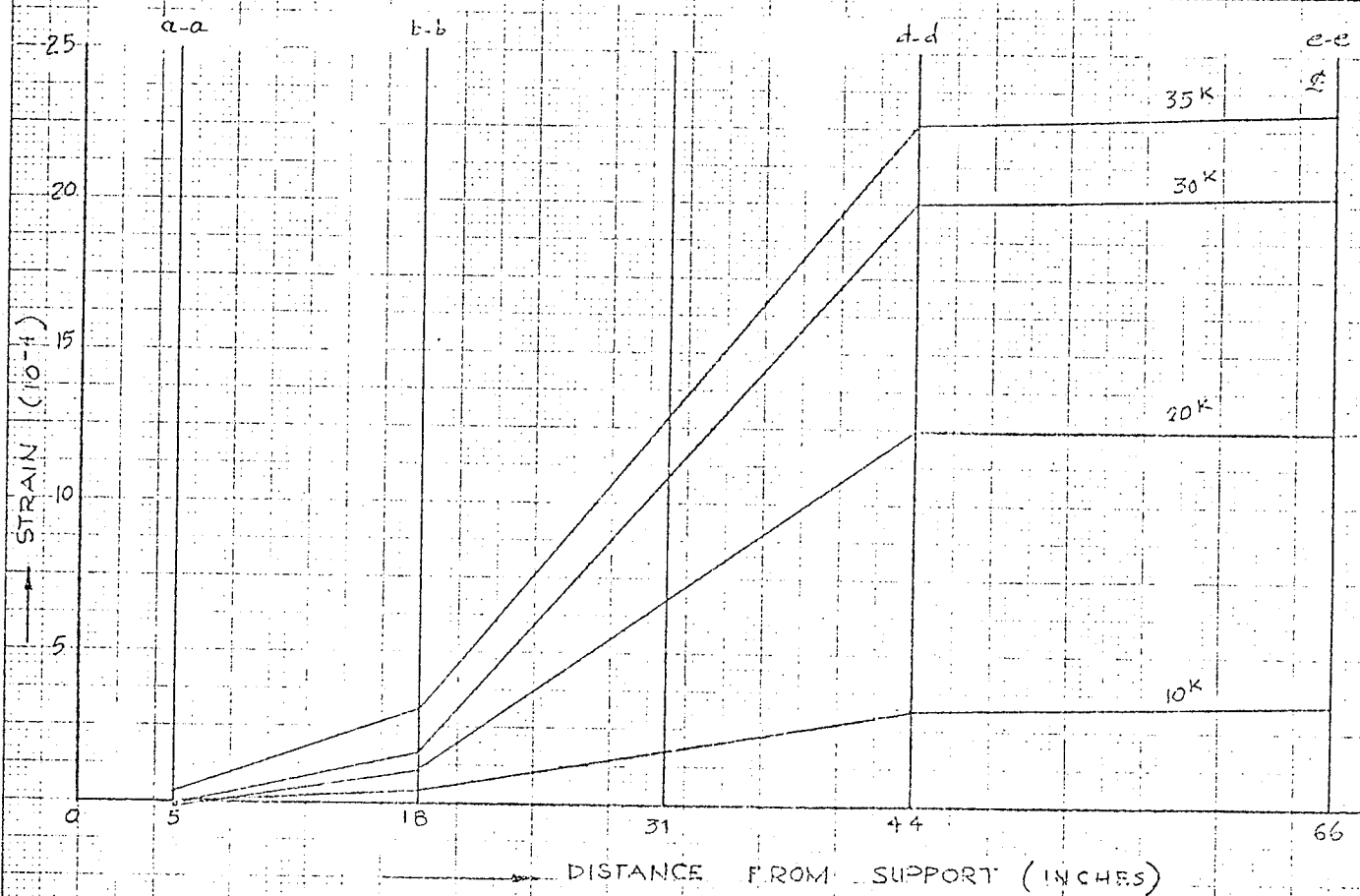


FIG. III.32 — BEAM IB-5: LONGITUDINAL STRAIN IN REINFORCEMENT

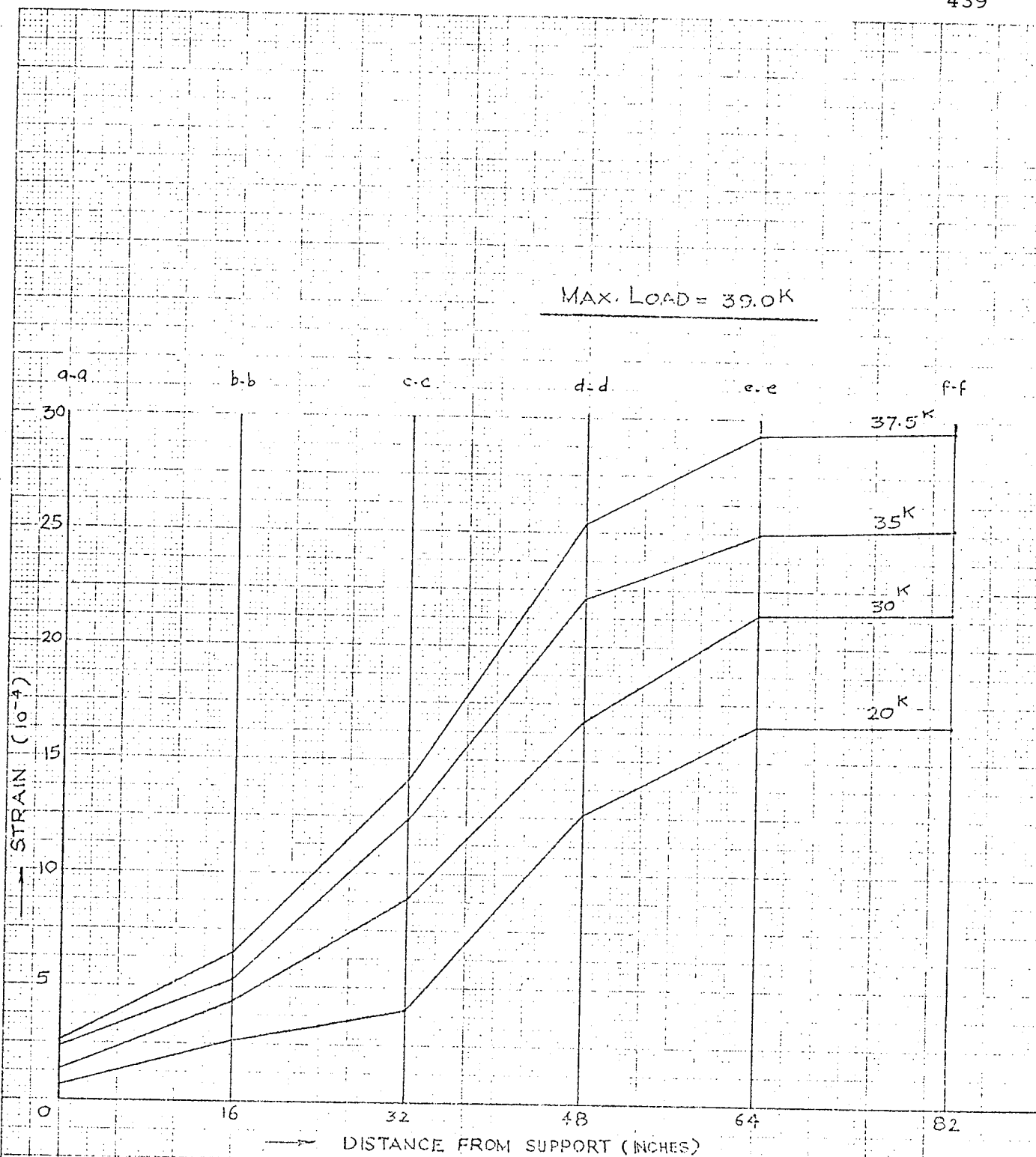


FIG. III.33 — BEAM IB-6: LONGITUDINAL STRAIN IN THE REINFORCEMENT

III.2.3 BEAMS OF SERIES IC (Figs.III.34 to III.36)

Beam IC-2 carried significant load after diagonal cracking. This coincided with an increase of tensile strains in the reinforcement over the supports and as failure approached, the tension force all along the reinforcement was constant and the reinforcement had yielded.

In beams IC-5 and IC-6, strains over support remained negligible. The strains at section d close to the load point in the shear span of the beam were even higher than at midspan.

After flexural cracking, bond forces in both beams in the inner regions of the beam reduced. This was observed from midspan of these beams upto the midshear span. Concrete strain distribution showed that compressive strains in the lower half of these beams also occurred only upto the midshear span, within which region the action of the bond force moment was not critical.

Beam IC-6 showed a flexural failure. The reinforcement at midspan upto the midshear span had yielded at failure.

The results show that bond forces do exist in the region compressive strains develop in the lower half of the beam after flexural cracking, though these are generally lower in the inner regions of the beam.

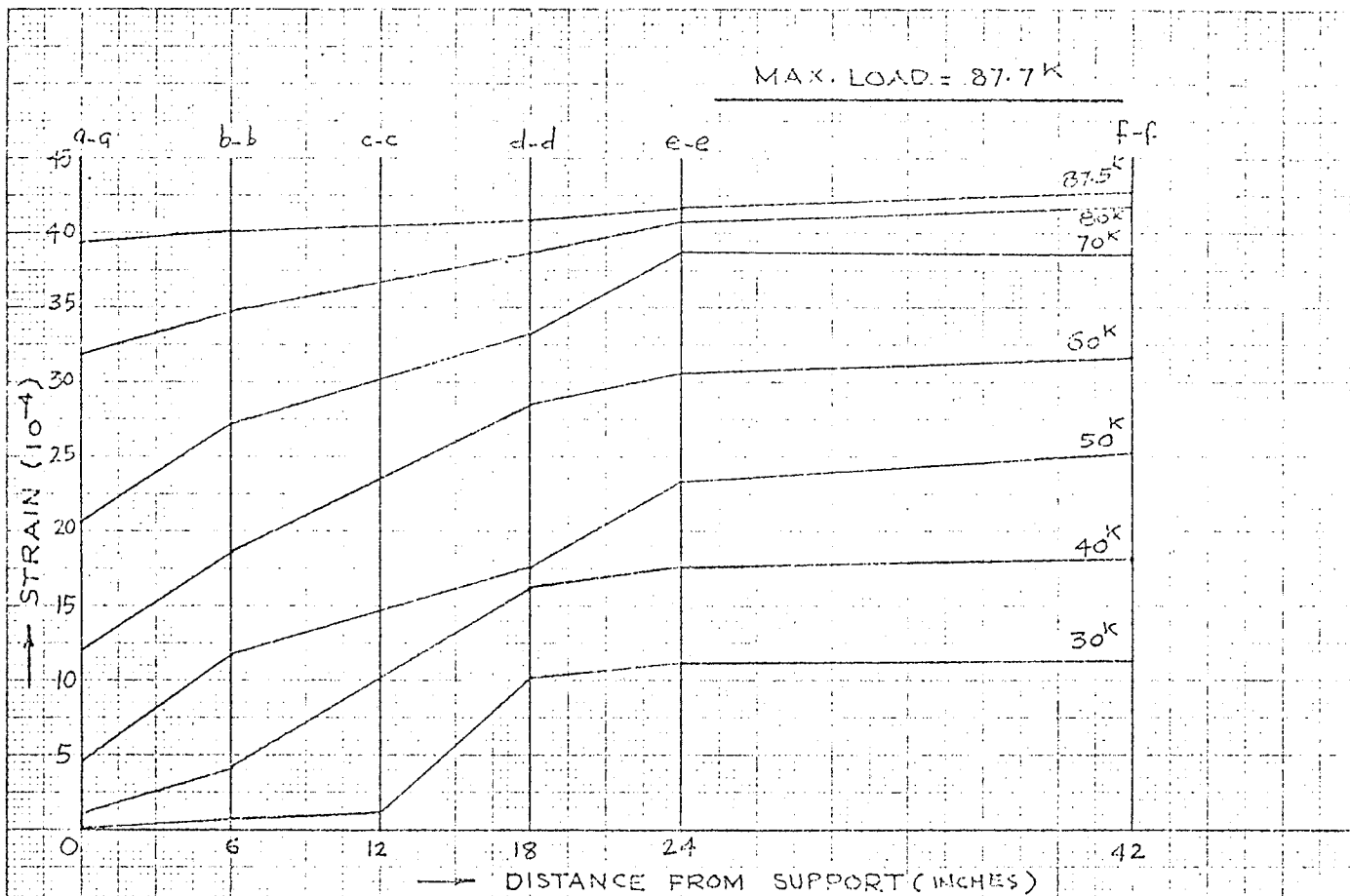


FIG. III.34 — BEAM IC-2: LONGITUDINAL STRAIN IN THE REINFORCEMENT

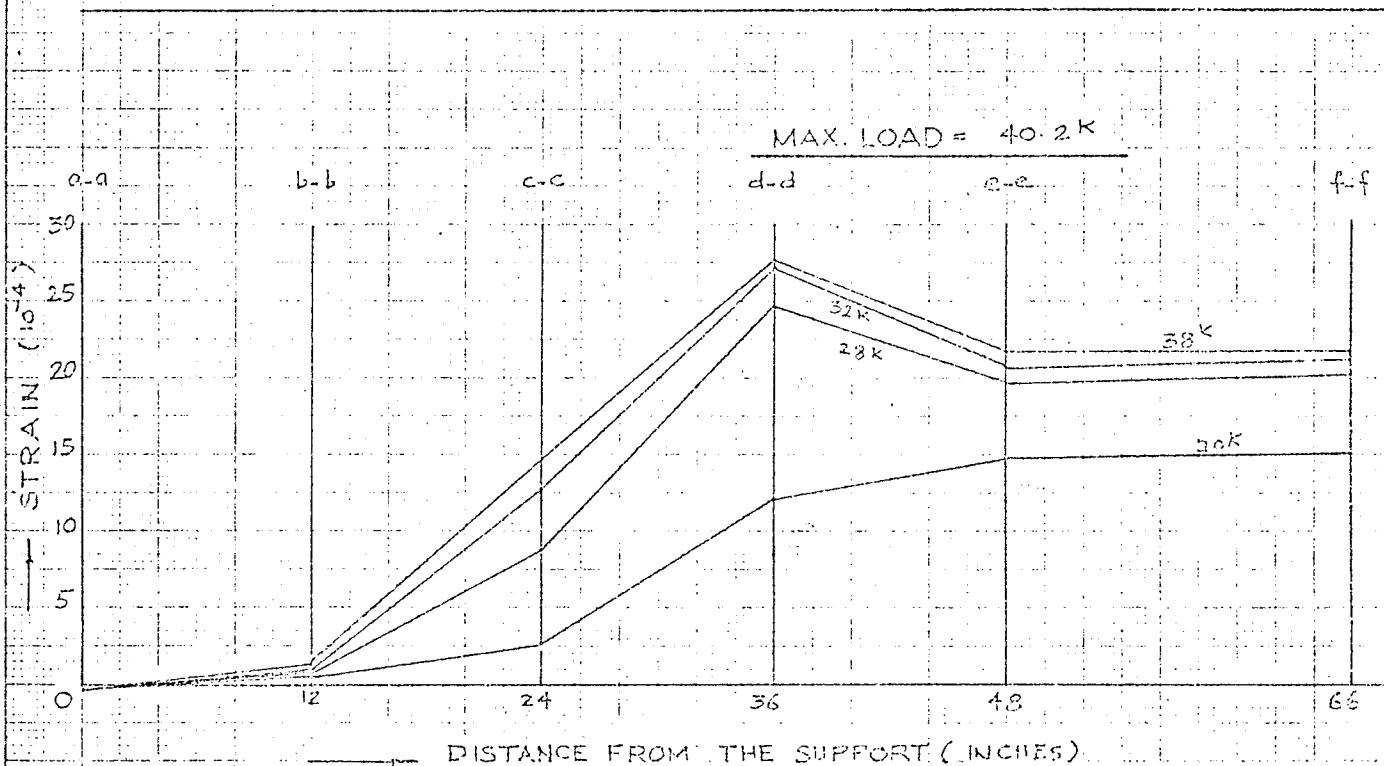


FIG. III.35 — BEAM IC-5: LONGITUDINAL STRAIN IN THE REINFORCEMENT

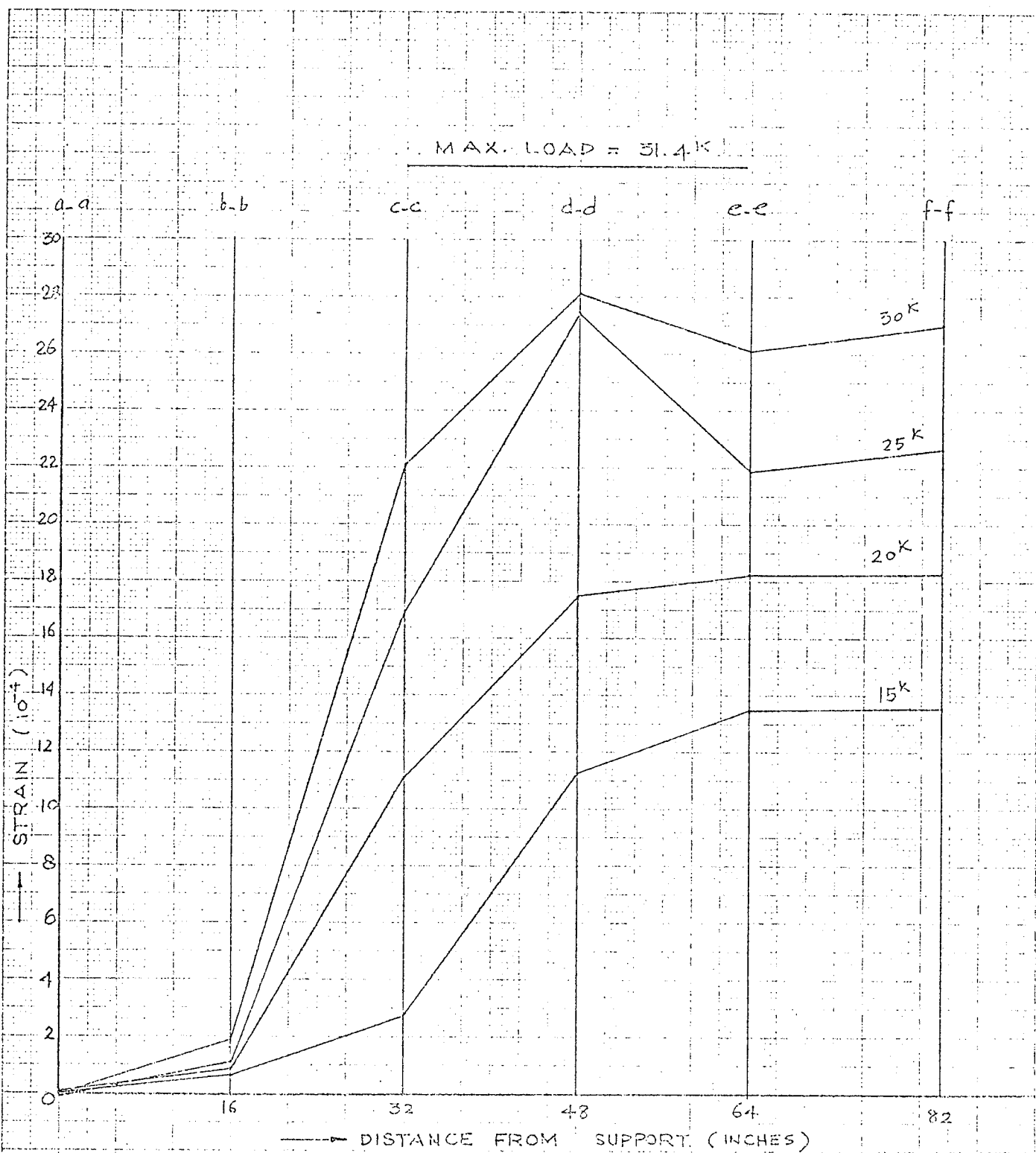


FIG. III.36 — BEAM IC-6: LONGITUDINAL STRAIN IN THE REINFORCEMENT

III.2.4 BEAMS OF SERIES IIA (Figs.III.37 to III.40)

It can be seen from Fig.III.38 that tensile strains at supports and sections close to it were just beginning to rise when premature failure of beam IIA-2 occurred at 55 kips. Reinforcement at this stage had not yielded at any point along the span. Beam IIA-2(b) (Fig.III.37), however, carried on more load after critical diagonal cracking. At this stage, a sharp rise in the strains in the reinforcement at sections close to the support occurred. Though the strain in the reinforcement over the support remained in the elastic range, stresses in excess of 30,000 psi existed at 78 kips, just 3 kips prior to failure. This shows a substantial reduction of bond forces after diagonal cracking. Since the loading was not directly applied over the compression face, unrestrained propagation of diagonal cracks occurred in the central position of the main beam. It appears that the reinforcement along a considerable portion yielded just prior to failure.

Strain diagrams of beams IIA-4 and IIA-6 (Figs.III.39 and III.40) show typical diagonal tension failures, strains remaining negligible over supports. Further, there is a consistent reduction of bond forces in the region between loading plane and the midshear span.

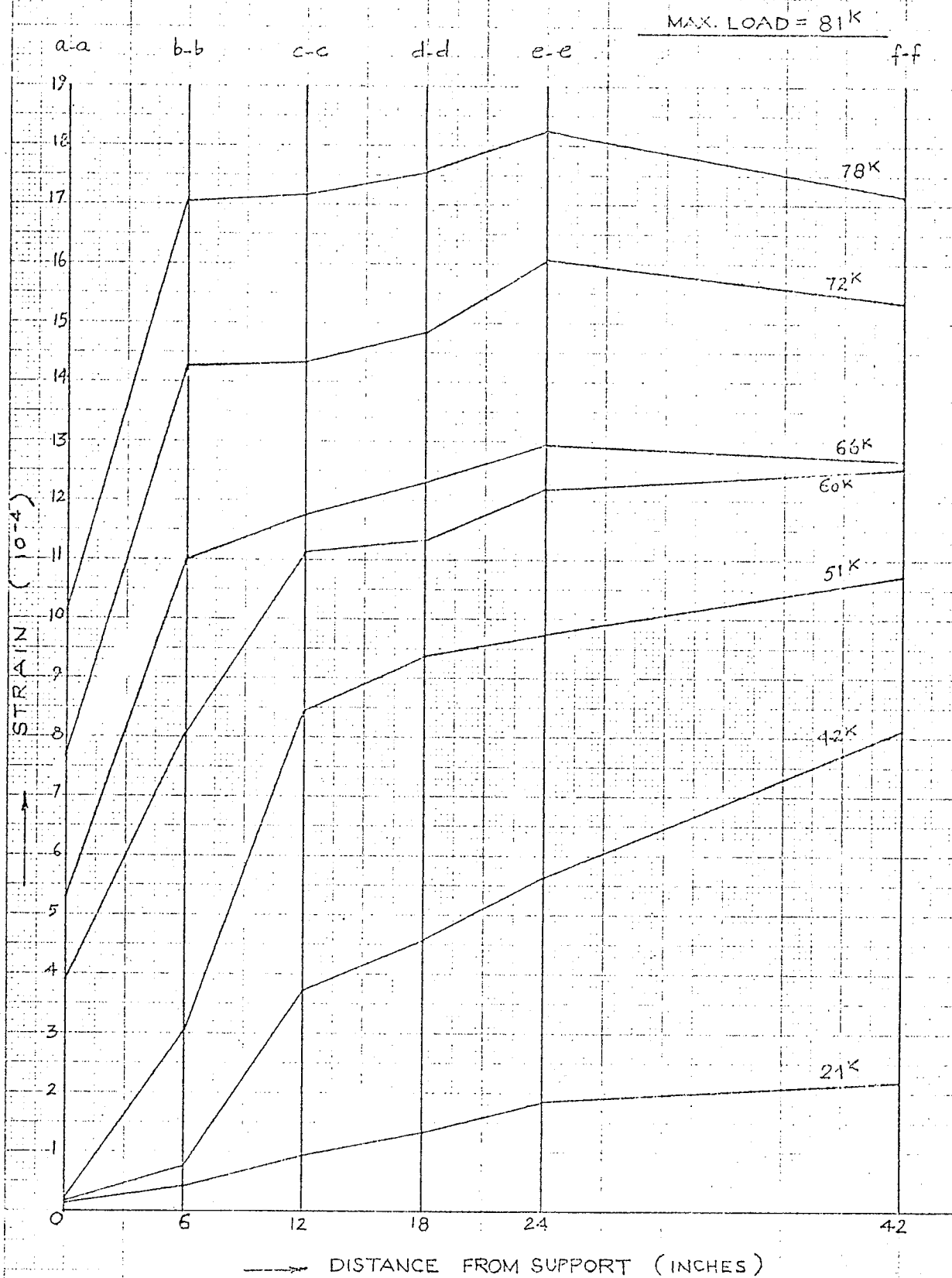


FIG. III.37— BEAM IIA-2 (b) — LONGITUDINAL STRAIN IN THE REINFORCEMENT

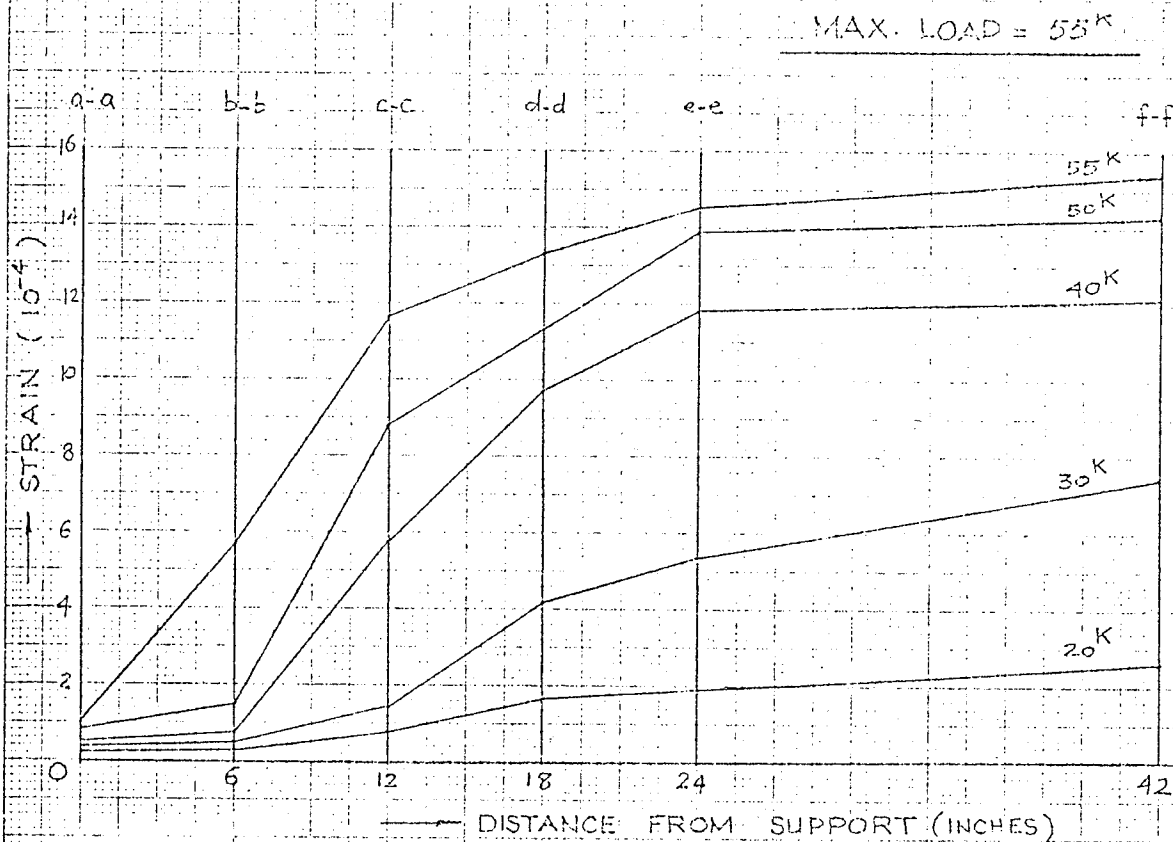


FIG. III.38 — BEAM IIA-2: LONGITUDINAL STRAIN IN THE REINFORCEMENT

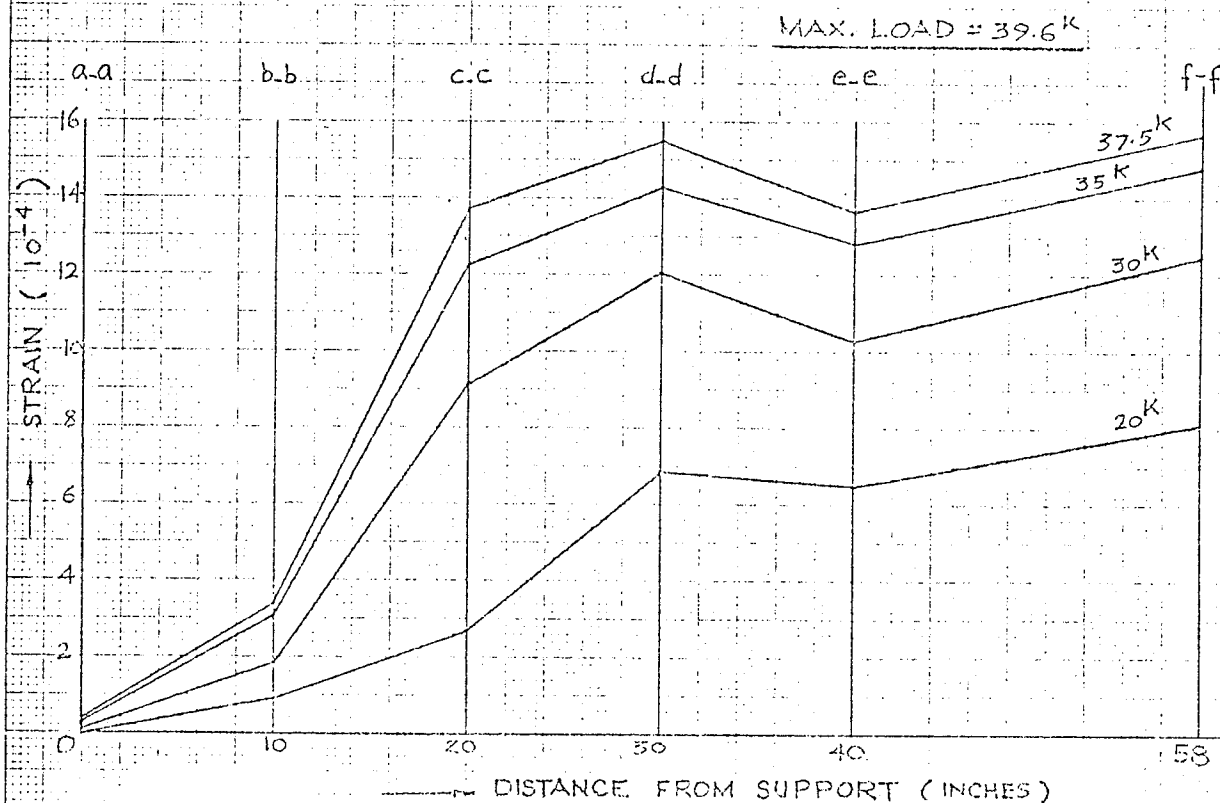


FIG. III.39 — BEAM IIA-4: LONGITUDINAL STRAIN IN THE REINFORCEMENT

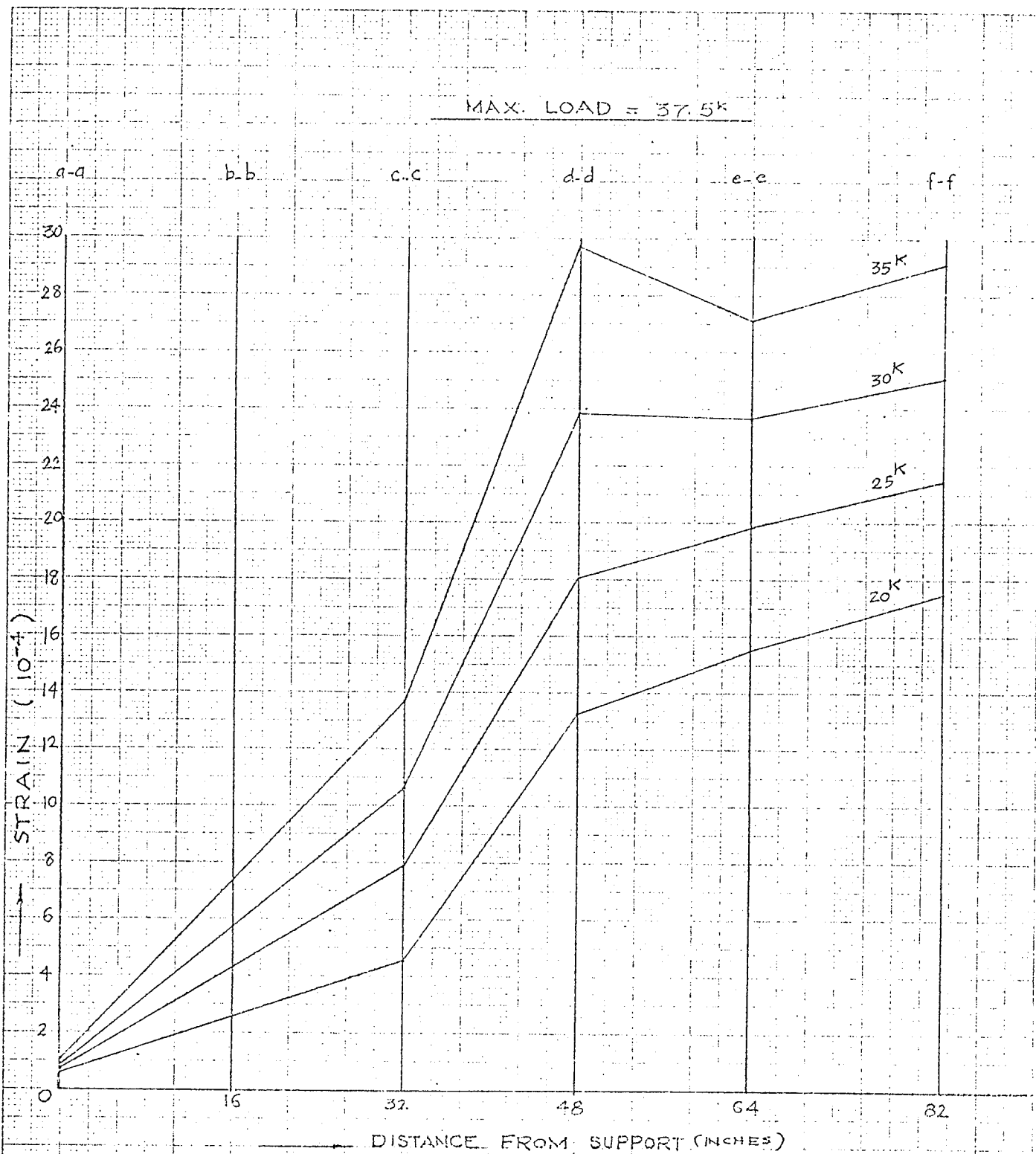


FIG. III. 40 BEAM IIA-6: LONGITUDINAL STRAIN IN THE REINFORCEMENT

III.2.5 BEAMS OF SERIES IIIA (Figs.III.41 to III.43)

Beam IIIA-3, which showed shear compression failure, continued recording negligible strains at supports until major diagonal cracking. At subsequent stages of loading, strain in the reinforcement at supports increased rapidly so that as failure approached, the entire length of reinforcement had yielded. The bond forces associated with distribution of tension force in the reinforcement also disappeared gradually towards failure.

Beam IIIA-6 had taken some load after critical diagonal cracking at a load of 50 kips. It can be seen that the reinforcement in the portion of the beam from section b to midspan had yielded at this stage. Bond forces within this region were also negligible. At subsequent stages of loading, the strain in the reinforcement at the support did increase but remained fairly low. Stresses of around 8,000 psi in the reinforcement existed over the supports prior to failure.

Beam IIIA-8 showed typical diagonal tension failure and the strains in the reinforcement associated with such failures. Strains over supports remained negligible.

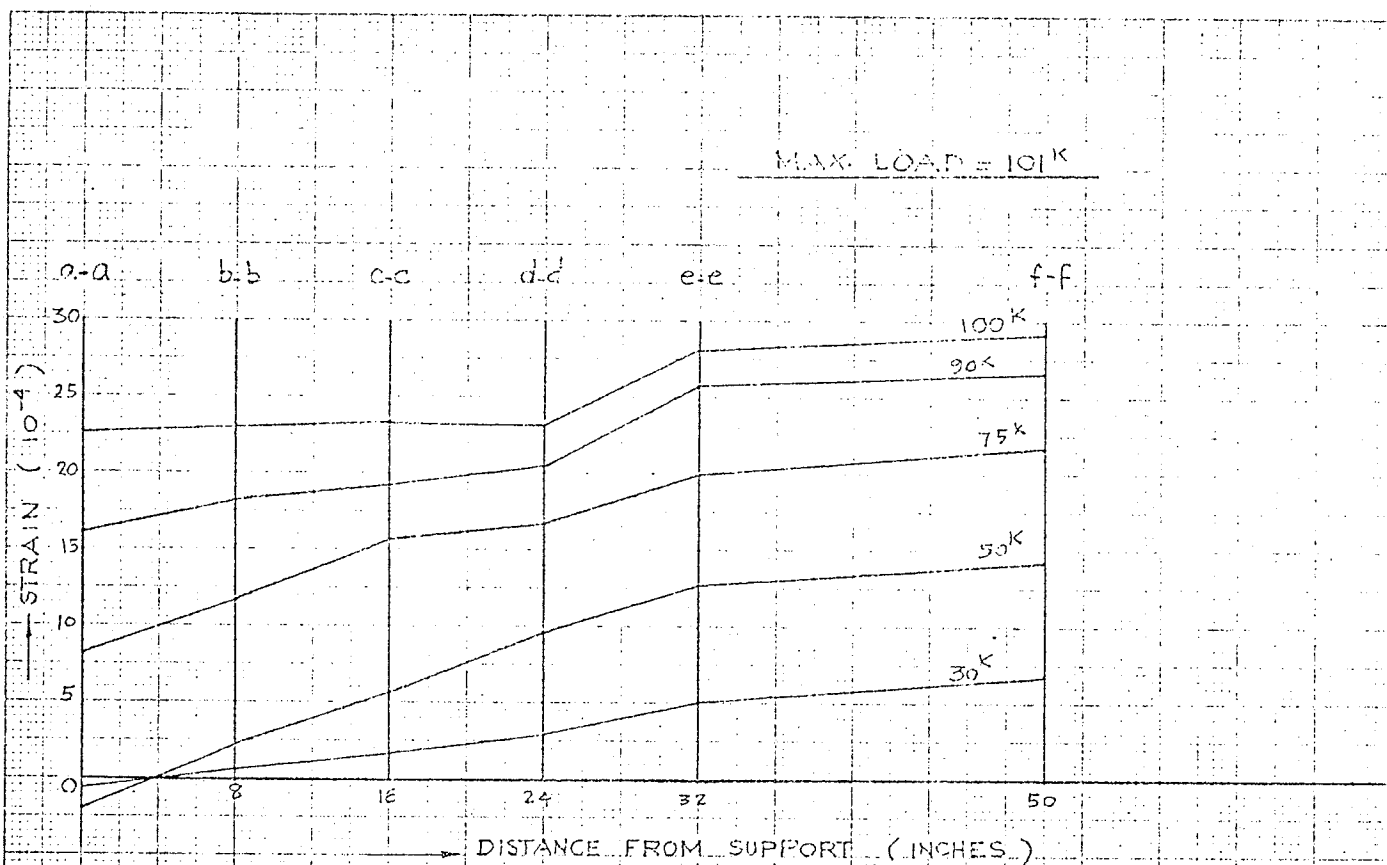


FIG. III.41 — BEAM IIIA-3: LONGITUDINAL STRAIN IN THE REINFORCEMENT

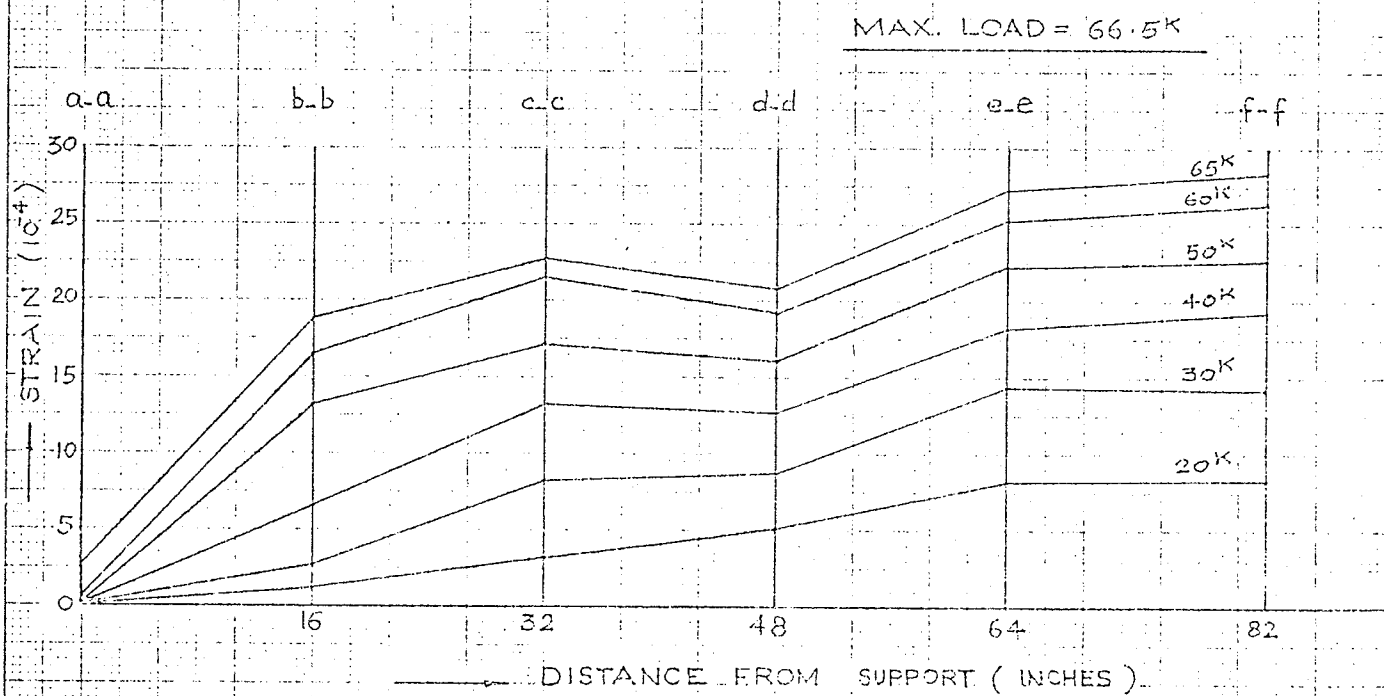


FIG. III.42 — BEAM IIIA-6: LONGITUDINAL STRAIN IN THE REINFORCEMENT

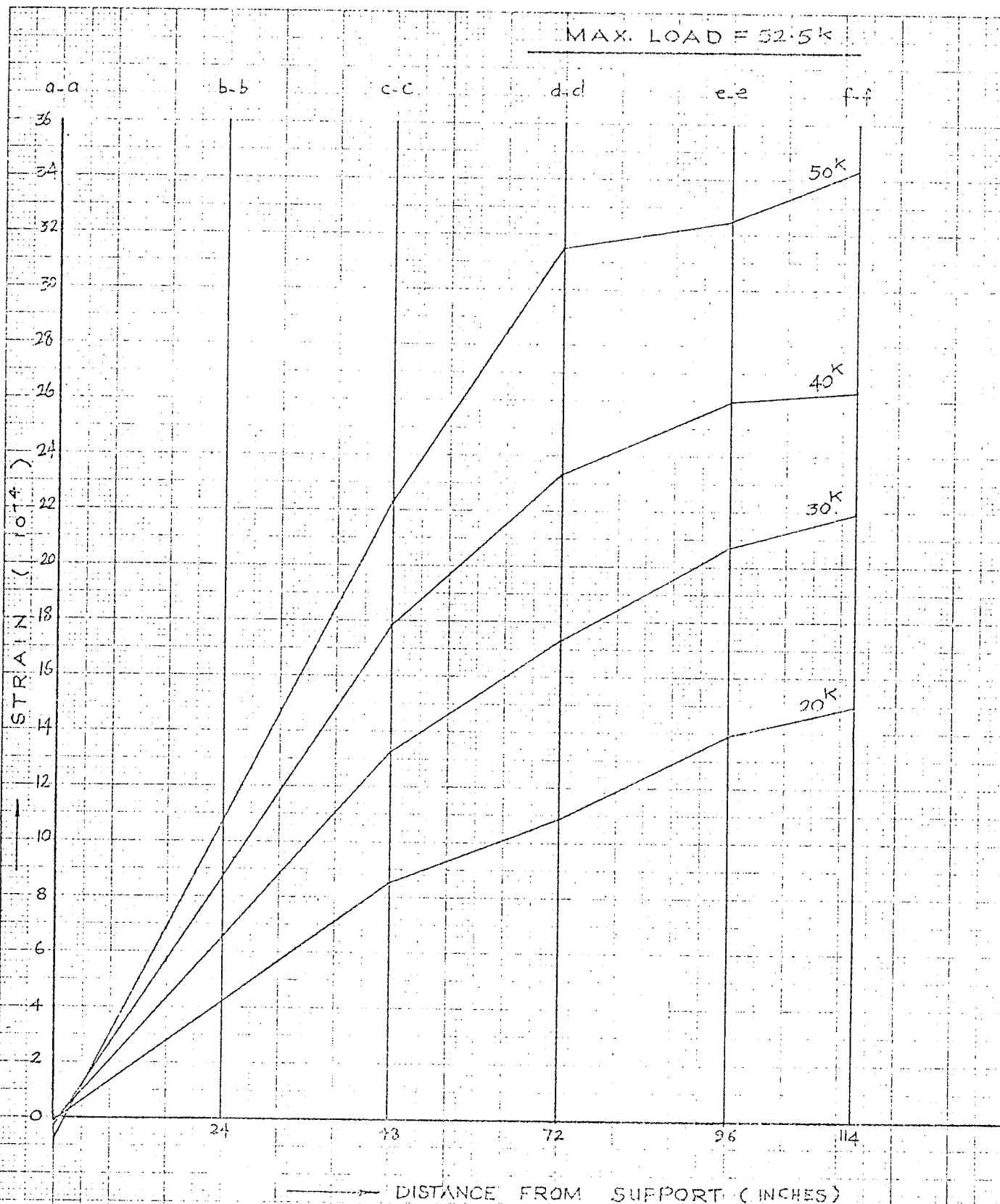


FIG. III. 43 — BEAM IIIA-8: LONGITUDINAL STRAIN IN THE REINFORCEMENT

III.3 DISTRIBUTION OF CONCRETE STRAINS OVER INCLINED GAUGE LINES

Figures III.44 to III.58 show the distribution of concrete strains on inclined gauge lines for the various beams tested. Each diagram also shows the location of the inclined DEMEC gauges, which were placed at 2-inch intervals, and each had a gauge length of 8 inches.

An examination of the strain distributions on these gauge lines shows a very consistent trend. In all those beams where a critical diagonal crack did not cause failure, a significant shift downwards of the centre of compression can be seen at the section between the midshear span and the supports after diagonal cracking. This happened for all beams within a/d ratios of 1 and 2. For all other beams, strain distribution on inclined gauge lines shows that maximum compressive strains at the compression face of the beam remained at the compression face of the beam throughout the whole test.

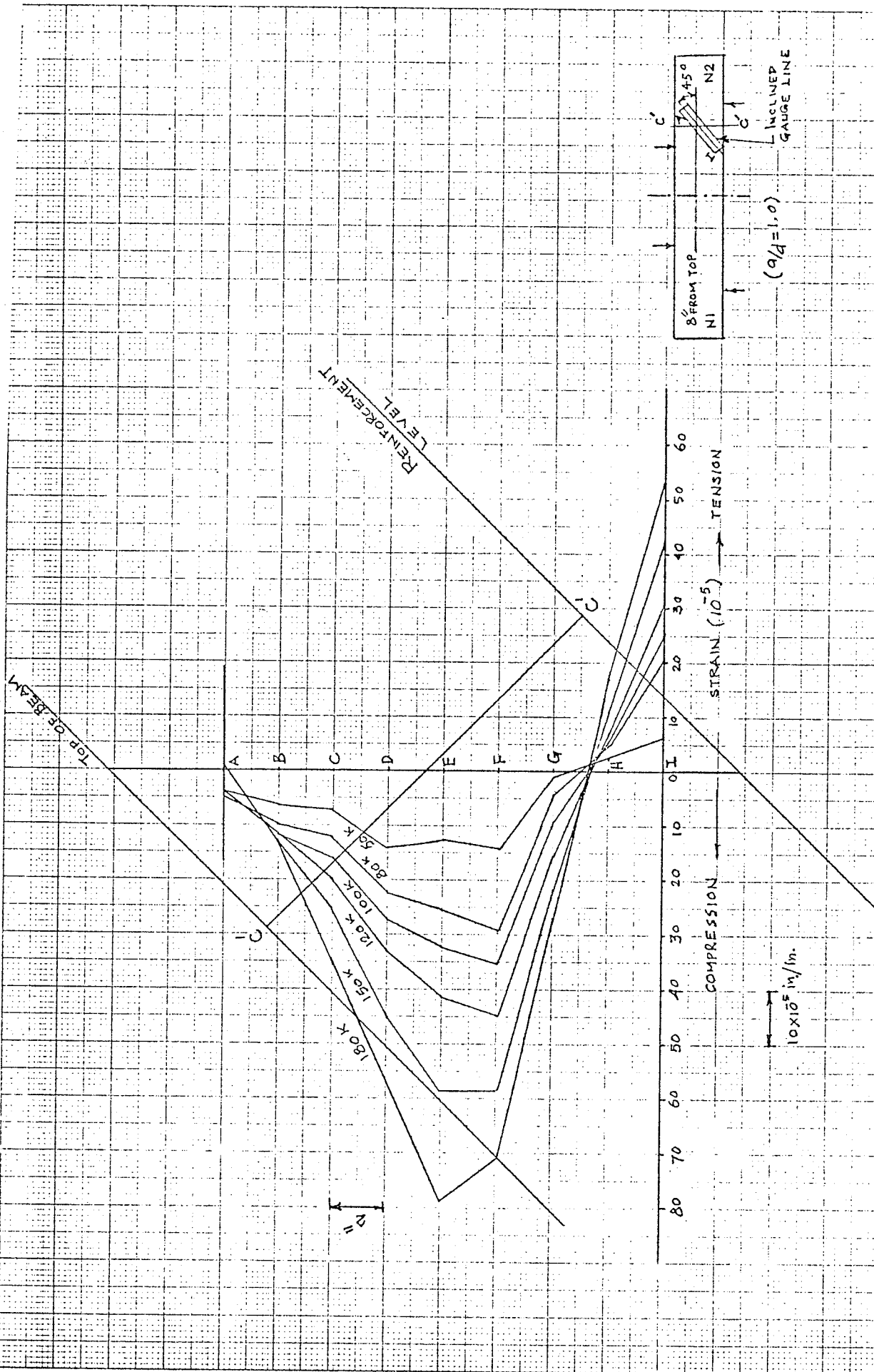
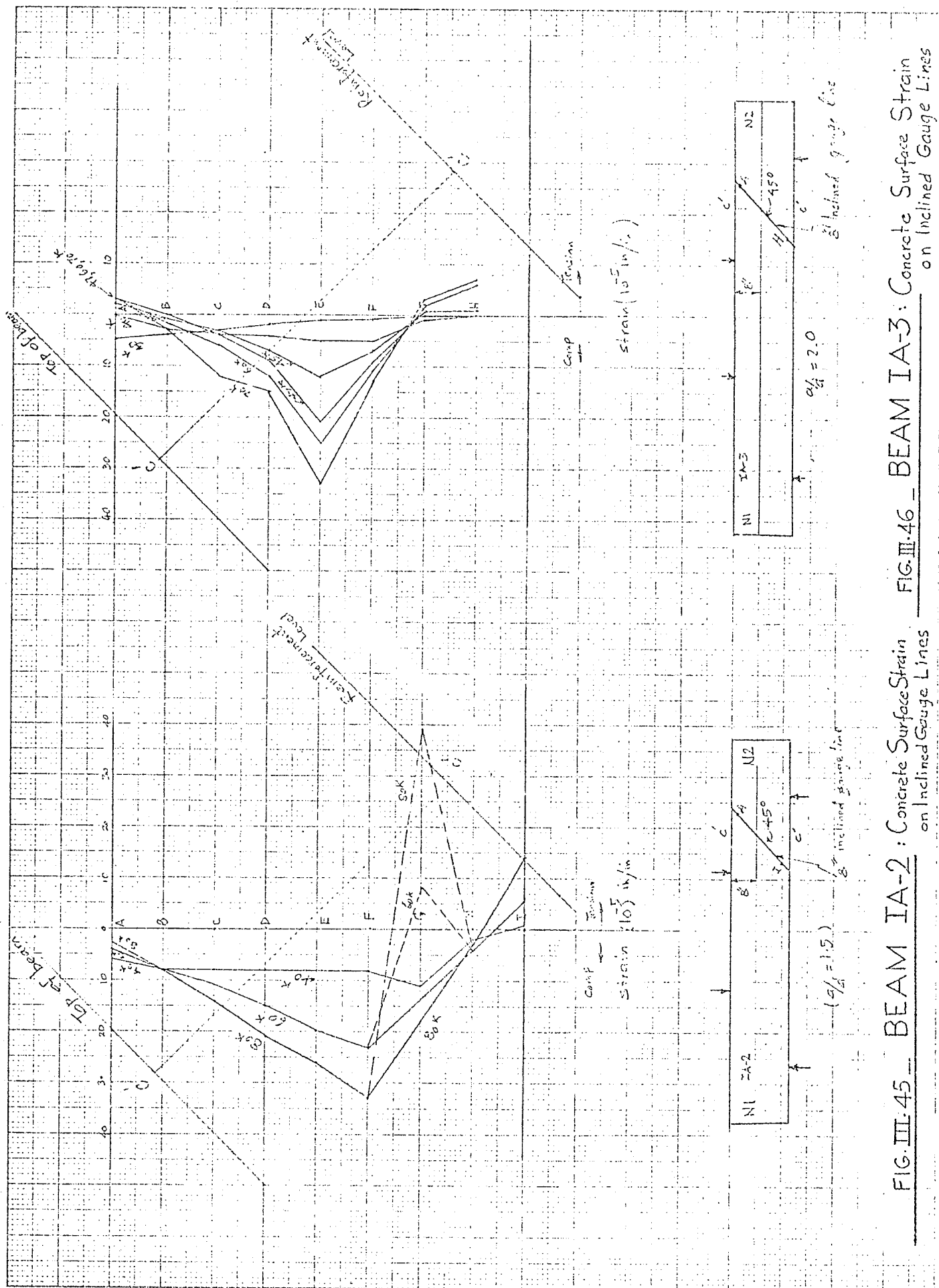


FIG. III-44-BEAM IA-1: Concrete Surface Strain on Inclined Gauge Lines



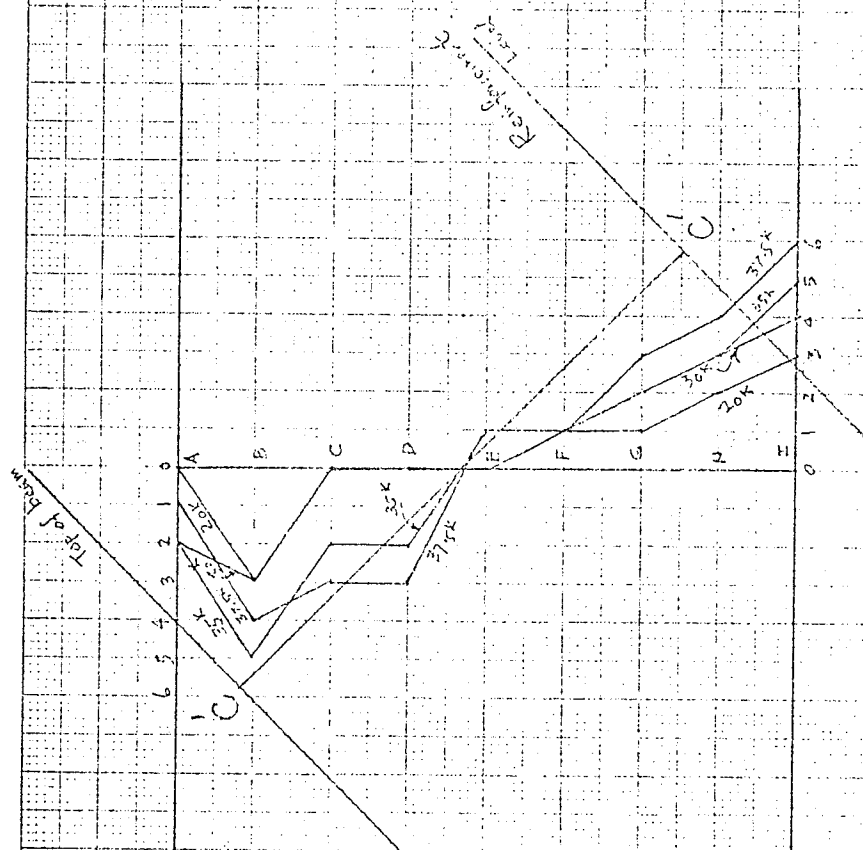


FIG. III.47_BEAM IA-4 — Concrete Surface Strain
on Inclined Gauge Lines

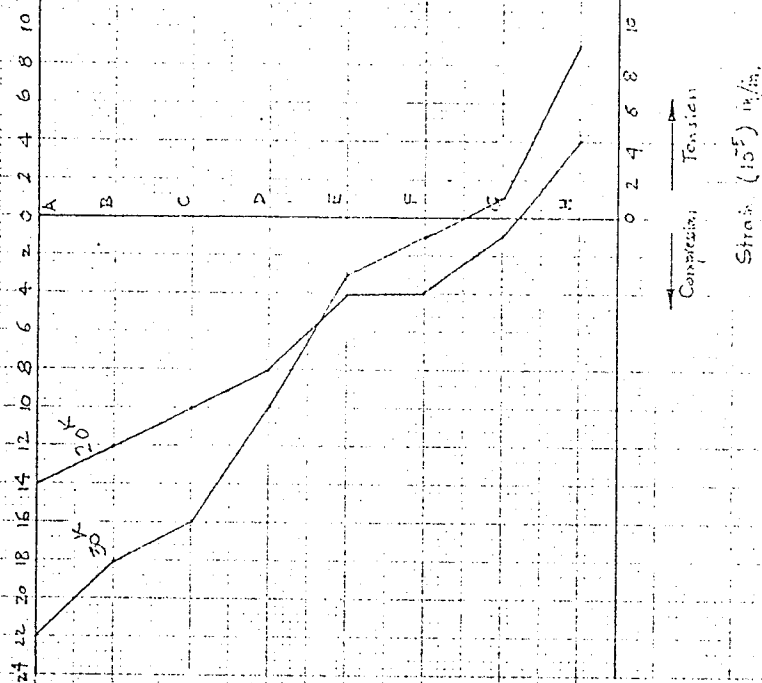
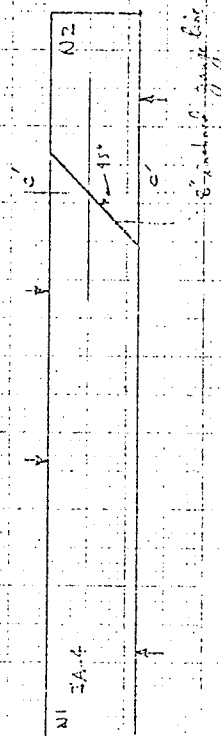
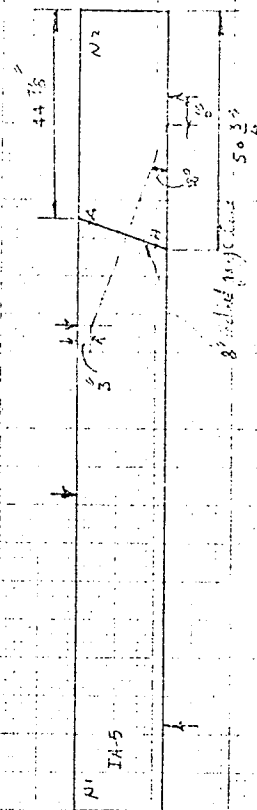


FIG. III.48 — BEAM IA-5: Concrete Surface Strain on Inclined Gauge Lines



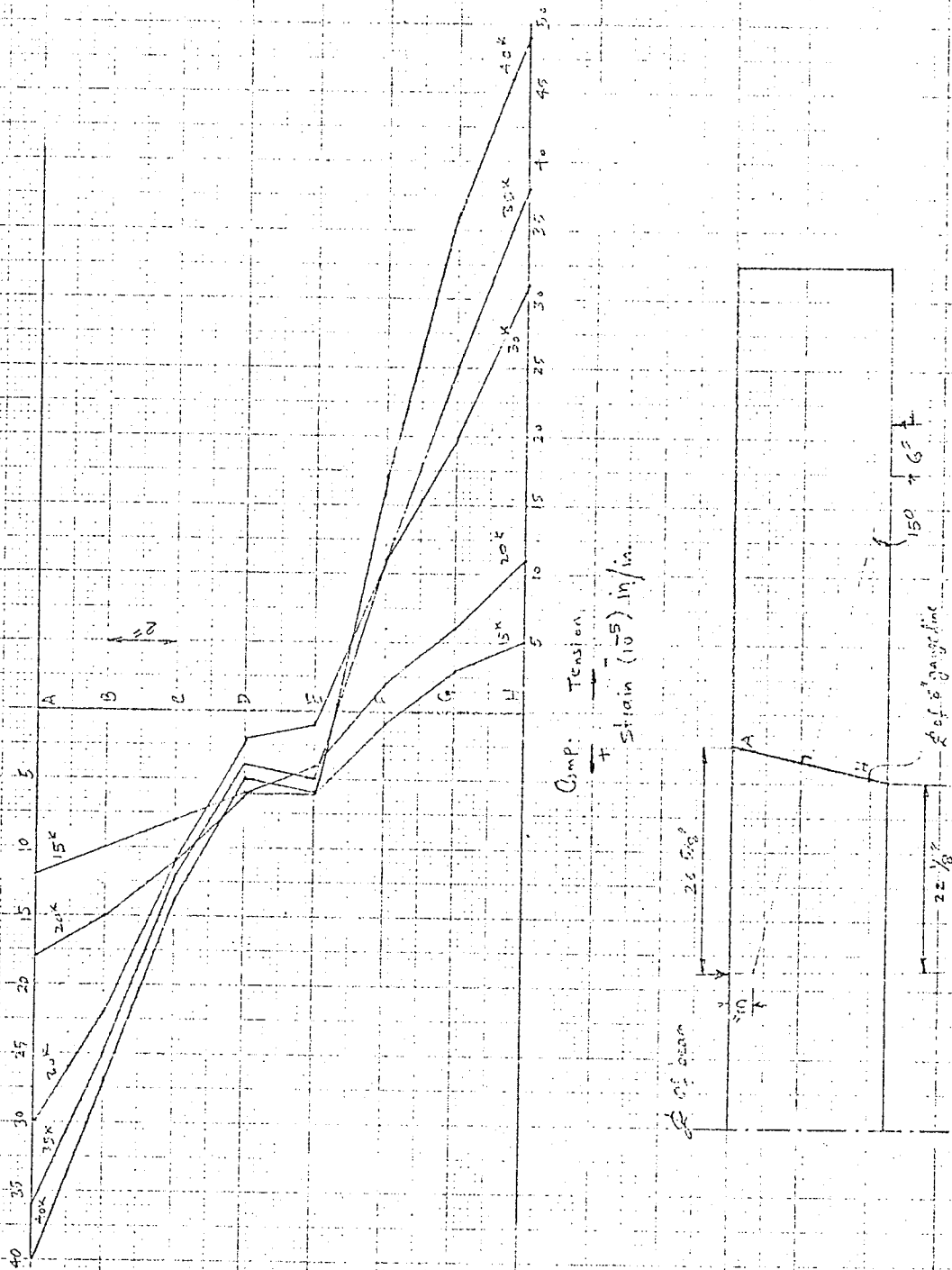


FIG. III.49 — BEAM IA-6 : Concrete Surface Strain Inclined Gauge Lines

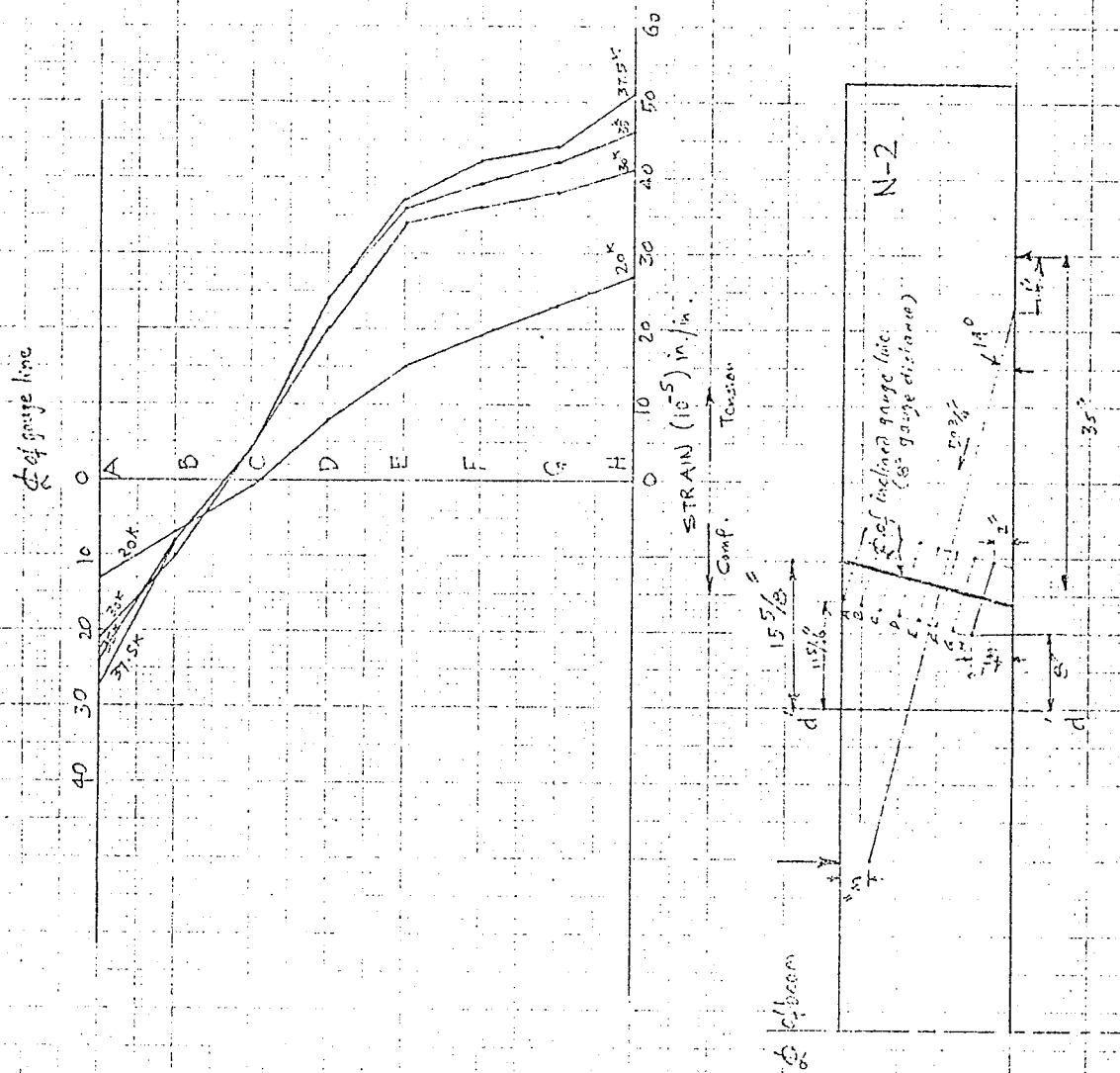
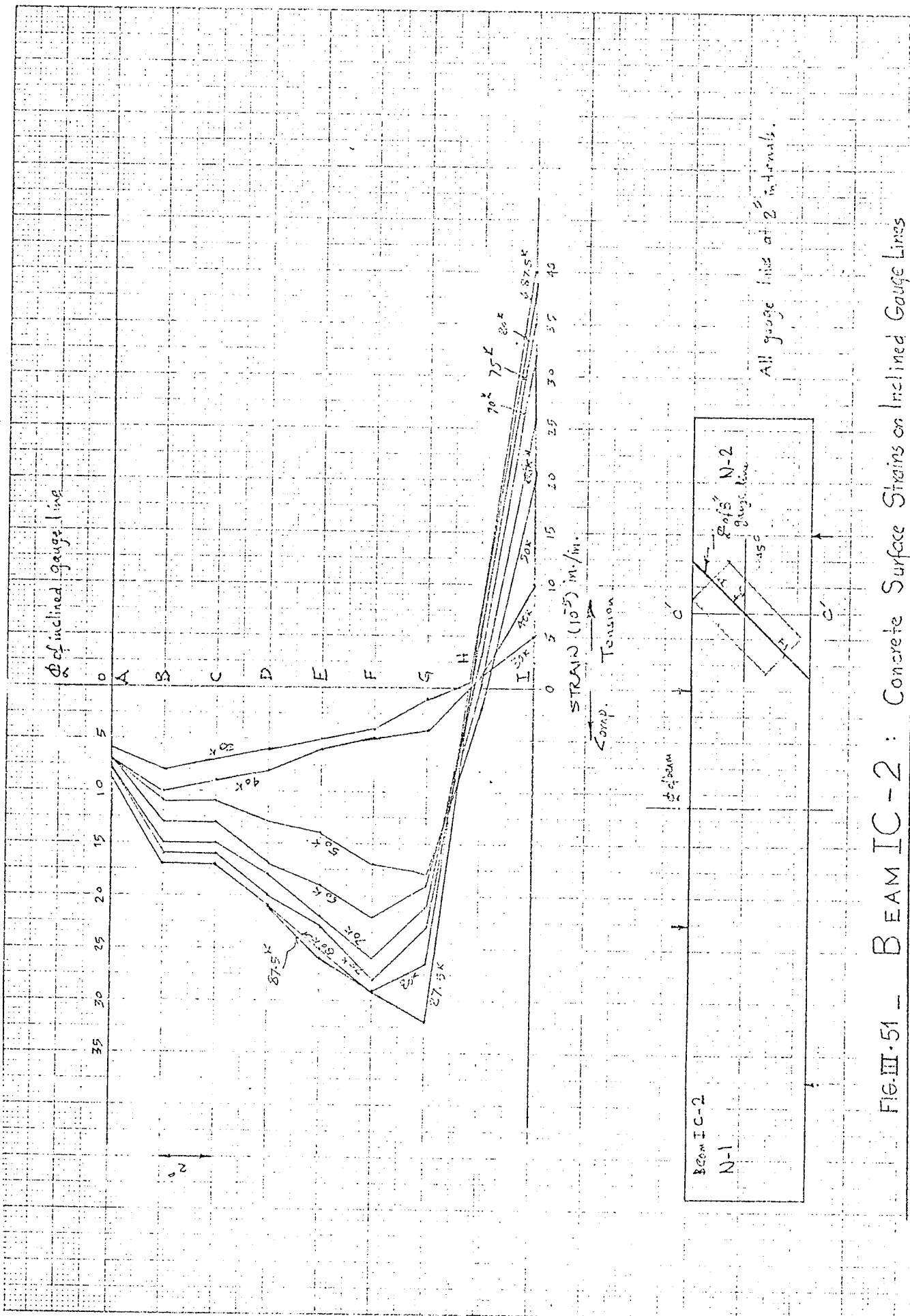


FIG. III-50 — BEAM IB-6: Concrete Surface Strain on Inclined Gauge Lines



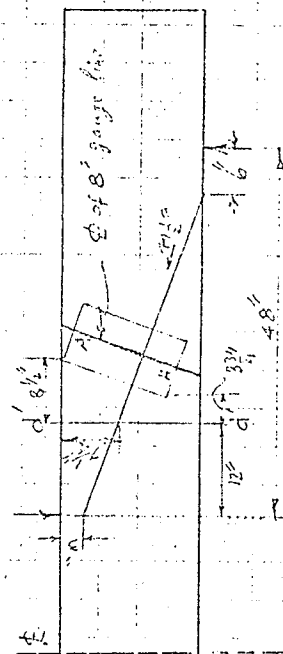
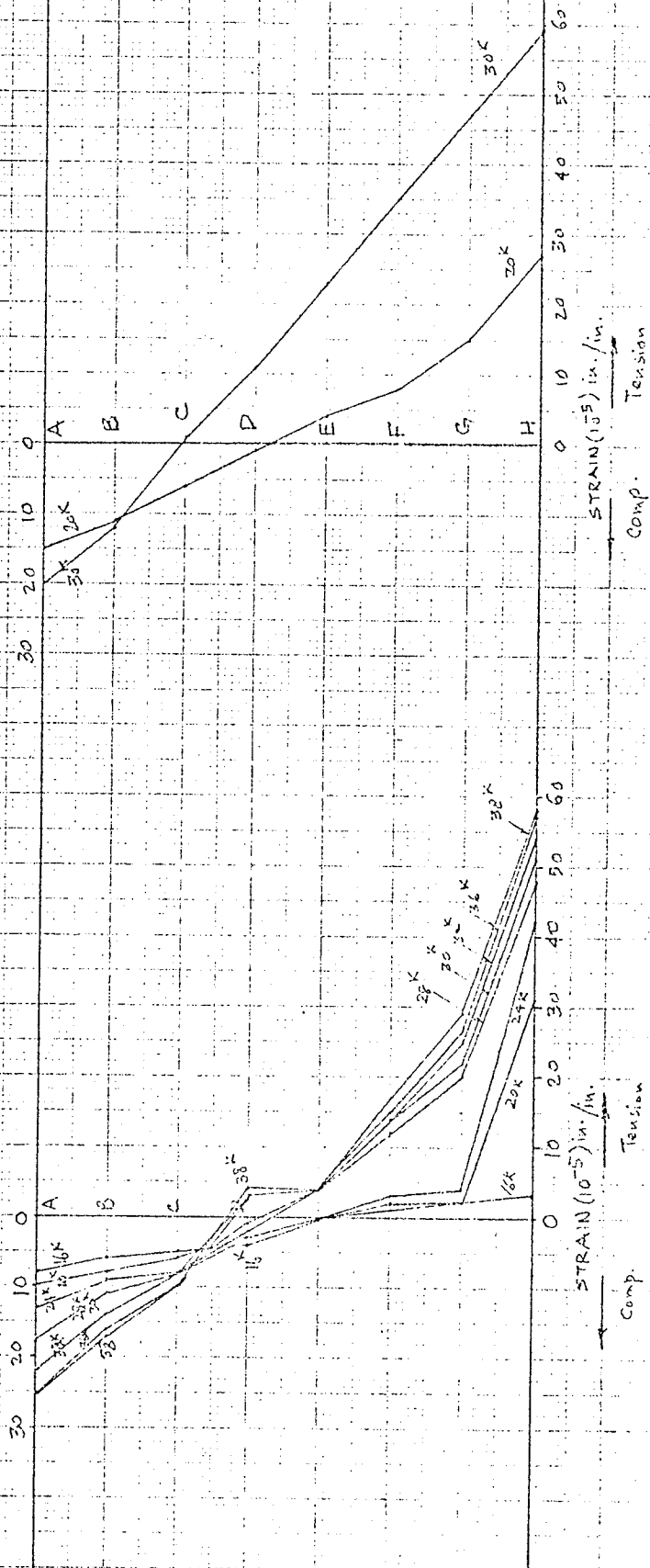


FIG. III-52 - Beam IC-5

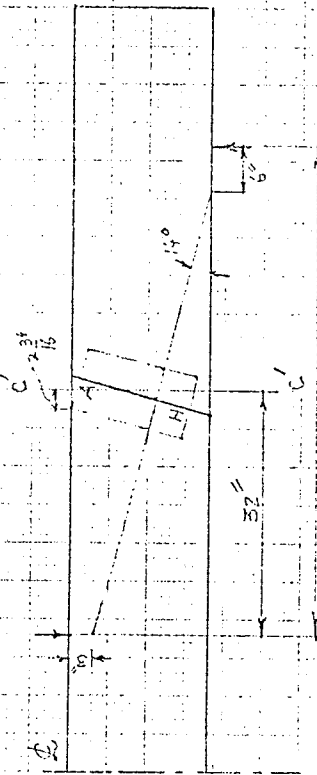


FIG. III-53 - Beam IC-6

BEAMS IC-5 & IC-6: Concrete Surface Strain on Inclined Gauge Lines

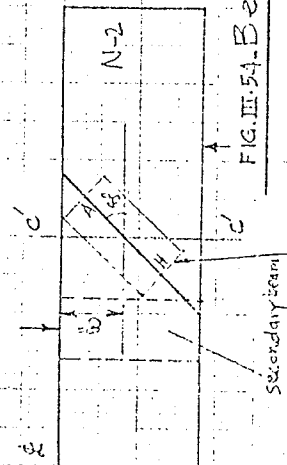
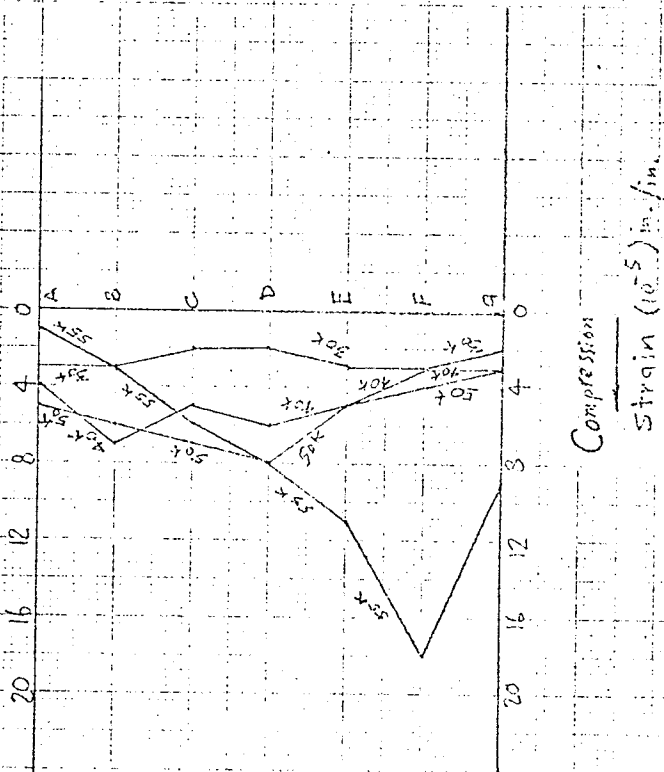


FIG. III-54-Beam IIA-2

Reading H-H could not be taken with DEMEC gauge, the locating disc on left being too close to Secondary beam.

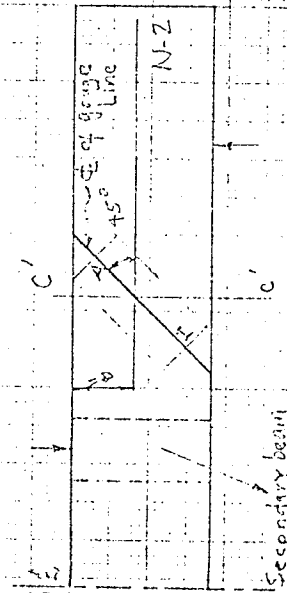
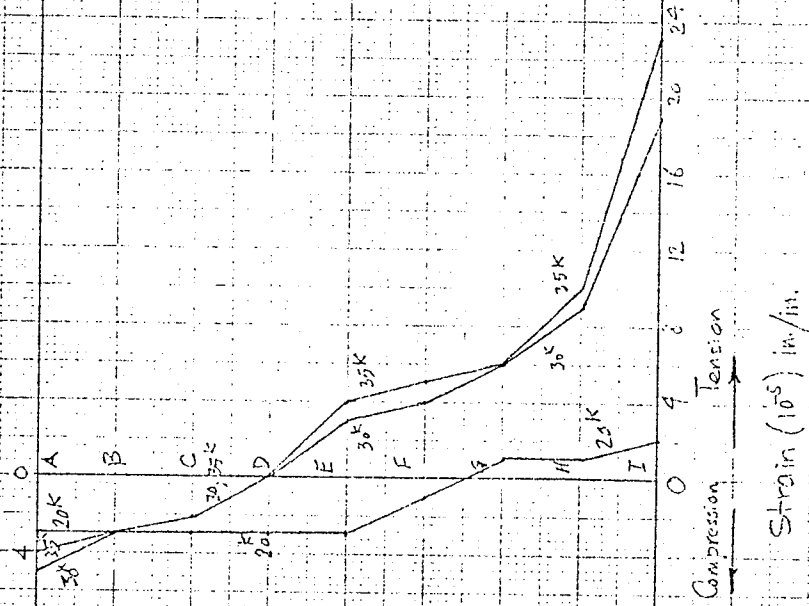


FIG. III-55-Beam IIA-4

Beams IIA-2 & IIA-4: Concrete Surface Strains on Inclined Gauge Lines

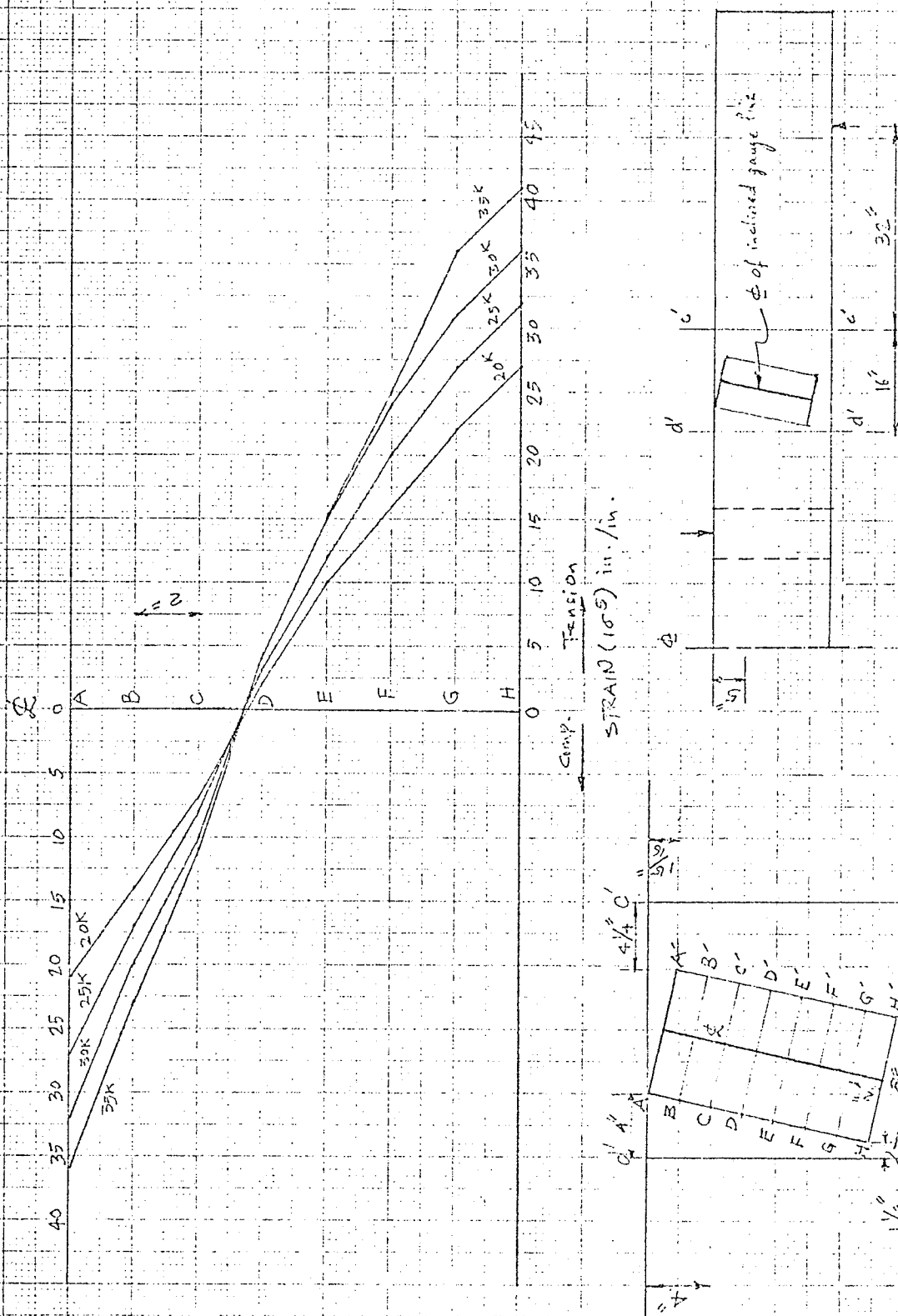


FIG. III-56 — Beam IIA-6: Concrete Surface Strain on Inclined Gauge Lines

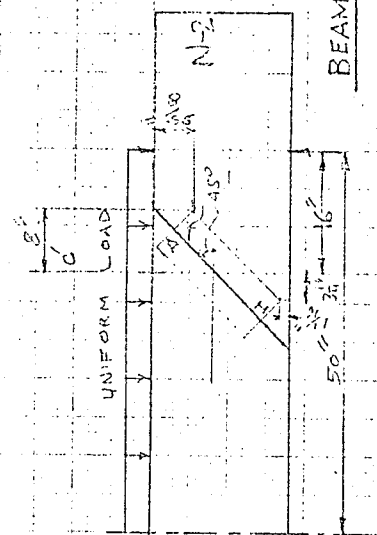
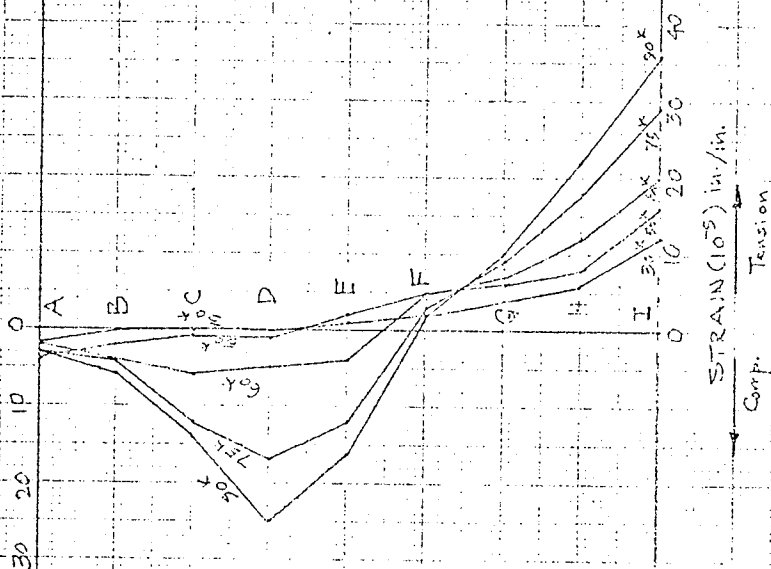


FIG. III-57

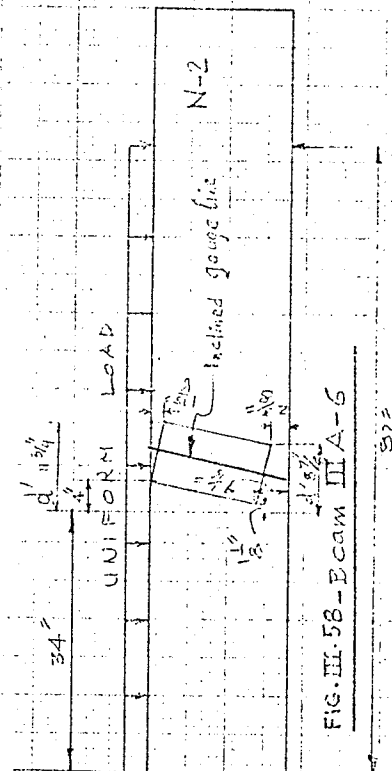
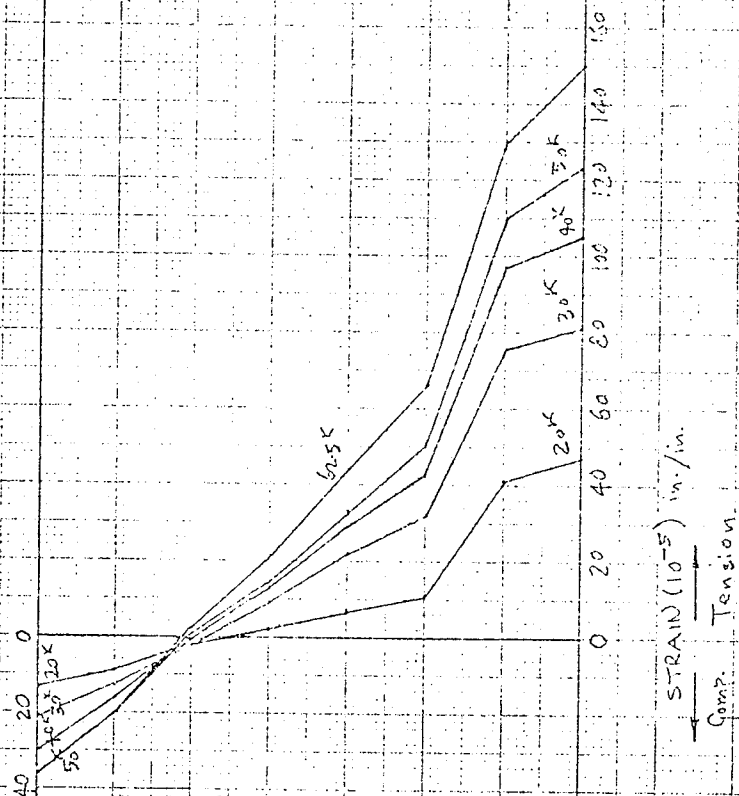


FIG. III-58-Beam IIIA-6

Beams IIIA-3 & IIIA-6: Concrete Surface Strains at Inclined Gauge Lines

III.4 DISPLACEMENTS RESULTING FROM BENDING OF CONCRETE CANTILEVERS AND ROTATION OF THE COMPRESSION ZONE

Horizontal displacements of the vertical sections throughout the beam tests were measured as follows.

Three horizontal lines, A, B and C at depths 2 in., 5 in., and 16 in. were run from the vertical axis of symmetry at midspan. [Section 5.5, Chapter 5]. The difference between the projected displacements of points at level C and those measured at this point, gives the total horizontal displacement of points at the level of the reinforcement due to bending of concrete cantilevers and rotations in the compression zone.

Results of these measurements for various beam tests are shown graphically in Figs.III.59 to III.73. No horizontal gauge lines were run for beams of series II due to the presence of secondary beams nor were these gauge lines run in the preliminary tests.

In all beams failing by shear compression, the displacements of vertical sections at the reinforcement level were found to be 3 to 4 times higher than the corresponding displacements in the diagonal tension failures. A substantial increase in displacement invariably occurred after critical diagonal cracking. Maximum displacements were generally recorded between the midspear span and the load point.

Results of individual beam tests are now briefly discussed. Location of gauge points is shown on plots of each beam.

BEAM IA-1 (Fig.III.59)

Upto critical diagonal cracking at a load of 50 kips, the displacements were generally small. At this load level, the displacement at C3 was 1.41×10^{-3} in., while that at C5 was 3.35×10^{-3} in. However, after critical diagonal cracking, these displacements increased considerably and though the beam was not loaded to failure, these displacements had relatively high values of 13.84×10^{-3} in. at C3 and 28.44×10^{-3} in. at C5 at a load of 180 kips.

BEAM IA-2 (Fig.III.60)

The displacements remained small upto major diagonal cracking, the maximum being 1.25×10^{-3} in. at a load of 40 kips. These displacements increased to 14.37×10^{-3} in. and 22.64×10^{-3} in. at a load of 60 and 70 kips respectively at the critical section (located at C4) as diagonal cracking developed.

BEAM IA-3 (Fig.III.61)

Maximum displacements of 7.92×10^{-3} in. (at C4) just prior to critical diagonal cracking increased to 13.89×10^{-3} in., 22.16×10^{-3} in., and 28.19×10^{-3} in., (at C5) at a load of 48, 60 and 70 kips respectively after the major diagonal crack occurred at a load of 45 kips.

BEAM IA-4 (Fig.III.62)

From a small displacement of 3.23×10^{-3} in. at a load of 30 kips, there was an increase in maximum displacement to

9.57×10^{-3} in. at a load of 37.5 kips before sudden diagonal tension failure of the beam. The displacement of 9.57×10^{-3} in. is comparable to the maximum displacement in beam IA-3 just prior to critical diagonal cracking. The displacement at failure in this beam, however, was about one-third of that at failure of beam IA-3.

BEAM IA-5 (Fig.III.63)

The displacements generally remained low in this beam, the maximum at a load of 30 kips being only 3.12×10^{-3} in.

BEAM IA-6 (Fig.III.64)

A maximum displacement of 7.20×10^{-3} in. at C5 was recorded at a load of 40 kips, near failure. Upto a load of 30 kips, the displacements remained fairly low, the maximum being only 1.79×10^{-3} in. This shows that substantial bending only occurred after significant flexural cracking. The ultimate displacement in this beam was about one-fourth of that for beam IA-2 at failure.

BEAM IA-7 (Fig.III.65)

The maximum displacement occurred at section C5 and at a load of 35 kips just prior to failure, it was 8.59×10^{-3} in. There was a significant increase in the value of displacement after a load of 30 kips.

BEAM IA-8 (Fig.III.66)

The maximum displacement developed at sections C5 and C11. At a load of 30 kips, just prior to failure, it was

8.03×10^{-3} in. at C5 and 13.17×10^{-3} at C11.

BEAM IB-6 (Fig.III.67)

The maximum displacement at a load of 35 kips was only 4.08×10^{-3} in.

BEAM IC-2 (Fig.III.68)

The maximum displacement was only 3.25×10^{-3} in. at a load of 40 kips prior to major diagonal cracking. Thereafter, it increased to a value of 26.05×10^{-3} in. at a load of 60 kips and 36.13×10^{-3} in. at a load of 80 kips. With a lower proportion of longitudinal reinforcement as compared to series IA, the ultimate displacement in this beam was significantly higher.

BEAM IC-5 (Fig.III.69)

A maximum displacement of 10.03×10^{-3} in. was recorded at a load of 36 kips. The displacement only became significant after diagonal cracking.

BEAM IC-6 (Fig.III.70)

A displacement of 4.69×10^{-3} in. was recorded at a load of 30 kips prior to failure in flexure.

BEAM IIIA-3 (Fig.III.71)

The maximum displacement was only 3.33×10^{-3} in. at a load of 50 kips as critical diagonal cracking developed. It increased rapidly thereafter and a high value of 30.83×10^{-3} in.

was recorded at a load of 90 kips before the beam failed at a load of 101 kips. This value is consistent with similar other beams failing in shear compression.

BEAM IIIA-6 (Fig.III.72)

The maximum displacement was only 8.13×10^{-3} in. at a load of 50 kips. Since the DEMEC readings at higher loads prior to failure are not available (the beam failed at 66.5 kips), it may have developed significant displacements after diagonal cracking.

BEAM IIIA-8 (Fig.III.73)

This beam failed at the appearance of a critical diagonal crack. The values of maximum displacement remain fairly low.

From the results of the horizontal displacements at the reinforcement level for all beam tests, it can be seen that large displacements invariably occurred after critical diagonal cracking and its stabilization. The final displacements in such beams near failure conditions were many times the displacements at failure for those beams which failed suddenly at the appearance of a diagonal crack.

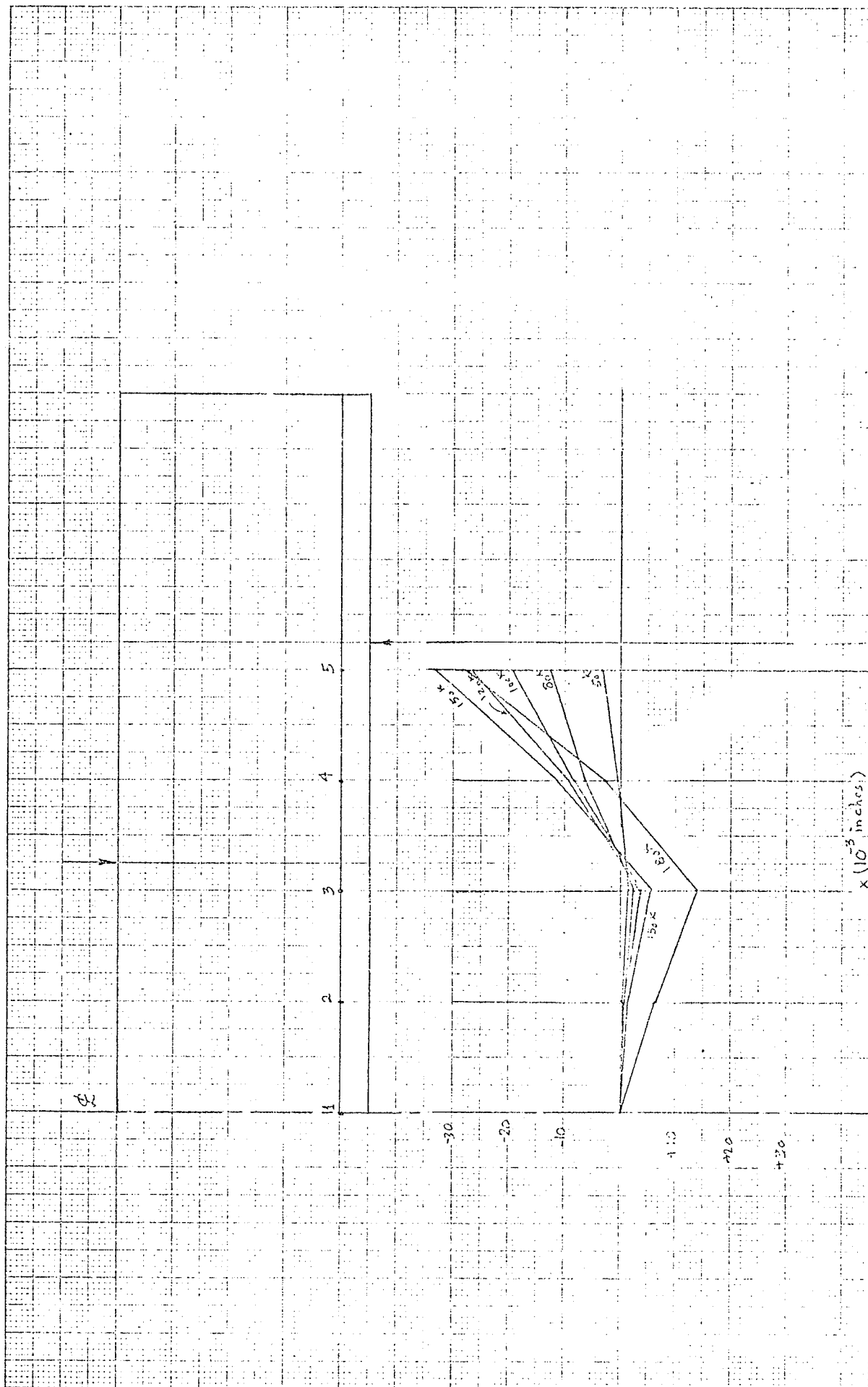


FIG. III-59 — BEAM IA-1 — Horizontal Displacement of Concrete Cantilevers

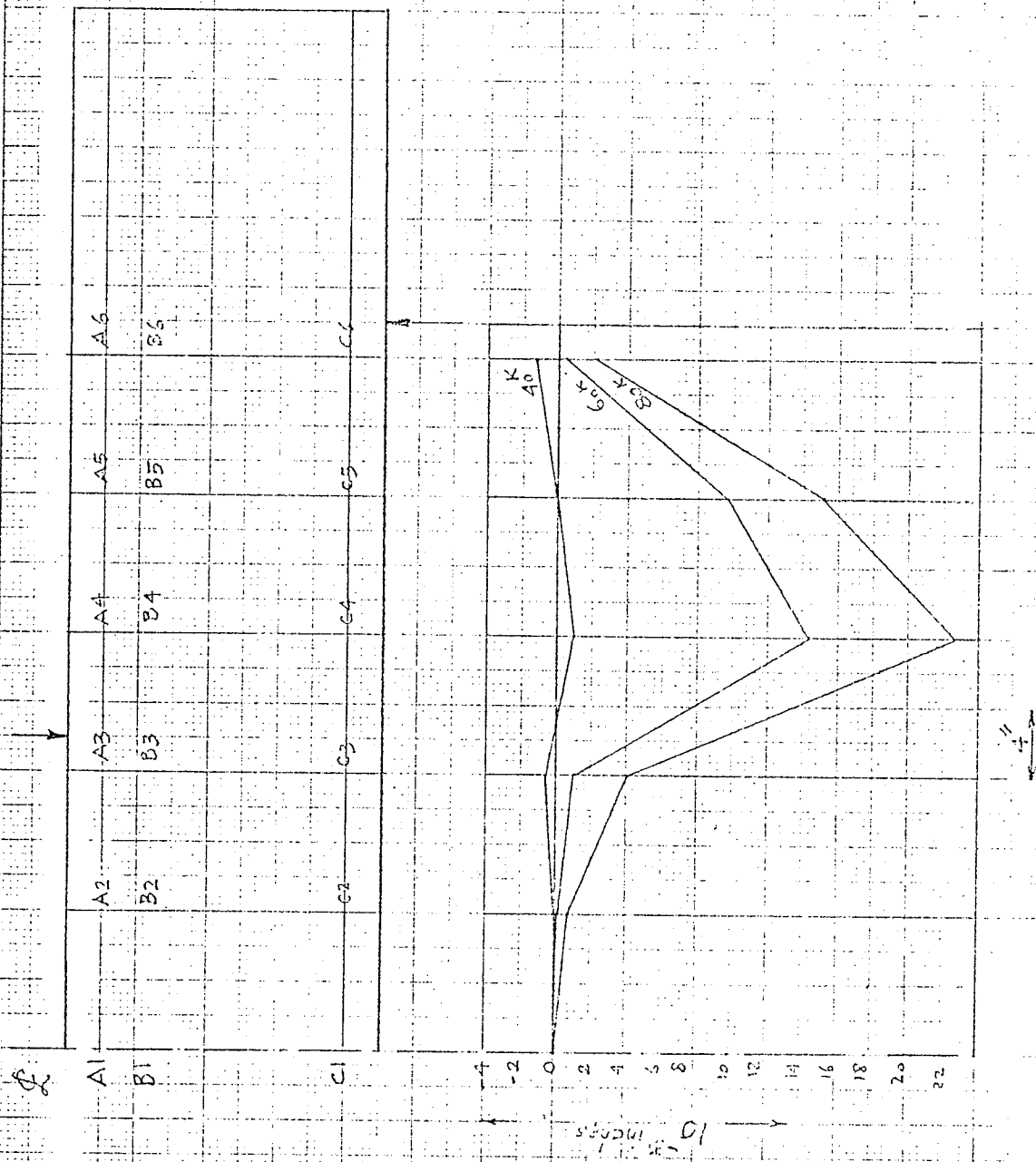


FIG. III-60 - Series IA: Horizontal Displacement of Concrete Cantilevers

BEAM IA-2

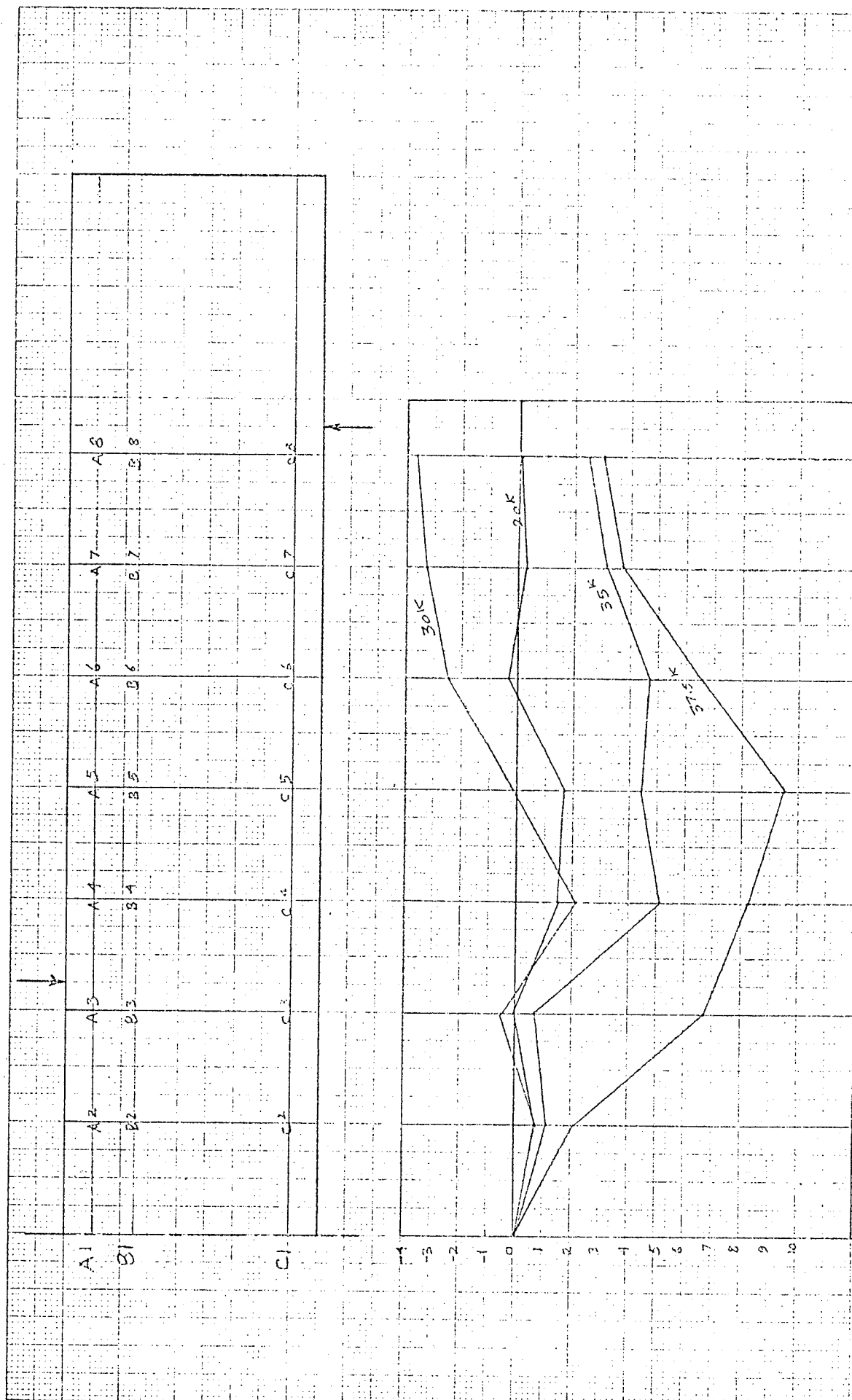


FIG. III-62 — Series IA: Horizontal Displacement of Concrete Cantilevers

BEAM IA-4

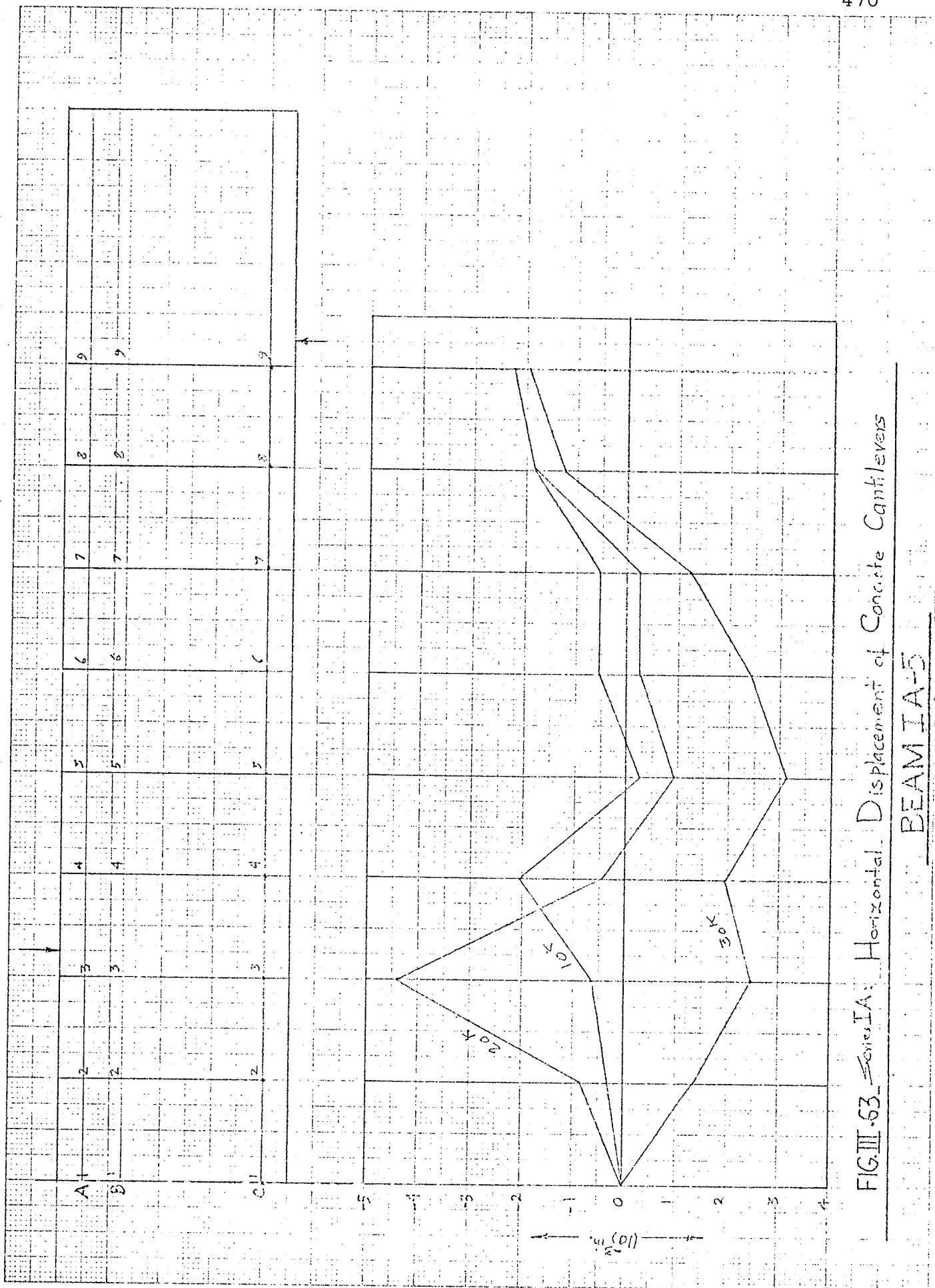


FIG. III-63. Series IA: Horizontal Displacement of Concrete Cantilevers

BEAM IA-5

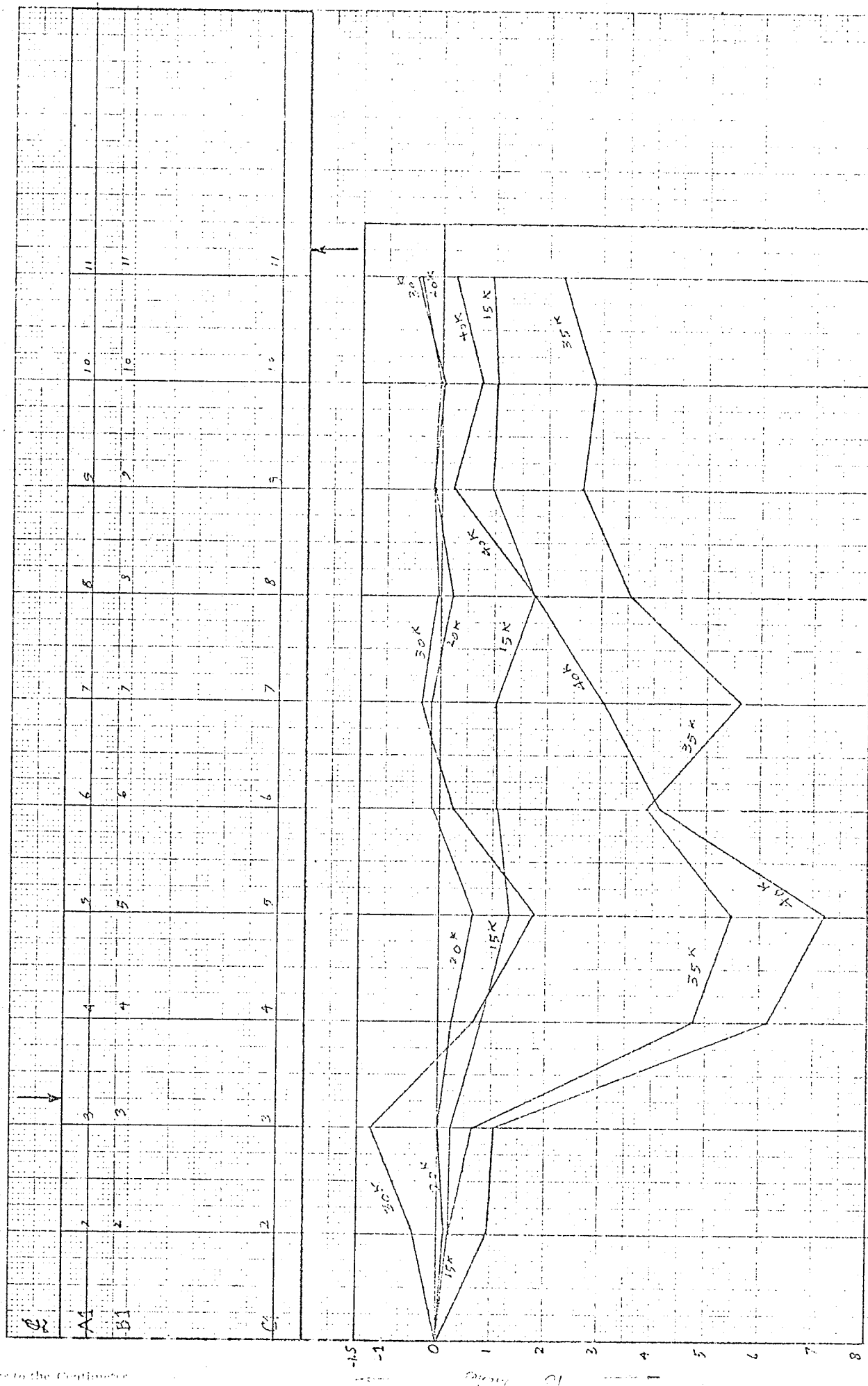


FIG. III.64— Series IA: Horizontal Displacement of Concrete Cantilevers
BEAM IA-6

L	↓												
	2	3	4	5	6	7	8	9	10	11	12	13	
A1	2	3	4	5	6	7	8	9	10	11	12	13	
B1	2	3	4	5	6	7	8	9	10	11	12	13	
C1	2	3	4	5	6	7	8	9	10	11	12	13	
→ 21													

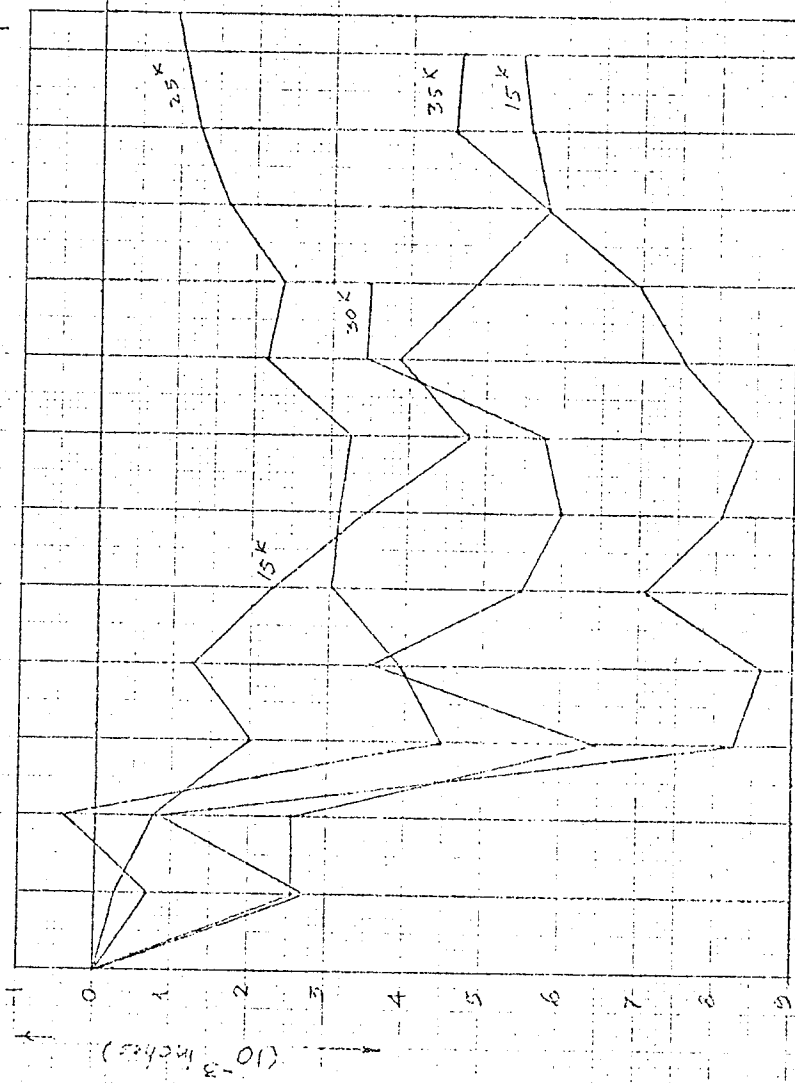


FIG. III-65 - Series IA: Horizontal Displacement of Concrete Cantilevers

BEAM IA-7

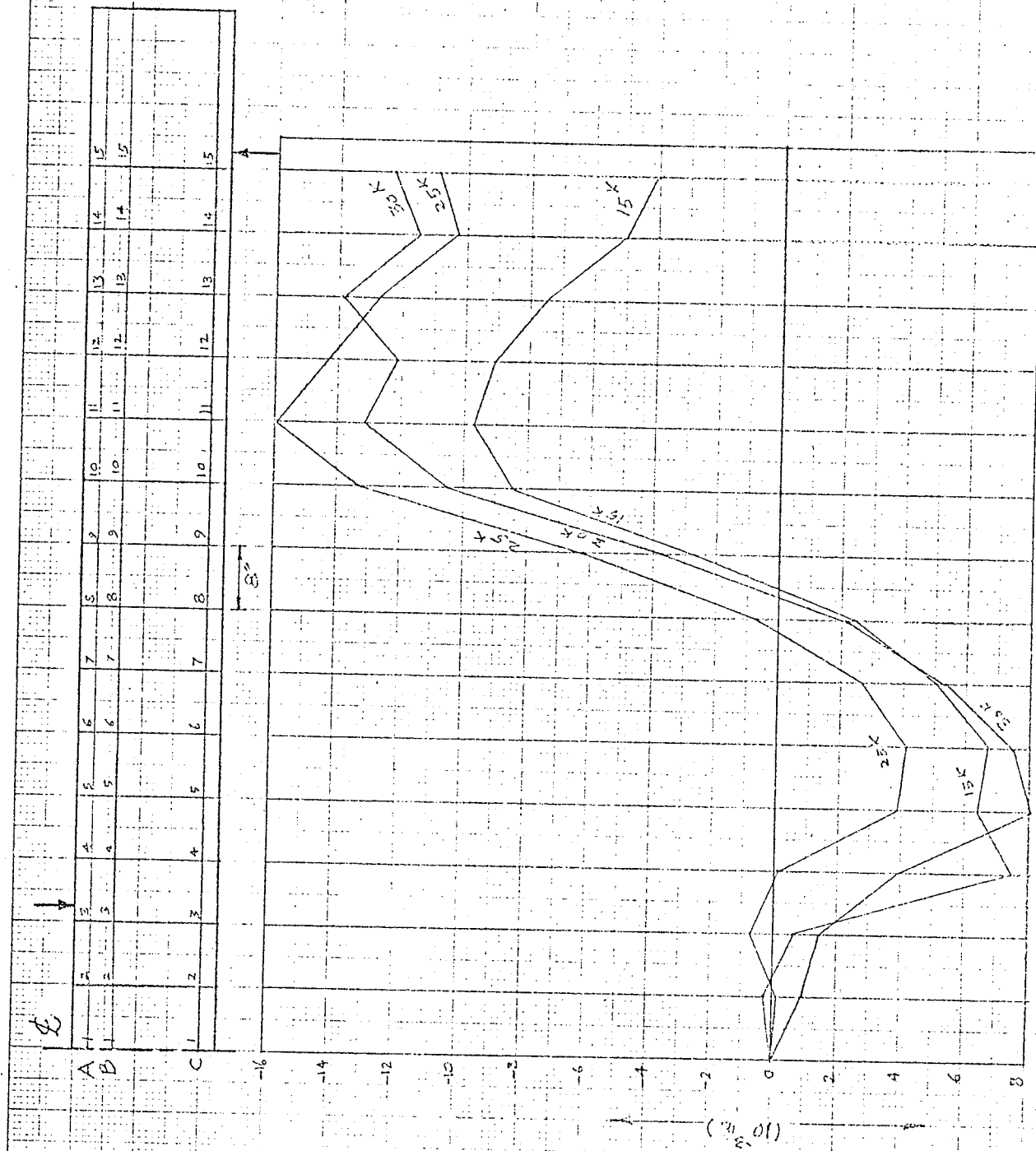


FIG. III-66. SERIES IA: Horizontal Displacement of Concrete Cantilevers

BEAM IA-8

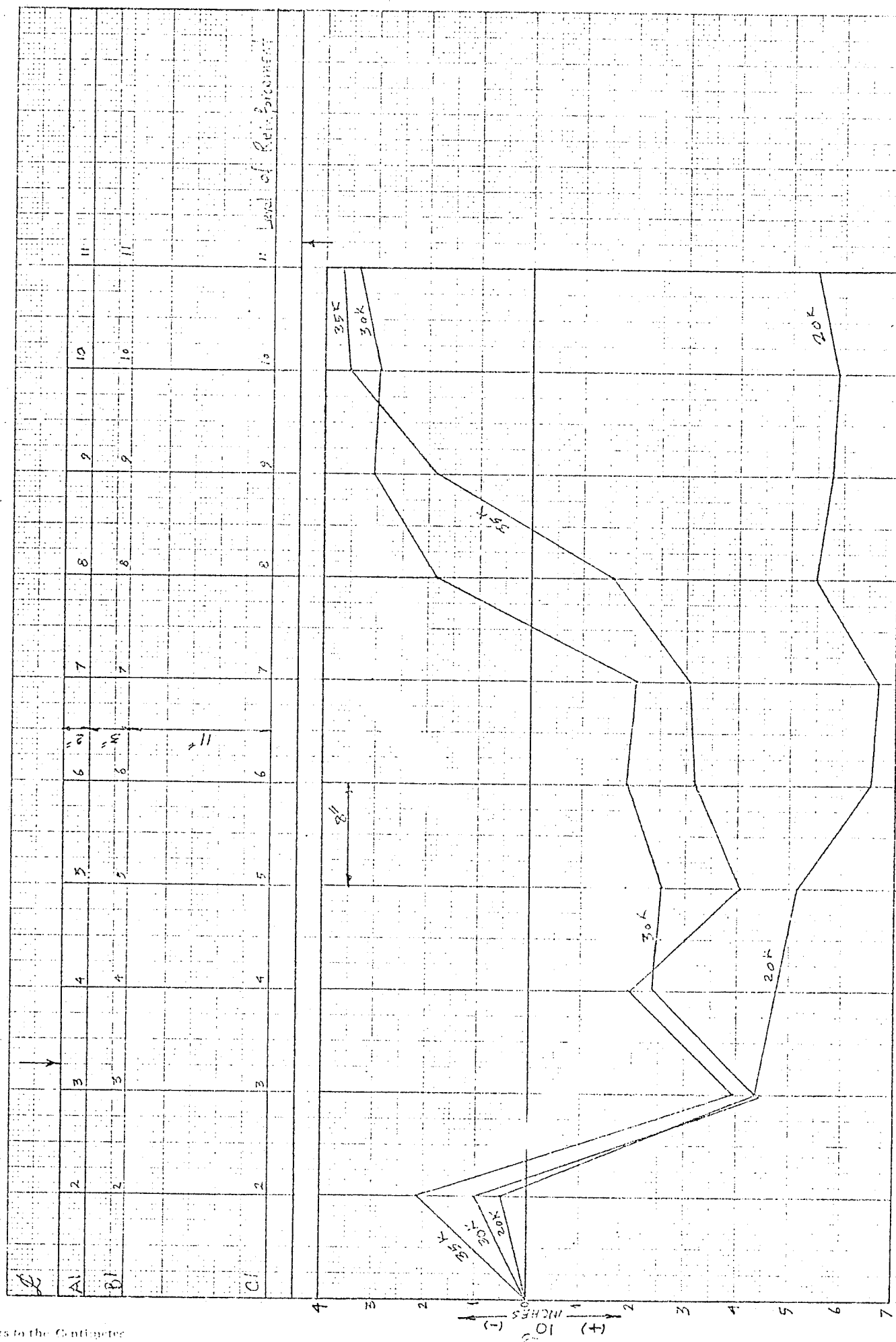
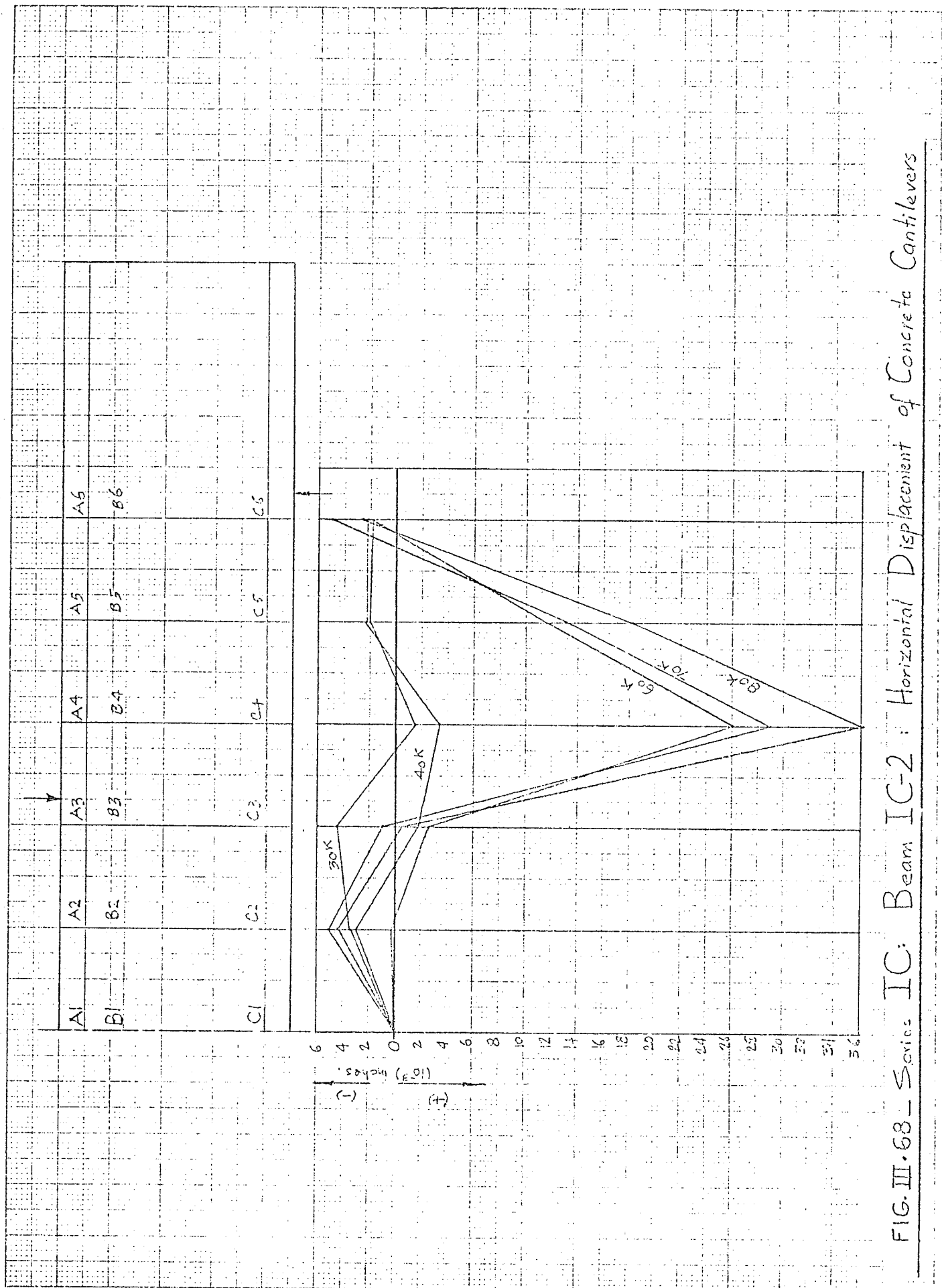


FIG. III.67 - SERIES B: BEAM IB-6 — Horizontal Displacement of Concrete Cantilevers



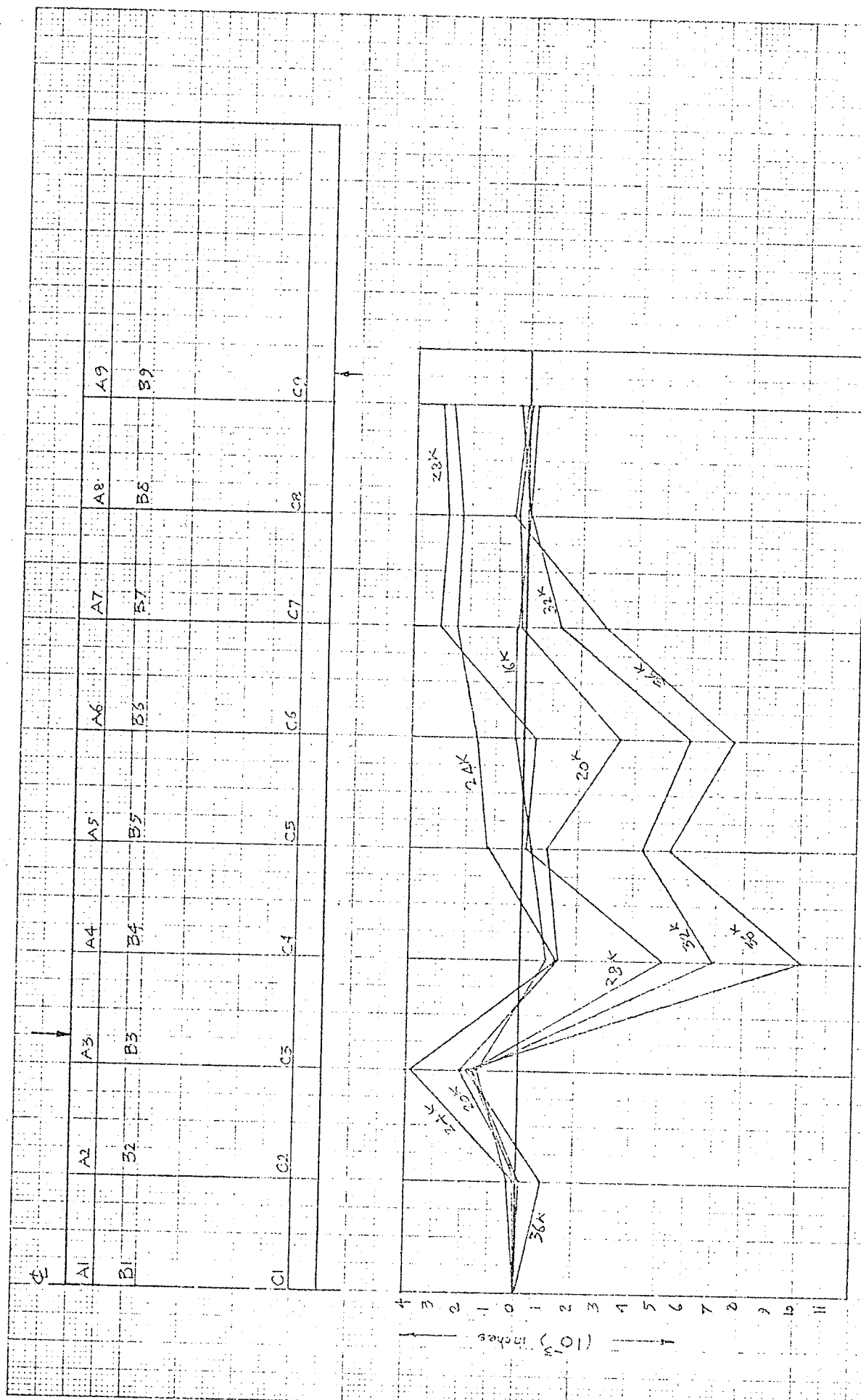
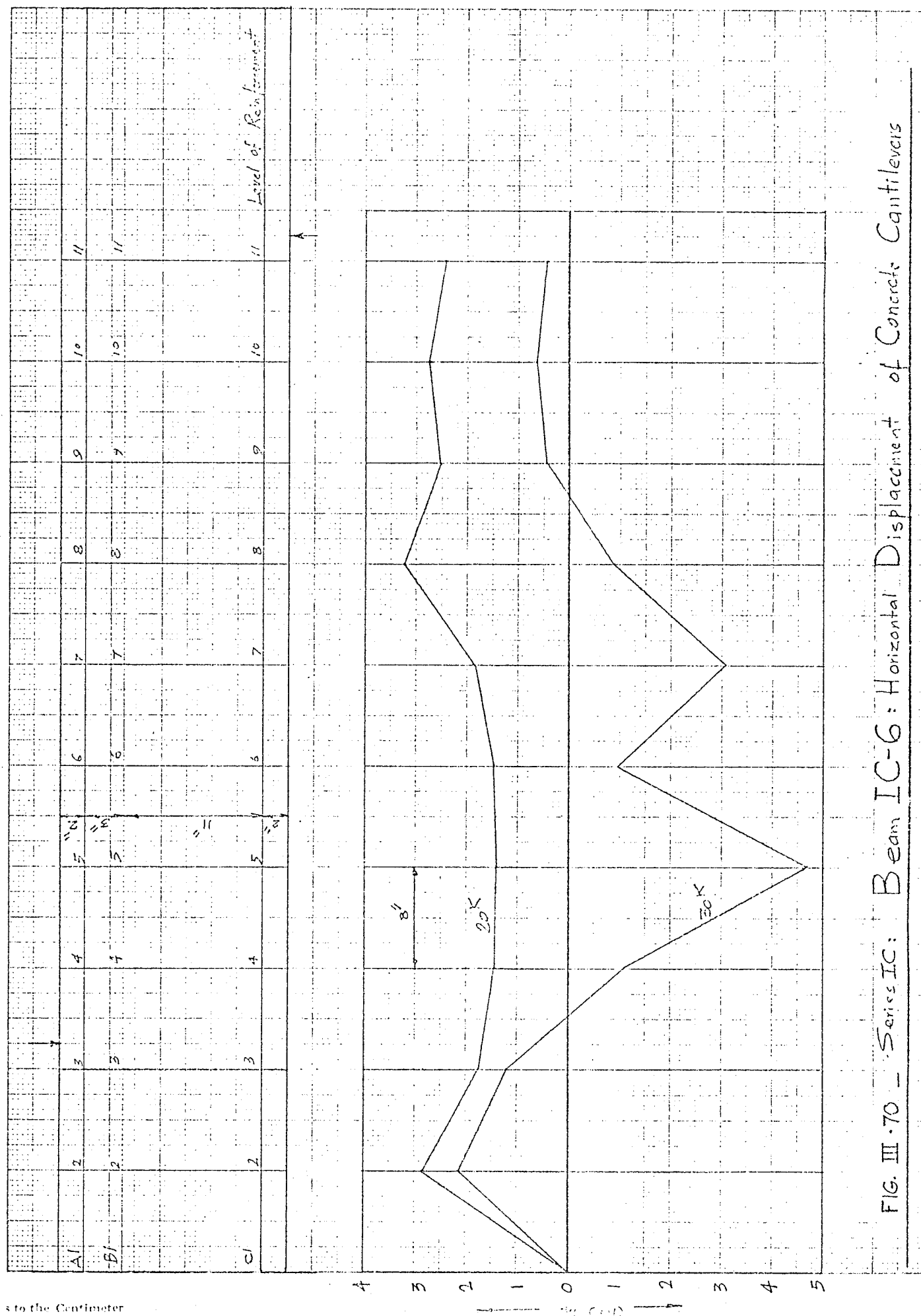


FIG. III.69 - Series IC: Beam IC-5: Horizontal Displacement of Concrete Cantilevers



to the Centimeter

A1	A2	A3	A4	A5	A6	A7
B1	B2	B3	B4	B5	B6	B7
C1	C2	C3	C4	C5	C6	C7

N-2

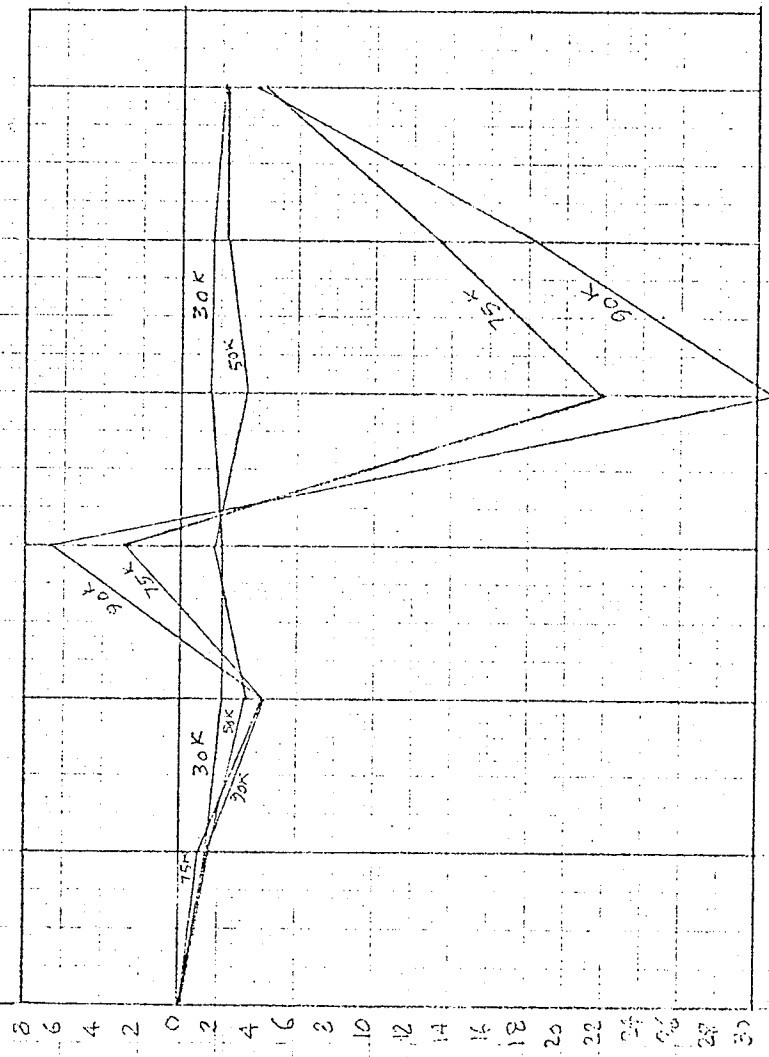


FIG. III.71 — SERIES III A: Horizontal Displacement of Concrete Cantilevers

BEAM III A-3

A1	A2	A3	A4	A5	A6	A7	A8	A9	A10	A11
B1	B2	B3	B4	B5	B6	B7	B8	B9	B10	B11
C1	C2	C3	C4	C5	C6	C7	C8	C9	C10	C11

N-2

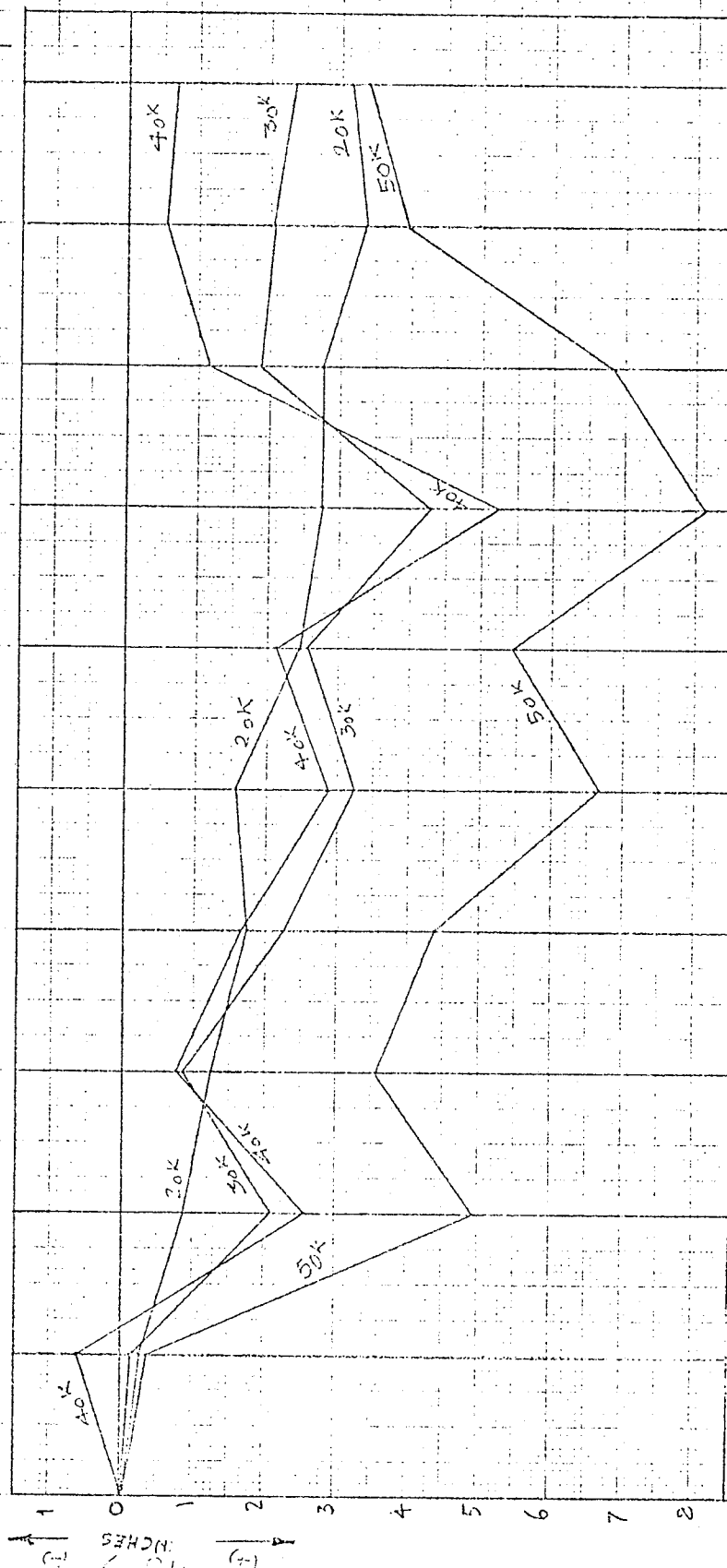


FIG. III-72 Series IIIA: Horizontal Displacement of Concrete Cantilevers - Beam III A-6

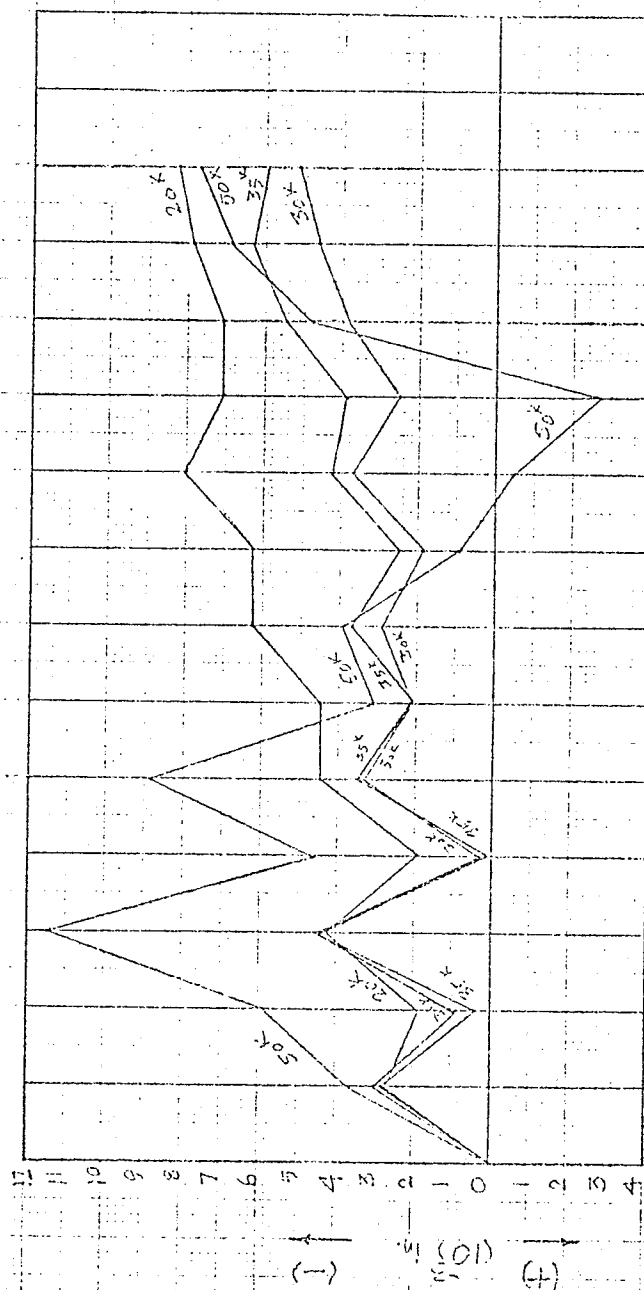


FIG. III.73 — Series III A: Horizontal Displacement of Concrete Cantilevers
Beam III A-8

III.5 CRACK WIDTHS AND INTERNAL ROTATIONS

Crack widths and internal rotations for individual beams were calculated from equations 3.4 and 3.5 (presented in Chapter 5) and are reported in this section.

III.5.1 SERIES IA

(i) BEAM IA-1

Results of this beam have already been discussed in Chapter 5.

(ii) BEAM IA-2

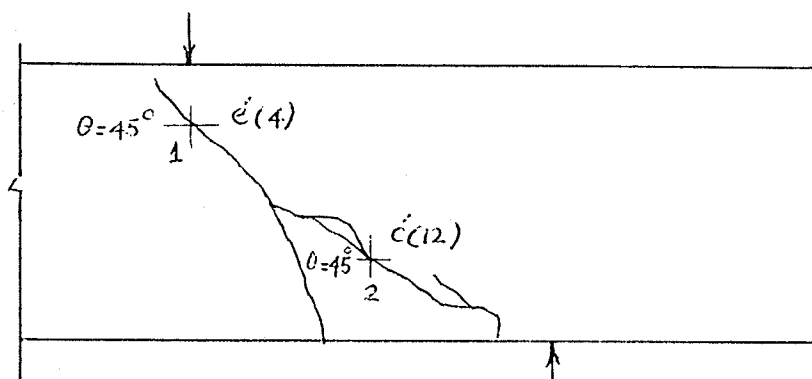


Fig.III.74 - BEAM IA-2: DEMEC ROSETTES
AND DIAGONAL CRACK

Figure III.74 shows that the diagonal crack crossed the DEMEC rosetts at $\epsilon'(4)$ and $\epsilon'(12)$ respectively, marked by points 1 and 2. In the rosette at $\epsilon'(12)$, only the inclined gauge line was crossed by the crack from which the crack width is found to be 14.24×10^{-3} in. and 25.274×10^{-3} in. at a load of 60 and 80 kips respectively. This shows progressive

widening of the crack after critical cracking. Further, the readings of the rosette at $\epsilon'(4)$ gives a crack width of 3.56×10^{-3} in. at 80 kips. Calculation of internal rotation from these crack widths gives θ_c as 1.46×10^{-3} in. radians. However, it is possible that the internal rotation was larger since the diagonal crack had branched off in the lower regions.

Inclined gauge line readings between the points the diagonal cracks cross them also show a rapid increase of crack width after critical diagonal cracking.

(iii) BEAM IA-3*

Failure did not occur on the side DEMEC gauges were placed. The only point where the critical diagonal crack crossed the DEMEC rosettes was $c'(12)$. Since the angle of the crack at this point was 45° , the 45° gauge reading perpendicular to the crack gives the crack width directly. It varied as follows:

Load (Kips)	40	45	46	47	48	52	54	60	70
$c_w (10^{-3})$ in.	2.838	10.160	16.086	18.128	19.920	22.806	25.000	31.324	41.632

Critical diagonal cracking occurred at a load of 45 kips. The width of crack increased rapidly at this stage with small increments of load. Maximum crack width at $c'(12)$ at 70 kips

* Where a sketch showing critical cracks does not accompany the description, refer to appendix II.

just prior to failure was 41.6×10^{-3} inches, which shows that the cracks had widened considerably. The points where this crack crossed inclined gauge lines between EF* and E'F'* give the following crack widths.

Crack Width (10^{-3}) Inches

Load (Kips)	40	45	48	52	54	60	70
$c_w(EF)$	1.29	10.20	22.56	27.72	31.50	40.20	59.40
$c_w(E'F')$	6.43	17.09	31.50	41.60	40.10	52.60	68.76

The width of crack between points E'F' was approaching .07 inches prior to failure. At the same time, considerable increase of compressive strain at top fibers under the load point was recorded.

(iv) BEAM IA-4

The diagonal crack causing ultimate failure only appeared at 37.5 kips and failure occurred at 39.7 kips. The width of this crack at c'(8) was only 1.74×10^{-3} in. prior to failure. One other flexural crack crossed d'(12), showing that its width remained constant at 2.14×10^{-3} in. from 25 kips to failure.

* Plots of inclined gauge line.

The diagonal crack close to the crack causing failure crossed the inclined gauge lines between H'I'* at 20 kips. The width of this crack increased from 0.85×10^{-3} in. at 20 kips to 2.64×10^{-3} in. at 30 kips and 3.44×10^{-3} in. at 37.5 kips. It suggests that the width of cracks and corresponding internal rotations remained small until the failure of the beam.

(v) BEAM IA-5

Failure was extremely sudden at the appearance of the critical diagonal crack and no significant rotations of the compression zone occurred. The maximum calculated crack width was only 0.55×10^{-3} inches prior to failure.

(vi) BEAM IA-6

No significant diagonal crack appeared on the side DEMEC gauges were placed. Only one rosette was crossed at c'(12), giving a maximum crack width of 4.5×10^{-3} inches prior to failure.

(vii) BEAM IA-7

The maximum crack width recorded on the side of beam where DEMEC gauges were placed was only 2.84×10^{-3} inches. Cracks did not open up and failure was sudden which occurred on the other end of the beam.

* Plots of inclined gauge line.

(viii) BEAM IA-8

No significant diagonal crack occurred on the side DEMEC gauges were placed and the maximum calculated width of flexural cracks was only 5.5×10^{-3} in. before sudden failure of the beam.

III.5.2 SERIES IB

Only one beam IB-6, had DEMEC gauges. Failure occurred extremely suddenly, crossing $c'(4)$ only at failure. No readings of the width of this crack prior to failure could be taken. Other smaller flexural cracks crossed gauge rosettes at $c'(12)$ and $d'(8)$. Maximum calculated width of crack at $c'(12)$ was only 5.58×10^{-3} in. while that at $d'(8)$ was only 3.48×10^{-3} in.

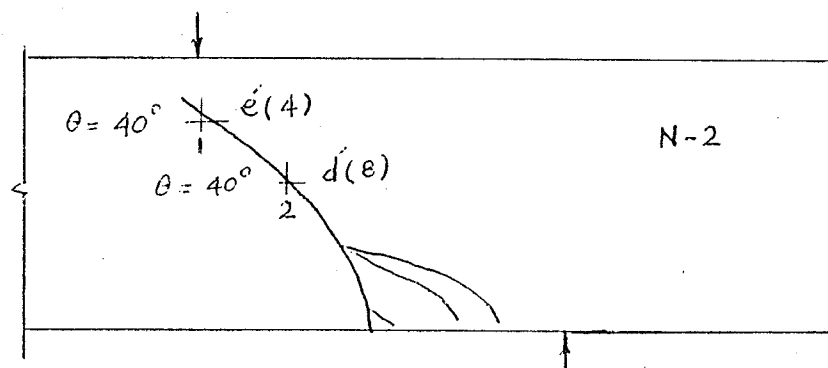
III.5.3 SERIES IC(i) BEAM IC-2

Fig.III.75 - BEAM IC-2: DEMEC ROSETTES AND DIAGONAL CRACK

Though failure occurred on end N1, a major inclined crack existed on end N2 where DEMEC gauges were used. Fig.III.75 shows the critical crack which crossed rosettes at $e'(4)$ and

$\bar{d}(8)$. A smaller diagonal crack crossed rosette at $\bar{d}(12)$ while a flexural crack under load point crossed the rosette at $\bar{e}(12)$. Critical diagonal crack was observed at a load of 50 kips.

Point $\bar{e}(4)$ gives the following crack widths.

$$\theta = 40^\circ$$

Load (Kips)	50	60	70	80
$c_w (10^{-3})$ in.	4.78	6.87	13.89	14.54

Point $\bar{d}(8)$ gives the following crack widths.

$$\theta = 40^\circ$$

Load (Kips)	60	70	80
$\delta_v (10^{-3})$ in.	16.234	21.414	26.792
$\delta_h (10^{-3})$ in.	10.956	13.844	16.732
$\Delta (10^{-3})$ in.	19.85	25.52	31.58
θ_1	$6^\circ 0'$	$70^\circ 10'$	$8^\circ 0'$
$c_w (10^{-3})$ in.	19.72	25.35	31.22

A maximum crack width of 31.22×10^{-3} in. was recorded at a load of 80 kips.

Diagonal cracks also crossed the inclined gauge lines. The main diagonal crack crossed the line between points FG* and F'G'*, giving the following crack widths.

* Plots of inclined gauge lines.

Load (Kips)	50	60	70	75	80	87.5
$c_w(FG) 10^{-3} \text{ in.}$	13.35	19.42	25.25	28.39	31.67	43.77
$c_w(F'G') 10^{-3} \text{ in.}$	16.13	23.26	30.78	35.71	39.09	54.38

From Fig.III.75, it can be seen that the main diagonal crack is split into various portion at its lower extremity. One of these cracks crosses the inclined gauge line between $G'H'^*$. A smaller diagonal crack under the main crack crosses the inclined gauge line between HI^* . The above table gives the following crack widths.

Load (Kips)	40	50	60	70	75	80	87.5
$c_w(G'H') 10^{-3} \text{ in.}$	4.43	7.07	7.57	7.92	8.32	8.32	13.74
$c_w(HI) 10^{-3} \text{ in.}$	3.88	4.58	4.43	4.58	4.78	4.93	4.83

From above, it can be seen that while the width of the main diagonal crack keeps on increasing, the lower diagonal crack increases in width very slowly, remaining almost constant in width from 50 kips onwards, when significant widening of main crack occurred. The maximum recorded width of the main diagonal crack at the inclined gauge line $F'G'^*$ occurred at 87.5 kips and was 54.38×10^{-3} inches. Calculations of internal rotation based on crack widths at $d(8)$ and the point between inclined gauge line $F'G'^*$ suggest that the maximum rotation was

* Plots of inclined gauge lines.

2.86×10^{-3} radians close to failure conditions. The width of cracks at $\epsilon'(4)$ was, however, larger than that compatible with the assumed centre of rotation located at the tip of the diagonal crack.

(ii) BEAM IC-5

Inclined cracking on end N2 of the beam where DEMEC gauges were placed remained insignificant. One flexural crack crossed $d'(12)$, recording a maximum crack width of 4.23×10^{-3} in. at 36 kips, just prior to failure of the beam. Another inclined crack crossed the inclined gauge line between $G'H'$ giving a maximum crack width of 6.2×10^{-3} in. at 38 kips. The beam failed at 40.2 kips with a diagonal crack on side N1. Crack widths remained small prior to failure of the beam.

(iii) BEAM IC-6

This was the only beam recording flexural failure. Widths of cracks remained small. One gauge rosette, $c'(8)$ showed a maximum crack width of 2.5×10^{-3} in. while inclined gauge line data gave a maximum crack width of 3.68×10^{-3} in.

III.5.4 SERIES IIA

(i) BEAM IIA-2

Only at 55 kips, just prior to premature failure, did the failure crack cross the gauge lines at $c'(12)$ and $d'(8)$. The maximum width of crack at this stage was 9.96×10^{-3} in. and 4.33×10^{-3} in. respectively at the above two locations. A

lower crack crossed $d'(12)$ at 55 kips giving a width of 3.39×10^{-3} in.

(ii) BEAM IIA-2 (b)

This beam alone had DEMEC rosettes at the level of the reinforcement as well. The critical diagonal crack developed at a load of 66 kips while failure occurred at a load of 81 kips. The diagonal crack crossed DEMEC rosette at $b'(16)$, showing a width of 6.47×10^{-3} in. at 66 kips. Another crack at $c'(16)$ was 3.83×10^{-3} in. wide at the same load. The width of cracks generally remained small, though the inclined gauge line data gave higher widths of cracks at sections removed from the tip of the diagonal crack. The widths immediately preceding failure, however, were not comparable to those recorded for shear-compression failures in beams loaded directly over their compression faces.

(iii) BEAM IIA-4

Diagonal failure was so sudden that the diagonal crack causing failure developed only at failure load above the existing flexural cracks. The maximum width of existing cracks did not exceed 2.98×10^{-3} inches.

(iv) BEAM IIA-6

Diagonal failure occurred suddenly on end N1 of the beam, the failure crack being an extension of two pre-existing flexural cracks. On end N2 of the beam where DEMEC gauges were placed, no major diagonal crack existed. Flexural cracks crossed $c'(12)$, $d'(12)$ and $e'(8)$ but the width of these cracks in

no case exceeded 5.83×10^{-3} in. which was observed at $d'(12)$. Significant internal rotations, therefore, did not take place.

III.5.5 SERIES IIIA

(i) BEAM IIIA-3

The results of this beam have already been discussed in Chapter 5.

(ii) BEAM IIIA-6

The major diagonal cracking occurred at 50 kips. At this load level the cracks were of the order of 2×10^{-3} inches. Enough DEMEC data is not available to find widths of cracks prior to failure at 66.5 kips, though the observations during the test clearly pointed towards opening of the cracks.

(iii) BEAM IIIA-8

The beam failed on end S2 where DEMEC gauges were placed on this beam. Critical diagonal cracking occurred just prior to failure and at that stage the maximum width of crack at $c'(8)$ was only 1.64×10^{-3} inches.

The results presented in this section clearly point out towards large internal rotations which take place in beams after the stabilization of the diagonal crack. These results are consistent with the conceptual model of diagonal failure presented in Chapter 3.

III.5 DEFLECTIONS OF BEAMS

Plots of deflections at midspan and under load point for various beam tests are shown in Figs. III.76 to III.85. Deflection readings are tabulated in Appendix II.

In diagonal tension failures, the deflections increased slightly more rapidly near failure but gave no advance warning of impending failure. However, in beams where a critical diagonal crack was stabilized, the deflections generally increased faster after critical diagonal cracking.

The deflections of comparable beams in different series increased with a decrease in the percentage of longitudinal reinforcement. The failure of beams in series IC ($p = 1.03\%$) was preceded by large deflections. One beam failed in flexure while two beams failed diagonally. In both of these beams large deflections were recorded before failure.

Beams IIA-2 and IIA-2(b) were alike except for a higher compressive strength of concrete in beam IIA-2(b). The deflections of this stiffer beam were consistently less than those of beam IIA-2 at all stages of loading.

Beams with uniform loading also show a higher rate of increase of deflections after critical diagonal cracking. Loading through secondary beams did not affect the beam deflections in any significant manner.

FIGURE 76: LOAD VS MIDSPAN DEFLECTION

(SERIES IA)

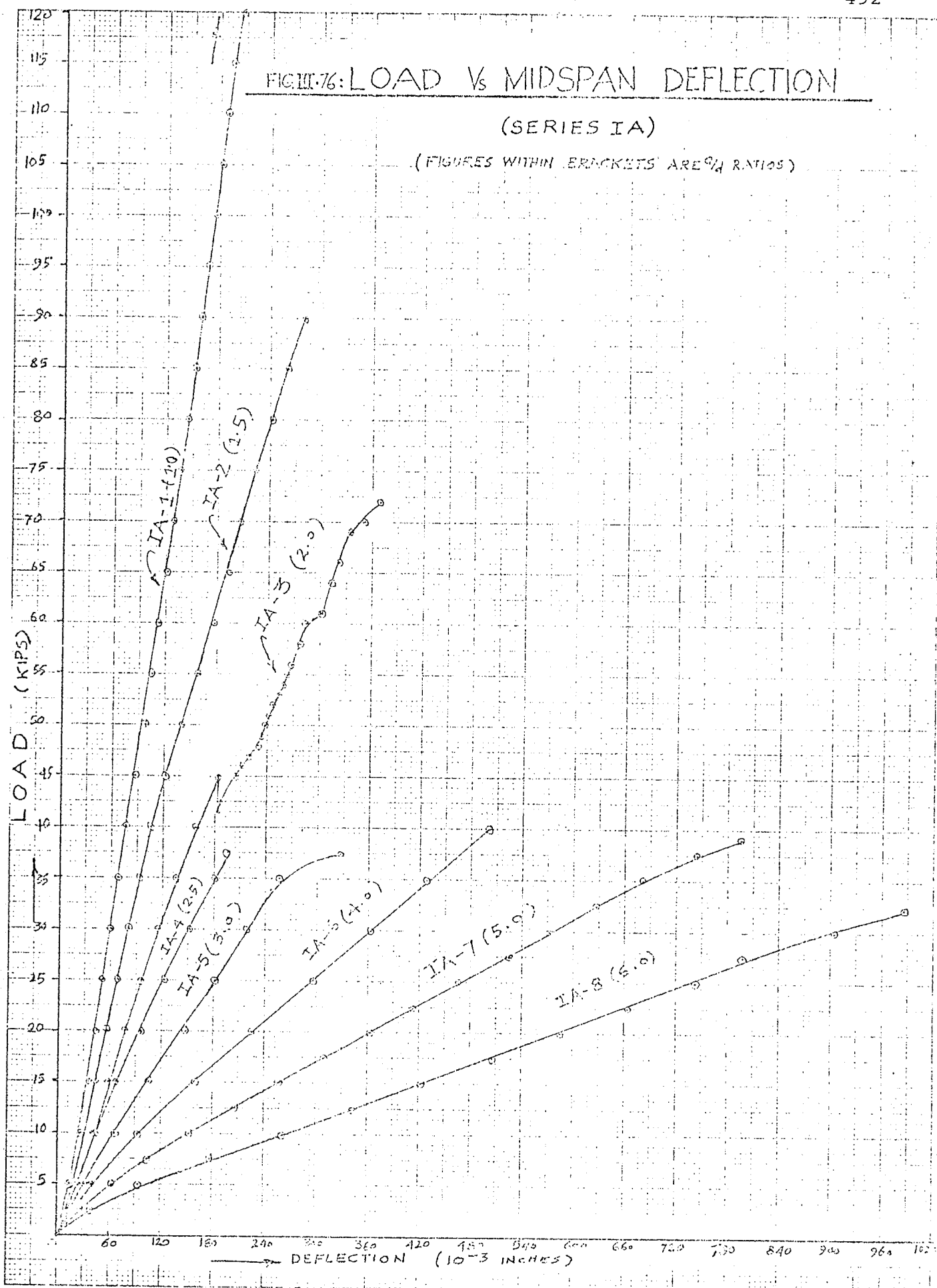
(FIGURES WITHIN BRACKETS ARE g/d RATIOS)

FIGURE 77 - LOAD V_s DEFLECTION (UNDER LOAD POINT)

(SERIES IA)

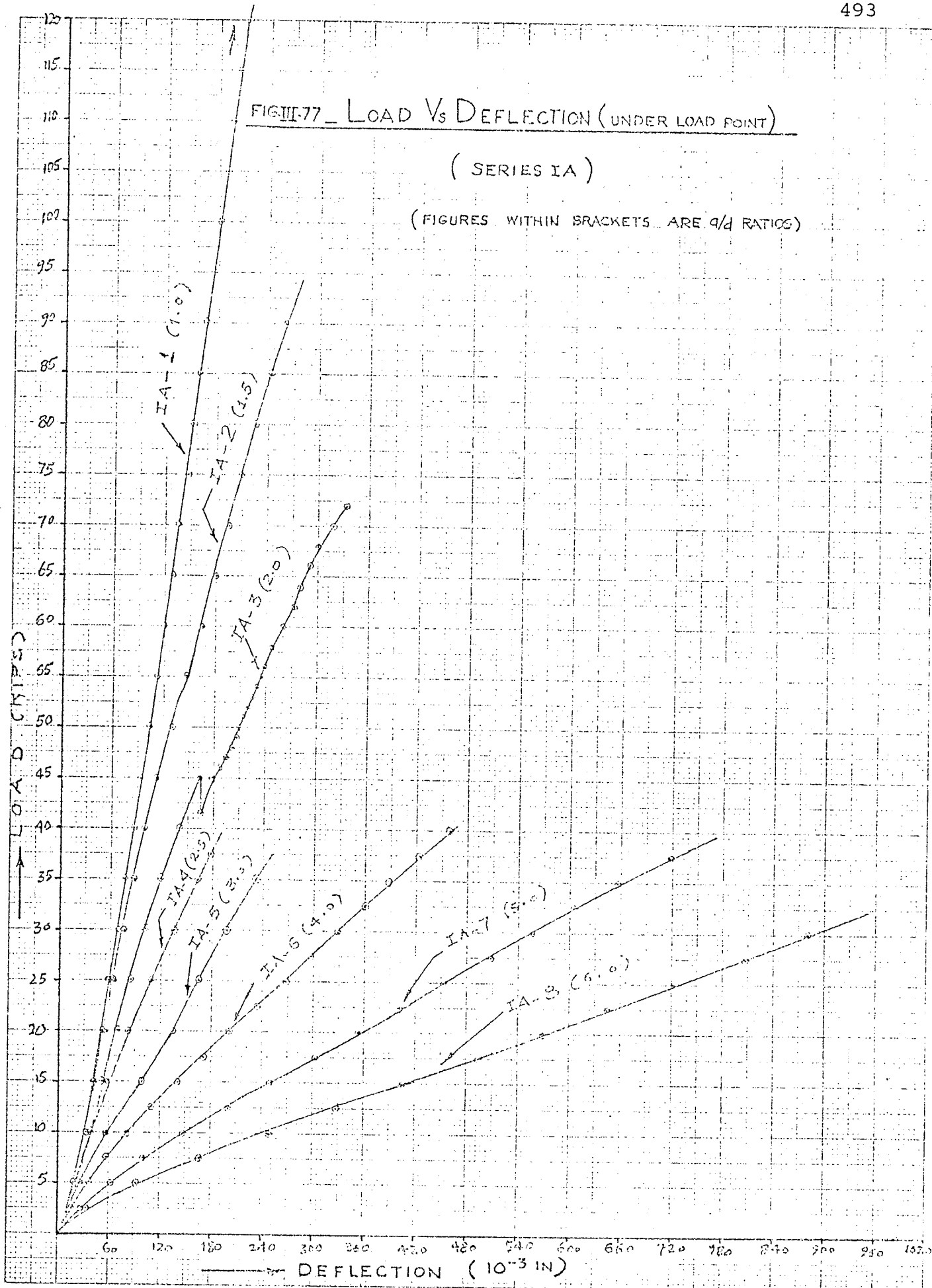
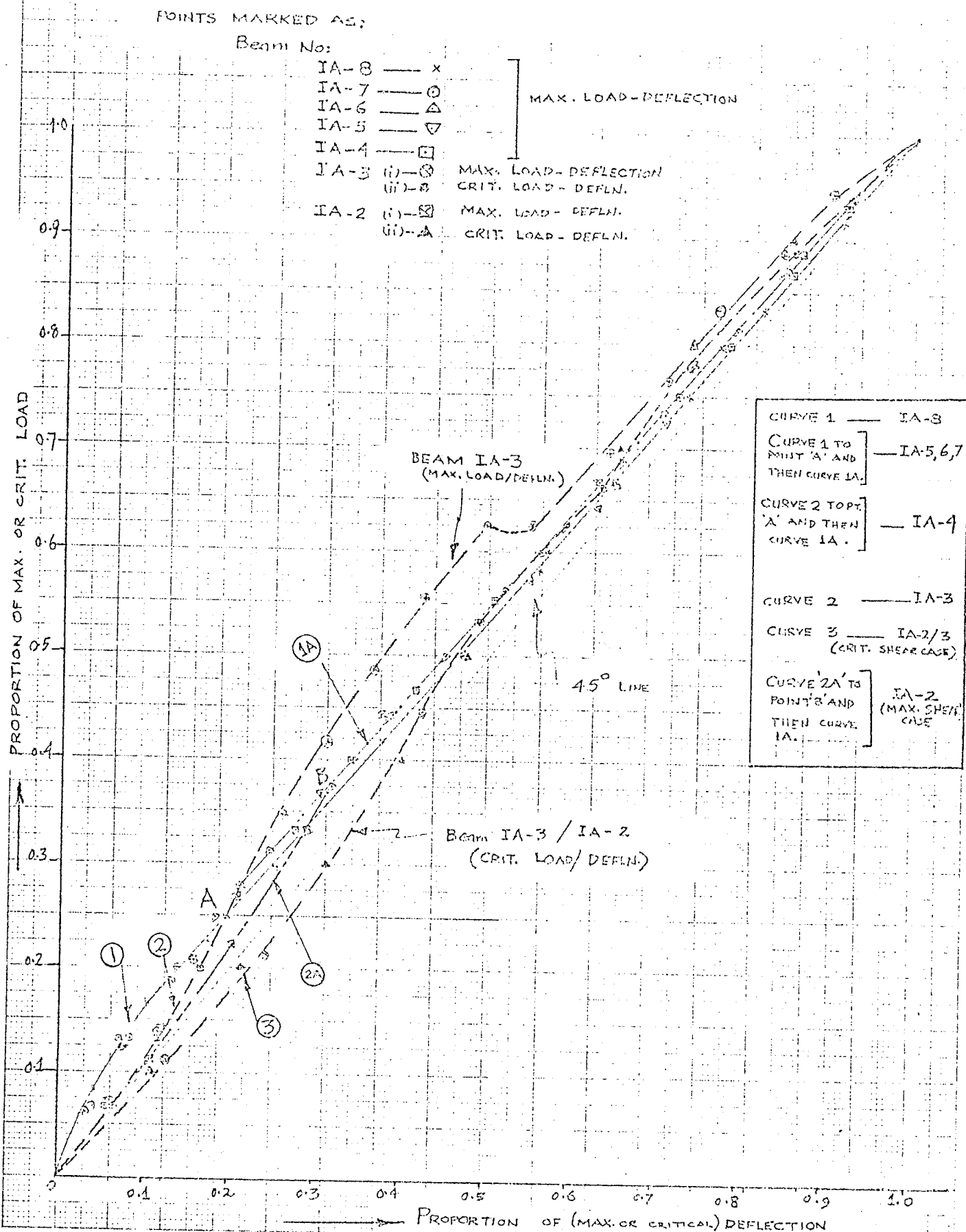
(FIGURES WITHIN BRACKETS ARE q/d RATIOS)

FIG. II-78. SERIES IA. COMPARATIVE LOAD-DEFLECTION CHARACTERISTICS AT MIDSPAN



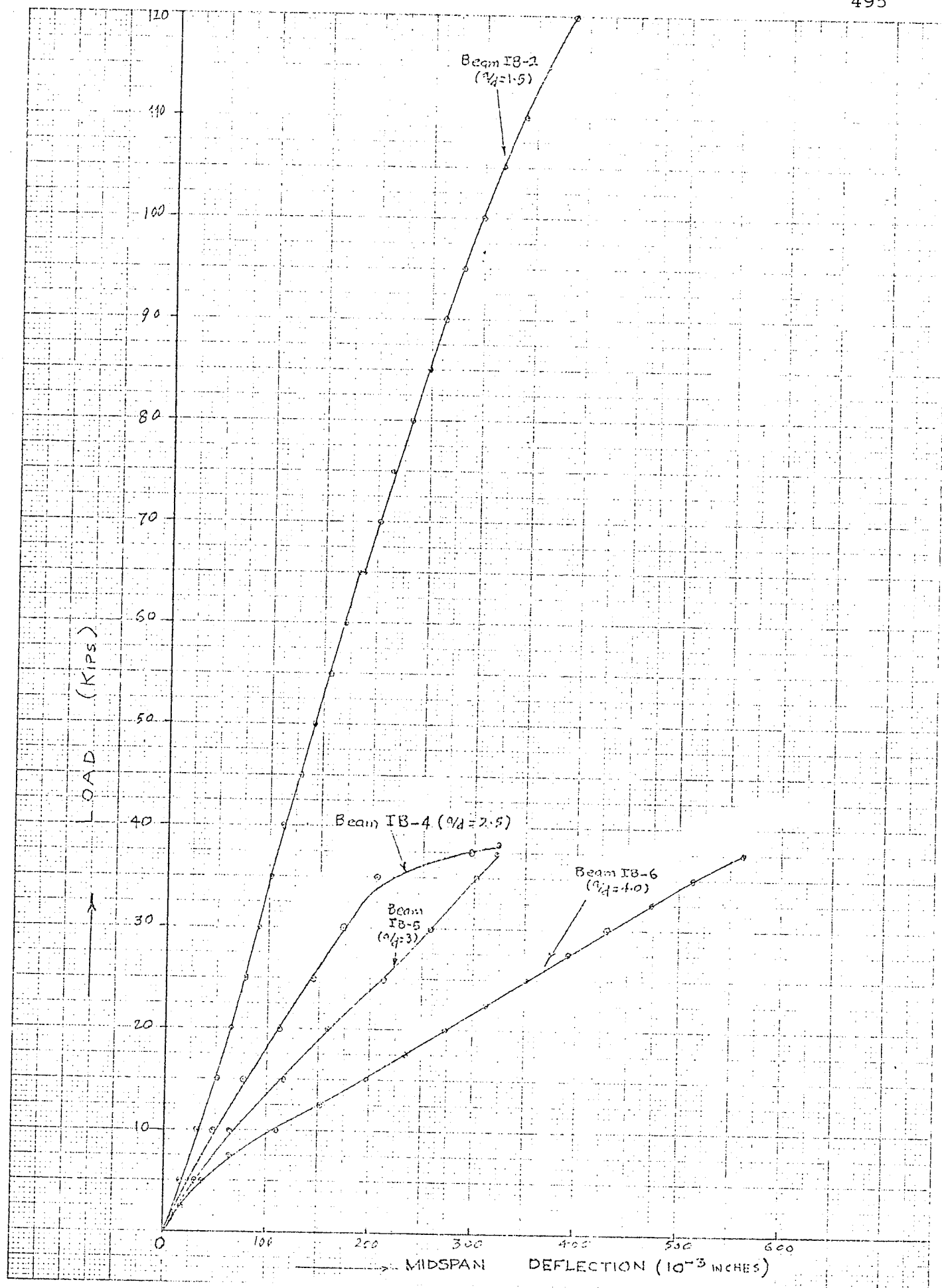


FIG. III-79 - SERIES IB — LOAD V_3 MIDSPAN DEFLECTION

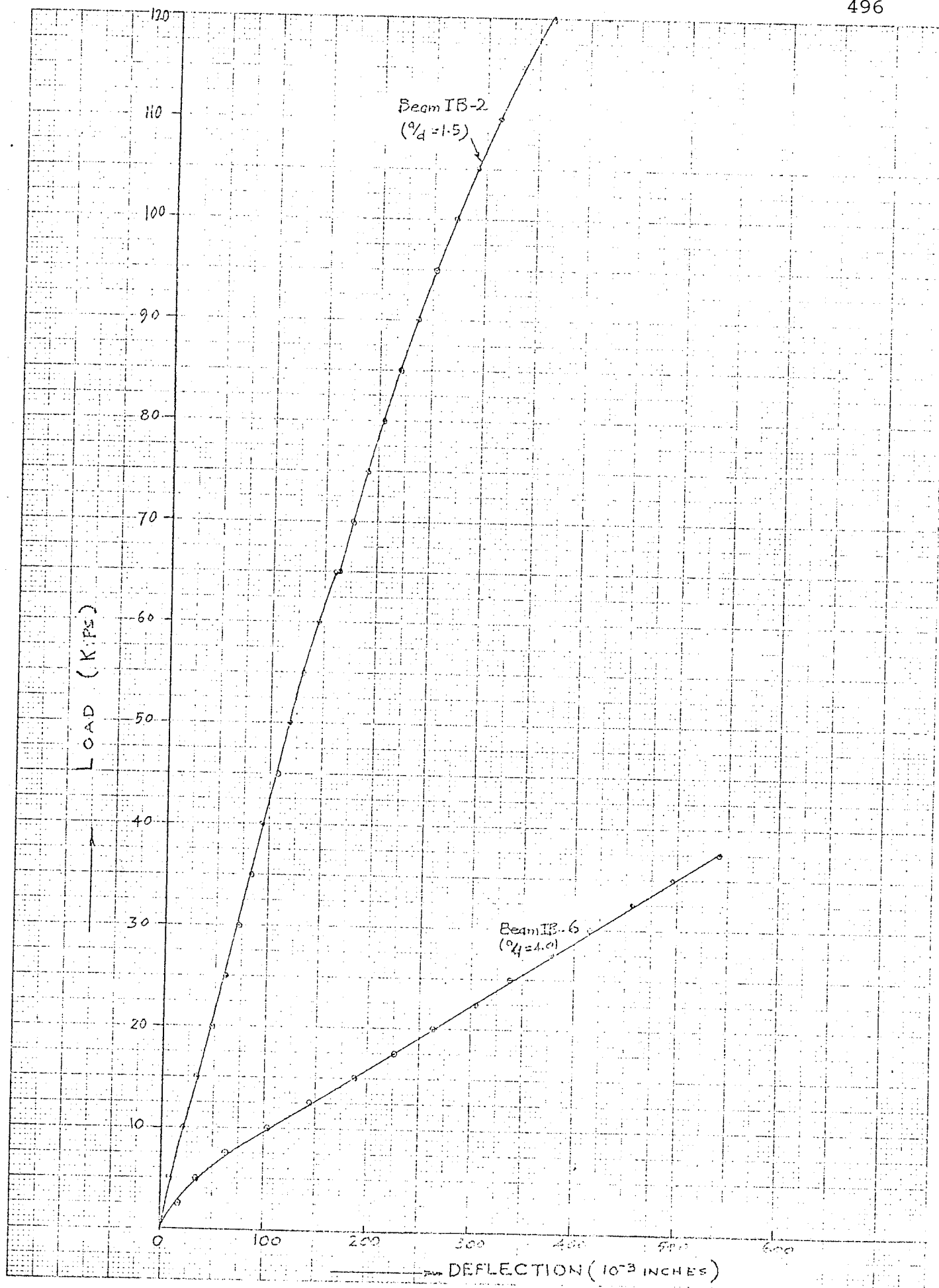


FIG. III.80-SERIES IB — LOAD VS DEFLECTION UNDER LOAD POINT

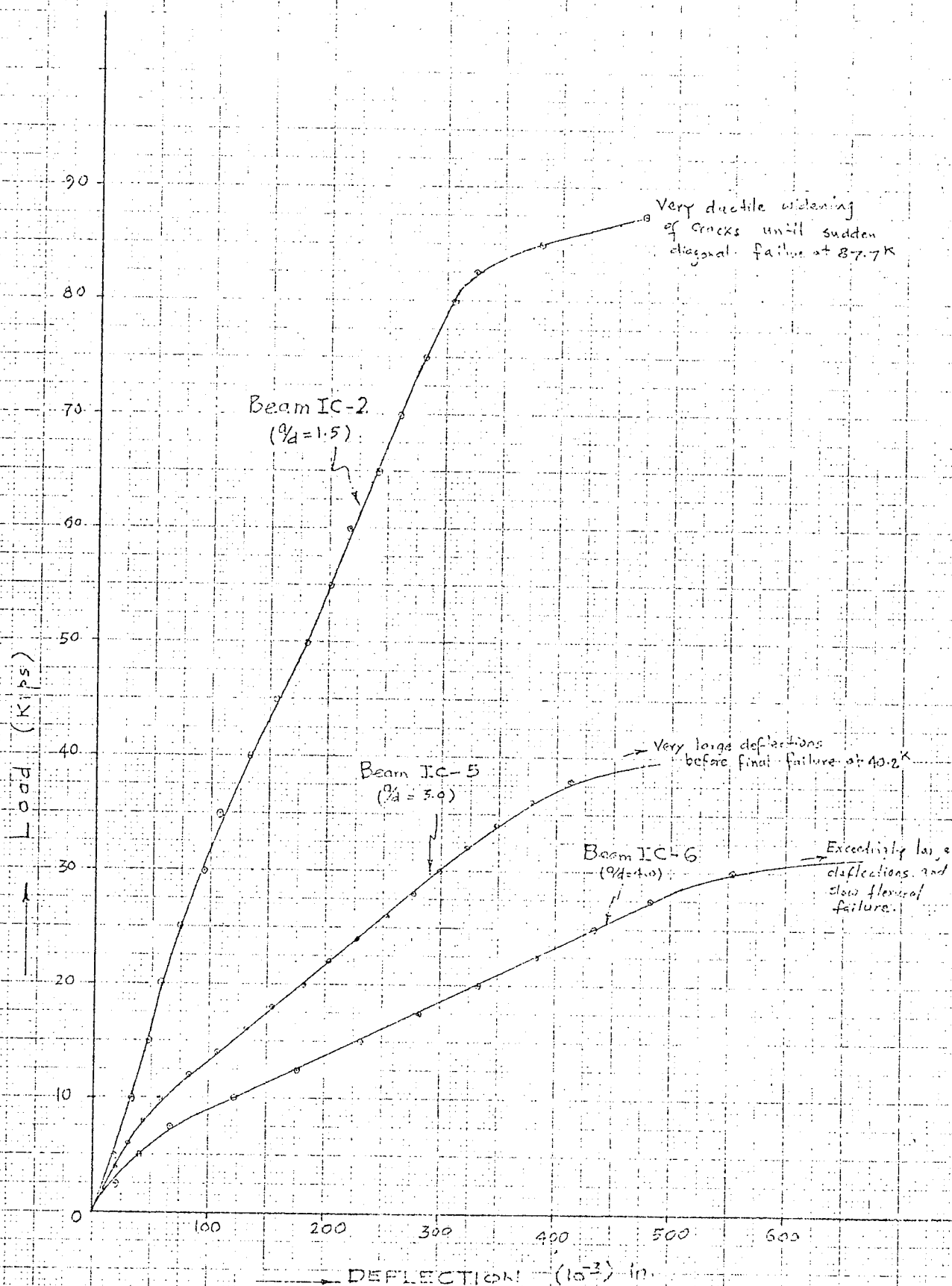


FIG. III-81

Series IC: Load Vs Midspan Deflection

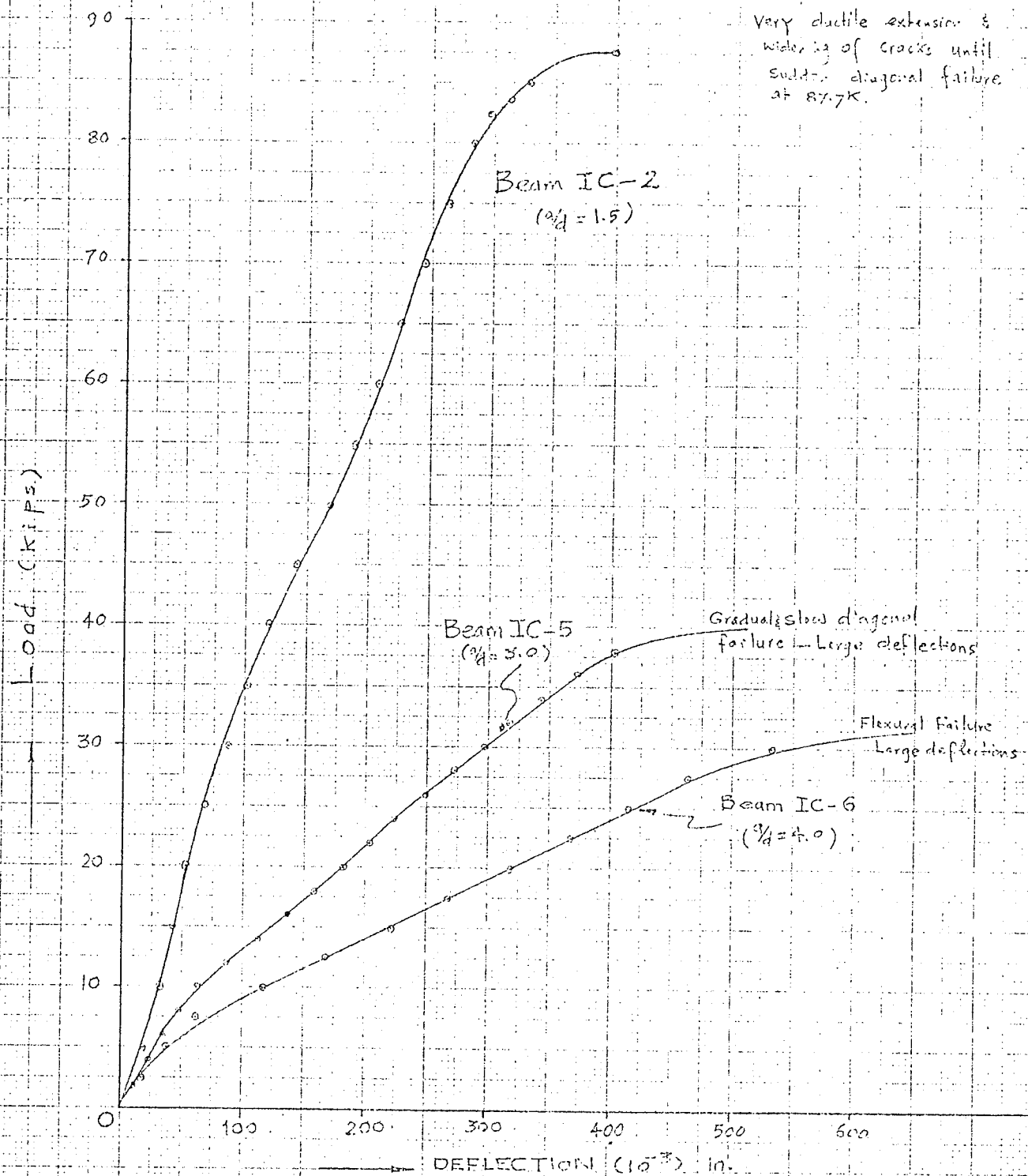


FIG. III-82

Series IC: Load Vs Deflection Under Load Point

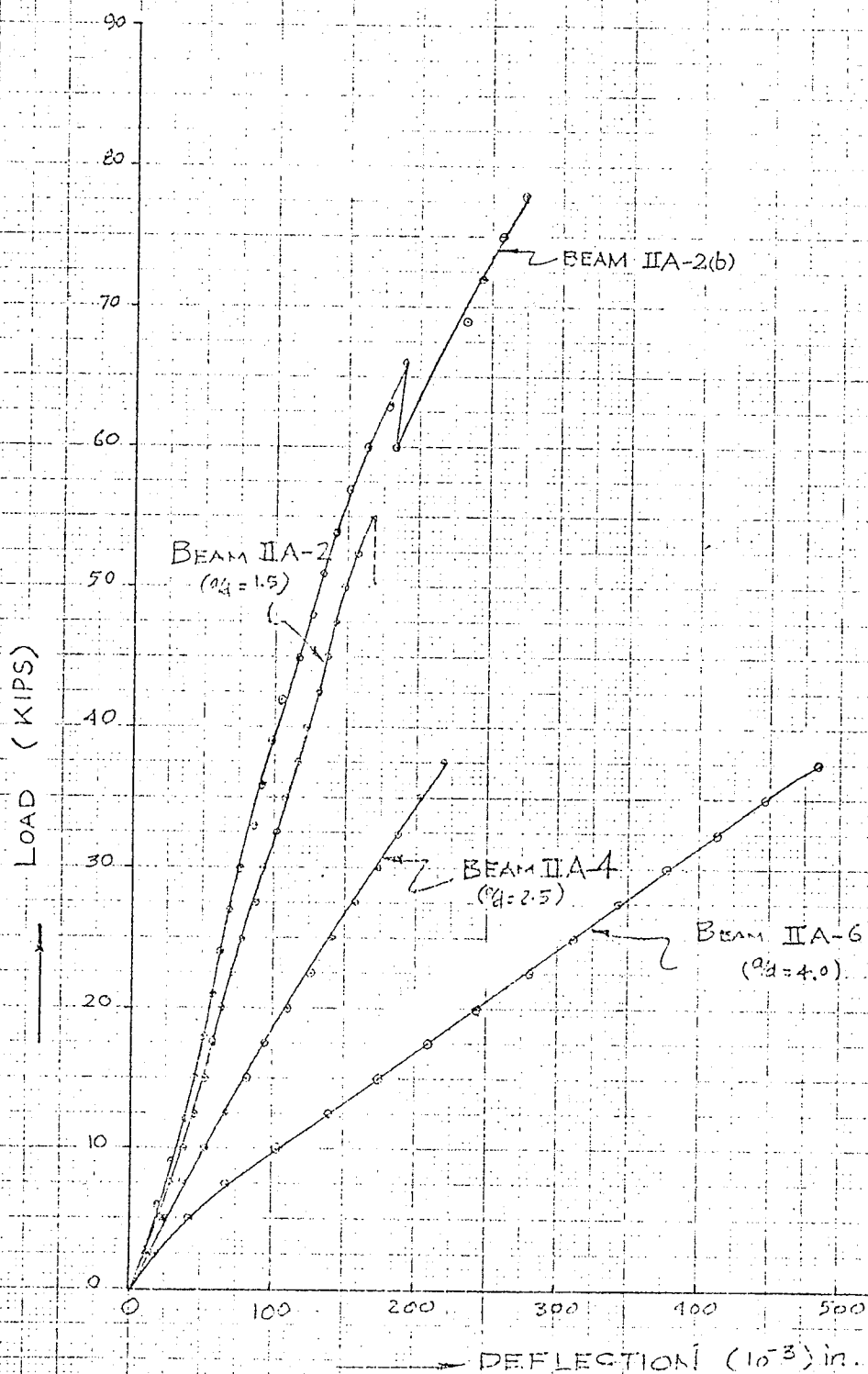


FIG. III-83

Series IIA: Load Vs Midspan Deflection

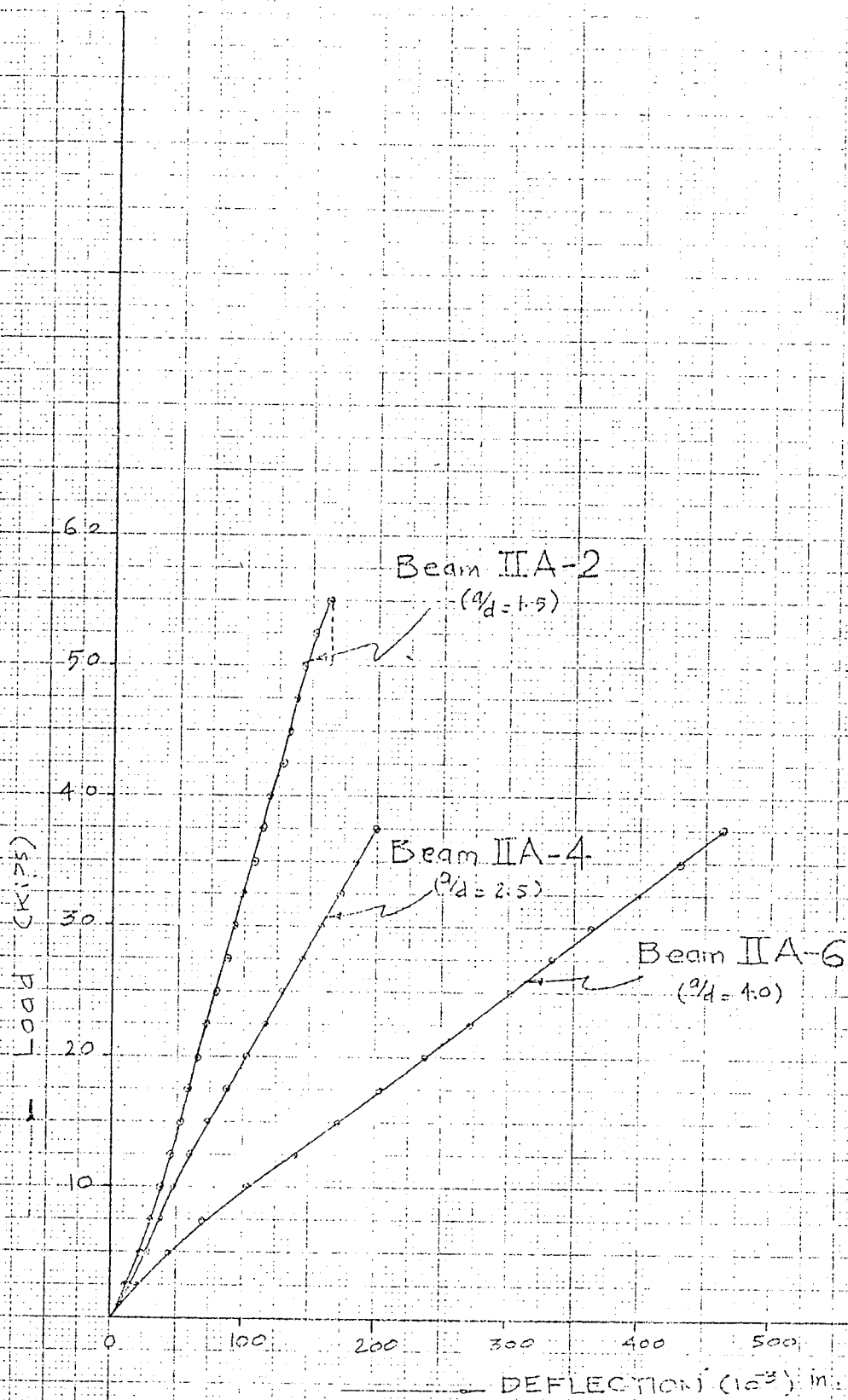


FIG. 84

Series IIA: Load Vs Deflection Under Load Point

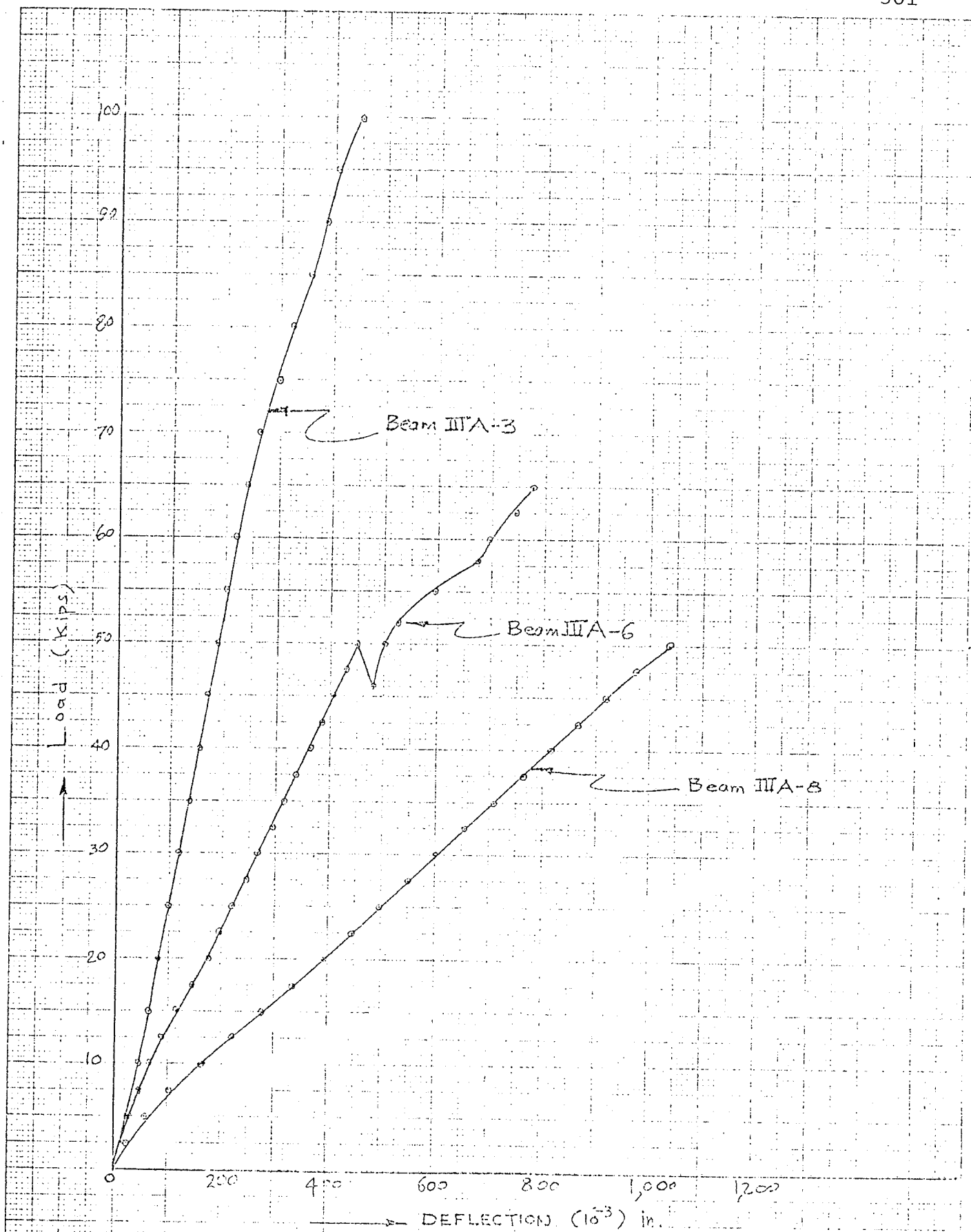


FIG. III-85

Series IIIA: Load Vs Midspan Deflection